Integration of Satellite System and Stratospheric Communication Platforms (SCP) for Weather Observation

by

Sihle S. Sibiya

A thesis submitted to the Information Technology (IT) Department in conformity with the requirements for the degree of

Doctor of Philosophy in Information Technology

at the

Durban University of Technology (DUT)

2016

Integration of Satellite System and Stratospheric Communication Platforms (SCP) for Weather Observation

by

Sihle S. Sibiya

A thesis submitted to the Information Technology (IT) Department in conformity with the requirements for the degree of

Doctor of Philosophy in Information Technology

at the

Durban University of Technology (DUT)

Supervisor: Prof. Dr. Dimov Stojče Ilčev
Research Group in Space Science

Co-supervisor: Waldo Kleynhans
Principal Researcher

Durban, 2016

Declaration

I, Sihle Sicelo Sibiya, declare that this dissertation is a representation of my own work both in conception and execution. This work has not been submitted in any form for another degree at any university or institution of higher learning. All information cited from published or unpublished works have been acknowledged.

Sihle Sicelo Sibiya	**30/06/2016**
Student Name	Date

Approved for final submission

Prof. Dimov Stojče Ilčev	**30/06/2016**
Supervisor	Date

Abstract

This doctoral research introduces an integration of satellite systems and new stratospheric platforms for weather observation, imaging and transfer of meteorological data to the ground infrastructures. Terrestrial configuration and satellite communication subsystems represent well-established technologies that have been involved in global satellite sensing and weather observation area for years. However, in recent times, a new alternative has emerged based on quasi-stationary aerial platforms located in the Stratosphere called High Altitude Platform (HAP) or Stratospheric Communication Platforms (SCP).

The SCP systems seem to represent a dream come true for communication engineers since they preserve most of the advantages of both terrestrial and satellite communication systems. Today, SCP systems are able to help, in a more cost effective way, developments of space Earth sensing and weather observation and weather sensing and observation. This new system can provide a number of forms ranging from a low altitude tethered balloon to a high altitude (18 – 25 km) fuel-powered piloted aircraft, solar-powered unmanned airplanes and solar-powered airship.

.

Acknowledgements

I thank the Lord for all His blessings bestowed on me in seeing this research work through; without which this research could not have become a reality. I would like to extend my sincere thanks to my supervisor Prof. Dimov Stojče Ilčev, for his advice, guidance and fatherly talks. He gave me courage to face the challenges in research and assisted me through. Thanks to him also for providing me with the amazing opportunity of being part of the Research Group in Space Science and the IT Department for accepting and supporting this research work.

I extend my special thanks to my co-supervisor, Dr. Waldo Kleynhans, who willingly assisted through this research.

I am indebted to my family, friends and all who have afforded me time and helped me in making this research work a great success in all aspects.

Preface

This research is providing essential practical and theoretical solutions for meteorological and weather observation via satellite and SCP systems. This study was conducted in order to form an integration of current satellite constellations and new SCP infrastructures as needs in the field of modern Earth monitoring and sensing for more cost effective meteorological and weather observation and collection of data.

This study includes meteorological and weather observations via existing Geostationary Earth Orbit (GEO) and Polar Earth Orbit (PEO) satellites and simultaneously sending data and images by satellite communication channels to the ground infrastructures. In the similar way, SCP aircraft or airships are able to provide metrological and weather observation and send data and images to the ground. At this point, SCP stations are able to provide integration with GEO or PEO satellites as bridges to receive and forward all observation data and images to the ground centres.

This thesis consists of 9 chapters on the following particular subjects:

Chapter 1: INTRODUCTION This chapter gives a short background to the development of Radio and Space systems, overview, concepts and applications of satellite communications in the functioning of transfer meteorological observation data and images.
Chapter 2: AIMS AND OBJECTIVES This chapter introduce the main scope and overview of this thesis for current and new space meteorological observation systems, together with the principal collections of data and images by space stations and their distribution to the ground processing fixed and mobile infrastructures.
Chapter 3: SPACE SEGMENT This chapter discusses the fundamental principles of the space platforms and orbital parameters, lows of satellite motions, new types of launching systems, satellite orbits and geometric relations, spacecraft configuration, payload structure, types of onboard antenna systems, satellite orbits and components of the satellite bus.
Chapter 4: THEORETICAL FRAMEWORK This chapter introduces an essential basic knowledge of baseband signals and processing, analog and digital transmissions, modulation, demodulation, coding, error corrections, multiple access techniques, fixed and mobile DVB-RCS standards, MPEG multimedia standards, audio and video broadcasting, direct-to-home digital broadcast system, transmission standards and DVB-S2 Architecture.
Chapter 5: ANTENNA SYSTEMS AND PROPAGATION This chapter provide research and introduce current and new proposed prototypes of antenna solutions for satellite and other radio meteorological communications systems, such as low-gain omnidirectional antennas, directional medium-gain antennas and high-gain directional aperture antennas. In addition, this chapter comprises all the particulars about propagation effects important for meteorological communication requirements such as: propagation fundamentals, refraction, absorption and non-LOS radio propagation, sky wave propagation, atmospheric effects on propagation, sky noise temperature contributions, path depolarization causes, propagation effects important for space communications and broadcasting, and so on.
Chapter 6: METEOROLOGICAL SATELLITE SYSTEMS This chapter introduces the history of the first types of meteorological satellites, current and new proposed meteorological satellites, such as Polar Earth Orbit (PEO), Geostationary Earth Orbit (GEO), Low Earth Orbit (LEO) and High Elliptical Orbit (HEO) developed by USA, Europe, Russia, China, India and Japan. In addition, this chapter presents the main types of meteorological imaging systems and meteorological satellite image interpretation.

Chapter 7: REGIONAL METEOROLOGICAL SERVICE VIA STRATOSPHERIC COMMUNICATION PLATFORMS (SCP) This chapter introduces all current and new developed SCP for multipurpose functions and meteorological observations and sending data to the ground. This chapter also gives details the proposed integrated architecture for weather observation and communication.

Chapter 8: GROUND SEGMENT This chapter describes **the** collection of daily environmental data from meteorological satellites or SCP by the Direct Readout Service (DRS) terminals, as one of the major functions of this subsystem. The weather satellite direct broadcasting system, or more commonly called DRS, was developed to overcome any problems caused by the previous distribution program. The description will also include Automatic Picture Transmission (APT), High Resolution Picture Transmission (HRPT) and Direct Sounder Broadcasts (DSB) from the PEO satellites, and Low-Rate Information Transmission (LRIT) and GOES Variable Format (GVAR) data from the GEO satellites. In addition, this chapter introduces Ground Earth Station (GES) mobile and user Earth stations infrastructures and antenna systems, including transmissions of meteorological data from Data Collection Platform (DCP) via satellites or SCP stations to the DRS ground terminals. Finally, this chapter explains Weather Ground Processing of Satellite Meteorological Data and its distribution to the different users and customers.

Chapter 9: SYSTEM ANALYSIS AND CONLUSION This chapter presents the system analyses, conclusion remarks, research limitations and future work.

Contents

List of Figures

List of Tables

CHAPTER ONE

INTRODUCTION

This chapter presents the principal structure of the space systems, functionality, media and applications for modern remote sensing, meteorological observation and transferring weather data from satellite or stratospheric platform sensors to the ground infrastructures. In such a way, satellites present “Eyes from the Space”, which can “see” the Earth and its atmosphere from global perspective and send all necessary observations, data and images via satellite onboard transponders to the Ground Earth Stations (GES) and processing facilities. On the other hand, it is very important to realize the idea of the project for the integration of satellite constellations, such as Geostationary Earth Orbit (GEO or Polar Earth Orbit (PEO), with Stratospheric Communication Platforms (SCP) or High Altitude Platforms (HAP).

However, the important link in this chain is the radio system as a predecessor to satellite and other wireless systems, which have been used as media for transmission of meteorological data and weather forecasts, namely, the weather radio is a network of radio stations in any country that broadcast continuous weather information directly from a nearby national weather forecast office of the service’s operator and service within one hypothetical country. The exploitation of the modern radio system began from the history of implementation of the first radio equipment invented by the great Russian professor, Alexandr Stepanovich Popov. For the first time in the world, Popov’s radio system was applied at shore and onboard ships for radio communication purposes as a part of today’s VHF, UHF and HF radio systems. Afterwards, the radio navigation and radar systems were developed as onboard radio equipment working on special frequencies for the determination position of mobiles on the Earth’s surface, such as radiolocation and radio determination systems.

Officially, the equipment for radiolocation, known as radar, was invented by the British Sir Robert Watson-Watt in 1935, and it then became the first radar used in battle. There was a race between Brittan and Germany as to who could produce the best radar for their national defense forces. Nevertheless, the Germans were unable to unlock its full potential.

The British had won the race and utilized the full power of the radar technology (Kramer, 2002). Radiolocation is the process of finding the location of some objects like ships through the use of radio waves, such as the surveillance radar. Radar is a measuring instrument in which the echo of a pulse of microwave radiation is used to detect and locate distant objects. Ground and space radars are serving today for Earth observation. However, this study will not include any type of radar remote sensing and meteorological observations.

1.1 Abstract

The weather observation and information has been an important part of life as long as history of mankind exists and weather measurements have been done for centuries. It is claimed that the first measurements of rainfall were reported as early as 500 B.C. from Greece. These measurements were aimed to estimate the expected growth of wheat and were used as a basis for taxation of the farmers. These primitive measurements were made by using bowls. The first actual rain gauges were developed much later in Korea (Bellis, 2011). The first early forecast services were established in England, France, Germany and USA during 1800’s to provide information about possible storms for seafarers (Hautala et al, 2007). Although there

is a long history of weather observations, their importance to everyday use has grown enormously during the last few decades and especially during the last ten years.

On the other hand, modern technological developments of the last few decades, such as improved telecommunications, Automatic Weather Stations (AWS) and various long range measuring systems, such as satellites, meteorological observation and weather radars, have enabled a range of new possibilities for utilizing weather information(Eumetsat, 2009). For a common person, these became evident in real time weather services tailored for individual customers, as well as the improved quality of the weather forecasts.

In the more than 30 years since the first meteorological and weather satellites were launched and deployed, they have become indispensable for the study of the Earth's atmosphere, climate and meteorological phenomenon for weather synopsis and prognoses. Indeed, together with their land and ocean-sensing forerunners, meteorological satellites view the Earth from a global perspective, which is unmatched and incomparable by any other observing system. In a similar way, Stratospheric Communication Platforms, as satellites in stratosphere, can provide more cost effective Earth monitoring, meteorological observation and remote sensing for local and even regional coverage (Aragon-Zavala et al, 2008, Ilcev 2011).

1.2 Overview of Space Age

The space age officially began on October 4, 1957, with the dramatic and historic launch of Sputnik 1 by the Soviet Union, but there are much deeper roots. In 1903, Russian high school mathematics teacher, Konstantin Tsiolkovsky (1857–1935), published "Investigation of outer space rocket appliances" (The Exploration of Cosmic Space by Means of Reaction Devices), the first serious scientific work on space travel. The Tsiolkovsky rocket equation known as the principle that governs rocket propulsion is named in his honour. He also advocated the use of liquid hydrogen and oxygen as fuel, calculating their maximum exhaust velocity. His work was essentially unknown outside the Soviet Union, but inside the country as a "Father of First Rocket", it inspired further research, experimentation and the formation of the Society for Studies of Interplanetary Travel in 1924. In the same year, Tsiolkovsky wrote a scientific work about Multi-stage Rockets in the "Cosmic Rocket Trains".

Thus, the twentieth century came with its great progress and the historical age of space program began to unfold. Thanks to Russian scientist Tsiolkovski and his early works on space program became a basis on virtually every aspect of space rocketing. He propounded the theoretical basis of liquid propelled rockets, put forward ideas for multi-stage launchers and manned space vehicles, space walks by astronauts and a large platform system that could be assembled in space for normal human habitation. In line with this strategy, on March 1, 1921, the Soviet authorities created the Gas Dynamic Laboratory (GDL), an institution for research in rocketry, to be led by Nikolai Tikhomirov. Researchers at GDL worked tirelessly on perfecting military missiles and developing new types of solid rocket fuel, which would allow the new weapons to compete with artillery. As Tsiolkovski was the first to discover that the reaction principle could reach space, it would make sense that the Russians would provide very significant developments in rockets. In early 1924, two new Russian rocket programs were founded. They were the Central Bureau for the study of the problems of rockets (TsBIRP), and the All-Union Society for the Study of Interplanetary Flight (OIMS). The main leader of these early Russian rocket efforts was Fridrikh Tsander, who developed liquid propellant rockets in the 1920s and 1930s.

A little later, the American, Robert H. Goddard, launched, on 16th March 1926, the first liquid propelled engine rocket. The German society for space travel or VfR, was founded in June of 1927, and it soon had around five hundred members and published its first journal "the Rocket".

At the beginning of the 1930s, the Soviet government sanctioned the creation of several research groups, which united rocket enthusiasts in organizations known as GIRD (Group for Investigation of Reactive Movement) with centres in Moscow, Leningrad and other cities.

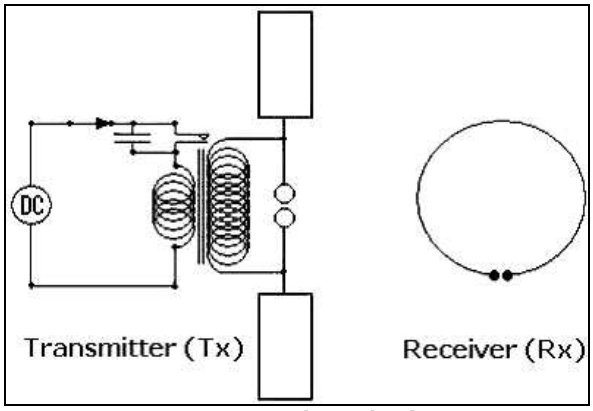

Figure 1. 1 First Spark Gap by Ilcev 2005

In Moscow, thanks to the efforts of Sergei Korolev (father of Soviet rockets) and Fridrikh Tsander, the government-sponsored Society for the Advancement of Defense, Aviation and Chemical Technology, Osaviakhim, agreed to fund GIRD. However, after Stalin took over the Soviet country, these rocket programs became Len-GRID and Mos-GRID, or "Group for the study of reactive motion", as the professional rocketry group in the world, based in Leningrad and Moscow, respectively. These two centres, in turn, soon became the State Reaction Scientific Research Institute. In 1933, a Soviet rocket with the hybrid engine (GIRD-09) is launched, which, in reality, started the cosmic era.

1.3 Development of Radio Communications

Communication satellites provide the bridges for a number of new, specialized markets in commercial and private telecommunications and make ties between nations. In the course of almost six decades, satellite communication systems have obtained global links in the public and private Terrestrial Telecommunication Network (TTN). In the meantime, the meteorological satellite system was developed and the US first satellite Explorer-1, which was launched on 31 January 1958, and 123 days later, the first Soviet satellite, Sputnik-1, was launched. Almost two decades later, the first truly global Mobile Satellite Communication (MSC) system was begun with the launch of the three Marisat satellites in 1976 by Comsat General.

The word **communications** is derived from the Latin phrase "**communication**", which stands for the social process of information exchange and covers the human need for direct contact, communications and mutual understanding. The word "**telecommunications**" means to convey and exchange information at a distance (**tele**) by the medium of electrical signals via space applications (Blonstein, 1987).
In general, telecommunications are the conveyance of intelligence in some form of signal, sign, sound or electronic means from one point to a distant second point. In ancient times,

that intelligence was communicated with the aid of audible callings, fire and visible vapour or smoke and image signals. We have come a long way since the first human audio and visual communications, used during many millennia. In the meantime, primitive kinds of communications between individuals or groups of people were invented. Hence, as impressive as this achievement was, the development of more reliable communications and so, wire and radio, had to wait a couple of centuries more.

The invention of the telegraph in 1844 and the telephone in 1876 harnessed the forces of electricity to allow the voice to be heard beyond visual and shouting distance for the first time. The British physicist, M. Faraday, and the Russian academic, E. H. Lenz, experimented with electric and magnetic phenomena and formulized a theory of Electromagnetic (EM) induction at the same time.

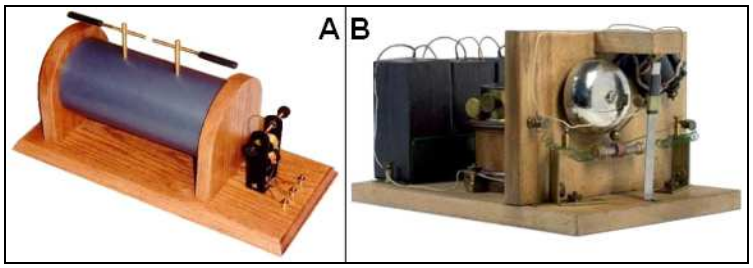

Figure 1. 2 First Rx/Tx Designed by Popov by Ilcev 2013

However, the British physicist, James C. Maxwell, published, in 1873, his classical theory of electromagnetic radiation, proving mathematically that electromagnetic waves travel through space with a speed precisely equal to that of light.

The famous German physicist, Heinrich Rudolf Hertz, during 1886, experimentally proved Maxwell's theoretical equations. He demonstrated that HF oscillations produce a resonant effect at a very small distance away from the source and that this phenomenon was the result of electromagnetic waves. Practically, Hertz used the damped oscillating currents in a dipole antenna, triggered by a high-voltage electrical capacitive spark discharge, as his Transmitter (Tx) source of Radiowaves (RW). Thus, his detector, in some experiments, was another dipole antenna connected to a narrow spark gap as Receiver (Rx). A small spark in this gap signified detecting of the radio waves. When he added cylindrical reflectors behind his dipole antennas, Hertz could detect radio waves about 20 meters from the Tx in his laboratory (see Figure 1.1) So, it is after Hertz that the new discipline of Radio technology is sourced and after whom the frequency and its measuring unit Hertz (Hz) are named.

An English physician, Sir Oliver J. Lodge, using the ideas of others, realized that the EM resonator was very insensitive and he invented a "coherer". A much better coherer was built and devised by a Parisian professor, Edouard Branly, in 1890. He put metal filings (shut in a glass tubule) between two electrodes and so a great number of fine contacts were created. This coherer suffered from one disadvantage, i.e., it needed to be "Shaken before use". Owing to imperceptible electric discharges, it always got "baked" and blocked.

The Russian professor of physics, Aleksandar S. Popov, in 1894, successfully realized the first practical experiments with EM waves for the transmission of radio signals. In the same year, he succeeded in making a reliable generator of EM waves, when the receiving or detecting systems in common use still were not at all satisfactory.

Using the inventions of his predecessors and on the basis of proper experiments, Popov elaborated the construction of the world's first radio receiver with a wire-shaped antenna system in the air attached to a balloon, shown in Figure 1.2 (A). Using the inventions of his predecessors and on the basis of proper experiments, Popov elaborated the world's first radio receiver with a wire shaped antenna in the air attached to a balloon, presented in Figure 1.2 (B). In 1895, Popov improved Branly's receiver by the insertion of choke coils on each side of the relay to protect the coherer and also by replacing the spark gap with a vertical antenna insulated at its upper end and connected to the ground through the coherer. He then mounted a small bell in serial connection with the coherer's relay anchor, whose ringing effected automatic destabilization and successive unblocked function of the receiver system. On 7 May 1895, he demonstrated his new apparatus to the members of the Russian Physic-Chemical Society: a lightning conductor as an antenna, a metal filings coherer and detector element with telegraph relay and a bell. The relay was used to activate the bell, which is announcing the occurrence of transmitting signals and, in this way, serving as a decoherer (tapper) to prepare the receiver to detect the next signals. This was the first telegraph station in the world, which could work without any wires. In May of the same year, he reported sending and receiving radio signals across a 550 m distance.

Figure 1. 3 Marconi with his first Radio by Ilcev 2005

Soon, instead of a bell he contrived to use a clock mechanism to realize direct, fast destabilization of metal filings in the coherer upon receipt of the signals. In December 1895, he announced the success of a regular radio connection and, on 21 March 1896 at the St. Petersburg University, he demonstrated it in public. Finally, on 24 May 1896, Popov installed a pencil instead of the bell and sent the first wireless message in the world at a distance of 250 m between two buildings, conveying the name "GENRICH GERZ" (the name of Hertz in Russian) by Morse code using his homemade transmitter and receiver.

In March 1897, Popov equipped a coastal radio station at Kronstadt and the Russian Navy cruiser Africa with his wireless apparatus and, in summer, 1897, Popov started to conduct experiments at sea, using radios on board ships. In 1898, he succeeded in relaying information at a distance of 9 km and, in 1899, a distance of 45 km between the island of Gogland and the city of Kotka, in Finland. With all his inventions, Popov made advances on the discoveries of Hertz and Branly and created the groundwork for the development of maritime radio.

In 1895, a few months later than Popov, a young Italian experimenter, Guglielmo Marconi, started to use radio and was the first to put EM theory into practical application. By the next year, he had sent Morse code messages at a distance of 2 miles. Moving to England to obtain patents on his equipment, he demonstrated radio reception over 8 miles. In 1897, he exhibited the use of radio between ship and shore and, according to Western literature, practically started the use of maritime radio. By the same year, Marconi succeeded in getting his wireless telegraphy transmissions officially patented for the first time in the world. The owners of the Dublin Daily Express in Ireland invited Marconi to conduct wireless reports of the Kingston Regatta of July 1898 from the steamer, Flying Huntress, the first ship equipped with a commercial wireless system.

Using an antenna hung from a kite to increase the effective height of his masts and a LF of 313 kHz at 10 kW of power, on 12 December 1901, Marconi crackled out the first wireless message to span an ocean in the form of Morse code; three dots forming the letter "s". This telegraph signal was sent from Newfoundland in Canada and received in Cornwall on the west coast of England (see photo of Marconi with his first Radio Equipment in Figure 1.3).
Unlike Popov, Marconi was a good businessman and was able to turn his research into a financial and manufacturing empire. He designed radio Sailor as a first used Morse Sender for transmitting distress messages and later for commercial ship to shore and vice versa direction at the turn of the 20 century.

In 1900, R. Fessenden made the first transmission of voice via radio in the USA, Fleming in 1904 discovered the diode valve, while their countryman and pioneer Lee de Forest developed and used a triode valve, which made it possible to use radio not only for radiotelegraphy but for voice communications. As early as 1907, he installed a triode valve mobile radio on a ferryboat operating on the Hudson River near New York City.

1.3.1 Evolution of Satellite Communications

The first known annotation about devices resembling rockets is said to have been used by Archytus of Tarentumin, who invented in 426 B.C. a steam-driven reaction jet rocket engine that flew a wooden pigeon around his room. Devices similar to rockets were also used in China during the year 1232. In the meantime, human space travel had to wait almost a millennium, until Sir Isaac Newton's time, when we understood gravity and how a projectile launched at the right speed could go into Earth orbit.

Finally, the twentieth century came with its great progress and the historical age of space communications began to unfold. Russian scientist, Konstantin Tsiolkovsky (1857–1935), published a scientific book on virtually every aspect of space rocketing. He propounded the theoretical basis of liquid propelled rockets, put forward ideas for multi-stage launchers and manned space vehicles, space walks by astronauts and a large platform system that could be assembled in space for normal human habitation. A little later, the American, Robert H. Goddard, launched, in 1926, the first liquid propelled engine rocket.

At the same time, between the two World wars, many Russian and former USSR scientists and military constructors used the great experience of Tsiolkovsky to design many models of rockets and to build the first reactive weapons, particularly rockets called "Katyusha", which one Soviet Red Army used against German troops at the beginning of the Homeland War (Second World War). Thus, towards the end of the Second World War, many military constructors in Germany started with experiments to use their series V1 and V2 rockets.

After that, in October 1945, the British radar expert and writer of science fiction books, Arthur C. Clarke, proposed that only three communications satellites in GEO could provide global coverage for TV broadcasting.

The work on rocket techniques in Russia and the former USSR was much extended after the Homeland War. The satellite era began when the Soviet Union shocked the globe with the launch of the first artificial satellite, Sputnik-1, on 4 October 1957. This launch marked the beginning of the use of artificial Earth satellites to extend and enhance the horizon for radiocommunications, navigation, weather monitoring and remote sensing and signified the announcement of the great space race and the development of satellite communications. As stated earlier, that was soon followed on 31 January 1958 by the launch of US first satellite Explorer-1, so the development of satellite communications and the space race began (Gordon et al, 1993).

The most significant progress in space technology was on 12 April 1961, when Yuri Gagarin, officer of the former USSR Air Forces lifted off aboard the Vostok-1 spaceship from Bailout Cosmodrome and made the first historical manned orbital flight in space.

1.3.2 Experiments with Active Communications Satellites

As stated, the first satellite equipped with onboard radio transmitter was the Soviet Union Sputnik-1, when de facto started era of Satellite Communications (Blonstein, 1987). Soon after the launch of Sputnik-1, a sustained effort by the USA to catch up with the USSR was started. The initiative of the US state and military forces was reflected in the first active communications satellite named SCORE, launched on 18 December 1958 by the US Air Force. This satellite provided relay by using a tape recorder to store and forward voice messages.

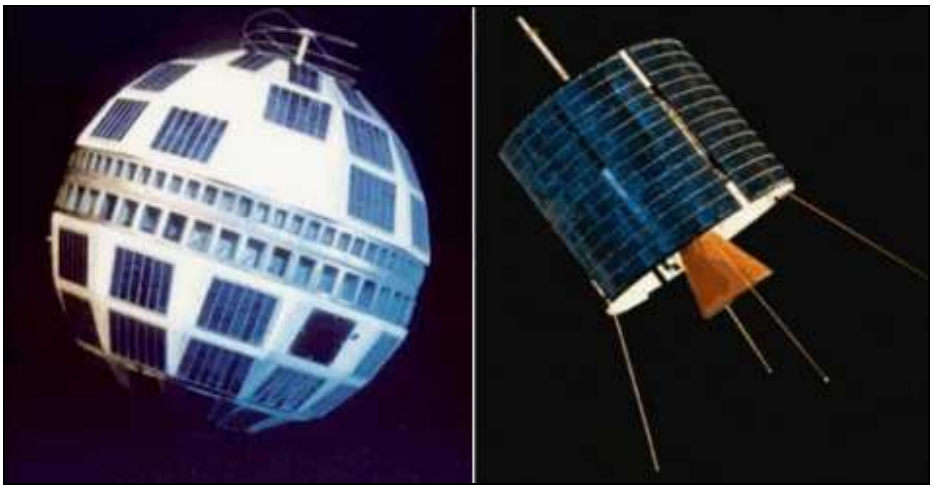

Figure 1. 4 Telstar-1and Intelsat-1 by Gunter 2015

The second satellite, Echo, was launched by NASA early in 1960, the 100-foot aluminized pet film balloon served as a passive reflector for radio communications. The third satellite, Courier, was launched on 4 October 1960 in High Elliptical Orbit (HEO) with its perigee at about 900 km and its apogee at about 1,350 km using solar cells and a frequency of 2 GHz. The maximum emission length was between 10 and 15 min for every successive passage.
The fourth satellite was Telstar-1, designed by Bell Telephone Laboratories engineers, and launched by NASA on the 10 July 1962 in HEO configuration with its perigee at about 100

km and apogee at about 6,000 km, shown in Figure 1.7 (Left). The plane of the orbit was inclined at about 45º to the equator and the duration of the orbit was about 2.5 hours. Due to the rotation of the Earth, the track of the satellite, as seen from the Earth stations, appeared to be different on every successive orbit. Otherwise, over the next two years, the spacecraft, Telstar I, was joined in the orbits by two new spacecrafts, Relay-1, Telstar-2 and Relay-2. All of these satellites had the same problem, because they were visible to widely separated GES terminals for only a few very short daily periods, so numbers of GES infrastructures were needed to provide full-time service. On the other hand, GEO satellites can be seen 24 hours a day from approximately 40% of the Earth's surface, providing direct and continuous RF and Microwave (MW) links between large numbers of widely separated locations.

The World's first GEO satellite, Syncom-1, was launched by NASA on 14 February 1963, which presented a prerequisite for the development of MSC systems (Calcutt & Tetley 2004). This satellite failed during launch but Syncom 2 and 3 were successfully placed in orbit on 26 July 1963 and 19 July 1964, respectively. Both satellites used the military band of 7.360 GHz for the uplink and 1.815 GHz for the downlink. Using FM or PSK mode, the transponder could support two carriers at a time for full duplex operation. Syncom 2 was used for direct TV transmission from the Tokyo Olympic Games in August 1964. These spacecraft continued successfully in service until some time after 1965 and they marked the end of the experimental period.

Technically, all these satellites were being used primarily for Fixed Satellite Service (FSS) experimental communications, which were used only to relay signals from Fixed Earth Stations (FES) at several locations around the world. Hence, one FES was actually located aboard a large transport vessel, the USNS Kingsport, home-ported in Honolulu, Hawaii. The ship had been modified by the US Navy to carry a 9.1 m parabolic antenna for tracking the Syncom satellites, thus ship terminal was the world's first Mobile Satellite Service (MSS).
Intelsat was founded in August 1964 as a global FSS operator. The first commercial GEO satellite was Early Bird (renamed as Intelsat-1), developed by Comsat for Intelsat, which is shown in Figure 1.7 (Right).

The spacecraft, Early Bird, was launched on 6 April 1965 and remained active until 1969. Routing operations between the US and Europe began on 28 June 1965, a date that should be recognized as the birthday of commercial FSS. The satellite had 2 x 25 MHz width transponder bands, the first with 2 Rx uplinks (centred at 6.301 GHz for Europe and 6.390 GHz for the USA) and the second 2 Tx downlinks (centred at 4.081 GHz for Europe and 4.161 GHz for the USA), with maximum transmission power of 10 W for each Tx. This GEO system used several GES terminals located within the USA and Europe and, so, the modern era of satellite communications had begun.

In the meantime, considerable progress in satellite communications had been made by the former USSR, the first of which was the Molniya-1 (Lightning) satellite, launched on 25 April 1965. These satellites were put into an HEO, very different to those used by the early experiments and were used for voice, Fax and video transmission from central FES near Moscow to a large number of relatively small receive only stations.

In other words, that time became the era of development of the international and regional FSS with the launch of many communications spacecraft in the USSR, USA, UK, France, Italy, China, Japan and other countries. At first, all satellites were put in GEO, but, later,

HEO and PEO were proposed, because such orbits would be particularly suitable for use with GES at high latitudes.

1.4 Development of Global Space Communications Systems

Once the principles of radio were understood, mobile radiocommunications have been a matter of steadily developing and perfecting the radio technologies, extending accessibility and the possibility of radio networks, enhancing range, extending coverage and reliability, reducing the size, cost and power consumption of radio devices and improving efficiency. With further MSS innovations, an age long barrier was eliminated between vessels and shore sites, including all mobiles, facilities were created to provide mobile offices in ships and all vehicles and to communicate with GES independently of space, place and time. The world is going to reduce communications barriers and move people across borders and so existing Fixed Satellite Communications (FSC) and new MSC systems including multipurpose satellite communications, navigation and meteorological services will be responsive to all these extraordinary changes and globalization trends, which scenario is shown in Figure 1.5.
The MSC systems and technology also offer other benefits and perspectives. In many developing countries, telephone density is still at a low level in urban and non-urban areas, because the cost of upgrading such facilities through wireless or TTN means is prohibitive for much of the world areas. Remote, rural and mobile service sectors in many regions are outside the reach of communications facilities, so the new MSS technology, with its instant ubiquitous coverage, may provide cost-effective solutions for developing countries.

1.4.1 Definition of Global Mobile Satellite Communications (GMSC)

The GMSC are deploying GEO or Non-GEO satellite systems, which refer to all mobile communications solutions that provide global MSC service directly to end users from a satellite segment, ground satellite network and TTN landline and/or radio infrastructures(Sheriff et al, 2001). The term GMSC means not only global coverage but also includes local or regional MSS solutions as an integral part of the worldwide telecommunications village. Hence, some of the regional and local MSC systems can be afterwards integrated worldwide to establish a Global MSC network. Thus, the GMSC solutions, as modern structures, began providing communication links to vessels initially in the 1970s and later to other mobiles via global and regional satellite coverages.

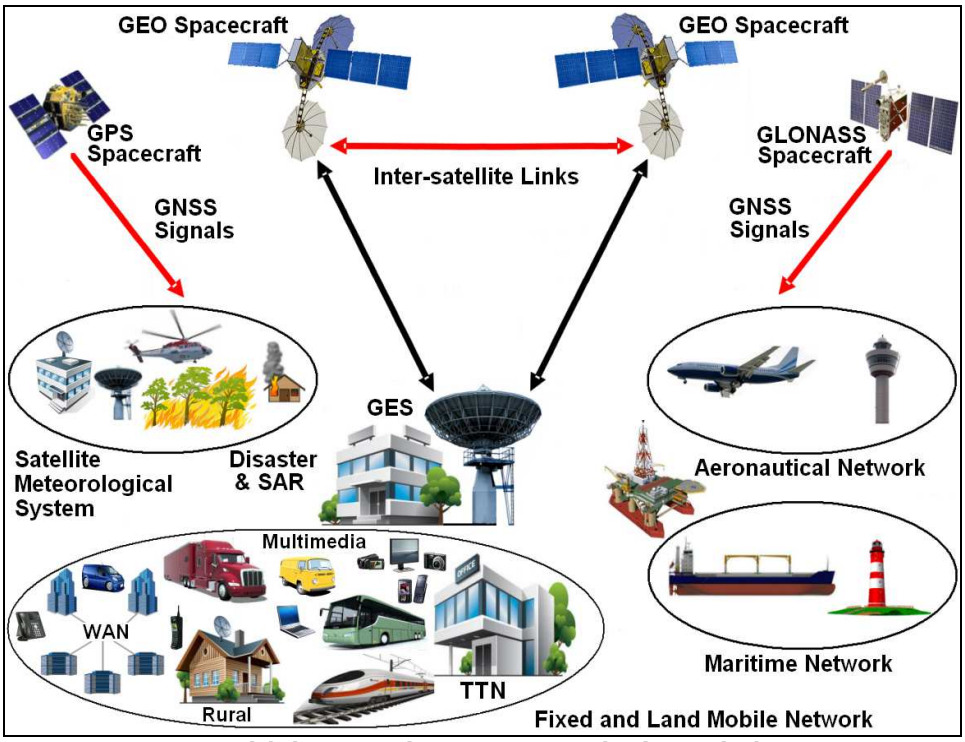

Figure 1. 5 Global Space Multipurpose Systems by Ilcev and Sibiya 2015

Old MSC technologies provided just voice and data communications, while using new Very Small Aperture Terminals (VSAT) of technology and a technique known as Digital Video Broadcasting-Return Channel via Satellite (DVB-RCS) standards improved global fixed, mobile and personal commercial and military communications. Recently, DVB-RCS has been for broadcasting of meteorological data and images.

In the meantime, GEO or Non-GEO Personal systems were developed and entered the field of MSC solutions, which, for the past 20 years, have been occupied predominately by Intergovernmental Satellite Organizations. In recent years, a growing number of international and private entities have been prepared to develop and invest in satellite technology, such as Inmarsat, Iridium, Globalstar and Orbcomm systems.

1.4.2 Definition of Communications via Stratospheric Communication Platforms (SCP)

Aerial telecommunications have been investigated for three decades through the design and evaluation of stratospheric platforms able to offer multiple types of wireless services. The SCP stations may be airplanes or airships and may be manned or unmanned with autonomous operation coupled with remote control from the ground(Antonini et al, 2003). There is increasing interest in the development of airspace platforms in recent years, for example, SCP carrying equipment for telecommunications, remote sensing or digital broadcasting. The multiple types of platform are able to carry a communication payload at different altitudes. Regarding the altitude of SCP aerial communication, there are three categories of balloons, i.e., High Altitude Platforms (HAP), Medium Altitude platform (MAP) and Low Altitude Platform (LAP).

Above all, the SCP systems provide an excellent option for broadcast and broadband fixed and mobile communications including a derived technique for DVB-RCS known as Digital

Video Broadcasting-Return Channel via Platform (DVB-RCP) (Ilcev, 2011). In addition, SCP stations can be deployed for meteorological observation and Earth monitoring, and are able to provide very reliable rural communications as backbone to cellular and TTN.

Finally, SCP stations are also suitable for disaster and emergency communications, and their survivability during a disaster and mobile ability to be continuously on station offer an ideal solution for an emergency communications capability. This thesis focused on the basic characteristics of SCP stations for meteorological observation and communication systems for transferring weather data and images from onboard platform instruments to ground processing and distribution centres.

In a similar way, SCP stations have to receive transmissions of meteorological data and images from the Data Collection Platform (DCP) and provide their retransmissions to the Direct Readout Service (DRS) ground terminals. Finally, the SCP stations may outline alternative network architecture scenarios for provision of wireless access to broadband communication services, and can coexist with WiMAX and WiFi service in the same coverage area (Emanuela et al, 2006).

The SCP systems are the newest space technique using top technologies for fixed and mobile applications including military solutions. This system uses solar or fuel energy for propulsion. Similar to spacecraft, SCP is carrying solar cells, payloads with transponders and antennas. The SCP network can be classified as the third layer of space communications infrastructure after satellite and terrestrial systems. The SCP stations are officially not used for weather observation, but can be implemented for local scenarios.

The SCP systems are using advanced digital transmission technologies offering cost-effective solutions such as, but not limited to, mobile voice, data and video over IP (VDVoIP) services with speed over 150 Mb/s and up to 10 GB/s (Knapek et al, 2008). SCP structures are at about 15 to 30 km above the Earth with the coverage between 600 to 1 000 kilometers, each SCP acts as a very low orbiting satellite, providing high density, capacity and speed of service with low power requirements and no latency to an entire coverage area. The SCP aircraft or airships do not require a launch vehicle, since they can move under their own power throughout the space or can remain stationary and, finally, while satellites cannot, they can be brought down to the Earth, refurbished and re-deployed without any service interruption (Everaerts et al, 2004). Similar to the satellite, each platform is independent for a dedicated area of coverage. The altitude enables the SCP system to provide a higher frequency reuse and a higher capacity then other wireless system.

1.4.3 Definition of Satellite Meteorological Observation Systems (SMOS)

Meteorological satellites have become essential for both meteorological and climatological observations, and continuing the two fundamental concepts of data and image exchange and international cooperation, which have been traditional for more than 150 years. They provide vital data at frequent intervals over wide areas, in the context of the international cooperation needed to ensure adequate worldwide data coverage. Cooperation and integration exist at two the following levels:
First at the worldwide level through those countries, which have come together to establish global Satellite Meteorology or Satellite Meteorological Observation Systems (SMOS) by integration of the USA, European, Russian, Chinese, Indian and Japanese meteorological satellite programs. In fact, this ensures the continuity of the SMOS constellations and ground

infrastructures in availability of data and images over the entire Earth. The SMOS network contribution to the global observing system required for both meteorology and climatology data and imaging system.

The second level of cooperation is on a regional scale, which ensures the availability of the individual meteorological satellite data and images of each above mentioned country alone and their availability over nearly one quarter of the planet. Thus, some of these countries are providing PEO and GEO meteorological satellite coverages, while, in addition, the US is providing LEO constellation and Russia is providing LEO and HEO additionally, totalling four satellite meteorological constellations.

The improvement in satellite technologies and advancements in satellite communication technologies have improved Earth observation, processing and transmission of data. Thus, the new-generation satellites are regenerative as they have onboard processing capability that enables the satellite to amplify, or reformat received uplink data and route the data to specified locations, or actually regenerate data onboard as opposed to simply acting as a relay station between two or more ground stations.

Both PEO and GEO weather satellites are the most important parts of the Global Observation System of the World Weather Watch program for WMO. Meteorological satellites help to visualize atmospheric condition, including Earth surfaces, sea surfaces, and clouds in a real-time basis.

The GEO satellites are looking as stationary platforms for observers, while PEO satellites for observers appear to be moving in a circle around the Earth. Observation instruments are installed on satellites for meteorological and remote sensing purposes. The meteorological satellite observation has been used not only for weather forecasting, but also for climate change detection and atmospheric research.

Both SCP and the weather observation satellite operate through the space. The difference between the two is the altitude in which they operate, cost to install and operation. SCP operates at the low altitude compared to satellites. Introducing SCP as part of the weather observation network can improve the quality of observation since it is closer to the Earth, offers cost effective, better, faster and greater speed of transmission. The use of SCP can improve weather observation especially in areas where it’s not possible to have ground infrastructure, especially in rural areas. This will highly contribute to understanding climate change issues and improve weather forecasts.

1.4.4 Definition of Global Navigation Satellite Systems (GNSS)

The GNSS systems are important for new developments in meteorological observations for weather distribution and forecasting. The first generation GNSS, as defined by the experts of the ICAO/GNSS panel, plans for some system augmentations in addition to the basic GPS and GLONASS constellations in order to achieve the level of performance suitable for augmented civil aviation applications in oceanic and approaching flight, for enhanced maritime routing applications worldwide, especially in narrow passages, coastal navigation and approaching ports, for land vehicles and also for ground positioning and surveying.
The GPS, as a first generation of GNSS network, is a satellite all-weather, full jam-resistant, continuous operation radio navigation system, which utilizes precise range measurements from the GPS satellites to determine the exact position and time anywhere in the world.

The Russian Federation (former USSR) provides the GLONASS service from space for accurate determination of position, velocity and time for mobile or fixed users worldwide and in all weather conditions anywhere. Therefore, a three-dimensional position and velocity determinations are based upon the measurement of transit time and Doppler Shift of RF signals transmitted by GLONASS satellites. The GLONASS satellite constellation, as a first generation of GNSS, will also provide signals for all RSAS infrastructures.

At this point, the GPS and GLONASS are parts of the first generation of operational GNSS known as GNSS-1, and there are, in the development phase, another two GNSS of second generation known as GNSS-2 systems, such as the Chinese operational systems Compass, and the still not operational European Galileo.

The GNSS consists of many players with similar GMSC systems and three major segments:
1) The Space Segment has 24 satellites (21 functioning satellites and 3 on-orbit spares) and is controlled by a proprietary satellite operator or service provider.
2) The Control Segment is operated by Master Control and Monitor Stations.

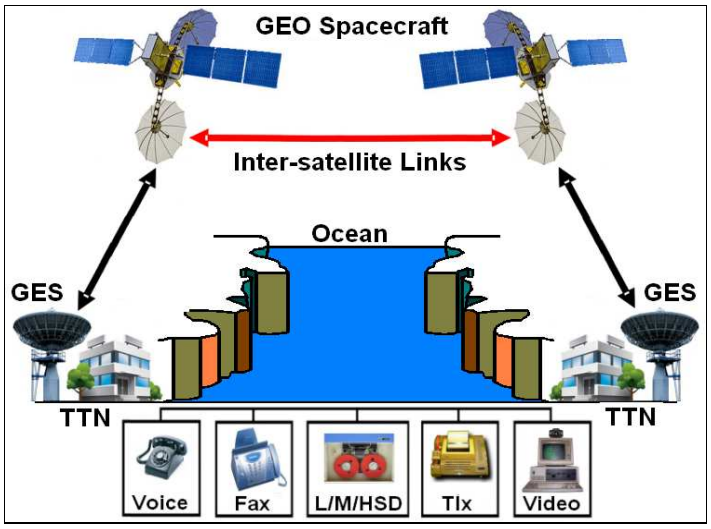

Figure 1. 6 Fixed Satellite Service by Gatenby et al, 1991

3) The User Segment is represented by the military and civilian authorities for maritime, land and aeronautical users located worldwide. This segment offers Standard Positioning Service (SPS) and Precise Positioning Service (PPS), available to all users around the world. Access to the SPS does not require approval by a certain service provider but PPS is only available to authorized users via the service provider administration.

1.5 Definition of Fixed Satellite Communications (FSC)

The FSC system enables a radiocommunications link between two or more FES or GES terminals at given positions, when one or more satellites are used, illustrated in Figure 1.6. In this sense, the given position may be a specified position or any fixed point within a particular area. In some cases, this particular service includes satellite-to-satellite links, which may also be operated in certain inter-satellite services. Moreover, the FSS solutions may also include feeder links for other space communication services, including MSS or MSS GES can provide service for FES as well.

The FSS signals are relayed between many FES, which are relatively large, complex and expensive systems(Widiawan et al, 2005). The FES terminals are connected to the conventional TTN and the service is intended for long distance voice, video and data communications. According to the WARC-85/88 principle plan, the FSS shares frequency bands with terrestrial networks in the 4/6, 12/14 and 20/30 GHz, which guarantees every country equal access to the GEO space constellations.

A typical example of FSS is the Intelsat, one of the pioneers in satellite communications. The first generation of Intelsat system operated in the C band (4/6 GHz). At present, many global systems, such as Intersputnik, Telesat, Eutelsat, PanAmSat and others, and regional systems such as Optus in Australia and JCSAT in Japan operate in the Ku band (30/14 GHz), which provides coverage throughout most of Europe and Japan, respectively. This service may include Satellite Voice and Voice, Data and Video (VDV) via VSAT networks.

1.5.1 Satellite Voice Network

Voice service is inherently interactive communication in nature providing global telephone infrastructures. In fact, the telephony system represents the first form of two-way wire or wireless communications on distance (Roddy, 2006).

Voice band channels are useful for relatively low data rate applications such as Fax, E-mail and low speed Internet access on less than 64 Kb/s. The digital standard for PSTN access at the subscriber level is ISDN service which provides 144 Kb/s of active data subdivided into two 64 Kb/s circuit switched bearer channels plus one data channel (2B+D).

The FSS voice network uses GEO satellite configuration and a bandwidth per channel from 8 to 64 Kb/s with FDMA and TDMA satellite transmissions. The system enables the international telephone trunks to extend the global coverage, thin route and to improve rural services in developing regions.

1.5.2 VSAT Network

The VSAT devices are quite similar to Inmarsat Mobile Earth Station (MES). This satellite equipment is small. Earth Stations are transceiver and capable of receiving from and transmitting and receiving (transceivers) to or from spacecrafts (Advantech, 2012). Therefore, VSAT devices are classified as a communications media with either one-way or two-way facilities.

In the broadest sense, the term one-way VSAT includes the data terminals designed for the reception only of DSB transmission and conventional TVRO, using PAL and similar TV systems. This device can also receive data using modulated sub carriers. Two-way VSAT can transmit and receive signals at rates of approximately 64 Kb/s. The low directivity of VSAT antennas limits the power and, hence, the boresight EIRP, which may be transmitted. The transceivers are usually in a completely solid state and can be highly integrated.

This equipment represents an important addition to the telecommunications world, because they can provide a service directly to their customers at virtually any geographic location covered by suitable satellite beams. They do not require any support from a local TTN and can even be run from a portable or alternative power supply. This system is useful for private

data network within countries and regions to promote business needs. Examples of such networks are Equatorial, Intelnet, Intelsat and other systems.
The VSAT system's main applications are serving for data and documents distribution, rural communities, business utilizations and for disaster area communications. Data distribution can be two-way between Central Hub stations for archive and data processing and all VSAT users. Documents distribution by VSAT can be only be a one-way satellite transmission from Hub library stations to all users. The users can be in touch with Hub via TTN.

Rural application of VSAT devices is very important for improving capability to transmit and receive much information from rural areas to central locations and vice versa. Rural communities would also like to provide speech service via VSAT systems, because of very limited telephone lines facilities, if they are available at all. The voice VSAT system operating at 4.8 Kb/s is already in use.

High quality speech can be carried on satellite channels with a data rate of 9.6 Kb/s using modern voice encodes and modems capable of operating at low C/N values, something like the Inmarsat aeronautical voice system. A voice circuit set up between two VSAT devices include a double hop and, accordingly, a delay of about 0,5 sec. A Hub located in a city can provide VDV and even VDV over IP (VDVoIP) to many fixed and mobile users.

Disaster areas and in generally for emergency needs VSAT devices for alert and security communications, for information regarding the terrain, locations and safety of life. The reason is that many ships, vehicles and aircraft now carry satellite distress beacons.

Business VSAT applications are of an essential interest because of their large potential to provide persons and companies with the competitive edge. Generally, business wants to establish private networks to link all their locations and move their information in a safe manner and for the lowest possible cost. The service can be numerous, like airlines and bus reservations, car rental conference facilities, insurance and newsgathering.

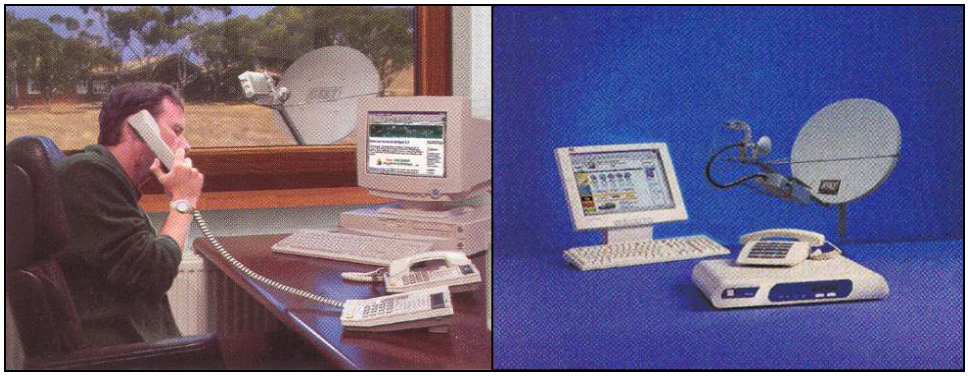

Figure 1. 7 VSAT Equipment for Multipurpose Applications by GT&T 2003

Although, the term VSAT equipment is generally used in connection with very small and fixed location terminals for business use, there are comparable developments in related fields. For example, very low cost TVRO, which can receive MAC signals from high power satellites, could offer a VSAT type service in higher data rates and less cost.

The VSAT technology brings all of the features and benefits of unit or bi-directional FSS down to an extremely economical and usable application for business data transmission. The

system can also provide meteorological data transfer and bypass with TTN for VDV services using sophisticated digital technology and advanced communication network protocols.
The VSAT system enables the use of one or more of 56 Kb/s data channels, each of which can be subdivided or applied directly. Voice communications is also possible using 16 or 32 Kb/s, depending on the compression algorithm. The VSAT network uses GEO configuration, a channel bandwidth from 64 to 512 Kb/s with FDMA and TDMA transmissions.

In Figure 1.7 (Left) is shown the GT&T Faraway SES100 VSAT cost-effective state-of-the-art satellite solution for companies having a high communication flow to their clients, agents or branch offices located abroad or for remote and rural areas where communication services are unavailable, unreliable or too expensive. This equipment uses a V-sat communication network with African C-Band and European, African and Middle East Ku-Band coverage. The system is providing on demand High-quality voice up to 8 telephone lines, Group III Fax, Data transfer compatible via external Hayes compatible modem with a rate from 4.8 up to 64 or 128 Kb/s, IP/X25/X400, Internet (E-Mail and Websites), Videoconference and Broadcasting (TV and Radio) services. The main unit with high capacity chassis allows several telephones (up to 8 interfaces), Fax and PCs to be connected simultaneously via parabolic antenna. The antenna is available with diameters of 65, 98, 120, 180 and 240 cm dishes depending on position in the coverage area and distance from subsatellite point. This configuration employs a full-mesh, DAMA and PAMA network architecture that maximize the use of available space and ground-based resources.

Mobile satellite users can also be included in this category of satellite communications. Most probably in the near future, the VSAT system will offer full MSS similar to Inmarsat-C or mini-M systems. With an additional mobile antenna, VSAT can offer MSS for maritime, land and aeronautical applications. Thus, another very last VSAT model is the GT&T IPsky2 of V-Sat two-way transceiver system together with Internet modem and router lunched in January 2002 that can be easily adapted in mobile unit with slight transformation of antenna system only, which is shown in Figure 1.7 (Right).

This equipment is a low cost and highly compact Internet dedicated DVB-RCS-MPEG2 solution that also offers prepaid VoIP and Fax by satellite. In reality, customers will have an ultra-fast asymmetric Internet interface that is directly connected to the Internet backbone of 155 Mb and 34 Mb fiber using an E-Mai, FTP, TCP and Web Access service available on a 24-hours basis.

The maximum available download (outbound) speed of service via GEO is 2 Mb/s including very high level of transmission and reception coding for high speed and reliability. The return path or inbound speed is 33, 76.8 or 153.6 Kb/s depending on the antenna size of 75, 96 or 1.2 m, respectively. Several PCs (from 5 to 13 or more, if necessary) and Ethernet LAN can be connected to the IPsky2 modem/router through a Proxy server, public IP network, private FTP, VPN, etc.

1.6 Space and Ground Segment for Space Systems

The space segment provides the connection between the subscribers on shore and mobile or fixed users via GES or Gateways. It consists in one or more operational or spare spacecraft in a corresponding constellation. The satellite constellation can be formed by a particular type of orbit, such as GEO, Non-GEO (LEO, PEO and HEO) or combinations of these orbits (Grace and Mohorcic 2011). The satellites can be independent or connected with each other

through Inter-Satellite Link (ISL) or Inter-Orbit Link (IOL). The space segment can be shared among different radio networks in different areas, which include satellite and SCP networks. There are also constellations of multipurpose satellites, whose platform can serve more than two payloads, such as a combination of Communication, Navigation and Surveillance (CNS) or GNSS, MSC and meteorological payloads.

The ground segment consists of three major network elements: GES terminals, ground support networks and user subsegments (Advantech, 2006). Users; subsystems can consist of fixed and mobile customers including personal terminals. The user network comprises many main categories of user terminals connected to TTN interfaces, whose characteristics are highly related to its applications and operational environments. The main part of meteorological ground segment is the Direct Readout Service (DRS) subsystem, which directly receives data and images from satellites or SCP and is known as GES terminals with antenna system. In addition, the part of ground infrastructure is a Data Collection Platform (DCP) as well, which transmits its collected meteorological data via satellites or SCP stations to the DRS ground terminals. The DRC terminals contain Weather Ground Processing of Satellite Meteorological Data and its distribution to the different customers.

1.7 International Coordination Organizations and Regulatory Procedures

International coordination in space systems has been carried out by the world International Coordination Organizations, which include ITU, WMO, IHO and others.

1. **International Telecommunications Union (ITU) and Radio Regulations (RR) –** The ITU organization of the UN with all member governments has carried out the entire international coordination and regulation of mobile radio and satellite communications by the ITU and RR. The ITU was inaugurated in 1932 and reorganized in 1992, with the head office, all committees and departments located in Geneva, Switzerland. The ITU consists of three sectors: firstly, Radiocommunication (ITU-R), which ensures optimal, fair and rational use of the Radio Frequency (RF) spectrum, secondly, Telecommunication Standardization (ITU-T), which formulates recommendations for standardizing telecommunication operations worldwide, and, thirdly, Telecommunication Development (ITU-D), which assists member countries in developing and maintaining internal communication operations, In fact, the World Administrative Radio Conference (WARC-92) covers the RF spectrum needs of numerous telecommunications services, from HF/VHF Broadcasting to satellite communications networks. The task of its International Radio Consultative Committee (CCIR) is to form study groups to consider and report on the operational and technical issues relating to the use of radio, space and all types of satellite communications.
2. **World Meteorological Organization (WMO) –** The WMO group coordinates all global scientific activity to allow prompt and accurate weather (WX) information, tropical storm forecasting and other services for public, private and commercial use, including the shipping and airline industries. The World Meteorological Convention, by which body the WMO was created and adopted at the 12th Conference of Directors of the International Meteorological Organization, met in the USA capital, Washington, in 1947. Although the Convention itself came into force in 1950, the WMO commenced operations as its successor in 1951 and, later that year, was established as an UN's specialized agency by agreement between the UN and the WMO. The main purposes of the WMO are to facilitate international cooperation in

the establishment of networks of stations for making meteorological, hydrological and other observations and to promote the rapid exchange of meteorological information by means of radio or satellite communications, the standardization of meteorological observations and the uniform publication of observations and statistics. The WMO also furthers specific weather and meteorology applications to maritime, aviation, agriculture and other human activities, climatology, atmospheric sciences, hydrology and instruments and methods of observation.
The main WMO task is to organize, control, collect and offer up-to-the-minute worldwide meteorological observations and weather information through many member-operated observation systems and telecommunication links with four PEO and five GEO satellites, about 10,000 land observation stations, 7,000 ship stations and 300 moored and drifting buoys carrying automatic weather stations. Each day, high-speed links transmit over 15 million data characters and 2,000 weather charts through 3 World, 35 Regional and 183 National Meteorological Centres cooperating with each other in preparing weather analyses and forecasts in an elaborately engineered fashion. Thus, transoceanic ships and airplanes, research scientists on sea/air pollution or global climate change, the media and the general public are given a constant supply of timely data, which are very important for safe navigation and flight. Moreover, it is through the WMO that the complex agreements on standards, codes, measurements and communications are internationally established.

Data from all over the world are needed to provide weather (WX) forecasts and warnings. An aircraft does not take off, nor does a ship sails, without a WX received via agent or by means of radio or satellite communications for safety utilization. Combining facilities and services provided by all members, the program's primary purpose of the system is to make available meteorological, geophysical and environmental information enabling countries to maintain efficient meteorological services. Facilities in the regions outside any national territory are maintained by members on a voluntary basis. Accordingly, the World Weather Watch System comprises the Global Observing System, the Global Data Processing System, the Global Telecommunication System, Data Management and System Support Activities. The Hydrology and Water Resources Program concentrates on promoting worldwide cooperation in the evaluation of water resources and the development of hydrological networks and services, including data collection and processing, hydrological forecasting and warnings very important for the safe navigation of ships and the flight of aircraft and the supply of meteorological and hydrological data for design purposes.

3. **International Hydrographic Organization (IHO) –** The IHO is also an international intergovernmental consultative and technical organization that was established in 1921 to support safety in maritime navigation and the protection of the marine environment.

1.8 Frequency Designations and Classification of Services

The assignment of a radiocommunications frequency, band or channels is performed by an authorized administration for radiocommunications via platform, satellite or space stations to use an RF spectrum or frequency channels under specified conditions.

At this point, in satellite communication fields, the frequency bands are often denoted with alphabetical symbols such as L to Ka-bands. Frequency band numbers and names are defined by the ITU RR, ITU Tables of Frequency Allocations, in general, or for a particular band and the mentioned alphabetic symbols by the IEEE Standard Radar Definitions. The radio spectrum shall be subdivided into nine RF bands and designated by progressive whole numbers, in accordance with **Table 1.1**.

Table 1. 1 Frequency Bands Designation in Dalgleish 1989

Band No.	Abbreviation	Band name	Name	Symbol	Frequency
4	VLF	Very Low Frequency	Myria m		3-30 kHz
5	LF	Low Frequency	Km		30-300 kHz
6	MF	Medium Frequency	Hm		300-3000 kHz
7	HF	High Frequency	Dam		3-30 MHz
8	VHF	Very High Frequency	m		30-300 MHz
9	UHF	Ultra High Frequency	dm		300-3000 MHz
				L-band	1-2 GHz
				S-band	2-4 GHz
10	SHF	Super High Frequency	cm		3-30 GHz
				C-band	4-8 GHz
				X-band	8-12 GHz
				Ku-band	12-18 GHz
				K-band	18-27 GHz
				Ka-band	27-40 GHz
11	EHF	Extremely High Frequency	mm		30-300 GHz
12	VEHF	Very Extremely High Frequency	deci mm		300-3000 GHz

In a more general sense, frequency designations for Meteorological Satellites (MetSat) are used by a number of different administrations for their national or international MetSat WX (Weather) networks and can be systematized into three main categories:

1. Allocated Frequency Bands for MetSat in the ITU Radio Regulations (RR) – This is the first frequency allocation for MetSat presented in **Table 1.2, which** provides RF allocations for Space Operations, GEO and Non-GEO MetSat Systems, and so on.

Table 1. 2 Allocated Frequency Bands for MetSat in the ITU Radio Regulations (RR) in ITU 1996

- 137 – 138 MHz (s-E)
- 400.15 – 401 MHz (s-E)
- 401 – 403 MHz (E-s)
- 460 – 470 MHz (s-E) ⇨ Secondary allocation
- 1670 – 1710 MHz (s-E) ⇨ 1670 – 1675 MHz no new MetSat use (Res. 670)
- 2025 – 2110 MHz (E-s) ⇨ Space Operation (SO), Earth Exploration Satellite (EESS)
- 2200 – 2290 MHz (s-E) ⇨ SO and EESS
- 7450 – 7550 MHz (s-E) ⇨ RR Footnote 5.461A limits use to GEO Satellites
- 7750 – 7850 MHz (s-E) ⇨ RR FN 5.461B limits use to Non-GEO Satellites
- 8025 – 8400 MHz (s-E) ⇨ EESS with stringent PFD limits in Region 1 and 3
- 8175 – 8215 MHz (E-s)
- 18.1 – 18.3 GHz (s-E) ⇨ Subject to extension to 300 MHz at WRC-2007
- 25.5 – 27 GHz (s-E) ⇨ EESS

2. Typical Applications in the Frequency Bands Allocated to the MetSat Service (1) – It is the second frequency allocation for MetSat presented in the **Table 1.3.**

Table 1. 3 Typical Applications in the Frequency Bands Allocated to the MetSat Service in ITU 2008

•	137 – 138 MHz (s-E)	⇨ Dissemination of low rate data from NGSO MetSat to user stations
•	401 – 403 MHz (E-s)	⇨ Data uplink from DCPs to GSO MetSat. The band is divided into regional and international channels
•	1670 – 1710 MHz (s-E)	⇨ The band is divided into several parts and is used for downlink of raw data, DCP data, dissemination
•	2025 – 2110 MHz (E-s)	⇨ Telecommand and ranging from main Earth and uplink of processes data for dissemination
•	2200 – 2290 MHz (s-E)	⇨ Telemetry and downlink of raw data to main station

3. Typical Applications in the Frequency Bands Allocated to the MetSat Service (2) – It is the third frequency allocation for MetSat presented in the **Table 1.4.**

Table 1. 4. Typical Applications in the Frequency Bands Allocated to the MetSat Servicein ITU 2008

•	7450 – 7550 MHz (s-E)	⇨ Downlink of medium rate raw data from GSO MetSat to main Earth station (not used on current generation MetSat systems)
•	7750 – 7850 MHz (s-E)	⇨ Downlink of raw data from NGSO MetSat to main Earth station, but also dissemination
•	8025 – 8400 MHz (s-E)	⇨ Downlink of sensor data from GSO and NGSO MetSat to main Earth station
•	18.1 – 18.3 GHz (s-E)	⇨ Downlink of high rate raw data to main Earth station
•	25.5 – 27 GHz (s-E)	⇨ Downlink of high rate raw data to main Earth station (currently no plans for next generation MetSat)

CHAPTER TWO

AIMS AND OBJECTIVES

The main aim of this thesis is to apply integration of current satellite weather observation system and new proposed regional Stratospheric Communication Platforms (SCP) systems, as a more reliable and cost effective solution. Terrestrial and satellite systems represent two well-established technologies that have been dominant in telecommunications area for a long time. However, in recent years, a new space alternative has emerged based on quasi-stationary aerial platforms located in the Stratosphere called SCP or High Altitude Platforms (HAP). The SCP stations seem to represent a dream come true for communication engineers since they preserve most of the advantages of both terrestrial and satellite systems (Fidler et al, 2010).

These stations can take a number of forms ranging from a tethered balloon to a high altitude solar powered pilot-less plane or powered airship, which keeps station in the winds at this altitude. This altitude means that the coverage of the antennas can be a footprint of diameter up to 100 km, thus catering for a significant number of different users including weather and meteorological observation.

The SCP stations give people more convenience and freedom to provide connections to many different communication networks and applications. It is thought that the demand for the capacity increases significantly when the next generation of multimedia applications is combined with future wireless communication systems for data and video transmissions. The platform can be divided into some types. Depending on the weight of the platform, SCP can be projected as lighter than air or heavier than air, and, on its operation, SCP can be divided as manned or unmanned.

2.1 Introduction

Satellites provide customers with a unique and long sought after opportunity to look at Earth from space. These spacecraft today enable all users to observe and measure the many forces of nature, which converge on the Planet. Since the 20th century, mankind is, for the first time, able to observe and investigate via remote sensing and meteorological satellites the global nature of the environmental factors, which interact to form the complex systems known as an Earth. From the unique vantage point of space, sophisticated environmental and weather satellites may bring to observers information about cloud formations and movements, precipitation amounts, air temperatures, ocean currents, sea surface temperatures, air and water pollutants, drought and floods, severe weather conditions, vegetation, insect infestations, ozone content of the atmosphere, volcano eruptions and other factors that affect our daily lives. They have also provided to scientists with less tangible aesthetic values that help shape attitudes about the environment of this planet. This global attitude is, perhaps, just as important as the hard data that the satellites provide.

Much of this information is transmitted from these satellite transponders via direct readout to ground stations where it can be displayed and analyzed. These Direct Readout Services were pioneered more than 45 years ago by the first weather satellites and have been expanded and operated by the US National Oceanic and Atmospheric Administration (NOAA) (Davis, 2011). Thus, the most popular of these services are the Automatic Picture Transmissions (APT) and High Resolution Picture Transmission (HRPT) of the US Polar Orbiting

Environmental Satellites (POES) and Low-Rate Information Transmission (LRIT) and GOES Variable (GVAR) data transmitted by the US Geostationary Operational Environmental Satellites (GOES).

Thousands of direct readout stations have been built, purchased and installed on the ground or mobile infrastructures to receive the direct readout transmissions from meteorological and weather satellites. Government and military agencies, corporations, industries and a variety of private individuals including ham radio operators, students and faculties are operating ground stations. However, the fastest growing use of this data today is within the educational communities. Many teachers with students at all levels within educational institutions have discovered the benefits of these satellites.

Thus, innovative teachers are using real time data to teach a variety of curriculum materials including the sciences, electronics, engineering, computer sciences, social studies, geography and art. Exposure to this exciting world of Earth remote sensing can help retain students, motivate them toward higher education, and expands career possibilities to areas unheard of a few years ago. This work provides a broad spectrum of potential users with the basic information needed to establish and operate a direct readout ground station and understand the imagery provided by Earth-orbiting weather satellites.

On the other hand, this study covers the recently developed and implemented modern space solutions known as Stratospheric Communication Platforms (SCP) or High Altitude Platforms (HAP).

2.2 Research Motivations and Goals

Telecommunication services by means of SCP have become a relevant topic of interest for the future generation system and many applications. The SCP stations have many benefits for different communication systems, including meteorological communication, such as large and stationary coverage area, simplified cell planning, low propagation delay, broadband capability, easy maintenance and upgrading, mobility on demand, payload reconfigurability, less ground-based infrastructure required, Line-of-Sight (LoS) propagation and the feasibility of integrating SCP stations with either communication systems.

Therefore, the SCP systems can be used in many applications such as cellular services, Communication, Navigation and Surveillance (CNS), Voice, Data and Video (DVD) for all types of digital broadcasting, Data and Video (DV) broadcasting of meteorological data and images, digital TV broadcasting, corporate and private communications, government and military solutions, emergency or disaster solutions and many other applications (Aragon-Zavala et al, 2008).

However, in comparison with SCP solutions, satellite systems are more expensive solutions, which deployments and operations are very complex and expensive. For such a reason, these space technologies are not affordable and suitable to many developing countries because of the high cost. At this point, SCP systems, as a more cost effective and suitable technology, can be considered as a good economical and practical substitute to satellite for these developing countries to use it in almost all the applications of satellite systems.

The platform used to close the information gap between developed and developing countries provides a very cost effective solution that produces a very high opportunity to use the higher

information application with an affordable price capacity on demand and low cost of installation and upgrading(Emanuela et al, 2006). From the above discussion, studying a SCP system is very important in the future for development and integration of satellite and platform constellations for the future generations of telecommunication systems for any kind of transmission applications including meteorological and weather services.

Nowadays, meteorological users are looking for broadcasting networks capable of supporting their platform communication needs and stationary in the stratosphere for a long time. The advantages of SCP include the fact that after launching the platform, it can be reconfigured on the ground for recovery and maintenance and redeployed. Other competitive advantages include rapid deployment, easy technology upgrades and station-keeping, minimum infrastructure build out, flexible deployment and redeployment, scalability and the ability to match investment to market demand.

The data and services are mainly focused on the requirements of operational meteorology, with the emphasis on support to operational weather forecasting. However, the data are of use for all areas of this discipline, including marine, agricultural and aviation meteorology, as well as, for example, climatology and the monitoring of planet Earth. The energy industries also vary the available capacity of their plants according to satellite weather-dependent predictions of demands. Accurate weather forecasts are a strong contributor to the efficiency of the way in which many industries work and to national economies. The variations in space weather and climate have enormous economic consequences, which are increasing as the world population grows and becomes more industrialized. Thus, the need to understand, monitor and predict the weather and the changing climate is becoming increasingly important.

The main goal of this research is to reveal the most effective solution for meteorological and weather observation, and to investigate how to effectively improve weather observation, especially in developing countries. More specifically, this research is proposing improvement of local and regional weather observation through an integrated, effective and reliable approach between satellite and SCP station models. This integration has to provide more effective meteorological observation in both developed and developing countries.

2.3 Research Aims and Objectives

Based on the research motivation and goal towards investigating how to effectively improve weather observation especially in developing countries, the following objectives were set towards attaining this goal:

1. To formulate a flexible, integrated and adaptive architecture for integrated satellite and SCP weather observation, especially for developing countries;
2. To demonstrate the utility and applicability of the architecture proposed in (1) above;
3. To provide integration interoperable and compatible between satellite and SCP stations onboard instruments, transmission systems and ground infrastructure; and
4. To contribute to knowledge and understanding of the use of SCP for delivery of weather observation, communications and other services.

2.4 Research Methodology

The following methodologies will be employed in fulfilling the above stated objectives:
1. Literature Survey: The aim of the literature survey is to establish a good theoretical foundation for the research. It will be necessary to start by exploring, from the literature, some recent trends in the area of satellite meteorological and weather satellite observation networks with special focus on communication subsystem. Thereafter, a comprehensive survey of some existing meteorological satellite observation systems and techniques will be carried out. In addition, relevant literature and conclusions will be provided in relation with meteorological observation via SCP stations.
2. Theoretical Framework: Based on a concrete real-life sample scenario and the insights that will be gained from literature on recent trends in the areas of meteorological satellite and SCP observation, a set of design criteria that an integrated and effective architecture should support will be drawn. Thus, this will then be transformed into an Efficient Meteorological Space Observation (EMSO) architectural model and design for weather observation by future integration of Satellite and SCP infrastructures.
3. Framework Experimentation: An experiment of the proposed theoretical framework will be carried out using tools identified from the literature. This experiment will provide us with mechanisms to elaborate and demonstrate the utility of our concepts in a real-life setting using weather applications.
4. Evaluation: To show the functionality of the proposed integration via EMSO architectural model, its performance needs to be theoretically evaluated. Testing the proposed satellite systems on a real infrastructure is a challenge because no single user has control on the entire system. In this regard, it will be possible by using empirical analysis and simulation experiments to conclude functionality and advantages of the proposed integrated system against related work in the literature. The aim will be to investigate how the design choices of each of the systems in proposed integration will be able to improve EMSO space and ground segments on the local and global scale.

2.5 Original key Contribution of the Thesis

The original key contribution of this research is to propose an integration of satellite and SCP systems for future meteorological observation and distribution of weather data and images via both observation and communication infrastructures.

2.5.1 Rationale and Benefits of Research

The research for this thesis is dedicated to solve technical problems with regards to physical equipment (hardware) and satellite networks for meteorological observation, rather than improving software or creating new techniques of data processing. It is important to conclude that all receiving and distributing ground devices of meteorological data and images cannot operate without applying adequate software and even IT and processing technology in direct readout ground stations.

Thus, every fixed or mobile ground terminal that is receiving meteorological or devices, satellite networks and data processing in control centres is using certain software, firmware and operation systems for data receiving, processing and distribution among of systems units. Essentially, the IT technology and techniques are debugged and perfectly operate in every node of any existing ground station's equipment. In such a way, software and firmware have

today surpassed previous evolution in the development of modern meteorological radio and satellite devices and networks.

In accordance with this fact, the most part of the work is dedicated to improve physical parts of the space and ground meteorological infrastructures and propose new application, solutions, networks and projects. Therefore, this study and research is proposing many new solutions in satellite and SCP meteorological observation, transmission systems and ground networks.

All theoretical and experimental framework, including experiments, provided in this research, can completely be applied as proposals and projects in real applications. Also theoretical and practical analyzes of meteorological integrated systems, equipment and networks can be useful for other researchers and operational developers. This research doesn't contain any science fiction study, but provides possibilities for development of real applications only. There are many new solutions and improvements by integration of space meteorological systems and networks.

2.5.2 Limitations of Study

Study and research in this thesis are limited only by practical implementation of proposed ideas in design and development of projects for tracking and detecting systems. These proposed projects of tracking and detecting systems could be considered and developed only by implementing theoretical proposals. To realize practical implementations of some projects explained in this thesis will require more technical details, a long period for developing them, adequate workshops and adequate funds. In addition, this specific research, proposals and projects need to involve different workshops and research groups, such as mechanical, electrical, computer and electronics engineering, IT and computers science, physics and others technical disciplines as well.

2.6 Research Problems

The combination of GEO and PEO meteorological satellites is one of the most important parts of the Global Space Observation and EMSO.

The GEO satellite constellation is in a circular orbit between 35 and 40 thousand kilometers above the Earth's equator and following the direction of the Earth's rotation. Thus, the satellite platforms are in GEO so far away from Earth that they cause communication latency to become significant.

The PEO satellite passes above or nearly above both poles once in a 12-hour period, and in such a way, that a satellite in such an orbit can observe the full Earth twice a day. The PEO satellites are at an altitude of approximately 1000 km.

Due to the importance of the real-time data set in weather observation, GEO satellites are mostly used because they provide observations every fifteen minutes while PEO satellites only provide two observations a day.

The ground station observations are expensive to have in all the corners of Earth, which contributes to low quality of observation and poor decision making. The current ground

communication is still inhibited by high latency, down times and it's not accessible in all the areas. At this point, all of the above mentioned factors indirectly affect the economy and the understanding of weather and climate change. The economy is affected where a budget is committed on poor decisions made due to poor observations.

Today, the important aspects for Weather Observation communication network are transmission speed (low latency), Quality of Service (QoS) and reliable clear coverage.
Most of these communication needs are not feasible especially from developing countries. This requires some innovative way to fulfill the above mentioned needs that will be affordable, reliable and easy to maintain that can be easily integrated with the current weather observation network.

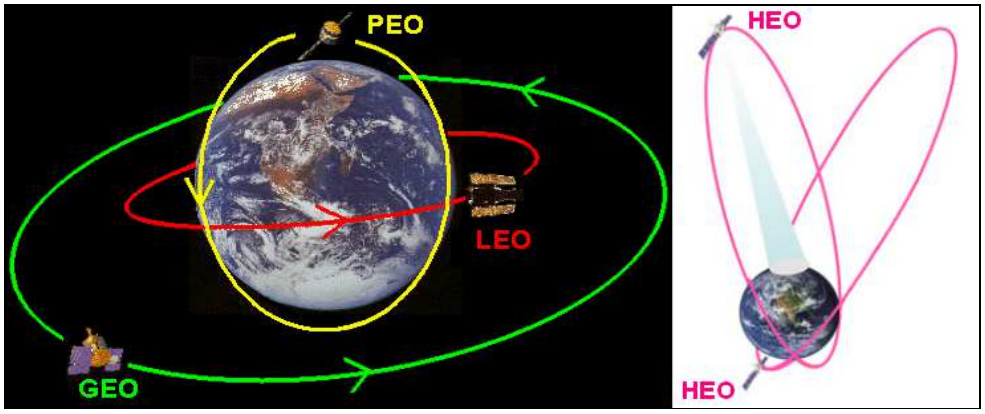

Figure 2. 1. Meteorological Satellite Constellations by Singh 2014

However, the SCP airships and aircraft can be used for weather observation to overcome these challenges imposed by the old communication infrastructure. In addition, SCP stations have especially to provide optical links from GEO satellites to the ground infrastructures and reduce the deployment of GES. This research seeks a way to introduce SCP systems for weather observations in integration with satellite and other space systems. The GEO and PEO meteorological satellite constellations, including new developed LEO constellation by USA and Russia are shown in Figure 2.1 (Left), while new HEO constellations developed by Russia alone, illustrated in Figure 2.1 (Right), can and do provide the necessary global weather coverage at the required intervals.

CHAPTER THREE

SPACE SEGMENT

This chapter describes orbital mechanics and their significance with regard to satellite use for weather observations and basic physical principles that reveal the shape of a satellite orbit and how to orient the orbital plane in space. To fully understand and use satellite meteorological data, it is necessary to understand the orbits in which satellites are constrained to move and the space geometry with which they view the Earth. This knowledge allows us to calculate the position of a satellite at any time, thus orbit perturbations and their effects on meteorological satellite orbits are then discussed. Next the geometry of satellite tracking and Earth locations of the measurements made from the satellites are explored. This leads to a discussion of space-time sampling.

This theoretical section also describes satellite orbits and their significance with regard to the meteorological observation, the fundamental laws governing satellite orbits and the principal parameters that describe the motion of artificial satellites of the Earth. The types of orbits are also classified and compared from a communication and meteorological system viewpoint in terms of Earth coverage performance and environmental and link constraints.

ThePolar Earth Orbit (PEO) satellites were developed five decades ago as a first solution for meteorological satellite applications. Thereafter, communication and meteorological satellite networks have utilized Geostationary Earth Orbit (GEO) satellites extensively to the point where portions of these orbits have become crowded and coordination between satellites is becoming constrained (Kongsberg, 2015). However, PEO, as Leo Earth Orbit LEO) satellite systems, have grown in importance, both because of their orbit characteristics and coverage capabilities in high latitudes. The chapter concludes with a brief overview of satellite launch vehicles and orbit insertion. Types of satellite orbits and perturbations are also classified and compared from the weather observation viewpoint in terms of coverage and link performances.

3.1 Platforms and Orbital Mechanics

The platform is an artificial object located in orbit around the Earth at a minimum altitude of about 20 km in the stratosphere and a maximum distance of about 36,000 km in the Space(Evans, 1991). The artificial platforms can have a different shape and designation but usually they have the form of aircraft, airship or spacecraft. In addition, there are special space stations and space ships, which are serving on more distant locations from the Earth’s surface for scientific exploration and research and for cosmic expeditions.

Orbital mechanics is a specific discipline describing planetary and satellite motion in the Solar system, which can solve the problems of calculating and determining the position, speed, path, perturbation and other orbital parameters of planets and satellites. In fact, a space platform is defined as an unattended object revolving around a larger one. Although it was used to denote a planet’s Moon since 1957, it is also a man-made object put into orbit around a large body (planet), when the former USSR launched its first spacecraft Sputnik-1. Accordingly, man-made satellites are sometimes called artificial satellites.
Orbital mechanics support a meteorological satellites project in the phases of orbital design and operations. The orbital design is based on a generic survey of orbits and, at an early stage, to identify the most suitable orbit for the objective metrological service. The orbital

operation is based on rather short-term knowledge of the orbital motion of the satellite and starts with TT&C maintenances after the satellite is located in orbit (Gordon et al, 1993).

3.1.1 Space Environment

The satellite service begins when a spacecraft is located as a platform in the desired orbital position in a space environment around the Earth. This space environment is a very specific part of the Universe, where many factors and determined elements affect the planet and satellite motions. The Earth is surrounded by a thick layer of many different gasses known as the atmosphere, whose density decreases as the altitude increases. There is no air and the atmosphere disappears at about 180 km above the Earth, where the Cosmos begins. The endless environment in space is not friendly and is extremely destructive, mainly because there is no atmosphere, the cosmic radiation is powerful, the vacuum creates high pressure on spacecraft or other bodies and there is the negative influence of low temperatures.

The Earth's gravity keeps everything on its surface. All the heavenly bodies such as the Sun, Moon, planets and stars have gravity and reciprocal reactions. Any object flying in the atmosphere continues to travel until it meets forces due to the Earth's gravity or until it has enough speed to surpass gravity and to hover in the stratosphere. However, to send an object into space, it first has to overcome gravity and then travel at least at a particular minimum speed to stay in space. In this case, an object travelling at about 5 miles/sec can circle around the Earth and become an artificial spacecraft (Kadish et al, 2000).

An enormous amount of energy is necessary to put a satellite into orbit and this is realized by using powerful rockets or launchers, which are defined as an apparatus consisting of a case containing a propellant (fuel) and reagents by the combustion of which it is projected into the space. As the payload is carried on the top, the rocket is usually separated and drops each stage after burnout and brings a payload up to the required velocity and leaves it in orbit. A rocket is also known as a booster, as a rocket starts with a low velocity and attains some required height, where air drag decreases and it attains a higher velocity.

3.1.2 Laws of Satellite Motion

A satellite is an artificial object located by a rocket in space orbit following the same laws in its motion as the planets rotating around the Sun. Johannes Kepler, a German mathematician, has contributed a great deal to the field of astronomy and astrology. The Laws of Planetary Motion formulated by Kepler proves that the orbits of the planets are ellipses and not circles, as believed by many. The ellipse is a geometrical shape that has two foci, such that, the sum of the distance from the focus to any point on the surface of the ellipse is constant. The orbits of planets have small eccentricities (flattening of ellipse), and they appear as circles. Based on the properties of ellipses, Johannes Kepler devised three laws that explain the motion of planets around the Sun (Ilcev, 2005).

A satellite is an artificial object launched and located by a rocket in orbit and follows the same laws in its motion as the planets rotating around the Sun (Maral et al, 2009). Thus, three important laws for planetary motion were derived by Johannes Kepler, as follows:

1. First Law – The first law is also known as The Law of Orbits. As discussed earlier, an ellipse has two foci. While studying the motion of planets around the Sun, Kepler explained

that the path followed was elliptical, with the Sun as one of the two foci. In simple terms, the law is stated as: The orbit of each planet follows an elliptical path or all planets move in elliptical orbits, with the Sun at one focus, as shown in Figure 3.1 (A). This indicates that the Sun is one focus, while the other focus is known as the vacant or empty focus. As seen in the diagram, the Sun and the empty focus lie on the major axis of the ellipse, and the planet lies on the surface of the ellipse. As the planet is continuously moving around the Sun, and as the Sun is not at the centre of the ellipse, the Planet-Sun distance will always keep on changing. The Law of Orbits proves that planet motion lies in the plane around the Sun (1602).

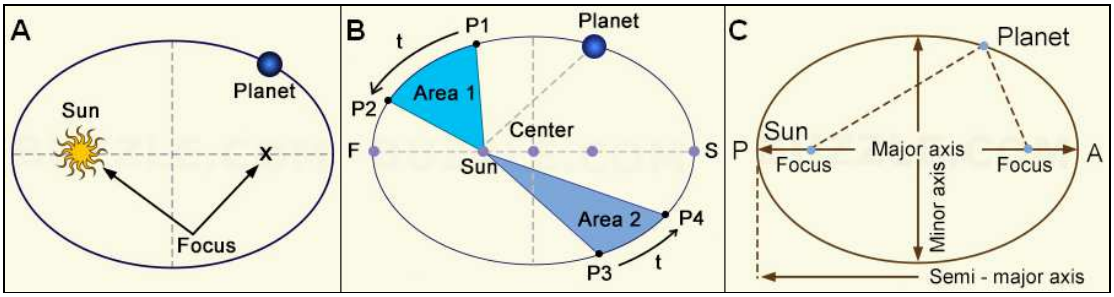

Figure 3. 1. Kepler's Laws of Satellite Motion by Ilcev 2011

2. Second Law – The second law is known as The Law of Equal Areas, shown in Figure 3.1 (B). As the Sun is one of the foci, it is clear that the Planet-Sun distance will be changing. However, the planet covers up for the increase in the distance by moving faster when it is closer to the Sun. This indicates that planets do not move at a uniform speed. This law states that: The line from the Sun to orbital planet or radius vector (r) sweeps out equal areas in equal intervals of time (t) as the planet travels around the ellipse. The point at which the speed of the planet is fastest is known as Perihelion or Perigee indicated with F (Fastest motion), while the distance with slowest speed is known as Aphelion (Apogee) indicated by S (Slowest motion). The distance measured from the Perihelion to the position of the Sun is known as Perihelion distance, while the distance from the Sun to the Aphelion is known as the Aphelion distance. The law says that, while moving in an elliptical path, the planet moves faster when it is closer to the Sun. In this way, the radius sweeps equal areas in equal amounts of time. If the planet is observed at successive times (P1, P2, P3, P4), it draws the radius vector during the first and second observations, showing that the two radius vectors have the same area. So, the area swept during the time (t) by the planet to move from P1 to P2 is the same as the area swept while moving from P3 to P4. This is the Law of Equal Areas (1605).

3. Third Law – The third law of planetary motion in ellipse with Perigee (P) and Apogee (A) is alternatively known as The Law of Periods and Harmonic Law, as shown in Figure 3.1 (C). This law relates the time required by a planet to make a complete trip around the Sun to its mean distance from the Sun. This law can be simply stated as: The square of the planet orbital period is directly proportional to the cube of the semi-major axis of its orbit. The square of the planet's orbital period around the Sun (T) is proportional to the cube of the semi-major axis (a = distance from the Sun) of the ellipse for all planets in the Solar system (1618).

Kepler's laws only describe the planetary motion if the mass of central body in so far as it is considered to be concentrated in its centre and when its orbits are not affected by other systems. However, these conditions are not completely fulfilled in the case of Earth motion

and its artificial satellites. The Earth does not have an ideal spherical shape and the different layers of mass are not equally concentrated inside of the Earth's body.

Therefore, the satellite motions are not ideally synchronized and stable. The motions are slower or faster at particular orbital sectors, which present certain exceptions to the rule of Kepler's Laws. Furthermore, in distinction from natural satellites, whose orbits are almost elliptical, the artificial satellites can also have circular orbits, for which the basic relation can be obtained by the equalizing the centrifugal and centripetal Earth forces.

Kepler's laws only describe the planetary motion if the mass of central body in so far as it is considered to be concentrated in its centre and when its orbits are not affected by other systems. These conditions are not completely fulfilled in the case of Earth motion and its artificial satellites. The Earth does not have an ideal spherical shape and the different layers of mass are not equally concentrated inside of the Earth's body. Therefore, the satellite motions are not ideally synchronized and stable. Thus, the motions are slower or faster at particular orbital sectors, which present certain exceptions to the rule of Kepler's Laws.

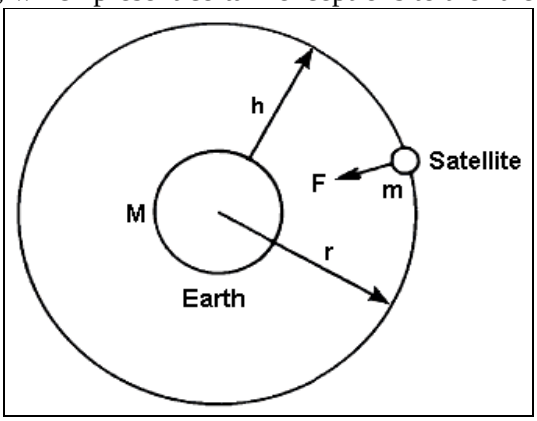

Figure 3. 2 Circular Satellite Orbit by Kidder and Ham 1995

Kepler's Laws were based on observational records and only described the planetary motion without attempting an additional theoretical or mathematical explanation of why the motion takes place in that manner. In 1687, Sir Isaac Newton published his breakthrough work "Principia Mathematica" with own syntheses, known as the Three Laws of Motion:

1. Law I – Every body continues in its state of rest or uniform motion in a straight line, unless it is compelled to change that state by forces impressed on it.

2. Law II – The change of momentum per unit time of a body is proportional to the force impressed on it and is in the same direction as that force.

3. Law III – To every action there is always an equal and opposite reaction.

On the basis of Law II, Newton also formulated the Law of Universal Gravitation, which states that any two bodies attract one another with a force proportional to the products of their masses and inversely proportional to the square of the distance between them. This law may be expressed mathematically for a circular orbit with the relations as follows:

$$F = ma = dv/dt \tag{3.1}$$

where F = force, m = mass of the satellite body, a = acceleration, v = velocity and t = time of satellite orbit.

The force of attraction between two distant point masses m_1 and m_2 separated by a distance *r* gives the following relation:

$$F = Gm_1m_2/r^2 \quad (3.2)$$

where G = Newtonian (or universal) gravitation constant.

Consider the simple circular orbit shown in Figure 3.2. Assuming that the Earth is a sphere, it is possible that can be treated a point mass. The centripetal force F_c required to keep the satellite in a circular orbit = mv^2/r, where ν = orbital velocity of the satellite. The force of gravity that supplies this centripetal force is GMm/r^2, where M = mass of the Earth and m is the mass of the satellite. Equating the two forces gives the following relation:

$$F_c = mv^2/r = GMm/r^2 \quad (3.3)$$

Division by m eliminates the mass of the satellite from the equation, which means that the orbit of a satellite is independent of its mass. Thus, the period of the satellite is the orbit circumference divided by the velocity: $T = 2\pi r/v$. Substituting in equation 3.3 gives the following relation:

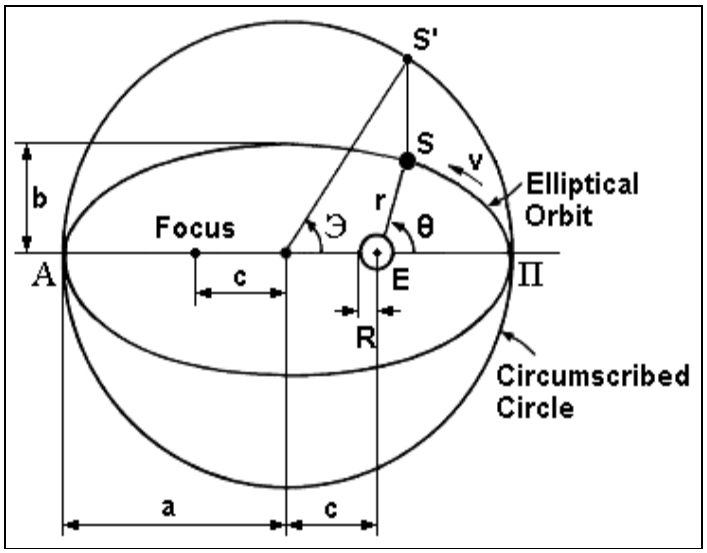

Figure 3. 3 Circular Satellite Orbit by Ilcev 2011

$$T^2 = (4\pi^2/GM)\, r^3 \quad (3.4)$$

The first generation NOAA meteorological satellites orbit at approximately 850 km above the Earth's surface. Since the equatorial radius of the Earth is about 6378 km, the orbit radius is about 7228 km. Substituting in equation 3.4 shows that the NOAA satellites have a period of about 102 min.

However, the radius required for a satellite in GEO has the same angular velocity as the Earth, so the angular velocity mean motion constant of a satellite shows:

$$\xi = 2\pi/T \quad (3.5)$$

Substituting equation. 3.5 in equation 3.4 results in the following formula:

$$r^3 = GM/\xi^2 \quad (3.6)$$

Inserting the angular velocity of the Earth, the required radius for a GEO is 42,164 km or about 35,786 km above the Earth's surface.

3.1.3 Geometry of Elliptical Orbit

The satellite in circular orbit undergoes its revolution at a fixed altitude and with fixed velocity, while a satellite in an elliptical orbit can drastically vary its altitude and velocity during one revolution. The elliptical orbit is also subject to Kepler's Three Laws of satellite motion.

Thus, the characteristics of elliptical orbit can be determined from elements of the ellipse of the satellite plane with the perigee (Π) and apogee (A) and its position in relation to the Earth (E), as shown in Figure 3.3. The parameters of elliptical orbit are presented as follows:

$e = c/a = \sqrt{[1 - (b/a)^2]}$ or $e = (\sqrt{a^2 - b^2}/a)$ $p = a(1 - e^2)$ or $p = b^2/a$

$c = \sqrt{(a^2 - b^2)}$ $a = p/1 - e^2$ $b = a\sqrt{(1 - e^2)}$ (3.7)

where e = eccentricity, which determines the type of conical section; a = large semi-major axis of elliptical orbit; b = small semi-major axis of elliptical orbit; c = axis between centre of the Earth and centre of ellipse and p = focal parameter.

The equation of ellipse derived from polar coordinates can be presented with the resulting trajectory equation as follows:

$r = p/1 + e \cos \Theta$ [m] (3.8)

where r = distance of the satellites from the centre of the Earth (r = R+h) or radius of path, Θ = true anomaly and $\Im$ = eccentric anomaly.

In this case, the position of the satellite will be determined by the angle called "the true anomaly", which can be counted positively in the direction of movement of the satellite from 0^o to 360^o, between the direction of the perigee and the direction of the satellite (S). The position of the satellite can also be defined by eccentric anomaly, which is the argument of the image in the mapping, which transforms the elliptical trajectory into its principal circle, an angle counted positively in the direction of movement of the satellite from 0 to 360^o, between the direction of the perigee and the direction of the satellite. The relations for both mentioned anomalies are given by the following equations:

$\cos \Theta = \cos \varepsilon - e/1 - e \cos \varepsilon$ $\cos \varepsilon = \cos \Theta + e/1 + e \cos \Theta$ (3.9)

The total mechanical energy of a satellite in elliptical orbit is constant, although there is an interchange between the potential and the kinetic energies. As a result, a satellite slows down when it moves up and gains speed as it loses height. Thus, considering the termed gravitation parameter μ=GM (Kepler's Constant $\mu = 3.99 \times 10^5$ km^3/sec^2), the velocity of a satellite is:

$v = \sqrt{[GM(2/r) - (1/a)} = \sqrt{\mu(2/r) - (1/a)]}$ (3.10)

Applying Kepler's Third Law, the sidereal time of one revolution of the satellite in elliptical orbit is as follows:

$$t = 2\pi \sqrt{(a^3/GM)} = 2\pi \sqrt{(a^3/\mu)} \quad (3.11a)$$

$$t = 3.147099647 \sqrt{(26{,}628.16 \cdot 10^3)^3 \cdot 10^{-7}} = 43{,}243.64 \quad [s] \quad (3.11b)$$

Therefore, the last equation is the calculated period of sidereal day for the elliptical orbit of Russian-based satellite Molnya with apogee = 40,000 km, perigee = 500 km, revolution time = 719 min and a = 0.5 (40,000 + 500 + 2 x 6,378.16) = 26,628.15 km

3.1.4 Geometry of Circular Orbit

The circular orbit is a special case of elliptical orbit, which is formed from the relations a = b = r and e = 0, as shown in Figure 3.3. According to Kepler's Third Law, the solar time (τ) in relation with the right ascension of an ascending node angle (Ω); the sidereal time (t) with the consideration that μ=GM and satellite altitude (h), for a satellite in circular orbit will have the following relations:

$$\tau = t / (1 - \Omega t / 2\pi) \quad (3.12)$$

$$t = 2\pi \sqrt{(r^3/\mu)} = 3.147099647 \sqrt{(r^3 \cdot 10^{-7})} \quad [s] \quad (3.13)$$

$$h = [\sqrt[3]{(\mu t^2/4\pi^2)}] - R = 2.1613562 \cdot 10^4 (\sqrt[3]{t^2}) - 6.37816 \cdot 10^6 \quad [m] \quad (3.14)$$

The time is measured with reference to the Sun by solar and sidereal day. Thus, a solar day is defined as the time between the successive passages of the Sun over a local meridian. In fact, a solar day is a little bit longer than a sidereal day, because the Earth revolves by more than 360^o for successive passages of the Sun over a point 0.986^o further.

On the other hand, a sidereal day is the time required for the Earth to rotate one circle of 360^o around its axis: t_E = 23 h 56 min 4.09 sec. Therefore, an artificial geostationary satellite must have an orbital period of one sidereal day in order to appear stationary to an observer on the Earth surface of subsatellite point.

During rotation, the duration of sidereal day t = 85,164,091 (s) and is considered in such a way for synchronous orbit that h = $35{,}786.04 \times 10^3$ (m). The speed is conversely proportional to the radius of the path (R+h) and for the satellite in circular orbit, it can be calculated from the following relation:

$$v = \sqrt{(MG/R + h)} = \sqrt{(\mu/r)} = 1.996502 \cdot 10^{-7}/\sqrt{r} = 631.65 \sqrt{r} \quad [m/s] \quad (3.15)$$

From equation 3.13 and using the duration of sidereal day (t_E) gives the relation for the radius of synchronous or geostationary orbits:

$$r = \sqrt[3]{[(\mu t) / 2\pi)^2]} \quad (3.16)$$

The satellite trajectory can have any angle of orbital planes in relation to the equatorial plane: in the range from PEO up to GEO plane.

If the satellite is rotating in the same direction of Earth's motion, where (t_E) is the period of the Earth's orbit, the apparent orbiting time (t_a) is calculated by the following relation:

$$t_a = t_E \cdot t/t_E - t \qquad (3.17)$$

This means, that, in as much as $t = t_{E,}$ the satellite is geostationary ($t_a = \infty$ or $\tau=0$). In **Table 3.1**, several values of parameters for times different than synchronous orbital time are presented in certain units.

Table 3. 1 The Values of Times Different than the Synchronous Time of Orbit

Parameter	Values of time					Unit
t	86,164.00	43,082.05	21,541.23	10,770.61	6,052.00	s
h	35,786.00	20,183.62	10,354.71	4,162.89	800.00	km
(R+h)	42,164.00	26,561.78	16,732.87	10,541.05	7,178.00	km
v	3,075.00	3,873.83	4,880.72	5,584.12	7,450.00	km/s^{-1}

According to **Table 3.1** and equation 3.14, it is evident that a satellite does not depend so much on its mass but decreases with higher altitude. In addition, satellites in circular orbits with altitudes of a 1,700, 10,400 and 36,000 km, will have t/ τ values 2/2,18, 6/8 and 24/zero, respectively. In this case, it is evident that only a satellite constellation at altitudes of about 36,000 km can be synchronous or geostationary.

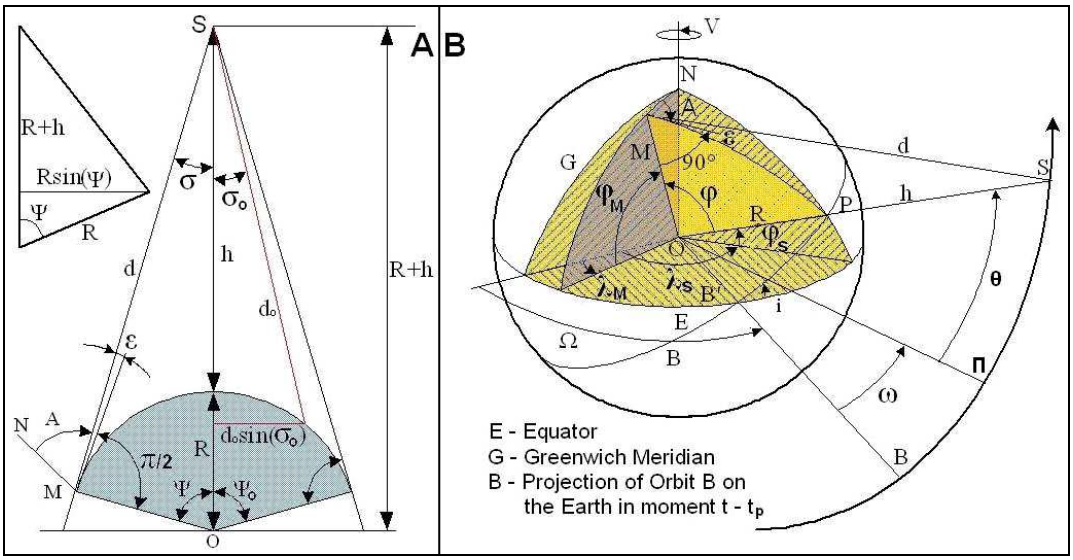

Figure 3. 4 Geometric Projection of Satellite Orbits by Ilcev 2011

3.2 Horizon and Geographic Satellite Coordinates

The geographical and horizon coordinates are very important to find out many satellite parameters and equations for better understanding the problems of orbital plane, satellite distance, visibility of the satellite, coverage areas, etc. The coverage areas of a satellite are illustrated in Figure 3.4 (A) with the following geometrical parameters: actual altitude (h), radius of Earth (R), angle of elevation (ε), angle of azimuth (A), distance between satellite and the Earth's surface (d) and central angle (Ψ) or sub-satellite angle, which is similar to the angle of antenna radiation (δ).

The geographical and horizon coordinates of a satellite are presented in Figure 3.4 (B) with the following, not yet mentioned, main parameters: angular speed of the Earth's rotation (ν), argument of the perigee (ω), moment of satellite pass across any point on the orbit (t_o), which can be perigee (Π), projection of the perigee point on the Earth's surface (Π'), spherical triangle (B'ΓP), satellite (S), the Point of the Observer or Mobile (M), latitudes of observer and satellite (φ_M and φ_S), longitudes of observer and satellite (λ_M and λ_S), inclination angle (i) of the orbital plane measured between the equatorial and orbital plane and the right ascension of an ascending node angle in the moment of t_o (Ω_o).

Otherwise, the right ascension of an ascending node angle (Ω) is the angle in the equatorial plane measured counter clockwise from the direction of the vernal equinox to that of the ascending node, while the argument of the perigee (ω) is the angle between the direction of the ascending node and the direction of the perigee.

3.2.1 Satellite Distance and Coverage Area

The area coverage or angle of view for each type of satellite depends on orbital parameters, its position in relation to the Ground Earth Station (GES) and geographic coordinates. This relation is very simple in the case where the sub-satellite point is in the centre of coverage, while all other samples are more complicated.

Thus, the angle of a GEO satellite inside its range has the following regular reciprocal relation:

$$\delta + \varepsilon + \Psi = 90^o \tag{3.18}$$

The circular sector radius can be determined by the following relation:

$$R_s = R \sin \Psi \tag{3.19}$$

When the altitude of orbit h is the distance between satellite and sub-satellite point (SP), the relation for the altitude of the circular sector can be written as:

$$h_s = R (1 - \cos \Psi) \tag{3.20}$$

From a satellite communications point of view, there are three key parameters associated with an orbiting satellite: **(1)** Coverage area or the portion of the Earth's surface that can receive the satellite's transmissions with an elevation angle larger than a prescribed minimum angle; **(2)** The slant range (actual LOS distance from a fixed point on the Earth to the satellite); and **(3)** The length of time a satellite is visible with a prescribed elevation angle. Elevation angle is an important parameter, since communications can be significantly impaired if the satellite has to be viewed at a low elevation angle, that is, an angle too close to the horizon line. In this case, a satellite close to synchronous orbit covers about 40% of the Earth's surface. Thus, from the diagram in Figure 3.4 (A), a covered area, expressed with central angle (2δ or 2Ψ) or with arc (MP≈RΨ) as a part of Earth's surface, can be derived with the following relation:

$$C = \pi (R_s^2 + h_s^2) = 2\pi R^2 (1 - \cos \Psi) \tag{3.21}$$

Since the Earth's total surface area is $4\pi R^2$, it is easy to rewrite C as a fraction of the Earth's total surface:

$$C/4\pi R^2 = 0{,}5\ (1 - \cos \Psi) \qquad (3.22)$$

The slant range between a point on Earth and a satellite at altitude (h) and elevation angle can be defined in this way:

$$z = [(R \sin \varepsilon)^2 + 2Rh + h^2]^{½} - R \sin \varepsilon \qquad (3.23)$$

This determines the direct propagation length between GES, (h) and (ε) and will also find the total propagation power loss from GES to satellite. In addition, (z) establishes the propagation time (time delay) over the path, which will take an electromagnetic field as:

$$t_d = (3.33)\ z \quad [\mu sec] \qquad (3.24)$$

To propagate over a path of length (z) km, it takes about 100 msec to transmit to GEO. If the location of the satellite is uncertain for ± 40 km, a time delay of about ± 133 μsec is always present in the Earth-to-satellite propagation path. When the satellite is in orbit at altitude (h), it will pass over a point on Earth with an elevation angle (ε) for a time period:

$$t_p = (2\Psi/360)\ (t/1 \pm (t/t_E) \qquad (3.25)$$

The quotations for right ascension of the ascending node angle (Ω) and argument of the perigee (ω) are as follows:

$$\Omega = 9{,}95\ (R/r)^{3.5} \cos i \quad \text{or} \quad \Omega = \Omega_o + \nu\ (t - t_o)$$

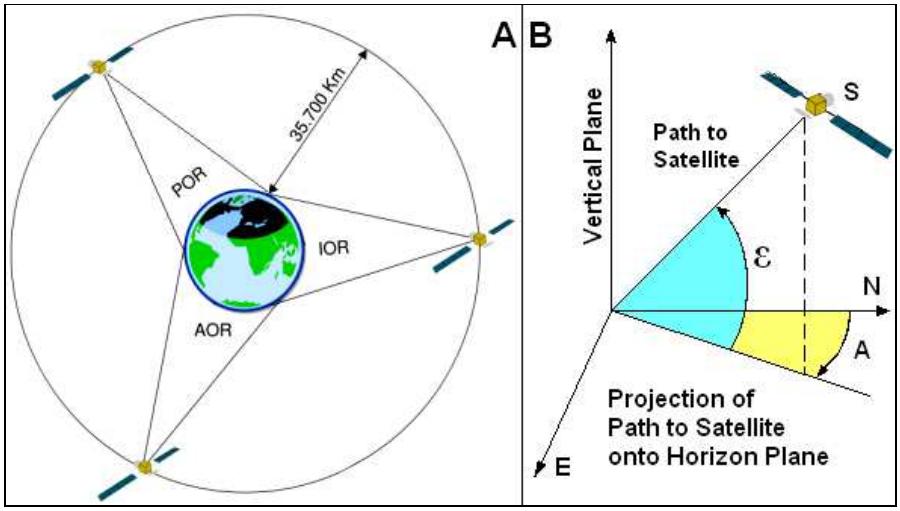

Figure 3. 5 GEO Configuration and Look Angle Parameters by Pratt 2002

$$\omega = 4{,}97\ (R/a)^{3.5}\ [5 \cos^2 i - 1/(1 - e^2)^2] \qquad (3.26)$$

The limit of the coverage area is defined by the elevation angle from GES above the horizon with angle of view $\varepsilon = 0^o$. In this case, the satellite is visible and its maximal central angle for GEO will be as follows:

$$\Psi = \text{arc cos}\ (R \cos \varepsilon / r) - \varepsilon \quad \text{or} \qquad (3.27)$$

$\Psi = \pi/2 - \arcsin(R/r) = \arccos(R/r) - \varepsilon = \arccos k - \varepsilon$

$\Psi = \arccos 6{,}376.16/42{,}164.20 = \arccos 0.15126956 = 81^o\ 17'\ 58.18"$

$C_{max} = 255.61 \cdot 10^6 (1 - 0.15126956) = 216.94 \cdot 10^6 \ (km^2)$ (3.28)

Therefore, all MES and GES, with a position above $\Psi = 81^{o,}$ will not be covered by GEO satellites. Since the Earth's square area is 510,100,933.5 km^2 and the extent of the equator is 40,076.6 km, only with three GEO mutually moved apart in the orbit by $120^{o,}$ it is possible to cover a great area of the Earth's surface, as shown in Figure 3.5 (A).

The zero angles of elevation have to be avoided, even to get maximum coverage, because this increases the noise temperature of the receiving antenna. Owing to this problem, an equation for the central angle with minimum angle of view between 5^o and 30^o will be calculated as follows:

$\Psi_s = \arccos(k \cos \varepsilon) - \varepsilon$ (3.29)

The arch length or the maximum distant point in the area of coverage can be determined in the following way:

$l = 2\pi R\ (2\Psi/360 = 222.64\Psi \quad [km]$ (3.30)

The real altitude of satellite over sub-satellite point is as follows:

$h = r - R = 42{,}162 - 6{,}378 = 35{,}784 \quad [km]$ (3.31)

The view angle under which a GEO satellite can see GES/MES is called the "sub-satellite angle". More distant points in the coverage area for GEO satellites are limited around $\varphi = 70^o$ of North and South geographical latitudes and around $\lambda = 70^o$ of East and West geographical longitudes, viewed from the sub-satellite's point. Theoretically, all Earth stations around these positions are able to see satellites by a minimum angle of elevation of $\varepsilon = 5^o$. Such access is very easy to calculate, using simple trigonometry relations:

$\delta_{\varepsilon=0} = \arcsin k \approx 9^o$ (3.32)

At any rate, the angle (Ψ) is in correlation with angle (δ), which can determine the aperture radiation beam. For example, the aperture radiation beam of satellite antenna for global coverage has a radiation beam of $2\delta = 17.3^o$. According to Figure 3.4 (A), it will be easy to find out relations for GEO satellites as follows:

$\operatorname{tg} \delta = k \sin \Psi / 1 - k \cos \Psi = 0.15126956 \sin \Psi / 1 - \cos \Psi / 1 - 0.15126956 \cos \Psi)$ (3.33)

$\delta_s = 90^o - \Psi_s = 8^o\ 42'\ 1.82"$

The width of the beam aperture ($2\delta_s$) provides the maximum possible coverage for synchronous circular orbit. The distance of GES and MES with regard to the satellite can be calculated using Figure 3.4 (A) and equations (3.18) and (3.27) by:

$d = R \sin \Psi / \sin \delta = r \sin / \cos \varepsilon$ (3.34)

The parameter (d) is important for transmitter power regulation of GES, which can be calculated by the following equation:

$d = \sqrt{[(R + r)^2 - 2R\, r \cos \Psi]}$ or

$d = h \sqrt{[1 + 2\,(1/k)\,(R/h)^2\,(1 - \cos \varphi \cos \Delta\lambda)]}$ or

$$d = r\,[1 - (R \cos \varepsilon / r)^2]^{1/2} - R \sin \varepsilon \qquad (3.35)$$

Accordingly, when the position of any MES is near the equator in sub-satellite point (P) or right under the GEO satellite, then its distance is equal to the satellite altitude and takes out value for d=H of 35,786 km. Thus, every MES will have a further position from (P) when the central angle exceeds $\Psi = 81^o$, when d_{max}=41,643 km.

3.2.2 Satellite Look Angles (Elevation and Azimuth)

The horizon coordinates are considered to determine satellite position in correlation with an Earth observer, GES and MES terminals. These specific and important horizon coordinates are angles of satellite elevation and azimuth, illustrated in Figure 3.4 (A and B) and Figure 3.5 (B), respectively.

The satellite elevation (ε) is the angle composed upward from the horizon to the vertical satellite direction on the vertical plane at the observer point. From point (M) shown in Figure 3.2 (A), the look angle of ε value can be calculated by the following relation:

$$\operatorname{tg} \varepsilon = \cos \Psi - k / \sin \Psi \qquad (3.36)$$

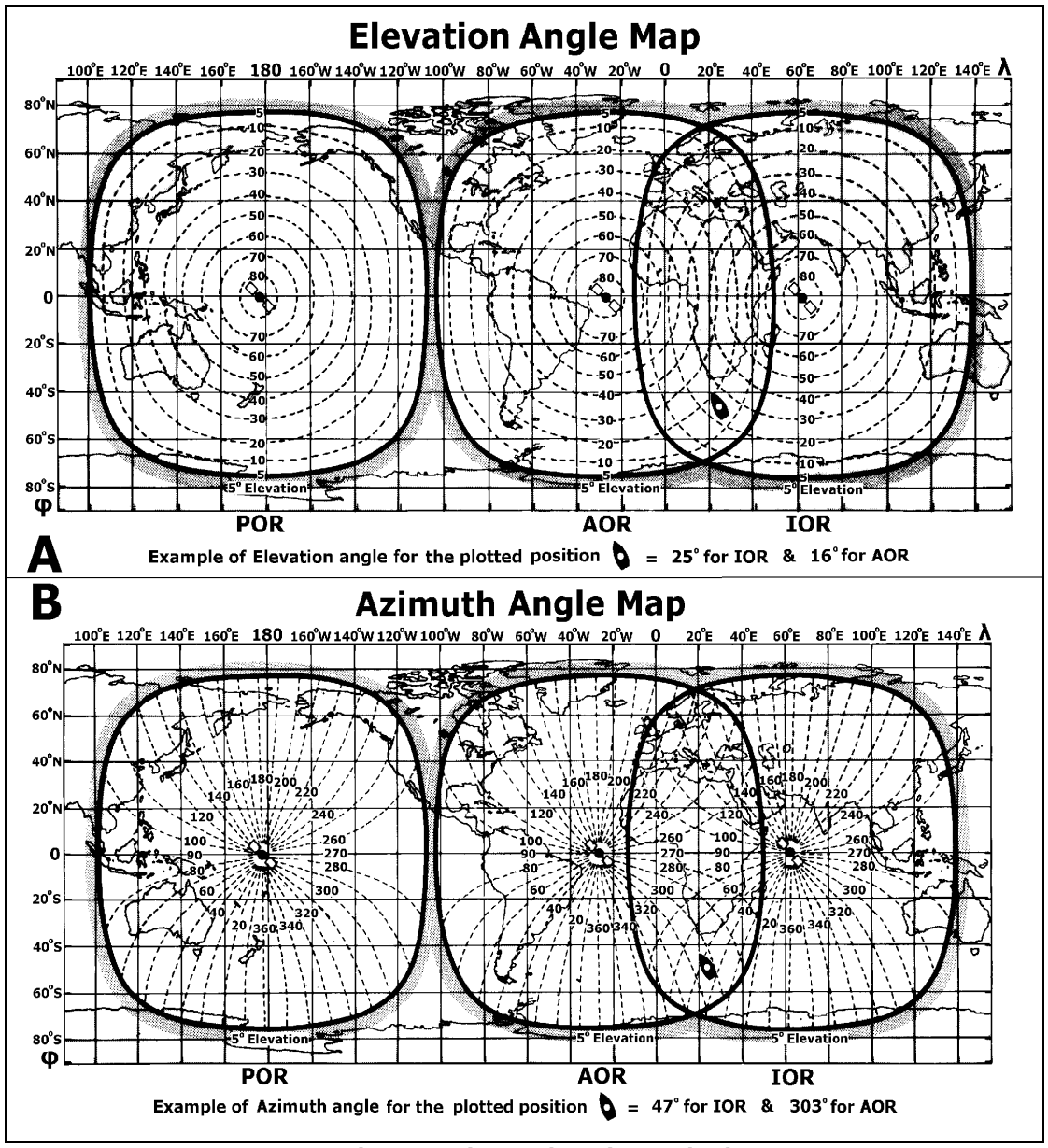

Figure 3. 6 Elevation and Azimuth Angle Maps by Ilcev 2005

Figure 3.6 (A) illustrates the Mercator chart of the 1st Generation Inmarsat space segment, using three ocean coverage areas with projection of elevation angles and with one example of a plotted position of a hypothetical ship (may also be aircraft or any mobile). Thus, it can be concluded that SES or any type of MES at designated position (ε=25^o for IOR and ε=16^o for AOR) has the possibility to use either GEO satellites over IOR or AOR to communicate with any GES inside the coverage areas of both satellites. The satellite azimuth (A) is the angle measured eastward from the geographical North line to the projection of the satellite path on the horizontal plane at the observer point. This angle varies between 0 and 360^o as a function of the relative positions of the satellite and the point considered.

The azimuth value of the satellite and sub-satellite point looking from the point (M) or the hypothetical position of MES can be calculated as follows:

$$\text{tg } A' = \text{tg } \Delta\lambda_M - k/\sin \Psi \quad (3.37)$$

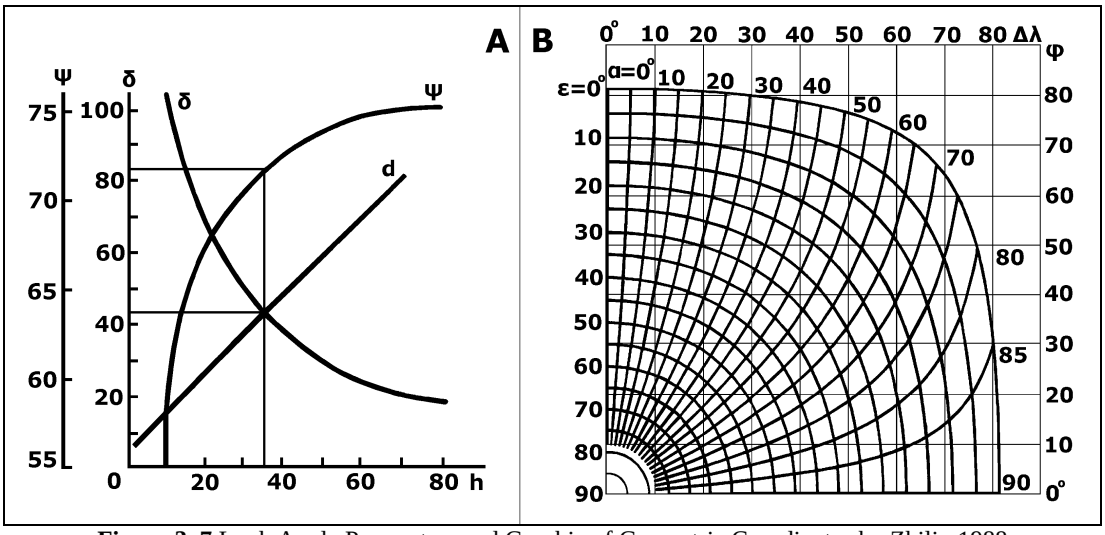

Figure 3. 7 Look Angle Parameters and Graphic of Geometric Coordinates by Zhilin 1988

Otherwise, the azimuth value, looking from sub-satellite point (P), can be calculated as:

$$\text{tg } A = \sin \Delta\lambda / \text{tg } \varphi \quad \text{or} \quad \sin A = \cos \varphi \sin \Delta\lambda \text{ cosec } \Psi \quad (3.38)$$

Figure 3.6 (B) illustrates the Mercator chart of the 1st Generation Inmarsat 3-satellite or ocean coverage areas with projection of azimuth angles, with one example for the plotted position of a hypothetical ship (ε=47° for IOR and ε=303° for AOR). Any mobile inside of both satellites' coverage can establish a radio link to the subscribers on shore via any GES.

However, parameter (A') is the angle between the meridian plane of point (M) and the plane of a big circle crossing this point and sub-satellite point (P), while the parameter (A) is the angle between a big circle and the meridian plane of point (P). Thus, the elevation and azimuth are, respectively, vertical or horizontal look angles, or angles of view, in which range the satellite can be seen.

Figure 3.7 (A) presents a correlation of the look angle for three basic parameters (δ, Ψ, and d) in relation to the altitude of the satellite. In as much as the altitude of the satellite is increasing as the values of central angle (Ψ), the distance between satellite and the Earth's surface (d) and the duration of communication (t_c) or time length of signals are increasing, while the value of sub-satellite angle (δ) is indirectly proportional. An important increase of look angle and duration of communication can be realized by increasing the altitude to 30 or 35,000 km, while an increase in look angle is unimportant for altitudes of more than 50,000 km. The duration of communication is affected by the direction's displacement from the centre of look angle, which will have maximum value in the case when the direction is passing across the zenith of the GES. The single angle of the satellite in circular orbit depends on the t/2 value, which, in area of satellite look angle, can be found in the duration of the time and is determined as:

$$t_c = \Psi\, t/\pi \quad (3.39)$$

The practical determination of the geometric parameters of a satellite is possible by using many kinds of plans, graphs and tables. It is possible to use tables for positions of SES (φ, λ), by the aid of which longitudinal differences can be determined between MES and satellite for four feasible positions of the ship: N/W, S/W, N/E and S/E in relation to GEO.

One of the most important practical pieces of information about a communications satellite is whether it can be seen from a particular location on the Earth's surface. In Figure 3.7 (B), a graphic design is shown which can approximately determine limited zones of satellite visibility from the Earth (MES) by using elevation and azimuth angles under the condition that $\delta = 0$. This graph contains two groups of crossing curves, which are used to compare (φ) and ($\Delta\lambda$,) coordinates of mobile positions.

Thus, the first group of parallel concentric curves shows the geometric positions where elevation has the constant value (ε=0), while the second group of fan-shaped curves starting from the centre shows the geometric positions where the difference in azimuth has the constant value (a = 0).

This diagram can be used in accordance with Figure 3.4 (B) and presented in the following order:
1) First, it is necessary to note the longitude values of satellite (λ_S) and mobile (λ_M) and the latitude of the mobile (φ_M), then calculate the difference in longitude ($\Delta\lambda$) and plot the point into the graphic with both coordinates (φ_M & $\Delta\lambda$);
2) The value of elevation angle (ε) can then be determined by a plotted point from the group of parallel concentric curves;
3) The difference value of azimuth (a) can be determined by a plotted point from the group of fan-shaped curves starting from the centre; and
4) Finally, depending on the mobile position, the value of azimuth (A) can be determined on the basis of the relations presented in **Table 3.2.**

Table 3. 2 The Form for Calculation of Azimuth Values

The GEO direction in relation to MES	Calculating of Azimuth Angles
Course of MES towards S & W	A = a
Course of MES towards N & W	A = 180^o – a
Course of MES towards N & E	A = 180^o + a
Course of MES towards S & E	A = 360^o – a

In as much as the position of SES is of significant or greater height above sea level (if the bridge or ship's antenna is in a very high position) or according to the flight altitude of AES, then the elevation angle will be compensated by the following parameter:

$$x = \arccos (1 - H/R) \qquad (3.40)$$

where H = height above sea level of observer or MES. Let us say, if the position of GES is a height of H = 1,000 m above sea level, the value of $x \approx 1^o$. This example can be used for the determination of AES compensation parameters, depending on actual aircraft altitude. The estimated value of elevation angle has to be subtracted for the value of the compensation parameter (x).

3.2.3 Satellite Track and Geometry (Longitude and Latitude)

The satellite track on the Earth's surface and the presentation of a satellite's position in correlation to the MES results from a spherical coordinate system, whose centre is the middle of Earth, is illustrated in Figure 3.4 (B). In this way, the satellite position, at any time, can be decided by the geographic coordinates, sub-satellite point and range of radius. At this point, the sub-satellite point is a determined position on the Earth's surface; above it is the satellite at its zenith(Ohmori et al 1998).

The longitude and latitude of satellite are geographic coordinates of the sub-satellite point, which can be calculated from the spherical triangle (B'ΓP) and implementing the following relations:

$$\sin \varphi = \sin (\Theta + \omega) \sin i$$

$$\operatorname{tg} (\lambda_S - \Omega) = \operatorname{tg} (\Theta + \omega) \cos i \qquad (3.41)$$

With the presented equation above, it is possible to calculate the satellite path or trajectory of sub-satellite points on the Earth's surface. The GEO track breaks out at the point of coordinates $\varphi = 0$ and $\lambda = \text{const}$.

Furthermore, considering geographic latitude (φ_M) and longitude (λ_M) of the point (M) on the Earth's surface presented in Figure 3.4 (B), which can be the position of the MES. Taking into consideration the arc (MP) of the angle illustrated in Figure 3.4 (A), the central angle can be calculated by the following relations:

$$\cos \Psi = \cos \varphi_S \cos \Delta\lambda \cos \varphi_M + \sin \varphi_S \sin \varphi_M \quad \text{or}$$

$$\cos \Psi = \cos \text{arc MP} = \cos \varphi_M \cos \Delta\lambda \qquad (3.42)$$

The transition calculation from geographic to spherical coordinates and vice versa can be computed with the following equations:

$$\cos \Psi = \cos \varphi \cos \Delta\lambda \quad \text{and} \quad \operatorname{tg} A = \sin \Delta\lambda / \operatorname{tg} \varphi, \quad \text{respectively}$$

$$\sin \varphi = \sin \Psi \cos A \quad \text{and} \quad \operatorname{tg} \Delta\lambda = \operatorname{tg} \Psi \sin A \qquad (3.43)$$

These relations are useful for any point or area of coverage on the Earth's surface, and for a centre of the area, if it exists, as well as for spot-beam and global area coverage for MSC systems. The optimum number of GEO satellites for global coverage can be determined by:

$$n = 180^o / \Psi \qquad (3.44)$$

For instance, if $\delta = 0$ and $\Psi = 81^o$, it will be necessary to put into orbit only 3 GEO, and to get a global coverage from 70^o N to 70^o S geographic latitude. Hence, in a similar way the number of satellites can be calculated for other types of satellite orbits.

The trajectory of radio waves on a link between an MES and satellite at distance (d) and the velocity of light ($c = 3 \times 10^8$ m/s) require a propagation time equal to:

$$T = d/c \quad (s) \tag{3.45}$$

The phenomenon of apparent change in frequency of signal waves at the receiver, when the signal source moves with respect to the receivers (Earth), was explained and quantified by Johann Doppler (1803–53). The frequency of the satellite transmission received on the ground increases as the satellite is approaching the ground observer and reduces as the satellite is moving away. This change in frequency is called Doppler Effect or shift, which occurs on both the uplink and the downlink. This effect is quite pronounced for LEO and compensating for it requires frequency tracking in a narrowband receiver, while its effect are negligible for GEO satellites. The Doppler shift at a transmitting frequency (f) and radial velocity (v_r) between the observer and the transmitter and can be calculated by the following relation:

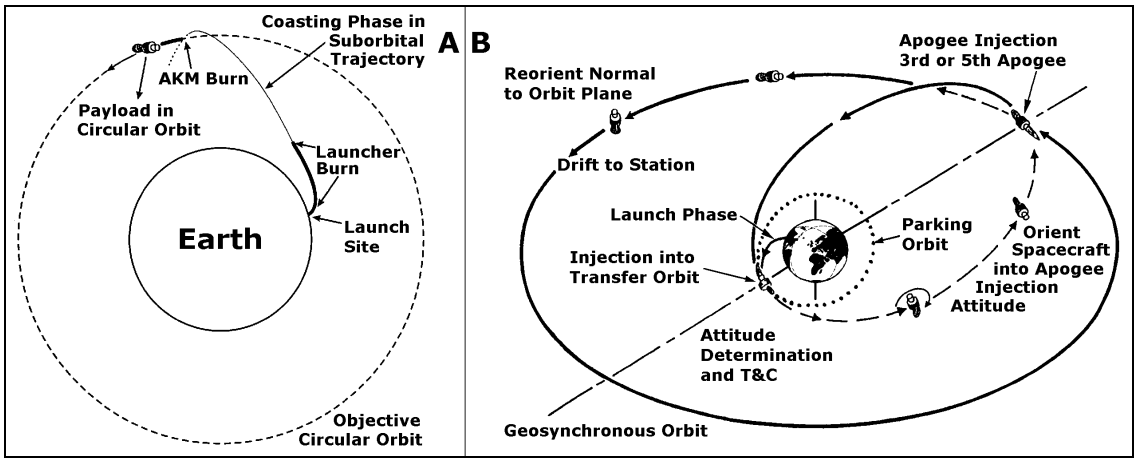

Figure 3. 8 Satellite Installation in Circular and Synchronous Orbit by Pascall 1997

$$\Delta f_D = f\, v_r / c \quad \text{where} \quad v_r = dR/dt \tag{3.46}$$

For an elliptical orbit, assuming that R = r, the radial velocity is given by:

$$v_r = dr/dt = (dr/\Theta)\,(d\Theta/dt) \tag{3.47}$$

The sign of the Doppler shift is positive when the satellite is approaching the observer and vice versa. Doppler Effect can also be used to estimate the position of an observer provided that the orbital parameters of the satellite are precisely known. This is very important for development of Doppler satellite tracking and determination systems.

3.3 Spacecraft Launching and Station-Keeping Techniques

The launch of the satellite and controlling support services are a very critical point in the creation of space communications and the most expensive phase of the total system cost. At the same time, the need to make a satellite body capable of surviving the stresses of the launch stages is a major element in their design phase. Satellites are also designed to be compatible with more then one model of launch vehicle and launching type. In a more determined sense, there are multi-stages expendable and manned or unmanned, reusable launcher systems (Maini and Agrawal, 2007).

Owing to location and type of site, there are land-based and sea-based launch systems. Additional rocket motors, such as perigee and apogee kick propulsion systems, may also be required. The process of launching a satellite is based mostly on launching into an equatorial circular orbit and after in GEO, but similar processes or phases are used for all types of orbits (Stacey 2008). The processes involved in the launching technique depend on the type of satellite launcher, the geographical position of the launching site and constraints associated with the payload. In order to successfully put the satellite into the transfer and drift orbit, the launcher must operate with great precision with regard to the magnitude and orientation of the velocity vector. On the other hand, launching operations necessitate either TT&T facilities at the launching base or at the stations distributed along the trajectory.

Satellites are usually designed to be compatible with more than one prototype of launchers. Launching, putting and controlling satellites into orbit are very expensive operations. The expenses of launcher and support services can exceed the cost of the satellites themselves.

The basic principle of any launch vehicle is that the rocket is propelled by reaction to the momentum of hot gas ejected through exhaust nozzles (Maini and Agrawal, 2007). Thus, for a spacecraft to achieve synchronous orbit, it must be accelerated to a velocity of 3,070 m/s in a zero-inclination orbit and raised a distance of 42,242 km from the centre of the Earth. Most rocket engines use the oxygen in the atmosphere to burn their fuel but solid or liquid propellant for a launcher in space must comprise both a fuel and an oxygen agent. There are two techniques for launching a satellite, namely, by direct ascent and by Hohmann transfer ellipse.

3.3.1 Direct Ascent Launching

A satellite may be launched into a circular orbit by using the direct ascent method, shown in Figure 3.8 (A). The thrust of the launch vehicle is used to place the satellite in a trajectory, the turning point of which is marginally above the altitude of the desired orbit. The initial sequence of the ascent trajectory is the boost phase, which is powered by the various stages of the launch vehicle. This is followed by a coasting phase along the ballistic trajectory, the spacecraft at this point consisting of the last launcher stage and the satellite. As the velocity required to sustain an orbit will not have been attained at this point, the spacecraft falls back from the highest point of the ballistic trajectory.

When the satellite and final stage have fallen to the desired injection altitude, having in the meantime converted some of their potential energy into kinetic energy, the final stage of the launcher, called the Apogee Kick Motor (AKM) is activated to provide the necessary velocity increase for injection into the chosen circular orbit. In effect, the AKM is often incorporated into the satellite itself, where other thrusters are also installed for adjusting the orbit or the altitude of the satellite throughout its operating lifetime in space. The typical launch vehicles for direct ascent satellite launching are US-based Titan IV, Russian-based Proton and Soyuz, as more used launchers today.

3.3.2 Indirect Ascent Launching

A satellite may be launched into an elliptical or synchronous orbit by using the successive or indirect ascent sequences, known as the Hohmann transfer ellipse method, shown in Figure 3.8 (B). The Hohmann transfer ellipse method enables a satellite to be placed in an orbit at the desired altitude using the trajectory that requires the least energy (Pascall, 1997). At the

first sequence, the launch vehicle propels the satellite into a low parking orbit by the direct ascent method. The satellite is then injected into an elliptical transfer orbit, the apogee of which is the altitude of the desired circular synchronous orbit. At the apogee, additional thrust is applied by an AKM to provide the velocity increment necessary for the attainment of the required synchronous orbit. In practice, it is usual for the direct ascent method to be used to inject a satellite into a LEO and for the Hohmann transfer ellipse to be used for higher types of orbits.

3.3.3 Satellite Launchers and Launching Systems

Two major types of launch vehicles can be used to put a satellite into PEO, GEO and other constellation: Expendable and Reusable Vehicles. There are also two principal locations or site-based types of launching centres: Land-based and Sea-based launch systems.

3.3.3.1 Expendable Launching Vehicles

The great majority of communication satellites have been launched by expendable vehicles and this is likely to continue to be the case for many years to come. There are two types of these vehicles: expendable three-stage vehicles and expendable direct-injection vehicles.

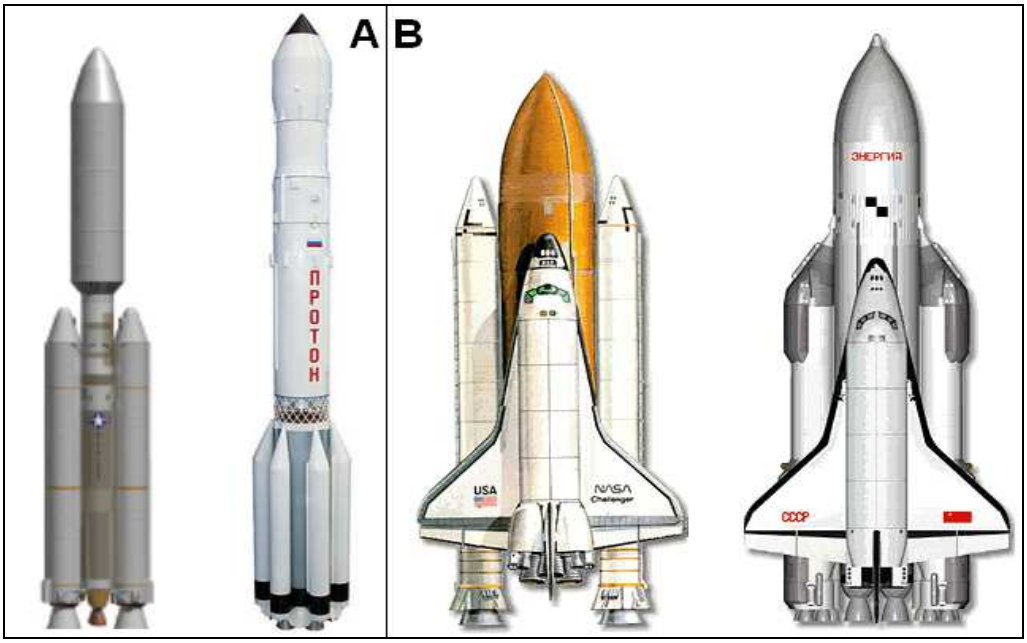

Figure 3. 9 Types of Launch Vehicles by Ilcev 2005

1. Expendable Three-Stage Vehicles – Typical series of three-stage launch vehicles are Delta and Atlas (USA), Ariane (Europe), Long March (China) and H-II (Japan). In addition, a new generation of launchers has already been developed with two-stages such as Delta III and Ariane 5. Both stages are propellant systems using cryogenic liquid fuel, while the first stage is assisted by nine strap-on solid-fuel motors.

The first and second stages of three-stage expandable launch vehicles are usually designed to lift them clear of the Earth's atmosphere, to accelerate horizontally to a velocity of about 8,000 m/s and enter a parking orbit at a height of about 200 km. The plane of the parking

orbit will be inclined to the equator at an angle not less than the latitude of the launch site. The most efficient way of getting from the parking orbit to a circular equatorial orbit is to convert the parking orbit into an elliptical orbit in the same plane, with the perigee at the height of the parking orbit and the apogee at about 36,000 km and then to convert the transfer ellipse to the GEO (Roshydromet, 2014). Thus, the third stage is fired as the satellite crosses the equator, which ensures that the apogee of the Geostationary Transfer Orbit (GTO) is in the equatorial plane. When the satellite is placed in the GTO, the third stage has completed its mission and is jettisoned. The final phase of the Hohmann transfer three-stage launch sequence is carried out by means of AKM built into the satellite. The propulsion of this motor is required to provide at the apogee of the GTO a velocity increment of such a magnitude and in such a direction as to reduce the orbit to zero and make the orbit circular. Once the satellite is in the GEO trajectory, the attitude is corrected, the antennas and solar panels are deployed and the satellite is drifted to the correct longitude (apogee position) for operation (Kongsberg, 2015).

2. Expendable Direct-Injection Vehicles – Typical models of direct-injection launchers are the USA-based Titan IV and the Russian-based Proton, illustrated in Figure 3.9. **(A-Left)** and **(A-Right)**, respectively, and the Soyuz (Russia and Zenit launcher (Ukraine). Otherwise, these types of vehicles do not need an AKM because direct-injection launchers have a fourth stage, which converts directly from GTO to GEO constellation. The Proton rocket is one of the most capable and reliable heavy lift launch vehicles in operation today. Proton D-1 and D-1-E launcher variants have three and four stages, respectively. At lift-off the total weight of Proton is about 688 tons and this vehicle has the capability of placing a maximum of 4,500 and 2,600 kg into GTO and GEO, respectively.

3.3.3.2 Reusable Launch Vehicles

Reusable launch vehicles have already been developed in the USA (Space Shuttle) and former USSR (Energia/Buran), which have as their aim the development of vehicles that could journey into space and return, all or much of their structure being reusable and, thus, the satellite launching will cost less. Moreover, in using these launchers, there will be less burnt-out upper stages than with expendable vehicles. What remains in space, the small pieces in transfer orbits for many years and much small debris, remains in LEO for a long time, adding to the growing space junk hazard for operational satellites and future space operations (Elbert, 2001).

There are other projects for development of similar vehicles such as a small manned reusable space shuttle called Hermes (Europe) and Hope (Japan). In the UK, an unmanned space plane, Hotol, is proposed, while, in Germany and the USA, two similar vehicles are projected: TAV (TransAtmospheric Vehicle) and Sanger Space plane, respectively. Thus, in the development of these small vehicles it is important to realize whether any of them could carry sufficient weight and be able to put communication satellites into the desired orbits.

1. Space Shuttle – The US-based NASA developed a fleet of manned reusable vehicles of Space Transportation System (STS) called Space Shuttle, which are capable of lifting a satellite of up to 29.5 tons into a parking orbit, inclined at 28.5^{o}, with an altitude of up to 431 km, shown in Figure 3.9 (B-Left). A Shuttle has three main elements: **(1)** the orbiter for carrying the satellite and crew; **(2)** a very large external tank containing propellant for the main engine of the orbiter; and **(3)** two solid-propellant boosters. The reusable Space Shuttle plane is 37.2 m long, the fuselage is 4.5 m in diameter, the wingspan is 23.8 m and the mass

is about 84.8 tons. This STS is designed to accommodate in total 7 crew members and passengers on board the plane.

The system came into service in 1981 and made over twenty successful operational flights until January 1986, when the Shuttle Challenger was destroyed by a fault in the solid-propellant booster and all the crew were killed in a tragic accident. Following this disaster, NASA redesigned the booster but decided to use STS only for regular launch programs of government and scientific vehicles. Criticism of the Space Shuttle program stems from claims that NASA Shuttle program has failed to achieve its promised cost and utility goals, as well as design, cost, management and safety issues. The biggest problem of the Space Shuttle was its Thermal Protection *S*ystem (TPS) made by the special isolation tiles for very high temperatures during entry in the atmosphere from space. Due to these problems, the retirement of the NASA Space Shuttle fleet took place from March to July 2011.

2. Energia/Buran Spaceplane – The launcher, Energia, was the most powerful operational reusable vehicle in the world, capable of carrying about 100 tons cargo into space, whose four first-stage booster units are recoverable for reuse. In particular, it can launch the Buran space plane, enabling it to acquire a LEO and to land with the aid of its own rocket engine, shown in Figure 3.9 (B-Right). The main purpose for which those very heavy lift vehicles were developed was to ferry personnel and supplies for the Russian space station, Mir, for other space operations, missions to the other planets and also to retrieve or repair satellites already in orbit.

The Energia vehicle can also carry into space a side-mounted canister containing an upper stage and a payload compartment suitable, for example, for a large heavy spacecraft or group of communication satellites to be placed in orbit. The Energia flew for the first time on 15 May 1987, carrying a spacecraft mock-up and later, on 18 November 1988, carrying an unmanned version of Buran space plane. The reusable Buran space plane is 36.3 m long, the fuselage is 5.6 m in diameter, the wingspan is 24 m and the mass is about 100 tons. It can be flown in automatic configuration or under the control of a pilot to place satellites in LEO or to retrieve them and come back to base for the next use.

Up to ten people, crew and passengers, can be accommodated and it can carry in the cargo bay up to 30 tons into an orbit of 200 km altitude and 51.6^{o} inclination. In fact, this plane enables large satellites to be put into orbit and construction of space stations to be considered for both for telecommunication purposes and for scientific missions.

The Energia Launch Vehicle was also the successor to the N-1 Moon Rockets, except that Buran was also used to launch Polyus from Baikonur Cosmodrome in Kazakhstan (former Soviet Union). The Energia was 60 m high and 18 m in diameter, consisting of a central core and four strap-on boosters, while the core was 58.1 m high and 7.7 m diameter. It used 4 RD-0120 rocket engines. The propellants were liquid hydrogen and oxygen. The strap-on boosters were then 38.3 m high and 3.9 m in diameter, with a single four-chamber RD-170 kerosene/liquid oxygen rocket engine.

In 1992, the Russian Space Agency (Roscosmos) decided to terminate the Energia/Buran Program due to Russia's economic difficulties after disintegration of the former Soviet Union. At that stage, the second Orbiter had been assembled and assembly of the third Orbiter with improved performance was nearing completion. Although the Energia project has been abandoned, it may return to service if a market or adequate partners are found.

Consideration is being given in Russia to the development of a more compact winged spaceplane designed to ferry personnel and their luggage into space. At this point, the Russian space company RSC Energia is developing a new partly reusable spaceplane known as Kliper (Clipper). Due to lack of funding from the ESA and RSA, the Kliper project has been indefinitely postponed as of 2006. Designed primarily to replace the Soyuz rocket, Kliper was proposed in two versions: as a pure lifting body design and as a spaceplane with small wings. In either case, the craft would have been able to glide into the atmosphere at an angle that produces much less stress on the human occupants than the current Soyuz. The Kliper will be able to carry up to six people and to perform ferry services between Earth and the International Space Station.

3.3.4 Land-Based Launching Systems

Most satellite launches have taken place from the following launch facilities:

1. US-Based Launch Centres – The USA launches satellites from two main locations, in Florida Cape Canaveral, suitable for direct equatorial orbit and the Vandenberg Air Force Base in California, suitable for polar orbit missions.

2. Russian Launch Centres – Russian satellites are launched from two main launch centres named Baikonur and Northern Cosmodrome. Baikonur lies north of Tyuratam, in Kazakhstan, with the all-launching support infrastructure for launching Proton and Energia heavy launchers. The Northern Cosmodrome is located near Plesetsk, south of the town Archangelsk, suitable for launching satellites for all purposes in high inclination orbits. This Cosmodrome is the world's busiest launch site.

3. European Launch Centres – The main European launch Cosmodrome is the Guiana Space Centre in French Guiana, using Ariane vehicles. The position of this Cosmodrome enables the best advantage to be taken of the Earth's rotation for direct equatorial orbit.

4. Chinese Launch Centres – The principal launch sites in China are Jiuquan and Xi Chang, for launching Long March vehicles. In the meantime, the Xi Chang launch centre has also become most used for launches into the GEO for the international market.

5. Japanese Launch Centres - The Japan's Tanegashima Space centre is situated in the prefecture of Kagashima. The facilities include the Takesaki Range for small rockets and the Osaki Range was used for the launch of H-I vehicles until the termination of the program in 1992. After renovation, the Osaki Range will be used as the launching for next generation of J-I Japanese vehicles. The new Yoshinobu launch complex has been constructed next to the Osaki centre to satisfy the requirements of the new H-II launcher.

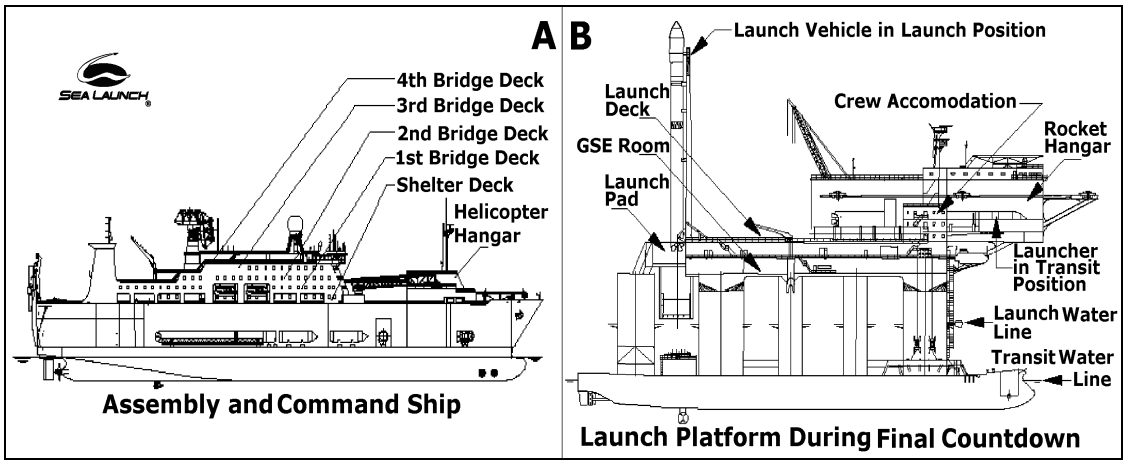

Figure 3. 10 Sea Launch Modules by Sea 1993

3.3.5 Sea-Based Launch Systems

The Sea Launch Multinational Organization was developed in March 1996 to overcome the cost of land-based launch infrastructure duplication around the world. The newly formed Sea Launch system is owned by the Sea Launch Partnership Limited in collaboration with international partners such as US Boeing Commercial Space Company, Russian RSC Energia, Ukrainian KB Yuzhnoye/PO Yuzhmash, Shipping Anglo-Norwegian Kvaerner Group and Sea Launch Company, LLC. The Sea Launch Company, partner locations and operating centres, has US-based headquarters in Long Beach, California, and is manned by selected representatives of each of the partner companies.

The System consists of two main modules: Assembly (Command and Control Ship) and Launch Platform, both illustrated in Figure 3.10 (A) and (B), respectively. However, transit for the ACV and the LP from Home Port in Long Beach to the launch site on the equator takes 10 to 12 days, based on a speed of 10.1 knots.

The Sea Launch Partners have the following responsibilities and tasks:

1) Boeing responsibilities include designing and manufacturing the payload fairing and adapter, developing and operating the Home Port facility in Long Beach, integrating the spacecraft with the payload unit and the Sea Launch system, performing mission analysis and analytical integration, leading operations, securing launch licensing documents and providing range services.

2) The RSC Energia is responsible for developing and qualifying the Block DM-SL design modifications, manufacturing the Block DM-SL upper stage, developing and operating the automated ground support infrastructure and equipment, integrating the Block DM-SL with Zenit-2S and launch support equipment, planning and designing the CIS portion of launch operations, developing flight design documentation for the flight of the upper stage and performing launch operations and range services.

3) The KB Yuzhnoye/PO Yuzhmash are responsible for developing and qualifying Zenit-2S vehicle design modifications, integrating the launch vehicle flight hardware, developing flight design documentation for launch with respect to the first two stages, supporting Zenit

processing and launch operations. Several significant configuration modifications have been made to allow the basic Zenit design to meet Sea Launch's unique requirements.

4) The Anglo-Norwegian Kvaerner Group is responsible for designing and modifying the Assembly and Command Vessel (ACV), designing and modifying the Launch Platform (LP) and integrating the marine elements. Furthermore, Barber Moss Marine Management is responsible for marine operations and maintenance of both vessels.

The partner team of contractors has developed an innovative approach to establishing Sea Launch as a reliable, cost-effective and flexible commercial launch system. Each partner is also a supplier to the venture, capitalizing on the strengths of these industry leaders. The Sea Launch Home Port complex is located in Long Beach, California. The Home Port site provides the facilities, equipment, supplies, personnel and other procedures necessary to receive, transport, process, test and integrate the spacecraft and its associated support equipment with the Sea Launch system. The Home Port also serves as the marine base of operations for both of the Sea Launch vessels. The personnel providing the day-to-day support and service during pre-launch processing and launch conduct to Sea Launch and its customers are located at the Home Port. The ACV performs four important functions for Sea Launch operations: **(1)** It serves as the facility for assembly, processing and checkout of the launch vehicle; **(2)** It houses the Launch Control Centre (LCC), which monitors and controls all operations at the launch site; **(3)** It acts as the base for tracking the initial ascent of the launch vehicle; and **(4)** It provides accommodation for the marine and launch crews during transit to and from the launch site. Therefore, the ACV is designed and constructed specifically to suit the unique requirements of Sea Launch. The ship's overall dimensions are nearly 200 m in length, 32 m in beam and a displacement of 34,000 tons.

Major features of the ACV include: a rocket assembly compartment; the LCC with viewing room; helicopter capability; spacecraft contractor and customer work areas and spacecraft contractor and customer accommodation. The rocket assembly compartment, which is located on the main deck of the ACV, hosts the final assembly and processing of the launch vehicle. This activity is conducted while the vessels are at the Home Port and typically in parallel with spacecraft processing. The bow of the main deck is dedicated to processing and fuelling the Block DM-SL of the Zenit launch vehicle. After the completion of spacecraft processing and encapsulation, the encapsulated payload is transferred into the rocket assembly compartment, where it is integrated with the Zenit-2S and Block DM. The launchers and the satellite are assembled horizontally in the ACV before sailing from the port of Long Beach to the designated launch site. A launcher with a payload will then be transferred in the horizontal position to the launch pad on LP and raised to a vertical position for fueling and launching.

During the launch sequence, the crew of the LP will be transferred to the ACV, which will initiate and control the launch from a position about 3 miles away from the LP pad. The LP is an extremely stable sea platform from which to conduct the launch, control and other operations. The LP rides catamaran-style on a pair of large pontoons and is self-propelled by a four-screw propulsion system (two in each lower hull,), which is powered by four direct-current double armature-type motors, each of which is rated at 3,000 hp. The LP in navigation has normal draft at sea water level but, once at the launch location, the pontoons are submerged to a depth of 22.5 m to achieve a very stable launch position, level to within approximately 1^{o}. The ballast tanks are located in the pontoons and in the lower part of the columns. Six ballast pumps, three in each pontoon, serve them. The LP has an overall length

of approximately 133 m at the pontoons and the launch deck is 78 by 66.8 m. The Zenit-3SL launcher is a two-stage liquid propellant launch vehicle solution capable of transporting a spacecraft to a variety of orbits. The original two-stage Zenit was designed by KB Yuzhnoye quickly to reconstitute former Soviet military satellite constellations. The design emphasizes robustness, ease of operation and fast reaction times. The result is a highly automated launch capability using a minimum complement of launch personnel. The launcher, as an integrated part of the Sea Launch system, is designed to place spacecraft into a variety of orbits and is capable of putting 5,250 kg of payload into GEO. The Sea Launch mission provides a number of technical support systems that are available for the customer's use in support of the launch process, including, most importantly, the following:

1. Communications – Internal communications systems are distributed between the ACV and LP. This system includes CCTV, telephones, intercom, video teleconferencing, public address and vessel-to-vessel radiocommunications, known as the Line-of-Sight (LOS) direct system. This system links with the external communication system and provides a worldwide network that interconnects the various segments of the Sea Launch program. The external communication system includes Intelsat and two ground stations. The LES are located in Brewster, Washington and Eik, Norway, and provide the primary distribution Gateways to the other communication nodes. Customers can connect to the Sea Launch communication network through the convenient Brewster site. The Intelsat system ties in with the ACV and launch platform PABX systems to provide telephone connectivity. Additionally, critical telephone, Fax, Tlx or data capability can be ensured by the Inmarsat system through SES Standard-B.

2. Tracking and Data Relay Satellite System (TDRSS) – The Sea Launch system uses a unique dual telemetry stream with the TDRSS. Telemetry is simultaneously received from the Zenit stages, the Block DM upper stage and the payload unit during certain portions of the flight. The Block DM upper stage and payload unit data are combined but the Zenit data is sent to a separate TDRSS receiver. Zenit data is received shortly after lift-off at approximately 9 sec and continues until Zenit Stage 2/Block DM separation, at around 9 minutes. These data are routed from the NASA White Sands LES to the Sea Launch Brewster LES and to the ACV. Otherwise, the data are also recorded at White Sands and Brewster for later playback to the KB Yuzhnoye design centre. When the payload fairing separates, the payload unit transmitter shifts from sending high-rate payload accommodation data by LOS to sending combined payload unit/Block DM by TDRSS. The combined data is again routed from White Sands to Brewster, where it is separated into Block DM and payload unit data and then sent on to the ACV. The data are received on board the ship through the Intelsat communications terminal and are routed to Room 15 for upper-stage data and Room 94 for PLU data. Simultaneously, Brewster routes Block DM data to the Energia Moscow control centre station. However, the TDRSS coverage continues until after playback of the recorded Block DM data.

3. Telemetry System – Sea Launch uses LOS telemetry systems for the initial flight phase, as well as the TDRSS for later phases. The LOS system, which includes the Proton antenna and the S-band system, is located on the ACV. Other telemetry assets include Russian ground tracking stations and the Energia Moscow control centre. The following subsections apply to launch vehicle and payload unit telemetry reception and routing.

4. Weather (WX) Data System and Forecast – The ACV unit has a self-contained WX station, which includes a motion-stabilized C-band Doppler radar equipment, surface wind

instruments, wave radar, upper-atmospheric balloon release station, ambient condition sensors and access to satellite imagery and information from an on-site buoy.

3.4 Types of Orbits for Meteorological and Other Satellite Systems

An orbit is the circular or elliptical path that the satellite traverses through space. This path appears in the chosen orbital plane in the same or different angle to the equatorial plane. All communication satellites always remain near the Earth and keep going around the same orbit, directed by centrifugal and centripetal forces. Each orbit has certain advantages in terms of launching (getting satellite into position), station keeping (keeping the satellite in place), roaming (providing adequate coverage) and maintaining the necessary quality of communication services, such as continuous availability, reliability, power requirements, time delay, propagation loss and network stability. There is a large range of satellite orbits but not all of them are useful for metrological or communication systems.

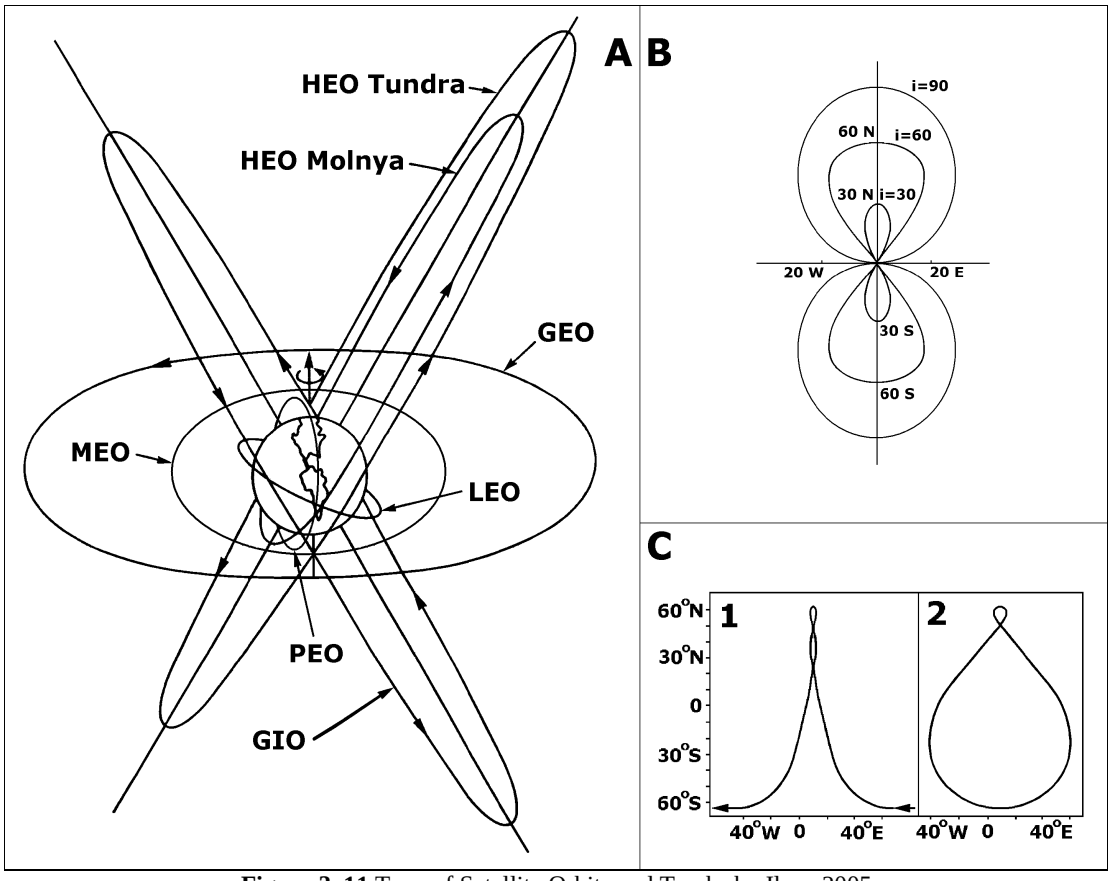

Figure 3. 11 Type of Satellite Orbits and Tracks by Ilcev 2005

In general, the one most commonly used orbit for satellite meteorology are GEO and PEO (LEO) constellations. In addition, the Highly Elliptical Orbit (HEO) and latterly Geosynchronous Inclined Orbits (GIO) and Medium Earth Orbit (MEO) can also be used, as shown in Figure 3.11 (A). Thus, it is essential to consider that satellites can serve all communication, navigation, meteorological and observation systems for which they cannot have an attribute such as fixed or mobile satellites and the only common difference is which type of payload or transponder they carry onboard.

After many years of research and experiments spent on finding the global standardization for spatial communications, satellites remained the only means of providing near global coverage, even in those parts which other communication systems are not able to reach. There is always doubt about the best orbital constellation that can realize an appropriate global coverage and a reliable communications solution. Unfortunately, there is no perfect system today; all systems have some advantages or disadvantages. The best conclusion is to abridge the story and to say briefly that, today, the GEO system is the best solution and has only congestion as a more serious problem (Schmetz, 2002).

The track of the satellite varies from 0 to 360^{o}, which is shown in Figure 3.11 (B). The track of the GEO satellite is at a point in the centre of the coordinate system; two tracks are apparent movements of the GIO satellite with respect to the ascending node of both 30^{o} and 60^{o} inclination angles and the last is the track of the PEO satellite with an inclined orbit plane to the equator of 90^{o}. The tracks of HEO Molniya (part of the track) and Tundra (complete track) orbits are shown in Figure 3.11 (C-1/C-2), respectively. These two tracks pass over the African Continent and almost all of Europe.

It is sufficient to see **Table 3.3** to understand that the major reasons for LEO problems are enormous satellite cost, complex network and short satellite visibility and lifetime. The LEO/PEO constellations are the same or similar and, because of differences in inclination angle of orbital plane and type of coverage, they will be considered separately.

Table 3. 3 The Properties of Four Major Orbits in Evans 1991

Orbital Properties	**LEO/PEO**	**MEO**	**HEO**	**GEO**
Development Period	Long	Short	Medium	Long
Launch & Satellite Cost	Maximum	Maximum	Medium	Medium
Satellite Life (Years)	3–7	10–15	2–4	10–15
Congestion	Low	Low	Low	High
Radiation Damage	Zero	Small	Big	Small
Orbital Period	<100 min	8-12 hours	½ Sidereal Day	1 Sidereal Day
Inclination	90^{o}	45^{o}	63.4^{o}	Zero
Coverage	Global	Global	Near Global	Near Global
Altitude Range (km^{-3})	0.5–1.5	8–20	40/A – 1/P	40 (i=0)
Satellite Visibility	Short	Medium	Medium	Continuous
Handover	Very Much	Medium	No	No
Elevation Variations	Rapid	Slow	Zero	Zero
Eccentricity	0 to High	High	High	Zero
Handheld Terminal	Possible	Possible	Possible	Possible
Network Complexity	Complex	Medium	Simple	Simple
Tx Power/Antenna	Low	Low	Low/High	Low/High
Gain	Short	Medium	Large	Large
Propagation Delay	Low	Medium	High	High
Propagation Loss	High	Medium	Low	Zero

3.4.1 Low Earth Orbits (LEO)

The LEO systems are either elliptical or more usually circular satellite orbits between 500 and 2,000 km above Earth surface and bellow the Inner Van Allen Belt. The orbit period at these altitudes varies between ninety minutes and two hours, as shown in Figure 3.11 (A). The radius of the footprint of a communications satellite in LEO varies from 3,000 to 4,000 km.

The maximum time during which a satellite in LEO orbit is above the local horizon for an observer on the Earth is up to 20 minutes. The traffic to a LEO satellite has to be handed over much more frequently than all other types of orbit. When an LEO satellite, which is serving particular users, moves below the local horizon, it needs to be able to quickly handover the service to a succeeding one in the same or adjacent orbit.

Due to the relatively large movement of a satellite in LEO constellation with respect to an observer on the Earth, satellite systems using this type of orbit need to be able to cope with large Doppler shifts. Satellites in LEO are not affected at all by radiation damage, but are affected by atmospheric drag, which causes the orbit to gradually deteriorate. Satellites in LEO and MEO constellation are subject to orbital perturbation. For LEO satellites, the aerodynamic drag is likely to be significant and, in general, some of the other perturbations, such as precession of the argument of the perigee, resolve to zero if the orbit is circular or polar. On the other hand, a perturbation is unlikely to have a serious effect on the operation of a multi-satellite constellation since it will usually affect all satellites of the configuration in equal measure (McGinnis and Dries, 2009).

3.4.2 Circular Orbits

The GEO satellite constellation has great advantages for meteorological observations, and, in the future, MEO satellites will have significant success in these fields.

3.4.2.1 Medium Earth Orbits (MEO)

The MEO satellite constellations, known also as Intermediate Circular Orbits (ICO), are circular orbits located at an altitude of around 10,000 to 20,0000 km between the Van Allen Belts. The MEO satellites are operated in a similar way to Big LEO systems providing global coverage, as shown in Figure 3.11 (A).

Thus, compared to a LEO system, a MEO constellation can only be in circular orbit. Doppler Effect and handover are less frequent and propagation delay is about 70 ms and free space loss is greater. These satellites are affected by radiation damages from the Inner Van Allen Belt only during the launching period.

Cosmic radiation in this orbit is lower, with subsequently longer life expectancy for the complete MEO configuration. Fewer eclipse cycles means that battery lifetime will be more than 7 years, higher average elevation angle from users to satellite minimizes probability of LOS blockage and higher RF output power required for both indoor and handheld MSC terminals. There is in exploitation a special model of MEO constellation known in practice as Highly Inclined Orbit. This particular orbit is of interest because it has been chosen for existing and proposed GNSS systems such as US GPS and Russian GLONASS (Ilcev, 2013). If it became operational, Galileo will use MEO configuration, which would have 24 satellites in 3 orbital planes equidistant from each other, at an altitude of 20,000 km and at an inclination of 55^{o}.

However, a MEO satellite configuration can be effective for metrological observations as well.

3.4.2.2 Geostationary Earth Orbits (GEO)

A GEO has circular orbit in the equatorial plane, with the orbital period equal to the rotation of the Earth of 1 sidereal day, which is achieved with the orbital radius of 66,107 (Equatorial) Earth Radii, or orbital height of 35,786 km, shown in Figure 3.11 (A). A Satellite in a GEO will appear fixed above the surface of the Earth and remain in a stationary position relative to the Earth itself. Thus, this orbit is with zero inclination and track as a point but, in practice, the orbit has small non-zero values for inclination and eccentricity, causing the satellite to trace out a small figure eight in the sky, whose track is shown in Figure 3.11 (B).

The footprint or service area of a GEO satellite covers almost 1/3 of the Earth's surface or 120^{o} in longitude direction and up to 75^{o}–78^{o} latitude North and South of the Equator but cannot cover the Polar Regions (Berlin 1988). In this way, near-global coverage can be achieved with a minimum of three satellites in orbit moved apart by 120^{o}, although the best solution is to employ four GEO satellites for better overlapping. This type of orbit is essentially used for communication, metrological and other services with the following advantages:

a). The satellite remains stationary with respect to one point on the Earth's surface and so the GES antennas can be beamed exactly towards the focus of the GEO satellite without periodical tracking.
b). The Inmarsat GEO space constellation consisting in three or four satellites can cover all three-ocean regions with overlapping longitudes, except for the Polar Regions beyond latitudes of 75^{o} North and South.
c). The Doppler shift, affecting synchronous digital systems caused by satellites to drift in orbit (affected by the gravitation of the Moon and to a lesser extent of the Sun) is small for GES/MES within satellite coverage.

The disadvantages of GEO compared with LEO and MEO operation are as follows:

a). The long signal delay is due to the large distance of about 35,800 km if the satellite is in zenith for MES and about 41,000 km at the minimum elevation angle of about 5^{o}. For the EM waves travelling at the speed of light, this causes a round-trip signal delay of 240-270 ms and full duplex delay of 480-540 ms.
b). The required higher RF output power and the use of directional satellite antennas system aggravate GEO operation slightly for use with handheld terminals, although it is not critical, because some GEO operators provide this service, such as Inmarsat, Thuraya and ACeS.
c). The launch procedure to put a satellite in GEO is expensive but the total cost of 4 satellites is less than the cost of a minimum of 12 or 40 for MEO and LEO, respectively.

An GEO satellite is at essentially fixed latitude and longitude, so even a narrow-beam Earth antenna can remain fixed. Satellites in GEO can use high and recently low-gain antennas, which help to overcome the great distances in achieving the required Effective Radiated Isotropic Power (EIRP) at ground level. Using satellite spot beam antennas, GEO coverage can be confined to smaller spot areas with bigger power and higher speed of transmission. The GEO satellites pass through both Van Allen Belts only on launch, so their effect is insignificant. After reaching the end of operational life, a satellite has to be removed from its orbital slots into a graveyard orbit some 200 km above the GEO plane. The GEO satellite constellation seems likely to continue to dominate in the satellite communications world,

especially in communication and meteorological systems, providing near global coverage with low and high-power transmission.

3.4.2.3 Geosynchronous Inclined Orbits (GIO)

The GIO orbit would consist of four satellites at six-hour intervals around the Earth orbit at an inclination of 45^o to the equatorial plane, as shown in Figure 3.11 (A). This orbit provides polar coverage for six hours on either side of their most Northerly and Southerly movement and needs special GES with full tracking antennas. The GIO satellite has a period of orbit equal to or very little different from a sidereal day (23h 56 min and 4.1 sec), which is time for one complete revolution of the Earth. The satellite movement speed has only very little difference from the angular velocity of the Earth. Therefore, this movement also has constant angular velocity.

Thus, the projection of this satellite movement on the equatorial plane is not at a constant velocity. There is an apparent movement of the satellite with respect to the reference meridian on the surface of the Earth and that of the satellite on passing through the nodes. The orbit may be inclined at any angle, which produces a repeating ground track. Figure 3.11 (B) presents tracks of 30^o and 60^o inclined orbits. The coupled N–S and E–W motion of GIO satellites is shown as a figure eight pattern, while the patterns could also be distorted circles. Depending on the inclination angle, the GIO satellite shows points on the equator at various longitudes.

A satellite may operate in this orbit for several reasons. First, it is often desirable to save the inclination control fuel required for the GEO circle. Second, usually there is no need to control inclination because tracking GES antennas are required for other reasons. Some GEO satellites may last beyond their planned lifetime if they run low on fuel and cease inclination control. In effect, the GIO constellation with non-zero inclination can be chosen because of easy launching and placing of the satellite into orbit. This satellite must move with an angular velocity equal to the Earth and be in a prograde orbit, that is, revolving eastward in the same direction as the Earth rotates. Otherwise, the only requirements for a GIO constellation are the right period and direction of rotation.

3.5 Polar Earth Orbits (PEO)

The PEO constellation is today a synonym for providing coverage of both Polar Regions for different types of meteorological observation and satellite determination services, shown in Figure 3.11. A satellite in this orbit travels its course over the geographical North and South Poles and will effectively follow a line of longitude.

Certainly, this orbit may be virtually circular or elliptical depending upon requirements of the program and is inclined at about 90^o to the equatorial plane, covering both poles. The orbit is fixed in space while the Earth rotates underneath and, consequently, the satellite, over a number of orbits determined by its specific orbit line, will pass over any given point on the Earth's surface (Dartcom, 2015). Therefore, a single satellite in a PEO provides, in principle, coverage to the entire globe, although there are long periods during which the satellite is out of view of a particular ground station. The track of PEO satellite with inclined orbit plane to the equator of 90^o is shown in Figure 3.11 (B).

Accessibility can, of course, be improved by deploying more than one satellite in different orbital planes. If, for instance, two such satellite orbits are spaced at 90^{o} to each other, the time between which satellites passes over any given point will be halved. The PEO system is rarely used for communication purposes because the satellite is in view of a specific point on the Earth's surface for only a short period of time. Any complex steerable antenna system would also need to follow the satellite as it passes overhead. This satellite orbit is acceptable for a communication, meteorological, determination and navigation systems.

There are four primary requirements for PEO systems as follows:

1) To provide total global satellite visibility for LEOSAR Cospas-Sarsat distress beacons;
2) To provide global continuous coverage for current or forthcoming GSNN systems;
3) To provide at L-band or any convenient spectrum for the communication requirements of ships and aircraft in the Polar Regions not covered by the Inmarsat GEO system; and
4) To provide global coverage for meteorological and synoptic observation stations.

There are two proposals for PEO satellite constellations, first, low altitudes up to 1,400 km and, second, high altitudes above 11,000 km. These two orbits are separated by the Inner Van Allen radiation belts, whose radiation level increases roughly exponentially with a height at around 1,000 km, reaching a peak at about 5,000 km altitude. Thus, a critical requirement to reduce high-energy proton damage to the solar cell arrays of the satellite system constrains both PEO altitudes. As is evident, another Outer Van Allen Belt has a negative influence on these two PEO constellations because it lies far away between the MEO and GEO planes (Festo, 2015).

3.6 Highly Elliptical Orbits (HEO)

Using inclined HEO configuration, both polar areas can be effectively covered with four satellites, two in each polar orbit, as shown in Figure 3.11. (A). The elevation angle to the HEO satellites remains high for most of the 12-hour period of visibility, which is especially required for continuous service over the Euro-Asian region. At this point, th blocking of the beam due to occlusion of the satellite by different obstacles is minimized (Roshydromet, 2014). Multiple trajectories caused by successive reflection of various obstacles are also reduced in comparison with systems operating with low elevation angles, like GEO.

The apogee altitude combines polar coverages with nearly synchronous advantages. Thus, a minimum of two special GES in both northern and southern Polar Regions are required to serve MES terminals. The GES tracking can be reached by a fairly directive fixed antenna while the satellite is in its slow apogee sector. The HEO space constellation is designed to cover the area under the apogee. Tracking of the satellite is facilitated on account of the small apparent movement and the long visibility duration. Otherwise, it is even possible to use antennas whose 3 dB bandwidth is a few tens of degrees, with fixed pointing towards the zenith, which permits the complexity and cost of the terminal to be reduced while retaining a high gain. A satellite in HEO constellation near the apogee can also use a high gain antenna to overcome the great distances in achieving the required EIRP values. The noise captured by the GES antenna, from the ground or due to interference from other radio systems and atmosphere, is also minimized due to the high elevation angles (Festo, 2015).

At any rate, these advantages have led the former USSR (today Russia) to design two HEO configurations and to use these orbits for a long time in order to provide coverage of their own high latitude territories for mobile systems.

The first prototype HEO Molnya satellite was launched in 1964 and, to date, more than 150 have been deployed, primarily produced by the Applied Mechanics NPO in Krasnoyarsk, former USSR. The Molnya satellites weigh approximately 1.6 metric tons at launch and stand 4.4 m tall, with a base diameter of 1.4 m. This satellite has initial perigees between 450 and 600 km fixed deep in the Southern Hemisphere and apogees near 40,000 km in the Northern Hemisphere.

The second Russian Tundra HEO system employs 2 satellites in two 24-hour orbits separated by 180^o around the Earth, with apogee distance at 53,622 km and perigee at 17,951 km, which provides visibility duration of more than 12 hours with high elevation angles.

The HEO satellite transmission has a similar delay as a GEO at the apogee of about 0.25 sec. Therefore, free space loss and propagation delay for HEO is comparable to that of the GEO constellation. Compared with GEO, the launch and satellite cost of the HEO constellation is reasonably low and this constellation is free of congestion because of only a few current and projected new HEO systems and provides high elevation angles for GES, which reduces atmospheric losses. Due to the relatively large movement of a satellite in HEO with respect to an observer on Earth, satellite systems using this model of orbit need to be able to cope with large Doppler shifts, 14 kHz for Molnya and 6 kHz for Tundra orbits in L-band 1.6 GHz. However, as the former USSR's experience has shown, satellites in this orbit tend to have rather a short lifetime due to the repetitive crossing of both Van Allen Belts.

The HEO satellite typically has a perigee at about 500 km above the Earth's surface and an apogee as high as 50,000 km. The orbits are inclined at 63.4^o in order to provide services to locations at high northern latitudes. The particular inclination value is selected in order to avoid rotation of the apses, i.e., the intersection of a line from the Earth's centre to the apogee and the Earth's surface will always occur at a latitude of 63.4^oN. Orbit period varies from eight to 24 hours. Owing to the high eccentricity of the orbit, a satellite will spend about two thirds of the orbital period near apogee and, during that time, it appears to be almost stationary for an observer on Earth (this is referred to as apogee dwell). After this period, a switchover needs to occur to another satellite in the same orbit in order to avoid loss of communications. There have to be at least three HEO satellites in orbit, with traffic being handed over from one to the next every eight hours at a minimum (Kidder and Ham, 1995).

When there is an orbit in the HEO plane of non-zero inclination, the satellite passes over the region situated on each side of the equator and will possibly cover the polar regions if the inclination of the orbit is close to 90^o. By orienting the apsidal line, namely, the line between perigee and apogee, in the vicinity of the perpendicular to the line of nodes (when ω is close to 90^o or 270^o), the HEO satellite at the apogee systematically returns above the regions of a given hemisphere. In this way, it is possible to establish satellite links with GES located at high latitudes. Although the satellite remains for several hours in the vicinity of the apogee, it does move with respect to the Earth and, after a time, dependent on the position of the GES, the satellite disappears over the horizon as seen from the mobiles. However, to establish permanent links it is necessary to provide several suitably phased satellites in similar orbits, which are spaced around the Earth (with different right ascensions of the ascending node and regularly distributed between 0 and 2π) in such a way that the satellite moving away from the

apogee is replaced (handover) by another satellite in the same area of the sky as seen from the GES. However, the problems of satellite acquisition and tracking by the GES are simplified. Finally, there only remains the problem of handover and switching the links from one satellite to other, so the RF link frequencies of the various satellites can be different in order to avoid interference.

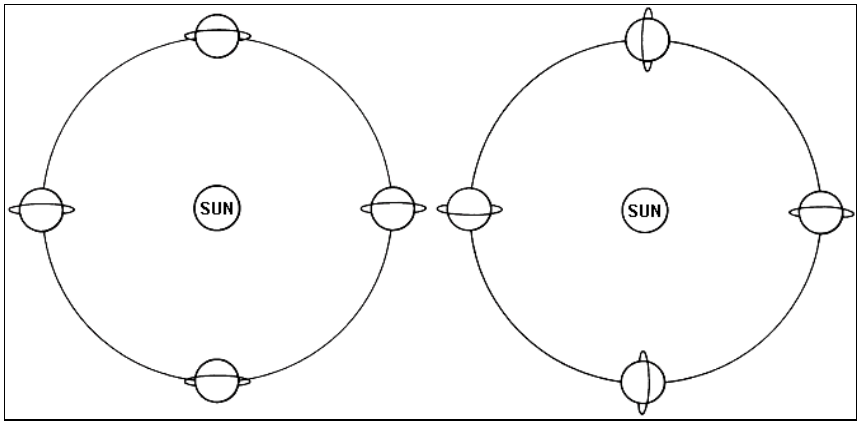

Figure 3. 12 Seasonal Changes for Keplerian and Sunsynchronous Orbit by Kidder and Ham 1995

3.7 Satellite Orbit Perturbations

After launching, a satellite in circular orbits undergoes uniform angular velocity. By Kepler's Second Law, however, a satellite in an elliptical orbit cannot have a uniform angular velocity, so it must travel faster when is closer to Earth. The position of the satellite as a function of time can be found by applying Kepler's equation:

$$M_a = Э - e \sin Э \qquad (3.48)$$

where M_a = means anomaly, Э = eccentric anomaly, and e = eccentricity

Thus, orbits, in which the classical orbital elements (except M_a) are constant, are called Keplerian orbits. More exactly, viewed from space, Keplerian orbits are simple. The satellite moves in an elliptical path with the centre of the Earth at one focus. The ellipse maintains a constant size, shape and orientation with respect to the stars, whose seasonal changes are shown in Figure 3.12, for Keplerian **(Left)** and Sunsynchronous Orbit **(Right).** Perhaps, surprisingly, the only effect of the Sun's gravity on the satellite is to move the focus of the ellipse (the Earth) in an elliptical path around the Sun (the Earth's orbit).
Viewed from the Earth, Keplerian orbits appear complicated because the Earth rotates on its axis as the satellite orbits the Earth. The orbit of a representative satellite, as viewed from a point rotating with the Earth, is shown in Figure 3.13.

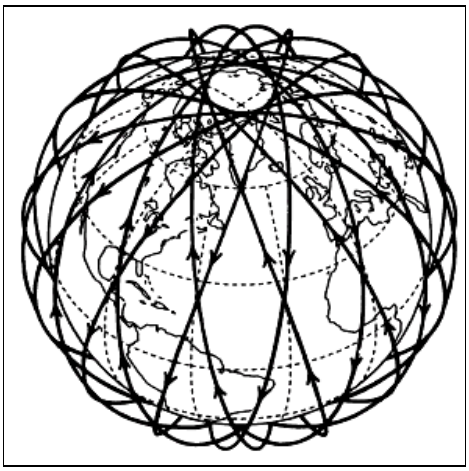

Figure 3. 13 Representative Satellite Orbit by Kidder and Ham 1995

The rotation of the Earth beneath a fixed orbit results in two daily passes of the satellite near a point on the Earth (assuming that the period is substantially less than a day and that the inclination angle is greater than the latitude of the point). Thus, one pass occurs during the ascending portion of the orbit; the other occurs during the descending portion of the orbit. This usually means that one pass occurs during daylight and one during darkness.

There is some variation in how the orbital elements are specified. For example, ESA system substitutes true anomaly for mean anomaly. Also, in less formal descriptions of satellite orbits, one frequently sees the height of the satellite above the Earth's surface substituted for the semimajor axis. Since the Earth is not round, the height of a satellite will vary according to its position in the orbit. Specifying the semimajor axis is a much better way to describe a satellite orbit.

The eccentric anomaly is useful to compute the position of a point moving in a Keplerian orbit. For instance, if the body passes the periastron at coordinates $x = a\,(1 - e)$, $y = 0$, at time $t = t_0$, then to find out the position of the body at any time, it will be firstly required to calculate the mean anomaly from the time and the mean motion n by the formula $M_a = n\,(t - t_0)$, then solve the Kepler equation above to get Э, and then get the coordinates from:

$$x = a\,(\cos Э - e) \quad \text{and} \quad y = b \sin Э \tag{3.49}$$

Therefore, Kepler's equation is a transcendental equation because sine is a transcendental function, meaning it cannot be solved by Э algebraically. Thus, numerical analysis and series expansions are generally required to evaluate Э.

Although satellites travel in nearly Keplerian orbits, these orbits are perturbed by a variety of forces, as indicated in **Table 3.4**.

Table 3. 4 Forces and Sources of Orbital Perturbations in Kidder and Ham 1995

Force	Source
Nonspherical gravitational field	Nonspherical, nonhomogeneous Earth
Gravitational attraction of auxiliary bodies	Moon, planets
Radiation pressure	Sun's radiation
Particle flux	Solar wind
Lift and drag	Residual atmosphere
Electromagnetic forces	Interaction of electrical currents in the satellite with the Earth's magnetic field

Forces arising from the last five processes are small and can be viewed as causing essentially random perturbations in the orbital elements. Operationally, they are dealt with simply by periodically observing the orbital elements and adjusting the orbit with on-board thrusters. Forces due to the nonspherical Earth cause secular (linear with time) changes in the orbital elements. These forces can be predicted theoretically and are useful. The gravitational potential of Earth is a complicated function of the Earth's shape, the distribution of land and ocean, and even the density of crystal material. As a first-order correction to a spherical shape, we may treat the Earth as an oblate spheroid of revolution. In cross section, the Earth is approximately elliptical (Kadish et al, 2000).

The distance from the centre of the Earth to the equator is, on average, 6378.140 km, whereas the distance to the poles is 6356.755 km. Thus, one can think of the Earth as a sphere with a 21 km thick "belt" around the equator. Therefore, the gravitational potential of the Earth is approximately given by the following equation:

$$U = - GM/r [1 + ½ J_2 (r_e/r)^2 (1 – 3 \sin^2 Д) + \ldots] \quad (3.50)$$

where r_e = equatorial radius of the Earth, Д = declination angle and J_2 = coefficient of the quadrupole term. The higher-order terms are more than two orders of magnitude smaller than the quadrupole term and will not be considered here, although they are necessary for very accurate calculations.

How does this belt of extra mass affect a satellite's orbit? One might expect it to cause the satellite to orbit at a different speed, and, indeed, it does. The time rate of change of the mean anomaly (dM_a/dt) is given by the mean motion constant n in the unperturbed orbit and by the anomalistic mean motion constant N, in a perturbed orbit. Considering only the quadrupole term anomaly can be formulated:

$$N = dM_a/dt = n [1 +3/2 J_2 (r_e/a)^2 (1 – e^2)^{-3/2} (1 – 3/2 \sin^2 i)] \quad (3.51)$$

where a = semimajor axis and i = inclination.

When the inclination angle is less than 54.7°, N is greater than n, so the satellite orbits faster than it would in an unperturbed orbit. However, for larger inclinations, the satellite orbits more slowly than it otherwise would.

Since the belt exerts an equator ward force, one might also expect that it would have an effect on the inclination angle. In such a way, this force affects the right ascension of the ascending node rather than the inclination angle.

Just as the force of gravity causes a top to precess rather than to fall over, so the attraction of the belt causes the orbit to precess about the α axis rather than to change its inclination angle. The rate of change of the right ascension of ascending node (Ω) can be determined by the following relation:

$$d\Omega/dt = - N [3/2 J_2 (r_e/a)^2 (1 - e^2)^{-2} \cos i] \quad (3.52)$$

The final effect of the belt is to cause the argument of perigee (ω) to rotate or precess, which relation is presented as:

$$d\omega/dt = - N [3/2 J_2 (r_e/a)^2 (1 - e^2)^{-2} (2 - 5/2 \cos^2 i)] \quad (3.53)$$

The other three orbital elements, a, e and i, undergo small, oscillatory changes that may be neglected. If SI Units are used, equations (3.5), (3.51), (3.52) and (3.53) result, respectively, in values of n, N, $d\Omega/dt$ and $d\omega/dt$ whose units are radians per second. The anomalistic period of a perturbed orbit is simply presented as:

$$T_a = 2\pi/N \quad (3.54)$$

However, because M_a is measured from perigee, the anomalistic period is the time for the satellite to travel from perigee to moving perigee. Of more use is the synodic or nodal period (T_s), which is the certain time for the satellite to travel from one ascending node to the next ascending node. An exact value of T_s must be calculated numerically; however, to very good approximation as follows:

$$T_s = 2\pi/[N + (d\omega/dt)] \quad (3.55)$$

In summary, therefore, the first-order effects of the nonspherical gravitational potential of the Earth consists of a slow, linear change in two of the classical orbital elements, than the right ascension of ascending node and the argument of perigee, and a small change in the mean motion constant.

3.8 Main Characteristics of Metrological Satellite Orbits

Nearly all-present meteorological satellites are in one of two orbits, such as sunsynchronous (PEO) or geostationary (GEO), but other orbits are also useful, such as LEO and HEO.

3.8.1 Sunsynchronous Orbits

The nonspherical gravitational perturbation of Earth, far from being a problem, has a very useful application. As shown in Figure 3.12 (Left), the angle between the lines that join the Sun and the ascending node to the centre of the Earth changes in a Keplerian orbit because the orbital plane is fixed while the Earth rotates around the Sun. This causes the satellite to pass over an area at different times of the day. For example, if the satellite passes over near noon and midnight in the spring, it will pass over near 6:00 am and 6:00 pm in the winter. Several problems result, such as: (1) the data do not fit conveniently into operational schedules; (2) orientation of solar cell panels is difficult; and (3) dawn or dusk visible images may not be as useful as images made at other times. Fortunately, the perturbations caused by the nonspherical Earth can be employed to keep the Sun-Earth-satellite angle constant.

The Earth makes one complete revolution about the sun (2π radians) in one tropical year (31,556,925.9747 s). Thus, the right ascension of the sun changes at the average rate of 1.991064×10^{-7} rad s^{-1} ($0.9856473° \text{ day}^{-1}$). If the inclination of the satellite is correctly chosen, the right ascension of its ascending node can be made to precess at this same rate. At this point, a satellite orbit that is so synchronized with the Sun is called a sunsynchronous orbit. For a satellite with a semimajor axis of 7228 km and zero eccentricity, equation (3.52) requires an inclination of 98.8° to be sunsynchronous. Figure 3.12 (Right) shows the change with season of a sunsynchronous orbit (Kramer, 2002).

Since the sun-Earth-ascending node angle is constant in a sunsynchronous satellite orbit, the satellite is often said to cross the equator at the same local time every day. Unfortunately, local time is an ambiguous term. This can be used to express equivalence as follows:

$$LT \equiv t_U + \lambda/15^0 \tag{3.56}$$

where t_U = coordinated universal time in hours and λ = longitude in degrees of a particular point. Equator Crossing Time (ECT) is the local time when a satellite crosses the equator:

$$ECT \equiv t_U + \lambda_N/15^0 \tag{3.57}$$

where λ_N = longitude of ascending or descending node. Therefore, if λ_N is constant, as it is for a sunsynchronous satellite, then ECT is constant.

Sunsynchronous satellites are classified by their ECT values. Thus, noon satellites (or noon-midnight satellites) ascend (or descend) near noon LT (local time). They must, therefore, descend (or ascend) near local midnight. Morning satellites ascend (or descend) between 06 and 12 h LT, and descend (or ascend) between 18 and 24 h LT. Afternoon satellites ascend (or descend) between 12 and 18 h LT, and descend (or ascend) between 00 and 06 h LT.

The highest latitude reached by the subsatellite point (in any orbit) is equal to the inclination angle (or the supplement of i, in the case of retrograde orbits). Since sunsynchronous orbits reach high latitudes, they are referred to as near polar orbits. This is frequently shortened to polar orbits, although they do not cross directly over the poles. These orbits are also called LEO to distinguish them from geostationary orbits (GEO). Note, however, that PEO is a general term for a satellite that passes near the poles, and LEO is a general term for a satellite that orbits not far above the Earth's surface (Maral et al, 2009).

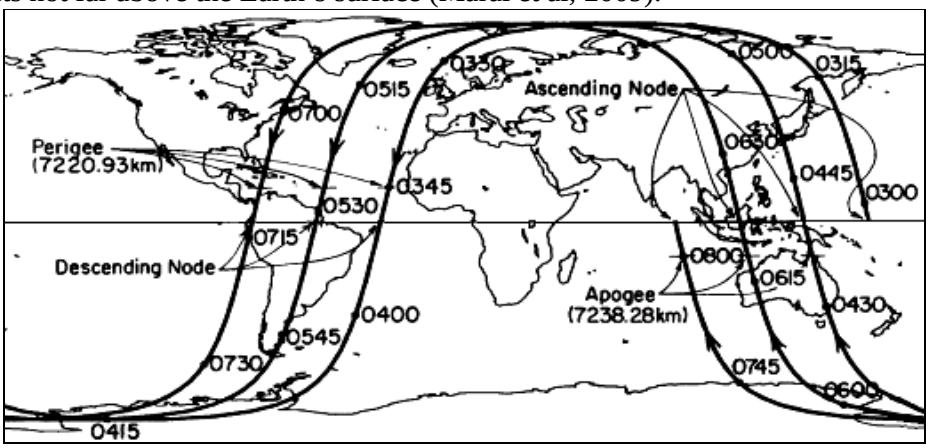

Figure 3. 14. Ground Track of Sunsynchronous Satellite by Kidder and Ham 1995

While sunsynchronous satellites are of necessity polar orbiters and LEO, the converse is not necessarily true. The ground track of a satellite is the path of the point on the Earth's surface that is directly between the satellite and the centre of the Earth (the subsatellite point*).* Figure 3.14 illustrates the ground track for three orbits of the typical sunsynchronous NOAA 11 satellite, whose main parameters are presenting the following values: a = 7229.606 km, i = 98.97446^0, e = 0.00110058, $M_a = 192.28166^0$, $\Omega = 29.31059^0$, $\omega_0 = 167.747540$, Epoch Time = 22 March 1990 1h 15 min and 55.353 sec UTC and Nodal Period = 102.0764 min.

3.8.2 Geostationary Orbits

Using equation (3.6), the radius of a geosynchronous orbit is calculated to be 42,164 km. Perturbations due to the nonspherical Earth, however, require a slight adjustment. The adjustment is small because the geosynchronous orbit is about 6.6 Earth radii, and the correction terms are inversely proportional to the square of this ratio. In fact, for an orbit with zero eccentricity and zero inclination, equations (3.51), (3.53) and (3.55) require a semimajor axis of 42,168 km to be geosynchronous (McGinnis and Dries, 2009).

The terms geosynchronous and geostationary are often used interchangeably. In fact, they are not the same. Geosynchronous means that the satellite orbits with the same angular velocity as the Earth. However, geostationary orbit is geosynchronous, but it is also required to have a zero inclination angle and zero eccentricity. Geostationary satellites, therefore, remain essentially motionless above a point on the equator. They are classified by the longitude of their subsatellite point.

Second-order perturbations cause an GEO satellite to drift from the desired orbit. Periodic maneuvers, performed as frequently as once a week, are required to correct the orbit. These maneuvers keep operational geostationary satellites very close to the desired orbit. For example, on 11 March 1990, the US GOES 7 satellite had an inclination angle of 0.05°; therefore, it did not venture more than 0.05° latitude from the equator. Figure 3.15 illustrates the ground track for a geostationary satellite that is no longer used for imaging and, therefore, its orbit is not so carefully maintained. Note that this satellite's orbit is not quite geostationary, because it drifts west slightly each day.

Thus, the principal GEO parameters are presented by the following values: a = 42171.798 km, $i = 1.97310^0$, e = 0.0003160, $M_a = 147.020^0$, $\Omega = 80.259^0$, $\omega_0 = 223.89100$, Epoch Time = 6 March 1990 4h 8 min and 20 sec UTC and Nodal Period = 1431.297 min.
As stated above, the satellite ground track is an imaginary line on the Earth's surface that traces the course of another imaginary line between Earth's centre (O) and an orbiting satellite (S).

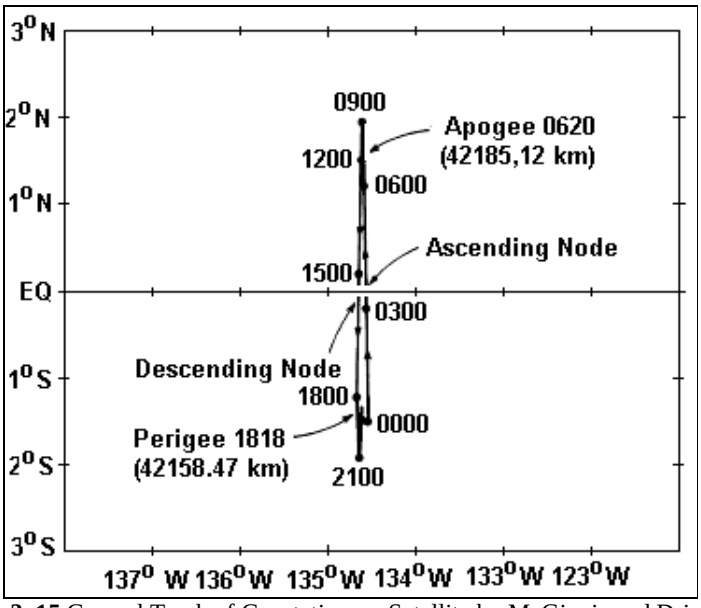

Figure 3. 15 Ground Track of Geostationary Satellite by McGinnis and Dries 2009

Near-circular orbits, which may be considered as circular in a first approximation, constitute a very important and frequently encountered case. Some notions developed specifically for these orbits, such as the equatorial shift or the apparent inclination. In this sense, when the orbit is circular, the motion of satellite is uniform with angular frequency (n), which is discussed earlier as mean motion.

The three Euler angles, θ, Φ and ψ, are serving to specify the orbit and its perigee in space. In this case, it is necessary to specify satellite (S). Obtaining the correspondence between the Euler angles and the orbital elements results in the following: $\theta = \Omega$, $\Phi = i$ and $\psi = \omega + Э$.

Although they are fixed for the Keplerian orbit, the ascending node angle (Ω); argument of the perigee (ω) and M−nt vary in time for a real orbit. The inclination *i* remain constant, however. The distance from *S* to the centre of attraction O or distance of the satellites from the centre of the Earth (r = R+h), known also as radius of path, is expressed in terms of semi-major axis (a), true anomaly (Э) eccentricity (e) as:

$$r = a\,(1 - e^2)/1 + e \cos Э \qquad (3.58)$$

Using the notation introduced above, the above stated value of $\psi = \omega + Э$ can be replaced by:

$$\psi = n\,(t - tAN) \qquad (3.59)$$

Therefore, the ground track of the satellite is determined by two quantities relating to the ascending node taken as origin, namely, its longitude λ_0 and the crossing time *t*AN, which constitutes the initial conditions of the uniform motion.

3.8.3 Other Satellite Orbits

Geostationary and sunsynchronous are only two of infinite possible orbits. Others have been and will become useful for meteorological satellites. The Earth Radiation Budget Satellite (ERBS) was launched from the vehicle Space Shuttle and orbits at an altitude of 600 km with an inclination angle of 57°. It was placed in this orbit so that it would precess with respect to the sun and sample all local times over the course of a month.

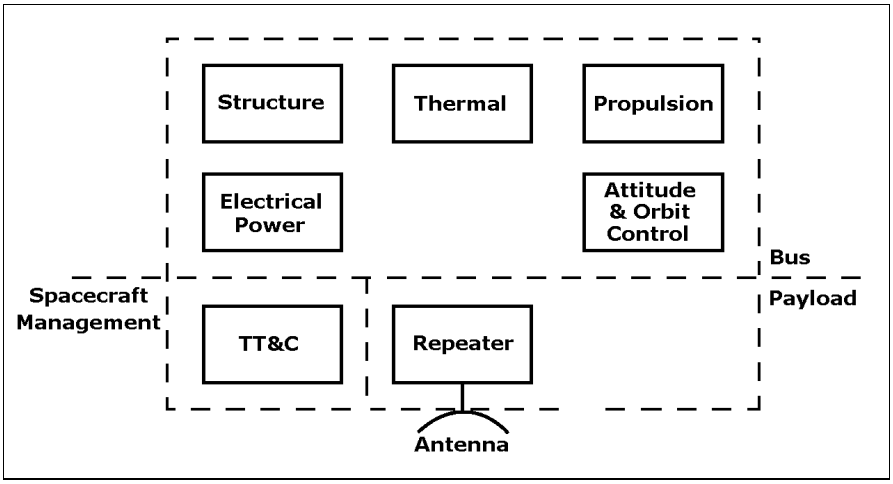

Figure 3. 16 Spacecraft Sub-System by Richharia 1995

The former Soviet Union placed its Meteor satellites in low Earth orbit with inclination angles of about 82°. The former Soviet Union also used a highly elliptical orbit for Molniya communications satellites. Thus, it has been suggested that this orbit would be useful for meteorological observations of the high latitudes (Kidder and Ham 1995). The Molniya has an inclination angle of 63.4°, at which the argument of perigee is motionless. Thus, the apogee, from which measurements are made, stays at a given latitude.

The semimajor axis is chosen such that the satellite makes two orbits while the Earth turns once with respect to the plane of the orbit. The eccentricity is made as large as possible so that the satellite will stay near apogee longer. However, the eccentricity must not be so large that the satellite encounters significant atmospheric drag at perigee. Á semimajor axis of 26,554 km and an eccentricity of 0.72 result in a perigee of 7378 km (1000 km above the equator), an apogee of 45,730 km (39,352 km above the equator), and a period of 717.8 min. The attractiveness of this orbit is that it functions as a high-latitude, part-time, nearly GEO satellite. For about 8 h centred on apogee, the satellite is synchronized with the Earth so that it is nearly stationary in the sky. For a meteorological satellite in a Molniya orbit, the rapid imaging capability, which is so useful from geostationary orbit, would be available in the high latitudes (Richharia, 1995).

As meteorological satellite instruments become more specialized, more custom orbits are likely to be used in the future.

3.9 Meteorological Satellite Payloads and Antenna Systems

A communication element of meteorological satellite consists mainly in two major functional units: payload and bus. The primary function of the payload is to provide communication between ground sensors known as Data Collection Platform (DCP) repeaters and ground

segment of Direct Readout Ground (DRG) Earth Stations. However the main function of satellite payload is to transmit collected meteorological data from onboard sensors to DRG, while the bus provides all the necessary electrical and mechanical support to the payload and all satellite missions, as illustrated in Figure 3.16.

The payload is made up of the multipurpose repeaters and antenna systems. The repeater performs the required processing of the signal and the antenna system is used to receive signals from LES and to transmit signals to MES in the coverage area and vice versa. Two main types of repeaters are possible for onboard utilization: Transparent and Regenerative transponders. However there are many other types for different satellite applications.

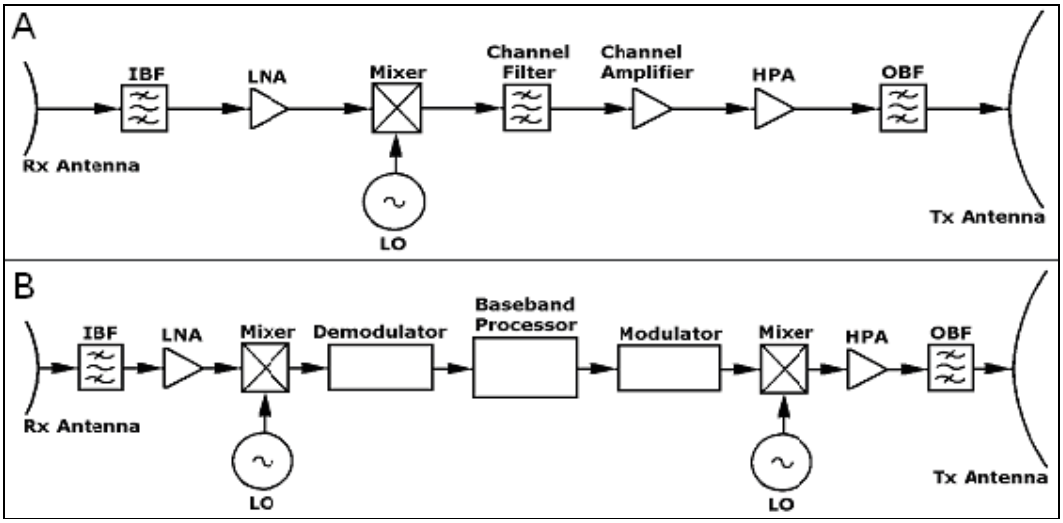

Figure 3. 17 Configuration of Spacecraft Transponders by ITU 1996

3.9.1 Transparent or Bent-pipe Communication Transponder

The basic function of the satellite transponder is to isolate individual carriers or groups of carriers of signals and to boost their power level before they are retransmitted to the ground stations. The carrier frequencies are also altered as the carriers pass through the satellite. Satellite repeaters that process the carrier in this way are typically referred to as transparent or bent-pipe transponders, shown in Figure 3.17 (A). Only the basic RF characteristics of the carrier (amplitude and frequency) are altered by the satellite.

The detailed signal carrier format, such as the modulation characteristics and the spectral shape, remains completely unchanged. Transmission via a transparent satellite transponder is often likened to a bent-pipe because the satellite simply channels the information back to the ground stations. A bent-pipe is a commonly used satellite link when the satellite transponder simply converts the uplink RF into a downlink RF, with its power amplification. Initially, the received uplink signals from ground-satellite-ground by Receiver (Rx) antennas are filtered in an Input Bandpass Filter (IBF) prior to amplification in a Low Noise Amplifier (LNA).
In addition, the output of the LNA is then fed into a Local Oscillator (LO), which performs the required frequency shift from uplink to downlink RF and the bandpass Channel Filter after the Mixer removes unwanted image frequencies resulting from the down conversion, prior to undergoing two amplification stages of signals in the Channel and High Power Amplifier (HPA).

Finally, the output signal of the HPA is then filtered in the Output Bandpass Filter (OBF) prior to transmission through Transmitter (Tx) antenna to the ground. The IFB is a bandpass filter which blocks out all other RF used in satellite communications. After that, the receiver converts the incoming signal to a lower frequency, using an LO which is controlled to provide a very stable frequency source (Fidler et al, 2010). This is needed to reduce all noises to facilitate processing of the incoming signal and to enable the downlink frequencies to be established.
The channel filter isolates the various communications channels contained in the waveband allowed through by the input filter. Filtering often leads to large power losses, creating a need for extra amplification, usually followed by a main amplifier. In order to attain the required gain of HPA, this segment may employ either a Solid-State Power Amplifier (SSPA) or a Traveling Wave Tube Amplifier (TWTA). In a more complex transponder design, in order to achieve higher RF power, it may be possible to combine the output of several amplifiers.

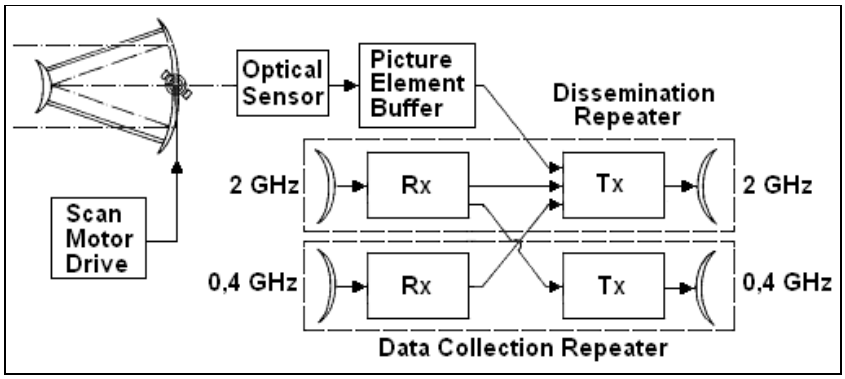

Figure 3. 18 Meteorological Satellite Payloads by Berlin 1988

3.9.2 Regenerative Communication Transponder

Other satellite system designs go through a more complex onboard process to manipulate the carrier's formats, by using on-board processing architecture. This payload architecture offers advantages over the transparent alternative, including improved transmission quality and the prospect of compact and inexpensive ground terminals. A typical on-board processing system will implement some or all of the functions that are performed by the ground-based Tx and/or Rx in a transparent satellite system.

Therefore, these functions may include recovery of the original information on board the satellite and the processing of this information into a different carrier format for transmission to the ground stations. In fact, any satellite transponder that recreates the signals carrier in this way is usually referred to as a regenerative transponder, as illustrated in Figure 3.17 (B). This type of satellite transponder provides demodulation and modulation capacity completely on board the satellite.

The received uplink signal goes along the down-converter segment prior to coming into the on-board demodulator, where it is demodulated and processed in the base band processor. This technology provides flexible functions, such as switching and routings. The downlink signal generated by an on-board modulator passes along the up-converter segment and is transmitted via the antenna. For this type of system, link design can be separately conducted for the uplink and downlink because link degradation factors are decoupled between the

uplink and downlink by the on-board demodulator and modulator, supported by the base band processor. A regenerative transponder with base band processing permits reformatting of data without limitation to ground Rx, while the bent-pipe system requires a satellite link design for the entire link, involving both uplink and downlink, but the forward link burst rate is limited by the ground Rx G/T and demodulation performance (Berlin, 1988).

3.9.3 Satellite Meteorological Communication Transponder

The meteorological payload is made up of the multipurpose repeaters and antenna systems. The repeater performs the required processing of the signal and the antenna system is used to receive signals from ground stations and to transmit signals to the ground receiving and processing facilities in the coverage area and vice versa (Haan, 2008).

Figure 3.18 illustrates the main components of meteorological satellite payloads, which contain the following main components of instruments: Scan Motor Drive, Optical Sensors, Picture Element Buffer and additional radiometers. In addition, meteorological satellite has communication payload, which contain two repeaters. First is the Dissemination Repeater, whose Receiver (Rx) and Transmitter (Tx) with both antennas use 2 GHz, while Rx and Tx with both antennas of Data Collection Repeater use 0.4 GHz.

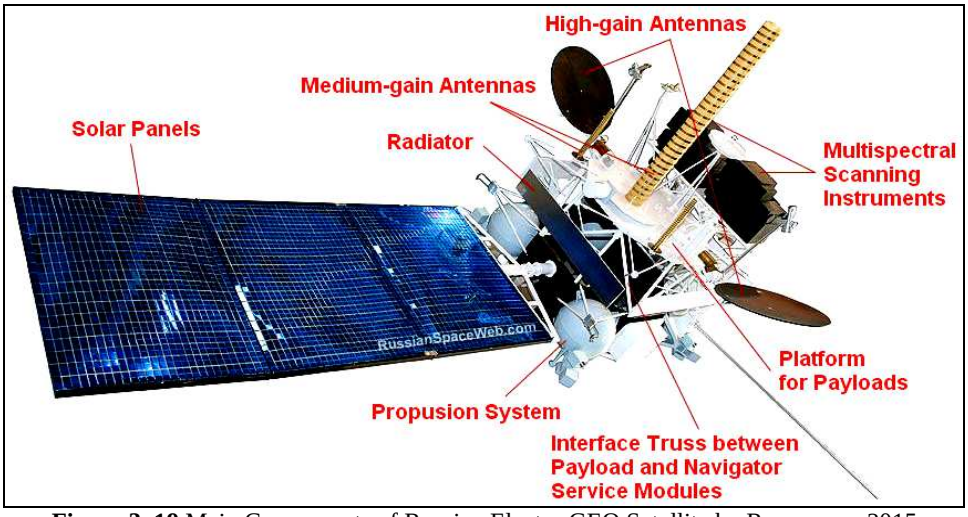

Figure 3. 19 Main Components of Russian Electro GEO Satellite by Roscosmos 2015

The duties of the meteorological payloads are to contain radio Rx, which acquire operational commands and meteorological data from the ground and retransmit this data via Tx in Data Collection Repeater to the ground receiving and processing facilities. However, second Tx in Dissemination Repeater can retransmit data from the ground and send data collected by the onboard instruments to Earth stations.

Then meteorological satellite may carry main components shown in Figure 3.19, including computers that process the data from the onboard instruments and the tape recorders on which data are recorded for later transmission to Earth. Usually, meteorological GEO satellites carry onboard several different payloads, not just one. The primary payloads are meteorological radiometer, which measures Earth radiances in the visible (0.4-1.0 μm) and thermal infrared (10-13 μm) spectral bands. The same satellites carry the additional payloads not related to meteorology.

For example, the Search and Rescue (SAR) payload of Cospas-Sarsat system detects signals from downed ships, land vehicles, persons and aircraft, giving the precise estimate of their location to aid in rescue operations. The Space Environment Monitor (SEM) measures energetic particles (protons, electrons and alpha particles) for solar and ionospheric studies. Finally, the Data Collection System (DCS) relays meteorological and other data transmitted from ground-based instruments (Cossu et al, 2009).

3.9.4 Repeaters for Stratospheric Communication Platform (SCP)

The SCP transponder, shown in Figure 3.20, illustrates a block diagram of a typical onboard architecture, which together with its associated antenna subsystem, would make a complete communications payload. In this case, the SCP transponder has a bandwidth of 500 MHz using a Code Division Multiple Access (CDMA) scheme. This transponder can accommodate up to 50 antenna beams with eight wideband carriers (assuming a carrier bandwidth of 1.25 MHz each). For the uplink, the carriers are received by the platform antenna subsystem and amplified by a LNA.

The bandwidth of these carriers is limited to only 10 MHz using passband filters, and multiplexed using Frequency Division Multiplexing (FDM). Before these multiplexed signals are transmitted to the ground station, they are amplified further by a High Power Amplifier (HPA) stage, filtered and multiplexed. For the downlink, the process is similar but in the reverse direction, and, instead of a multiplexer, a demultiplexer is used [ITU-F1500, 00].

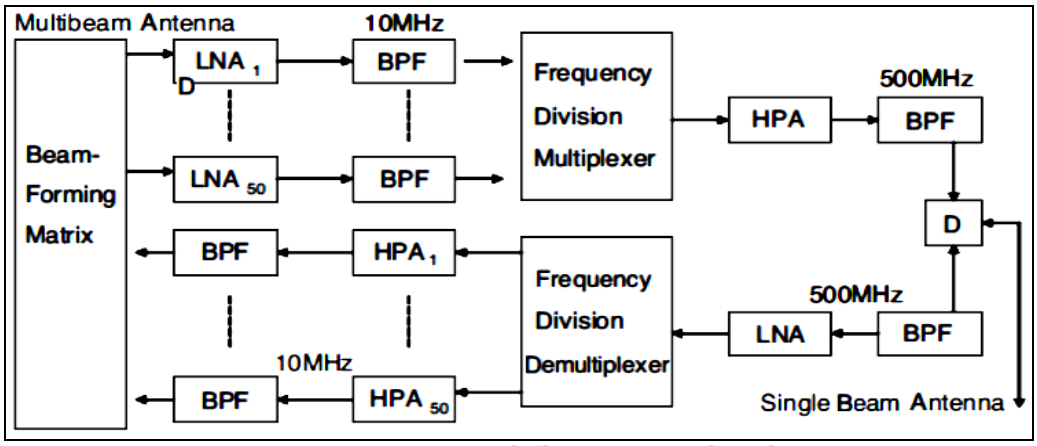

Figure 3. 20 SPSCP Transponder by Aragon-Zavala et al, 2008

Other transponder components play an important role in the system performance, and their design and selection should not be underestimated. The Low Noise Amplifier (LNA) element having low-noise temperature and sufficient gain, ensure that noise contributions from the succeeding stages are kept small via By-Pass Filter (BPF). Frequency converters serve as frequency-change devices (also known as mixers), which either up-convert or down-convert the signals in the SCP to differentiate between uplink and downlink.

Noise performance is also important for these frequency converters, although not as critical as the noise figure for the LNA, since this is the first element in the front-end and so is the one that contributes most to the overall noise. The Intermediate Frequency (IF) processors have the main functions of providing most of transponder gain defining a frequency response of each channel and, whenever required, performing beam-to-beam routing functions. Filters are in charge of limiting adjacent spurious signals as well as noise that can be generated by

the payload itself. Their design is crucial for the performance of the communications payload. Transmitters are in charge of amplifying the signals to the level required for downlink transmissions.

Examples of well-known transmitters used for satellite communications are the TWT and power transistors, the latter being used for specific applications in lower frequency bands. Payload system performance or performance parameters of individual equipments need to be specified so that the required SCP payload performance is achieved by the Antenna Coverage Area**,** Figure of Merit G/T, EIRP, Power per Backhaul Carrier, Isolation Between Channels, Spurious Outputs, Amplifier Linearity and Group Delay Variation values (Gagliardi, 1984).

However, the SCP payload can carry onboard all kind of meteorological instruments and components for weather and climatological observations.

3.9.5 Antenna System onboard Metrological Satellites

The antenna systems of onboard meteorological satellites can be many types and may have different shapes. The spacecraft antenna system mounted on the spacecraft structure, similar to the transponders, is composed of two main integrated elements: the receiving antennas, which detect all signals from the ground stations, and transmitting antennas, which send data and video signals to the ground receiving and processing stations.

The transmit antenna systems provide a global (wide) beam on the Earth's surface via GEO satellites, and local footprint via PEO satellites. However, narrow circular beams from GEO or Non-GEO can be used to provide spot beam coverage. For instance, from GEO, the Earth subtends an angle of 17.4^{o}. Antenna beams of 5.8^{o} wide can reuse three frequency bands twice in providing Earth disc coverage.

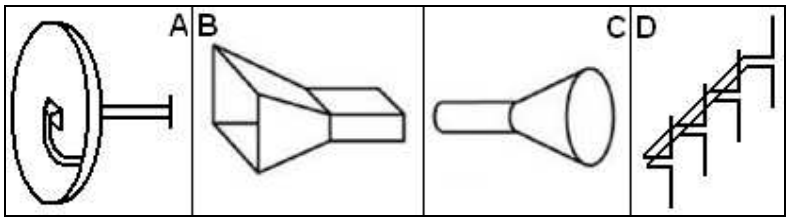

Figure 3. 21 Four Types of Satellite Antennas by Ilcev 2013

For instance, from GEO, the Earth subtends an angle of 17.4^{o}. The following are four types of Satellite Antennas:

1. Reflector Antennas – The parabolic reflector is a good example of reflectors at radio microwave frequencies, shown in Figure 3.21 (A). In the past, parabolic reflectors were used mainly in space applications onboard spacecraft, but today they are very popular and are used by almost everyone who wishes to receive a large number of television or broadcasting channels transmitted all over the globe providing gain in values of 20 – 30 dB.

Reflector antennas are typically used when very high gain or a very narrow main beam is required. Gain is improved and the main beam narrowed with increase in the reflector size. Large reflectors are, however, difficult to simulate as they become very large in terms of wavelengths. Reflector antennas are usually illuminated by one or more horns and provide a larger aperture than can be achieved with a horn alone, whose prototype made by the US

company, Lockheed Martin, is shown in Figure 3.22 (Left). For maximum gain, it is necessary to generate a plane wave in the aperture of the reflector. This is achieved by choosing a reflector profile that has equal path lengths from the feed to the aperture, so that all the energy radiated by the feed and reflected by the reflector reaches the aperture with the same phase angle and creates a uniform phase front. One reflector shape that achieves this with a point source of radiation is the paraboloid, with a feed placed at its focus, shown in Figure 3.22 (Right).

The paraboloid, however, is the basic shape for most reflector antennas, and is commonly used for earth station antennas. Satellite antennas often use modified paraboloidal reflector profiles to tailor the beam pattern to a particular coverage zone. The preferred way of making directional Antennas is to make a dish to reflect the waves rather then to refract them with a lens. These dishes are easy to make and, unlike a lens, which needs to be solid, they need only a very thin reflective surface (Reckeweg and Rohner, 2015). When the reflector is given a specific shape called a parabola and the receiver is placed at the focus, the waves received are parallel. This makes this antenna the preferred type for radio telescopes and other extreme range applications.
However, the the waves leaving the reflector dish are parallel to each other and, therefore, will go great distances with out scattering. While this works, it has problems mostly with its transmission since waves moving to the left are unaffordable.

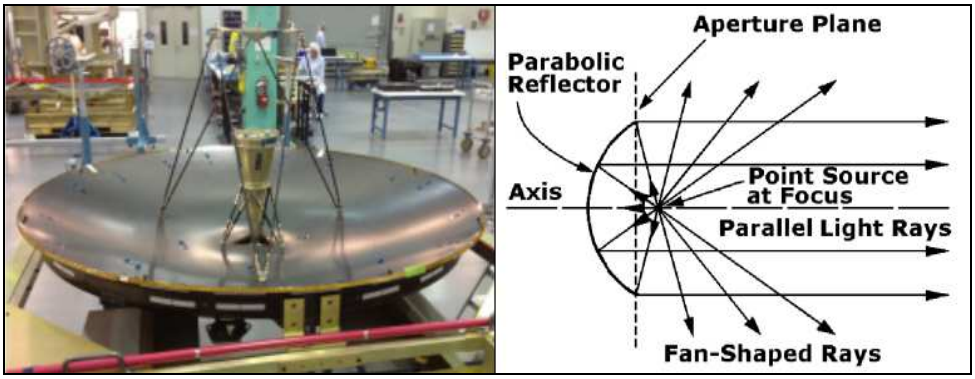

Figure 3. 22 Parabolic Reflector Antenna Systems by Ilcev 2011

2. Aperture Antennas (Horn Antennas) – A horn is an example of aperture antennas, which are used in satellite spacecraft more commonly. The pyramidal horn is shown in Figure 3.21 (B), while the conical horn is shown in Figure 3.21 (C). The rectangular or pyramidal horn antenna is one of the simplest and most widely used antennas. Horns have been used for more than a hundred years, and, today, they are used in satellite communications, radio astronomy, in communication dishes as feeders, in measurements, etc. Horn antenna is used at MW while for global coverage relatively wide beams are required. A horn is a flared section of waveguide that provides an aperture several wavelengths wide and a good match between the waveguide impedance and free space. It is also used as feeds for reflectors, either singly or in clusters. Horns and reflectors are examples of aperture antennas that launch a wave into free space from a waveguide. Therefore, it is difficult to obtain gains much greater than 23 dB or beam widths narrower than about 10^{o} with horn antennas. Thus, for higher gains or narrow beam widths, a reflector antenna or array must be used (Fujimoto, 2008).

3. Array Antennas – A grouping of several similar or different antennas form a single array antenna is shown in Figure 3.21 (D). The control of phase shift from element to element is

used to scan electronically the direction of radiation. Antenna arrays are able to produce combined radiation patterns that have characteristics that a single antenna would not. The antenna elements can be arranged to form a 1 or 2 dimensional antenna array. A number of antenna array specific aspects will be outlined using 1 dimensional arrays for simplicity reasons. Antennas exhibit a specific radiation pattern, and the overall radiation pattern changes when several antenna elements are combined in an array. The array factor quantifies the effect of combining radiating elements in an array without the element specific radiation pattern taken into account. The overall radiation pattern results in certain directivity and thus gain linked through the efficiency with the directivity. Directivity and gain are equal if the efficiency is 100%.

An antenna pattern is a plot of the field strength in the far field of the antenna when a transmitter drives the antenna. The gain of an antenna is a measure in dB of the antenna's capability to direct energy in one direction, rather than all around. A useful principle in antenna theory is reciprocity, which means that an antenna has the same gain and pattern at any given frequency whether it transmits or receives. An antenna pattern measured when receiving is identical to the pattern when transmitting.

As stated earlier, the antenna is providing global, spot and multiple beam coverages, but it can provide scanning and orthogonally polarized beams or coverage zones as well. The pattern is frequently specified by its 3-dB beam width, the angle between the directions in which the radiated (or received) field falls to half the power in the direction of maximum field strength. However, a satellite antenna is used to provide coverage of a certain area or zone on the Earth's surface, and it is more useful to have contours of antenna gain with maximum strengths of the signal in the middle of the coverage area and with decreasing signals to the peripheries (Festo, 2015).

When computing the signal power received by a GES from the satellite, it is important to know where the station lies relative to the satellite transmit antenna contour pattern, so that the exact EIRP can be calculated. If the pattern is not known, it may be possible to estimate the antenna gain in a given direction if the antenna boresight or beam axis direction and its beam width are known.

Furthermore, a greater power density per unit area for a given input power can be achieved very well, when compared with that produced by a global circular beam, leading to the use of much smaller receiving MES antennas. The equation that determines received power (P_R) is proportional to the power transmitted (P_T) separated by a distance (R), with gain of transmit antenna (G_T) and effective area of receiving antenna (A_R) and inverse proportional with 4π and square of distance. The relations for P_R and G_T are presented as follows:

$$P_R = P_T G_T A_R/4\pi R^2$$

$$G_T = 4\pi A_T/\lambda^2 \qquad (3.60)$$

where G_T = effective area of transmit antenna and λ = wavelength. The product of P_T and G_T is gain, generally as an increase in signal power, known as an EIRP. Signal or carrier power received in a link is proportional to the gain of the transmitting and receiving antennas (G_R) presented as:

$$P_R = P_T G_T G_R \lambda^2/(4\pi R)^2 \quad \text{or} \quad P_R = P_T G_T G_R/L_P L_K \quad [W] \qquad (3.61)$$

The last relation can be derived with the density of noise power giving:

$$P_R/N = P_T G_T (G_R/T_R) (1/K L_P L_K) \quad (3.62)$$

where L_P = coefficient of energy loss in free space, L_K = coefficient of EMW energy absorption in satellite channels, T_R = temperature noise of receiver, G_R/T_R is the figure of merit and K = Boltzmann's Constant (1.38×10^{-23} J/K or its alternative value is –228.6 dBW/K/Hz).

At any rate, P_R has a minimum allowable value compared with system noise power (N), i.e., the Carrier and Noise (C/N) or Signal and Noise (S/N) ratio must exceed a certain value. This may be achieved by a trade-off between EIRP ($P_T G_T$) and received antenna gain (G_R). If the received antenna on the satellite is very efficient, the demands on the LES/MES are minimized. Similarly, on the satellite-to-Earth link, the higher the gain of the satellite transmit antenna, the greater the EIRP for a given transmitter power. Satellites often have parabolic dish antennas, though there are also other types, such as phased arrays. The principal property of a parabolic reflector is its ability to turn light from a point source placed at its focus into a parallel beam, as illustrated in Figure 3.22 (Right). In practice, the beam can never be truly parallel, because rays can also be fan-shaped, i.e., a car headlamp is a typical example. In a microwave antenna, the light source is replaced by the antenna feed, which directs waves towards the reflector. The length of all paths from feed to aperture plane via the reflector is constant, irrespective of their angle of parabolic axis. The phase of the wave in the aperture plane is constant, resulting in maximum efficiency and gain. The gain of an aperture (G_a) and parabolic (G_p) type of antennas are:

$$G_a = \eta (4\pi A/\lambda^2) = 4\pi A_E/\lambda^2$$

$$G_p = \eta (\pi D)^2 /\lambda^2 \quad (3.63)$$

where η = efficiency factor, A = projected aperture area of antenna, $A_E = \eta^A$ is the effective collecting area and D = parabolic antenna diameter. Thus, owing to correlation between frequency and wavelength, $f = c/\lambda$ is given the following relations:

$$G_p = \eta (\pi D f/c)^2 = 60{,}7 (D f)^2 \quad (3.64)$$

where the second relation comes from considering that $\eta \approx 0.55$ of numerical value. If this value is presented in decibels, the gain of antenna will be calculated as follows:

$$G_T = 10 \log G_p \quad (3.65)$$

For example, a parabolic antenna of 2 m in diameter has a gain of 36 dB for a frequency at 4 GHz and a gain of 38 dB for a frequency at 6 GHz. Parabolic antennas can have aperture planes that are circular, elliptical or rectangular in shape. Thus, antenna with circular shape and homogeneous illumination of aperture with a gain of –3 dB has about 47.5% of effective radiation, and the rest of the power is lost. To find out the ideal characteristics, it is necessary to determine the function diagram of radiation in the following way:

$$F(\delta_o) = s(\delta_o)/s(\delta_o=0) \quad (3.66)$$

where parameter s (δ_o) = flow density of radiation in the hypothetical satellite angle (δ_o) and s (δ_o=0) = flow density in the middle of the coverage area. The geometrical relations in Figure 3.4 (A) follows the relation:

$$F(\delta_o) = d_o/h = \cos\delta \sqrt{(k^2 - \sin^2\delta_o)}/l - k \quad (3.67)$$

where, as mentioned, k = R/(R + h) = sin δ and if $\delta_o = \delta$, the relation is defined by the following equation:

$$F(\delta) = k \cos\delta \quad (3.68)$$

For the GEO satellite, the value of ΔL is given as a function of angle δ, which is the distance from the centre of the coverage area, where the function diagram of the radiation is as follows:

$$F(\delta) = \Delta L = 20 \log = 20 \log R/(R + h) \cos\delta = 10 \log R/(1 + 2R/h) \quad [dB] \quad (3.69)$$

Therefore, in the case of GEO satellites, the losses of antenna propagation are greater around the periphery than in the centre of the coverage area for about 1.32 dB. The free-space propagation loss (L_P) and the input level of received signals (L_K) are given by the equations:

$$L_P = (4\pi\, d/\lambda)^2$$

$$P_R/S = P_T G_T/4\pi d^2 L_K \quad (3.70)$$

The free-space propagation loss is caused by geometrical attenuation during propagation from the transmitter to the receiver.

3.9.6 Satellite Bus

The satellite bus is usually called a platform and consists of several sections, shown in Figure 3.16. The function of the satellite platform is to support the payload operation reliably throughout the mission of primary construction section, such as Structure Platform (SP), Electric Power (EP), Thermal Control (TC), Attitude and Orbit Control (AOC), Telemetry, Tracking and Command (TT&C) and Propulsion Engine.

3.9.6.1 Structure Platform (SP)

The structure has to house and keep together all components of bus and communications modules, enable protection from the environment and facilitate connection of the satellite to the launcher.

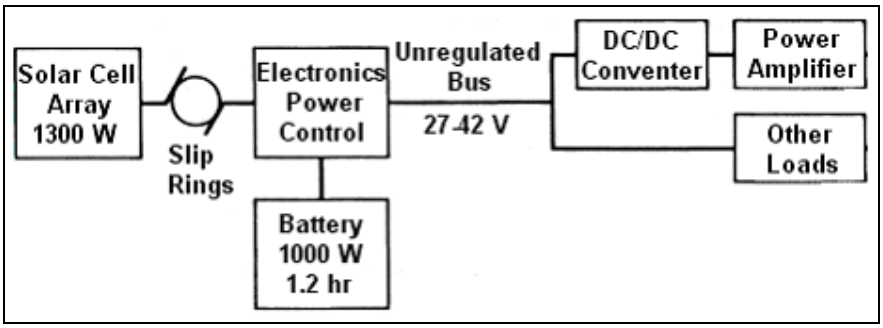

Figure 3. 23 Satellite Electric Power Subsystem by Gordon et al, 1993

It comprises a skeleton on which the equipment modules are mounted and a panel, which covers and provides protection for sensitive parts during the operational phase from micrometers and helps to shield the equipment from extremes of heat, coldness, vacuum and weightlessness, including the relatively small dynamic forces produced by the station-keeping, attitude control engines and inertial momentum devices (Gordon et al, 1993).

The spacecraft is protected during the launch phase with an enclosure, or nose cone. At the end, the nose cone is jettisoned, at which time the spacecraft must survive the inertial and thermal stress of an additional propulsion stage until it is inserted into orbit. In this sense, a spacecraft is virtually free of gravitational stress when in orbit, which allows the use of very large deployable arrays, which would collapse under their own weight on the Earth's surface without problems. Thus, large stresses are developed during launch as a result of massive acceleration and intense vibration, so the SP body must be sufficiently strong to withstand all external forces. On the other hand, all large structures such as antenna and solar arrays have to be folded and protected during a launch sequence and must have a deployable mechanism. The deployment of structures requires a special technique in the vacuum of space because of the lack of a damping medium, such as air.

3.9.6.2 Electric Power (EP)

The primary source of power for a communications satellite is the Sun. Hence, solar cells are used to convert energy received from the Sun into an electrical source. The principal components of the power supply system include: **(1)** The power electric generator, usually solar cell arrays located on the spinning body of a spin-stabilized satellite or on the paddles for a three-axes stabilized satellite; **(2)** Reliable electrical storage devices, such as batteries, for operating during periods of solar eclipses; **(3)** The electrical harness for conducting electricity to all of the devices demanding power; (**4)** The special converters and regulators delivering regulated voltage and currents to the devices on board the spacecraft; and (**5)** The electrical control and protection section is associated with the remote TT&C satellite system. The solar arrays are the motor during the entire life of the satellite, providing sufficient power to all active components. Occasionally, the Earth or Moon blocks the Sun, then researchable batteries provide secondary electrical power. A typical satellite power subsystem is shown in Figure 3.23. Most components are duplicated for redundancy. On spinning satellites, the rings are between the power subsystem, on the rotating part, and the satellite bus.

Each cell delivers about 150 mA at a few hundred millivolts and an array of cells must be connected in series or parallel together to give the required voltage and current for operating the equipment until the end of its life and to recharge the batteries when the satellite moves

out of an eclipse. Charge is applied via the main electric power bus or a small section of the solar cell. During exploitation, batteries are sometimes reconditioned by intentionally discharging them to a low charge level and recharging again, which prolongs their life.

The operational status of batteries including recharge, in-service or reconditioning is remotely controlled by a special ground segment. Thus, the mass of a battery constitutes a significant portion of the total satellite mass. Therefore, a useful figure of merit to evaluate the performance of a battery is capacity in W/h per unit weight taken at the end of its life. Until recently, virtually all satellites used Ni-Cd (Nickel-Cadmium) batteries because of their high reliability and long lifetime. These batteries provide a low specific energy of about 30 to 40 Wh/kg. The latest type of Ni-H (Nickel-Hydrogen) batteries can store at least 50% more energy per kilogram.

When a satellite passes through the Earth's shadow, the solar arrays stop producing power and the satellite structures use the energy from batteries. The GEO satellite undergoes around 84 eclipses in a year, with a maximum duration of 70 min. Thus, the eclipse occurs twice a year for 42 consecutive days each time. The percentage of eclipses' duration for GEO and HEO is much less than for lower satellite orbits. The LEO satellites can undergo several thousand eclipses in a year. For example, a LEO satellite in equatorial orbit at an altitude of 780 km can remain in the Earth's shadow for 35% of the orbital period. For a MEO under similar conditions, the maximum eclipse duration would be about 12.5% of the orbital period and a total duration of about 3 hours a day, with about 4 eclipses per day. Otherwise, the Sun can also be sometimes eclipsed by the Moon's shadow, which is less predictable.

3.9.6.3 Thermal Control (TC)

There is not air at satellite orbit surrounded by very harsh space environment. The average satellite temperature is determined by the absorbed solar energy, different thermal radiation into space and internal electric dissipation, what depends on the satellite shape and surface.
Thermal control of a communication satellite is a very important factor during an entire satellite's lifetime, which is necessary to achieve normal temperature balance and proper performance of all subsystems. Thermal stress results from high temperature effects from the Sun and from low temperatures occurring during the eclipse period. The obvious objective of the TC is to assure that the spacecraft structure and all equipment are maintained within temperatures that will provide successful operations (Feher, 1983). Thus, a satellite undergoes different thermal and other conditions during the launch and operational phase. The vacuum in space limits all heat transfer mechanisms to and from a spacecraft and its external environment to that of radiation.

However, some main parts are usually in direct sunlight with a flux density of over 1 kW/m^2, while other parts are facing the shadow side at a temperature of about -270^oC. In addition, an eclipse causes temperature variation from around -180^o to $+60^oC$, when the ambient temperature falls well below 0^oC and rises rapidly from the moment the satellite emerges from the eclipse. All these extremes have to be eliminated or moderated for normal satellite operations, especially because all electronic devices need optimum temperatures between -5^o and $+45^oC$.

These problems can be solved by remote TC techniques, using both passive and active means of controlling and regulating the temperature inside the spacecraft. The passive means are simple and reliable, using surface finishes, filters and insulation blankets. The active means

are necessary to supplement the passive systems, which include louvers and blinds operated by bimetallic strips, heat pipes, thermal louvers and different electrical heaters. Heat pipes are used to transfer heat from internal hot spots or devices to remote radiator surfaces or must be transported to the outside surface where it can be dissipated. On the other hand, special electric heaters are used to maintain minimum component or structure temperatures during cold conditions. Accordingly, the TC subsystem ensures temperature regulation for optimum efficiency and satellite performance.

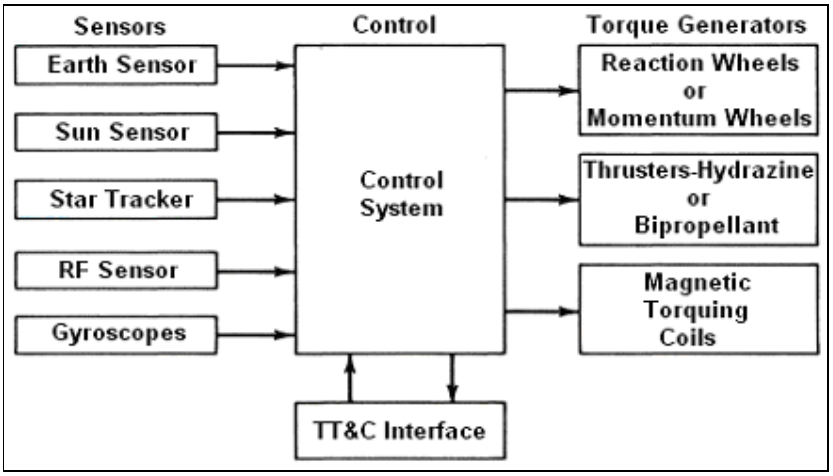

Figure 3. 24 Satellite AOC Subsystem by Gordon et al, 1993

3.9.6.4 Attitude and Orbit Control (AOC)

The attitude and orbital control subsystem checks that a spacecraft is placed in its precise orbital position, and maintains, thereafter, the required attitude throughout its mission. Control is achieved by employing momentum wheels, which produce gyroscopic torques, combined with an auxiliary reaction control gas thruster system. Many sensors are employed to detect attitude errors, including the Sun's initial orientation purposes.

The satellite antennas require an AOC system that will keep them pointed always at the Earth, frequently within 0.1º and 0.01º. Figure 3.24 shows a block diagram of the AOC system. The sensors direct any pointing errors and correct them by changing the speed or direction of a rotating wheel. The main performance specification of an AOC system is determined by the disturbance torques and the required pointing accuracy.

The AOC system performs satellite orientation and accurate orbital positioning throughout its lifetime, because loss of attitude renders a spacecraft useless. There are in use two common AOS in use, namely, attitude control and orbit or station keeping control systems. The objective of attitude control is to keep the antenna RF beam pointing at the intended areas on the Earth.The attitude control process comprises the following steps:
a) Measuring the attitude of the satellite by sensors;
b) Comparing the results of measurements with the required values;
c) Calculating the corrections to reduce eventual errors; and
d) Introducing these corrections by operating the appropriate torque units.

1. Attitude Control – Currently, all types of attitude stabilization systems have relied on the conservation of angular momentum in a spinning element, which can be classified into the

two categories already mentioned, such as spin-stabilized and three-axis stabilization. The satellite is rapidly spun around one of its principal axes of inertia. Thus, in the absence of any perturbing torque, the satellite attains an angular momentum in a fixed direction in an absolute frame of reference. For the GEO satellite, the spin (pitch direction) axis must be parallel to the axis of the Earth's rotation. The perturbation torques reduce the spin of the satellite and they affect the orientation of the spin axis. The second system of attitude control is a body-stabilized design in a three-axis stabilized satellite, whose body remains fixed in space (Maini and Agrawal, 2007). This solution is the simplest method of attitude control using a momentum wheel, which simultaneously acts as a gyroscope, in a combination of spin and drive stabilization. Certain perturbing torques can be resisted by changing its spin speed and the resulting angular momentum of the satellite.

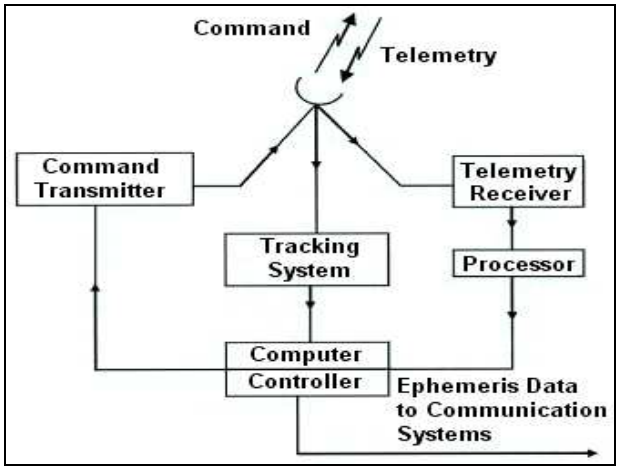

Figure 3. 25 Satellite TT&C by Maini and Agrawal, 2007

2. Orbit or Station-Keeping Control – On-board propulsion requirements for both GEO and Non-GEO are important to keep a satellite in the correct orbital attitude and position. For this reason, several types of propulsion systems are used, such as arc jet thrusters, ion and solar electrical propulsion, pulsed plasma thrusters, iridium-coated rhenium chambers for chemical propellants, etc. In order that the appropriate station-keeping corrections can be applied, it is essential that the orbit and position of a satellite are accurately determined. This may be done by making measurements of the angular direction and distance of the satellite from the Earth station, or a number of LES. When the orbit and position of the satellite have been determined, it is possible to calculate the velocity increments required to keep the N–S and E–W excursion of the satellite within the tolerated limits. The frequency with which N–S correction must be made depends on the maximum allowable value of the orbital inclination but the total increment required each year to cancel out the attraction of the Sun and Moon is 40 to 50 m/s. Otherwise, E–W station-keeping is usually achieved by allowing the satellite to drift towards the nearest point of equilibrium until it reaches the maximum tolerable error in longitude. Then the process is repeated on the other side of the nominal longitude and, finally, the satellite drifts back once more towards the point of equilibrium and the process is repeated. The frequency and magnitude of the velocity increments required depend on the angular distance between the satellite and the points of equilibrium and on the tolerable error, which is a maximum of about 2 m/s (Roscosmos, 2015).

3.9.6.5 Telemetry, Tracking and Command (TT&C)

The telemetry, tracking, command and communication equipment enable data to be sent continuously to the Earth stations, received from these stations and allow ground control stations to track the spacecraft and to monitor the health of the spacecraft and also to send commands to carry out various tasks like switching the transponders in and out of service, switching between redundant units, etc.

The TT&C subsystem monitors and controls the satellite functions right from the lift-off stage to the end of its operational life in space. The TT&C subsystem is, therefore, very important, not only during orbital injection and the positioning phase but also throughout the operational life of the satellite. During the orbital injection and positioning phase, the telemetry link is primarily used by the tracking system to establish the satellite-to-Earth station communication channel. After the satellite is put into the desired slot in its intended orbit, its mission is to monitor the health of various subsystems onboard the satellite (Evans, 1991).

Figure 3.25 shows the block schematic arrangement of the basic TT&C subsystem. The TT&C system supports the function of spacecraft management for successful operation of payload and bus sub-systems. The main functions of a TT&C are as follows:

1. Telemetry Sub-System – The function of telemetry is to monitor various spacecraft parameters and performances such as voltage, current, temperature, output from attitude sensors, reaction wheel speed, pressure of propulsion tanks and equipment status and to transmit the monitored data to the Satellite Control Centre (SCC) on the Earth. At this point, the telemetered data are analyzed at the SCC and used for routine operational and failure diagnosis purposes, to provide data about the amount of fuel remaining, and to support determination of orbital parameters, etc.

2. Tracking Sub-System – The function of tracking is to provide necessary sources to Earth stations for the tracking and determination of orbital parameters. To maintain a satellite in its assigned orbital slot and provide look angle information to LES in the network, it is necessary to estimate the orbital parameters regularly. These parameters can be obtained by tracking the communications satellite from the ground and measuring its angular position and range. Most SCC employ angular and range or range-rate tracking to control satellite orbits.

3. Command Sub-System – This sub-system receives commands transmitted from the ground SCC, verifies reception and executes commands to perform various functions of the satellite during its operational mission, such as: Satellite transponder and beacon switching, Antenna pointing control, Switch matrix reconfiguration, Controlling direction and speed of solar arrays drive, Battery reconditioning, Thruster firing and Switching heaters of the various systems.

3.9.6.6 Propulsion Engine (PE)

The functions of the propulsion motors are to generate the thrust required for the attitude and orbital control of errors caused by solar and lunar gravity and other influences, or possibly the adequate assistance of the satellite into its final orbit.
Hence, these errors are normally corrected at set intervals in response to commands from the SCC. The necessary impulse is provided by thrusters, which operate by ejecting hot or cold

gas under pressure. The thrust requirements for orbital control are provided by mono or bi-propellant fuels. The attitude control thrusters are positioned away from the centre of the mass to achieve the maximum thrust, the thrust being applied perpendicularly to the direction of a spacecraft's centre of mass. The orbit control thrusters are mounted so that the thrust vector passes through the centre of mass. The relocation of a satellite from transfer orbit into GEO may be performed by apogee boost motor. In some satellite configurations, this is achieved by a solid or liquid fuel engine. Moreover, the choice between these two motors has a significant effect on the internal arrangements of the satellite.

CHAPTER FOUR

THEORETICAL FRAMEWORK

This chapter explains the theoretical framework of baseband signals and transmission systems between meteorological satellites and ground Earth stations infrastructures which are a very important segment in distributing weather data.

Early satellite systems, primarily communication and, later, meteorological networks were used in the analog transmission technique. Although modern satellite communication networks are still using the analog technique, the rapid development of high-speed digital satellite equipment is fostering a new trend towards completely digital satellite transmissions. This chapter includes techniques and technology that enable data, facsimile and image signals to be transmitted from satellite sensors to ground weather fixed and mobile infrastructures (Space-to-Earth), fixed service (point-to-point and point-to-multipoint) systems and data from meteorological cites or other platforms on the Earth surface to be relayed via meteorological satellite to a ground central receiving weather sites.

There are several methods of modulation, multiplexing and multiple access techniques used in satellite transmission and their reverse processes, with some overlapping. Modulation is the process by which the baseband signal in EM form can be impressed upon a carrier, so Phase (PM) and Frequency (FM) modulations are used heavily in satellite communications because of their positive ability to deal with nonlinear distortion, noise and interference. The amplitude of the PM and FM carrier is held constant, so there is no apparent change in the power level. Most nonlinear distortions are the result of amplitude variations on the carrier, so PM and FM is able to perform better in this environment than Amplitude Modulation (AM), which has a major limitation in directly using AM for satellite fixed and mobile systems (Lasaponara and Masini, 2012).

Multiplexing and multiple access require sharing the resources of the satellite. Facilities are shared based on spectrum assignment (frequencies), by time sharing (time domain) and by spatial separation (antenna beam and polarization). Theoretically, any method can be used for the transmission of analog and digital signals. In practice, frequency is easier used with analog signals, whereas time division is easier to use with digital signals. Multiplexing consists in combining the signals from several users into a single signal, which then forms the signal used for modulation of the carrier. After demodulation, the individual signals are separated by an inverse operation called the demultiplexing system (Grace et al, 2005). Then, all types of coding, decoding, error corrections and compression, including Digital Video Broadcasting-Return Channel via Satellite (DVB-RCS) system and protocols are discussed.

4.1 Baseband Signals

The information transmitted over an RF communications link consists of signals conveyed from one user to another one or two ways transmissions. Such signals are called baseband signals, which consist in basic electrical impulses carried by the radio path of a satellite or via other communication networks. If the baseband signal is analog, the voltage, which it represents, can take any value within a given range but if the signal is digital, the voltage takes discrete values within a given range. The type of baseband signals is determined by the communication requirements of the final users and the nature of the network, which can be voice, data and video (image) signals. Note that voice (speech) transmission is not used in

meteorological transmissions so far, but, perhaps, voice satellite channels can be used for transmissions of data, video (image) and facsimile transfer (Dartcom, 2015).

Each of these radio signals has to be arranged in a form suitable for transmission over some physical layer (air or wire) and such a technique is called baseband signal processing. The modified baseband signal is then superimposed onto a higher frequency carrier wave, when the signal modulates the carrier to a value suitable for propagation over the many different transmission links, such as radio, satellite, etc. The analog process at the transmit end of the link is called modulation and the circuit that performs modulation is the modulator, while at the receive end of the link, it is called demodulation and the circuit that recovers the baseband information is the demodulator (NOAA/NESDIS, 2008). Digital systems use a modulator for transmission and demodulator for reception of the RF carriers within one unit, known as a modem.

The process of modulation/demodulation applies to radio, satellite and terrestrial links by applying analog or digital transmission methods. The encryption device can be attached to Tx providing secure and secret service from eavesdroppers almost anywhere in the world.

The bandwidth classifiers and a brief description of system characteristics are as follow:

1. Narrowband – It uses low data of 10 Kb/s by channel bandwidths of 12.5-25 KHz;
2. Wideband – It is developed to provide higher data rate services by channel bandwidths of 50, 100 or 150 KHz and provides data rates that are measured in 100 Kb/s; and
3. Broadband – It provides megabits per second of data. The current allocation is 50 MHz of spectrum at 4.9 GHz band.

This thesis considers the following most common baseband signals:
- Telephone or Voice Signal;
- Data and Multimedia Signals;
- Sound Signals; and
- Television or Video Signals.

4.1.1 Voice Signals

The first commercial voice service via satellites was established by Intelsat at a time when underwater cables could not keep pace with the rapid growth of telephone traffic. In spite of data traffic growth in recent years, voice traffic has become dominant and will remain in the future integrated with videophones. In general, signals from most telephone sets are analog but these signals can be transformed into digital mode and multiplexed at a local telephone exchange for transmission on trunk routes(Launius, 2014).

In addition, satellites are effective for broadcast distribution Voice, Data and Video (VDV) signals anywhere and anytime, including voice (Tel) modems are able to send digital data over satellite voice channels or via an 3.3 KHz analog voice channel interfaced to the landline voice equipment.

Based on extensive studies of voice signals, it is now well known that most of the speech energy during normal conversation lies between 0 and 3400 Hz and the range of voice frequency that can be registered by the human ear is up to about 20 kHz. Therefore, a bandwidth of 3 to 4 kHz is allocated to each voice channel. The CCITT recommends the

range of telephony signals as 300–3400 Hz. The maximum energy of a signal representing speech is in the range of 800 Hz and about 99% of the energy is situated below 3000 Hz. The signal power of an average talker implied to a zero relative level point is given by:

$$P_m = P_a + 0.115\sigma^2 + 10\log\tau \quad [dBm_o] \tag{4.1}$$

where $P_a = -12{,}9$ dBm_o represents the average power of the speech signal; $\sigma = 5.8$ dB is the standard deviation of the normal distribution of the active speech power; $\tau = 0.25$ is the active factor of a talker. Thus, in total, the value of $P_m = -15$ dBm_o (Article G.223 of CCITT Recommendation).

The quality of a received analog voice signal has been specified by the CCITT to give a worst-case baseband signal-to-noise ratio for voice (Tel) signals, for transmission over a long distance, as 50 dB and with the maximum allowable noise in the baseband of 10,000 picowatts. Speech is characterized by having a large, dynamic range of up to 50 dB to accommodate the volume difference between a whisper and a shout.

4.1.2 Data and Multimedia Signals

Data transmission is composed using digital signals consisting of a series of bits. Actually, bits are bi-state pulses with low state called "0" (–V) and high state "1" (+V). Information is superimposed on a digital stream by arranging groups of bits called words, which can be used for the transmission of analog signals from a telephone or alphanumeric characters from a PC keypad. Therefore, facsimile, telex, data and PC E-mail networking terminals are used for the transfer of data through the medium of different transmission techniques and applications that are expanding rapidly (CHEOS, 2012).

Data signals used by satellite systems can be broadly classified into three ranges:

1) Narrowband data of about 300 b/s can be transmitted via ground stations TDMA 24 Kb/s Tlx channel with possibly 16 data bursts directed to Ground Earth Stations (GES) or User Earth Stations (UES) and PSTN via a modem;

2) Full duplex voice and 9.6 Kb/s data signals can be transmitted in the Single Channel Per Carrier (SCPC) data channel with a rate of 24 Kb/s in O-QPSK modulation scheme. In fact, the data channel enables packet data transfer using the CCITT X.25 recommendation for interface Data Terminal Equipment (DTE) and Data-Circuit Terminating Equipment (DCTE) operating in packet mode to the PSDN by dedicated circuits. This channel also supports CCITT Group-3 Fax, which is also available in the SCPC voice channel; using a 2.4 b/s data rate and APC voice codes; and

3) Wideband one-way High Speed Data (HSD) transmission can be supported with a rate of 64/56 Kb/s via voice channels on a dedicated frequency with a special type of V.32 (9600 b/s) modem. This service can be used for the transfer of PC data, high quality digital audio and compressed video. The Duplex HSD will offer a two-way 492 Kb/s via standard IP service for aircraft in both directions. The two-way HSD can be also used for digital multiplexing data channels and video conferencing between ships and shore.

There are several known techniques in transmitting digital data, facsimile, E-mail and PC networking data applications, whose utility is also expanding rapidly for fixed and mobile

systems. The new Global Area Network (GAN) portfolio of the HSD service developed by Inmarsat offers a cost-effective extension to corporate LAN and WAN even in the world's most rugged regions. Moreover, mobile packet data allow users to pay according to the amount of data they send rather than how long they spend online suited to Internet web-based applications such as Intranet access and E-commerce via satellite.

Meanwhile, the quality of data service provided by some satellite systems enables speed of transmission up to 7.2 Kb/s and the contributed Bit Error Rate (BER) is less than 1×10^{-6}. Hence, a higher satellite terminal rate of about 9.6 Kb/s can be processed if the equipment incorporates an elastic buffer to accommodate the required flow control (Calcutt and Tetley, 2004).

Therefore, data is becoming the most common vehicle for information transfer related to a large variety of services, including voice telephony, video and PC-generated information exchange. One of the most appealing aspects of data is the ability to combine, onto a single transmission, support data generated by a number of individual sources, which results in a single data stream called aggregate traffic. This is paramount for the transfer of multimedia traffic integrating VDV signals that often display a reduced bit rate variance versus traffic generated by the individual sources due to the embedded statistical multiplexing.

A network operator uses this opportunity to dimension its links (and particularly satellite links) with a capacity that is less than the sum of the peak bit rate of the individual sources. This dimensioning considers both the burstiness of the data traffic and the multiplexing techniques in use. The traffic is typically transported by packets, so the data structure (transport stream) developed for conveying TV program components could be used to carry any type of data, taking advantage of the well-recognized standard and mass-market production of equipment.

For example, the Moving Picture Experts Group (MPEG-2) transport stream (MPEG-TS) packets are used with DVB-S data transmission. As for video program, MPEG-2 transport stream (MPEG-TS) packet has a fixed size of 188 bytes of which 4 bytes are used for the packet header and 144 bytes for the payload. The header consists of a synchronization (sync) byte, a Packet Identifier (PID), transport error indication and a field of adaptation options. The Asynchronous Transfer Mode (ATM) data format is used in high data rate, terrestrial networks. The ATM packet, called an "ATM cell", is a fixed size of 53 bytes, of which 5 bytes are used for the header and 48 bytes for the payload. The header consists of a Virtual Channel Identifier (VCI), a Virtual Path Identifier (VPI), a payload type, and priority and Header Error Check (HEC) fields (Kadish et al, 2000).

4.1.3 Sound (Audio) Signals

A high-quality radio sound program occupies a band from 40Hz to 15 kHz. The test signal is a pure sinusoid at a frequency of 1 kHz. Its power relative to the zero reference level for an impedance of 600W is 1mWor 0 dBm0s (the "s" suffix indicates that the value relates to the sound program test signal). The mean power of a sound program is 3.4 dBm0 and the peak power (exceeded for a fraction less than 10^{-5} of the time) is equal to 12 dBm0.

For the emission of digitally encoded audio signals, the analogue sound program must go through an analogue-to-digital converter. This implies sampling, quantization and source encoding. Two encoding techniques, Pulse Code Modulation (PCM) and adaptive delta

modulation (ADM) are considered. Some formats have been defined using sampling rates of 32 kHz, 44.1 kHz or 48 kHz of different audio signals (Gordon et al, 1993).

For instance, where satellites are used for broadcasting of audio program to mobile receivers, Digital Audio Broadcasting (DAB) and Orthogonal Frequency Division Multiplexing (OFDM) can be used. This transmits data by dividing the stream into several parallel bit streams, each at lower bit rate, then uses these sub-streams to modulate several carriers. The OFDM time-domain waveforms are chosen such that mutual orthogonality is ensured, even though the spectra from several subcarriers may overlap. Thus, Coded OFDM (COFDM) is able to combat the time dispersion due to multipath, frequently encountered over mobile satellite channels.

4.1.4 Video and Television signals

Prior to the advent of satellite communications, it was very impracticable to relay video and TV programs across oceans because of the limited bandwidth of submarine coaxial cables. Today, optical fiber cables have enough channels but cannot, like satellite systems, transmit Digital Broadcasting Satellite (DBS) TV video to many widely separated fixed or Very Small Aperture Terminal VSAT stations in rural or remote areas and especially to mobile terminals. Direct broadcast by satellite has been in use for about 15 years, because the first such European satellite was launched in 1987. The demand for this type of satellite service continues to gain interest for the distribution of TV programs direct to homes (households) or other fixed stations and, later, to provide a service for mobile stations.

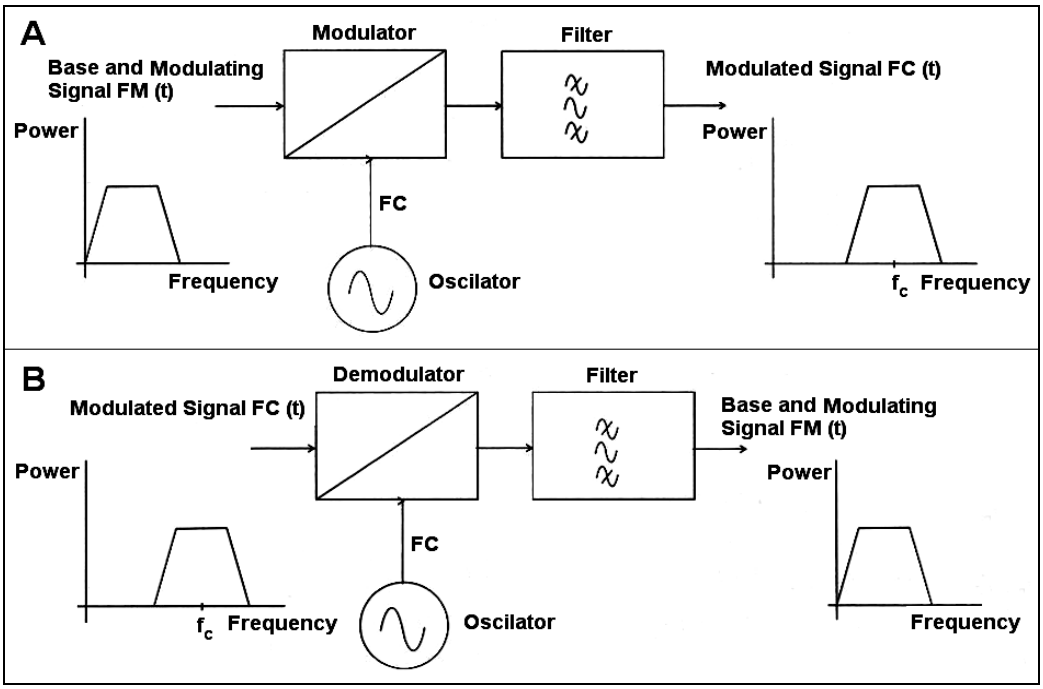

Figure 4. 1 Basic Modulator and Demodulator by Stacey 2008

There are various inexpensive ways in which it is possible to add data transmissions to the DBS and to provide cheap information services and E-mail for both domestic and business purposes, to onshore or offshore TV subscribers.

More then a decade ago, Inmarsat started to provide still pictures mode from the oil fields to any office using a wide range of analog and digital portable devices for transmitting, receiving and processing high resolution colour photographs in less then five minutes. In addition, Inmarsat developed the HSD Store-and-Forward video system. With the aid of advanced video codecs, it is possible to digitize and compress video material and then transmit it at 492 Kb/s to a receiver, which decompresses and buffers the data in almost full motion video. The store-and-forward technique also ensures that the received material is error-free, since the data transmission is achieved by using error detection and repeat transmission mode (Stacey, 2008).

There is a new possibility recently to use Integrated Services for Digital Network (ISDN) interfaces as well for the transfer of intensive data interactive applications such as Video Conferencing (VC) and Digital Image Transfer (DIT). Therefore, utility of standard ISDN interfaces will enable one to easily connect mobile fleet offices with corporate applications. Video baseband allows Inmarsat users to relay video from almost anywhere on the globe. This provides an effective flexible solution for media companies and the growing number of corporation who also use the VC system to facilitate “real time” discussion on a regular basis. Users benefit from ISDN speeds and easy-to-use portable equipment, which delivers immediate live action, training or medical and equipment diagnostic support, as required.

The Multiplexed Analogue Components (MAC) standard was proposed in the 1980s for satellite broadcasting (DBS) television and video, but was never developed into a successful commercial service. Fully digital techniques based on video compression were developed in the 1990s resulting in the widely recognized MPEG standards. The TV signal has a baseband signal of a few Mb/s, hence, the transmission of digital television and video is possible without requiring a huge amount of radio-frequency spectrum. At the same time, standards for DVB-RCS, and, in particular, the satellite versions of (DVB-S and DVBS2, have been adopted, making satellite broadcasting television a successful commercial service.

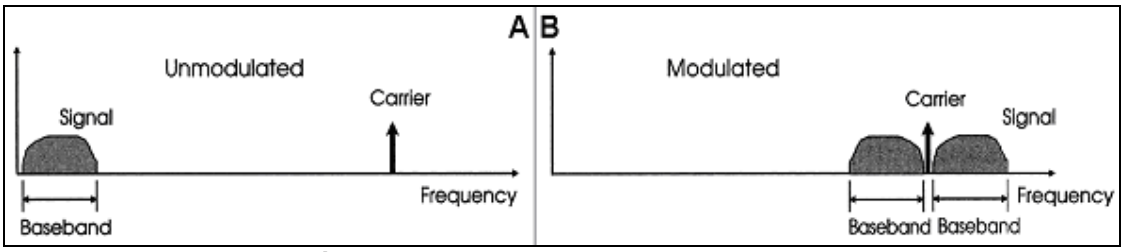

Figure 4. 2 Frequency Domain by Stacey 2008

4.1.5 Basic Concept of Modulation

Modulation is when the signal message that is to be conveyed is transposed in baseband, signals, such as voice or raw PC data, into a suitable form so that it can be transmitted over the media involved, usually plain air with absorbing gases, as described earlier. The raw data or voice signal can be modulated onto a carrier frequency as illustrated in Figure 4.1.

A frequency carrier is selected to suit propagation conditions, then spectrum and frequency management constraints and ITU radio regulations and efficient and reliable transportation of the information across the media. There are mathematical equations that describe this modulation process. The reverse process demodulation is when the useful information is extracted from the unuseful carrier.

There are many different types of modulation schemes available to the radio designers. In principle, these can be broken down into analogue modulation such as Amplitude or Frequency Modulation (AM or FM) schemes or variants of these, as can be used to modulate voice signals (Stacey, 2008). More recently, digital modulation such as Frequency Shift Keying (FSK), Phase Shift Keying (PSK) or advanced variants of these can be used to convey digital messages and/or digitized voice streams, or, of course, both. The selections of appropriate modulation schemes for an application are usually dependent on, but not necessarily limited to, the following factors: 1.Required ranges of propagation; 2. Frequency of operation and propagation properties; 3. Spectral efficiency; 4. Equipment complexity, reliability, size weight and cost; and 5. Required data or voice throughput rate and regulatory constraints.

The Modulation Conundrum is shown in Figure 4.2. The figure shows how baseband unmodulated signal is transformed into modulated baseband signal in frequency domain. There is a relationship between all of these aspects. Mathematically, it is Shannon's law, and it is usually necessary to trade off one requirement against the others to achieve the best overall engineering solution. In reality, for low-specification systems where performance is not so critical, rugged and rudimentary low-order modulation schemes can work very efficiently, and this keeps cost and complexity down. For some of the more sophisticated systems where data throughput in a limited bandwidth is premium, some of the more sophisticated and elaborate modulation schemes pushing the limits of Shannon's law become applicable, if not essential.

4.1.6 Analog and Digital Domains

Before detailing the modulation schemes it is worth momentarily to look at the Analog-to-Digital (A/D) aspects of signal modulation. Modern satellite systems generally digitize voice, data and images and transmit them via a digital medium, where quality can generally be kept, before putting them back in their original analogue domains. With data, there is never any A/D and it stays entirely in the digital domain. The modulation process can be considered as the inverse of this process; i.e., data are modulated onto a carrier conversion, which is akin to Digital-to-Analog (D/A) version, and then it is transmitted over the media and converted back to digital via A/D conversion at the end, as shown in **Table 4.1**.

Table 4. 1 Analog and Digital Domains

Analog-to-analog conversion (anolog speech to analog radio)	Digital-to-analog conversion (data or digitized speech to radio)
Amplitude modulation	Amplitude shift keying
Frequency modulation	Frequency shift keying
	Phase shift keying

With voice over legacy radio systems, it is never even coming into the digital domain. It is analog when it starts, it goes through an analog-to-analog conversion as it is modulated and then, at the end, it is an analog-to-analog demodulation process (Njoku, 2000). Analog modulation supports emissions of Double Side Band-Amplitude Modulation (DSB-AM), Single Side Band-AM (SSB-AM), Suppressed Carrier-AM (SC-AM) and the Frequency Modulation (FM) modulation scheme supports emissions of Phase Shift Keying (PSK), Frequency Shift Keying (FSK), Differential Phase Shift Keying (DPSK), Differential

Frequency Shift Keying (DFSK), Quadrature Amplitude Modulation (QAM) and Trellis Coded Modulation (TCM).

4.2 Analog Transmission

Analog transmission is characterized by processing performed on the baseband signal before and after modulation in order to improve the quality of the link. The carrier can support only one or few channels for the transmission of baseband signals. A SCPC transmission takes place iin the case of a carrier transmitted from the station representing only a single user channel. On the other hand, a Frequency Division Multiplexing (MCPC) transfer occurs if the carrier represents a number of multiplexed users, is designated Multiple Channel Per Carrier (MCPC) and uses several channels.

A signal needs to be impressed on an RF carrier for transmission through the satellite and for this purpose uses a process known as modulation. The objective of any communications is to transmit the modulated carrier to Rx as reliably as possible, so that the demodulated signals can be satisfactorily recovered. In analog transmission systems, the information waveform in the form of voice, data or video signal, are modulated directly from the source onto the carrier at the modulator of Tx, by using methods of Amplitude (AM), Frequency (FM) and Phase Modulation (PM). Frequency and phase modulation are used most widely for direct analog transmission in satellite communications, while amplitude modulation is a process used indirectly in the satellite link (Roddy, 2006).

Modulation may also be used at very low frequencies, like the more common and various forms of PSK modulation scheme. In addition, modulation is often done on a carrier with an RF of about 70 MHz lower than the transmission RF. This RF is then up-converted to the transponder frequencies on 6/4 GHz for amplification and retransmission. However, previous types of satellite do not change the received modulation before retransmission. Satellites are now being designed to allow only one modulation method to be employed in the uplink and another for the downlink; each link can be optimized. The space link between two GES can generally be accomplished by the combination of modulation and multiplexing techniques.
In the context of analog modulation will be included specific schemes as well as DSB-AM, SSB-AM and SC-AM.

As stated before, in satellite data communications, analog signals are used to transmit data over the telephone or voice systems. Alternatively, analog signals can be converted to digital information using a codec (coder/decoder), which process is called digitizing. Phones that connect to all-digital communication links use codecs to convert analog voice signals to digital signals.

4.2.1 Baseband Processing

The purpose of baseband processing is to improve the quality of the space (satellite) link using different methods whose cost is less than that arising from modification of one of the parameters involved in the link budget (Stacey, 2008). The principal methods of baseband processing for telephone transmission are speech activation, pre- and de-emphasis and companding and for TV transmission pre- and de-emphasis only.

1. Speech Activation - The principle of speech activation is to establish the space link only when the subscriber is actually speaking. As the activity factor is $\tau = 0.25$, its application to a

multicarrier SCPC system should permit a reduction of the power required on the satellite by about 6 dB. In practice, the reduction is only in the order of 4 dB, allowing guard times for activation and deactivation of the carrier and the sensitivity of S/N spikes. Therefore, the activation threshold parameter has to be from –30 to –40 dBm_o, the carrier activation time can be 6 to 10 ms and deactivation time can be 150 to 200 ms.

2. Pre- and De-Emphasis - The noise at the output of the demodulator of a FM transmission has a parabolic spectral density, when the high frequency components of the signal are more affected by noise than the low frequencies.

3. Companding Process - Companding is a process of compression and expansion for reducing the effect of noise on speech channels in accordance with the specification of CCITT Recommendations G.162 and article G.166. In effect, a compandor comprises a compressor and an expander and an improvement in the S/N ratio at the output of the demodulator is obtained by reducing the dynamic range of the signal before modulation (compression) and performing the inverse operation after demodulation (expansion) in order to restore the original speech signal to its correct relative level. These circuits perform the task of modifying the speech signal in analog voice channels. Thus, when the gain of the compressor and expander are controlled by the speech power at a syllabic rate, the technique is referred to as syllabic companding.

4.2.2 Analog Modulation and Multiplexing

Source waveforms of analog signals are directly modulated onto RF or IF carriers at the transmitter, using any form of three types of modulation: AM, FM or PM.

Analog modulation is a process in which some characteristics of a HF carrier are varied in accordance with the baseband signal, which is the creation, transmission and reception of EM fields (Huurdeman, 1997). In reality, EM fields and waves can be used to communicate all kinds of information from place to place. Therefore, an analog modulated signal can be represented as the following sinusoidal wave:

$$c(t) = A \cos[2\pi f t + \varphi] \qquad (4.2)$$

where A = amplitude, $2\pi f$ = form of ω_c = angular frequency of the carrier, f = frequency and φ = carrier phase. Modulation can be achieved by altering the amplitude, frequency or phase of the wave in accordance with the information signals. Consequently, AM, FM and PM analog carriers are simply forms of modulated carriers in which either the amplitude, frequency or phase is modulated by the information waveform. In such a way, by changing the amplitude, frequency or phase results in AM, FM or PM, respectively, as illustrated in Figure 4.3. Thus**,** since EM fields are vector fields, it is also possible to modulate the polarization of a wave to communicate information. However, polarization modulation is only normally used for special purposes, as the polarization state of a wave can easily be “scrambled” during free space transmission by effects such as unwanted reflections from buildings.

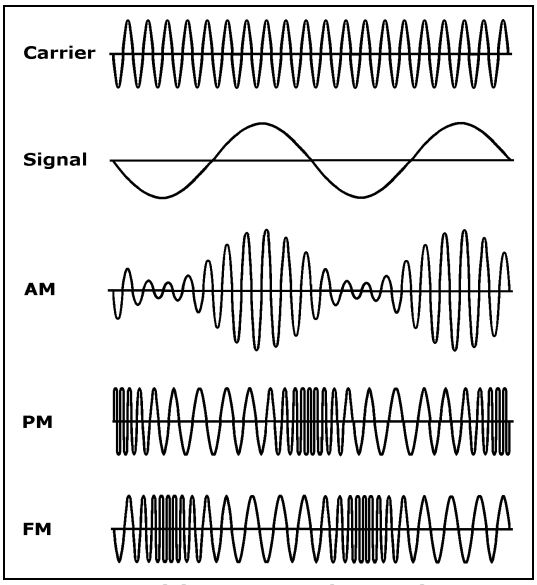

Figure 4. 3 Modulation Options by Huurdeman 1997

The AM system is a type of linear modulation in which the baseband signal is linearly related to the modulated signal, while FM and PM are kinds of angle modulation in which the baseband signal is angularly related to the modulated signal. However, angle modulated FM and PM signals require more carrier bandwidth than AM but achieve a higher demodulated C/N ratio for the same carrier C/N value. The reverse process of recovering the information signal from the modulated carrier at the demodulator of the receiver is known as demodulation. Multichannel operation of FM for analog high-capacity satellite telephone transmission is normally accomplished by a system called FDM scheme. In such a system, different channels are separated from one another by being assigned different subscribers, which are then combined to fill the total bandwidth of the transponder.

4.2.2.1 Amplitude Modulation (AM)

Amplitude modulation is a type of linear modulation and is not used as a transmission modulating process in the satellite link. However, it can be used to modulate individual voice channels before combining them using FDM technique.

In AM, the amplitude of the carrier frequency is modified by the amplitude of a modulating signal, namely, a carrier has to be amplitude modulated when the amplitude of the carrier varies in accordance with the signals. The side bands are displaced at either side of the carrier frequency by the magnitude of the modulation frequency and the amplitude depends on the modulation amplitude. The fundamental equation of AM modulation signals is:

$$c(t) = A[1 + \Delta_a m_{AM}(t)] \cos(\omega_c t + \varphi) \quad (4.3)$$

where $m_{AM}(t)$ = AM signal represents the information waveform to be transmitted and Δa = AM index (coefficient giving the degree of modulation of angular frequency of the carrier).
The AM method is employed usually in AM radio broadcasting and radiocommunication transmissions. In these systems, the intensity or amplitude of the carrier wave varies in accordance with the modulating signal. When the carrier is modulated, a fraction of the power is converted to side band extending above and below the carrier frequency by an amount equal to the highest modulating frequency.

If the modulated carrier is rectified and the carrier frequency filtered out, the modulating signal can be recovered. This form of AM is not a very efficient way to send information because the power required is quite large and because the carrier, which contains no information, is sent along with the information. In AM, the information is carried only in the side bands and, therefore, power in the carrier remains unutilized. In a Double Side Band Suppressed Carrier (DSB-SC), modulation of the carrier is suppressed and only side bands are used. The amplitude of this wave does not follow the signal amplitude and, consequently, the inherent simplicity of using envelope detection is lost. Therefore, this modulation is not used in satellite communications.

In a variant of amplitude modulation, called Single Side Band (SSB), the modulated signal contains only one side band and no carrier. Hence, the information can be demodulated only if the carrier is used as a reference. This is normally accomplished by generating a wave in the receiver (Rx) at the carrier frequency. The SSB is used for long-distance HF radiotelephony and telegraphy over land, such as in the maritime HF radio frequency bands and submarine cables. In the other words, the SSB scheme is called an SSB Suppressed Carrier (SSB-SC) when the carrier is suppressed (Huurdeman, 1997).

In fact, the most common application of SSB modulation in satellite communications is to multiplex voice carriers into a composite baseband signal. Thus, the required C/N ratio and the occupied bandwidths are two aspects considered in assessing the suitability of SSB for satellite transmission. The occupied RF bandwidth of an SSB transmission is the same as the baseband bandwidth, which is 4 to 5 kHz for a single telephone channel transmission. Typical bandwidth of –30 kHz is necessary for FM and 20 kHz for the O-QPSK, so both schemes are widely used in satellite communications.

However, a typical satellite communication link can economically provide C/N ratios in the order of 10 to 12 dB, making SSB transmission inefficient from power considerations. That is to say, this disadvantage can be offset to a large extent by the use of compandors, which offer an S/N ratio advantage of about 15 to 20 dB and in such a manner that SSB transmission appears attractive. This scheme is called Amplitude Companded SSB (ACSSB). Bandwidth efficiency is essential for mobile satellite service and, for this reason, ACSSB has been considered favourably for such applications.

4.2.2.2 Frequency Modulation (FM)

In FM scheme, the amplitude of the carrier frequency is modified by the frequency deviation of a modulating signal. The side bands are displaced at either side of the carrier frequency with an infinite number of separate bands, most resolving near zero (Stacey, 2008). The amplitude depends on the modulation frequency change and the frequency depends on the rate of frequency change of the modulation. Therefore, the fundamental equations of FM modulation are given below:

$$c(t) = A \cos[\omega_c t\, 2\pi\Delta_f \int m_{FM}(t)dt + \varphi] \quad (4.4)$$

where $m_{FM}(t)$ = FM signal representing the information waveform to be transmitted and Δf = FM index (coefficient giving the degree of modulation angular frequency of the carrier).
Using FM, the frequency of the carrier wave is varied in such a way that the change in frequency at any instant is proportional to another signal that varies with time. The FM band has become the choice of music listeners and for the audio portion of TV broadcasting

because of its low-noise and wide-bandwidth qualities However, the FM schemes are also extensively used in satellite communications. Examples of FM applications are multiplexed telephony, SCPC systems and TV broadcasting.

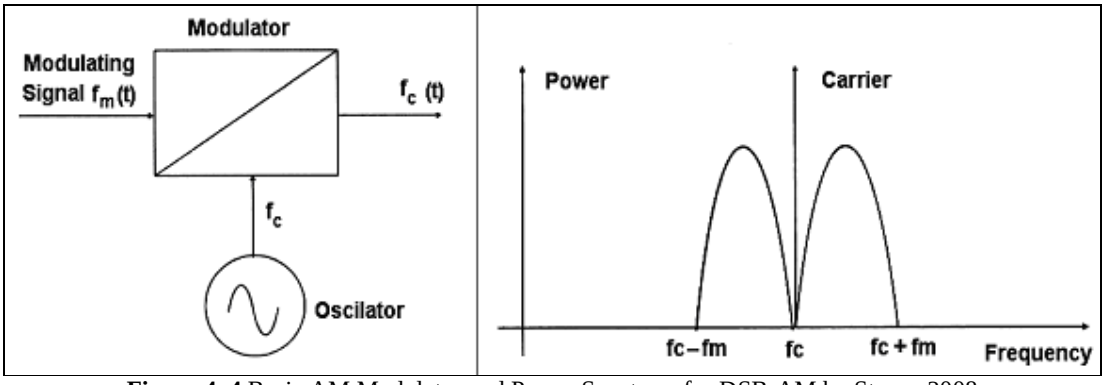

Figure 4. 4 Basic AM Modulator and Power Spectrum for DSB-AM by Stacey 2008

Thus, FM systems are well suited for those cases where the baseband signal is in analog form. An example is FM with companding used in Rx and Tx voice channels of the analog Inmarsat-A system of the SES transceiver.

Furthermore, this scheme also offers advantages for transmission of digital data in applications where simple receivers are essential, such as the Inmarsat paging system. At any rate, an important requirement of a paging system is the need for simple, low cost and rugged receivers.

4.2.2.3 Phase Modulation (PM)

Phase modulation (PM), like frequency modulation, is a form of angle modulation, so-called because the angle of the sine wave carrier is changed by the modulating wave. The two methods are very similar in the sense that any attempt to shift the frequency or phase is accomplished by a change in the other. The PM relation can be expressed with:

$$c(t) = A \cos[\omega_c t + \Delta_p m_{PM}(t) + \varphi] \quad (4.5)$$

where $m_{PM}(t)$ = PM signal representing the information waveform to be transmitted and Δp = PM index (coefficient giving the degree of modulation angular frequency of the carrier).

4.2.3 Double Side Band-Amplitude Modulation (DSB-AM)

AM is when the amplitude of the carrier is directly proportional to the modulating signal. Probably the simplest form of AM is DSB-AM mode, which is illustrated in Figure 4.4 (Left). The DSB-AM emission is described mathematically with the following equation:

$$f_c(t) = A \cos(2\pi f_c t + \varphi)\, \pi \quad (4.6)$$

where $f_c(t)$ is the modulated signal output. This relation results in the following equation:

$$A = K + f_m(t) \quad (4.7)$$

where K is the unmodulated carrier amplitude and $f_m(t)$ is the Baseband signal, and than is getting the following relations:

$$f_m(t) = a\cos(2\pi f_m t) \quad (4.8)$$

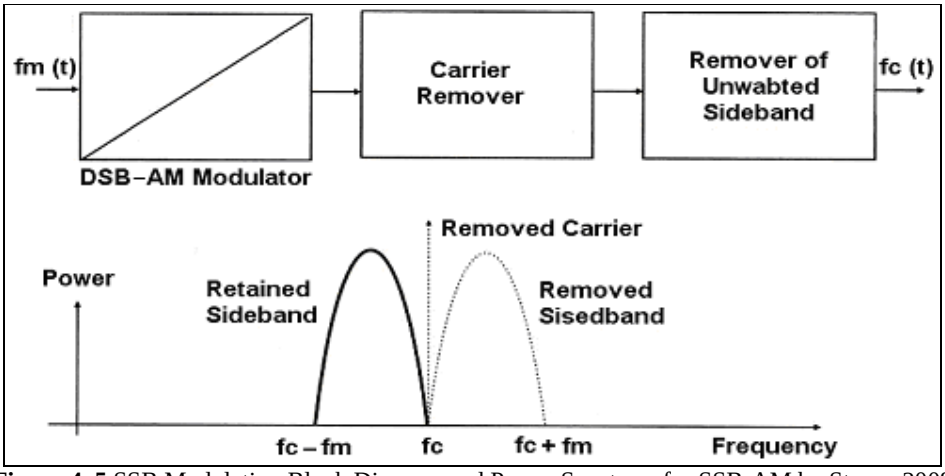

Figure 4. 5 SSB Modulation Block Diagram and Power Spectrum for SSB-AM by Stacey 2008

$$f_c(t) = [K + a\cos(2\pi f_m t)]\cos(2\pi f_c t + \Phi) \quad (4.9)$$

When $\Phi = 0$, then multiplying out the cos function:

$$f_c(t) = K\{\cos(2\pi f_c t) + 0.5\ m\cos[2\pi (f_c - f_m)\ t] + 0.5\ m\cos[2\pi (f_c + f_m)t]\} \quad (4.10)$$

At this point, depth of modulation (m) = modulating signal amplitude (a)/unmodulated carrier amplitude (K). In the frequency domain, these discrete components can be seen in Figure 4.4 (Right) and are called upper and lower sidebands, respectively. It is interesting to note that the modulated bandwidth of DSB-AM is twice the size of the minimum baseband bandwidth or the frequency component. It is independent of the depth of modulation.

4.2.4 Single Side Band-Amplitude Modulation (SSB-AM)

With DSB-AM practical work, it is found that the upper sideband is a perfect reflection of the lower sideband, i.e., the same information is carried by both. Thus, by removing one of the sidebands and by removing the carrier, therefore, no information is lost and the S/N (signal-to-noise radio) increases for a given transmit power as all the transmitted energy is concentrated into the information signal. This is the basis for the SSB-AM block diagram and power spectrum illustrated in Figure 4.5.

The construction of an SSB is fractionally more complicated than that of DSB-AM. It can be in synthesized two different ways.

Method 1 – As SSB relates to indirect synthesis and filtering, a SSB signal can be synthesized either by using basic DSB-AM or DSB-SC-AM modulator and filtering out the unwanted carrier and sideband (usually done at a IF).

Method 2 – Arguably, a more elegant way of modulation is to use the Hilbert modulator as SSB direct synthesis, which essentially cancels out the unwanted sideband and carrier.

Mathematically, this is described with the following quotation:

$$V_{out} = 0.5k \cos[2\pi (2f \pm f_m)t + \varphi] \pm 0.5k \cos(2\pi f_m t - \varphi) \quad (4.11)$$

The HF component is filtered out and expressed as:

$$V_{out} = 0.5k \cos(2\pi f_m t - \varphi) = 0.5k \cos(2\pi f_m)t \cos\Phi \pm 0.5k \sin(2\pi f_m) \sin\varphi \quad (4.12)$$

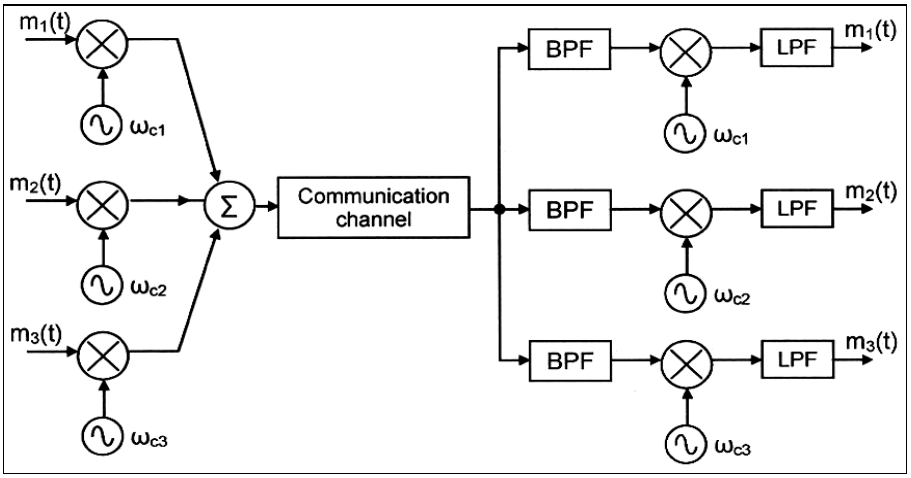

Figure 4. 6 Frequency Division Multiplexer by Maini and Agrawal 2007

More sophisticated demodulation is required (coherent detector with PLL, costas loop).
It can be prone to phase distortions (due to Tx and Rx oscillators beating and Φ changing). Therefore, a high oscillator specification is required at both endsWhich are not really heard by listeners (quality not high). The HF and other SSB systems use SSB modulation for reasons of spectral efficiency and a limited resource. Also a number of earlier military systems are known to have used SSB as a basis.

Suppressed Carrier Double Side Band AM (SCDSB-AM) is a modulation technique also used in aeronautical radio traffic. Worth mentioning in passing, there is an intermediate version of modulation called suppressed carrier double side band AM, which lies between DSB-AM and SSB-AM. In its basic form, it is the same as DSB-AM, with the carrier filtered out. It has the advantage of concentrating more power into the useful sidebands, so there is an S/N improvement; however, there is no bandwidth saving and it requires a more complex synthesis. It is rarely used, as most applications will do a full conversion to the SSB, where power and spectral efficiency become important and there are no mainstream applications of this in the aeronautical bands.

4.2.5 Frequency Division Multiplexing (FDM)

The process of combining baseband signals and sharing the communication channels is known as multiplexing, while the reverse process of extracting individual baseband signals is called demultiplexing. The CCITT (French: Comité Consultatif International Téléphonique et Télégraphique) proposed all multiplexing standards including FDM, which is applicable only to telephony baseband signals, whereas the digital Time Division Multiplexing (TDM) standard is applicable to all types of baseband signals.

Each type of GES usually transmits and receives many kinds of signal transmissions to and from spacecraft. Multiplexing enables the division of channels or the combination of two or more input signals into a single output for transmission. The most common and known analog multiplexing method is FDM, used in satellite communication transmissions. The simplest approach to multiplexing is to assign a specific part of the available frequency or bandwidth spectrum to each signal. If two signals initially have the same spectrum, the frequency of one or both is shifted, in such a way that they will not overlap. The FDM is a multiplexing solution where signals occupy the channel at the same time but on different frequencies, namely, different message signals are separated from each other in frequency. The multiplexing scenario of FDM is shown in Figure 4.6, which illustrates the simultaneous transmission of three message signals over a common communication channel. It is clear from the block schematic arrangement shown that each of the three messages signals modulates a different carrier.

As stated earlier, frequency modulation is when the carrier frequency is modulated by the baseband signal. The FM mode is used for some specialist military systems, in aeronautical telemetry and, finally, in the adjacent band to the VHF aeronautical communications for broadcasting information. It is mainly used by broadcasting in the band between 88 and 108 MHz, just below the VHF navigation and communication bands 108.000-117.975 MHz and 117.975-137.000 MHz, respectively. However, a clear understanding of FM is potentially useful for adjacent channel compatibility work. In addition, it is synthesized using a voltage-controlled oscillator. Also, it is more susceptible to Doppler shifts, which, even although these have been shown to be very minor in a previous section, make it impractical for mobile aeronautical communications. Historically, FM gives a better quality of voice service. The FM modulation is used by entertainment systems on board aircraft where channels are FDM into time slots. Otherwise, the most common used modulation technique in aeronautical telephony is SSB (Stacey, 2008).

4.3 Digital Transmission

Before providing any explanation about solutions of digital transmission, it will be necessary to introduce some relations:

1. Shannon's Theory – Shannon's theory provides a theoretical relationship between bits per second, baud and S/N for error-free transmission, as presented in **Table 4.2.**

Table 4. 2 Shannon's Law in Maini and Agrawal 2007

M	2^M	Minimum S/N required	Maximum spectrum efficiency (maximum capacity)
1	2	3	1 bits/Hz
2	4	15	2 bits/Hz
3	8	63	4 bits/Hz

$$R\ (b/s) = M\ (\text{number of signal states}) \times r\ (\text{baud or signal rate}) \quad (4.13)$$

$$C = B \log_2 [(1 + S/N)] \quad (4.14)$$

where C is channel capacity in b/s, B is bandwidth in Hz, S/N is signal to noise ratio, R is the data rate and is always < *C* for errorless transmission. If R > C, errors will occur. The theoretical relationship between *M* and S/N is as follows:

$$M = [(1 + S/N)]^{0.5} \quad \text{or} \quad S/N = M^2 - 1 \tag{4.15}$$

2. Non-Errorless Transmission –Shannon's law does not apply if it is decided to push past this theoretical limit of data throughput if errors can be tolerated. Actually, it is sometimes a prudent approach to tolerate the errored environment and to make facilities for correcting them by Forward Error Correction (FEC) and Cyclic Redundancy Coding (CRC); FEC and CRC too are overhead and not useful data payload. However, this can be a more efficient way to operate and maximize data throughput. Alternatively, the errors can just be tolerated and the application layer of the data system can be designed to tolerate this or to correct it. Also, in a number of digital systems, errors will be present from the propagation problems already present and these have to be tolerated.

Digital transmission relates to the link for which the GES is designed to produce the digital signals by PC or modem and to send them through Tx. It is possible to transmit analog signals (voice or broadcast) in digital form. Although this choice implies an increased baseband, it permits signals from diverse origins to be transmitted on the same satellite channels and the satellite link to be incorporated in ISDN, which implies the use of TDM. The digitization of analog signals implies the stages of sampling, quantization and coding. The simple digital transmission chain includes a transmitting and receiving segment. The first unit of the transmitting segment is TDM with input signals from digital (direct) and analog (via encoder) sources and after multiplexed signals pass devices such as: Data Encryption, Channel Encoding, Scrambling and Digital Modulation, where the digital signal is transmitted through up or down satellite links. In the receiving segment of reverse mode, incoming signal goes through devices such as: Demodulator, Descrambling, Channel Decoding, Data Decryption and TDM Demultiplexing in its direction to different users.
Digital signals use the same principle to modulate a carrier as analog signals. The AM, FM and PM schemes are all applicable to digital modulation; digital equivalents are ASK, FSK and PSK and special hybrid modulation solutions have also been developed to optimize digital modulation, such as QAM (Sheriff et al, 2001).

4.3.1 Delta Modulation (DM)

Analog signals, such as speech and video signals, generally have a considerable amount of redundancy, namely, there is a significant correlation between successive samples. Thus, when these correlated samples are coded, as in the Pulse Code Modulation (PCM) system, the resulting digital stream contains redundant information. The redundancy in these analog signals makes it possible to predict a sample value from the preceding sample values and to transmit the difference between the actual sample value and the predicted sample value estimated from the past samples. This result in a technique called difference encoding. One of the simplest forms of this is DM, which provides a staircase approximation of the sampled version of the analog input signal. This type of modulation is a way of digitizing a voice waveform, transmitting the digits and reconstructing the original analog waveform that avoids the quantizer and the A/D and D/A converters employed in PCM. In Linear Delta Modulation (LDM), a circuit of DM determines the difference between an incoming waveform or message signal m(t) and estimated waveform or error signal e(t), where a difference of signal error voltage is as:

$$\Delta m(t) = m(t) - e(t) \quad (4.16)$$

The quantizer output is a positive constant when Δm(t) is positive and vice versa. Therefore, the difference between the input and the approximation is quantized into two levels, +Δ and –Δ, corresponding to a positive and a negative difference, respectively. Moreover, at any sampling instant, the approximation can be increased or decreased by step size (Δ) value, depending on whether it is below or above the analog input signal (Maini and Agrawal 2007).

Furthermore, a digital output of 1 or 0 can be generated according to whether the difference is +Δ or –Δ. These pulses go to a conventional PSK digital modulator for transmission. Increasing the step size (Δ) will result in poor resolution and increasing the sampling rate will lead to a higher digital bit rate. In LDM, the step size is fixed at a value that provides performance near the peak, while better final performance may be achieved through a scheme of Adaptive Delta Modulation (ADM) in which the value of step size is varied during the modulation process. On the other hand, it is difficult to make comparisons between the performance of PCM and DM because the latter is continually improving.

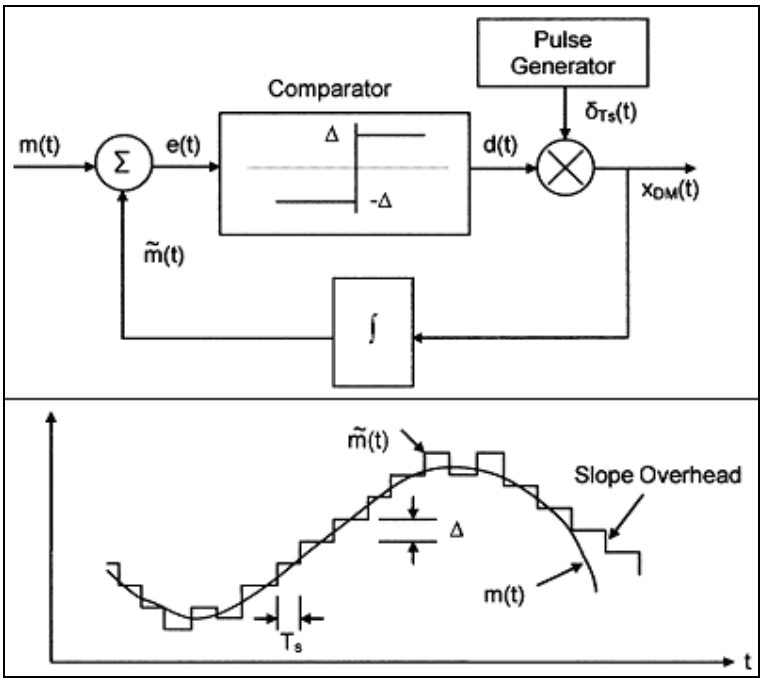

Figure 4. 7 DM and Output Waveform of DM System by Maini and Agrawal 2007

The DM mode has various forms. In one of the simplest forms, only one bit is transmitted per sample just to indicate whether the amplitude of the current sample is greater or smaller than the amplitude of the immediately preceding sample. It has extremely simple encoding and decoding processes but, then, it may result in tremendous quantizing noise in case of rapidly varying signal. In Figure 4.7 (above) is illustrated a simple delta modulator system, where m(t) is added to a reference signal with the polarity shown, while in Figure 4.7 (below) is presented its output waveform.

The reference signal is an integral part of the delta modulated signal. The error signal is fed to comparator, and at output of comparator is (+Δ) for e(t)>0 and (-Δ) for e(t)<0. Thus, the

output of DM is a series of impulses with the polarity of each impulse depending upon the signal of e(t) at the sampling instants of time. A DM signal can be demodulated by integrating the modulated signal to obtain the staircase approximation and then passing it through lower filter. The smaller the Δ value, the better is the reproduction of the message signal.

4.3.2 Coded Modulation (CM)

The CM is a combination of modulation and error correction codes without degrading the power of bandwidth efficiency. Thus, using FEC, such as block and convolutional codes, the bit error performance is improved by expanding the required bandwidth (Maini and Agrawal 2007). Obtaining the power efficiency requires twice the bandwidth of the original uncoded signal because of the increase in the symbol rate of modulation and complex implementation.

This can be done by increasing the number of phases in PSK modulation without expanding signal bandwidth. In this case, the 8-PSK signals with 2/3 rate of convolutional code have the same bandwidth as uncoded 4-PSK. However, the bit error performance degrades by about 4 dB due to an increase in phase but will be referable if the coding gain becomes more than 4 dB. There are two practical CMs in use for MSS: the Trellis Coded Modulation (TCM) and the Block Coded Modulation (BCM).

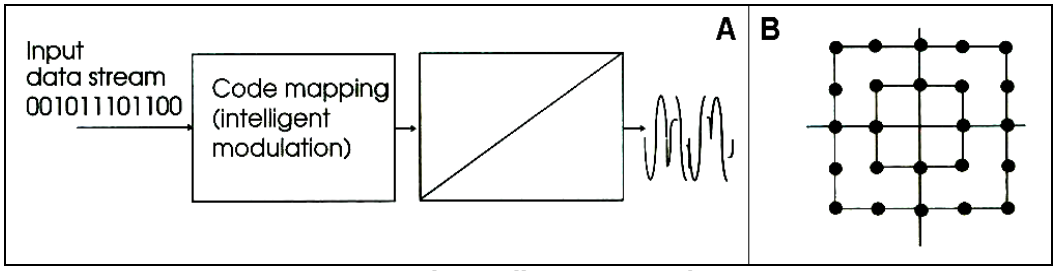

Figure 4. 8. TCM and Constellation Diagrams by Stacey 2008

4.3.2.1 Trellis Coded Modulation (TCM)

The TCM scheme uses the combination of convolutional coding and expanded signal sets of 8-PSK to transmit two information bits per symbol. The modulation signals in TCM are assigned to each one- or two-satellite trellis branch, although binary code symbols are assigned in the convolutional codes. Here is a very important definition of measuring the distance between modulation signals assigned to each trellis branch. The modulation signal assignment in TCM can be designed either by the Euclidean or Hamming distances.

Initially, the modulator states are based on a trellis shown in Figure 4.8 (A). This scheme is intelligent and involves more signals processing theory than the simpler prior modulation schemes. This sample works on the principle of putting states that are likely to occur simultaneously as far apart on the constellation diagram shown in Figure 4.8 (B), with maximum distance of separation employing Euclidean distance. This sample shows variable phase and amplitudes determining Euclidean distance as the distance between two points in constellation. Similarly, a binary sequence that is unlikely to occur can be put together on the constellation diagram with minimum Euclidean distance. This offers an effective coding gain over the simpler QAM and for a given BER and data throughput would consequently require a lower SNR than QAM.

The performance of TCM scheme can be improved by increasing the number of states or by modifying the signal constellation. Thus, one solution is provided by multidimensional signals and another is performed by multiple-
coded modulations, known as Multiple TCM (MTCM). A TCM 8-DPSK modem with a rate of 2/3 and 16 states for 4800 b/s has been implemented in the NASA MSAT-X experimental program for ground communications.

4.3.2.2 Block Coded Modulation (BCM)

Instead of convolutional coding, this scheme uses short binary block codes, which could be simpler and faster to decode. Similar to TCM, this type of modulation can improve performance by using Multiple BCM (MBCM). Thus, MBCM with two symbols per branch has a coding gain of 3 dB relative to conventional BCM. The two symbols per branch MBCM has a performance for coding gains of 1.1 dB and 2.2 dB at BER = 10^{-3} relative to the BCM 8-PSK and the uncoded QPSK, respectively.

4.3.3 Pulse Code Modulation (PCM)

The digitization starts with the conversion of analog voice signals into a digital format. An analog can be converted into a digital signal of equal quality if the analog signal is sampled at a rate that corresponds to at least twice the signal's maximum frequency.

The peak-to-peak amplitude rate of the modulating signal in PCM is divided into a number of standard levels, which, in the case of binary systems, is an integral power of 2. The amplitude of the signal to be sent at any sampling instant is the nearest standard level.

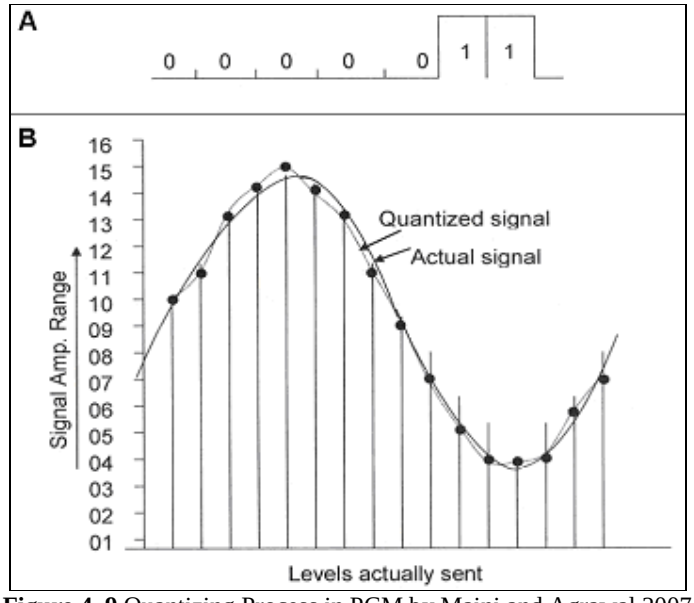

Figure 4. 9 Quantizing Process in PCM by Maini and Agrawal 2007

So, if at a particular sampling instant, the signal amplitude is 3.2 V, it will not be sent as a 3.2 V pulse, as can be the case of Pulse Amplitude Modulation (PAM). Instead, it will be sent as the digit 3, if 3 V is the nearest standard amplitude. Thus, where the signal range has been divided into 28 levels, it will be transmitted as 0000011, whose coded waveform is shown in Figure 4.9 (A). This scheme is known as a quantizing process in PCM shown in Figure 4.9 (B), where the number of bits for 2^n chosen standard levels per code group is n+1. In fact, it

is evident that the quantizing process distorts the signals. This distortion is referred to as a quantizing noise, which is random in nature as the error in the signal's amplitude and that is actually sent after quantizing is random. The maximum error can be as high as half of the sampling interval, and the number of the level is 16 or 1/32 of total signal amplitude range.

A technique for converting an analog signal to a digital form is PCM, which requires three operations:

1. Sampling – This operation converts the continuous analog signal into a set of periodic pulses, the amplitudes of which represent the instantaneous amplitudes of the analog signal at the sampling instant. Thus, the process of sampling involves reading of input signals at discrete points in time. Hence, the sampled signals consist in electrical pulses, which vary in accordance with the amplitude of the input signal. In accordance with the Nyquist sampling rate, an analog signal of bandwidth B Hz must be sampled at a rate of at least 1/2B to preserve its wave shape when reconstructed.

2. Quantizing – This technique is the process of representing the continuous amplitude of the samples by a finite set of levels. If V quantizer levels are employed to represent the amplitude range, it takes the $\log_2$ V bit to code each sample. In voice transmission, 256 quantized levels are employed. Hence, each sample is coded using $\log_2 256 = 8$ bits and, thus, the digital bit rate is 8,000 x 8 = 64,000 b/s. Therefore, the process of quantization introduces distortion into the signal, making the received voice signals raspy and hoarse. This type of distortion is known as quantization noise, which is only present during speech. However, when a large number of quantization steps, each of ΔS volts, are used to quantize a signal having an rms signal level S_{rms}, the signal-to-quantization noise ratio is given by:

$$S_{qn} = (S_{rms})^2/(\Delta S)^2/12 \qquad (4.17)$$

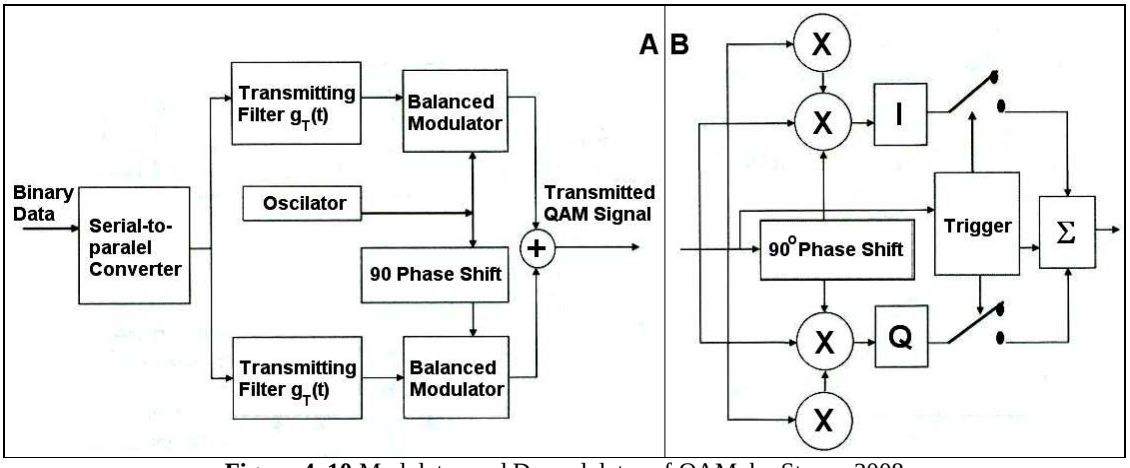

Figure 4. 10 Modulator and Demodulator of QAM by Stacey 2008

A large number of bits are necessary to provide an acceptable signal-to-quantization noise ratio throughout the dynamic amplitude range. Some analysis of speech signals show that smaller amplitude levels have a much higher probability of occurrence than high levels.

3. Coding – This solution protects message signals from impairment by adding redundancy to the message signal.

Another important approach in digital coding of analog signals is Differential PCM. This is basically a modification of DM where the difference between the analog input signals and their approximation at the sampling instant is quantized into V levels and the output of the encoder is coded into $\log_2$ V bits. In this way, the encoder combines the simplicity of DM and the multilevel quantizing feature of PCM mode and, in many applications, can provide a good reproduction of analog signals comparable to PCM, with a considerable reduction in the digital bit rate.

4.3.4 Quadrature Amplitude Modulation (QAM)

Each higher PSK modulation requires a better S/N ratio performance, which is difficult to achieve without special schemes. Instead of 16, a higher PSK modulation QAM is used, which is a combination of amplitude and phase modulation. In effect, modulation can be achieved in a similar manner to that of QPSK, by which the in-phase and quadrature carrier components are independently amplitude modulated by the incoming data streams. The incoming signals are detected at the receiver using matched filters. In terms of bandwidth, it is a highly efficient method for transmitting data flow. However, the sensitivity of the QAM method to variation in amplitude limits its applicability to satellite communication systems in practice, where non-linear payload characteristics may distort the waveform, resulting in the reception of erroneous messages (Ilcev, 2013).

The QAM scheme is a combination of the phase domain. The number of possible states = 360/number of phase changes used. The functional block diagram of modulator for QAM is shown in Figure 4.10 (A). The demodulation and detection process for QAM signals, shown in Figure 4.10 (B), becomes quite complex, but is not unachievable with modern technology. It is used frequently in high-capacity data point-to-point radio links. 64QAM, 128QAM, 256QAM and even 518QAM are not uncommon. Obviously, these have high spectral efficiency in the amount of data per unit RF bandwidth they are able to pass. However, consequently, a very good SNR is needed to retain a high BER. Figure 4.14 (d) shows a 16-QAM signal space diagram with a 16-state grid that permits both carrier amplitude and phase change. This scheme is not yet considered favourable for satellite communication.

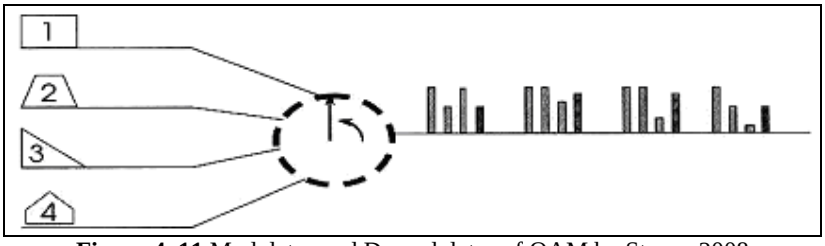

Figure 4. 11 Modulator and Demodulator of QAM by Stacey 2008

4.3.5 Time Division Multiplexing (TDM)

Satellite links normally relay many signals from different UES but, to avoid interfering with each other, it is necessary for some kind of separation or division. This separation is known as multiplexing and its common forms are FDM (already explained) and TDM. The TDM is easier to implement with digital modulation and to form hybrid solutions applicable to all type of baseband signals.

The TDM is a time multiplexing solution where a group of various transmission signals on the same frequency at different times take turns using a channel. In this way, a group of pulses from a number of channels may be interleaved to form a single high rate bit stream of multiplexed assembly directly modulated onto the RF carrier. Since digital signals are precisely timed and consist in short pulse groups with relatively long intervals between them, TDM is the only natural way to combine digital signals for transmission. This system has the advantage that less equipment is required than is needed to modulate each channel onto a separate carrier and that the transmission efficiency of a satellite is usually better when it is carrying a few transmissions on many channels and vice versa. Accurate timing is essential to the correct operation of digital systems. Thus, for that reason the TDM system uses a synchronous clock, which controls the timing of all slave clocks and plesiochronous independent clocks with very good accuracy. If the transmission is without errors and breaks in the synchronous system it would be only necessary to provide single markers at the beginning of transmission where the decoder could identify all streams of bits (Stacey, 2008).

The TDM is used when there is one RF channel shared in time between the different users. If a suitable TDM repetition frequency is chosen, the user does not need to be aware of the discontinuity shown in Figure 4.11. This is the principle deployed in modern ground cable and fiber networks to which the radio systems need to interface.
However, in any practical communication system, regular markers must be provided in the bit stream so that the decoder can extract groups of digitally representative samples, identify the channels of a TDM assembly and resynchronize the system after errors, breaks of transmission or drift of the clock. Therefore, when plesiochronous time multiplexes are combined to form higher order of TDM, it is necessary, in order to preserve synchronism over the long-term, to allow for the occasional addition of dummy or padding bits.

4.3.6 Types of Digital Shift Keying

Digital signals can be used to modulate the amplitude, frequency and phase and, therefore, the solutions of shift keying available for digital modulation are Amplitude Shift Keying (ASK), Frequency Shift Keying (FSK) and Minimum Shift Keying (MSK) as applications of FSK and Phase Shift Keying (PSK) (Sheriff et al, 2001). In terms of performance, ASK and FSK, both illustrated in Figure 4.12 (A) and (B), respectively, require twice as much power to attain the same BER performance as PSK, as shown in Figure 4.12 (C). At the top of the same figure, a stream of a digital signal with 1 and 0 binary state is presented. Consequently, the vast majority of MSS employ a method of phase modulation known as PSK.

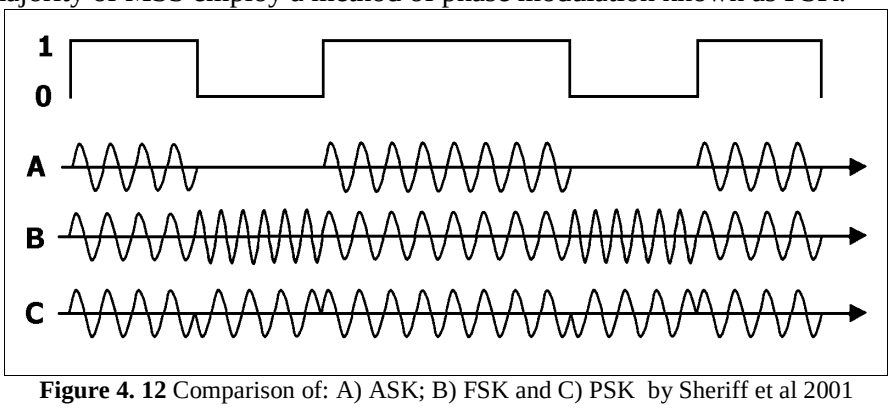

Figure 4. 12 Comparison of: A) ASK; B) FSK and C) PSK by Sheriff et al 2001

4.3.6.1 Amplitude Shift Keying (ASK)

This scheme can be accomplished simply by the on-off gating of a continuous carrier. The simplest ASK technique is to represent one binary level (binary 1) by a single signal of fixed amplitude and the other level (binary 0) by switching off the signal. The absence of the signal for one of the binary levels has the disadvantage that, if fault conditions exist, it could be misinterpreted as received data. Waveform for ASK, using different amplitude signals for the logic levels, is an alternative method to prevent this disadvantage (Sheriff et al, 2001). As with speech telephony circuits, the upper side band and carrier may be suppressed to reduce the bandwidth requirement and concentrate the available power on the signal containing the information.

4.3.6.2 Frequency Shift Keying (FSK)

This solution may be used whereby the carrier frequency has one value for a 1 bit and another for a 0 bit. The main difficulty in the use of this FM technique is that the gap between the frequencies used must be increased as the modulation rate increases. More exactly, for a restricted channel bandwidth, especially using in-band supervisory signaling, there is a limit to the maximum bit rate that is possible with this technique.

4.3.6.3 Minimum Shift Keying (MSK)

The MSK is a binary form of Continuous Phase Frequency Shift Keying (CPFSK), where the frequency deviation (Δf) from the carrier is set at half the reciprocal data rate of 1/2T. The MSK scheme may also be viewed as a special form of Offset-QPSK, consisting in two sinusoidal envelope carriers, employing modulation at half the bit rate. For this reason, the MSK demodulator is usually a coherent quadrature detector, similar to that for QPSK. The error rate performance is the same as that of BPSK and QPSK. Similarly, differentially encoded data have the same error performance as D-PSK. This solution can also be received as an FSK signal using coherent or non-coherent methods, however, this will degrade the performance of the link. At any rate, the side lobes of MSK are usually suppressed, using Gaussian filters and the modulation method scheme adopted by GSM cellular systems.

4.3.6.4 Phase Shift Keying (PSK)

The PSK scheme is a technique using a multistate signaling stream in which the rate of data transmission can be increased without having to increase the bandwidth. In this shift keying system, the phase of the carrier changes in accordance with the baseband digital stream or information content, whose general form of a PSK scheme is given by:

$$s_m(t) = A \cos(\omega t + \phi) \quad \text{and} \quad \phi = (2m + 1)\,\pi/M \qquad (4.18)$$

where A = amplitude; ω = frequency angle; ϕ = phase angle varied in accordance with the information signal; m = integer in the range from 0 to (M – 1) and M = number of states. Depending on how many bits can be combined in a group of information as a symbol, there are a number of combination possibilities for PSK digital carriers.

4.3.7 Combinations of PSK Digital Carriers

There are several types of hybrid solutions used for the combination of PSK Digital Carriers. The PSK family is most popular for satellite communications and especially for mobiles. A

real-valued band bass signal s(t), which has a common form for these types of PSK methods, is expressed as follows:

$$s(t) = A(t) \cos [2\pi f_c t + \phi(t)] = A(t) \cos [2\omega_c t + \phi(t)] \quad [V] \tag{4.19}$$

where A (t) = amplitude; f_c = carrier frequency of signal s(t); ϕ (t) = phase angle and ω_c = frequency angle varied in accordance with the signal s(t). Including information waveform m(t), the previous relation can be determined as follows:

$$s(t) = Re [m(t)] e^{j2\pi fct} \tag{4.20}$$

In linear modulation methods such as pulse, PAM and PSK can be expressed by:

$$m(t) = A(t) \exp [j\phi(t)] = \sum_{n=0}^{\infty} a_n p(t) (t - nT) \tag{4.21}$$

where Re = real part of the complex in the next bracket; a_n = information carrying symbols; p(t) = signal pulse and T = time interval of symbol.

4.3.7.1 Binary PSK (BPSK)

The simplest form of PSK is Binary PSK (BPSK), where the digital information modulates a sinusoidal carrier (Ohmori et al, 1998). For a general case of M-ary PSK (number of states) in BPSK, M=2, so the baseband bit rate and the symbol rates are the same. Binary data are expressed by $a_n = \exp (j\phi_n)$ for $\phi_n = 0$ or π and the phase changes every data bit of duration period T_b. When p(t) is a rectangular pulse over symbol duration $T = T_b$, the BPSK signal is expressed by the following quotation:

$$s(t) = Aa_n \cos 2\pi f_c t = A \cos (2\omega_c t + \phi_n) \quad \text{for} \quad nT \leq t < (n + 1) T \tag{4.22}$$

In Figure 4.13 (A), a diagram is illustrated of how, theoretically, the phase of the carrier changes instantaneously by 180^o when the baseband signal switches from 0 to 1, while Figure 4.14 (a) represents the two states of the carrier by two vectors with a phase difference of 180^o. In this sense, where $\phi = 0^o$ and $\phi = 180^o$ when the baseband signal is 0 and 1, respectively, and where A = +V and A = –V when the baseband signal is 0 and 1, respectively.
The TDM/BPSK scheme is used by many satellite communication and broadcasting systems for processing such as Forwarding Signaling/Assignment Channels, while Return Request Channels use Aloha BPSK.

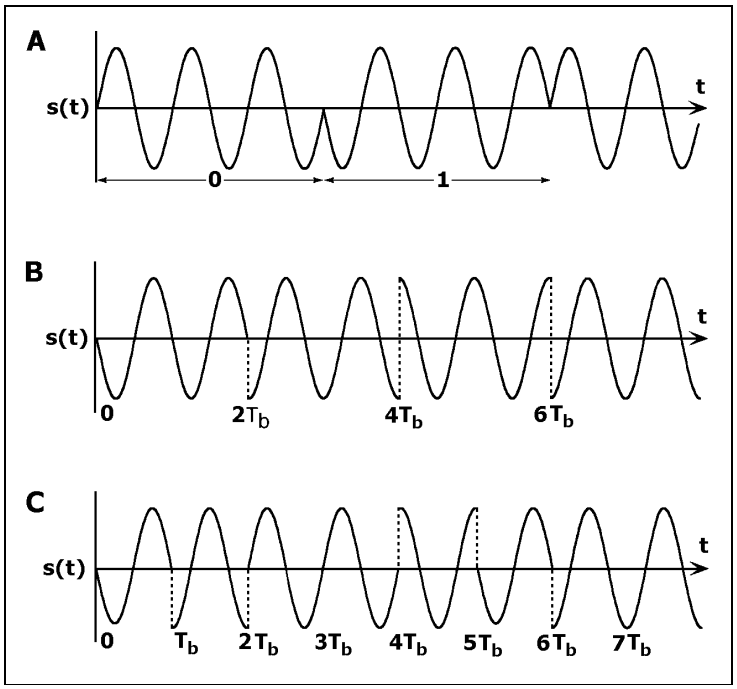

Figure 4. 13 Hybrid PSK Modulations: A) BPSK; B) QPSK and C) O-QPSK by Ohmori et al 1998

4.3.7.2 Quadrature PSK (QPSK)

For M-ary, PSK is selected from M signals like: exp [j2π (m – 1)/M], where m = 1, 2,..., M and the resulting signal s(t) is written as follows:

$$s(t) = A \cos [2\pi f_c t + 2\pi/M\ (m - 1)] \quad \text{for } m = 1, 2,..., M \tag{4.23}$$

A slightly more complex form PSK is QPSK or 4-PSK, for which ϕ_n is a set of 0, π/2, π and 3/2π. Then, the signal s(t) is given by:

$$s(t) = A/\sqrt{2}\ (a^I_n \cos (2\pi f_c t + \pi/4) + A/\sqrt{2}\ (a^Q_n \cos (2\pi f_c t + \pi/4) \tag{4.24}$$

where a^I_n and a^Q_n are the ±1 value data, which are converted from input data sequence a_n into the in-phase channel (I channel) and quadrature channel (Q channel), respectively. However, the relation (a^I_n, a^Q_n) is (1, 1) for $\phi_n = 0$; (1, –1) for $\phi_n = \pi/2$; (–1, –1) for $\phi n = \pi$ and (–1, 1) for $\phi_n = 3\pi/2$.

In Figure 4.13 (B), the shape of QPSK modulated signals is presented and a QPSK scheme in the I-Q plane is shown in Figure 4.14 (b).

Only two binary digits are needed to describe four possible states as follows: the ϕ values of 45^o, 135^o, 225^o and 315^o correspond to 00, 01, 11 and 10, respectively. In fact, each state of the signal carries two bits of information. Thus, a combination of two bits or more, which corresponds to a discrete state of a signal, is called a symbol, in the case of QPSK; the symbol rate is half the bit rate. Therefore, a bit rate of 120 Mb/s corresponds, with QPSK, to a symbol rate of 60 Mb/s or Mbauds (Ohmori et al, 1998).

The QPSK schemes of modulators are basically dual channel BPSK modulator and demodulator equipment. At this point, one channel processes the u_i (I) bits and uses the

reference carrier and the other process the u_q (Q) bits using a 90º phase shifted version of the reference.

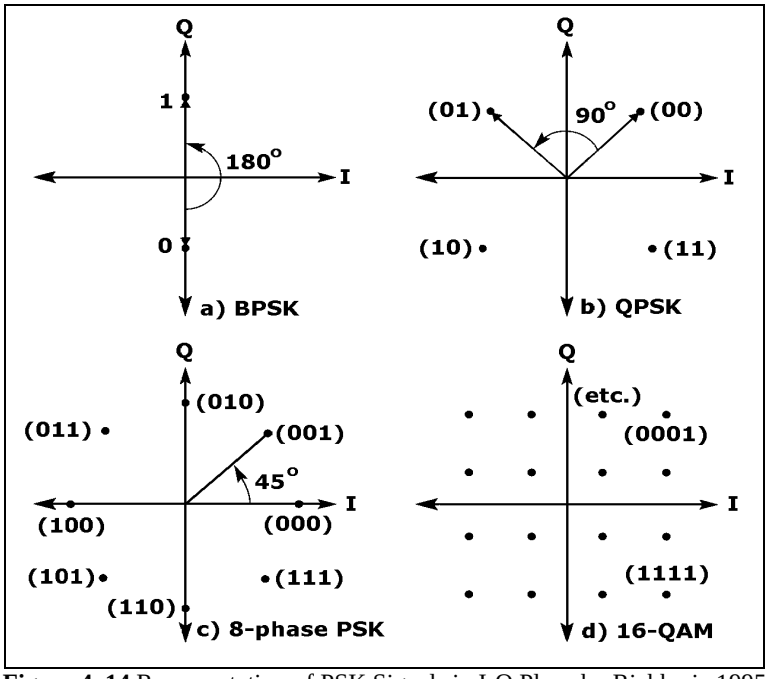

Figure 4. 14 Representation of PSK Signals in I-Q Plane by Richharia 1995

The demodulation signals are passing out via Low Power Filter (LPF) and Logic circuit. The bits values u_i and u_q are selected alternately from the input bit stream. For example, u_i may represent the odd number bits and u_q the even number bits. In this case, one binary data channel enters the QPSK modulator and the outgoing symbol rate is equal to half of the incoming bit rate. The octal phase modulation, known as 8-phase PSK, is a constant amplitude scheme with a higher bandwidth efficiency of 3 b/s/Hz, as shown in Figure 4.14 (c). Thus, **t**he demands of high bit-rate applications are related to images, video, TV and High Definition Television (HDTV) transmissions.

4.3.7.3 Offset QPSK (O-QPSK)

The O-QPSK scheme delays the quadrature bit stream by T sec relative to the in-phase bit stream to restrict the phase transition to phase changes of 0 or $\pi/2$ every T sec. Using a^I_n and a^Q_n, the equivalent low-pass and resulting signals are expressed by:

$$u(t) = \sum_{n=0}^{\infty} a^I_n\, p(t)\,(t - 2nT) - j a^Q_n\, p(t)\,(t - 2nT - T)\, e^{j\pi/4}$$

$$s(t) = [\sum_n a^I_n\, p(t)\,(t - 2nT)] \cos(2\pi f_c t + \pi/4) + [\sum_n a^Q_n\, p(t)\,(t - 2nT - T)] \sin(2\pi f_c t + \pi/4) \quad (4.25)$$

The data transmission occurs in the conventional QPSK at the same time in both I and Q channels. This scheme has larger phase changes than O-QPSK, which has phase changes of, at most, $\pm\pi/2$ data transmission and large envelope fluctuations do not occur as they do with Π-phase changes in QPSK. Figure 4.13 (C) shows the O-QPSK modulated signal's shape.

The Aloha O-QPSK (1/2-FEC) serves in return request channels by a transmission speed of 24 Kb/s, while 16 Kb/s or 9.6 Kb/s uses the APC O-QPSK scheme in voice channels.

4.3.7.4 Differential PSK (DPSK)

Channel conditions in mobile communications are more severe than additive white Gaussian noise channels due to multipath fading, shadowing and Doppler effects. These problems can be solved by using differentially coherent detection of encoded signals. The received signal phase is generally an 180^o ambiguity sign, which cannot be resolved unless some known reference signal is transmitted and a comparison made. In the worst case, if such a case is left unresolved, the received signal could end up being the complement of the transmitted signal. When the phase condition is constant for 2T seconds, the DPSK demodulator can obtain the optimum a posteriori probability. The DPSK scheme can also be used to remove sign ambiguity at the receiver. Differentially encoding data prior to modulation occurs when a binary 1 is used to indicate that the current message bit and prior code bit are of the same polarity and 0 to represent the condition when the two pulses are of opposite polarity (Richharia, 1995). The equivalent low-pass signal in the interval of m is given by:

$$v_m = \alpha e^{j(\phi m-\phi)} u_m(t) + n_m(t) \quad (4.26)$$

where α = loss factor; ϕ_m = phase difference in m interval; $u_m(t)$ = signal in m interval and $n_m(t)$ = Gaussian noise in m interval. The non-coherent detection technique is useful when the carrier phase is difficult to estimate at the receiver. In satellite channels, the transmitting oscillator that generates the carrier cannot be completely stabilized and a satellite link has a low S/N ratio. Besides, for coherent detection, the bandwidth of the carrier-tracking loop at the Rx must be decreased in the proper manner to increase the S/N and obtain a good phase reference.

Since propagation characteristics such as multipath fading and the Doppler effect cause rapid phase variation, the carrier phase of the Rx signal does not remain fixed long enough to be estimated. The problem can be solved with non-coherent detection, which is equivalent low-pass signal in relation to random phase value (ϕ_n) and Gaussian noise is:

$$v_m = \alpha e^{-j\phi n} u_n(t) + n(t) \quad (4.27)$$

Therefore, non-coherent detection results in the degradation of the bit error performance with respect to coherent detection. In this case, the BER probability (P_b) for binary DPSK is determined with the following relation:

$$P_b = \tfrac{1}{2} \exp(-\gamma_b) \quad (4.28)$$

where $\gamma_b = E_b/N_0$ is the value of the S/N density ratio per bit signal. In this sense, when considering the use of DPSK schemes, a trade-off between simplified receiver complexities against reduced performance characteristics in the presence of noise, particularly when employing higher order modulation techniques, needs to be made.

4.3.7.5 π/4-QPSK

Recently, π/4-QPSK, or π/4 shift QPSK, has become very popular for mobile satellite as well as for cellular systems because it has a compact spectrum with small spectrum restoration

due to non-linear amplification and can perform differential detection. The phase point of this scheme always shifts its phase over successive time intervals by ±π/4 or ±3π/4. The spectrum of this scheme is the same as that of a QPSK that undergoes an instantaneous ±π/24 or ±π phase transition.

The π/4-QPSK signal can reduce the envelope fluctuation due to band-limited filtering or non-linear amplification more than can QPSK. In a more general sense, this is because differential detection can be used since π/4-QPSK is not an offset scheme.
For mobile channels, a strong line-of-sight signal can be expected even in the Rician fading channel, so, coherent demodulation is desirable for improved power efficiency. The bit error performance of coherently detected π/4-QPSK is the same as that of QPSK. On the other hand, differential detection is also desirable for simple hardware implementation. The bit error probability for differential coherer detected π/4-QPSK is given by:

$$P_b = e^{-2\gamma b} \sum_{k=0}^{\infty} (\sqrt{2} - 1)^k I_k (\sqrt{2\gamma_b}) - 1/2\, I_0 (\sqrt{2\gamma_b})\, e^{-2\gamma b} \quad (4.29)$$

where $\gamma_b = E_b/N_0$ and I_k = modified Bessel function of the first kind in k interval order. Thus, the differential detection is about 2 to 3 dB inferior to the coherent detection in AWGN and fading channels and non-coherent detection is also applicable. Due to these advantages, π/4-QPSK has been chosen as the standard modulation technique for several systems of cellular and satellite-based mobile communications. Some experimental results show that, in fully saturated amplifier systems, π/4-QPSK still has significant spectral restoration. In effect, to reduce this restoration, π/4-controlled transition QPSK (CTPSK) uses both sinusoidal shaping pulses and timing offsets of the phase transition between I and Q channels.

4.4 Channel Coding and Decoding

Voice, video, data and telex information are transmitted in digital form through a channel that can cause degradation of these transmission signals. The noise, interference, fading and other obstacle factors experienced during transmission could increase the probability of bit error at the receiver. On the contrary, the data signal may be encoded in such a way as to reduce the likelihood of bit error. Anyway, the coding process uses redundant bits, which do not contain information to assist in the detection and correction of errors. The subject of coding emerged following the fundamental concepts of information theory laid down by Shannon in 1948, which is the relationship between communication channel and the rate at which information can be transmitted over it. Basically, the theorems laying down the fundamental limits on the amount of information flow through a channel are given (Ohmori et al, 1998).

4.4.1 Channel Processing

Channel processing is composed of special activities, which can improve the transmission techniques throughout satellite channels in connection with gain, errors, noise, interference, concentration and authenticity.

4.4.1.1 Digital Speech Concentration and Channel Multiplication

The system for digital speech concentration (interpolation) uses the activity factor of telephone channels in order to reduce the number of satellite channels required to transmit a

given number of terrestrial channels. The Digital Speech Interpolation (DSI) technique is based on the fact that, in a normal telephone conversation, each participant monopolizes the circuit for only around half the time.

As the silence between syllables, words and phrases increases, so does the unoccupied time. Hence, on average, the activity time of a circuit is from 35% to 40% of the connection time. By making use of the actual activity of the channels, several users can be permitted to share the same telephone circuit. Certain numbers of terrestrial satellite channels require only half the satellite channels and the gain is about 2. By adding a low rate encoder to the digital speech concentrator, the gain can be further increased.

For example, with encoding at 32 Kb/s, a gain increase by a factor of 2 can be obtained in voice channels used alternately for speech or data transmission. The theoretical DSI gain is defined by the ratio between the actual number of speakers (input trunks) and the number of transmission channels (bearers) required to service them.

On the other hand, the function of the Digital Circuit Multiplication (DCM) equipment is to concentrate a number of input digital lines (trunks) onto a smaller number of digital output channels (bearers), thereby achieving a higher digital efficiency of the link or channels. This technique is qualified by the circuit multiplication gain, which is defined as the ratio of the input channels' number over the number of DCM output channels. It is used in digital circuit multiplication equipment of the Intelsat/Eutelsat system.

4.4.1.2 Channel Encoding

The two fundamental problems related to reliable transmission of information via channels were identified by C.E. Shannon as follows:

1) The use of minimal numbers of bits to represent the information given by a source in accordance with a fidelity criterion. In reality, this issue is usually identified as a problem of inefficient channels, to which the source coding provides most practical solutions.
2) The recovery as exactly as possible of the information after its transmission through a communication channel in the presence of noise and other interference. This is a problem of unreliable satellite systems, to which channel (error) coding is the basic solution.

Shannon proved that, by proper encoding, these two objectives can always be achieved, provided that the transmission rate (R_b) verifies the fundamental expression $H<R_b<C$, where H = source entropy and C = channel capacity. The BER of a digital system may be improved either by increasing E_b/N_0 or by detecting and correcting some of the errors in the received data. For the Additive White Gaussian Noise (AWGN) channel, the Shannon Hartley law states that capacity of a channel is given by the following relation:

$$C = B \log (1 + C/N) \quad [b/s] \tag{4.30}$$

where B = channel bandwidth in Hz and S/N = signal-to-noise ratio at the receiver. Thus, the channel capacity is the measure rate of the maximum information quantity that two parties can communicate without error via a probabilistically modeled channel. This chain of channels is composed of information data on input rate (R_b), channel encoder with redundancy data (r) and encoded data symbols on output rate (R_c). A reverse channel model contains input encoded data symbols, channel decoder and output information data symbols.

According to Shannon, if information is provided at rate R, which is less than the capacity of the channel, then a means of coding can be applied such that the probability of error of the received signal is arbitrarily small.

If this rate is greater than the channel capacity, then it will not be possible to improve the link quality by means of coding techniques. Indeed, its application could have a detrimental effect on the link. Rearranging the above equation in terms of energy-per-bit and information rate, where the information rate is equal to the channel capacity, results in the following:

$$C/B = \log (1 + E_b\, C/N_0 B) \qquad (4.31)$$

where E_b = information bit rate; E_b = related to the carrier power and the information bit rate and C/N_0 = Carrier-to-Noise Density Ratio. Moreover, the above expression can be utilized to derive the Shannon limit, the minimum value of Eb/N_0 below which there can be no error-free transmission of information. As C/B tends to zero, this can be shown to be equal to – 1.59 dB ($1/\log_2 e$). The code rate and input rate can be defined as:

$$c = n/n + r \quad \text{and} \quad R_c = R_b/n \quad [b/s] \qquad (4.32)$$

The capacity of the channel is independent of the coding/modulation scheme used. Hence, Shannon's channel coding theorem exactly stated that, for a given carrier-to-noise ratio, the error probability could be made as small as desirable, provided that the information rate (R_b) is less than the capacity (C) and a suitable coding is used.

In any case, channel coding is especially interesting because of the severe power, bandwidth and propagation limitations. Moreover, the considerable progresses in multiple access modulation schemes, resource assignment algorithms, signal processing techniques and advanced error control coding provide the most efficient means to realize highly reliable information transmission.

4.4.1.3 Digital Compression

Digital transmission, in general, uses compression techniques for data and video signals. The effective data transfer can be significantly increased by using data compression software. Essential results were provided on PC by the PKZIP/PKUNZIP program developed by US-based PKWARE, which, in a fraction of a second, gives a 2 to 3 times reduction in size of ASCII files and 1.5 times reduction for many types of binary files. The ARJ compression software from Robert K. Jung is slower but more effective than PKZIP. It can also be recommended for the compression of data files containing graphic information. Thus, the real-time data compression incorporated into the most advanced modems can also increase the effective data rate of ASCII files transmission but, for transmission of already compressed files with information, it is better not to use the compression in the modem.

Their use in compressed video systems, where a TV Receive Only (TVRO) can also receive many channels of video from one transponder (about 6 to 8), has become very widespread, first in the USA and then in Europe. The compression system that has now become standard refers to an MPEG standard, formed under the auspices of the ISO and the International Electrotechnical Commission (IEC). In such a system, a number of digitized videos are combined into a single bit stream in a source coder. That bit stream is then sent to a channel coder for FEC and then to a QPSK modulator, an up-converter, amplifier and an antenna for

up linking to the satellite transponder. Since only one signal is present in the transponder at any on time, there is no need for back-off and full transponder power is used. At the reverse side, the compressed video downlink comprises a line in the chain of an antenna, tuner including down-converter and QPSK demodulator, then FEC detector, demultiplexer and MPEG decoder. The MPEG is determined to provide standard compression that allows video and accompanying audio signals to be compressed in channel width. The packetizer function is to enter a suitable code in the bit stream for the individual digitized TV program so that it can be separated in the receiving chain, allowing the enabled user to select the desired program. Thus, the BER is determined from the (E_b/N_0) obtained for a combination of whatever transponder EIRP, FEC coding, transmission symbol rate and receiver system are used.

If a plot of that FEC system is not available, then the Viterbi mode FEC coding performance could be used for a good estimate of results. This type of compression has effects like: MPEG-2 compression results in the removal of most audio and video redundancy; the FES utilization scheme resulting in a rapid BER increase and the resultant (E_b/N_0) should be high enough to achieve a BER of 10^{-6} for a TVRO.

4.4.1.4 Voice Encryption

Encryption is used when it is wished to prevent exploitation or tampering with transmitted messages or voice conversation by unauthorized users, in the form of algorithmic operation in real time, bit-by-bit, on the binary stream.

Thus, the set of parameters, which defines the transformation, is called a key. Its use is often associated with military communications but commercial satellite systems are increasingly induced by customers to propose encrypted links, particularly for administrative and government sectors. In fact, due to the extended coverage of satellite networks and the easy access to them by small UES, eavesdropping and message falsification are potentially within the reach of a large number of agents of modest means.

The encryption transmission chain is composed of an encryption unit with plain text input, satellite channel with intruder and key distribution for retransmission of cipher (encrypted) text and de-encryption with a unit for production of plain output text. The encryption and de-encryption units operate with a key provided by the key generation unit. Acquisition of a common key implies a secure method of key distribution. This key is entered into the encryption unit through a key injector about the size of a matchbox. Without this key, a potential eavesdropper attempting to listen in on the conversation would hear nothing but a noise made up of digital signals (Sheriff et al, 2001).
The technique used for most voice encryption consists in speech compressing and digitizing, using a very complicated coding process. In such a way, the voice signal is sliced into small bits, which are processed by an algorithm into bits of voice with a very complex structure. At the other end of the process, using the same key pattern, the voice is reproduced as it was before the encryption.

A typical example of voice encryption is Satsec A1 for secure satellite voice transmission, of Inmarsat standard-A UES. This unit is housed in a modern smart telephone, which uses a very sophisticated Swiss encryption technique. The Satsec A1 features include full digital voice and facsimile encryption and LPC voice compression, using full duplex operations CCITT V.22bis and V.27 Modem with a rate of 2400 b/s, giving business users a security

level comparable to that used by government agencies. In case of transmission only in half duplex mode, the unit automatically falls back to the built-in VOX-controlled quasi-duplex operational mode (Ilcev, 2009).

Hence, this device should not be confused with a voice scrambler, even a digital one, which is no longer a competitive alternative to high level encryption. The unit digitizer uses linear predictive coding and has, unlike self-synchronizing stream ciphers, no bit error multiplication. In a more general sense, under the same circumstances, this device may even have an enhanced effect on the channel is quality of transmission.

The aspects of encryption are confidential to avoid exploitation of the voice/message by unauthorized persons and to provide authentic protection against any modification of the message by an intruder. This system uses the following techniques:

1. On-line encryption (Stream Cipher) - Each bit of the original binary message stream (plain text) is combined using a simple operation, for example, modulo-2 addition, with each bit of a binary stream (keystream) generated by a key device. Otherwise, the latter could be a pseudorandom sequence generator whose structure is defined by the key.
2. Encryption by Block (Block Cipher) - The transmission of the original binary stream message into an encrypted stream is performed simply block-by-block, according to the logic defined by the key. Besides, encryption is commonly used in direct TV broadcasting to avoid illegal reception and military applications to minimize the probability of message interception. The principle of encryption and decryption unit for text is that both operate with a key generation unit. At this point, a key generation unit provides the necessary key outputs to encryption and decryption units.

4.4.2 Coding

As is known, satellite communication systems are generally limited by the available power and bandwidth. Thus, it is of interest if the signal power can be reduced while maintaining the same grade of service (BER). As mentioned, this can be achieved by adding extra or redundant bits to the information content by using a channel coder. Otherwise, except for several main classes of channel coder, the three most widely used in satellite communications are block, cyclic and convolutional encoders (Calcutt and Tetley, 2004).

4.4.2.1 Block Codes

Binary linear block codes are expressed in the (n, k) form, where (k) is the information bits number that is converted into (n) code word bits. There are (n, k) party bits in each encoded block, where the difference between (n) and (k) bits are added by the coder as a number of redundancy bits (r). In other words, a coded block comprising (n) bits consists in (k) information and (r) redundant bits expressed as follows:

$$n = k + r \tag{4.33}$$

Such a code is designated as a (n, k) code, where the code rate or code efficiency is given by the ratio of (k/n). Mapping between message sequences and code words can be achieved using look-up tables; although, as the size of the code block increases, such an approach

becomes impractical. This is not such a problem as linear code words can be generated using some form of linear transformation of the message sequence. Thus, a code sequence (c) comprising of the row vector elements (c_1, c_2,…, c_n) is generated from a message sequence (m), comprising the row vector elements (m_1, m_2,…, m_k) by a linear operation:

$$c = m\,G \tag{3.34}$$

where G = generator matrix. Thus, in general, all (c) code bits are generated from linear combinations of the (k) message bits.

A special category known as a systematic code occurs when the first (k) digits of the code are the same as the first (k) message bits, namely, if input message bits appear as part of the output code bits. The remaining (n-k) code bits are then generated from the (k) message bits using a form of linear combination, and they are termed the party data bits.

The generator matrix for a linear block code is one of the bases of the vector space of valid codewords. The generator matrix defines the length of each codeword (n), the number of information bits (k) in each codeword and the type of redundancy that is added; the code is completely defined by its generator matrix. The generator matrix is a (k · n) matrix, that is, the row space of V_k.

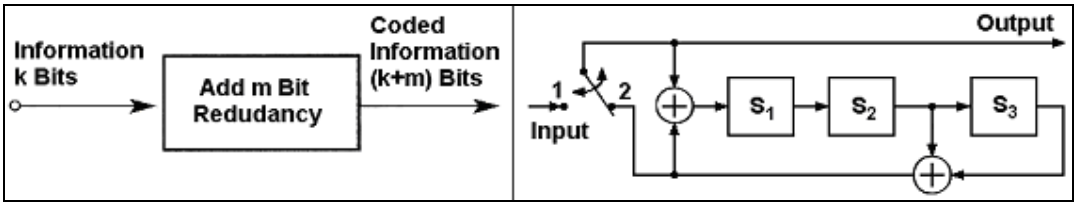

Figure 4. 15 Block and Cyclic Coders by Calcutt and Tetley 2004

Thus, one possible generator matrix for a typical (7, 4) linear block code has to be presented in four rows as blocks: G = 1101000/0110100/1110010/1010001. The distance between two coded words (for example, first 2 and second 2 digits) in a block is defined as the number of bits in which the words differ and is called the Hamming distance (d_h). The Hamming distance has the capability to detect all coded words having errors (e_d), where $e_d < (d_h - 1)$; to detect and correct (e_{dc}) bits, where $e_{dc} = (d_h - 1)/2$ and to correct (t) and detect (e) errors, where the Hamming distance, as a minimum space between two coded blocks, is given by:

$$d_h = t + e + 1 \tag{4.35}$$

In the detection process, two coded words separated by (d_h) are most likely to be mistaken for each other. The extended Golay code offers superior performance to Hamming codes but at a cost of increased receiver complexity. In practice, code words are conveniently generated using a series of simple shift registers and modulo-2 adders.

Figure 4.15 (Left) shows the concept of block codes and rate, which operate on groups of bits organized as blocks, namely, information bits are assembled as blocks before coding.

4.4.2.2 Cyclic Codes

The cyclic code methods are a subclass of linear codes, whose code word is generated simply by performing a cyclic shift of its predecessor, as shown in Figure 4.15 (Right). In other

words, each bit in a code sequence generation is shifted by one place to the right and the end bit is fed back to the start of the sequence, hence, the term cyclic. Both the linear Hamming and extended Golay codes have equivalent cyclic code generators. Thus, non-systematic cyclic codes are generated using a unique generator polynomial g(p) and message polynomials in the forms presented by the following relations:

$$g(p) = p^{n-k} + g_{n-k}p^{k-1} + \ldots g_1 p + 1 \quad (4.36)$$

$$m(p) = m_{k-1}p^{k-1} + m_{k-2}p^{k-2} + \ldots + m_1 p + m_0 \quad (4.37)$$

where the generator polynomial is a factor of p^{n+1} and the value ($m_{k-1}\ldots m_0$). When this is multiplied by the generator polynomial, it results in the generation of a code word by:

$$c(p) = (m_{k-1}p^{k-1} + m_{k-2}p^{k-2} + \ldots + m_1 p + m_0)\, g(p) \quad (4.38)$$

Thus, an alternative to this approach is to generate systematic cyclic codes, which can be generated in three steps, involving the use of feedback shift register:

a) The message polynomial is multiplied by p^{n-k}, which is equivalent to shifting the message sequence by (n – k) bits. This is necessary to make space for the insertion of the party bits;
b) The product of step 1, $p^{n-k}m(p)$ is divided by the generator polynomial, g(p); and
c) The remainder from step 2 is the party bit sequence, which is then added to the message sequence prior to transmissions.

The cyclic codes scheme has two methods used in satellite communications, naamely: Bose-Chadhury-Hocquenghem (BCH) and Reed-Solomon (RS).

1. BCH Codes – The BCH codes are the most powerful of all cyclic codes with a large range of block length, code rates, alphabets and error correction capability. These codes have been found to be superior in performance to all other codes of similar block length and code rate. Most commonly used BCH codes have a code word block length as $n = 2^m - 1$, where (m = 3, 4 …). For instance, the Inmarsat standard-A uses 57 bits plus 6 party bits encoded with BCH (63, 57 code in TDM channels and for the return request channel burst employs Aloha BPSK (BCH) 4800 b/s.

2. RS Codes – The RS codes are a subset of the BCH codes specially suited for correcting the effect of the burst errors. The latter consideration is particularly important in the context of the satellite channels and, hence, RS codes are usually incorporated into the system design. This set of codes has the largest possible code minimum distance of any linear code with the same encoder input and output block length. At this point, the RS codes are specified using the convention RS (n, k), where n = number of code symbols word length per block; k = data symbols encoded and the difference between (n) and (k) is the number of parity symbols added to the data. The code minimum distance is given by:

$$d_{min} = n - k + 1 \quad (4.39)$$

The code is capable of correcting errors such as: $e = 1/2\,(d_{min} - 1)$ and $e = (n - k)/2$, or to use an alphabet of 2^m symbols with: $n = 2^m - 1$ and $k = 2^m - 1 - 2e$, where m = 2,3 … and so on. The advantage of RS codes is the reduction in the number of words (n) symbols, which are code words, producing a possibly large value of minimum distance (d_{min}).

4.4.2.3 Convolutional Codes

The second family of commonly used codes is known as convolution codes. Unlike block codes, which operate on each block independently, these codes retain several previous bits in memory, which are all used in the coding process. They are generated by a typed-shift register and two or more modulo-2 adders are connected to a particular stage of the register. The number of bits stored in the shift register is termed the constraint length (K). Bits within the register are shifted by (k) input bits. Each new input generates (n) output bits, which are obtained by sampling the outputs of the modulo-2 adders. The ratio of (k) to (n) is known as the code rate. These codes are usually classified according to the following convention: (n, k, K), for example, (2, 1, 7) refers to a half-rate encoder of constraint length 7. It is important to know what sequence of output code bits will be generated for a particular input stream. There are several techniques available to assist with this question, the most popular being connection pictorial, state diagram, tree diagram and trellis diagram (Richharia, 1995).

However, to illustrate how these methods are applied, the simple example of half-rate (1/2) encoder will be considered with constraint length k = 3. The system has two modulo-2 adders, so that the code rate is 1/2. The input bit (m) placed into the first of the shift register causes the bits in the register to be moved one place to the right. The output switch samples the output of each modulo-2 adder, one after the other, to form a bit pair for the bit just entered.

The connections from the register to the adders could be one, two or three interfaces for either adder. The choice depends on the requirement to produce a code with good distance properties. A similar encoder used by the Inmarsat standard-A is a half-rate convolutional encoder. Therefore, in terms of connections to the modulo-2, adders can be defined using generator polynomials in the encoder configuration.

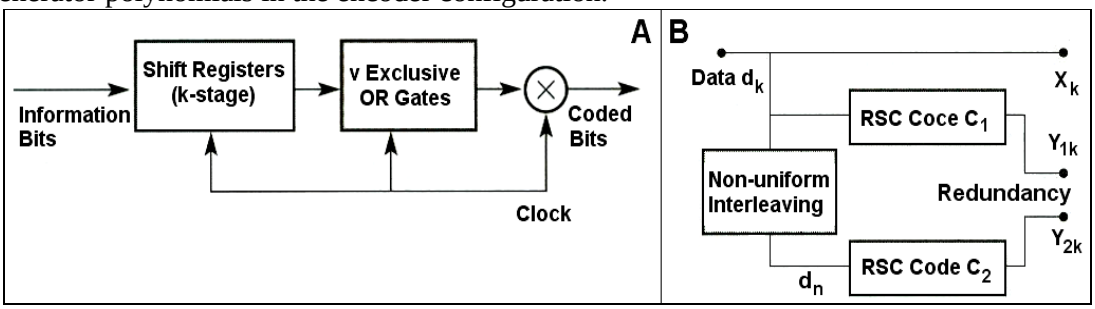

Figure 4. 16 Convolutional and Turbo Coders by Richharia 1995

Thus, convolutional codes form in a convolutional coder by convolving information bits R with the impulse response of a shift register encoder, which is shown in the block diagram in Figure 4.16 (A). These types of codes use previous information bits in memory (v) and continuously produce coded bits. The constraint length of convolutional code defines the number of information bits, which influence the encoder output. Therefore, the constraint length is decided by the number of shift registers or code memory. The error correcting property of the convolutional code depends on the constraint length and its value improves as code memory is increased, and, in such a way, decoding complexity increases.

The polynomial for the generating arm (n) of the encoder value $g_n(p)$ and the generator polynomials representing encoder $g_1(p)$ can have the following relations:

$$g_n(p) = g_0(p) + g_1p^1 + \dots g_np^n \quad (4.40)$$

$$g_1(p) = 1 + p + p^2 = 1 + p^2 \quad (4.41)$$

where the value of g_1 takes on the value of 0 or 1 and 1 is used to indicate that there is a connection between a particular element of the shift register and the modulo-2 adder. Thus, to provide a simple representation of the encoder, generator polynomials are used to predict the output coded message sequences for given input sequences. For instance, the input sequence 10110 can be represented by the polynomial relation:

$$m(p) = 1 + p^2 + p^3 \quad (4.42)$$

The output code sequence c(p) is obtained by interleaving the above two products presented in the following quotation:

$$c(p) = [1,1]p^0 + [1,0]p^1 + [0,0]p^2 + [0,1]p^3 + [0,1]p^4 + [1,1]p^5 \quad (4.43)$$

Here, the number between brackets represents the output code sequence.

The Inmarsat analog standard-A uses a HSD channel encoding configuration for the information data stream at 56 Kb/s. The scrambling sequence on the input data stream shall be provided by the scrambler before the convolutional encoder described in CCITT Recommendation V.35 scheme.

The data stream then passes differential encoder state stage 1 followed by 1/2 (half) convolutional encoding with constant length k = 7. The half (1/2) rate convolutional encoder can provide two data streams to the QPSK modulator using two generator polynomials rates as follows: $G_1 = 1 + x^2 + x^3 + x^5 + x^6$ and $G_2 = 1 + x + x^2 + x^3 + x^6$. The encoder provides two parallel data streams to the modulator: I and Q, while (Q) should lag (I) by 90^o in the modulator.

The punctured coding is used to derive 3/4 and 1/2 rates. All BPSK channels are differentially encoded outside the FEC. The Inmarsat maritime and aero standard-M for all transmissions, with the exception of those fields carrying digitally coded voice, employs FEC with convolutional encoding of constraint length k = 7 and 8-level soft decision Viterbi decoding.

There are two generator polynomials rates: G_1 (133 octal) and G_2 (171 octal). The transmitted bit is nominated by 1 and deleted by 0. However, the first bit in each transmission frame is the output from the G_1 polynomial and all bits are transmitted at the rate of 1/2 code. Finally, the output data from the bit selector are punctured coded data of 3/4 rate.

4.4.2.4 Concatenated Codes

These codes were originally developed for deep space communications and occur when two separate coding techniques are combined to form a large code. The inner decoder is used to correct most of the errors introduced by the channel, the output of which is then fed into the outer decoder, which further reduces the BER to the target level. That is to say, a typical concatenated coding scheme would employ half-rate convolutional encoding of constraint length 7 (2, 1, 7) – Viterbi decoding as the inner scheme and RS (255, 223) block encoding

and decoding as the outer scheme. Interleaving between the inner and outer coders can be used to further improve the performance.

4.4.2.5 Turbo Codes

Turbo Codes are a new class of error correction codes that were introduced in 1993 by a group of researchers from France, along with a practical decoding algorithm. Figure 4.16 (B) **s**hows a basic rate 1/3 turbo coder. At this point, it feeds data stream d_k directly into a Recursive Systematic Convolution (RCS) coder c_1 after interleaving into another RCS coder C_2, which is not necessarily identical to C_1. In addition, the transmitting bit stream compresses symbol X_k and redundancies Y_{1k} and Y_{2k}, and is, therefore, a rate 1/3 code or it may be punctured to give a higher code rate. The major importance of these codes is that they enable reliable transmission with power efficiencies close to the theoretical limit predicted by Claude Shannon.

Since their introduction, turbo codes have been proposed for low-power applications such as deep space and satellite communications, as well as for interference limited applications such as third generation cellular/personal communication services. Due to the use of a pseudo-random interleaver, turbo codes appear randomly to the channel, yet possess enough structure so that decoding can be physically realized. Developed for deep space and satellite communication applications, turbo codes offer a performance significantly better than concatenated codes. However, they are generated using two or more recursive systematic convolutional code generators concatenated in parallel.

Here, the term recursive implies that some of the output bits of the convolutional encoder are fed back and applied to the input bit sequence. The first encoder takes the information bits as input. The key to the turbo code generation is the presence of a permuter, which performs a function similar to an interleaver; with the only difference being that the output sequence is pseudo-random. The permuter takes a block of information bits, which should be large to increase performance, for example more than 1 000 bits and produces a random, delayed sequence of output bits, which is then fed into the second encoder. In such a manner, the outputs of the two encoders are partly bits transmitted along with the original information bits. In order to reduce the number of transmitted bits, the party bits are punctured prior to transmission.

From various simulation results, it is recognized that turbo codes are capable of achieving an arbitrarily low BER of 10-5 at an Eb/No ratio of just 0.7 dB. For instance, in order to achieve this level of performance, large block sizes of 65,532 data bits are required. Due to this prohibitively enlarged block size, an original turbo code is not well suited for real time Tel communication systems such as IS-95 CDMA cellular standard. For that reason, the work on this problem has focused on the design of short block length codes, compatible with IS-95 standard.

4.4.3 Decoding

The complete transmission loop requires any type of encoder followed by modulation and transmitter via transmission channel to receiver, namely, to demodulator and decoder. In such a manner, decoding is the reverse method of coding and every type of decoding on the transmit side needs the same convenient decoding method on the receive side.

4.4.3.1 Block Decoding

The simplest means of decoding block codes is by a method of correlation whereby the decoder makes a comparison between the received code word and all permissible code words, selecting that word that gives the nearest match. This decoding scheme will also depend on whether error detection or error correction is required, since decoders generally cannot use soft decision outputs from the demodulator, unlike the decoders for convolutional codes

4.4.3.2 Convolutional Decoding

The effect of the transmission channel on the signal and the probability of detection of a 1 or 0 in the presence of Gaussian noise are important factors during detection. In such a manner, an output from the demodulator unit can be configured to give a correct decision regarding whether the incoming signal is 1 or 0. The process of decoding then depends on the two state inputs it receives (Richharia, 1995).

An alternative demodulator configuration allows quantization of the predicted level which gives the decoder more necessary information regarding the probable state of the demodulator output. For example, if 3 bit ($2^3 = 8$ levels) quantization occurs then 0 0 0 would suggest a firm valuation of the level received as a 0. On the other hand, a 0 0 1 scheme suggests the 0 is received close to the threshold and this valuation as a 0 is made with less certainty. The reason for quantization is to provide the convolutional decoder with more information in order to correctly recover the transmitted information with better error performance probability.

4.4.3.3 Turbo Decoding

The turbo decoder operates by performing an interactive decoding algorithm, resulting in the partial transfer of an a priori likelihood estimate of the decoded bit sequence between the constituent decoders. Initially, the received information bits, which may be in some error due to the influence of the channel, are used to perform a priori likelihood estimates by the respective decoders(Fujimoto, 2008).. In a more precise sense, the decoders employ a Maximum a Posteriori (MAP) algorithm to converge on the likely sequence of data transfer, after which the interaction between decoders ceases and the output sequence is obtained from one of the decoders

An interleaver can be placed between the output of Decoder 1 and the input of Decoder 2, to provide an additional weighted decision input into Decoder 2; similarly, a de-interleaver is placed at the output of Decoder 2, to provide feedback to Decoder 1. The decoding time is proportional to the number of interactions between decoders.

4.4.3.4 Sequential Decoding

A sequential decoder may be used for convolutional decoding and it operates in a similar manner to the Viterbi decoder. On receipt of the incoming code word sequence, this decoder will penetrate into the tree according to a decision made regarding the best path to follow. For that reason, using a trial and error technique, the decoder will progress as long as the chosen path appears correct, otherwise it will backtrack to try a different route. Thus, either

soft decision or hard decision decoding is possible with the sequential decoder, although a soft decision would considerably increase the computational time and storage space required.

4.4.3.5 Viterbi Decoding

Viterbi maximum likelihood decoding of convolutional codes provides the best possible results in the presence of random errors. Thus, in an attempt to match the output sequence received by the decoder, Viterbi's algorithm models the possible state transition through a trellis identical to that used by the encoder.

Accordingly, the Viterbi decoding algorithm is a maximum likelihood path algorithm that takes advantage of the remaining path structure of convolutional codes. This method works by modeling the possible state transitions of the encoder and finding the output sequence that matches most closely to that received by the decoder. Its task is to realize that not all paths through the encoder states can contribute to the final decoded output and that many paths can be rejected after each frame is received, which keeps the problem to manageable proportions. If the encoder remembers (v) bits, then there are 2^v possible memory states to be modeled by the decoder. Hence, this term dominates expressions for speed, complexity and cost of the decoder and currently imposes an upper limit of 8 to 10 on constraint length. By path maximum likelihood decoding means that of all the possible paths through the trellis, a Viterbi decoder chooses the convenient path, most likely in the probabilistic sense to have been transmitted (Richharia, 1995). Viterbi decoders easily make use of either hard or soft decision making. This decoding can incorporate soft decisions very simply, which will almost double the error correction power of the code and this can provide an additional gain of up to 3 dB. Otherwise, the procedure for choosing the best Viterbi scheme is to maximize constraint length within the limits of cost and speed, to find a nonsymmetrical code with the best value of d_∞ and to use soft decisions. The maritime Inmarsat standard-B and multipurpose M utilize an 8-level soft decision Viterbi decoding in their channels (constraint length = 7).

4.4.4 Error Correction

There are several methods (such as ADPCM) that reduce the number of redundant bits in speech, audio and visual signals in order to make more economic use of bandwidth. First of all, it is necessary to consider methods that require the deliberate addition of redundant bits to messages. The added bits are very carefully chosen and error correction systems make it possible to achieve large savings in the power required to realize low BER. At the receiver, the additional bits are used to detect any errors introduced by channels. To achieve this technique in satellite communications, FEC, ARQ and Pseudo-noise and Interleaving are employed.

It is also possible to combine FEC and ARQ in an integration form known as a Hybrid Error Correction (HEC) transmitting scheme. At this point, however, the HEC method is used to reduce BER and the number of retranslated blocks. Such an arrangement could also be used to provide feedback information to the transmitter regarding slow variations, such as a fading.

4.4.4.1 Forward Error Correction (FEC)

The FEC is a technique where errors are detected and corrected at the receiver. Thus, this scheme requires only a one-way transmission link, since the message contains parity bits used for detection and correction of errors. This technique only receives Tlx mode in radio and satellite one-way transmissions (Huurdeman, 1997).

The basic FEC technique used in satellite communications can be classified into two major (already explained) categories such as Convolutional and Block codes. The FEC coding resulting from convolutional coding is used in Inmarsat standards for some voice, telex and signaling channels. For example, Inmarsat standard-B uses a convolutional encoder of constraint length 7- and 8-level soft decision Viterbi decoder. The coding rate is either 3/4 or 1/2, while, for voice channel, the code rate 3/4 is used and is derived by puncturing the rate 1/2 with k = 7 convolutional code.

The association of both basic coding techniques results in an even more powerful FES scheme known as the concatenated coding system. This powerful FEC scheme has been introduced in recent years, resulting in a considerable increase of the service quality without appreciable expansion of bandwidth. Whereas the inner code, together with Viterbi decoding, can correct a large part of the random errors and very short error bursts, the residual errors at the outputs of the Viterbi decoder tend to be grouped in bursts.

Using a properly chosen interleaving that cuts the error bursts into shorter ones, a high rate Reed-Solomon code can be used as the outer code in order to correct most of these dispersed error bursts to achieve a very low BER. Thus, the introduction of concatenated coding and trellis-coded modulation into satellite communications is the most remarkable event in the domain.

An FEC scheme can improve the quality of a digital transmission link by the following two aspects: **a)** An BER reduction, closely related to the service quality criterion; and **b)** a saving in the E_b/N_0 or C/N_0 to be considered in the link budget. The E_b/N_0 or C/N_0 saving is often called the coding gain, expressed in dB as a difference at certain BER values, of the coded system and the reference non-coded one. In the comparison between different transmission schemes, E_b/N_0 is usually used because it is independent of the coding scheme, where the gain is given as follows:

$$G = (E_b/N_0)\,\text{ref} - (E_b/N_0)\,\text{cod} \quad [\text{dB}] \tag{4.44}$$

The merit of a coding system can also be appreciated in terms of the savings in C/N_0 and C/N, Then, considering information rate (R_b) and information transmission bandwidth, the equations for Carrier-to-Noise Density Ratio (C/N_0) and the Carrier-to-Noise Ratio (C/N) are:

$$(C/N_0) = (E_b/N_0) + \log R_b \quad \text{and} \quad (C/N) = (E_b/N_0) + \log R_b - 10 \log W \quad [\text{dB}] \tag{4.45}$$

A coding gain in E_b/N_0 means, in general, a gain in C/N but the coding in C/N depends on the bandwidth expansion with respect to the reference system. It is, however, possible to have a coding gain without bandwidth expansions using Trellis Coded Modulation (TCM).

4.4.4.2 Automatic Request Repeat (ARQ)

The ARQ is a technique with which a high degree of data integrity is required and latency is not a significant factor. In reality, the ARQ scheme, based on error detection coding and a retransmission protocol, is well adapted to the situation where a two-way channel is available (Maral et al, 2009).

Typical examples of such systems can be encountered in a computer data network using satellite links. However, it is worthy of notice that the ARQ and improved ARQ, as well as HEC techniques, are widely used in modern digital communications and storage systems.
The ARQ method requires a two-way link, since a receiver, detecting an error, does not attempt to correct it but simply requests the transmitter to retransmit the message. Thus, the ARQ scheme basically works with the following modus:

1. Stop and Wait ARQ – After each message block is sent via satellite link, the transmitter waits for acknowledgement. If the message block received is in error, the transmitter will retransmit that block but if this message is correctly received, the next message block is transmitted. A half-duplex link is required, and transmission on the link is possible in both directions but not at the same time.
2. Continuous ARQ with Repeat – The transmitter sends and the receiver acknowledges message blocks continuously. Hence, any message block not correctly received causes the transmitter to return to the block in question (incorrect received block) and recommences continuous retransmission from there. A full-duplex link is necessary for transmission in both directions simultaneously.
3. Continuous ARQ with Selective Repeat – In this ARQ arrangement, only the block received in error is retransmitted and the transmitter continues from where it left off at the last block, instead of repeating all the subsequent even correctly received messages. However, a full-duplex link is also necessary for transmission in both directions simultaneously.
A major advantage of ARQ mode compared with FEC is that decoding equipment for error corrections can be simpler and the redundancy in the total message stream is less. The ARQ efficiency is good for low error ratios but for high ratios requiring retransmission of a large number of message blocks, the system becomes inefficient.

A disadvantage of ARQ is the variability of the delays experienced from end-to-end of the link and the possible requirement for large data stores of incoming data blocks.

4.4.4.3 Pseudo Noise (PN)

The PN generator will produce a set of cyclic codes with good distance properties. Thus, the name of the sequence is given, because the sequence, although deterministic, appears to have the properties of sampled white noise.

Furthermore, a PN sequence is easily generated using shift registers, and has a correlation function that is high packet for zero delay and approximates to zero for other delays. The PN sequence, being deterministic, is usually for synchronization purposes between a transmitter and receiver.

The scrambler/descrambler circuits are clocked at the rate of one shift per information bit. The first bit into the scrambler at the beginning of a frame is modulo-2, added with the output

of the scrambler shift generator, corresponding to the initial state-scrambling vector. The initial state of the shift register is located at the beginning of a burst and a frame.

Considering the Inmarsat standard-M, the initial state of the scrambler shift registers at the GES (for SCPC channel operating in voice mode) and is sent to the GES by the UES at the start of a call as part of a call set-up sequence.

The UES chooses any initial state (except all zeros) on a random basis for each call and signals this scrambling vector message (8D in hexadecimal form or 10001101) for implementation at the GES with the Least Significant Bit (LSB) in shift register No 1 and the Most Significant Bit (MSB) in shift register No 15 of the scrambler. The UES simultaneously sets the descrambler shift register with the same scrambling vector. Otherwise, for MES-to-GES channels, a fixed initial state default value of 6,959 in hexadecimal form or 110100101011001 is used in UES scramblers and GES descramblers.

4.4.4.4 Interleaving

As is well known, the satellite transmission channel introduces errors of a bursting nature. Hence, in the short term, the errors introduced by the channel cannot be considered to be statistically independent of memory less, the criterion upon which most coders (block and convolutional) optimally operate. In order to mimic a statistically independent channel, a technique known as interleaving is incorporated into the transmitter chain after the output of the encoder and from the interleaver the input signal passes via the modulator. In reverse mode, the output signal goes through the demodulator, deinterleaver and channel decoder. This circle presents the interleaver/deinterleaver segment within the transmission/reception chain in the satellite link. Hence, the role of the interleaver is to re-order the transmission sequence of the bits that make up the code words in some predetermined fashion, such that the effect of an error burst is minimized (Richharia, 1995).
Interleaving can be performed for both block and convolutional codes. Block interleaving is achieved by firstly storing the output code words of the encoder into a two-dimensional array. Consider the case of an $(m \cdot n)$ array, where (m) is the number of code words to be interleaved and (n) is the number of code word bits. Thus, each row of the array comprises a generated code word. Once the array is full, the contents are then output to the transmitter but, in this case, data is read out on a column-by-column basis. Generally speaking, the transmission of each symbol of a particular code word will be non-sequential. The input signal goes via the input sequence into the interleaver block and after processing the output sequence would correspond to the chain starting with C_{11}, C_{21}, C_{31}, C_{41}, C_{51}, C_{61}, C_{71}, C_{12}-C_{72}, … until C_{18}-C_{78}. At this point, the effect of any error bursts will have been dispersed in time throughout the transmitted code words. Convolutional interleavers work along similar lines, achieving performance characteristics similar to block interleaving.

At the receiver, the inverse of the interleaving function is performed by a deinterleaver and the original code words are reconstituted prior to feeding into the encoder. A burst of error affecting the transmitted bits indicated by the chain coming from the interleaver block would be dispersed among the code words at the receiver.

4.5 Multiple Access Technique

In satellite communication systems, as a rule, many users are active at the same time. The problem of simultaneous communications between many single or multipoint satellite users,

however, can be solved by using the Multiple Access (MA) technique. Since the resources of the systems such as the transmitting power and the bandwidth are limited, it is advisable to use the channels with complete charge and to create a different MA to the channel (Ilcev, 2013).

This generates a problem of summation and separation of signals in the transmission and reception parts, respectively. Deciding this problem consists in the development of orthogonal channels of transmission in order to divide signals from various users unambiguously on the reception part. There are five principal forms of MA techniques:

1) Frequency Division Multiple Access (FDMA) is a scheme where each concerned GES or UES is assigned its own different working carrier radio frequency inside the spacecraft transponder bandwidth.
2) Time Division Multiple Access (TDMA) is a scheme where all concerned Earth stations use the same carrier frequency and bandwidth with time sharing, non-overlapping intervals.
3) Code Division Multiple Access (CDMA) is a scheme where all concerned Earth stations simultaneously share the same bandwidth and recognize the signals by various processes, such as code identification. Actually, they share the resources of both frequency and time using a set of mutually orthogonal codes, such as a Pseudorandom Noise (PN) sequence.
4) Space Division Multiple Access (SDMA) is a scheme where all concerned Earth stations can use the same frequency at the same time within a separate space available for each link.
5) Random (Packet) Division Multiple Access (RDMA) is a scheme where a large number of satellite users share asynchronously the same transponder by randomly transmitting short burst or packet divisions.

Currently, these methods of multiple access are widely in use with many advantages and disadvantages, together with their combination of hybrid schemes or with other types of modulations. Hence, multiple access technique assignment strategy can be classified into three methods as follows: **(1)** Preassignment or fixed assignment; **(2)** Demand Assignment (DA); and **(3)** Random Access (RA). The bits that make up the code words in some predetermined fashion, such that the effect of an error burst is minimized.

In the preassignment method, channel plans are previously determined for chairing the system resources, regardless of traffic fluctuations. Therefore, this scheme is suitable for communication links with a large amount of steady traffic. However, since most mobile users in satellite communications do not communicate continuously, the preassignment method is wasteful of the satellite resources. In Demand Assignment Multiple Access (DAMA), satellite channels are dynamically assigned to users according to the traffic requirements. Due to high efficiency and system flexibility, DAMA schemes are suited to satellite systems. In RA, a large number of mobile users use the satellite resources in bursts, with long inactive intervals. In effect, to increase the system throughout, several mobile Aloha methods have been proposed.

Therefore, the MA techniques permit more than two Earth stations to use the same satellite network for interchanging information. Several transponders in the satellite payload share the frequency bands in use and each transponder will act independently of the others to filter out its own allocated frequency and further process that signal for transmission.

Thus, this feature allows any GES located in the corresponding coverage area to receive carriers originating from several UES and vice versa and carriers transmitted by one UES can

be received by any GES. This enables a transmitting Earth station to group several signals into a single, multi-destination carrier. Access to a transponder may be limited to single carrier or many carriers may exist simultaneously. The baseband information to be transmitted is impressed on the carrier by the single process of multi-channel modulation.

4.5.1 Frequency Division Multiple Access (FDMA)

The most common and first employed MA scheme for satellite communication and other satellite transmission systems is the FDMA concept where transmitting radio signals occupy non-overlapping frequency bands with guard bands between signals to avoid interchannel interference. The bandwidth of a repeater channel is, therefore, divided into many sub-bands, each assigned to the carrier transmitted by an Earth station. The UES terminals transmit continuously and the channel transmits several carriers simultaneously at a series of different frequency bands.

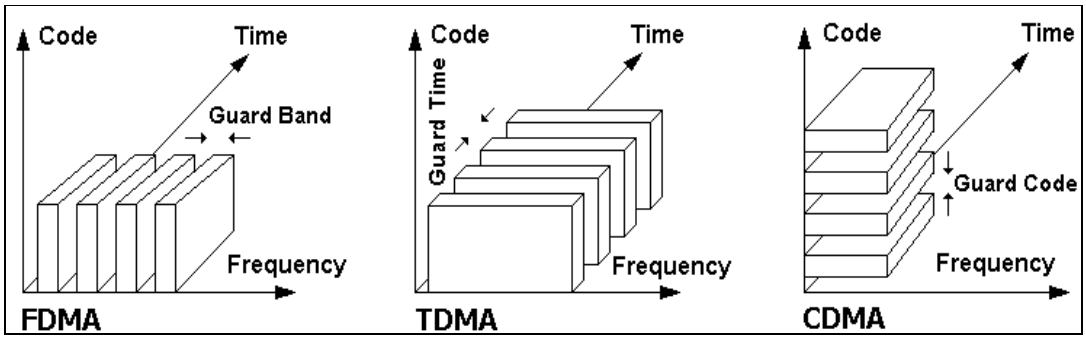

Figure 4. 17 Multiple Access Techniques by Ilcev 2013

Due to interchannel interference, it is necessary to provide guard intervals between each band occupied by a carrier to allow for the imperfections of oscillators and filters. The downlink Rx selects the required carrier in accordance with the appropriate frequency. When the satellite transponder is operating close to its saturation, non-linear amplification produces Intermodulation (IM) products, which may cause interference in the signals of other users. In order to reduce IM, it is necessary to operate the transponder by reducing the total input power according to input back off and the IF amplifier provides adequate filtering.

Therefore, FDMA allocates a single satellite channel to one user at once, as shown in Figure 4.17 (FDMA). In fact, if the transmission path deteriorates, the controller switches the system to another channel. Although technically simple to implement, FDMA is wasteful of bandwidth because the voice channel is assigned to a single conversation, whether or not somebody is speaking. Moreover, it cannot handle alternate forms of data. It can only handle voice transmissions. This system's advantages are that it is a simple technique using equipment proven over decades to be reliable and it will remain very commonly in use because of its simplicity and flexibility.

However, it does have the following disadvantages:

1) A FDMA method is a relatively inflexible system and if there are changes in the required capacity, then the frequency plan has to change and, thus, involve many GES.
2) Multiple carriers cause IM in both the UES HPA and in the transponder HPA. Reducing IM requires back off of the HPA power, so it cannot be exploited at full capacity.

3) As the number of carriers increase, the IM products between carriers also increase and more HPA back off is needed to optimize the system. The throughput decreases relatively rapidly with the number of transmission carriers. Therefore, for 25 carriers, it is about 40% less than with 1 carrier.
4) The FM system can suffer from what is known as a capture effect, where if two received signals are very close in frequency but of different strengths, the stronger one tends to suppress the weaker one. For this reason, the carrier power has to be controlled carefully.
Therefore, with the FDMA technique, the signals from the various users are amplified by the satellite transponder in a given allocated bandwidth at the same time but at different frequencies. Depending on the multiplexing and modulation techniques employed, several transmission hybrid schemes can be considered and, in general, may be divided into two categories, based on the traffic demands of GES on Multiple Channels Per Carrier (MCPC) and Single Channel Per Carrier (SCPC).

The main elements of the MCPC are multiplexer, modulator and transmitter using a satellite uplink, when GES multiplexes baseband data to the terrestrial network and destined for various UES. The multiplexed data are modulated and transmitted to the allocated frequency segment, when the bandwidth of the transponder is shared among several UES, each with different traffic requirements. The transponder bandwidth is divided into several fixed segments, with several time frequency divisions allocated to these UES terminals.

Between each band segment is a guard band, which reduces the bandwidth utilization efficiency and the loss is directly related to the number of accessing UES in the network, as shown in Figure 4.17 (FDMA). Depending on the number of receiving UES, a total number of carriers will pass through the satellite transponder.

The SCPS scheme is used for certain applications, such as the provision of satellite service to remote areas or individual UES. Traffic requirements are low. In reality, assigning multiple channels to each UES is wasteful of bandwidth because most channels remain unutilized for a significant part of the day. For this type of application, the SCPC type of FDMA is used. In the SCPC system, each carrier is modulated by only one voice or by low to medium bit rate data channel. Some old analog systems use Companded FM but most new systems are digital PSK modulated. In the SCPC scheme, each carrier transmits a single carrier.

There are several important hybrid schemes of multiplexed FDMA in combination with SCPS, PSK, TDM and TDMA techniques, such as SCPC/FM/FDMA, SCPC/PSK/FDMA, TDM/FDMA and TDMA/FDMA.

4.5.2 Time Division Multiple Access (TDMA)

The TDMA application is a digital MA technique that permits individual Earth station transmissions to be received by the satellite in separate, non-overlapping time slots, called bursts, which contain buffered information. The satellite receives these bursts sequentially, without overlapping interference and is then able to retransmit them to the UES terminals. Synchronization is necessary and is achieved using a reference station from which burst position and timing information can be used as a reference by all other stations. Each UES must determine the satellite system time and range so that the transmitted signal bursts, typically QPSK modulated, are timed to arrive at the satellite in the proper time slots. Thus, to improve the imperfect timing of TDMA bursts, several synchronization methods of random access, open-loop and closed-loop have been proposed.

In Figure 4.17 (TDMA), a concept of TDMA is illustrated, where each satellite terminal transmits a data burst with a guard time to avoid overlaps. Since only one TDMA burst occupies the full bandwidth of the satellite transponder at a time, input back off, which is needed to reduce IM interference in FDMA, is not necessary in TDMA. At any instant in time, the transponder receives and amplifies only a single carrier. Thus, there can be no IM, which permits the satellite amplifier to be operated in full HPA saturation and the transmitter carrier power need not be controlled. Since all UES transmit and receive at the same frequency, tuning is simplified. This results in a significant increase in channel capacity. Another advantage over FDMA is its flexibility and time-slot assignments are easier to adjust than frequency channel assignments. The transmission rate of TDMA bursts is about 4,800 b/s, while the frame length is about 1.74 seconds and the optimal guard time is approximately 40 msec, using the open-loop burst synchronization method.

There are some disadvantages, because TDMA is more complex than FDMA:

1) Two reference stations are needed and complex computer procedures, for automated synchronizations between MES terminals; and
2) Peak power and bandwidth of individual MES terminals need to be larger than with FDMA, owing to high burst bit rate.

Therefore, in the TDMA scheme, the transmission signals from various users are amplified at different times but at the same nominal frequency, and are spread by the modulation in a given bandwidth. Depending on the multiplexing techniques employed, two transmission hybrid schemes can be introduced for use in satellite systems.

There are several important hybrid schemes of multiplexed TDMA in combination with TDM, FDMA and TDMA techniques, such as TDM/TDMA and FDMA/TDMA.

4.5.3 Code Division Multiple Access (CDMA)

The CDMA solution is based on the use the modulation technique also known as Spread Spectrum Multiple Access (SSMA), which means that it spreads the information contained in a particular signal of interest over a much greater bandwidth than the original signal. In this MA scheme, the resources of both frequency bandwidth and time are shared by all users employing orthogonal codes, as shown in Figure 4.17 (CDMA). Therefore, the CDMA is achieved by a PN (Pseudo-Noise) sequence generated by irreducible polynomials, which is the most popular CDMA method. In this way, a SSMA method, using low-rate error correcting codes, including orthogonal codes with Hadamard or waveform transformation, has also been proposed. Concerning the specific encoding process, each user is actually assigned a signature sequence, with its own characteristic code, chosen from a set of codes assigned individually to the various users of the system. This code is mixed, as a supplementary modulation, with the useful information signal. On reception, from all the signals that are received, a given user is able to select and recognize, by its own code, the signal, which is intended for it, and then to extract useful information.

The other received signal can be intended for other users but they can also originate from unwanted emissions, which give CDMA a certain anti-jamming capability. For this operation, where it is necessary to identify one CDMA transmission signal among several others sharing the same band at the same time, correlation techniques are generally

employed. From a commercial and military perspective, this MA is still new and has significant advantages. Interference from adjacent satellite systems, including jammers, is better solved than with other systems. This scheme is simple to operate as it requires no synchronization of the transmitter and is more suited for a military MES. Small mobile antennas can be very useful in these applications, without the interference caused by wide antenna bandwidths. Using multibeam satellites, frequency reuse with CDMA is very effective and allows good flexibility in the management of traffic and the orbit/spectrum resources. The Power Flux Density (PFD) of the CDMA signal received in the service area is automatically limited, with no need for any other dispersal processes. It also provides a low probability of intercept of the users and some kind of privacy, due to individual characteristic codes. The main disadvantage of CDMA by satellite is that the bandwidth required for the space segment of the spread carrier is very large, compared to that of a single unspread carrier, so the throughput is somewhat lower than with other systems (Ilcev, 2013).

Therefore, in the CDMA scheme, the signals from various users operate simultaneously, at the same nominal frequency but are spread in the given allocated bandwidth by a special encoding process. Depending on the multiplexing techniques employed, the bandwidth may extend to the entire capacity of the transponder but is often restricted to its own part, so CDMA can possibly be combined in the hybrid scheme with FDMA and/or TDMA. The SSMA technique can be classified into two methods: Direct Sequence (DS) and Frequency Hopping (FH). A combined system of DC and FH is called a hybrid CDMA system and the processing gain can be improved without increases of chip rate. The hybrid system has been used in the military Joint Tactical Information Distribution System (JTIDS) and OmniTRACS, which is Ku-band satellite system developed by the Qualcomm Company. In a more precise sense, the CDMA technique was developed by experts of the Qualcomm Company in 1987. At present, the CDMA system advantages are practically effective in new satellite systems, such as Globalstar, also developed by Qualcomm, which is devoted to MSS handheld terminals and Skybridge, involved in FSS. This type of MA is, therefore, attractive for handheld and portable MSS equipment with a wide antenna pattern.

There are several two combined schemes of multiplexed CDMA, such as Direct Sequence CDMA (DS-CDMA) and Frequency Hopping CDMA (FH-CDMA).

4.5.4 Space Division Multiple Access (SDMA)

Previous systems have used frequency, time and code domains to achieve multiple access schemes, while SDMA uses spatial separation.

The significant factor in the performance of MA in a satellite communications system is interference caused by different factors and other users. In other words, the most usual types of interference are co-channel and adjacent channel interference. The co-channel interference can be caused by transmissions from non-adjacent cells or spot beams using the same set of frequencies, where there is minimal physical separation from neighbouring cells using the same frequencies, while the adjacent channel interference is caused by RF leakage on the subscriber’s channel from a neighbouring cell using an adjacent frequency. This can occur when the user’s signal is much weaker than that of the adjacent channel user. Signal-to-Interference Ratio (SIR) is an important indicator of call quality; it is a measure of the ratio between the mobile phone signal (the carrier signal) and an interfering signal. A higher SIR ratio means increasing overall system capacity (Richharia, 1995).

Taking into account that, within the systems of satellite communications, every user has their own unique spatial position. This fact may be used for the separation of channels in space and, as a consequence, to increase the SIR ratio by using SDMA. In effect, this method physically makes the separation of paths available for each satellite link.

Terrestrial telecommunication networks can use separate cables or radio links but, on a single satellite, independent transmission paths are required. Thus, this MA control radiates energy into space and transmission can be on the same frequency: such as TDMA or CDMA and on different frequencies, such as FDMA.

This MA is usually used in mobile radio and satellite systems, which provide three hybrid schemes, such as SDMA/FDMA, SDMA/TDMA and SDMA/CDMA.

4.5.5 Random Division Multiple Access (RDMA)

For data transmission, a bit stream may be sent continuously over an established channel without the need to provide addresses or unique words if the channel is not charred. In fact, where charring is implemented, data are sent in bursts, which require unique words or synchronization signals to enable time-sharing with other users, to be affected in the division of channels. Each burst may consist of one or more packets comprising data from one or more sources assembled over time, processed and made ready for transmission. The RDMA scheme is also known as Packet MA. Packet access can be used in special RDMA solutions, such as Aloha, where retransmission of blocked packets may be required. There are two types of Aloha: Slotted Aloha and Slot Reservation Aloha.

Random access can be achieved to the satellite link by contention and, for that reason, it is called a contention access scheme. This type of access is well-suited to satellite networks containing a large number of stations, such as UES, where each station is required to transmit short randomly-generated messages with long dead times between messages. The principle of RDMA is to permit the transmission of messages almost without restriction, in the form of limited duration bursts, which occupy all the bandwidth of the transmission channel. This is MA with time division and random transmission, so RDMA is quite assessable (Ilcev, 2013).

A user transmits a message irrespective of the fact that there may be other users equally in connection. The probability of collisions between bursts at the satellite is accepted, causing the data to be blocked from receipt by the Earth station. In case of collision, the destination Earth station receiver will be confronted with interference noise, which can compromise message identification and retransmission after a random delay period. The retransmissions can occur as many times as they are probably carried out, using random time delays.

4.6 Digital Video Broadcast-Return Channel via Satellite (DVB-RCS) Transmission

The DVB-RCS transmission satellite system is a European standard formalized by the European Telecommunication Standard Institute (ETSI) and is envisaged to become the de facto standard for two-way (interactive) satellite networks. This satellite system provides the user with an interactive satellite service via Very Small Aperture Terminal (VSAT). Accordingly, there are two elements to the system: Receive and Transmit capability.

The forward link is shared among a population of terminals using either DVB-S (EN 300 421) or the highly efficient DVB-S2 standard (EN 302 307). Adaptive transmission to

overcome variations in channel characteristics (e.g., rain fade) can be implemented in both the forward and return links. The DVB-RCS return link or uplink to the satellite utilizes a Multi Frequency TDMA (MF-TDMA) transmission scheme. This form of scheme enables the system to provide high bandwidth efficiency for multiple users of meteorological data. A key to the high efficiency of the system is the demand-assignment scheme which uses several capacity mechanisms to allow optimization for different classes of applications, so that voice, video streaming, file transfers and web browsing can all be handled efficiently.

The DVB-RCS standard supports several access schemes making the system much more responsive, and thus more efficient, than traditional demand-assigned satellite systems. These access schemes are combined with a flexible transmission scheme that includes turbo coding, several burst size options and efficient Internet Protocol (IP) encapsulation options. These tools allow systems to be fine-tuned for the best use of the power and bandwidth satellite resources. The user terminal offers an Ethernet interface that can be used for wired or wireless interactive IP connectivity for a local home or office network ranging from one to several users. In addition to providing interactive DVB services, broadband and IPTV, the DVB-RCS systems can provide full IP connectivity anywhere there is suitable satellite coverage. As most of the satellites that can provide DVB-RCS are likely to be GEO, this effectively means anywhere closer to the equator than either 80^0 North in the Northern hemisphere or 80^0 South in the Southern Hemisphere (Ilcev, 2009).

Beyond the basic hub-and-spoke architecture, the DVB-RCS air interface has also been deployed in systems that provide direct terminal-to-terminal "mesh" connectivity, either through satellite on-board processors that mirror the functions of a ground-based hub, or through transparent satellites, using terminals equipped with an additional demodulator.

4.6.1 Fixed DVB-RCS

According to a recent Satellite Industry Association's report, over 130M direct satellite TV subscribers are spread around the world. The key enablers attributed to this success include modern satellite systems capable of powerful transmissions over vast expanses, efficient transmission, highly integrated, low-cost receiver systems and a vast variety of rich content at an affordable price. Current audio and video compression techniques dwell specifically on the MPEG multimedia standards, which constitute the industry's standards for compression and transport. At this point, a majority of direct broadcast satellite systems beaming Standard-Definition TV (SDTV) either use or can support the MPEG-2 standard, while HDTV and multimedia broadcast systems rely firmly on the standard's upgraded version, MPEG-4 mode. Thus, in last two decades, the new DVB-RCS standard was implemented.

To encourage mass-scale acceptance, regulatory bodies promote standardization of the satellite broadcast service. At this point, ITU recognizes at least six Direct to Home (DTH) broadcast systems that encompass television, data and multimedia. Modern satellite and handheld receiver technologies enable television and radio broadcasts to handheld and portable personal devices.

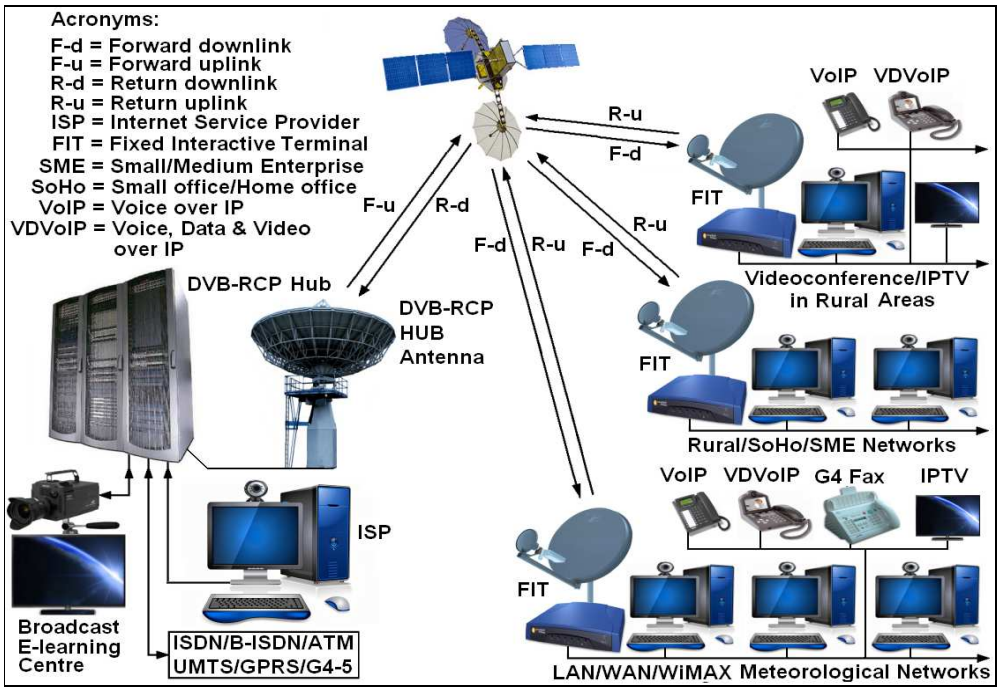

Figure 4. 18 Mixed DVB-RCS for Meteorological Solutions by Ilcev 2013

In the meantime, numerous commercial systems that offer sound and television services to the individual and groups have emerged in the last decade. The final developments of this technique offer the new personal and mobile solutions that will be, in the future, recognized as Digital Video Broadcast-Satellite Personal (DVB-SP) and as well as Digital Video Broadcast-Satellite Mobile (DVB-SM) standards, both of which support commercial mobile broadcasting and television services.

The major development in satellite broadcasting technology was the standardization of the DVB-RCS, which allows the users within direct broadcast terrestrial network (DVB-T) to communicate directly with the broadcast satellite network (DVB-S) through an assigned return channel. The DVB-T cell can be comprised by UMTS/GPRS, ISDN, B-ISDN, and ATM broadband networks and the DVB-S cells may include rural, Consumer broadcasting SoHo/SME LAN, Corporate WAN and multicasting networks(Ilcev, 2009). This greatly simplifies the overall network architecture and associated network management procedures, in that now all kinds of communication solutions take place over the same access network. Thus, the DVB-RCS system has been specified for indoor use only. It can be envisaged that, very soon, research and standardization efforts will be directed towards establishing a suitable mobile standard that be enough to develop a corresponding mobile satellite antenna, and this could open up significant new opportunities in the mobile satellite sector.

A sample of a fixed DVB-RCS system is illustrated in Figure 4.18. The DVB-RCS network enables via HUB as a GES with C, Ku or Ka-band antenna to interface the DVB-T cell via corresponding satellite connections (C, Ku or Ka-band GEO) to the Satellite Interactive Terminals (SIT) or Remote (DVB-S) cells for the following services:

1) Regenerate rural communications: VoIP, IPTV, Internet access and interactive TV/radio two separate way broadcasting (Telephony/Broadband/Broadcast);

2) Broadband access: Asymmetric Digital Subscriber Line (ADSL) anywhere and anytime, Internet access/E-mail, Consumer, SoHo/SME LAN, Corporate WAN, Intranet/VPN, File Transfer Protocol (FTP) and Hyper-Text Transfer Protocol (HTTP); The FTP scheme is a service

for moving and copying an electronic file of any type from one computer to another over the Internet. In addition, it can be used both for downloads and uploads;
3) Teleservice of all E-solutions, which include E-medicine and E-education and others: Videoconference, Image/Video/Audio transfer and Interactive distance learning;
4) Multicasting: Web casting, Video streaming, Satellite newsgathering and Push/Pull data delivery and Voice Data and Video over IP (VDVoIP);
5) Transmissions of meteorological data from a DVB-RCS transponder installed onboard of meteorological satellite, including of retransmissions of weather data send by Data Collection Platform (DCP) ground stations via DVB-RCS transponders to the Direct Readout GES;
6) Transmissions of meteorological data from DVB-RCS transponder installed onboard of meteorological satellite to the fixed or mobile VSAT terminals; and
7) Retransmissions of weather data sent by Data Collection Platform (DCP) ground stations via DVB-RCS satellite transponders to the Direct Readout GES.

The Hub terminal supports existing DVB-RCS compliant Forward Link System (FLS) and provides all the ground required interfaces and management functions necessary to set up a DVB-RCS service over 100 Mb/s downstreams. The Hub operator can interface DVB-RCS terminals to a terrestrial network or service provider, and manage all the operational aspects of the system. The Hub station design is optimized for robustness and stability in operations and can be delivered in a number of different configurations to suit customers' precise applications. Its architecture is also designed to accommodate upgrades and expansions of DVB-RCS network and offer to DVB-RCS providers a choice of C, Ku or Ka-band antenna and RF equipment, so one ordinary DVB-RCS configuration can handle 1 to 10 forward link transmitters and from one to several hundred return link receivers.

The DVB-RCS Satellite Interactive Terminal (SIT) for rack mounting is composed by Outdoor Unit (ODU) of antenna and Indoor Satellite Unit (ISU) of Remote transceiver to provide the most attractive and reliable DVB solutions and ensures full compatibility with any DVB-RCS system via fixed VSAT modem, ETSI/CE approval. The DVB-RCS Remote consists of desktop terminals and a router that provide two-way IP communications via satellite at C, Ku and Ka-Band frequencies. These terminals for corporations, institutions, home offices and householders offer an open-interface for high-capacity broadband access that bypasses the "last mile" bottleneck associated with terrestrial infrastructure. The DVB-RCS system offers broadband access to core IP networks using standard technologies such as DVB-RCS, DVB-S, latest DVB-S2 and IP interfacing DVB-T with fixed and mobile user terminals. The broadband network delivers two-way IP connectivity both between user terminals in the satellite system and between user terminals and the terrestrial network coming in a scalable choice of performance with a range of data IP throughputs from 4 Mb/s to 40 Mb/s (Ilcev, 2013).

The broadcast MPEG2/DVB-S service is available in one-way (unidirectional) from the HUB to the users' terminals. With very low cost per bit, service prices become comparable to those offered by terrestrial networks and can be delivered where other technologies cannot reach. This network can provide solutions in a variety of user segments, such as: Enterprises and Private Networks, Broadcasting and Content Distribution (BCD), Satellite News Gathering, Satellite Emergency and Security Management, Satellite Meteorological Data, Defense Information Management, and so on.

4.6.2 Mobile Digital Video Broadcasting-Return Channel over Satellite (DVB-RCS)

The convergence of Satellite Mobile and Internet technique has opened many opportunities to deliver new multimedia service over hybrid satellite systems to Mobile Interactive Terminals (MIT). The interactive nature of the Internet has paved the way for new generation MSS to support interactivity. Apart from the convergence between mobile and Internet technologies, the other major technical driver is the convergence between mobile and fixed technologies.

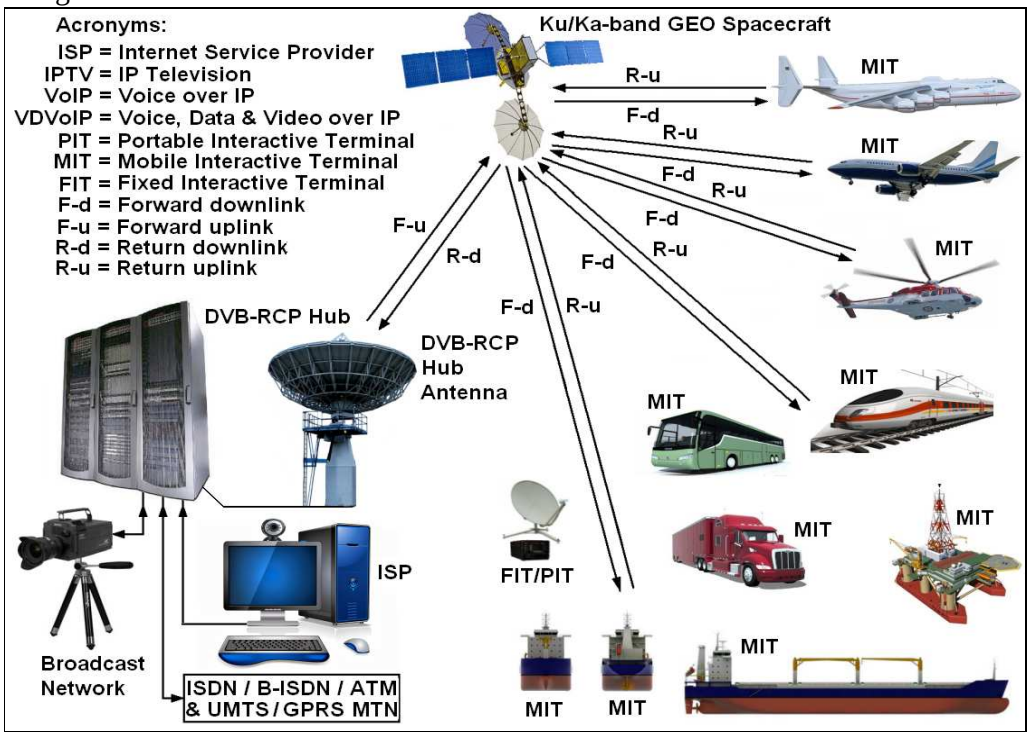

Figure 4. 19 Mobile DVB-RCS for Meteorological by Ilcev 2013

By supplementing broadcasting systems with a narrowband uplink, new interactive services can be facilitated in DVB and DAB solutions. This is foreseen for fixed network operation and could equally be adopted onto a mobile network such as the UMTS, thus demonstrating the concept of convergence of personal and mobile communications, Internet, IPTV, video and data broadcasting technology for meteorological transmissions.

A configuration of mobile DVB-RCS system, shown in Figure 4.19, is designed in 2000. The DVB-RCS mobile network includes a HUB as a GES with C, Ku or Ka-band antenna to interface the TTN (DVB-T) cell via corresponding satellite connections (C, Ku or Ka-band GEO) to the Mobile Interactive Terminals (MIT) or Remote (DVB-S) cells for the following services: Maritime and Offshore Installations, Land (Road and Rail) solutions and Aeronautical service. This infrastructure is the best solution for the establishment of a network for connection of all seaports or airports in one hypothetical country or region. In any case, however, the modern Aeronautical DVB-RCS network is the most reliable communication link between aircraft and airports for commercial and security purposes.

4.7 MPEG Multimedia Standards

The encoding of both high-fidelity (non-speech) audio signals and video signals today is dominated by the standards defined by the International Standards Organization (ISO) MPEG, subsequently adopted by both the ISO/IEC and the ITU. The first standard, MPEG-1, "Coding of moving pictures and associated audio for digital storage media at up to about 1.5 Mb/s, issued in 1992, and its successor MPEG-2, "Generic coding of moving pictures and associated audio information", issued in 1994, define generic coding for both moving pictures (i.e., video) and associated audio information. Work on an MPEG-3 standard was discontinued. More recently, MPEG-4 primarily focuses on new functionality, but also includes improved compression algorithms, and for the first time includes speech compression algorithms, such as CELP.

Each standard comprises a number of parts, for example, MPEG-4 has 23 parts, each of which focuses on a particular aspect of the encoding (video, voice, audio, data encapsulation, and so on).

Significantly, MPEG standards only define in detail the source decoder, providing a toolbox of algorithms, and standardized bit stream formats. The detailed encoder architecture is typically not defined (although example implementations are given), thereby allowing equipment manufacturers to differentiate their products while ensuring compatibility of a user's equipment.

4.7.1 Audio Broadcasting

With reference to the audio broadcasting, in general, it is necessary to turn attention to the general audio waveform, and, in particular, to the high fidelity audio, including stereo music, multichannel surround-sound content and speech encoding.

4.7.1.1 MPEG-2 Audio Layer II (MP2) Encoding

MPEG-1 provided for three different types of audio encoding with sampling rates of 32 kHz (kSamples/s), 44.1 and 48 kHz for monophonic (mono), dual mono and stereophonic (stereo) channels. MPEG-2 added support for up to five audio channels and sampling frequencies down to 16 kHz.

Subsequently, MPEG-2 Advanced Audio Encoding (AAC) added sampling from 8 to 96 kHz with up to 48 audio channels (and 15 embedded data streams). MPEG-2 audio layer I is the simplest encoding scheme and is suited for encoded bit rates above 128 kb/s per channel (Pan, 1995).

Audio layer II, known as MP2 audio file format, has an intermediate complexity and is targeted at bit rates around 128 kb/s. On the other hand, MP2, also known as Musicam, forms the basis of the Digital Audio Broadcasting (DAB) system and is incorporated into the DVB standard.

4.7.1.2 MPEG-2 Audio Layer III (MP3) Encoding

MPEG-2 audio layer III, known as MP3, provides increased compression (or, alternatively, improved quality at the same data rate) compared with MP2 at the expense of slightly

increased complexity and computational effort. Today, MP3 is widely used for the storage and distribution of music on personal computers via the Internet and for digital satellite broadcasting by 1 worldspace.

The MP3 psychoacoustic model uses a finer-frequency resolution than the MP2 polyphase quadrature filter band provides (Pan, 1995). MP3 divides the audio spectrum into 576 frequency bands and processes each band separately. It does this in two stages.

First, the spectrum is divided into the normal 32 bands, using a polyphase quadrature filter, in order to ensure compatibility with audio layers I and II. In MP3, however, each band is further divided into 18 sub-bands using a Modified Discrete Cosine Transform (MDCT). The MP3 MDCT is a variant of the discrete cosine transform that reuses a fraction of the data from one sample to the next.

It is obvious that following the transformation into the frequency domain, component frequencies can be allocated bits according to their audibility using the masking levels in each filter. We also noted that MP3 exploits inter-channel redundancies, for example, in situations when the same information is transmitted on both stereo channels. Typically, MP3 permits compression of CD-quality sound by a factor of –12.

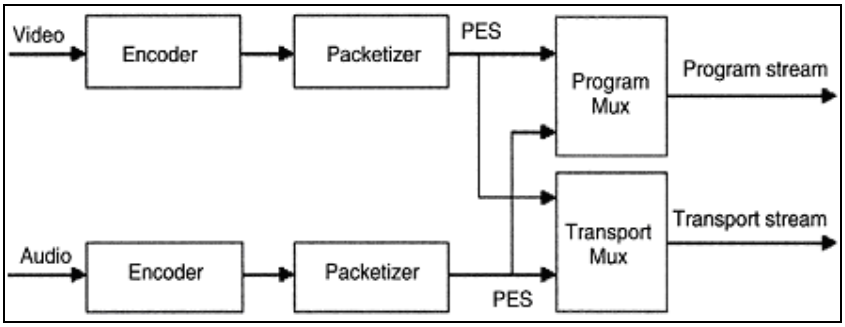

Figure 4. 20 MPEG Programme and Transport Stream by Richharia 1995

4.7.2 Video Broadcasting

As with audio encoding, the dominant video encoding standards are currently the MPEG standards, notably MPEG-2 for standard-definition video and, increasingly, MPEG-4 for high-definition video. The MPEG-2 video decoders contain a 'toolbox' of compression algorithms grouped into a number of subsets called 'profiles'. Furthermore, profiles support a number of levels (combinations of image size, frame rate, etc.), and decoders may implement a subset of profiles (Richharia, 1995).

4.7.2.1 MPEG-2 Video Encoding

MPEG video encoding algorithms aim to transmit differences between frames where possible and use a DCT (a form of Fourier transform) to encode the different information into the frequency domain, discarding insignificant high spatial frequency information that would not normally be noticeable. For this reason, they are sometimes referred to as hybrid block interframe Differential PCM (DPCM)/Discrete Cosine Transform (DCT) algorithms. A video buffer is used to ensure a constant bit stream on the user side. Typical bit rates for MPEG-2 encoded standard-definition video are in the region of 3–15 Mb/s, which is around 10–50:1 compression is achieved over the raw PCM bit rate.

4.7.2.2 High-Definition TV and MPEG-4

Even greater compression ratios are required for the transmission of high-definition TV video. HDTV frame resolutions of up to 1920 x 1080 pixels are in use (at 25 Hz) – with up to 5 times as many pixels per frame compared with SDTV. While MPEG-2 High Level can support resolutions of up to 1920 x 1080 (sometimes referred to as full-HD), HDTV generally requires the increased compression available in MPEG-4 to be viable. MPEG-4 Advanced Video Coding (MPEG-4 part 10 AVC), jointly developed with the ITU Video Coding Experts Group (as H.264), employs additional techniques to achieve compression ratios greater than those for MPEG-2, and is used by several satellite services for broadcasting HDTV. MPEG-4 AVC is utilized in BluRay videodiscs. Specifically, MPEG-4 AVC utilizes a number of features to achieve higher compression than MPEG-2. Some of the more significant features of MPEG-4 AVC are:

1. Up to 32 reference pictures may be used for motion compensation, rather than just 1 (I-Pictures) or 2 (B-Pictures);
2. The macroblock size used for motion compensation may be varied from 16 x 16 to 4 x 4 pixels with subpixel precision, and new 4 x 4 and 16 x 16 pixel block transforms; and
3. Improved non-linear quantization size control and improved entropy encoding.

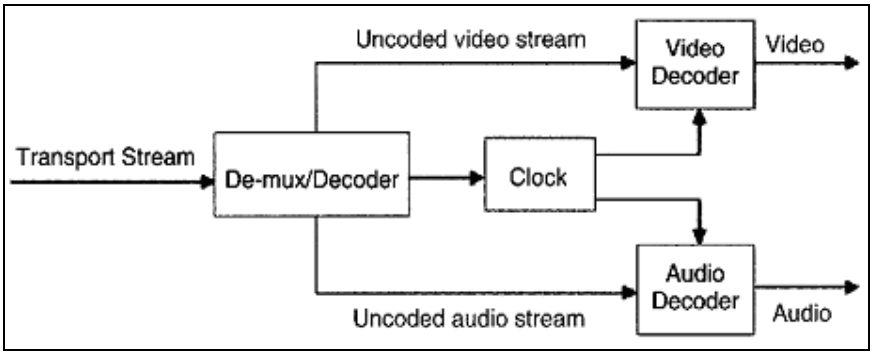

Figure 4. 21 Demultiplexing and Decoding of MPEG by Richharia 1995

4.7.2.3 Multiplexing and Transporting

In Figure 4.20 illustrates packetization of encoded video and audio elementary streams to produce a Packetized Elementary Stream (PES). The PES packets are next combined with system-level information to form Transport Streams (TS) or Programme Streams (PS).

The systems part of the MPEG-2 specification (ISO/IEC 13818-1:2000(E)) specifies all syntactical and semantic rules to combine MPEG-2 video and audio elementary streams (output of an encoder), including other types of data content, into a single or multiple streams to enable storage or transmission.

The program stream consists of one or more streams of PES packets of common time base into a single stream. The stream is useful for operation in relatively error-free environments such as interactive multimedia applications.

The transport stream consists of one or more independent programs into a single stream. This type of stream is useful in error-prone environments as satellite broadcasts. Packets are 188 bytes in length. Transport stream rates may be fixed or variable. Values and locations of

Programme Clock Reference (PCR) fields define the stream rate. The transport stream design is such as to facilitate: retrieval and decoding of a single program within the transport stream, extraction of only one more program or contents from a transport stream and conversion of a program into a transport stream including recovery at Rx.

Figure 4.21 illustrates the concept of demultiplexing and decoding of a single program from a received transport scheme containing one or more program streams. The input stream to the demultiplexer/decoder includes a system layer wrapped about a compression layer. The system layer facilitates the operation of the demultiplexer block, and the compression layer assists in video and audio decoding. Note that, although audio and video decoders are illustrated, these may not always be necessary when the transport stream carries other classes of data.

4.8 Direct-to-Home Broadcast System

Recognizing the advantages of digital television transmissions, and their potential to transport HDTV efficiently, considerable effort was directed in the 1980s and 1990s (notably in the United States, Europe and Japan) towards the development of digital transmission systems, resulting in the design of several terrestrial and satellite systems. The convergence of computing, telecommunications and broadcast disciplines led the developers to adapt a generic architecture that would offer a variety of enabling satellite services in addition to SDTV and HDTV.

Enabling technology and services include a digital video recorder to facilitate the recording of a program directly in a digital format, interactivity (e.g., multichannel display or multiple camera angle displays), receiver-enabled home networking and reception onboard mobiles.
Broadcast Satellite Service (BSS) radio frequency plan of ITU provides a useful framework with guaranteed availability of spectrum in Ku-band to each member country, allowing high-power radio transmissions amenable for reception at home via small non-obtrusive antenna on low-cost receivers. It is necessary to highlight the technology of the DVB-S2 satellite system, as it incorporates a wide range of recent technology advances to provide a highly flexible and efficient medium, and, moreover, it is uniquely identified by the ITU as a broadcast system for digital satellite broadcasting system with flexible configuration.

4.8.1 Transmission System Architecture

A typical direct-to-home system comprises incoming signals to the uplink facility from one or more transmission sources, such as a studio, local terrestrial broadcast signal feed, pre-recorded material, etc. Occasionally, additional material, such as advertisements, may be added locally at pre-agreed points of the incoming program. The incoming signals are monitored, routed within the facility and, if necessary, readjusted and synchronized. The prerecorded material is checked for quality, edited, when necessary, and read into video file servers to be played at the broadcast time.

Commercial systems incorporate a facility known as conditional access to facilitate reception solely by the authorized users. Other functionalities include additions of Service Information (SI) and Electronic Programme Guide (EPG), analogue-to-digital conversion, compression, multiplexing to create a suitable transport stream, error control and modulation. The SI and EPG equipment creates signals for displaying program-related information, for example, program title, start/end time, etc. The compression equipment is typically MPEG-2, although

migration to MPEG-4 is endemic because of its tighter encoding. Several channels are multiplexed to provide a single high-rate channel for transmission. The stream is FEC mode, modulated and transmitted.
The ITU BSS plan recommends uplink transmissions in the 17.5 GHz band and downlink transmissions to the user community in the 12.5 GHz band, but their transmission powers are restricted by the FSS regulations. The BSS satellites are placed in geostationary orbits. The satellites use transparent transponders capable of transmitting very high powers through spot, and often, shaped beams to be able to provide the high signal quality necessary for reception on small DTH receivers.

The DTH receivers typically use a 45-60 cm dish at Ku-band, depending on satellite EIRP. The relatively high gain of the receive antenna in conjunction with high-power satellite transmissions provides sufficient link margins to counter rain fades common in this band.

4.8.2 Generic Reference Integrated Receiver Decoder (IRD) Model

The indoor unit housing the electronics is known as the Integrated Receiver Decoder (IRD). The core functions of all the direct-to-home television systems are nominally identical, and, hence, a generic model of the IRD is feasible. Operators may tailor the remaining functions around these core functional entities. The ITU proposes reference architecture of the IRD on this premise. The model provides a structured definition of functionalities to facilitate a generic receiver design. As observed in the preceding section, the core functions relate generically to a transmission system. The additional essential functions relate to the service provision, operation of the system and additional or complementary features, which may differ depending on implementation.

These functions and units include: a satellite tuner, output interfaces, an operating system and applications, EPG, Service/system Information (SI), Conditional Access (CA), a display, a remote control, Read Only Memory (ROM), Random Access Memory (RAM), FLASH memory, an interactive module, a microcontroller and units to support teletext, subtitling, etc. Software-reconfigurable receivers are common as they simplify an upgrade to the receiver. The upgrade may, for example, become necessary to repair a software anomaly, add a new functionality or reconfigure receiver subsystems when a new satellite transponder is deployed.

Modern receivers typically include a digital video recorder permitting users to record a program directly in a digital format, or to store content, ready for an ‘instant’ video-on-demand display, thereby avoiding the interactive delay. Often L-band IF, signals from a single dish/LNB flow to one or more receivers in the customer’s home. Home networking systems permit interworking between receivers, thereby permitting programs recorded on one set to be viewed by other sets elsewhere in the house, and, in addition, support features such as security and quality of service management.

4.9 Transmission Standards

The development of digital television has evolved independently around the world, and, hence, several types of transmission systems are in use. The majority operates in the 11/12 GHz downlink band. Being digital, the systems can support numerous applications and services efficiently, be it television, multimedia, data services or audio. To assist in the

selection of an appropriate system, ITU recommends four systems – system A, system B, system C and system D.

4.9.1 Digital Video Broadcast-Second Generation (DVB-S2) Standard

The DVB transmission project, initiated in Europe, but subsequently extended worldwide, defines digital broadcast standards by consensus among the participants representing the manufacturing industry, broadcasters, program providers, network operators, satellite operators and regulatory bodies. The DVB standards embrace broadcast transmission technology across all media of cable, terrestrial and satellite. The DVB-S specifications were standardized in 1993. A second-enervations specification, DVB-S2, was produced in 2003 in response to a growing demand for more capacity and services, taking advantage of the advances in technology.

The DVB-S2 system was standardized by the European Telecommunication Standard Institute (ETSI) as EN 302 307 (ETSI Online). In August 2006, the ITU's study group on satellite delivery issued a recommendation (BO.1784) that DVB-S2 be the preferred option for a Digital Satellite Broadcasting System with Flexible Configuration (Television, Sound and Data), entitled system E.

The DVB-S standards support up to 12 categories of transmission medium encompassing a plethora of media contents, among others, standard- and high-definition television, radio and data with or without user interactivity. The standard includes specifications for Internet Protocol (IP) data, software downloads and transmissions to handheld devices. The standards, namely, DVB-Satellite (DVB-S), DVB-Return Channel Satellite (DVB-RCS) and DVB-Second Generation (DVB-S2) apply to fixed user terminals. The DVB-Satellite Handheld (DVB-SH) standard, discussed later in the chapter, applies to handheld terminals.
Many parts of the DVB-S specifications are shared between various transmission media. The source coding of video and audio and formation of the transport stream comprises MPEG-2 tailored for satellite systems (MPEG specifications are too generic).

The DVB-S STANDARD also supports H.264/AVC video and MPEG-4 high-efficiency AAC audio, and additionally, audio formats such as Dolby AC-3 and DTS coded audio. Guidelines are also available for transporting IP content. The specifications support teletext and other data transmitted during the vertical blanking period, subtitles, graphical elements, service information, etc. Thus, DVB-S's enhanced version, DVB-S2, is based on three key concepts: 1. Best transmission performance; 2. Total flexibility; and 3. Reasonable receiver complexity.

The specifications enable delivery of services that could never have been delivered by DVB-S. According to the developers, the DVB-S2 standard is not intended to replace DVB-S in the short-term for conventional TV broadcasting applications but is rather aimed at new applications such as the delivery of HDTV and IP-based services, fly-away small DSNG stations, low-cost Internet access to rural areas and in developing countries, etc. The DVB-S2 specifications, in conjunction with recent advances in video compression, have enabled the widespread commercial launch of HDTV services.

The supported applications are as follows: 1. Standard and high-definition television broadcasts; 2. Interactive services, including Internet access for consumer applications; 3. Professional applications: Digital TV Contribution (DTVC) facilitating point-to-multipoint

transmissions, and Digital Satellite News Gathering (DSNG); 4. Content distribution; and 5. Internet trunking.
In addition to MPEG-2 video and audio coding, DVB-S2 is designed to handle a variety of advanced audio and video formats, which the DVB Project is currently defining. In fact, DVB-S2 accommodates the most common digital input stream format, including single or multiple MPEG transport streams, continuous bit streams, IP as well as ATM packets. It is 30% spectrally more efficient than its predecessor, employing an adaptable modulation scheme consisting of QPSK and 8-PSK for broadcast applications and also 16-APSK and 32-APSK for professional applications such as newsgathering and interactive services.

In addition, the modulation and coding schemes may be dynamically adapted to variable channel condition on a frame-by-frame basis scheme. The coding arrangement consists of a Bose-Chaudhuri-Hocquenghem (BCH) outer code scheme and a Low-Density Parity Check (LDPC) inner code. The communication performance lies within 0.7 dB of the theoretical limit. The flexibility offered by variable coding and modulation provides different levels of protection to services as needed(Ilcev, 2013).

The specifications support the operation on any type of satellite transponder characteristics with a large variety of spectrum efficiencies and associated C/N requirements. Thus, the DVB-S2 broadcast services comprise a backward compatible mode and a more optimized version, which is not backward compatible. The system allows interactive services by return channels established either via satellite or another medium incorporating the added flexibility of Adaptive Coding and Modulation (ACM) to the forward channel through feedback. Structured as a toolkit, DVB-S2 attempts to optimize transmission efficiency and flexibility, keeping receiver costs at an acceptable level.

4.9.2 DVB-S2 Architecture

Figure 4.22 illustrates a block schematic of functional components of a DVB-S2 transmission system. Thus, there are two levels of framing structures, one at Baseband (BBFRAME) and the other at Physical Layer (PLFRAME).

Thus, BBFRAME includes signaling to configure the receiver for the given specification and service. The PLFRAME comprises a regular sequence of frames, each coded and modulated for the given channel condition and application, containing a few signaling bits for synchronization and physical layer signaling.

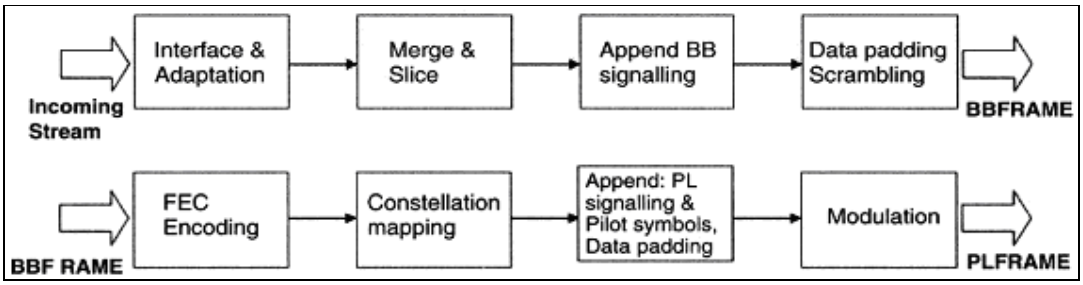

Figure 4. 22. DVB-S2 Transmission System by Richharia 1995

Referring to BBFRAME, shown in Figure 4.22, the mode and stream adaptation block interfaces with the incoming stream, provides synchronization and supports the adaptive coding-modulation schemes. It merges multiple streams and slices them into blocks, each of which is modulated and coded homogeneously. A header of 80 bits containing transmission

characteristics is next appended to the baseband data block to assist reception. The information within the header, for example, informs the receiver as to whether the transmission stream is single or multiple, the type of coding modulation schemes, signal format, etc. When the volume of data is insufficient to fill the frame, data padding is introduced, and, finally, the frame is scrambled and passed over for coding (Richharia, 1995).

The FEC coding-modulation schemes are instrumental in high transmission efficiency. The FEC code comprises a Low-Density Parity Check (LDPC) code that exhibits a low distance from the Shannon limit for the specified decoder complexity (equating to 14 mm^2 of silicon 0.13 μm technologies). The LDPC codes are suitable for iterative decoding at reasonable complexity because of their easily parallelizable decoding algorithm, which can use simple operations resulting in reduced complexity and storage. To avoid error floors at low error rates, a BCH outer code of the same block length as the LPDC code is concatenated
.
The coded payload modulates the carrier with a QPSK, 8-PSK, 16-APSK or 32-APSK scheme, as required by the given application data rate and link conditions. In fact, the corresponding spectral efficiency ranges from 0.5 to 4.5 b/symbol. Typically, the QPSK and 8-PSK schemes are applied for broadcast applications through non-linear transponders, whereas 16 and 32-APSK schemes are better suited for professional and other applications operating through transponders driven in the quasi-linear region. The DVB-S2 provides backward compatibility with DVB-S through a hierarchical modulation scheme.

The Physical Layer (PL) signals are composed of a regular sequence of frames, within each of which the modulation and coding schemes remain unchanged, that is, a homogeneous operation. A header of 90 bits preceding the payload assists in synchronization at the receiver, detection of modulation and coding parameters, etc. This header must be made particularly robust, as the LPDC/BCH scheme is not applied here and the packet will not be detectable unless the header is detected correctly. An interleaved first-order Reed-Muller block code in tandem with the π/2-BPSK modulation scheme was found to be suitable.

CHAPTER FIVE

ANTENNA SYSTEMS AND PROPAGATION

In the beginning of radio development, radio communication systems were conceived for the transmission and receiving of telegraphy and telephony signals via antenna systems. The consideration of antenna transmission is inevitable where their propagation characteristics are much affected by different and changeable local environments during movement of mobile and differ greatly from those observed in fixed satellite systems. To create antenna hardware for mobile and fixed systems, engineers have to consider all related factors in order to realize full mechanical and transmission potentials.

This chapter describes antenna characteristics, requirements and basic relations of antenna systems for mobile and fixed applications, such as low-gain omnidirectional antennas, three principal divisions of medium-gain directional antennas and high-gain directional aperture antennas and, finally, the major practical type of antenna used in meteorological satellite communications for transmitting and receiving Ground Earth Stations (GES) are presented.

In addition propagation and interference characteristics, which are very important for providing quality and reliability of satellite propagation channels, will be introduced. To design an effective satellite communications model, it is necessary to consider the quantum of all propagation characteristics, such as signal lost in normal environment, path depolarization causes, transionospheric contribution, propagation effects important for mobile systems, including reflection from the Earth's surface, fading due to sea and land reflection, signal blockage and to the different local environmental interferences for all mobile and handheld applications. At any rate, the local propagation characteristics on the determinate geographical position have very specific statistical proprieties and results for ground transmitting and receiving satellite stations and infrastructures, which are related to the Carrier-to-Noise-density ratio (C/N_o).

5.1 Evolution of Antenna Systems for Radio Communications

The oldest existing antennas were used by Heinrich Hertz in 1888 at a very short distance in his first experiments for proving the existence of electromagnetic (EM) waves. The antennas were neither physically nor functionally separated from high-frequency generators, and, up to the present day, resonant circuits are taken as models for illustrating certain antenna characteristics.

The Russian professor of physics, Popov, designed his first world's ever radio receiver in 1895 with an antenna in the shape of wire mounted on a balloon in the air and a transmitter with a lightning conductor as an antenna, including a metal filings coherer and a detector element with telegraph relay and a bell. The antenna was clearly separated and regarded an independent unit in a radio system as transmitting and receiving stations were set up. Later, Marconi started commercially to deploy radio and antenna equipment and to establish his own company for the production of radio and antenna equipment (Rohner, 2013).

5.1.1 Overview of Antennas for Radio and Satellite Communications

The satellite systems introduced new complexities into the design of ground-based antennas. The direct line-of-sight between antenna and satellite requires the antenna to see from

horizon to overhead (zenith – 90^o) in elevation and 360^o in azimuth angle, with total hemispherical coverage. This is fulfilled in the case of transceiver antenna through the use of tracking rotatable high-gain antennas, often installed in the premises of GES.

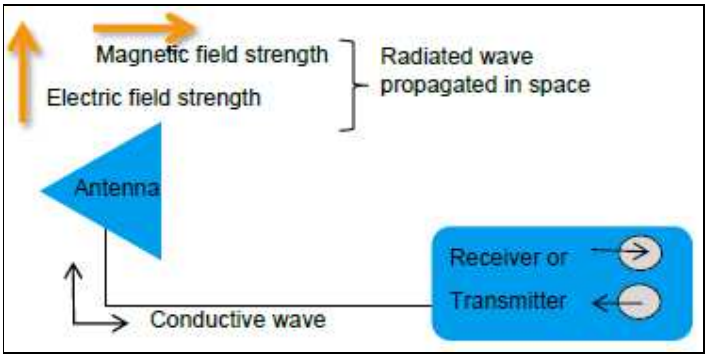

Figure 5. 1 Basic Antenna Functionality by Rohde 2013

Antennas act as converters between conducted waves and electromagnetic waves propagating freely in space, as shown in Figure 5.1. Their name is borrowed from zoology, in which the Latin word antennae are used to describe the long, thin feelers possessed by many insects. In Figure 5.2, it can be seen that the antenna is an important element in any radio system because it acts like a link of a chain. So the overall performance is significantly influenced by the performance of transmit and receive antennas.
At first glance, modern antennas may still look very similar to the ancient model developed by Hertz and Prof. Popov. However, they are nowadays optimized at great expense for their intended application. Communications antenna technology primarily strives to transform one wave type into another with as little loss as possible.

This requirement is less important in the case of test antennas, which are intended to provide a precise measurement of the field strength at the installation site to a connected test receiver; instead, their physical properties need to be known with high accuracy. The explanation of the physical parameters by which the behaviour of each antenna can be both described and evaluated is probably of wider general use; however, the following chapters can describe only a few of the many forms of antenna that are in use today.

5.1.2 Satellite Antennas Geometry

Communication via satellites is always done using different types of antenna and, in particular, is employed a directional parabolic reflector. Since it is directional, the antenna must be accurately pointed toward the satellite and then fixed in place. On the other hand, some ground and mobile antennas have automatical tracking and pointing mechanism, which always is providing antenna in the focus of satellite. Tracking mechanism of mobile antenna is most sophisticated, because it has to follow the heading of a moving ship or aircraft.

All Geostationary Earth Orbit (GEO) satellites are positioned over equator and at the same altitude in the region of space known as the Clarke belt. Before attempting to align an antenna with GEO satellite, it is useful to imagine what the Clarke belt would look like if the observer could see in the sky from different locations on the Earth.

An antenna using Low Earth Orbiting (LEO) satellites presents a different sort of challenge. While a geostationary satellite appears to "hang" in a single spot in the sky all the time, LEO satellites "rise" and "set" again and again relative to a single location on the ground.

Figure 5. 2 Block Diagram of Radio Link by Rohde 2013

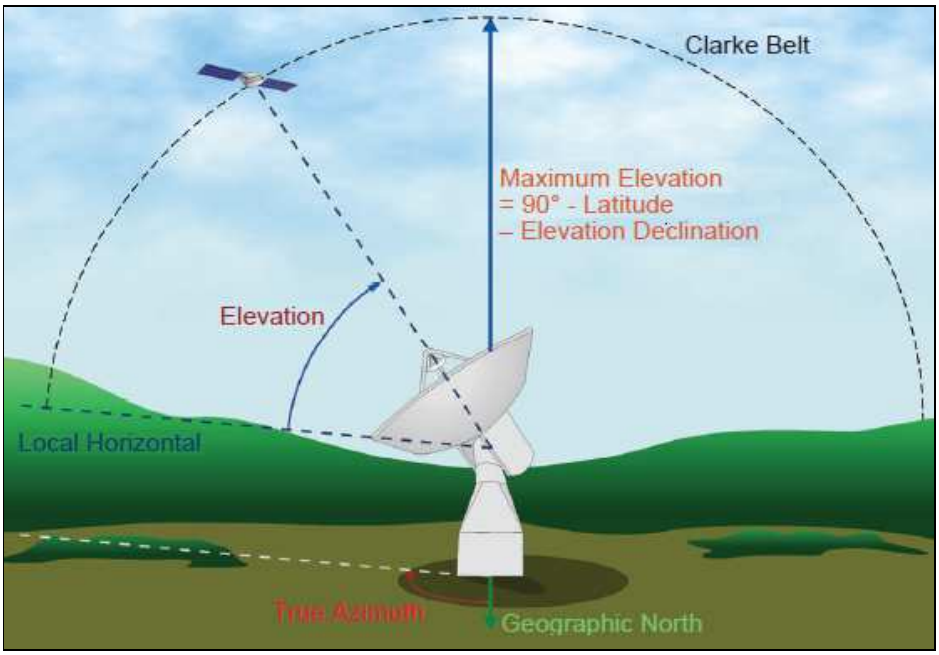

Figure 5. 3 Clarke Belt and Antenna Look Angles in the Northern Hemisphere by Rohde 2013

In most cases, it is impractical to install an antenna that tracks the movements of these spacecraft, and, at this point, omnidirectional antennas are normally used. Power levels for these types of installations must be carefully calculated so that a sufficient level of energy reaches the satellite regardless of its position in the sky at any given moment.

The Clarke belt forms an imaginary arc in the sky. Figure 5.3 shows Azimuth and Elevation angles of antennas in the Local Horizontal plane in the geographical North. If an observer is at the equator, the belt passes directly overhead. If an observer is in the Northern Hemisphere, the belt stretches from the horizon a little South of due east, rising to its maximum height directly towards the South, and then reaching the horizon a few degrees South of due West. If an observer is in the Southern hemisphere, the maximum height of the arc appears directly North of his location.

The true Azimuths of all GEO satellites that are visible from a location in the Northern Hemisphere range from a little more than 90^0 to a little less than 270^0. For locations in the Southern Hemisphere, the true Azimuths are greater than 270^0 or less than 90^0.

The Elevation of the GEO satellite can range from a little more than 0^0 in local horizon to a maximum Elevation that depends on the latitude of the Earth station antenna. For an antenna at the equator, the maximum possible elevation is equal to 90^0 minus the latitude (φ) minus the apparent declination (d).

5.1.3 Antennas Requirements and Technical Characteristics

This section describes the following important general requirements for fixed and mobile antenna solutions used in any satellite transmissions:

1. Mechanical Characteristics – The communication antennas have to satisfy significant requirements of mechanical characteristics in relation to construction strength and easy installation. Easy installation and appropriate physical shape are very important requirements in addition to compactness and lightweight. In the case of fixed antennas, the installation requirements are not as severe compared to that of mobile antennas because, even in big ships, there is no a comfortable space to install an antenna set.

2. Electrical Characteristics - Mechanical design of antenna is perfect because of some functional or electrical characteristics; however, designers of antenna have to keep in mind that the compact design of antenna has two major disadvantages in electrical characteristics, such as low-gain and wide beam coverage. The gain is closely related to the beamwidth and a Low-Gain Antenna (LGA) should have a wide beamwidth. As the gain of antenna is theoretically determined by its physical dimensions, reducing the size of antenna means decreasing its gain. Due to low-gain and limited electric power supply, it is very difficult for antennas to have enough receiving capability of Gain-to-noise-Temperature (G/T) and transmission Equivalent Isotropically Radiated Power (EIRP). These disadvantages of GES antenna can be compensated by a satellite that has a large antenna and High Power Amplifier (HPA) with enough electrical power. A powerful satellite with high G/T and EIRP performance should permit the fabrication of compact and lightweight antennas. The next disadvantage is that a wide beam antenna is likely to transmit undesired signals to and them from an undesired direction, which will cause interference in and from other systems.

5.2 Basic Relations of Antennas

The basic relations of antenna systems are very important parameters to easily understand the mode of antenna functions in two-way (duplex) satellite transmission systems, such as GES transceiving antennas. Moreover, these characteristics of antenna systems are needed for link budget calculations and for good satellite up and downlink design, which can provide reliable and acceptable quality satellite communications. At this point, this implies that the signal transmitted via the Transmitted (Tx) antenna must reach the Receiving (Rx) antenna of other communication antennas at a carrier level sufficiently above the unwanted signals generated by various unavoidable sources of noise and interference (SCISYS, 2014).

5.2.1 Frequency and Bandwidth in Meteorological Satellite Communications

In almost all present and forthcoming satellite communication systems using GEO and LEO or Polar Earth Orbit (PEO) satellites, the L-band 1.6/1.5 GHz is used for a link between the satellite and GES terminals. The required frequency bandwidth in L-band in mobile satellite systems is about 8% to cover transmission and receiving channels. In using a narrow-band satellite antenna, such as an omnidirectional patch antenna, some efforts have to be made to widen the bandwidth. Thus, the S and L-band are allocated in WARC-92 for the Big LEO Iridium and Globalstar systems, which require frequency bandwidths of about 5%.

In general, Radio Frequency (RF) is any of the Electromagnetic Wave (EW) frequencies that lie in the range extending from around 3 kHz to 300 GHz, which include those frequencies

used for communications or radar signals. The RF usually refers to electrical rather than mechanical oscillations, while mechanical RF systems do exist.

In particular, Meteorological Satellite (MetSat) systems are using the following RF spectar:

- 137 – 138 MHz in Satellite to Earth (S-E) direction - Dissemination of low rate data from Non-GEO (PEO or LEO) MetSat to user stations, GEO or User Earth Station (UES);
- 401 – 403 MHz in Earth to Satellite (E-S) direction - Data uplink from Data Collection Platform (DCP) to GEO MetSat, which frequency band is divided into regional and international channels;
-1670 – 1710 MHz (S-E) - The band is divided into several parts and is used for downlink of raw data, DCP data, and dissemination;
- 2025 – 2110 MHz (E-S) - Telecommand and ranging signals from main Earth and uplink of processes data for dissemination;
- 2200 – 2290 MHz (S-E) - Telemetry and downlink of raw data to main station;
- 7450 – 7550 MHz (S-E) - Downlink of medium rate raw data from GEO MetSat to main Earth station (not used on current generation MetSat systems);
- 7750 – 7850 MHz (S-E) - Downlink of raw data from Non-GEO (PEO or LEO) MetSat to main Earth station, but also dissemination;
- 8025 – 8400 MHz (S-E) - Downlink of sensor data from GEO and Non-GEO MetSat to main Earth station;
-18.1 – 18.3 GHz (S-E) - Downlink of high rate raw data to main Earth station; and
- 25.5 – 27 GHz (S-E) - Downlink of high rate raw data to main Earth station (currently no plans for next generation MetSat).

The bandwidth of an antenna is defined as the range of usable frequencies within which the performance of the antenna with respect to some characteristics conforms to a specified standard. The parameter most commonly taken into account here is the impedance match, where. Voltage Standing Wave Ratio (VSWR) < 1.5, - but other parameters like gain or side lobe suppression may serve as a bandwidth criteria here, too.

Radio and satellite antennas are usually designed with a specific frequency, and their performance characteristics, e.g., gain and radiation pattern, are generally specified with that specific frequency. These characteristics change, generally deteriorate, as the operating frequency deviates from the specified frequency. The frequency range within which the performance characteristics maintain a certain level with respect to the specified performance characteristics, e.g., 90%, is referred to as the antenna bandwidth.

Many different types of antennas, e.g., wire or aperture antennas have different bandwidth characteristics. In general, wire antennas have narrower bandwidths than aperture antennas. For instance, the bandwidth of a simple linear wire antenna is about 8–16% of its designed frequency. Therefore, much effort had been spent to develop broadband wire antennas by changing the physical shapes of the antennas.

For broadband antennas, the bandwidth is usually expressed as the ratio of the upper-to-lower frequencies of acceptable operation. For example, a 10:1 bandwidth indicates that the upper frequency is 10 times greater than the lower. A ratio of 2:1 is called an octave and a ratio of 10:1 is a decade, whose broadband bandwidth is expressed by relation:

$$BW_b = f_H/f_L \quad (5.1)$$

where f_H is the highest usable frequency and f_L is the lowest usable frequency. An antenna is said to be broadband when BW is equal to or greater than 2.
For narrowband antennas, the bandwidth is expressed as a percentage of the frequency difference (upper minus lower) over the center frequency of the bandwidth. For example, a 5% bandwidth indicates that the frequency difference of acceptable operation is 5% of the center frequency of the bandwidth. There exists also a different definition of bandwidth which is valid only for narrowband antennas:

$$BW_n\,(\text{in }\%) = (f_H\text{-}f_L/f_C) \cdot 100 \qquad (5.2)$$

where f_C is the center frequency. Values here can range from 0 to 200%, thus, in practice this definition is only used up to about 100%.

5.2.2 Gain and Directivity

The required antenna gain is determined by a link budget, which can be calculated by taking into consideration the required channel quality and the satellite capability. The channels are expressed as C/N_o and depend on the G/T and EIRP values of the satellite and GES.

In the case of present GEO satellite systems, a medium gain between 8 to 15 dBi is required for voice and High Speed Data (HSD) channels of 24 Kb/s. On the other hand, in the case of High-Gain Antenna (HGA), minimum 24 dBi is required, due to the difference in satellite capabilities. Thus, Low Gain Antenna (LGA) of about 0 to 4 dBi is used in omnidirectional antenna systems to provide Low Speed Data (LSD) of only about 600 to 1,200 b/s.

There are no exact definitions to differentiate between characteristics of Low, Medium and High-gain antenna systems, except by the gain quantum, shape of the antenna and type of service. For instance, the classification of L-Band GES antenna systems by their receiving and service capabilities is illustrated in **Table 5.1**.

Table 5. 1 Classification of L-Band Satellite Antenna Systems

Type of Antenna	Gain Class	Typical Gain [dBi]	Typical G/T [dBK]	Typical Antenna (Dimension)	Typical Satellite Communication Services
Omnidirectional	Low	0 – 4	–27 to –23	Quadrifilar Drooping-dipole Patch	LSD (Messages)
Semidirectional (Only in Azimuth)	Medium	4 – 8 8 – 16	–23 to –18 –18 to –10	Array (2–4 elements) Helical, Patch SBF (0,4m Φ) Phased Array (20 elements)	Voice/HSD
Directional	High	17 – 20 20 – 24	– 8 to –6 –4	Dish (0,8m Φ) Dish (1m Φ)	Voice/HSD

The ideal antenna gain can be defined with an isotropic (hypothetical) antenna, which has an isotropic radiation pattern without any losses and, therefore, radiates power in all directions in uniform intensities. Thus, if input power (P_{in}) is put into an isotropic antenna, the power

flux-density per ideal unit area (P_{id}) at distance (r) from the antenna is given by the following relation:

$$P_{id} = P_{in}/4\pi r^2 \quad [W/m^2] \tag{5.3}$$

However, if radiated power density is $P(\theta, \phi)/r^2$ in directions (θ = angle between the considered direction and the one in which maximum power is radiated, known as boresight; and ϕ = phase) at distance (r) from the antenna under elevation, the gain of the antenna can be defined by the following equations:

$$G(\theta, \phi) = P(\theta, \phi)/r^2/P_{id} = P(\theta, \phi)/r^2/P_{in}/4\pi r^2 = 4\pi\ P(\theta, \phi)/P_{in} = P(\theta, \phi)/\ P_{in}/4\pi \quad [dBi] \tag{5.4}$$

The above-defined gain is called an absolute gain or directive gain, which is determined only by the directivity (radiation pattern) of the antenna without taking account of any losses in the antenna system, such as impedance mismatch loss or spillover loss. Thus, if direction is not specified and the gain is not given a function of (θ, ϕ), it is assumed to be maximum gain (Evans, 1991). There is a general relationship between absolute gain and the physical dimensions of the antenna and this is given by the equation as follows:

$$G = 4\pi/\lambda^2\ \eta a \tag{5.5}$$

where η = aperture efficiency and a = physical aperture, which will denote the effective aperture of the antenna.

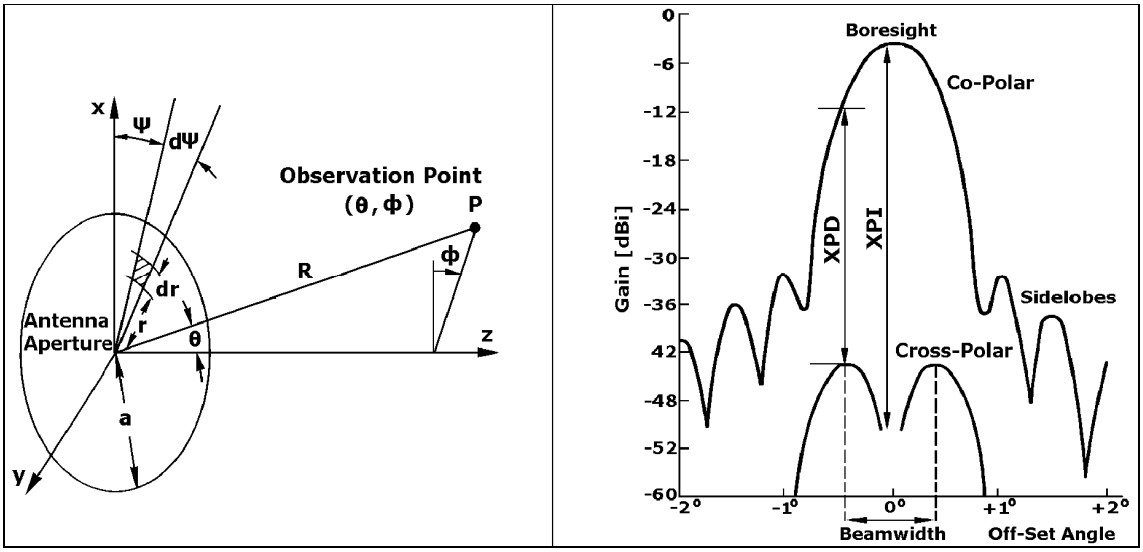

Figure 5. 4 Geometrical Parameters of Antenna Pattern and Gain Characteristics by Evans 1991

According to the above relation, it can be realized that compact antennas with small apertures must have low gain. If an antenna aperture is a dish, a known diameter (d), can be written in normal and in decibel expression as follows:

$$G = (\pi d/\lambda)^2\ \eta = 10 \log \eta\ (\pi d/\lambda)^2 \quad [dBi] \tag{5.6}$$

Thus, it can be calculated that the gain in the Inmarsat shipborne antenna with a diameter of d = 1 m operated at 1.5 GHz is about 21 dBi.

The directivity of the antenna $D(\theta, \phi)$ does not include dissipative losses and is defined as the ratio of $P(\theta, \phi)$ to the power per unit solid angle from an isotropic antenna radiation, with the same total antenna radiated power (P_r). The antenna directivity can be expressed by:

$$D(\theta, \phi) = P(\theta, \phi)/P_r/4\pi \quad (5.7)$$

The definition of antenna directivity does not take the efficiency of an antenna into account because ($P_r/4\pi$) is related to the actual power launched into space. The ratio of $G(\theta, \phi)$ to $D(\theta, \phi)$ is termed the radiation efficiency of the antenna.

5.2.3 Radiation Pattern, Beamwidth and Sidelobes

Radiation calculation is possible in principle if the EM field can be described quantitatively at all points of the antenna surface whose boundaries are those of the apertures. For an antenna that generates a single focused beam, the principal parameter affecting the antenna radiation pattern $E(\theta, \phi)$, after the aperture size (a), is the aperture illumination distribution $E_a(r, \psi)$, which is the amplitude of the far field radiation pattern E, at the point (θ, ϕ), being essentially the Fourier transform of the illumination distribution and is given by:

$$E(\theta, \phi) = 1/\pi a^2 \int_0^{2\pi} \int_0^{a} E_a(r, \psi) \exp [-jkr \sin \theta \cos (\phi - \psi)] \, rdrd\psi \quad (5.8)$$

An example considers a satellite communication antenna, which utilizes a circular aperture, where for circularly symmetric aperture illumination distribution, this relation reduces:

$$E(\theta) = 2/a^2 \int_0^{a} E_a(r) \, J_0 (kr \sin \theta \cos (\phi - \psi)] \, rdr \quad (5.9)$$

where a = d/2 denotes the radius of antenna aperture; J_0 = first kind and order zero of the Bassel function and k = 2 π/2 denotes the wave number. The other notations that denote distance and angles in coordinates are defined in the geometry illustrated in Figure 5.4 (Left). The antenna radiation pattern is three-dimensional in nature, so it usually has to be represented from the point of view of a single-axis plot.

The characteristics of the satellite antenna radiation pattern affect interference levels directly. Any improvement in the pattern will, therefore, be fully reflected in the interference level and such improvement constitutes a very effective means of solving interference problems. To improve the pattern, one can either increase the antenna diameter or, with a constant diameter, use a specific technique for reducing the sidelobes. This method is, therefore, applicable when the satellite network is in the initial stages of development.

The antenna gain is normally calculated with reference to the boresight, i.e., the direction at which the maximum antenna gain occurs, in the case when $\theta, \phi = 0^o$. Gain is usually expressed in (dBi), where component (i) refers to the fact that it is relative to the isotropic gain. In this instance, the matter of moment in a dual polarization frequency re-use satellite communication system is polarization discrimination between the co-polar and cross-polar signals, especially in the antenna main beam region, as illustrated in Figure 5.4 (Right). An important parameter that is used in an antenna's specification is the beam width evaluated by

Half Power Beam width (HPBW) $2\theta_{HP}$, where θ_{HP} is the half-power angle when radiated power becomes half the maximum level (-3 dB). The HPBW (θ_0) is given by the following equation:

$$\theta_0 = 65\ (\lambda/d) \qquad (5.10)$$

Here it is possible to realize that the half-power bandwidth is inversely proportional to the operating frequency and the diameter of the antenna. For example, a 1 m receiver antenna operating in the C-band (4 GHz) has a 3 dB bandwidth of roughly 4.9^o, while the same antenna operating in the Ku-band (11 GHz) has a 3 dB bandwidth of approximately 1.8^o.

The antenna systems have co-polar and cross-polar gains, where the reception of unwanted, orthogonally polarized cross-polar signals will add as interference to the co-polar signal. The ability of an antenna to discriminate between a wanted polarized waveform and its unwanted orthogonal component is termed as its Cross-Polar Discrimination (XPD). When dual polarization is employed and the antenna's ability to differentiate between the wanted polarized waveform and the unwanted signal of the same polarization, introduced by the orthogonal polarized wave, it is termed as the Cross-Polar Isolation (XPI). In this context, an antenna typically would have an XPI > 30 dB.

The level of the antenna pattern's sidelobes is also important, as this tends to represent gain in an unwanted direction. For a transmitting gain, this leads to the transmission of unwanted power, resulting in interference to other systems, or in the case of a receiving antenna, the reception of unwanted signals or noise. The sidelobe characteristic of GES is one of the main factors in determining the minimum spacing between satellites and, therefore, the orbit and spectrum utilization efficiency. The ITU-R S.465-5 recommendation gives a reference radiation diagram for use in coordination and interference assessment, which is defined by:

$$G = 32 - 25 \log \phi \quad [\text{dBi}] \quad \text{for } \phi_{min} \leq \phi < 48^o$$

$$= 10 \text{ dBi} \qquad \text{for } 48^o \leq \phi \leq 180^o \qquad (5.11)$$

where G = gain relative to an isotropic antenna; ϕ = off-axis angle referred to the main lobe axis and $\phi_{min} = 1^o$ or 100 λ/d degrees, whichever is the greater. In this context, most of the effective power radiated by an antenna is contained in the so-called main lobes of the radiation pattern, while some residual power is radiated in the sidelobes. Sidelobes are an intrinsic property of antenna radiation and diffraction theory shows that they cannot be completely suppressed. However, sidelobes are also due partly to antenna defects which can be minimized by proper design. Conversely, due to the reciprocity theorem, the receive antenna gains and radiation patterns at the same frequency, are identical to the transmit antenna gains and radiation patterns. Unwanted power can also be picked up by the antenna sidelobes during reception.

For large satellite antennas, with a diameter over 100 λ (wavelengths), a reference radiation pattern is recommended by the CCIR for interference to and from other satellite and terrestrial communication systems. At this point, the diameters of the vehicle antennas under discussion are, in many cases, below five wavelengths in the L-band. Further, CCIR action is expected to define a reference radiation pattern for mobile antennas in MSC.

5.2.4 Polarization and Axial Ratio

The antenna and the EM field, received or transmitted, have polarization properties. Thus, the polarization of an EM wave describes the shape and orientation of the locus of the extremities of the field vectors as a function of time. A wave may be described as linearly, circularly or elliptically polarized. Linear polarization is such that the electric E-field is oriented at a constant angle as it is propagated and can be either vertical or horizontal.

If a plane wave is propagated along the (z) axis and electric field (E) is on the (x-z) or (y-z) planes, relations for linear vertical and horizontal polarization can be written as follows:

$$E_x = E_a \cdot e^{j(\omega t - kz + \phi a)} \text{ and } E_y = E_b \cdot e^{j(\omega t - kz + \phi b)} \quad (5.12)$$

where E_a; ω; k and ϕ_a denote the maximum amplitude of electric field, angular frequency ($2\pi f$), wave number and initial phase, respectively, while E_b and ϕ_b are the maximum amplitude and the initial phase of the wave.

Circular polarization is the superposition of two orthogonal linear polarizations, such as vertical and horizontal, with a 90^o ($\pi/2$) phase difference. The tip of the resultant E-field vector may be imagined to rotate as it propagates in a helical path. There is a Left-Hand Circularly Polarized (LHCP) wave with anticlockwise rotation and a Right-Hand Circularly Polarized (RHCP) wave with clockwise rotation.

An elliptically polarized wave may be regarded as the result either of two linearly or two circularly polarized waves with opposite directions. This type of polarization is the case when the amplitudes and phase difference between the two waves are not equal ($\pi/2$).

As discussed in a previous section, the signal fields can contain co- and cross-polar components. In this way, the cross-polarization of a source becomes of increasing interest to satellite antenna designers. In the case of Tx or Rx antennas with a linearly polarized field, the cross-polar component is the field at right angles to this co-polar component. If the co-polar component is vertical, then the cross-polar component is horizontal. Circular cross-polarization is that of the opposite hand to the desired principal or reference polarization. Impure circular polarization is, in fact, elliptical (Kantor et al, 1988). The level of impurity is measured by the elliptical and known as the Axial Ratio (AR). The AR can be defined as the ratio of the major axis electric component to that of the minor axis by:

$$|AR| = |E_1/E_2| \; (1 \leq |AR| \leq \infty) \quad (5.13)$$

The signal for AR denotes the direction of rotation, however, an absolute value is usually used to evaluate circular polarized radiated waves and can be expressed in decibels by the following equation:

$$|AR| = 20 \cdot \log(|E_1/E_2|) \quad [\text{dB}] \quad \text{for} \quad (0 \leq |AR| \leq \infty) \quad (5.14)$$

Accordingly, the AR is determined by the performance of the antenna, so the AR is one of the most important parameters of circular polarized antennas. It can easily be understood that the AR depends on direction with respect to the axis of the antenna. In general, the AR is best (smallest) in the boresight direction and is progressively worse further away from the boresight.

Circular polarized waves are used in order to eliminate the need for polarization tracking. RHCP has been used in the Inmarsat transmission system. Otherwise, in the case of aperture-type antennas, such as the parabolic reflector antenna, which is commonly used as a shipborne antenna in the current Inmarsat-A and B terminal, an axial ratio of below 1. 5 dB in the boresight direction is so easy to achieve that polarization mismatch loss is almost negligible. However, in the case of phased array antennas, a degradation of the axis ratio caused by beam scanning must be taken into account.

5.2.5 Figure of Merit (G/T) and EIRP

Although gain is an essential factor in considering antennas, the figure of merit ratio of a gain-to-noise temperature (G/T) is more commonly specified from the standpoint of MSS and satellite communications, in general. The figure of merit for the receiving station is defined as the ratio between the gain of the antenna in the direction of the receiving signal and the receiving system noise temperature, the gain-to-noise temperature ratio (G/T) is generally given for the maximum gain derived from gain formula (5.15.) as follows:

$$G_{max} = P_{max}/P_0/4\pi = 10 \log G \quad [dB] \tag{5.15.}$$

The G_{max} is often called the antenna gain expressed in dB, where the total radiated power in all directions can be determined by the following integration:

$$P_0 = \int_0^{2\pi} \int_0^{\pi} P(\theta, \phi) \sin\theta \, d\theta \, d\phi \tag{5.16}$$

The G/T value for satellite antenna is expressed in decibels per Kelvin [$dB(K^{-1})$] by the following relation:

$$(G/T) = 10 \log G - \log T_{SA} = 10 \log G - \log T_S \quad [dB(K^{-1})] \tag{5.17}$$

The Earth station G/T typical values range from 35 $dB(K^{-1})$, for instance, an LES receive antenna with a 15 to 18 m diameter has some 15.5 $dB(K^{-1})$. The G/T is a very important parameter of an Earth station, so the methods used for its measurement and the contribution to the noise temperature are the subject of the ITU-R S.733 Recommendation.

The noise temperature measured at the terminals of antenna pointed to the sky depends upon frequency of operation, elevation angle and the antenna sidelobe structure. In more formal terms, the noise temperature will be derived from a complete solid angle integration of the noise power received from all noise sources (terrestrial and galactic) and determined for clear weather conditions by the following integral:

$$T_A = 1/4\pi \int_\Omega P(\theta, \phi) \, T(\theta, \phi) \, d\theta \, d\phi \tag{5.18}$$

Thus, to produce a low noise antenna, its sidelobes must be minimized, especially in the direction of the Earth's surface, where T = noise temperature.

System total noise temperature of the system (T_{SR}) at an input port of receiver LNA or at the antenna output (T_A), taking account of losses caused by tracking, feed lines and a radome is defined by:

$$T_{SR} = T_R + T_a (1 - 1/a) + T_A/a \quad \text{or} \quad T_{SA} = T_A + T_a (a - 1) + a\, T_A \tag{5.19}$$

where T_R = noise temperature of the receiver (LNA) with a typical value of about 80 K to 100 K in the L-band; T_a = temperature of the environment of about 300 K; L_f = total loss of feed lines and components such as diplexer, cables and phase shifters if a phased-array antenna is used; a = attenuation expressed as a power ratio ($a \geq 1$ or in decibels $a_{dB} = 10 \log a$); T_A = antenna noise temperature that comes from such effects as the ionosphere and the Earth, which value of about 200 K depends on factors such as frequency and bandwidth and T_{SA} = antenna with a noise temperature. In such a manner, the noise of the antenna temperature must be kept as low as possible by proper design solution in order to obtain a high figure of merit (G/T)

.

With reference to the previously expressed formula ($P_{id} = P_{in}/4\pi r^2$) of transmitting antenna power density on the spherical surface if it has a transmitting gain (G_T) and where (P_{in}) is equal to the transmitted power (P_T), the power density (P_D) can be written by the following equation:

$$P_D = G_T \cdot P_T/4\pi r^2 \ [W/m^2] \tag{5.20}$$

where ($G_T \cdot P_T$) related values are considered to be the radiation power transmitted by an ideal omnidirectional antenna. Therefore, this term is considered as an Effective (or also Equivalent) Isotropically Radiated Power (EIRP), which can be expressed in antilogarithm and decibel expressions, respectively, as follows:

$$EIRP = G_T \cdot P_T \ [W] \quad \text{and} \quad EIRP = [G_T] + [P_T] \ [dBW] \tag{5.21}$$

The EIRP value is an important parameter in evaluating the transmitting performance of a GES terminal including an antenna. However, the EIRP amount (dBW) is defined by the sum of the antenna gain (dB) and the output power of HPA (dBW), taking account of feed losses such as feed lines, cable and a diplexer.

5.2.6 Classification of Satellite Antennas

In many respects, the mobile satellite antennas currently available for satellite applications constitute the weakest links of the system. If the mobile antenna has a high gain, it has to track the satellite, following both mobiles and satellite orbital motions. Thus, sometimes this is difficult and expensive to synchronize.

Therefore, if the vehicular antenna has low gain, it does not need to perform tracking but the capacity of the communications link is limited. In general, according to the transmission direction, there are three types of satellite antennas: **1)** transmitting and receiving or so-called transceiving, as a part of all types of MetSat antennas; **2)** only receiving is part of the special MetSat receivers in spacecraft payloads or on the ground; and **3)** only transmitting is built in spacecraft payloads and ground transmitters of Data Collection Platform (DCP).

5.3 Low-Gain Omnidirectional Antennas

As stated, the satellite antenna systems are classified into omnidirectional and directional. For instance, the gain of omnidirectional antennas is low and generally from 0 to 4 dB in the L-band, which does not require the capability of satellite tracking. Thus, there are three types of low-gain omnidirectional antennas, which are very attractive owing to the small size, light

weight and circular polarization properties. These antennas are also used as elements of directional antennas for special configurations.

5.3.1 Quadrifilar Helix Antenna (QHA)

The QHA low-gain model is composed of four identical helixes wound, equally spaced, on a cylindrical surface. The helix elements are fed with signals equal in amplitude and 0, 90, 180 and 270^o in relative phase. This antenna can easily generate circular polarized waves without a balloon or a 3 dB power divider, which are required to excite a balanced fed dipole and circular polarized cross-dipoles. It can also be operated on a wide frequency bandwidth of up to 200% because it is a travelling-wave-type antenna (Calcutt and Tetley, 2004).

The components of QHA are ground plane **(g)**, pitch **(p)**, pitch angle **(a)**, length **(l)** and diameter **(d)**, presented in Figure 5.5 (A). The diameter of the ground plane is usually selected to be larger than one wavelength and the number of turns is N = l/p. However, it is well known that the parameters for (a) are about 12 to 15 and the circumference of the helix (πd) is about 0.75 to 1.25 wavelengths. Circular polarized waves with good axial ratios can be transmitted along the (z) axis direction (axial mode). The gain of a helical antenna depends on the number of (N) turns and typical gain and half-power beam width are about 8 dBi and 50^o when N = 12 ~ 12 but is usually about 3 dBi.

In general, QHA has two advantages over a conventional unifilar helical antenna. The first is an increase in bandwidth, namely, it can generate axial mode circular polarized waves in the frequency range from 0.4 to 2.0 wavelengths of the helix circumference. The second is lowered frequency for axial mode operation. The principle disadvantage is an increase in the complexity of the feed system. The area of the ground plane is usually about 3 times the diameter of the helix.

5.3.2 Crossed-Drooping Dipole Antenna (CDDA)

A dipole antenna with a half-wavelength (λ/2) is the most widely used and it is also the most popular, having been used in antenna systems such as the parabolic antenna for MSC. A half-wavelength dipole is a linear antenna whose current amplitude varies one-half of a sine wave, with a maximum at the centre. As a dipole antenna radiates linearly polarized waves, two crossed-dipole antennas have been used in order to generate circular polarized waves. The two dipoles are geometrically orthogonal and equal amplitude signals are fed to them with π/2 in-phase difference (Ilcev, 2013). In order to optimize the radiation pattern, a set of dipole antennas is bent toward the ground, as illustrated in Figure 5.5 (B) and, for that reason, it is called a drooping dipole antenna. Otherwise, the CCDA as a transceiver antenna for L-band satellite applications can be mounted inside a radome.

The CDDA is the most interesting for ground applications, where the required angular coverage is narrow in elevation and is almost constant in azimuth angle. By varying the separation between the dipole elements and the ground plane, the elevation pattern can be adjusted for optimum coverage for the region of interest. The general characteristics of this antenna are: gain is 4 dBi minimums, axial ratio is 6 dB maximum and the height of the antenna is about 15 cm. This antenna has a maximum gain in the boresight direction.

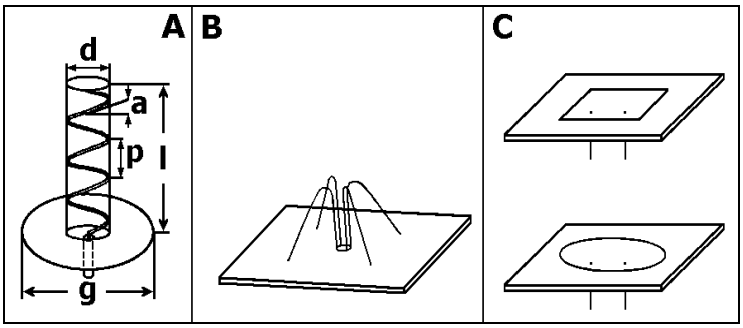

Figure 5. 5 Types of Low-Gain Omnidirectional Antennas by Ilcev 2013

5.3.3 Microstrip Patch Antenna (MPA)

A microstrip disc (patch) antenna is very low profile and has mechanical strength, so it is considered to be the best type for mobiles such as cars and especially in aircraft at the hybrid L to Ku-band, which requires low air drag. In general, a circular disk antenna element has a circular metallic disc supported by a dielectric substrate material and printed on a thin dielectric substrate with a ground plane. In order to produce a circularly polarized wave, a patch antenna is excited at two points orthogonal to each other and fed with signals equal in amplitude and 0 and 90^o in relative phase. Thus, a higher mode patch antenna can also be designed to have a similar radiation pattern to the drooping dipole. To produce conical radiation patterns (null on axis) suitable for land mobile satellite applications, the antenna is excited at higher mode orders. Figure 5.5 (C) illustrates the basic configuration for a circular patch antenna (above it is shown square patch with the same characteristics), which has two feed points to generate circular polarized waves. The resonant frequency is excited by basic mode and given as:

$$f= 1{,}84c/2\pi a \sqrt{\epsilon_r} \qquad (5.22)$$

where (a), (c) and (ϵ_r) are the radius of circular disc, the velocity of light in free space and the relative dielectric constant of the substrate, respectively. The MPA antenna with higher order excitation is considered better because it can optimize the gain in elevation angle to the satellite in the same way as a CDDA. In fact, the area of a higher mode circular MPA is about 1.7 times larger in radius and the gain is about 6 to 8 dBi. The circular patch is also suitable as a satellite navigation-receiving antenna for GPS receivers.

5.4 Medium-Gain Directional Antennas

The medium-gain directional antennas are solutions with a typical gain between 12 and 15 dBi, although some antennas can have even bigger gains. These antennas can provide voice, Fax and data (HSD) in satellite communications.

5.4.1 Aperture Reflector Antennas

The aperture reflector antennas are good solutions with medium-gain characteristics used in satellite communications, with three basic representatives such as SBF, modified SBF and improved SBF antennas, illustrated in Figure 5.6 (A), (B) and (C), respectively. The main characteristics of these three antennas are shown in **Table 5.2.**

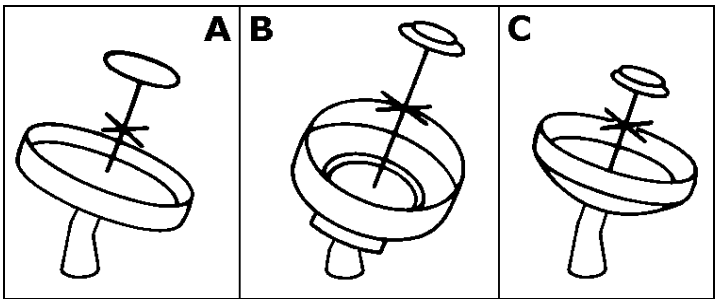

Figure 5. 6 Types of Directional Medium-Gain Aperture Antennas by Fujimoto 2008

Moreover, due to the excellent radiation characteristics of SBF antennas, all three types of aperture antenna with half-power beam width of about 34^o have been in their time proposed for shipborne antenna of Inmarsat-M. The SBF antennas consist of the stabilized platform with two gyroscopes for azimuth and elevation angles, diplexer, HPA and LNA, which are enclosed under the protective cupola of a radome. In order to stabilize the antenna, two gyro wheels rotate in opposite directions on a platform.

1. Short Backfire (SBF) Plane Reflector Antenna – The SBF plane reflector antenna that was developed experimentally by H.W. Ehrenspeck in the 1960s is well known as a highly efficient antenna of distinctly simple and compact construction. Its high directivity and low sidelobe characteristics make it a single antenna with high, even values, which are applicable to satellite communications, tracking and telemetry. Thus, an SBF antenna is very attractive for gains in the order of 13 - 15 dBi peak RHCP and can be mounted primarily for any type of environment.

Table 5. 2 Particulars of Aperture Types of Antennas in Fujimoto 2008

Characteristics	SBF Antenna	Modified SBF Antenna	Improved SBF Antenna
Effective Gain	14.5 dB	15 dB	15 dB
Half-Power Bandwidth	34^o	34^o	34^o
Directive Gain	14.8 dB	15,5 dB	15.5 dB
First Sidelobe Level	–21 dB	–22 dB	–22.5 dB
Axial Ratio	–1.3 dB	–1.1 dB	–1.1 dB
Aperture Efficiency:			
Effective - Directive Gain	65% – 75%	75% – 80%	76% – 85%
RF/VSWR Bandwidth, under 1,5	3%	7%	9%
Diameter of Large Reflector (D_R):			
Bigger ($D_{R\,1}$)	40 cm (2,05λ)	40 cm (2,05λ)	40 cm (2.05λ)
Smaller ($D_{R\,2}$)	-	27 cm (1.38λ)	-
Diameter of Small Reflector (D_r):		-	
Bigger (D_{r1})	9 cm (0.46λ)	9.5 cm (0.48λ)	9 cm (0.46λ)
Smaller (D_{r2})	-	8.5 cm (0.43λ)	8 cm (0.41λ)
Width of a Rim	4.9 (0.25 λ)		4.9 (0.25 λ)
Distance Between (D_R) and (D_r)	9.7 cm (0.49λ)	19.5 cm (0.99λ)	12.9 cm (0.66λ)
Distance Between Exciter & D_r	4.9 cm (0.25λ)	-	5.7 cm (0.29λ)
Distance Between (D_{r1}) & (D_{r2})	-	-	1.8 cm (0.09λ)
Slanting Angle of a (D_R)	0^0	-	15^0

Otherwise, this type of satellite antenna consists of two circular planar reflectors of different diameter, separated generally by about one-half wavelength, forming a shallow leaky cavity resonator with a radiation beam normal to the small reflector. The antenna is fed by a dipole at around the midpoint between two reflectors and it has almost a quarter-wavelength rim on the larger reflector. It has the problem of a narrow bandwidth of about 3% because of its

leaky cavity operation. The Rx terminal G/T is –12 dBK and the EIRP of the Tx terminal is 28 dBW

.

The basic configuration of the SBF antenna consists of a cross-dipole element, which is required to generate a circularly polarized wave, large and small reflectors and a circular metallic rim. The antenna has the strong directivity normal to the reflector and its performance is superior to that of other types of mobile antennas with the same diameter, however, it has the problem of narrow frequency band characteristics. This antenna has many beneficial characteristics, such as efficiency and the simplicity of construction and is also considered a favourite option for a compact and high-efficiency shipboard antenna.

2. Modified SBF Plane Reflector Antenna - This antenna differs from the conventional SBF antenna in that there is either an additional step on the large reflector or a change in the shape of the large reflector from a circular to a conical plate in order to improve the gain characteristics and the frequency bandwidth of the VSWR. The dual reflector improves the input impedance characteristics covering the frequency range between transmitting and receiving sides (Fujimoto, 2008). The conventional SBF model is a resonant-type antenna, producing input impedance characteristics that are narrow in bandwidth, so for instance, wider bandwidth is required to cover the 1.6/1.5 GHz RF range. In such a way, the improvement in the antenna input impedance is greatly dependent on the size and the separation of the small reflectors. The VSWR can be reduced from 1.7 and 1.5 (at 1.54 and 1.64 GHz) to below 1.2 for each RF band.

3. Improved SBF Conical Reflector Antenna – The main research activities of the ETS-V satellite program have been focused on studying the reduction of fading, using compact and high-efficiency antennas with a gain of around 15 dBi, so the electrical characteristics of a simple SBF antenna have been improved by changing its main reflector from a flat disk to a conical or a step plate and by adding a second small reflector. The gain is improved by 1 dB without changing sidelobe levels.

5.4.2 Wire Antennas

The wire antenna systems are monosyllabic construction or combinations of elements, such as different shapes of wire spirals and helixes, dipoles and patches. These types of antennas have a very simple construction, with any reflector specified for medium-gain directional antennas and, with some modification, respond well to the demands of satellite systems.

1. Helical Wire Antennas – Since an axial mode of helical wire antenna has good circular polarization characteristics over a wide frequency range, it has been put into practical use as a single wire antenna or as an array element. With respect to the structure, this antenna can be considered a compromise between the dipole and the loop antennas and the radiation mode varies with the pitch angle and the circumference of the helix. In particular, a helix with a pitch angle of 12 to 15^{o} and a circumference of about 1 λ has a sharp directivity towards the axial direction of the antenna. This radiation mode is called the axial mode, which is the most important mode in helical antennas. Several studies have been carried out on the properties of the axial mode helical antenna with a finite reflector. The current induced on the helix is composed of four major waves, which are two rapidly attenuating waves and two uniform waves along the helical wire. These waves include the travelling wave and the reflected wave. Thus, in a conventional helical antenna, the uniform travelling wave will be dominant when the antenna length is fairly large, with typical versions such as a conical helix

shown in Figure 5.7 (A) and a cylindrical helix in Figure 5.7 (B). A conical helix is interesting for all RF bands and especially for L-band satellite communications enabling HPBW in the order of 100^o and circular polarization without hybrid gains of 4 to 7 dBi. Cylindrical antennas can be monofilar or multifilar, also suited for satellite communications, while in a short-cut cylindrical helix antenna, the rapidly attenuating travelling wave will be dominant, especially in a two-turn (N = 2) helical antenna.

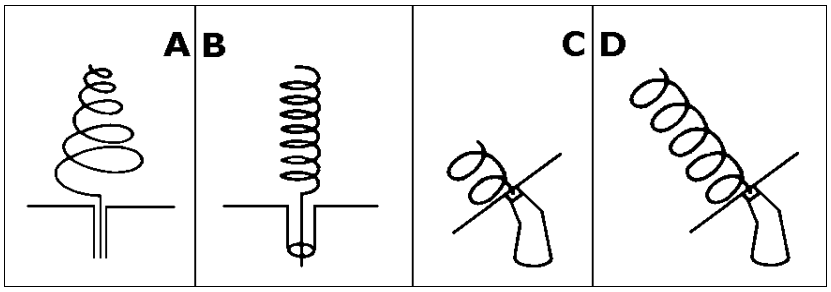

Figure 5. 7 Types of Helical Wire Antennas by Fujimoto 2008

a) Conical Helix Antenna can be regarded as a low-gain development of the cylindrical helix antenna and is suitable for wide-beam width applications with good efficiency. Thus, with suitable choices of cone angle and turn spacing, it is possible to achieve a beam width in the order of 100^o. This type of antenna can also achieve an input VSWR of 1.5:1 or better than 5% frequency bandwidth merely by incorporating a simple quarter-wavelength transformer. The typical size for an L-band application is in the order of 15 cm in length and the ground plane is about 20 cm in diameter. The resultant gain is approximately 4 to 7 dBi, which is between low and medium-gain requirements.

b) Two-Turn Cylindrical Helix Antenna has two-turns of wires, forming a simple helical antenna solution with reflector, illustrated in Figure 5.7 (C). This model has relatively high antenna gain and excellent polarization characteristics for its size. Radiation patterns characteristically are calculated with respect to (E_0) and (E_ϕ) planes. The gain of this antenna is 9 dBi and the axial ratio is about 1 dB, with reflector diameter (d) around 1λ. Such types of antenna have comparatively high performance in spite of their small size and compact construction.

c) Five-Turn Cylindrical Helix Antenna is shown in Figure 5.7 (D). The main electrical characteristics are: gain is 12.5 dBi of peak RHCP for Tx and 11.5 dBi for Rx; sidelobe level has value of about –13 dB; axial ratio is 3 dB; beam width of 3 dB has angle of $–47^o$; terminal G/T has –16 dBK and terminal EIRP has 29 dBW. This antenna solution is designed and developed by the European research institution ESTEC. In addition, stabilization of this antenna is obtained by gravity elevation on double-gimbaled suspension.

2. Inverted V-Form Cross Dipole Antenna – This antenna is an advanced circularly polarized antenna with tick V-elements, shown in Figure 5.8 (A). The resonance of this antenna is obtained when the length is somewhat shorter than a free-space half wavelength. Thus, as the thickness is increased, the resonant length is reduced. Circular polarization can be produced by a pair of orthogonally positioned dipoles driven in quadrature phase with equal amplitudes. The crossed-dipole antenna arrangement cannot provide a good axial ratio off boresight because the radiation patterns for the straight dipole are different in both principal planes, called the H and E-planes. This shortcoming can be improved by modifying the straight dipoles to a non-straight version, such as the V and U-forms. The improved dipoles are called V and U-type dipoles. According to some conducted measurements, the U-type provides better electrical performance than the V-type, though the V-type is simpler in mechanical structure and is less complex. The crossed-dipole can also produce circular

polarization without using any external circuits, such as the hybrid component. The condition to excite the circularly polarized waves can be established by a balun and the self-phasing of four radiating elements. Two of the elements are at a 0^o phase angle and the other two are at an 180^o phase angle. Thus, the desired 90^o phase difference is obtained by designing the orthogonal elements such that one is larger relative to making it inductive, while the other is smaller to make it capacitive. This type of antenna is a good model for Ku-band satellite communications.

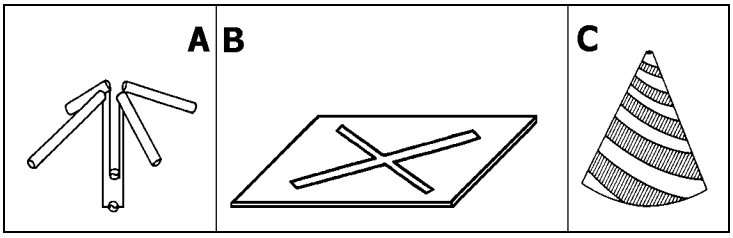

Figure 5. 8 Types of Cross Dipole, Slot and Conical Wire Antennas by Ilcev 2013

3. Crossed-Slot Antenna - These antennas are useful for L-band satellite communications, as illustrated in Figure 5.8 (B). The slot antenna is circularly polarized and is complementary with the corresponding dipole antenna, so that the radiation pattern is the same as that for the horizontal dipole. There are only two differences: first, is the property that the electric and magnetic fields are interchanged and, second, is that the slot electric field component normal to the perfectly conducting sheet is discontinuous from one side of the sheet to the other because the direction of the field reverses. In this case, the tangential component of the magnetic field is, likewise, discontinuous. This antenna can be also complementary with the corresponding crossed-dipole antenna, although the feeding method for the circular polarization is more complicated. Thus, on a model of this antenna, known as a cavity-backed, it needs one 90^o hybrid to produce the circular polarization. This feed technique is effective not only to suppress undesired coupling between the cross slots but also to match the input impedance over a wider frequency band.

4. Conical Spiral Antenna – This type of antenna has spiral wire elements on a cone with circular polarization and is suitable for L-band LMSC and GPS applications, while the bifilar version is also used in Ku-band satellite communications, which is shown in Figure 5.8 (C). In comparison with a conical helix antenna, this type of antenna provides better performance and is more versatile, though the geometry is somewhat complex. Its radiation mechanism can be understood by regarding the two spirals as a transmission line. When two conductor arms are fed in antiphase at the cone apex, waves travel out from the feed point and propagate along the spirals without radiating until a resonant length has been traversed. Strong radiation occurs at that point and very little energy is reflected by the outer limits of the spiral.

5. Planar Spiral Antennas – Cavity-backed planar spiral antennas are commonly divided into three main categories: equiangular, logarithmic and Archimedean spiral antennas. These types of antennas are useful for L to Ku-band satellite communications. In general, this antenna has been fed by using the external balun but it can also be fed at the centre point, or apex, from a coaxial cable bonded to one of the arms, without any external baluns, like the conical spiral antenna.

a) Equiangular Spiral Antenna corresponds to the special case of the conical spiral antenna, bifilar with logarithmic period and cavity-backed. This antenna needs no external hybrid circuits to produce circular polarization and the example shown in Figure 5.9 (A) can radiate LHCP waves outward from the page and RHCP waves into the page when the pair of spirals

is excited in antiphase at the centre. Otherwise, according to experimental measurements, the axial ratio is near unity and the HPBW is in the order of 90^o over a decade bandwidth or even more. As for the input impedance, the resistive part on the thickness of the antenna elements and thin elements lead to high impedance values. This implies that the impedance depends on the arm width when the structure is planar. If the angular extent (Δ) is chosen to be 90^o, the geometries of the arm and the space between arms are identical, except for a rotation of 90^o around an axis. This structure is defined as self-complementary, just like the conical spiral antenna but it should be noted that the planar spiral antenna has a constant impedance of 60π [Ω] for the two arm configurations.

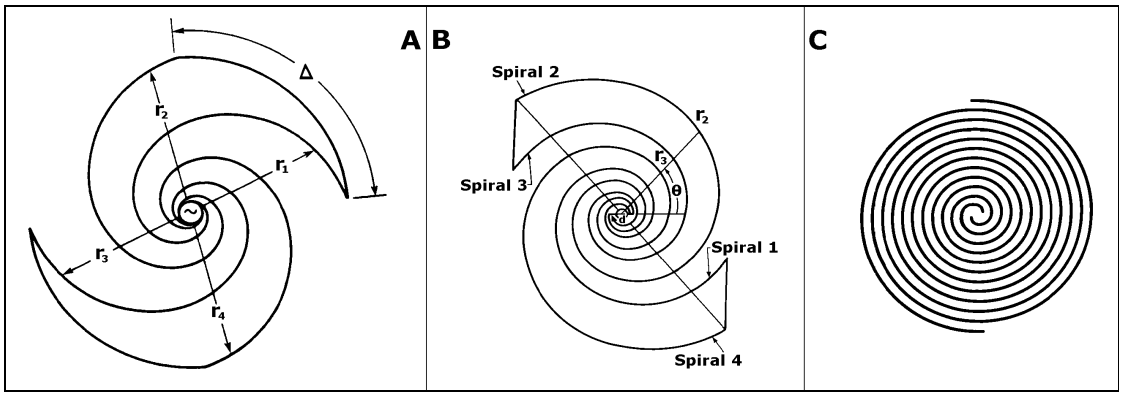

Figure 5. 9 Types of Spiral Wire Antennas by Fujimoto 2008

b) Logarithmic Spiral Antenna has bifilar design with logarithmic period and cavity-backed, as shown in Figure 5.9 (B). It can radiate RHCP waves outward from the page and LHCP waves into the page without any external hybrid circuits, as a pair of spirals is excited with an antiphase at the centre.

c) Archimedean Spiral Antenna thin-wire bifilar cavity-backed antenna, as shown in Figure 5.9 (C), is another geometry of the planar spiral. This antenna is broadband and it has superior bandwidth properties when fully optimized and typically consists of a pair of thin wire arms. It also needs no external hybrid circuits to produce circular polarization and can radiate RHCP waves outward from the page and the LHCP waves into the page if the pair of thin wire arms is excited in antiphase at the centre. When placed in a quarter-wave cavity, this antenna can achieve near-octave bandwidth, even when the cavity consists in a metal-based cylinder without any absorber. Thus, if an absorber-loaded cylinder is employed in the cavity, a greater-than decade bandwidth may be achieved, although about half the power is dissipated into heat by the absorber. A typical Archimedean spiral antenna has an octave bandwidth for a VSWR less then 2, an axial ratio of less then 2 dB and a beam width of about 70^o, while a gain of 7 to 8 dBi is achieved without an absorber. The structure has several mechanical advantages: it is compact and fairly simple to construct and the spiral arms can be easily fed, using a suitable impendence-transforming balun.

5.4.3 Array Antennas

Several different type of antenna can be arrayed in space to make a directional pattern or one with a desired radiation pattern. This type of integrated and combined antenna is called an array antenna consisting in more than two elements, such as microstrip, cross-slot, cross-dipole, helixes and other wire elements. Each element of an array antenna is excited by equal amplitude and phase and its radiation pattern is fixed.

1. Microstrip Array Antenna (MAA) – This is a nine-element flat antenna, disposed in three lines spaced at 94 mm, namely, about a half wavelength at 1.6/1.5 GHz and whose antenna volume is about 300 x 300 x 10 mm (see Figure 5.10 (A). As shown in this figure, the element arrangements of the antenna solutions are 3 x 3 rows square arrays in order to obtain similar radiation patterns in different cut planes. The MAA beam scanning is performed by controlling four-bit variable phase shifters attached to each antenna element.
2. Cross-Slot Array Antenna (XSA) – This is a 16-element solution with 97 mm spacing and their volume is about 560 x 560 x 20 mm, as shown in Figure 5.10 (B). The element arrangement of the XSA is a modified 4 x 4 square array in order to obtain similar radiation patterns in different cut planes. The XSA antenna beam scanning is carried into effect to control four-bit variable phase shifters associated to each antenna element.

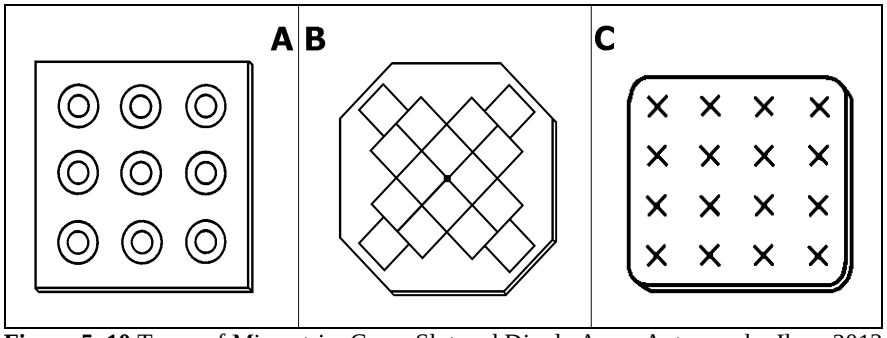

Figure 5. 10 Types of Microstrip, Cross-Slot and Dipole Array Antennas by Ilcev 2013

3. Cross-Dipole Array Antenna - This is composed of 16 crossed-dipoles fed in phase with a peak gain of 17 dBi and with the feeding circuit behind the radiating aperture, as shown in Figure 5.10 (C). The main electrical characteristics of this antenna are: gain is 15 to 17 dBi with peak RHCP transmit; axial ratio has a value of 0.7 dB; beam width of 3 dB is -34^{o}; terminal G/T is –9.5 dBK and EIRP terminal value is 32 dBW. It consists in a stabilization mechanism, diplexer, HPA and LNA, which are all protected by a plastic radome.
4. Four-Element Array Antennas – There have been several four-element antenna models developed, such as Yagi-Uda, Quad-Helix and four elements SBF array.
a) Yagi-Uda Crossed-Dipole Array Antenna has been developed for use on board ships and is protected with a radome, as shown in Figure 5.11 (Left). The feeder of this antenna is a simple formation of four in-line crossed-dipoles fixed in the middle of the reflector. This endfire array has circular polarization and the gain is between 8 and 15 dBi.
2. Quad-Helix Array Antenna – The quad-helix array antenna solution is composed of four identical two-turn helical wire antennas in the shape of a square and whose elements are oriented in the manner illustrated in Figure 5.11 (Middle). According to previous studies, the effect of mutual coupling between each element of this antenna is not negligible and this mutual coupling mainly degrades the axial ratio. The axial ratio of a single helical antenna is about 1 dB but this value is degraded to about 4.5 dB in the case of the array antenna with an array spacing of 0.7λ. However, the best properties of antenna gain and axial ratio can be obtained at a rim height of about 0.25λ. The antenna gain is improved by 0,4 dB and the axial ratio is also improved by 3.5 dB, compared to that of the quad-helix array antenna without rims. The performance characteristics of this small antenna are essentially: gain is about 13 dB (HPBW is 38^{o}) and aperture efficiency is about 100%.
3. Four-Element SBF Array – This antenna is developed on the basis of a conventional SBF antenna as an integrated array with four SBF elements, as shown in Figure 5.11 (Right). The antenna provides high aperture efficiency, circular polarization and almost high-

performance gain between 18 and 20 dBi. Due to the high gain characteristics, this array is very suitable for maritime applications as a shipborne antenna.

Figure 5. 11 Four-Element Arrays by Ilcev 2013

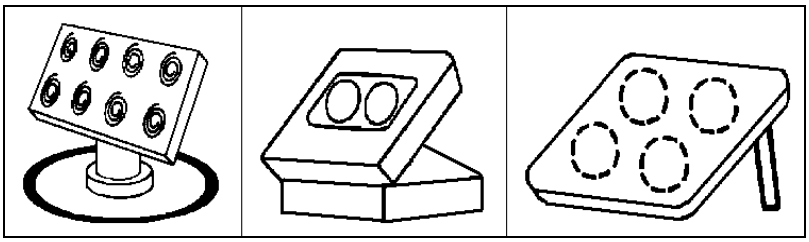

Figure 5. 12 Types of Spiral, Two and Four-Patch Array Antennas by Ilcev 2013

4. Spiral Array Antenna – This is directional antenna expected to provide voice and HSD links. The cost is an important factor to be taken into account in designing antenna systems. Thus, it may be replaced by a phased array antenna in the near future because it has many attractive advantages, such as low profile, high-speed tracking and potential low cost. It has a mechanical steering antenna with eight spiral elements and with adopted closed loop tracking method gives about 15 dBi in system gain, as shown in Figure 5.12 (Left). The antenna is 30 cm in radius, 35 cm in height and 1.5 kg in weight. The array consists of 2 x 4 spiral elements and it forms a fan beam with a half-power beam width of 21^{o} in the azimuth and 39^{o} in the elevation plane at L-band. Its peak gain is about 15 dBi, including the feeder losses, and is suitable to track the satellite for MSC, because elevation angles to the satellite are not as varied as those of the azimuth angles. In effect, the antenna beam direction can be shifted in two azimuth directions, from the E or W side, by switching the pin diode phase shifters. Consequently, the difference between the received signals in both directions is used to drive the antenna system towards the satellite. The beam-shifting angle is set to approximately 4^{o}.

5.4.4 Patch Array Antennas

The main feature of the future MSC will be portability, which means that a person can directly access the satellite to establish a link using a very small TES transceiver with an antenna system. Even in the present Inmarsat L-band system, great efforts have been made to develop transportable and portable terminals with corresponding antennas.

1. Two-Patch Array Antenna – This antenna for TES and briefcase portable terminals is developed in the Inmarsat and ETS-V programs, as illustrated in Figure 5.12 (Middle). This antenna has two microstrip patch elements (one for Rx and another for Tx), gain is 6 dBi, EIRP is 6 dBW and G/T is –21 dBK. The reason for adopting separate Rx and Tx antennas is to eliminate a diplexer, which is too large and heavy for a compact and lightweight terminal. The antenna beam width on the lid is wide enough to point to a satellite by manual tracking.

2. Four-Patch Array Antenna – Several types of this antenna were developed for universal satellite communications, which may have a mechanically steered, tilted 1 x 4 patch array

and two electrically steered planar-phase array antennas. Otherwise, the mechanically steered four-square patch arrays can be fixed in one line, similar to two-patch array or can have the shape of a four-circular patch array manually steered antenna, which arrangement is shown in Figure 5.12 (Right).

These three medium-gain antennas. shown in Figure 5.12, feature beams that are narrow in azimuth angle, hence, they require azimuth steering to keep the beam pointed toward the desired satellite. They provide 9 to 12 dBi gain, reject multipath signals outside their beam pattern and allow two satellites separated by 30^o in a GEO satellite arc and to reuse the same frequency. A dither-tracking four-element, circular, polarized array has been designed, 10.16 cm high, 50.8 cm in diameter, with 20 – 60° elevation coverage and with a minimum of 10 dBi gain. The rotating antenna platform of these antennas is mounted on the fixed platform that includes the motor drive and pointing system hardware.

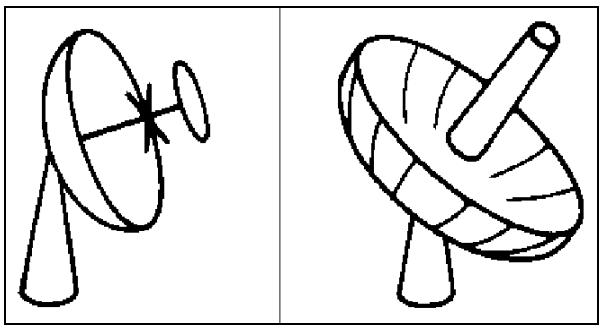

Figure 5. 13 High-Gain Directional Reflector Antennas by Fujimoto 2008

5.5 High-Gain Directional Aperture Antennas

High-gain directional aperture antennas are more powerful transmission reflectors and panels used in any kind of satellite communications for fixed, mobile and ground applications. The typical gain of these antennas is more than 20 dBi, EIRP is a maximum of 33 dBW and G/T is about –4 dBK. In fact, there are two basic types of directional parabolic antennas: dish and umbrella and the third new solution for Inmarsat transportable units is the Quad flat panel antenna designed by the South African-based company OmniPless.

5.5.1 Parabolic Dish Antenna

The first generation of parabolic dish antennas used a reflector in diameter of max 1.2 m, whereas on newer models it is likely to have reduced in size to approximately 0.7 to 0.8 m, as shown in Figure 5.13 (Left). Since a large proportion of the Rx signal gain and Tx EIRP is produced by the antenna, the area of the dish can only be reduced if the transmitting power from the satellite transponder is increased, when the receive preamplifier gain can be increased without an appreciable increase in noise. The parabolic reflector is most often used for high directivity for radio signals travelling in straight lines, as do light rays. They can also be focused and reflected just as light rays can, namely, a microwave source can be placed at the focal point of the antenna reflector. The field leaves this antenna as a spherical wave front. As each part of the wave front reaches the reflecting surface, it is phase-shifted 180^o. Each part is then sent outward at an angle that results in all parts of the field traveling in parallel paths. Due to the special shape of a parabolic surface, all paths from the focus to the reflector and back into space line are the same length. When the parts of the field are reflected from the parabolic surface, they travel to the space line in the same amount of time.

This antenna is a large microwave parabolic consisting in the reflector of dish shape, feeder structure, waveguide assembly, servo and drive system and protective radome.

1. Stable Platform – This is the antenna support assembly, which must remain perfectly stable when the ship is pitching and rolling in extremely bad weather conditions. It is essential that the stable platform hold the reflector in its Azimuth/Elevation (A/E) angular positions despite movement of the ship. The platform usually consists of a large solid bed mounted in such a way that four gyro compasses are able to sense movement and correct any errors detected, holding the platform level. In practice, it is a form of electronic gimbal.

2. Tracking System – The antenna is controlled in A/E angles by stepping motors, which, in turn, are electronically controlled in a simple feedback system. This electromechanical antenna arrangement enables the dish to maintain a lock on a satellite despite navigation course changes. In such a way, as the ship changes course, both A/E control corrections must be made automatically.

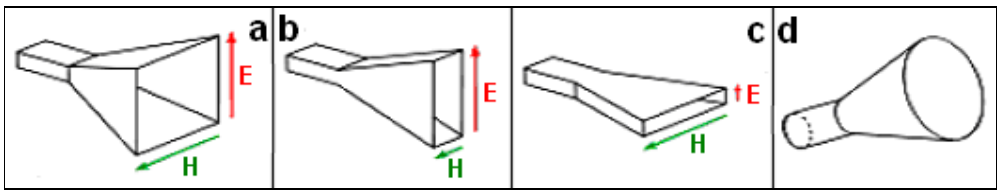

Figure 5. 14 High-Gain Directional Horn Antennas by Ilcev 2013

3. Computer Control – The antenna unit processor controls all antenna functions, which include satellite tracking and electronic control.

4. RF Electronics – This segment contains the Tx HPA and the Rx RF front-end LNA stages, plus all the critical Bandpass signal filter stage.

5. Multiplexer Unit – In modern equipment, it is common practice to reduce the number of cables between antenna and transceiver equipment. Hence, this is achieved by multiplexing up/down signals or commands between antenna and transceiver onto the one coaxial feeder. Therefore, this antenna can be connected in fixed, mobile and ground satellite stations.

5.5.2 Parabolic Umbrella Antenna

An umbrella-type antenna is a deployable, compact and lightweight parabolic type suitable for transportable and ground transceivers, as shown in Figure 5.13. (Right). Otherwise, this antenna has almost all the same technical characteristics as a parabolic dish antenna.

5.5.3 Horn Antennas

Horn antennas are very popular at UHF (300 MHz-3 GHz) and higher frequencies, such as up to 140 GHz. Horn antennas often have a directional radiation pattern with a high antenna gain, which can range up to 25 dB in some cases, with 10-20 dB being typical. Horn antennas have a wide impedance bandwidth, implying that the input impedance is slowly varying over a wide frequency range. However, the bandwidth for practical horn antennas can be on the order of 20:1 (for instance, operating from 1 GHz-20 GHz), with a 10:1 bandwidth not being uncommon.

The gain of horn antennas often increases, while beamwidth decreases as the frequency of operation is increased. This is because the size of the horn aperture is always measured in wavelengths; at higher frequencies, the horn antenna is “electrically larger”. This is because a higher frequency has a smaller wavelength. Since the horn antenna has a fixed physical size

(say a square aperture of 20 cm across, for instance), the aperture is more wavelengths across at higher frequencies. Moreover, a recurring theme in antenna theory is that larger antennas (in terms of wavelengths in size) have higher directivities (Fujimoto, 2008).

Horn antennas have very little loss, so the directivity of a horn is roughly equal to its gain. Horn antennas are somewhat intuitive and relatively simple to manufacture. In addition, acoustic horn antennas are also used in transmitting sound waves (for example, with a megaphone). Horn antennas are also often used to feed a dish antenna, or as a "standard gain" antenna in measurements. Horns can have different flare angles as well as different expansion curves (elliptic, hyperbolic, etc.) in the E-field and H-field directions, making possible a wide variety of different beam profiles.

Below are introduced the following main types of horn antennas:

1. Pyramidal Horn – This is a major horn antenna with the horn in the shape of a four-sided pyramid, with a rectangular cross section, as illustrated in Figure 5.14 (a). They are a common type of this antenna, used with rectangular waveguides, and radiate linearly polarized radio waves.

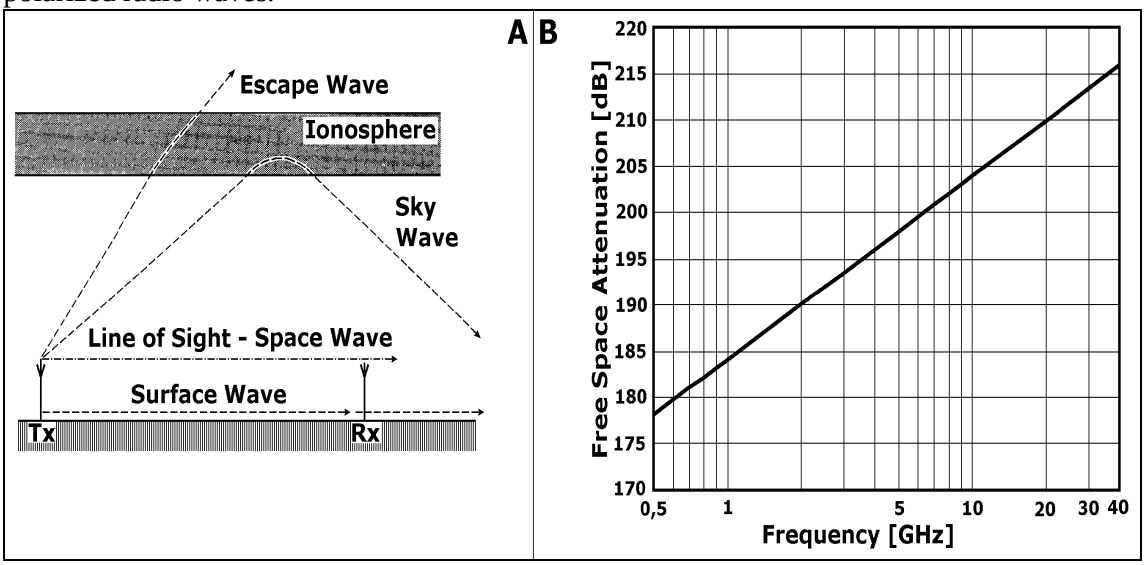

Figure 5. 15 Radiowave Modes of Propagation and Free Space Loss by Ohmori et al, 1998

2. E-plane Horn – This is a sectoral four-sided horn antenna flared in the direction of the electric or E-filed in the waveguide, as shown in Figure 5.14 (b).
3. H-plane Horn – This is a sectoral horn flared in the direction of the magnetic or H-field in the waveguide, as shown in Figure 5.14 (c).
4. Conical Horn – This is a horn in the shape of a cone, with a circular cross section, as shown in Figure 5.14 (d). They are used with cylindrical waveguides.

5.6 Propagation and Interference Consideration

Propagation and interference characteristics are very important for providing quality and reliability of satellite propagation channels. The Quality of Service (QoS) can be expressed in terms of the Bit Error Rate (BER) performance, which depends on the Carrier-to-Noise C/N_0 density ratio, while the service reliability is manifested in the relation of service availability. Thus, the intervening medium between UES within the network and satellites is termed a transmission channel. The fixed satellite services have two constant channels between a

minimum of two UES using the same spacecraft, which have many different characteristics, which need to be taken into account during the system design examination (Ohmori et al, 1998).

The common satellite channel environment affects radiowave propagation in changeless ways. The different parameters influenced are mainly path attenuation, polarization and noise. The factors to be considered are gaseous absorption in the atmosphere, absorption and scattering by clouds, fog, all precipitation, atmospheric turbulence and ionospheric effects. Thus, several measurement techniques serve to quantify these effects in order to improve reliability in the system design. Since these factors are random events, satellite system designers usually use a statistical process in modeling their effects on radiowave propagation.

5.6.1 Radiowave Propagation

Radiowaves travel in space as electrons at the speed of light approximately 300,000,000 m/sec. When radiowaves are propagated from a transmitter antenna, they form three modes of propagation path: surface, sky and space wave propagation, shown in Figure 5.15 (A). Radiowaves are generally transmitted from an antenna omnidirectionally but transmission can be also modified in a directional path by using a directional dish or antenna arrays.
The surface wave is a radiowave that is modified by the nature of the terrain over which it travels. The surface wave propagation predominates at all radio frequencies up to 3 MHz for VLF, LF and MF bands. Hence, sky waves are severely influenced by the action of free electrons, called ions, in the upper atmosphere, known as the ionosphere and are caused to be attenuated and reflected and possibly returned to Earth. In fact, sky wave propagation predominates in the HF band between 3 and 30 MHz.

Above 30 MHz, the predominant mode of propagation of radiowaves is by the space wave. This wave, when propagated between 30 and 300 MHz into the troposphere by an Earth VHF or UHF radio station, is subject to deflection by variations in the refractive index structure of the air through which it passes, which will cause the radiowave to follow the Earth's curvature for short distances up to about 100 km. However, space waves above 300 MHz propagated upwards, away from the troposphere, may be termed free space waves and are primarily used for satellite communications.

Whilst all transmitting antenna systems produce one or more of the three main modes of propagation, one of the modes will predominate. The predominant mode may be equated to the frequency used, as all other constraints remain constant. Therefore, for the purposes of this explanation of propagated radiowaves, it is assumed that the mode of propagation is dependent upon the frequency used in an adequate system, for that is the only parameter, which may be changed by an operator.

The simplest situation involving the transmission of information by EM waves is when the Tx antenna transmits directly to the Rx antenna, without any obstacles in the path through which the EM waves must travel. This situation occurs when both antennas are located at a relatively short distance on the Earth's surface with full mutual visibility. As the distance between the two antennas increases due to the Earth's curvature, the EM waves are no longer in a direct path (line-of-sight).

In order to increase the path length, the antenna can be fitted on a higher mast but only to the extent that the costs do not become prohibitive. In this way, the problem can be solved by

means of forthcoming stratospheric platforms or communications satellite payloads. Since these satellites are placed at very high altitudes, their reach is far superior to that of the higher towers that can be built on the Earth's surface, sea altitudes and other parameters illustrated in **Table 5.3**.

Table 5. 3 Altitude Location of Stratospheric Platforms and Spacecraft in Ilcev 2013

System	Altitude (h) in Km	Angle in degrees	Distance (d) in Km
International Flight	10	3.313	368.4
Stratospheric Platforms	30	5.549	617.1
Amateur Satellites	150	12.320	136.2
LEO Satellites/Low	780	27.008	3003.6
LEO Satellites/High	2000	40.438	4497.1
MEO Satellites	10000	67.095	7461.7
GEO Satellites	35600	81.268	9037.8

When two antennas situated on the Earth are very far apart and there is no visibility between them, stratospheric platforms or satellites can be used to relay the signals. There is otherwise visibility between the Tx antenna and the spacecraft (platforms) and vice versa, between spacecraft (platforms) and Rx antenna. At this point, the ways these signals will travel on their line-of-sight depend on propagation characteristics and conditions of interference in the hypothetical environment.

Since communications satellites are located at higher altitudes relative to the Earth's surface than stratospheric platforms and masts, they cover a wider area, which is beneficial for ocean spaces, continents and for countries with large dimensions.

5.6.2 Propagation Loss in Free Space

It is necessary to define the loss between Tx and Rx antenna separated by a distance from the transmission medium, assumed to be a vacuum and the antenna is isotropic. It may serve either as Tx or Rx antenna in the radiation field where it is situated.

Considering that the isotropic radio antenna radiates signals in all directions of its spherical surface with total power flow P_T in Watts, including receiving antenna gain, at a sufficiently large distance (r) in meters away from the centre to the surface of the sphere, the power flux of hypothetical antenna per unit area through any portion of the spherical surface must be as follows:

$$P_f = P_T/4\pi r^2 \tag{5.23}$$

The amount of power that the receiving antenna absorbs in relation to the RF power density of the EM field is determined by its effective aperture, which is defined as the area of the incident EM wave front that has a power flux equal to the power dissipated in the load connected to the receive antenna output terminals. Following the previous (5.1.) equation, the receiving power at a receiving antenna can be expressed by:

$$P_r = P_T (\lambda/4\pi r)^2 = P_T/L_f \tag{5.24}$$

where λ = wavelength and L_f = free space transmission loss, which can be given in dB as is presented in the following relation:

$L_f = 10 \log_{10} (P_T / P_r = 32{,}40 + 20 \log f_{MHz} + 20 \log r_{km}$ (5.25)

where f = frequency of the emitted radio field in dB and r = distance in km between Tx and Rx antenna. Thus, free space loss is related to operating frequency and transmission distance. Figure 5.15 (B) illustrates free space loss as a function of frequency in GHz for a distance of 36,000 km.

5.6.3 Atmospheric Effects on Propagation

This study deals with propagation effects in all regions of the atmosphere and free space, including the Earth's ionosphere. Most of the Earth's weather precipitation and hydrometeors occur in the troposphere, which is the non-ionized region from the Earth's surface up to a height of about 15 km above the surface at the Equator. The thickness of the troposphere decreases towards the poles. Therefore, propagation effects in the troposphere tend to increase in importance as the RF increases above 1 GHz. For satellite systems, the effects of reflection from the Earth's surface are critically important at even lower RF.
At frequencies below about 1 GHz, the most important region of the Earth's atmosphere is the ionosphere, the ionized region above the stratosphere, within which low RF propagation effects are quite strong. Propagation effects within the ionosphere have an influence on the terrestrial and Earth space paths from VLF to SHF bands. However, it should be borne in mind that for an RF band range below a certain number of GHz, the ionospheric propagation effects can be quite important and for frequencies above a certain number of GHz, tropospheric effects may be negligible (Schott, 1997).

At this point, radiowave signals passing through the atmosphere or over the surface of the Earth begin to lose strength. The decrease of signal due to the medium through which it passes is called attenuation.

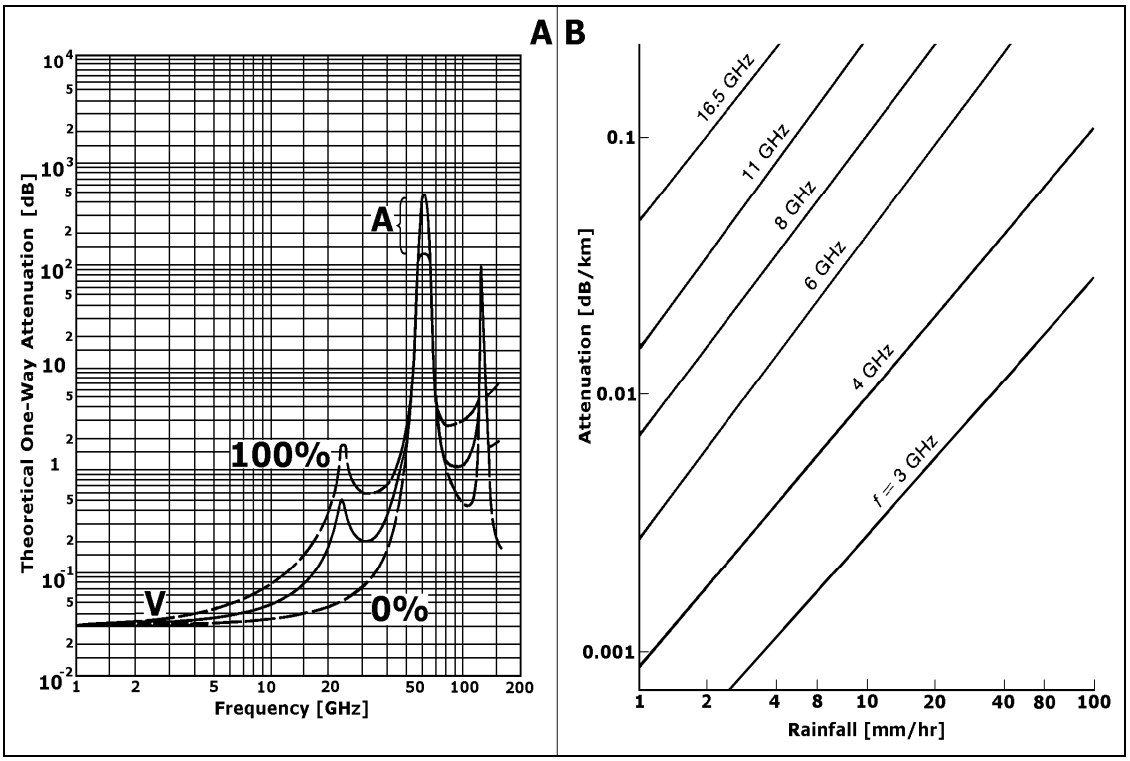

Figure 5. 16 Theoretical One-Way and Rainfall Attenuations by Richharia 1995

5.6.4 Propagation Effects of the Troposphere

The troposphere extends upwards from the Earth's surface to a height of approximately 15 km, where it meets the stratosphere. More exactly, at the boundary between the two spaces, there is a region called the tropopause, which possesses a different refractive index to each neighbouring layer. The effect exhibited by the tropopause on a space wave is to produce a downward bending action, causing it to follow the Earth's curvature. Hence, the bending radius of the radiowave is not as severe as the curvature of the Earth, nevertheless, the space wave will propagate beyond the visual horizon. In practice, the radio horizon exceeds the visual horizon by approximately 15% (Gagliardi, 1984).

5.6.4.1 Attenuation due to Atmospheric Gases

The different types of gases present in the atmosphere may attenuate the electromagnetic waves, which are caused by the molecular absorption of the atmospheric constituents and are strongly frequency dependent. The main contributors to this attenuation below 70 GHz are water vapour and oxygen. Thus, absorption increases as the elevation angle is reduced. The elevation angle. at any frequency, is a function of temperature, pressure, humidity of the atmosphere and the elevation angle of the satellite.

At sufficiently high frequencies, EM waves interact with the molecules of atmospheric gases to cause attenuation. These interactions occur at resonance radio frequencies and are apparent in plots of zenith (90^o elevation angle) attenuation versus frequency, as shown in Figure 5.16

(A). This is the theoretical total estimated one-way attenuation for vertical paths through the atmosphere, where solid curves are for moderately humid atmosphere, dashed curves represent the limits for 0% and 100% relative humidity, V is vertical polarization and A denotes limits of uncertainty, for a vertical Earth space path as a function between 1 and 200 GHz at 45^o North latitude using US standard atmosphere.

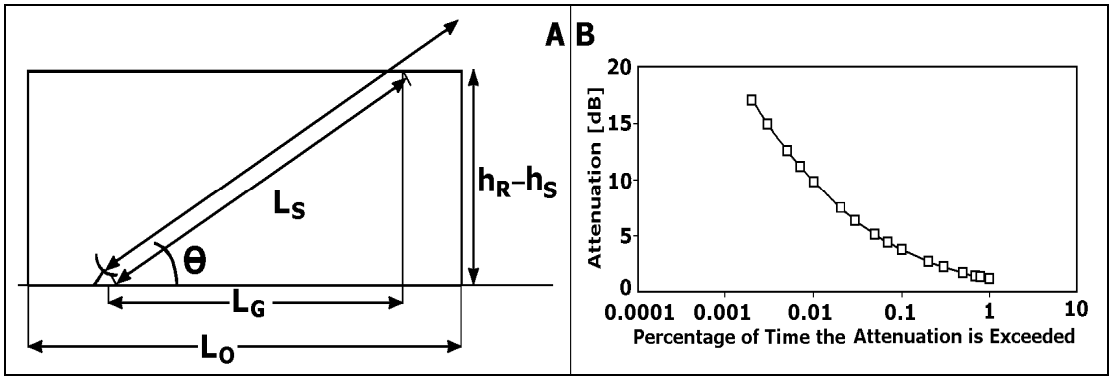

Figure 5. 17 Equivalent Rain Cell of Rainfall Rate and Rain Attenuation Statistics by ITU 1996

It may be noted that the specific frequency bands where the absorption is high are about 22.23 GHz caused by vapour (left peak in the curve) and centered between 53.50 and 65.20 GHz caused by oxygen (right peak in the curve). Meanwhile, in the frequency range of current interest about 1–18 GHz, the zenith one-way absorption is in the range of 0.03–0.20 dB and 0.35–2.30 at 5^o elevation. The corresponding upper limit for 100% humidity is 0.7 dB at zenith and 8 dB at 5^o elevation (ITU, 1996).

5.6.4.2 Attenuation by Precipitation and Hydrometeors

Hydrometeors are condensed water vapours existing in the atmosphere, such as cloud, fog, rain, hail and snow. The last three forms of atmospheric water are called precipitation. They produce transmission impairments and attenuation by absorbing and scattering the energy of radiowaves.

1. Clouds and Fog – Cloud and fog may cause attenuation but much less than that caused by light rain of about 10 mm/h. Clouds and fog are suspended water droplets, usually less than about 0.10 mm in diameter, whose effect is significant only for systems operating above 10 GHz. It is important to note that attenuation to radiowaves depends on the liquid water content of the atmosphere along the propagation path. Clouds have liquid contents from 0.05 to 5 g/m^3 and their formation shape can be due to a variety of atmospheric processes, which result in cloud layer types for each of three cloud heights: low, middle and high. Thunderstorm cumulo-nimbus high clouds cause the maximum attenuation. The fog liquid content is in the order of about 0.40 g/m^3 and typically fog extends from 2 to 8 km. The attenuation from fog is negligible for satellite communications.

2. Rain – Rain precipitation is the most significant contribution to atmospheric attenuation, which is caused by radiowave absorption and scattering from raindrops. First of all, to evaluate this additional rain loss, it is necessary to obtain the expected rainfall rate in mm/hr for the region of the communication link. For this reason, Figure 5.16 (B) presents six curves, which can be used to read off dB losses per EM path length at the operating frequencies. These curves are generated from a combination of empirical data and mathematical models that fit this data. Rainfall rate distribution is inhomogeneous in space and time and can impair a satellite communications link at frequencies above 10 GHz, as well as increase the noise temperature and impairment, or cross-polarization discrimination. Rain gauge records show

short intervals of higher rain rates occurring in longer periods of lighter rain. Various precipitation methods have been proposed for predicting rain attenuation statistics calculations from rainfall rate measurements near the signal path. The slant path rain attenuation prediction is based on the estimation of the attenuation exceeded at 0.01% of the time $A_{0.01}$ from the rainfall rate $R_{0.01}$ (mm/h), exceeding at the same time percentage.

The effective path length is given by the formula:

$$A_{0.01} = {}_{\gamma R} \cdot L_e = {}_{\gamma R} \cdot L_s \cdot r_{0.01} \quad [dB] \tag{5.26}$$

Where γ_R (dB/km) = specific attenuation, L_e is the effective path length, L_s = slant path length and $r_{0.01}$ = path reduction factor. The spatial structure of rain can be modeled by an equivalent rain cell of uniform rainfall rate with a rectangular cross-section of equivalent length L_0 and effective height h_R-h_S in the plane of the path, as shown in Figure 5.17 (A).

The relation for slant path length for elevation angles above 5^o is as follows:

$$L_s = h_R\text{-}h_S/\sin\theta \quad [km] \tag{5.27}$$

and for elevation angles less than 5^o is:

$$L_s = 2(h_R - h_S)/ [\sin^2\theta + 2(h_R\text{-}h_S)/R_e]^{½} + \sin\theta \quad [km] \tag{5.28}$$

where θ = path elevation angle and R_e = effective radius of the Earth (8,500 km). Using simple trigonometry relations, the horizontal projection is given by the formula:

$$L_G = L_s \cos\theta \quad [km] \tag{5.29}$$

The reduction factor has the following relation:

$$r_{0.01} = 1/1 + L_G / L_0 \tag{5.30}$$

For example, the specific attenuation using the frequency-dependent coefficients k and α gives the following expression:

$$\gamma_R = k(R_{0.01})^{\alpha} \quad [dB/km] \tag{5.31}$$

Values of the frequency-dependent coefficients are shown in **Table 5.4.** Values not given there can be obtained by interpolation using logarithmic scales for frequency and k and a linear scale for α. For linear and circular polarization, these parameters can also be obtained by the following equations:

$$k = [k_h + k_v + (k_h - k_v) \cos^2\theta \cos2\tau] / 2$$

$$\alpha = [k_h\alpha_h + k_v\alpha_v + (k_h\alpha_h + k_v\alpha_v) \cos^2\theta \cos2\tau] / 2k \tag{5.32}$$

where θ = path elevation angle and τ = polarization tilt angle relative to the horizon ($\tau = 45^o$ for circular polarization).

The attenuation value predicted for a percentage in the range of 0.001 to 1% can be obtained by relation:

$$A_p = A_{0.01}\, 0{,}12 \cdot p^{-(0{,}546+0{,}043\log P)} \quad (5.33)$$

For percentages of the time outside the 0.001 to 0.1% is a relatively complicated procedure, while the predicted attenuation exceeded for 0.01% for an average year is $A_{0.01}$ = 9.8 dB. Finally, the estimated attenuation exceeded for any other percentages of the time P may be calculated from $A_{0.01}$ by the expression:

$$A_p = A_{0.01}\,(P/0.01)^{-\alpha} \quad [\text{dB}] \quad (5.34)$$

The cumulative distribution of the rain attenuation statistics is illustrated in Figure 5.17 (B).

3. Hail and Snow – Hail depolarization often precedes or follows rain and the presence of hail above rain is one factor that causes wide variations in the instantaneous value of Cross Polarization Discrimination (XPD), which may accompany a given attenuation. Hail, with its ice meteors, causes a small loss due to scattering but not due to absorption.

Dry snow, likewise, does not absorb radiowave energy, however, the water content of wet snow dropping slowly through the ray path causes more absorption than would arise if the same amount of water were falling as rain.

5.6.4.3 Site Diversity Factors

Path diversity in satellite systems involves the provision of alternate propagation paths for signal transmission, with the capability to select the least-impaired path when conditions warrant. In this case, implementation of path diversity requires the deployment of two or more interconnected Earth terminals at spatially separated sites, hence, the use of the term “site diversity”. This combination is considerable when a GES is being used for a commercially or militarily important purpose, where an outage is considered more serious, e.g., at the head end of a cable system, the probability of an outage can be reduced by having a second GES a few kilometers away and using whichever has the better signal at that moment. Therefore, this is because heavy rain, in particular, tends to be quite localized and would probably not impact both stations at the same time (Richharia, 1995).

Without an ability to increase the margin (e.g., through the application of power control via additional transmit gain and power, or increased resource allocation in the TDMA frame), there are basically three types of diversity schemes that can be used by satellite systems to overcome impairments at a given GES:

1. Orbital Diversity – This diversity is different from site diversity in that only one GES site is used. To achieve a measure of diversity, the GES uses two antennas that can access different satellites simultaneously and is not necessarily the diversity-interconnecting link between sites that is required for site diversity. However, to obtain significant decorrelation of concurrent attenuations along the two paths, the angle between the two paths at the GES must be large. In as much as this angle is large, at least one or even both of the links will be at a relatively low elevation angle and, therefore, encounter a greater degree of impairment than at higher elevation angles. In general, the achievable diversity gain is very small, with values of about 2 to 3 dB in the 14/11 GHz bands.

2. Frequency Diversity – Path losses caused by particulates on the path increase as the frequency increases, particularly for rain. In effect, at 6/4 GHz, attenuation due to rain is

negligible; at 14/11 GHz, it can be significant in high rainfall regions of the world; at 30/20 GHz, it is the dominant link impairment nearly everywhere. At this point, if it is possible to switch communication transmissions to a lower-frequency band, significant increases in availability might be achieved. This capability requires that both frequency bands (the higher, impaired one and the lower one to which the communication channels are to be switched) be simultaneously available at the GES in question. Furthermore, there must be spare capacity available in the lower frequency spectrum whenever needed, implying that significant spare capacity must be provided if the link is a high-capacity channel and that the complete network need to be under dynamic control. Both elements require significant investment. Should such dynamic network control features be in place and the additional capacity in the lower frequency band be available on-call, frequency diversity can, therefore, undoubtedly provide large increases in availability.

3. Time Diversity – Severe rain events do not usually last long at a given location. Thus, this characteristic can be used in any communication RF link that does not require interaction between the caller and the receiver. The service can be said to be acceptable if, for example, a Fax is successfully sent without any error within a two-hour period. The delay in sending the Fax can be considered a form of time diversity. This feature could also be used with advantage to determine the capacity requirement of a given RF link for optimal economic performance. Thus, if a link is sized for a maximum anticipated capacity, it will have excess capacity for most of the time. If some transmissions can be delayed and sent, for example, at off-peak times, the capacity requirements can be reduced. The time delay could, therefore, be used either at times of peak capacity (i.e., the equivalent of call-blocking) or when the GES is undergoing a severe rain event.

5.6.5 Clear-Sky Effects on Atmospheric Propagation

Radio signals travelling through the atmosphere layers suffer attenuation even during fine weather. In any event, the clear-sky attenuation is mainly the result of absorption of energy from the transmission by water vapour and oxygen molecules; although there are other modes of clear-sky effect that have influences on propagation (Pratt et al, 2002).

1. Defocusing and Wave-Front Incoherence Contribution – Several expressions have already been evaluated and are provided in No 2.3.2 of ITU-R P.618 recommendation to estimate the defocusing (beam-spreading) losses on paths at very low elevation angles. Otherwise, the loss is implicitly accounted for in the prediction methods for low-angle fading found in articles No 2.4.2 and 2.4.3 of the Recommendation. Hence, small-scale irregularities of the refractive index structure of the atmosphere cause incoherence in the wave front at the receiving antenna. In any case, this will result in both rapid radio signal fluctuations and an antenna-to-medium coupling loss that can be described as a decrease of the antenna gain. In practice, signal loss due to wave-front incoherence is, therefore, probably only significant for large-aperture antennas, high frequencies and elevation angles below 5^o. Measurements made in Japan with 22 m antenna suggest that, at 5^o elevation angle, the loss is about 0.2 to 0.4 dB at 6/4 GHz, while measurements with a 7 m antenna at 15.5 GHz and 31.6 GHz gave losses of 0.3 and 0.6 dB, respectively, at a 5^o elevation angle.

2. Scintillation and Multipath Influence - Small-scale irregularities in the atmospheric refractive index cause rapid amplitude variations. Thus, tropospheric effects in the absence of precipitation are unlikely to produce serious fading in space telecommunication systems operating at a frequency below about 10 GHz and at elevation angles above 10^o. At low elevation angles and at a frequency spectrum above about 10 GHz, tropospheric scintillations can, on occasion, cause serious degradations in performance. The atmosphere scintillation

measure model includes frequency, elevation angle and antenna diameter, but also including meteorological parameters, can be used to account for regional and seasonal dependencies.
3. Propagation Delays – Additional propagation delays superimposed on the delay due to free space propagation are produced by refraction through the troposphere precipitation and the ionosphere. Therefore, at a frequency above 10 GHz, the ionospheric time delay is generally less than that for the troposphere.
4. Angle of Arrival Values – The gradient of the refractive index of the atmosphere causes a bending of the radio ray and the angle of arrival varies from that calculated based on the geometry of the path. Since the relative index varies largely with altitude, the angle-of-arrival variation is much greater in the elevation than in the azimuth angle. In addition, turbulent irregularities of the refractive index can give rise to angle-of-arrival scintillations. Both of these effects decrease markedly with elevation angle and are generally insignificant for elevation angles above 10^o. The effects are independent of frequency.

5.6.6 Transionospheric Propagation

Radiowaves at frequencies of VHF and above are capable of penetrating the ionosphere and, therefore, they provide transionospheric telecommunications. The ionosphere consists of a layer somewhere between 80 and 150 km altitude, where the density of the atmosphere is very low. Radiation from the Sun ionizes some molecules and it takes a long time for them to be neutralized by other ions. The concentration of ions varies with height, time of day, the season and in what part of its 11-year sunspot cycle the Sun happens to be.

5.6.6.1 Faraday Rotation and Group Delay

Ionospheric effects are significant for frequencies up to about 10 GHz and are particularly important for GEO and Non-GEO satellite constellations operating below 3 GHz. At the frequencies used for satellite transmission, signals pass right through and are subject to negligible refraction, less than 0.01^o at 30^o elevation.

The Total Electron Content (TEC) accumulated through the transionospheric transmission path results in the rotation of the linear polarization of the signal carrier and a time delay in addition to the anticipated propagation path delay. Given knowledge of the TEC, Faraday rotation and group delay can be estimated for communication applications. Therefore, this delay is known as the group delay, while the rotation of the linear polarization of the carrier is known as Faraday rotation. The TEC, denoted by N_T, can be evaluated by the formula:

$$N_T = \int_s N_e(s)\, ds \quad [\text{electrons/m}^2] \tag{5.35}$$

where N_e = electron density [electrons/m^2] and s = propagation path length through the ionosphere [m]. Typically, N_T varies from 1 to 200 TEC units (1 TEC unit = 10^{16} el/m^2). N_T has typical values in the range of 10^{16} and 10^{18} el/m^2. Even when the precise propagation path is known, the elevation of N_T is difficult to determine because N_e is highly variable in space and time. When propagating through the ionosphere, a linearly polarized wave will suffer a gradual rotation of its plane of polarization due to the presence of the geomagnetic field and the anisotropy of the plasma medium.

This trend slows down the signal because the Earth's magnetic field penetrates the ionosphere when ions (charged particles), subject to the alternating electric field of a signal, tend to gyrate around the local line of force. The magnitude of Faraday rotation will depend

on the frequency of the radiowave, the geomagnetic field strength and the electronic density (concentration) of the plasma as:

$$\Phi = N_T\,(KM/f^2) = 2.36 \times 10^2\, B_E N_T f^2 \ \text{[radians]} \qquad (5.36)$$

where K = 2.36 x 10^4 [MKS units]; M = value of (B_E secϕ) at 420 km of height; B_E = longitudinal component of the Earth's magnetic induction along the ray path [Tesla]; ϕ = zenith angle of the ray and f = frequency [Hz]. Typical values of Φ as a function of frequency for representative TEC values are shown in Figure 5.18. Hence, the occurrence of Faraday is well understood and can be predicted with a high degree of accuracy and compensated for by adjusting the polarization tilt angle at the GES. The GPS and similar satellite navigation systems, which use the 1 to 2 GHz frequency spectrum and depend on measuring the travel time of EM signals, has to correct for this effect.

The presence of charged particles in the ionosphere slows down the propagation of radio signals along the path and produces a phase advance. Thus, the time delay in excess of the propagation time in free space is called the group delay and is given by:

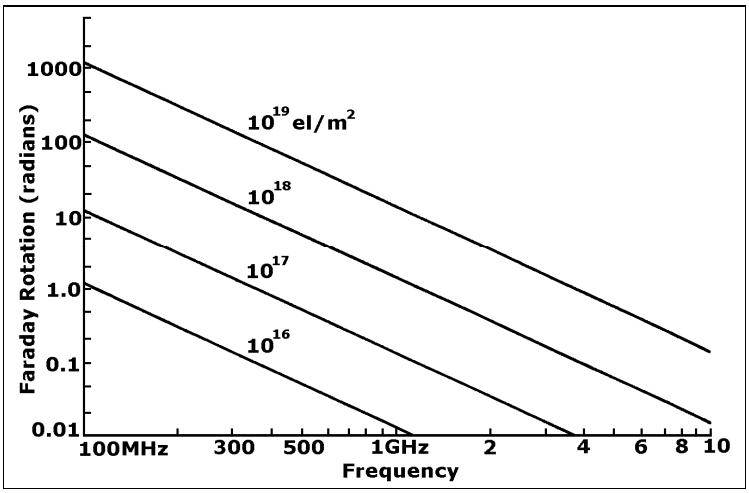

Figure 5. 18 Faraday Rotation as a Function of TEC and RF by ITU 1996

$$T_g = 1{,}34 \times 10^{-7}\, N_T/f^2 \ \text{[sec]} \qquad (5.37)$$

Accordingly, the time delay with reference to propagation in vacuum is an important factor to be considered for digital communication and navigation positioning systems.

5.6.6.2 Ionospheric Scintillation

Ionospheric effects are important at frequencies below 1 GHz, although they may even be important at frequencies above 1 GHz and are dependent on location, season, solar activity (sunspots) and local time. Thus, ionospheric scintillation occurs as short-term, rapid signal fluctuations and is mainly caused by irregularities in the ionosphere ranging from altitudes of 200 to 600 km. In fact, the frequency-dependence depends on the ionospheric conditions but the attenuation varies approximately at the same rate as the square of the wavelengths. The effect is greater for lower frequencies and at lower latitudes; while high latitude areas near the Arctic polar region bounded between ± 20^o are susceptible to intense scintillation activity. In the L and S-band, this effect can be ignored at medium latitudes except during periods of solar activity. When the Sun is very active, L-band enhancement and fading of 6 dB and –36

dB, respectively, were observed even at 37^o latitude. Scintillation activity is at a maximum during the night, lasting from 30 minutes to a number of hours (Lasaponara and Masini, 2012).

5.6.6.3 Other Ionospheric Effects

1. Dispersion – When transionospheric radio signals occupy a significant bandwidth, the propagation delay, being a function of frequency, introduces dispersion. The differential delay across the bandwidth is proportional to the integrated electron density along the ray path. Hence, for an integrated electron content of 5×10^{17} el/m^2, a signal with a pulse length of 1 μs will sustain a differential delay of 0.02 μs at 200 MHz, while at 600 MHz delay would be only 0.00074 μs.
2. Refraction – When radiowaves propagate obliquely through the ionosphere layer, they undergo refraction, which produces a change in the direction of arrival of the ray.
3. Absorption – For equatorial and mid-latitude regions, radiowaves of frequencies above 70 MHz will assure penetration of the ionosphere without significant absorption, while for frequencies below 70 MHz the ionospheric absorption loss is significant.
4. Doppler Frequency Shift – The special effects of frequency change due to the temporal variability of the ionosphere layer upon the apparent frequency of the carrier (the Doppler shifted carrier). For example, at f = 1.6 GHz (GPS system), the observed frequency change Δf at high latitude is: $\Delta f/f<10^{-9}$.

5.6.6.4 Sky Noise Temperature Contributions

The mechanism that causes absorption of energy from a wave passing between space and the Earth also causes the emission of thermal noise at RF. In fact, some radio noise is added to the emission reaching the receiver, whereas the Earth itself radiates noise, which can enter the transmission path via satellite or the GES receiving antennas. Therefore, the radio noise emitted by all matter, while used as a source of information in radio astronomy and remote sensing, may be a limiting factor in communication services. Otherwise, sources of radio noise of interest on Earth-to-space paths are the atmosphere, clouds, rain, extraterrestrial sources and noise from the surface of the Earth. Prediction methods are given in the ITU-R P.372 Recommendation. The thermal noise power N, available from a blackbody having a noise temperature of the source T [K], measured in bandwidth B [Hz], is given by the form:

$$N = kTB \quad [W] \tag{5.38}$$

where k = Boltzmann's Constant. The special power density N_0 of noise from source is:

$$N_0 = N/B = kT \quad [WHz^{-1}] \tag{5.39}$$

In considering the level of noise received at a GES or satellite from sources external to the environment, it is convenient to identify a brightness temperature T_B for each separate source and a coefficient (η), which represents the efficiency that receiving antenna captures noise from that source. The noise temperature component (t) due to the identified source is given:

$$t= \eta T_B \quad [K] \tag{5.40}$$

Therefore, the total noise entering the system from all of these sources, expressed as a noise temperature, can be obtained by summing all the component noise temperatures.

5.6.6.5 Environmental Noise Temperature Sources

The GES antennas in GEO satellite infrastructures are typically designed and sited so that the main lobe does not intersect the local terrain or obstructions, such as mountains or large buildings. Side lobes are also minimized to reduce the effect of the Earth's temperatures on the system performance. However, in satellite systems, the antenna beam may pass through vegetation and be obstructed by buildings or mountain terrain. Measurements suggest that the impact of the additional terrestrial noise is greater when the antenna has a low internal noise temperature, that is, for less directive antennas. Although these obstructions will raise the noise temperature seen by the antenna, they will also cause shadowing or multipath effects, which are likely to be more significant in the total link performance(Maral et al, 2009).

Industrial man-made sources of noise affect VHF and UHF frequencies for all but the quietest rural areas. Unlike other noise effects, there is a polarization dependence in that the vertical component is higher than the horizontal. In general, the median level of noise will decrease linearly with log (f). There are significant variations with location and time and little data are available to develop models to predict levels.

Thus, considering the noise received at a GES from the ground, the sea, etc., and buildings nearby, T_B typically lies between 100 and 250K, approaching the lower limit at sea at low angles of elevation angles and the upper limit on land. The relation for this noise temperature component t_{gr} is same as for t.

If the angle of elevation of the main beam and the gain of the antenna are both high and the antenna design is good, with well-suppressed side lobes and little sub reflector spillover, the corresponding value of η will be small and t_{gr} may be no more than 20K. If, however, the gain of the antenna is very low, as is typical of GES, η may reach 0.5 and t_{gr} may exceed 100K.

On the other hand, satellite antennas directed towards the Earth, having sufficient gain for the main lobe to be filled by the Earth, will also receive terrestrial noise with $\eta \approx 1$, while T_B will be about 210K if land occupies a large fraction of the beam footprint. However, except in the atmospheric absorption bands, T will be somewhat less, perhaps as little as 160K, if the sea occupies a large part of the footprint.

5.6.6.6 Atmospheric Noise Temperature Elements

The noise temperature of a satellite-based antenna is dominated by the high temperature emitted by the Earth, which fills, or mostly fills, the main beam of the antenna. Additional noise from precipitation or other variables is insignificant in this case. For a global beam, the noise temperatures are dependent both on frequency and on the position of the satellite with relation to the major landmasses of the Earth (Sheriff et al, 2001).

The ground antenna observes the relatively cool sky and, therefore, the presence of clouds and rain can significantly raise the noise temperature of the antenna. In general, the brightness temperature of the atmosphere due to the permanent gases and rain if it is present and seen by an antenna, is given as:

$$T_B = T_m (1 - 10^{-A/10}) \quad [K] \qquad (5.41)$$

where T_m = effective temperature of the attenuating medium (atmosphere, clouds, rain), typically about 270K and A = total attenuation due to the medium. The effect of rain on a satellite downlink is not just the attenuation but also decrease in C/N due to the higher noise temperature seen in rainy conditions, compared to clear sky conditions. In some cases, the noise temperature increase can have more effect on the link than the attenuation itself.

5.6.6.7 Galactic and Other Interplanetary Noise Effects

Noise from interplanetary sources, particularly the Sun, the Moon and from the galactic background, is well understood and the effect on the total extraterrestrial noise temperature of a system can be calculated with the following relation:

$$T_B = T_g \times 10^{-A/10} \quad [K] \qquad (5.42)$$

where T_g = temperature of any interplanetary radio sources, including background Galactic noise (about 3K above 3 GHz). Thus, the brightness temperature of the Sun decreases with increasing frequency, from about 10^6 at 30 MHz to 10^4 at 10 GHz under quiet conditions. At 20 GHz, an antenna of 2 m diameter and a beam width of about 0.5^o would have an increase in noise temperature of about 8.100K with a quiet Sun. The Sun and Moon each sub tend an angle of about 0.5^o, so that if the antenna beam is significantly larger than that, the effect t of the Sun or Moon is averaged with a larger portion of a relatively cool sky.

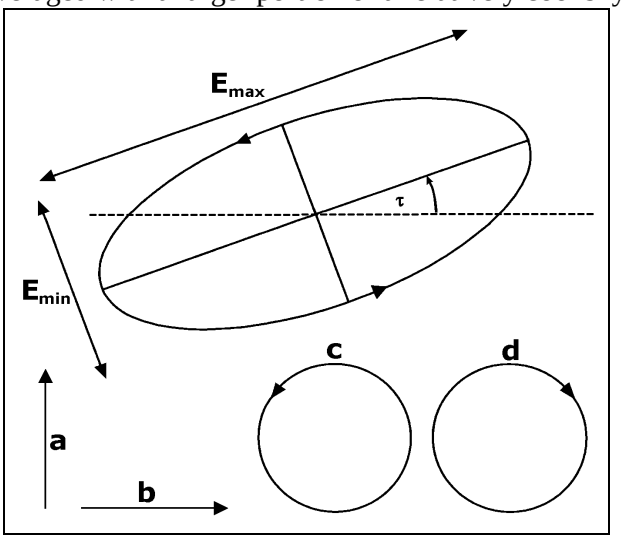

Figure 5. 19. Generalized Elliptical Waveform by Sheriff et al 2001

5.6.7 Path Depolarization Causes

The atmosphere behaves as an anisotropic medium for any radio propagation. Consequently, power from one polarization is coupled to its orthogonal component, causing interference between the channels of a dual polarized system.

In this sense, depolarization or cross-polarization may occur when EM waves propagate through media that are anisotropic, namely, asymmetrical with respect to the incident of polarization. Meanwhile, depolarization, in the form of Faraday rotation of the plane of linear polarization, occurs in the ionosphere because of the presence of the Earth's magnetic fields. At this point, the resulting impairments are typically circumvented by using circular polarization at frequencies below 10 GHz, for which the effect can be significant.

Depolarization is often the most significant path impairment for 6/4 GHz satellite systems and can be the limiting performance factor for some 14/11 GHz satellite paths, especially at lower path elevation angles in moderate rain climates.

On the other hand, depolarization in precipitation is caused by differential attenuation and phase shifts that are induced between orthogonal components of an incident wave by anisotropic hydrometeors. Orthogonally polarized radiowaves, propagating in a medium that causes only differential phase shift, are depolarized but maintain orthogonality. If the medium induces differential attenuation, the waves are also deorthogonalized.

5.6.7.1 Depolarization and Polarization Components

The importance of depolarization for satellite communications systems depends on a few components: f = frequency signal, geometry of path (θ = elevation angle and τ = tilt angle of the received polarization), local climatic factors (severity of the rain) and sensitivity to cross-polar interference (whether the system employs frequency reuse).

The EM waves comprise both the electric and magnetic field vectors. Therefore, these two components travel in the direction of the transmission path and are orthogonal, while the orientation of the electric field vector defines the polarization of the transmitted waves. In general, as the wave progresses in time, the tip of the electric vector traces an ellipse in a plane perpendicular to the propagation direction. A representative polarization ellipse of representative elliptically polarized radiowave is displayed in Figure 5.19.

Two important parameters in this figure are the axial ratio and τ = the inclination tilted angle with respect to the reference axis. The polarization ellipse may be tilted at an angle (τ) with respect to the particular coordinate frame. Thus, the general form of a polarized wave, when viewed perpendicular to the direction of travel, is elliptical in shape.

The polarization state of a wave is completely specified by its polarization ellipse, i.e., the amplitudes of the major axis (E_{max}), the minor axis (E_{min}) and the sense of rotation of the vector also defines the axial ratio by using the following expression:

$$A_R = 20\log (E_{max}/ E_{min}) \ [dB] \quad (5.43)$$

In satellite communications, four types of polarization are employed, as shown in Figure 5.19:
(a) Vertical Linear Polarization (VLP); **(b)** Horizontal Linear Polarization (HLP); **(c)** Left-Hand Circular Polarization (LHCP) and **(d)** Right-Hand Circular Polarization (RHCP). The direction of the travel is symbolical “into the paper”.

Horizontal and vertical polarizations are defined with respect to the horizon, LHCP has an anticlockwise and RHCP has a clockwise rotation when viewed from the antenna in the direction of travel.

Therefore, if E_{max} and E_{min} are equal in magnitude, the polarization state can be RHCP or LHCP, depending on the sense of rotation and in the case where E_{max} is nonzero and E_{min} is zero, the value of electric vector maintains a constant orientation defined by E_{max} and the polarization state is said to be linear.

The polarization quantity of interest for frequency re-use communication systems is the Cross-Polar Isolation (XPI), defined as the decibel ratio of the (desired) co-polar power received in a channel to the (undesired) cross-polar power received in that same channel. In practice, however, XPI is difficult to measure because the cross-polarized components cannot be distinguished from noise in the co-polar channel. The quantity usually measured is the Cross-Polar Discrimination (XPD), defined as the ratio of the co-polarized power received in one channel to the cross-polarized power detected in the orthogonal channel, both arising from the same transmitted signal. Moreover, theory predicts that XPD and XPI components are equivalent for most practical situations (Elbert, 2001).

In fact, a polarized wave will comprise the wanted polarization together with some energy transmitted on the orthogonal polarization. The degree of the coupling of energy between polarizations is given by:

$$XPD = 20\log |E_{cpr}/E_{xpr}| \quad [dB] \tag{5.44}$$

where parameters E_{cpr} = received co-polarized electric field strength and E_{xpr} = received cross-polarized electric field strength. For the case of coexisting circular polarized waves, the XPD can be determined from the axial ratio by the expression:

$$XPD = 20\log (A_R + 1/A_R - 1) \quad [dB] \tag{5.45}$$

5.6.7.2 Relation between Depolarization and Attenuation

The ITU provides a step-by-step method for the calculation of hydrometer-induced cross-polarization, which is valid for frequencies within the range 8 GHz < f < 35 GHz and for elevation angles less than 60^o. In addition to operating frequency and elevation angle, the attenuation due to rain exceeded for the required percentage of time p and the polarization tilt angle τ, with respect to the horizontal, also needs to be known. The XPD due to rain is given by the following equation:

$$XPD_{rain} = C_f - C_A + C_\tau + C_\theta + C_\sigma \quad [dB] \tag{5.46}$$

where C_f = frequency-dependent term or 30 logf [GHz]; C_A= rain-dependent term or V(f) logA_p; C_τ = polarization improvement factor or $-10\log [1-0.484 (1+\cos 4\tau)]$; C_θ = elevation angle-dependent term or $-10\log (\cos\theta)$ and C_σ = canting angle term or 0.0052σ. In the above, the canting angle refers to the angle at which a falling raindrop arrives at the Earth with respect to the local horizon. Terms τ, θ and σ are expressed in degrees, while σ has value of 0^o, 5^o, 10^o and 15^o for 1, 0.1, 0.01 and 0.001% of the time, respectively. Taking ice into account, the XPD not exceeded for p% of time is given by:

$$XPD_p = XPD_{rain} - C_{ice} \quad [dB] \tag{5.47}$$

where C_{ice} = ice depolarization or XPD_{rain} x (0.3+0.1 logp)/2.

5.6.8 Surface Reflection and Local Environmental Effects

Surface reflections and local environmental effects are important for satellite communications because such factors generally tend to impair the performance of satellite communications links, although signal enhancements are also occasionally observed. Local

environmental effects include shadowing and blockage from objects and vegetation near the UES.

At this point, surface reflections are generated either in the immediate vicinity of the UES terminals or from distant reflectors, such as mountains and large industrial infrastructures. The reflected transmission signal can interfere with the direct signal from the satellite to produce unacceptable levels of signal degradation. In addition to fading, signal degradations can include intersymbol interference, arising from delayed replicas (Fujimoto, 2008).

The impact of the impairments depends on the specific application. In the case of typical UES or GES links, all measurements and theoretical analysis indicate that the specular reflection component is usually negligible for path elevation angles above 20^{o}. Moreover, for handheld terminals, specular reflections may be important as the low antenna directivity increases the potential for significant specular reflection effects. For satellite system links, design reflection multipath fading, in combination with possible shadowing and blockage of the direct signal from the satellite, is generally the dominant system impairment.

5.6.9 Reflection from the Earth's Surface

Prediction of the propagation impairments caused by reflections from the Earth's surface and from different objects (buildings, hills, vegetation) on the surface is difficult because the possible impairment scenarios are quite numerous, complex and often cannot be easily quantified. For example, the degree of shadowing in UES satellite links frequently cannot be precisely specified. Therefore, impairment prediction models for some complicated situations, especially for UES links, tend to be primarily empirical, while more analytical models, such as those used to predict sea reflection fading, have restricted regions of applicability (Ilcev, 2013). Nevertheless, the basic features of surface reflections and the resultant effects on propagating signals can be understood in terms of the general theory of surface reflections, as summarized in the following classification:

1. Specular Reflection from a Plane Earth – Here, the specular reflection coefficient for vertical polarization is less than or equal to the coefficient for horizontal polarization. Thus the polarization of the reflected waves will be different from the polarization of the incident wave if the incident polarization is not purely horizontal or purely vertical. For example, a circularly polarized incident wave becomes elliptically polarized after reflection.
2. Specular Reflection from a Smooth Spherical Earth – Here, the incident grazing angle is equal to the angle of reflection. The amplitude of the reflected signal is equal to the amplitude of the incident signal multiplied by the modules of the reflection coefficient.
3. Divergence Factor – When rays are specularly reflected from a spherical surface, there is an effective reduction in the reflection coefficient, which is actually a geometrical effect arising from the divergence of the rays.
4. Reflection from Rough Surface – In many practical cases, the surface of the Earth is not smooth. When the surface is rough, the reflected signal has two components: one is a specular component, which is coherent with the incident signal, while the other is a diffuse component, which fluctuates in amplitude and phase with a Rayleigh distribution.
5. Total Reflected Field – The total field above a reflecting surface is a result of the direct field, the coherent specular component and the random diffuse component.
6. Reflection Multipath – Owing to the existence of surface reflection phenomena signals may arrive at a receiver from a multiple of apparent sources. Thus, the combination of the direct signal (line-of-sight) with specular and diffusely reflected waves causes signal fading

at the receiver. The resultant multipath fading, in combination with varying levels of shadowing and blockage of the line-of-sight components, can cause the received signal power to fade severely and rapidly for UES and is really the dominant impairment in the satellite service.

CHAPTER SIX

METEOROLOGICAL SATELLITE SYSTEMS

This chapter provides an introduction to global meteorological satellites for weather observation and imaging. As already stated, satellites are objects that orbit larger objects, such as planets or moons. The Earth's Moon is an example of a natural satellite and Earth itself is a natural satellite of the Sun. Thus, communication, navigation, weather and other artificial satellites are the result of human ingenuity.

There are two main types of weather satellites, defined by their orbital characteristics: Polar Earth Orbit (PEO) and Geostationary Earth Orbit (GEO) (Tan, 2014). Thus, most satellite images seen on the local television news or the weather TV channels are produced by GEO satellites. The GEO satellites orbit the Earth above the equator at the same speed as the Earth rotates around its axis, so they can transmit a continuous picture of the region below. However, the PEO satellites are significantly lower and shorter, taking about 100 minutes to travel from pole to pole and produce high-resolution snapshots of the Earth.

Meteorological global services are today utilized by every nation in the world in the frame of World Meteorological Organization (WMO). These services include weather forecasts, public warnings and providing products, images and information for the purposes of protection and safety. Weather forecasting and severe weather warnings services are essential to the success of the public and private sectors, including business and commerce, agriculture, forestry, marine and fisheries, aviation, military and applications under urban infrastructure management. However, the timely collection of data related to current weather or information required for forecasting future conditions is essential to any weather forecast. In fact, weather forecast will only be as good as the data and knowledge that is available.

Meteorological satellites carry sensors that point towards the ground, enabling them to have bird's eye view of the entire globe from the space. The two types of meteorological satellites characterized by their orbits, such as GEO and PEO are illustrated in Figure 6.1. Recently, WMO and their member nations started to use Low Earth Orbits (LEO) satellites.
As the name suggests, a GEO satellite is stationary relative to the Earth, that is, it moves above the equator at the same rate as the Earth's rotation so that all the time the satellite is above the same geographical area on the globe. In this manner, it is capable of taking cloud images of the same area continuously, 24 hours a day. As it is some 35,800 km from the Earth, the GEO satellite is capable of taking cloud pictures covering part of the whole globe and observing the perspective areas on the Earth from North to South for 25 minutes.

Figure 6. 1 Main GEO and PEO Meteorological Satellite Constellations by Ilcev 2013

Figure 6. 2 Blue Marble Photography by NASA 2014

The PEO satellites are low flying path circling the Earth in a nearly North to South orbit, at several hundred kilometers above the Earth and most of them pass over the same place a couple of times a day. As they operate at a distance closer to the Earth, they are only capable of taking cloud and other images of a limited area of the globe each time of their passage. Compared with GEO meteorological satellites, PEO satellites offer fewer and smaller cloud and other pictures. However, the advantage of PEO satellites is that the cloud and other pictures obtained are of much higher resolution.

6.1 History of Satellite Meteorology

In the more than 30 years since the first meteorological satellites were launched, they have become indispensable for study and observing of the Earth's atmosphere. Indeed, together with their land- and ocean-sensing cousins, meteorological satellites view the Earth from a global perspective that is unmatched and unmatchable by any other observing system.

It is human nature to want to find out about our surroundings, to explore our neighbourhood, our planet Earth and beyond. Until the twentieth century, viewing Earth from a space-based perspective could only be accomplished by imagination. From ancient times, astronomers have looked up at the sky, recorded their observations and made up stories about how the universe was created and what it was like. Ancient Greeks were more aware of the truth of

their surroundings than other cultures in that time period. They helped to discover that Earth was a sphere and developed observational and mathematical techniques to measure the circumference of the planet. During recent times, with increasingly powerful ground-based telescopes, came the discovery of the Milky Way and other galaxies and our understanding that the universe is expanding (Tan, 2014).

The practice of Earth observation involves the gathering of information about the planet's physical, chemical and biological systems, usually by remote sensing systems, which have grown technologically more and more sophisticated over time. Thus, the famous "Big Blue Marble" photograph of Earth, taken in 1972 by astronauts onboard Apollo 17, demonstrated the dramatic impact of viewing Earth from space, as shown in Figure 6.2. This emphasized the importance of minimizing the negative impact of modern human civilization to improve social and economic well-being.

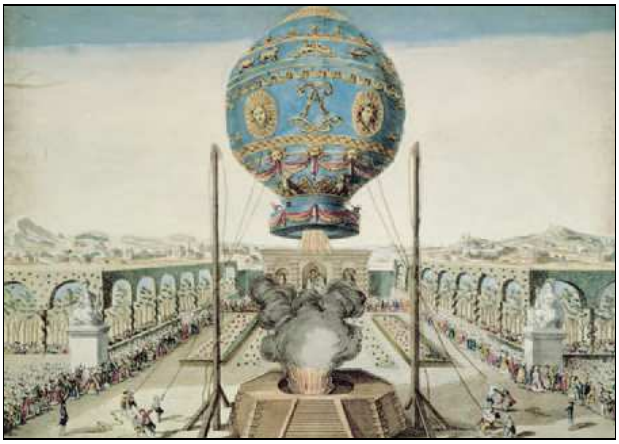

Figure 6. 3 Drawing of the First Hot-air Balloon by Tan 2014

The art of weather observation and forecasting, which began with early civilizations and was based on recurring astronomical and meteorological events, was used to monitor and predict seasonal changes in the weather situation. In 650 BC, the Babylonians attempted to predict short-term weather based on cloud patterns and astrological observations, while Chinese weather prediction dates back to 300 BC, when annual calendars were developed according to repeated patterns of weather events. This experience accumulated over generations to produce weather lore.

In about 340 BC, Greek philosopher and scientist Aristotle described weather patterns in a treatise entitled "Meteorologica". This writing contained Earth science theories, such as on cloud formations, wind, rain, and other weather phenomena. This later led to his pupil, Theophrastus, compiling "The Book of Signs", which documented weather lore and forecast signs. These texts served as definitive weather forecasting references for more than 2,000 years and helped to establish meteorology as a distinct discipline of study and developments. Weather forecasting advanced little from these ancient times until the Renaissance, despite many of Aristotle's claims being erroneous.

6.1.1 Early Meteorological Instrumentation

Over the centuries, it became apparent that forecasts based on weather lore, philosophical speculations and personal observations alone were not always reliable. In order to advance knowledge and understanding of the atmosphere, instruments were needed to measure

properties, such as air, moisture, temperature and pressure. The first device to measure the humidity of air, called the hygrometer, was invented by Leonardo da Vinci in the fifteenth century. About 1593, Galileo Galilei, often deemed the father of modern observational astronomy, invented an early thermometer for temperature measurement using the expansion and contraction of air in a bulb to move water in an attached tube. His student, Evangelista Torricelli, invented the barometer for measuring atmospheric pressure in 1643.

In subsequent centuries, these meteorological instruments were refined and improved, and were being applied in association with observational platforms launched in the air, such as balloons and aircrafts, for taking from a height atmospheric meteorological measurements. A significant historical development was the invention of the first air balloon in 1783 by the French brothers, Étienne and Joseph Montgolfier, as illustrated in Figure 6.3. This discovery represents a precursor to the development of modern baluns, aircraft, stratospheric platforms and artificial satellites, which represent the future integration components for meteorological observations as well.

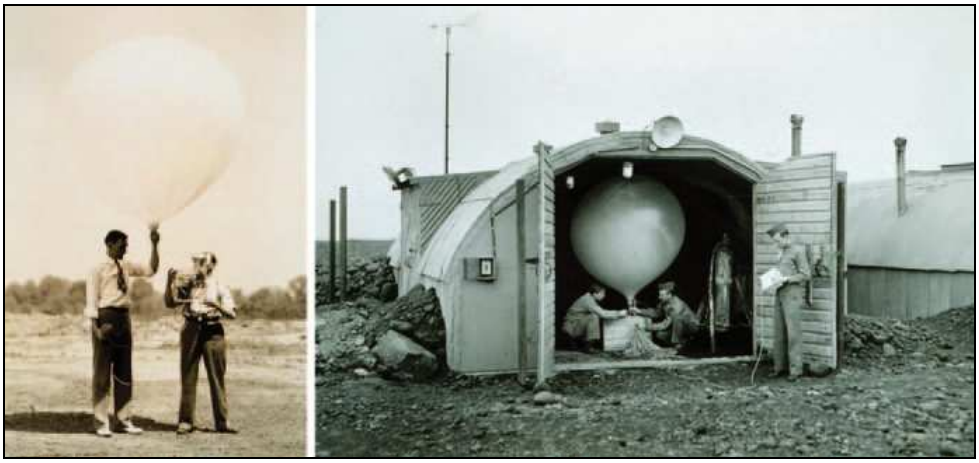

Figure 6. 4 Early Launch of Radiosondes and Preparing Hydrogen-filled Balloon in the Hangar by Tan 2014

With advancements in meteorological measurement instrumentation in the eighteenth century came experimentation of many different airborne platforms to measure physical properties of the atmospheric column, including pressure, temperature, wind speed, wind direction and other properties.

They experimented with hydrogen-filled paper bags, which led to the correct notion that a buoyant force should cause ascent of the bags, if the inside gas was lighter than air. Since gas diffused out quickly and hydrogen was produced in small quantities, they subsequently tried "gas" produced by the combustion of a mixture of moistened straw and wool. This designed the first hot-air balloon in the world, which attained a height of about 1,950 m.

In the same year, J.A.C. Charles and the Robert brothers designed and constructed a new hydrogen-filled balloon, but inflation was achieved only with great difficulty over a period of four days. Balloon flights began carrying animals and then, subsequently, men. Furthermore, balloons were improved to descend and ascend at will, and, in time, were improved with safe landing devices and better direction control. As techniques of the hydrogen manned balloon evolved rapidly, they offered the possibility to investigate Earth's atmosphere. The first manned hydrogen balloon flight conducted by Charles and the Robert brothers carried a barometer and thermometer to measure the pressure and the temperature of the air, making it

the first atmospheric meteorological measurements above Earth's surface. Also in 1784, Charles rose again and measured temperature variation along with altitude in the atmosphere. After 1850, the application of balloons for measuring meteorological parameters was widely practised. To monitor favourable weather conditions for balloon ascent, Charles also inaugurated the practice of launching a small pilot balloon prior to flight in order to determine the wind vector at different altitudes.

Subsequent technical advances in the use of unmanned air balloons made it possible to sound the atmosphere. Thus, Colonel William Blaire in the US Signal Corps performed primitive experiments with weather measurements from a balloon, while the first really useful radiosonde was invented in France by Robert Bureau in 1929. This device sent precise encoded telemetry from weather sensors to the ground. Subsequent developments enabled radiosonde instruments to become smaller, lighter and more accurate. Figure 6.4 shows the early launch of radiosondes developed by the US Bureau of Standards in 1936 **(Left)** and the US Army Air Force meteorologists preparing a hydrogen-filled balloon equipped with a radiosonde in 1944 **(Right)**.

Radiosondes have also been used for exploring atmospheres of other planets, such as in the Soviet Union's Vega program, where probes dropped radiosondes to study the atmosphere of Venus. Up to the present day, radiosondes are still launched worldwide all year-round.

The US National Weather Service releases about 75,000 radiosondes each year, not including soundings made by military facilities and for other specialized scientific purposes. Collective agreements have formed a global radiosonde station network worldwide (about 900 stations) that make an average of 1,209 soundings each day to support weather forecast activities.

The modern age of weather forecasting began with the invention of the electric telegraph in 1835, which allowed for routine and instantaneous transmission of weather observations. It was possible to develop crude weather maps and to study surface wind patterns and storm systems. Synoptic weather forecasting was made possible by the compilation and analysis of data collected simultaneously from weather observing stations and conveyed across the globe via telegraph in the1860s. Data collected by land locations are now conveyed worldwide via phone or wireless technology, enabling information to be communicated quickly for weather forecasts and studies of the atmosphere and climate.

Thereafter, pilot balloons were superseded by free-flight sounding balloons, which carried sensors and radio telemetry transmitters. Sensors launched by weather balloons to measure atmospheric profiles of pressure, temperature, and relative humidity are carried in a unit commonly referred to as a radiosonde. Usually contained in a small, expendable instrument package suspended below a large balloon, the radiosonde provided an efficient way to systematically and regularly measure various atmospheric parameters to heights of over 30,000 meters, without the necessity of considering weather conditions. Nowadays, received meteorological information is transmitted to a ground-based station for data users via a radio transmitter and radiosondes are still used by national weather services for capturing high vertical resolution flight data (Davis, 2000).

In addition, kites were frequently used for capturing meteorological observation data in the second half of the nineteenth century. A meteographic device, which is a chart recorder for measuring humidity and temperature, was usually attached. However, kites were linked to the ground and were highly unstable due to windy conditions. During World War I,

meteorological observations from kite flights were largely substituted by new developed aircraft. Flying weather forecasts for aircraft were not required prior to World War I, since pilots mostly flew at low altitudes.

During wartime, however, aircraft were often required to fly in clouds, in bad weather conditions, and at high altitudes. Meteographs were often mounted on the wings of military aircraft to obtain meteorological information for monitoring flying conditions. Observations were recorded on a cylindrical chart that was retrieved after the landing of the aircraft, and meteorological parameters were read from the chart. Pilots were often required to reach a flying altitude of at least 4,000 meters, where they could black out from lack of oxygen, making this a very dangerous enterprise. It was often impossible to fly in bad weather, which unfortunately was when observations were needed the most.

6.1.2 Evolution of PEO Meteorological Satellites

The vast array of radiosonde stations, weather reconnaissance aircraft and newly developed observing systems have provided a significant amount of information about meteorological parameters and weather conditions. Sensors are measuring atmospheric constituents directly, such as thermometers, barometers, and humidity sensors, have been sent aloft on balloons, rockets or dropsondes for many years. Although precise in their measurements, these instruments have limited capabilities to provide regional or even global coverage, which is necessary for making accurate weather forecasts (Uesawa, 2006). Thus, the global network of radiosonde observing stations tend to have a highly concentrated dispersion in the northern hemisphere temperate zone for large land masses, whereas the density of observations for the southern hemisphere, tropical regions, the Arctic and most of the northern Pacific is relatively sparse.

Figure 6. 5 Early Meteorological Satellites Vanguard-2 and Explorer-7 by Ilcev 2013

Consequently, there is a high degree of uncertainty with tracking main tropical storms over the North Pacific Ocean, areas around Madagascar and Florida in the US. Since the Earth's atmosphere is a single and closely interacting mass of air, disturbances can propagate throughout at a speed much faster than winds. The real-time synoptic monitoring of large areas of the Earth is necessary for improved meteorological data collection via satellites. Extended and long-range weather forecasts require data to be collected and distributed globally. Earth-observing satellites are able to collect meteorological data at synoptic scales and in remote locations, tracking cloud cover, relative motion of storm systems and the jet stream, and maximum heights of clouds and vertical temperature profiles. Satellite imagery can identify cloud patterns associated with different types of weather conditions and patterns (e.g., spiral cloud patterns and convective cells), which are difficult to capture and monitor using conventional weather observations alone. Developments in satellite technologies have

resulted in enormous improvements in the accuracy of weather forecasting. Satellites have particularly provided routine access to observations and data from remote areas of the globe. These efforts were intensified after the launch by the Soviet Union on 4 October 1957 of the first successful Earth satellite, Sputnik-1. The first successful U.S. satellite, Explorer-1, was launched 123 days later on 31 January 1958. The cosmic era and race over the globe began. The first weather satellite with meteorological instruments, Vanguard-2, was launched on 17 February 1959 by NASA, as shown in Figure 6.5 (Left). In fact, it was designed to measure cloud cover and resistance, but a poor axis of rotation kept it from collecting a notable amount of useful data. On 13 October 1959, NASA launched Explorer-7 and made the first meteorological measurements from the satellite Suomi's net flux radiometer, shown in Figure 6. 5 (Right).

The first real weather satellite to be considered a success was TIROS-1, launched by NASA on 1 April 1960, shown in Figure 6.6 (Left). In 1964, an important series of meteorological satellites, Nimbus, was initiated. Nimbus-1 satellite, as shown in Figure 6.6 (Right) was launched on 28 August 1964.

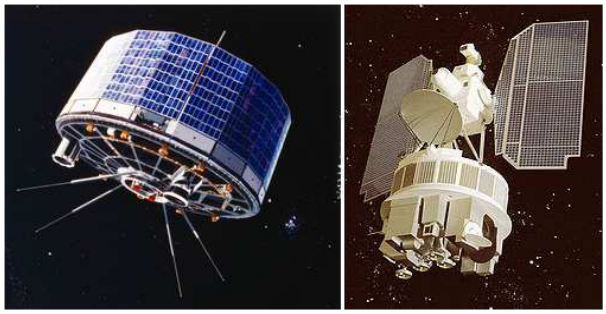

Figure 6. 6 Meteorological Satellites TIROS-1and Nimbus-1 by Ilcev 2013

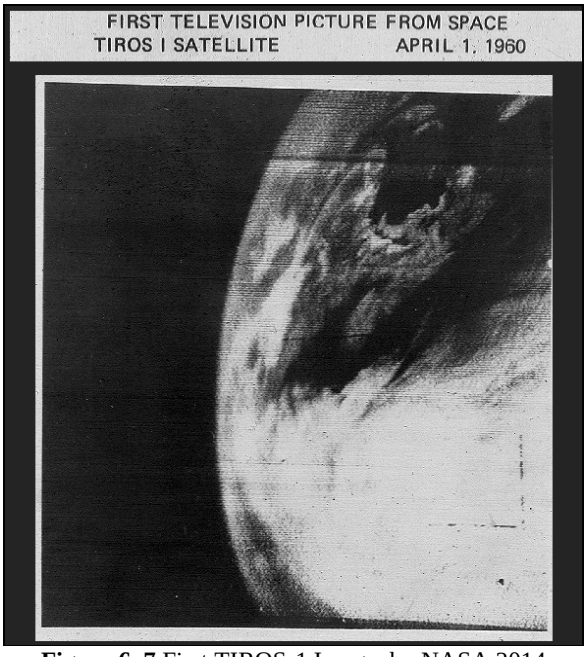

Figure 6. 7 First TIROS-1 Image: by NASA 2014

The meteorological satellite TIROS (Television and Infrared Observational Satellite), was operated for 78 days and proved to be much more successful than Vanguard-2. It released

fuzzy images of thick bands and clusters of clouds over the United States. One of the first images captured by the TIROS-1 satellite is shown in Figure 6.7. This satellite would forever change weather forecasting and climate research in the field of Earth system science.

The TIROS satellite data was directly transmitted in real-time to ground stations within signal range of the satellite linked to forecasting centers. By 1965, TIROS imagery had been combined to generate the first global view of worldwide weather. The success of these meteorological observations proved to be effective for meteorological and environmental surveillance, paving the way for the Nimbus program, whose technology and findings are the heritage of most Earth-observing satellites(NASA, 2014).

To maintain their orientation in space, many satellites spin. In the absence of external torques, angular momentum is conserved, and the spin axis points in a constant direction in space as the satellite orbits the Earth. Thus, TIROS spun at about 12 revolutions per minute (rpm). This caused a viewing problem with the first eight TIROS, however. The vidicon cameras on these satellites were on the “bottom” of the craft; that is, they pointed parallel to the spin axis and, therefore, in a constant direction in space. Thus, the Earth was in their field of view only about 25% of the time of each orbit. During the remaining 75% of each orbit, they viewed space and could produce images.

In 1964, the Nimbus series, an extremely important series of experimental meteorological satellites was initiated.. The first in a series of second-generation meteorological research and development satellites, Nimbus-1, had two notable firsts. It was the first three-axis stabilized meteorological satellite that used momentum special wheels, namely, flywheels inside the spacecraft controlled by horizon sensors. It rotated once per orbit (by placing torque on the appropriate momentum wheels), so that its instruments constantly pointed toward Earth. It was designed to serve as a stabilized, earth-oriented platform for the testing of advanced meteorological sensor systems and for collecting meteorological data. The polar-orbiting spacecraft consisted of three major elements, namely: a sensory ring, solar paddles, and the control system housing.

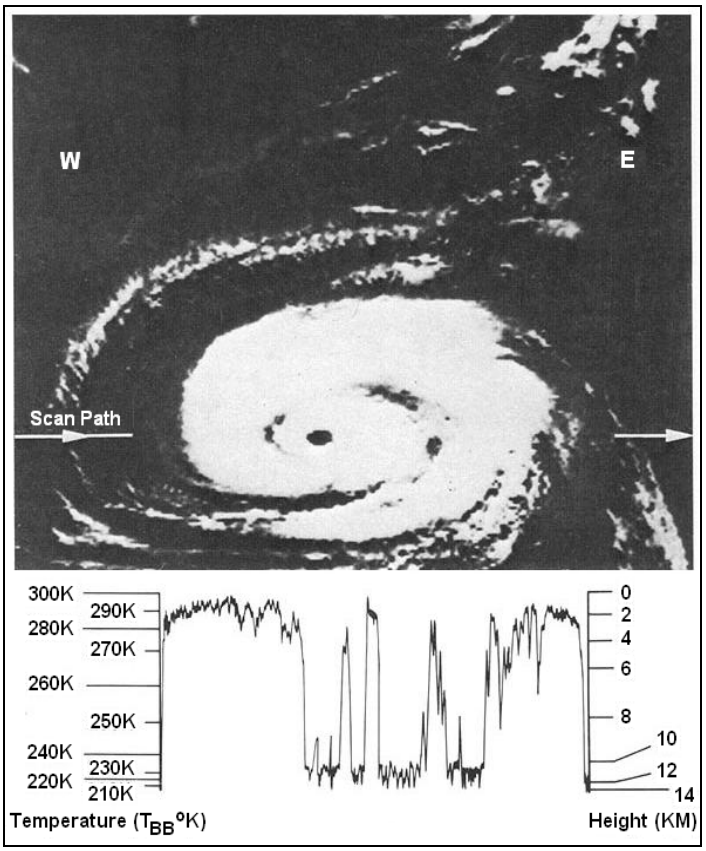

Figure 6. 8 Nimbus-1 HRIR image of Hurricane Gladys by NASA 2014

The Nimbus-1 meteorological satellite also was the first artificial sunsynchronous satellite, which means that it passed over any point on Earth at approximately the same time each day. This regularity increased its utility in operational forecasting, so the sunsynchronous orbit has been used ever since for US operational meteorological satellites in near-polar orbits. The High Resolution Infrared Radiometer (HRIR) of Nimbus-l has a scanning radiometer quite similar to those in operational use today, and provided night and day coverage. Figure 6.8 shows an HRIR image of Hurricane Gladys. Its Automatic Picture Transmission (APT) camera was, therefore, much more useful than that of TIROS-8, which only viewed the Earth 25% of the time. ANimbus-1 APT photo is shown in Figure 6.9.

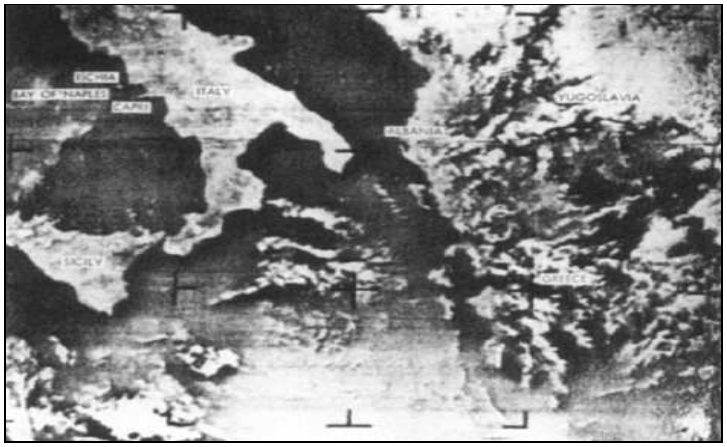

Figure 6. 9 Nimbus-1 APT Photo by NASA 2014

Figure 6. 10 TIROS-9 Earth mosaic by NASA/NOAA 2014

Hence, an important accomplishment of satellite meteorology is that, since sometime in the mid-1960s when meteorological satellite coverage became continuous, there have been no undetected tropical cyclones anywhere on Earth. These ocean-born storms, which for centuries menaced seafarers and coastal and island dwellers, can no longer surprise potential victims. Lives are still lost to tropical cyclones, but many are now saved because of the warnings that meteorological satellites make possible (Kramer, 2002).

The TIROS-9 is ninth in the group of 10 TIROS satellites, launched on 22 January 1965, which introduced a new construction known as "cartwheel" configuration. The satellite's spin axis was tilted to be perpendicular to the orbital plane, and the cameras were reoriented to point out the side of the spacecraft. Thus, the satellite "rolled" like the wheel of a cart in its orbit about the Earth. With each rotation of the satellite, the cameras would point towards Earth, and a picture could be taken. This situation allowed global composite images to be made, as shown in Figure 6.10.

Figure 6.11 illustrates ground antenna **(Left)** and ground receiving equipment **(Right)** from inside building 9162 at the Camp Evans Diana site while receiving the first weather satellite photos. In fact, this is a sample of one of the first NOAA Ground Earth Station (GES) serving meteorological satellites TIROS in 1962. These first pictures, received from TIROS spacecraft and processed by ground infrastructures, were immediately flown to Washington where the head of NASA presented them to President Eisenhower for public release. Later, even more impressive images were obtained from many parts of the globe, among them pictures of the Baja California Peninsula and the Suez-Canal-Red Sea area, which are still vividly in the memory from this time.

Figure 6. 11 TIROS Ground Antenna and Station by Evans 1991

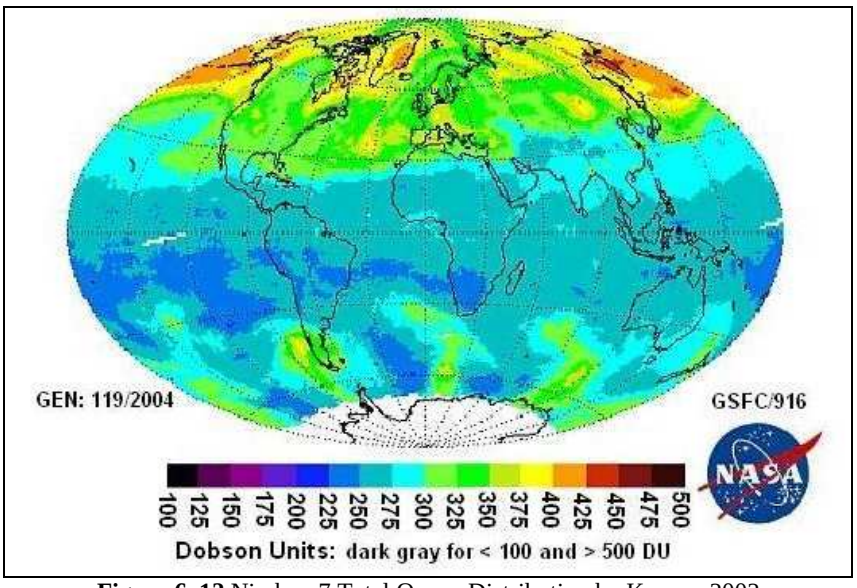

Figure 6. 12 Nimbus-7 Total Ozone Distribution by Kramer 2002

In total, seven Nimbus satellites were launched. Some experiments on the last one, Nimbus-7, launched 24 October 1978, were operational until late 1995. Figure 6.12 illustrates Nimbus-7 TOMS Total Ozone Distribution on 6 May 1993. The Nimbus series of PEO meteorological satellites tested many new concepts that have lead to the operational instruments in use today. This PEO satellite served as a stabilized, Earth-oriented platform for the testing of advanced systems for sensing and collecting data in the pollution, oceanographic and meteorological disciplines. It had three major structures: (1) a hollow torus-shaped sensor mount; (2) solar paddles; and (3) a control-housing unit that was connected to the sensor mount by a tripod truss structure.

Similar in appearance to the Nimbus satellites, the Landsat satellite series was designed for land remote sensing. Landsat-1, also called the Earth Resources Technology Satellite (ERTS), was launched on 23 July 1972. Its sensors have extremely high resolution, 80 m in the first satellite and up to 30 m in the Landsat-5 satellite, launched on 1 March 1984, which is shown in Figure 6.13 (Left). A more modern Landsat-8 satellite was launched on 11 February 2013 with the Extended Payload Fairing (EPF) and its satellite payload consists of two science instruments: Operational Land Imager (OLI) and Thermal Infrared Sensor (TIRS), shown in Figure 6.13 (Right). The images of Landsat data are also used in meteorology primarily to study small clouds and surface features that may influence weather.

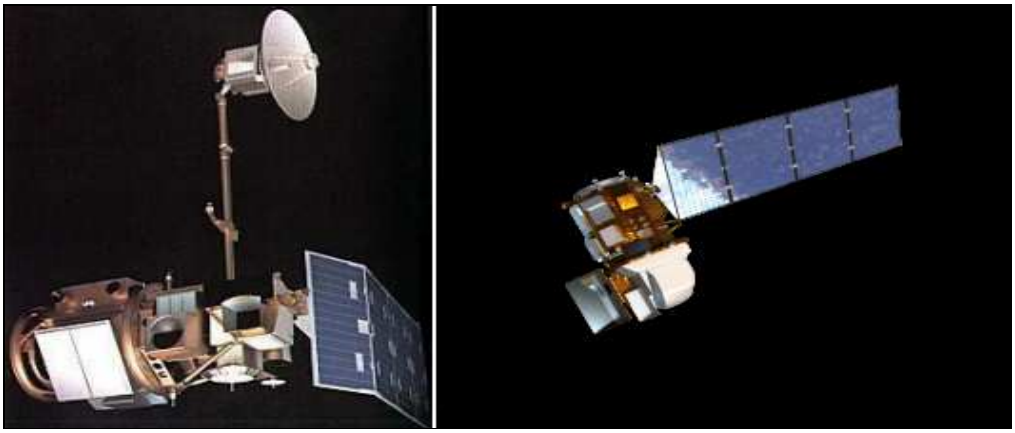

Figure 6. 13 Landsat-5 and Landsat-8 Spacecraft by NASA 2014

Figure 6. 14 Soviet Meteor 1-1 and Chinese FY 1-1 Polar Orbiting Meteorological Satellites by Ilcev 2015

In the meantime, the Soviet Union (subsequently Russia) Space Agency developed a series of PEO satellites for science, technology, radiation and meteorology. The first spacecraft to be given a Kosmos-1 (Sputnik-11) designation was launched on 16 March 1962. On 26 March 1969. the Soviet Union Meteor 1-1 was launched as the first fully operational weather satellite, shown in Figure 6.14 (Left). It weighed between 1,200 and 1,400 kilograms, and was originally placed in orbit at an altitude of 650 km. Two solar panels were automatically oriented towards the Sun. This spacecraft ceased operations in July 1970. It was the first of 25 similar spacecraft series from 1969 to 1977. The second series of operational Soviet meteorological satellites began on 11 July 1975 with the launch of Meteor 2-1.

India has been quite active in satellite meteorology. Thus, two Indian polar orbiters have been launched, Bhaskara-1 on 7 June 1979 and Bhaskara-2 on 20 November 1981. Bhaskara-1, weighing 444 kg at launch, was launched from Kapustin Yar aboard the Intercosmos launch vehicle. It was placed in an orbital perigee and apogee of 394 km and 399 km, respectively, at an inclination of 50.7°. The satellite consisted of 2 TV cameras operating in visible (600 nanometre) and near-infrared (800 nanometre) and collected data related to hydrology, forestry and geology. SAtellite MIcrowave Radiometer (SAMIR) was operating at 19 and 22 GHz for study of ocean-state, water vapour, liquid water content in the atmosphere and other solutions.

In 1988, on 6 September, and again in 1990, on 3 September, China launched FY 1-1 (Feng Yun - Wind and Cloud) meteorological satellites into approximately 900 km, 99^0 inclination orbits by CZ-4 boosters from Taiyuan, as shown in Figure 6.14 (Right). The spacecraft was designed to be comparable to existing international PEO meteorological and remote sensing systems, including APT technique in the 137 MHz band. The satellite structure and support systems were designed and created by the Shanghai Satellite Engineering and Research Center of the China Space Technology Institute, whereas the payload was developed by the Shanghai Technical Physics Institute of the Chinese Academy of Sciences.

6.1.3 Evolution of GEO Meteorological Satellites

On 7 December 1966, the US Applications Technology Satellite (ATS) was launched. ATS-1 was the first of six spacecrafts used to test the feasibility of placing a satellite into GEO Geosynchronous orbit. At the beginning, it was originally intended to be a communications satellite, but also provided a platform for meteorological and navigation equipment. It was designed to test GEO orbit techniques and applications at this special orbit that circles Earth once a day. This satellite orbit is exactly 22,236 miles (or 35,786 km) above Earth's surface.

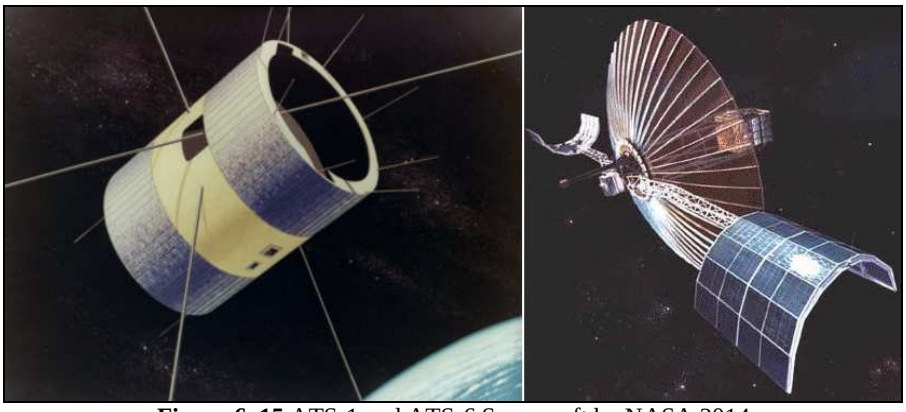

Figure 6. 15 ATS-1 and ATS-6 Spacecraft by NASA 2014

In satellite GEO orbit within Earth's equatorial plane, the ATS-1 satellite transponder was able to transmit information to surface ground stations that are constantly pointed towards the satellite without tracking, which is shown in Figure 6.15. (Left). This makes the orbit excellent for telecommunications, video broadcasting, and Earth observation. Figure 6.15 (Right) illustrates the sixth ATS satellite, named ATS-6.

Temporally continuous GEO satellite images offer the ability to track clouds and tropical depressions. With this information, wind speeds at cloud altitude can be inferred. Research into tracking clouds using image sequences began almost immediately, especially with the successful operation of the ATS-1 spin-scan camera. This imaging device provided the first high quality cloud-cover pictures and afforded a continuous watch of global weather patterns. The success of meteorological experiments carried aboard the ATS series of satellites led to NASA's development of two weather satellites designed specifically to make images of atmospheric observations, called the Synchronous Meteorological Satellites (SMS-1 and SMS-2). These two Geosynchronous meteorological satellites were launched in 1974 and 1975, respectively, and carried the first Data Collection Platform (DCP) repeater, which later evolved into the GOES program.

Data from meteorological or other platforms on the surface could be relayed by the satellite to a central receiving site, so data from meteorological remote ground sites could be easily obtained for the first time. The DCP sites are shown in Figure 6.16. The cloud cameras on the ATS satellites made images in the visible portion of the spectrum only, and to provide images during the night, SMS and the succeeding GOES have an infrared radiometer as well.

Figure 6. 16 DCP Ground Sites by Ilcev 2015

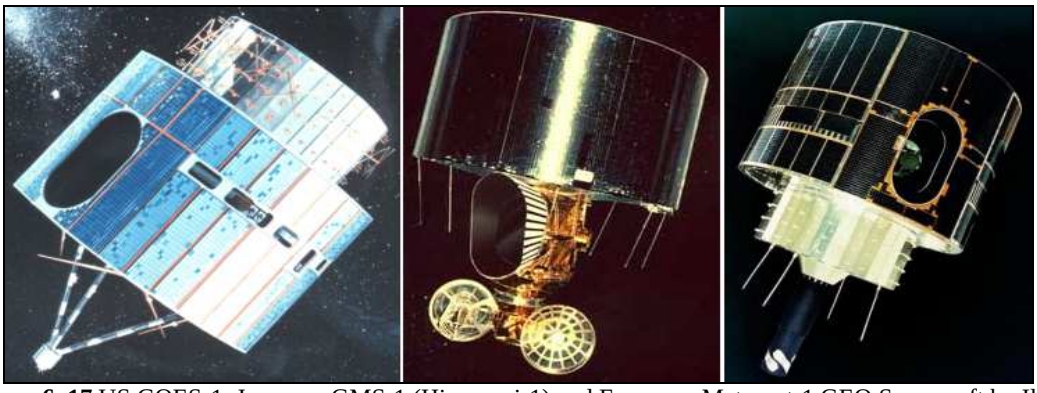

Figure 6. 17 US GOES-1, Japanese GMS-1 (Himawari-1) and European Meteosat-1 GEO Spacecraft by Ilcev 2015

Since 27 June 1974, when SMS-1 became operational, the world meteorological consumers have had continuous, uninterrupted, 24-hour-per-day observation and monitoring of most of the Western Hemisphere from space. The US Geostationary Operational Environmental Satellites (GOES) program was formally initiated with the first operational spacecraft GOES-1 launched on 16 October 1975, which is shown in Figure 6.17 (Left). Its ability is to orbit synchronously with Earth's rotation, along with the Polar Operational Environmental Satellites (POES) and Defense Meteorological Satellite Program (DMSP) satellites enhanced NOAA forecasting capabilities. The next deployed GOES-2 and -3 were similar to GOES 1. Since the launch of SMS-2, the US has generally maintained two GEO satellites in orbit, one at 75° West longitude and one at 135° west longitude.

In the following year, 1977, Japan and Europe launched their first GEO weather satellites. These were, respectively, the Geostationary Meteorological Satellite (GMS-1), shown in Figure 6.17 (Middle), and the European Meteorological Satellite (Meteosat-1), shown in Figure 6.17 (Right). Meteosat-1 provided visible imagery with a spatial resolution of 2.5 km and infrared window band imagery and water vapour band imagery, both at 5 km spatial

resolution. Its water vapour imagery provided a very different view of Earth. It primarily observed upper tropospheric humidity and high cloud features, which indicated synoptic scale circulations. In 1979, three GOES and one Meteosat satellites were used as part of a Global Atmospheric Research Program (GARP) to define global atmospheric circulations.
Meteosat-1 spacecraft of European Space Agency (ESA) was the first GEO meteorological GEO satellite to make in 1977 images of mid to upper-troposphere water vapour at 6.7 m in addition to visible and 10 – 12 m infrared, as shown in Figure 6.18.

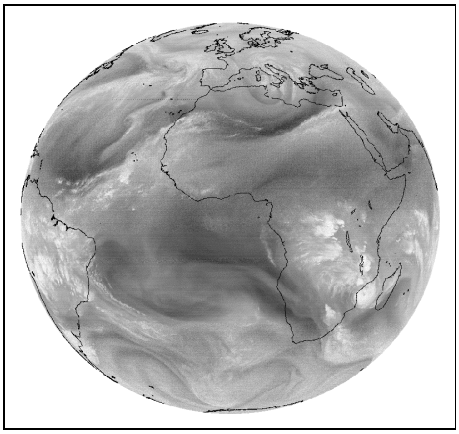

Figure 6. 18 Meteosat-1 Water Vapor Image by SSEC 2006

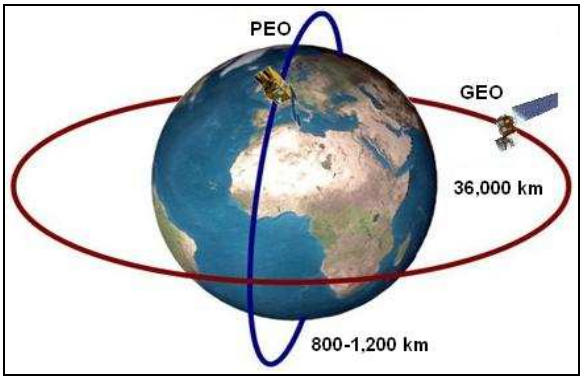

Figure 6. 19 Two Main Satellite Orbits: GEO and PEO by Ilcev 2015

6.2 Classification of Meteorological Satellites

As stated earlier, in general, meteorological satellites fall into two categories defined by classes of orbit, namely, polar-orbiting (PEO) or, based on US appointments, are called Polar Operational Environmental Satellites (POES) and geostationary (GEO) or the basis of US nominations is Geostationary Operational Environmental Satellites (GOES). Both orbits are illustrated in Figure 6.19.

Most satellite images seen on the local television news or the weather channel are produced by GOES satellites, which orbit the Earth above the equator at the same speed as the Earth rotates and they can transmit a continuous picture of the region below. On the other hand, POES orbits are significantly lower and shorter, taking about 100 minutes to travel from pole to pole and produce high resolution “snapshots” of the Earth. Since both types of satellites produce different types of data and information, they are better suited for different

applications. Combining usages and integrating data products from both systems have also been extensively implemented with new data fusion techniques.

6.2.1 Introduction of Polar Meteorological Satellites

Polar-orbiting satellites provide coverage of Earth's polar regions beyond the view of GEO satellites and fly at altitudes typically between 800 and 1,200 km above Earth in a north to south (or vice versa) path, as shown in Figure 6.19 (Vertical Projection). Polar orbiting satellites travel in a circular orbit moving from pole to pole. These satellites collect data in a swath beneath them as the earth rotates on its axis. In this way, a polar orbiting satellite can "see" the entire planet twice in a 24 hour period. The basic operational mode deploys two polar orbiting satellites continuously, one passing north to south (descending) and the other passing south to north (ascending), circling the earth every 12 hours.

Polar Orbiting Satellites are inserted into sun-synchronous orbits, which place the spacecraft in a relatively constant relationship to the Sun so that the ascending node will remain at a constant solar time, permitting images and data to be received by direct broadcast at the same time each day. This proximity results in high-resolution images and atmospheric profiles. Therefore, polar orbiting satellites are in Sun-synchronous orbits, observing Earth with the Sun at a constant angle to the satellites every day throughout the year. The angle relative to the Sun is determined by the satellite equator-crossing time, which is chosen at the time of launch of the satellite. These Sun-synchronous satellites are able to observe almost any place on Earth, including Polar Regions, and will view every location twice in 24 h with constant general lighting conditions due to the near-constant local solar time. Recording conditions stay constant and scenes from different time periods can be easily compared (SSEC, 2006).

Polar satellite orbits are able to image Polar Regions more frequently than areas at low latitudes due to the increasing overlap in adjacent swaths as the orbit path comes closer together near the poles. The areas of coverage (swaths) are usually about 2,600 km wide. In such a way, polar orbiting satellites tend to provide higher spatial resolution images due to their proximity to Earth, as well as regular data collection at consistent times for long-term comparisons.

Satellite orientation and stabilization in space is highly important for solar cells receiving solar radiation and antenna communicating information. Satellites intended for weather and telecommunication purposes usually require to be earth pointing and it is necessary to control the satellite's position in both east-west and north south directions. However, once in orbit, a satellite experiences perturbing torques, including gravitational forces, magnetic fields, and solar radiation pressures, which can affect satellite orientation.

An attitude and orbit control system maintains a satellite's position and orientation, usually using a set of thrusters that are fired to achieve a desired rate of rotation around the Earth and to reach a desired position. At this point, polar satellites can be classified by their techniques used for attitude control, including most typically either (a) spin-stabilized satellites, or (b) three-axis stabilized satellites.

The US typically operates two polar orbiting satellites called POES and one European polar-orbiting satellite called Metop. Other satellites in PEO orbit are the Russian Meteor and Chinese PEO FY-3.

The POES instruments include the Advanced Very High Resolution Radiometer (AVHRR) instrument and the Advanced TIROS Operational Vertical Sounder (ATOVS) suite. The Eumetsat-provided Microwave Humidity Sounder (MHS) instrument completes the ATOVS suite. The AVHRR/ATOVS provides visible, infrared, and microwave data, which are used for a variety of applications such as cloud and precipitation monitoring, determination of surface properties, and humidity profiles.

Therefore, data from the POES constellation series support a broad range of environmental monitoring applications including weather analysis and forecasting, climate research and prediction, global sea surface temperature measurements, ocean waves dynamics research, atmospheric analyses and soundings of temperature and humidity, forest fire detection, volcanic eruption monitoring, global vegetation analysis, search and rescue and many other applications.

6.2.2 Introduction of Geostationary Meteorological Satellites

The GEO satellites orbit the Earth's axis as fast as the Earth spins. They hover over a single point above the Earth at an altitude of about 36,000 kilometers (22,370 miles). The orbit is shown in Figure 6.19 (Horizontal Projection**)**. However, to maintain constant height and momentum, a geostationary satellite must be located over the equator**.**

At this particular altitude, GEO satellites complete one orbit in 24 hours synchronized with Earth's rotation about its own axis and its movement around the Sun. Consequently, they remain over the same location on the equator, thereby enabling continuous surveillance of Earth and space. Thus, the primary advantage of geostationary satellites is the high temporal resolution of their data.

As stated in Chapter 3, scientists determined this position by using Newton's Law of Gravity. The same force that makes apples fall from trees on Earth is the force that keeps the satellite in its orbit. At this point, Sir Isaac Newton realized that the force of gravity depends on the masses of the objects involved (more massive objects feel a stronger gravitational force), and the distance between the objects involved (objects which are close together feel a stronger gravitational force).

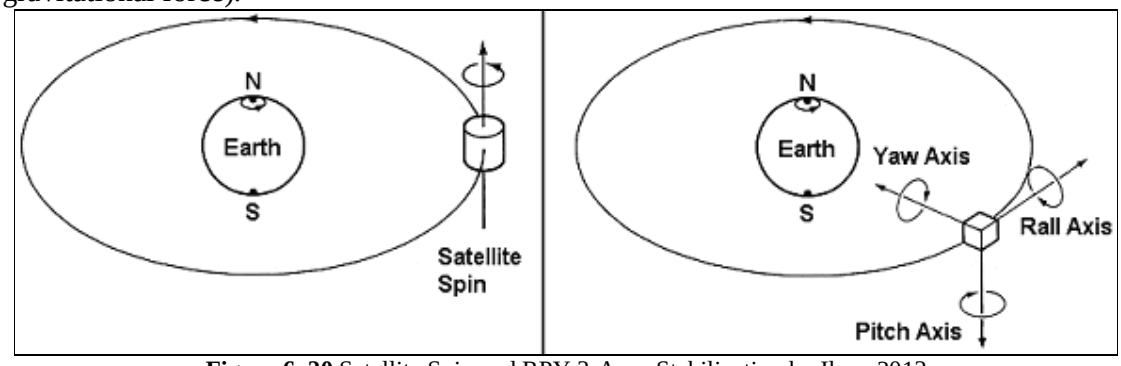

Figure 6. 20 Satellite Spin and RPY 3-Axes Stabilization by Ilcev 2013

Due to their high altitude, some GEO meteorological satellites are monitoring weather and cloud patterns covering an entire hemisphere with a fresh image of the full disk of the Earth available every 30 min. For example, Meteosat is a GEO satellite that provides high temporal resolution, which enables continuous monitoring of clouds and weather conditions.

However, GEO satellites have limited spatial resolution when compared to PEO satellites due to their high altitude. Another disadvantage is incomplete geographical coverage, since ground and mobile stations at latitudes higher than 60° have difficulty receiving signals at low elevations.

The US typically operates two geostationary satellites called GOES. One has a good view of the East Coast and the other is focused on the West Coast. Other satellites in GEO orbit are the EU Meteosat (Meteorological Satellite), which views the eastern Atlantic Ocean, Africa and Europe, the Japanese GMS (Geostationary Meteorological Satellite) has a good view of Asia, Australia and the western Pacific Ocean areas, while the Russian Elektro Geostationary Operational Meteorological Satellite (GOMS), Chinese GEO FY-2 and Indian GEO Kalpana are covering almost the same areas of Russia, Indochina and Indian Ocean.

6.3 Attitude Control and Stabilization of Meteorological Satellites

The attitude of satellite refers to its orientation in space. Much of the equipment carried aboard the satellite is there for the purpose of controlling its attitude. In fact, attitude control is necessary, for example, to ensure that directional antenna point in the proper direction. In the case of Earth environmental or meteorological satellites, the Earth sensing instruments must cover the required region of the Earth, which also needs attitude control. To provide attitude control, satellites must take precise measurement from their place in orbit. The attitude of a satellite is its position in space, namely its orientation.

Attitude determines what a satellite looks at, which way its cameras are facing and the angle the satellite makes with the object it is orbiting. To stabilize a satellite, the satellite must have a system that keeps it moving evenly through its orbit. At this point, satellites often use the spinning or gyroscopic motion to keep them stable, so a satellite's measurements and pictures will be inaccurate and fuzzy if they are not stabilized. If it is not stabilized, a satellite's orbit is more likely to decay, slowly change course either toward the Earth or out into space.
In stabilizing a satellite, the direction that onboard satellites' instruments and solar panels are facing is also important. It is easier and cheaper to power a satellite that has solar panels that are constantly exposed to the sunlight, which is necessary for satellites with extraordinarily high-energy requirements; however, this is not possible if the satellite is spinning. There are several ways to stabilize a satellite. In general, most satellites are either cylindrically shaped and are stabilized by spinning the whole of the main body, as illustrated in Figure 6.20 (Left), or box shaped three-axis body stabilized, as illustrated in Figure 6.20 (Right).

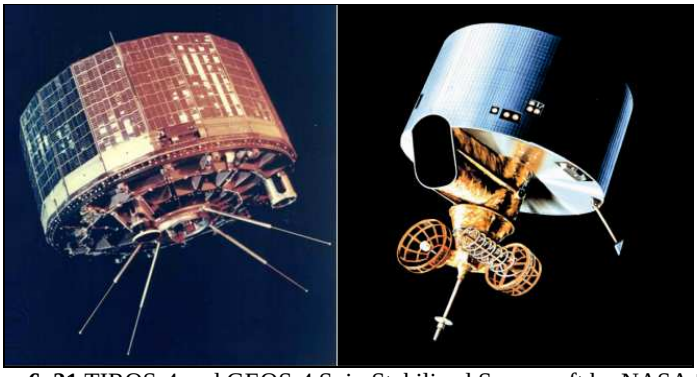

Figure 6. 21 TIROS-4 and GEOS-4 Spin Stabilized Spacecraft by NASA 2014

Materials in space are not subject to gravitational stress or atmospheric corrosion and the effects of the space environment are not all benign by any means. The high vacuum causes some materials to sublime or evaporate and some to weld together on contact. The latter behaviour means that special attention has to be given to the materials used for bearings. The basic materials for the main frame are aluminum or magnesium alloys and special plastic or fiber materials and, for other components, carbon fiber, epoxy resins and carbon nanotube filaments are used.

Satellite stabilization of meteorological satellites usually takes three possible forms: (1) Spin Stabilization, whereby the satellite is spun at 10-30 rpm; (2) Inertial Stabilization is using heavy wheels rotating at high speed, typically three wheels, one for each axis and providing Three-axis Stabilization; and (3) Gravity Gradient Stabilization using a large weight attached to the satellite by a length of line.

6.3.1 Spin Stabilized Satellites

This is a simple and effective method of keeping a spacecraft pointed in a certain direction. Any spinning spacecraft resists perturbing forces in the same way that a spinning gyroscope or a top does. Also, because, in space, different forces that slow the rate of spin are negligible, once a spacecraft is set spinning, the rate of rotation stays the same. With a spinner, there are inherent inefficiencies because only some of the solar cells are illuminated at any one instant and because most of the radio wave energy, radiating from the non-directional antennas in all directions, is not directed at Earth. Thus, thrusters are fired to make desired changes in the spin-stabilized attitude. They may require complicated systems to de-spin antennas or optical instruments which must be pointed at targets.

Therefore, spin-stabilized satellites have the motion of one axis relatively fixed by spinning the satellite around the major axis by the gyroscopic effect offering inertial stiffness, much like a spinning top. This prevents the satellite from drifting from its desired orientation and keeps the spacecraft pointed in a certain direction. The spinning spacecraft effectively resists perturbing forces, which tend to be small in space. Spin-stabilization design was applied to most early satellites and typically have a cylindrical shape.

Figure 6.21 (Left) presents the TIROS-4 satellite as an example of the US POES early design of TIROS series 1-4 with spin stabilization solution in 1981. In this configuration, solar arrays are mounted around the spinning cylindrical drum. One disadvantage of this design is that the satellite is limited in terms of the size of solar arrays that can be used to obtain solar energy, which results in large battery power requirements. Another disadvantage is that instruments or antennae must also perform “de-spin” maneuvers, so that the satellite antenna can point at the appropriate Earth ground terminals, that were visible at that time.

Moreover, this design suffers from the fact that instruments on the satellite spend much of their time looking away from Earth and only a small part of their time facing Earth. Finally, since the spin rate of the satellite decays with time, constant readjustment is required. This readjustment can be achieved by firing thrusters tangentially to the circumference of the spinning drum.

In the 1980s, the capability was added to obtain vertical profiles of temperature and moisture throughout the atmosphere by the series of GOES 4-7 or D-H satellites. Figure 6.21 (Right) shows the design of the US GEO spin stabilized spacecraft GEOS-4. This type of satellite is

not experiencing problems mentioned for previous POES, because it is always facing to the Earth's surface and has normal sized solar arrays. However, spin-stabilized satellites are often simpler in design, lighter in mass, and usually less expensive.
Spin stabilized structures have a cylindrical part, which rotates at a speed of 50–100 rpm and the despun stabilized part has mounted antennas always facing to the Earth. The spin axis lies along the pitch axis parallel to the Earth's N-S axis. Thus, spin is initiated during the launch phase by means of small gas jet (Harris, 2015).

The spinning part of the cylinder is covered with solar cells and its spin axis is oriented perpendicularly to the Sun. Body stabilized structures rotate once for every rotation of the Earth, so that the side with mounted antenna will always face the Earth. This platform utilizes a deployed set of solar panels with solar cells mounted on one side of the panel surface relative to the Sun.

The box shaped body stabilized satellite has three-axis known as Roll, Pitch and Yaw (RPY), which define the attitude of satellite. Thus, all three axes pass through the centre of satellite gravity. The Yaw axis is directed towards the Earth's centre, the Pitch axis is normal to the orbital plane and Roll axis is perpendicular to the other two. In fact, the Roll axis is tangential to the orbit and lies along the satellite velocity vector.

6.3.2 Three-Axis Stabilized Satellites

The three-axis solution is a type of satellite stabilization in which a spacecraft maintains a fixed attitude relative to its orbital track. This is achieved by nudging the spacecraft back and forth within a dead-band of allowed attitude error, using small thrusters or reaction wheels. With a three-axis stabilized spacecraft, solar panels can be kept facing the Sun, a directional antenna can be kept pointed at Earth, and cameras can be kept pointed at desired targets without having to be de-spun. On the other hand, rotation maneuvers may be needed to best utilize fields and particle instruments. Figure 22 (Left) illustrates a GEOS I-M (8-12) sample of three-axis stabilized satellites series, launched in 1994. Other examples of weather satellites belonging to the category of three-axis stabilized systems include GOES-8, GOES-9, and series of TIROS-N satellites.

These satellites brought real improvement in the resolution, quantity, and continuity of the data, i.e., three-axis stabilization of the spacecraft and separate optics for imaging and sounding. Three-axis stabilization meant that the imager and sounder could work simultaneously. Forecasters had much more accurate data with which to better pinpoint locations of storms and potentially dangerous weather events such as lightning and tornadoes (SCISYS, 2014). The satellites could temporarily suspend their routine scans of the hemisphere to concentrate on a small area of quickly evolving events to improve short-term weather forecasts for that area.

For this stabilization, the body of the satellite remains fixed in space relative to a constant Earth orientation. The movement of the satellite is controlled along all three axes, i.e., RPY. Small spinning wheels (called reaction wheels or momentum wheels) rotate to maintain the spacecraft in the desired orientation in relation to Earth and the Sun. Corrective forces are applied by the active control system on the wheels to correct for satellite orbit perturbations.

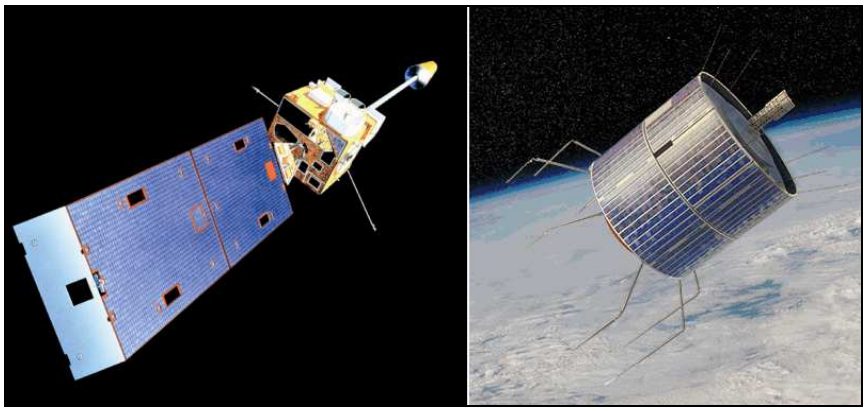

Figure 6. 22 GEOS I-M (8-12) Three-Axis and ATS 2-5 Gravity Gradient Stabilized Satellites by NASA 2014

Once satellite sensors detect that the satellite is moving away from the proper orientation, momentum wheels immediately speed up or decelerate to provide the dynamic force required to keep it within a specific range. Some spacecraft also use small propulsion-system thrusters to continually nudge the spacecraft back and forth until the correct position is achieved. In comparison to spin-stabilized, three-axis stabilized satellites can view Earth continuously, but are somewhat more difficult to maintain a perfect relationship or orientation to Earth.

They also have an extendible solar array that is unable to provide power when the satellite is in the transfer orbit, while it is still stored inside the satellite. However, three-axis stabilized satellites have potential for more power generation capability with large solar arrays during operation, as well as additional mounting areas available for complex antennae structures (Harris, 2015). In addition, they are able to point optical instruments and antennae without having to de-spin them, unlike spin-stabilized satellites.

6.3.3 Gravity Gradient Stabilized Satellites

A useful passive method to achieve stabilization of satellites is also possible by using the gravity gradient of the primary body. An orbiting spacecraft will tend to align its long axis (more precisely, the axis of minimum moment of inertia) with the local vertical, that is, in a radial direction. Therefore, gravity-gradient stabilization, or "tidal stabilization", is a method of stabilizing satellites in a fixed orientation using only the orbited body's mass distribution and gravitational field. The main advantage over using active stabilization with propellants, gyroscope or reaction wheels is the low use of power and resources.

The idea is to use the Earth's gravitational filed and tidal forces to keep the spacecraft always aligned in the desired orientation. The gravity of the Earth decreases according to the inverse-square law and by extending the long axis perpendicular to the orbit, the "lower" part of the orbiting structure will be more attracted to the Earth. The effect is that the satellite will tend to align its axis of minimum moment of inertia vertically.

The first experimental attempt to use the technique on a human spaceflight was performed on 13 September 1966, on the US Gemini-11 mission, by attaching the Gemini spacecraft to its Agenda target vehicle by a 100 feet (30 m) tether. The attempt was a failure, as insufficient gradient was produced to keep the tether taut. The technique was first successfully used in a Near-GEO on the Department of Defense Gravity Experiment (DODGE) satellite in July 1967. It was first used for LEO and tested unsuccessfully for GEO in the series of ATS 2-5 satellites from 1966 until 1969. The sample of the satellite is shown in Figure 22 (Right). An

example of gravity-gradient stabilization was demonstrated during NASA's TSS-1R mission. Just prior to tether separation, the tension on the tether was about 65 N (14.6 lbs).

6.3.4 Inertially Stabilized Satellites

Inertial stabilization is a type of stabilization in which a spacecraft maintains a fixed attitude along one or more axes relative to the stars. Inertially stabilized platforms (ISP) are routinely used onboard vehicles, ships, aircraft and spacecraft for diverse missions including aerial photography, battle reconnaissance, antenna stabilization, missile guidance and so on.

Therefore, this platform requires accurate angular velocity estimation at a relatively high bandwidth to achieve stable control of the lines of sight of optical imaging sensors. An inertial platform, also known as a gyroscopic platform or stabilized platform, is a system using gyroscope to maintain a particular orientation in space despite the movement of the vehicle they are attached to.

6.4 Comparison of PEO and GEO Meteorological Satellites

Since 71 % of Earth's surface is covered by water, and large regions are sparsely inhabited, PEO satellite systems produce data that compensate for the deficiencies in conventional observing networks. The polar-orbiting spacecraft offers the advantages of acquiring data from almost all locations on the globe in the course of successive revolutions (e.g., TIROS series and POES series satellites). The primary advantages of this type of satellite are observing daily global cloud cover, accurate quantitative measurements of surface and vertical temperature, and atmospheric water vapour.
Moreover, Sun-synchronous PEO satellites offer the advantages of moderate to high spatial resolution, and nearly constant daily equatorial crossing times. They are able to track weather conditions, atmospheric variables, and cloud cover. However, observations of instant changes from these platforms are spatially and temporally fragmented due to the swath width and revisit times of the orbital ground tracks. A method to mitigate this loss is to fly sensors on twin satellites, so that the sensor can sample every 6 hours from a near-polar orbit. Nevertheless, a good combination of spatial and temporal resolution is still required for adequately sampling and monitoring a phenomenon of interest. In contrast, GEO satellites provide a continuous view of weather systems necessary for intensive data analysis, thereby recording the motion, development and decay of changing atmospheric conditions. However, GEO satellites "hover" continuously over a fixed position on the Earth's surface. For example, severe thunderstorms with a lifetime of only a few hours can be successfully detected and recognized in the early stages, making it possible to issue warnings to the general public of the time and area of the storm's maximum impact (Kidder and Ham, 1995). Then GEO satellite imagery can also be used to estimate rainfall during thunderstorms, flash floods during hurricanes, and snowfall accumulations in the winter. Due to this capability, geostationary spacecraft has been primarily used for short-term natural disaster warnings. **Table 6.1** summarizes and compares basic features of geostationary and polar orbiting satellites.

Table 6. 1 Comparison of GEO and PEO Meteorological Satellites in Tan 2014

	Geostationary weather satellites	Polar-orbiting weather satellites
Image resolution	Relatively low	Relatively high
Scan coverage	Whole globe disk	Limited areas
Altitude of orbit	About 36,000 km (22,370 miles) above the equator	About 800–1,200 km (497–746 miles)
Movement of satellite	Orbit in synchronization with the Earth	Circling the Earth in a roughly north-south orbit
Frequency of image capture	Continuous viewing of one location	One to two times a day for the same place

Figure 6. 23 TIROS-1 Preparing for Launching and Onboard Components by NASA/NOAA 2014

Given the opposing advantages and disadvantages of PEO and GEO satellites, it has been suggested that the strengths of each platform complement each other and could be greatly exploited by merging datasets. Analyzing satellite imagery collected from multiple sensors and/or multiple platforms is a common technique that has been used to increase the sampling frequency of Earth observations. For example, the GOES space program is applied for national, regional, short-range warnings and real-time forecasts, while POES is usually applied for global, long-term forecasting and environmental monitoring (Tan, 2014).

Producing image composites by combining GEOS and PEOS observations is challenging due to the need to deal with differences in calibration, viewing geometry and temporal offsets from a variety of satellites. Temporally, two major factors to contend with are the timeliness of the data and time interval between composite images. Thus, advances in multi-sensor data fusion techniques optimize the use of current meteorological satellite systems and integrate data for global weather monitoring and improved forecasts. Combined together, both types of satellites constitute a truly global meteorological network, evolving into an integrated environmental observing system with capabilities to observe, assess, and predict the total Earth system, including atmosphere, ocean, land and space environments.

6.5 Evolution of Sensing Techniques

In the early 1960s, television cameras were on-loaded onto meteorological satellites to view and monitor Earth from low orbit altitudes of approximately 720 km. Pictures taken by a 10 mm lens at a speed of 5 frames per set achieved a spatial resolution of 0.15 km under full sunlight with 25 % contrast. These parameters permitted a transverse strip approximately 550 km wide to be photographed when a satellite orbited Earth.

The PEO TIROS-1 was the first successful dedicated weather satellite ready for launching, as shown in Figure 6.23 (Left), and it was marked the world's first weather satellite to test the experimental TV techniques. The main components of TIROS-1 with two TV cameras are shown in Figure 6.23. (Right).

It carried two 6-inch long television cameras on-board, which were rugged and lightweight devices weighing only about 2 kg. One of the cameras had a low-resolution wide-angle lens providing views of approximately 1,200 km on a side, while a narrow angle camera had a higher resolution telephoto lens with a view that was about 130 km on a side.

However, a magnetic tape recorder for each camera was supplied for storing photographs when the satellite was beyond the range of a ground station, containing 122 m of tape and recording up to 32 pictures. When within range of a ground station, the cameras took pictures every 10–30 s. In addition to vidicon camera systems for daytime visible imaging, TIROS satellites also carried passive infrared radiometers for sensing during both day and night conditions. TIROS-8, launched in December 1963, carried a 1.27-cm vidicon camera and a 2.54-cm Automatic Picture Transmission (APT) camera. The latter utilized a very slow-scan vidicon compared to the former and was designed for real-time picture transmission of cloud cover conditions to be received by fairly simple and inexpensive ground stations anywhere in the world. Whereas the vidicon camera required 2 s to scan its 500-television-line image, the APT camera required 200 s for read-out of its 800-television-line image. Thus, over 1,600 pictures were obtained in the 3½ weeks of mission lifetime. The APT cameras were subsequently used on Nimbus-1 and -2, then on the operational ESSA series and the initial NOAA satellites.
In the Environmental Satellite Service Administration (ESSA) series (also called the TIROS operational System – TOS series), satellites from ESSA 3 began to apply a modified Nimbus camera, the Advanced Vidicon Camera System (AVCS). This system combined APT transmission and onboard data storage for the collection of daytime imagery (visible and thermal infrared) and night-time imagery (thermal infrared only). The AVCS consisted of three cameras, a tape recorder, and an S-band transmitter that produced a three-segment composite picture. It provided higher resolution imagery and a larger picture area than the 1.27 cm vidicon for TIROS. It also yielded a linear resolution of better than 1 km at nadir from an altitude of 800 km. The 2 kHz bandwidth of the system enabled the satellites to transmit direct, real-time television pictures to the inexpensive APT ground stations located around the world. AVCS provided more near-global and high-resolution cloud cover imagery than had ever been assembled prior to that time.

The ESSA system was followed by the Improved TOS (ITOS, or TIROS-M series), which allowed the global coverage and APT services to be combined on one satellite. Launched in January 1970, ITOS-1 was the first of an operational series of three-axis stabilized satellites. This allowed scanning radiometers (SR) to be flown on the satellites and provided routine infrared window coverage both day and night. These devices were used to further evaluate

and develop global sea-surface temperature mapping, as well as other thermal patterns, which led to significant contributions to radiation budget and space weather applications.

Only about three years later, the launch of NOAA-2 (or ITOS-D) marked the end of the vidicon era and the start of the era of multi-channel high-resolution radiometers, which were an improvement over the SR. The Very High Resolution Radiometer (VHRR), a calibrated scanning radiometer, was installed on the TIROS-M satellite series initially only to capture information from the visible and infrared window. As part of international weather data exchange, NOAA introduced the direct reception of VHRR data at no charge to ground stations built by an increasing number of users, beginning in 1972. ITOS-1 and NOAA-1 were transitional satellites of the ITOS series. The NOAA-2, through NOAA-5 satellites that were launched in 1972–1976, carried the VHRR instrument. The next milestone of the development of imaging technologies occurred on October 1978 with the launch of TIROS-N. This satellite included an across-track scanning instrument, in the form of a four spectral channel radiometer called the Advanced VHRR (AVHRR). This advanced radiometer covered the visible, near-infrared, mid-wave infrared, and thermal spectral channels. All four channels had a spatial resolution of 1.1 km. The infrared window channels had a precise thermal resolution of 0.12 K at 300 K. The AVHRR installed on later satellites were applied for global daytime and night-time sea surface temperature determination, heat budget components estimation, cloud delineation, and snow and sea ice identification.

The AVHRR subsequently improved to a five and six spectral channel system, with all channels providing imagery at 1.09 km resolution at nadir. Thus, the data have also been used for a variety of other studies, including mapping marine oil pollution, monitoring volcanic eruptions, and assessing vegetation vigour on an international scale. Information reported from NOAA about the wavelength and typical applications of the six bands of AVHRR/3 sensor channel characteristics and typical applications are listed in **Table 6.2.**

Table 6. 2 Comparison of GEO and PEO Meteorological Satellites in Tan 2014

Channel #	Wavelength (μm)	Applications
1	0.58–0.68	Daytime cloud and surface mapping
2	0.725–1.00	Land-water boundaries
3A	1.58–1.64	Snow and ice detection
3B	3.55–3.93	Night cloud mapping, sea surface temperature
4	10.30–11.30	Night cloud mapping, sea surface temperature
5	11.50–12.50	Sea surface temperature

A second primary sensor on-board the TIROS-N was a vertical sounder, referred to as the Vertical Atmospheric Sounder (VAS). This is a type of radiometer that measures infrared or microwave radiation. This device provided vertical profiles of temperature, pressures, water vapour, and critical trace gases (e.g., carbon dioxide or ozone) in Earth's atmosphere. Apart from the VHRR, NOAA 2 (launched in 1972) also allowed operational thermodynamic soundings with the Vertical Temperature Profile Radiometer (VTPR). This instrument was an 8-channel TIR/FIR filter radiometer that scanned perpendicular to the satellite motion with a horizontal resolution of 55 × 57 km at the nadir and 67 × 91 km at the edges of the radiometer's scan.

In the same period, it was recognized that the optimum temperature profiles would be obtained by taking advantage of the unique characteristics offered by taking soundings at the

4.3 μm, 15 μm, and 0.5 cm wavelength regions. Consequently, the High Resolution Infrared Radiation Sounder (HIRS) experiment of Nimbus-6 (launched in 1975) was designed to accommodate channels in both the 4.3 and 15 μm infrared regions. The 7-channel HIRS was about 25 × 25 km in spatial resolution. It was also designed to measure scene radiance to permit the calculation of the vertical temperature profile from Earth's surface all the way up to about 40 km in altitude. This was subsequently complemented by the 0.5-cm microwave wavelength channels of a Scanning Microwave Spectrometer (SCAMS), which provided nearly full Earth coverage every 12 hours. The combination of instruments on-board the Nimbus-6 satellite provided improved sounding capabilities as compared to the infrared sounders alone.

The TIROS-N/NOAA satellites series that began in 1978 not only carried the AVHRR but also an atmospheric sounding system called the TOVS-TIROS Operational Vertical Sounder (TOVS). This sounder provided vertical profiles of temperature and water vapour from Earth's surface to the top of the atmosphere. A solar proton monitor detected the arrival of energetic particles for applications in solar storm prediction. The TOVS incorporated a suite of instruments, including a HIRS, the Microwave Sounding Unit (MSU), and the Stratospheric Sounding Unit (SSU).

An operational Solar Backscatter Ultraviolet Radiometer (SBUV/2) used to monitor the distribution of ozone in the atmosphere was flown on NOAA-9, -11, -13, and -14 satellites. Since NOAA-15 (launched in 1998), all sounding units have greatly improved, including the deployment of the Advanced TOVS (ATOVS) system for NOAA 15 and subsequent satellites. The ATOVS used the HIRS and AMSU-A to generate atmospheric profiles, while the AVHRR instrument was used for cloud detection.

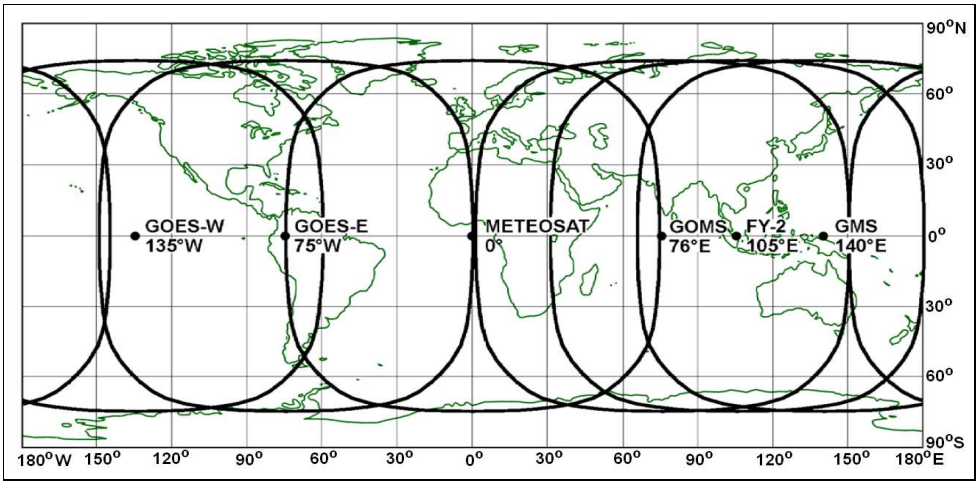

Figure 6. 24 Global Observation Coverage by International GEO Meteorological Satellites by Eumetsat 2009

The ATOVS from NOAA 15 (launched in 1998) generated about 300,000 retrievals every 24 h with a 60-km spatial resolution. It was the first in a series of five satellites with improved imaging and sounding capabilities.

NOAA-15 also first carried the AVHRR/3 sensor (**Table 6.2**), which is an across track scanner that senses Earth's outgoing radiation in six channels. Three channels operate in the visible-near infrared region and three channels in the Thermal Infrared (TIR), with a spatial resolution of 1 km at nadir. The data from the six channels, after processing, permits multi-spectral analysis for more precisely defining hydrologic, oceanographic, and meteorological

parameters. AVHRR/3 data have been used widely for measuring temperature and various environmental parameters of land, water, sea surfaces, and cloud cover.

6.6 Data Synthesis and International Data Exchange

Researchers have increasingly applied data fusion methods to integrate and display data from multiple space-borne sensors in order to analyze complementary remote sensing imagery and thus to fulfill research objectives. For example, a model yielding the probability of rainfall was established based on GOES visible/infrared imagery and simultaneous radar data for eastern Canada in 1980.

A similar approach has been applied for daily evapo-transpiration mapping implemented by the Atmosphere-Land Exchange Inverse (ALEXI) model, which is a multi-sensor TIR approach. This model was developed for estimating and mapping surface fluxes and surface moisture variables at the regional scale. The TIR imagery is derived from any type of GOES data, depending on the resolution required by a given application. The ALEXI model has potential for global applications by integrating data from multiple GEO meteorological satellites systems, such as the US GOES, the European Meteosat satellites, the Chinese Feng-yun-2B series, and the Japanese GMS. Observation covering scales of these international GEO satellites are shown in Figure 6.24.

In addition, synthetic application of multi-sensor data can be found in many research studies and applications. For example, the International Satellite Cloud Climatology Project (ISCCP), the first project of the World Climate Research Program (WCRP), established in 1982, has the goal of examining global distribution of cloud radiative properties. Thus, by collecting and analyzing satellite radiance measurements, global cloud distribution, and other data, it is possible for temporal (diurnal, seasonal, and yearly) variations to be inferred, as shown in Figure 6.25.

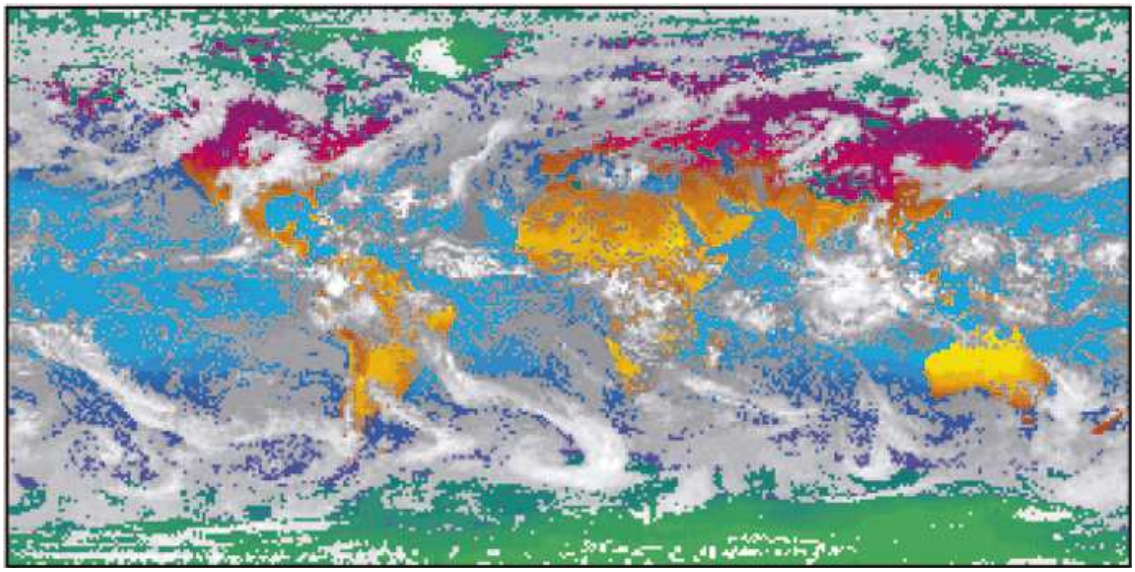

Figure 6. 25 NASA ISCCP Data Product Image of Global Cloud Coverage by NASA 2014

Data applied in this project have been sought from five GEO meteorological satellites, including GOES-E, GOES-W, GMS, INSAT (Indian National Satellite System), and

Meteosat, as well as, at least, two polar-orbiting satellites (NOAA/TIROS-N and Meteor class satellites). The primary datasets have been derived from two standard visible (0.6 μm) and infrared (11 μm) channels from all of these satellites. The ISCCP cloud data are used to determine cloud effects on Earth's radiation balance. This has greatly enhanced understanding of cloud formation processes and the global water cycle.

Otherwise, another example of international satellite data exchange is the International Space Environment Service (ISES). This global service facilitates near-real-time international monitoring and prediction of the space environment. The ISES system comprises a network of globally distributed Regional Warning Centers. A permanent service of the Federation of Astronomical and Geophysical Data Analysis Services (FAGS), the ISES has an important role in coordinating the exchange of data between organizations around the world, which are involved in forecasting solar terrestrial conditions and reducing the impact of space weather on activities of human interest.

The data exchanged are highly varied in nature and in format, ranging from simple forecasts or coded information up to more complicated information, such as satellite imagery. An important strength of the ISES data exchange system is the network of Regional Warning Centers and access to data from unique instrumentation available from the scientific community in each center's region. Exchange via the ISES enables such data sets to be available to the wider international scientific and user community. A data exchange schedule operates with each center providing and relaying data to other centers. A center in Boulder, Colorado (USA), plays a special role as a "world warning agency" and acts as a hub for data exchange and space weather forecasts. The ISES plays a key role in international data exchange based on cooperation in space weather services. Within the European Space Agency (ESA), data are exchanged on a regular basis among the member states().

The UN's WMO serves as the global authoritative voice on the state and behaviour of Earth's atmosphere. The WMO is thus concerned with the atmosphere and its interaction with the oceans, the impacts on the climate that Earth's oceans and atmosphere actually produces, and the resulting distribution of water resources.

Established in 1950, the WMO comprises of 191 member states and territories (as of January 1, 2013). The WMO is the United Nations' specialized agency for meteorology (weather and climate), operational hydrology, and related geophysical sciences. In such a way, the WMO promotes cooperation between member states for making meteorological observations. It carries out its mission by facilitating the free and unrestricted exchange of data and information, processing and standardization of related data, and assisting with technological transfer, training and research.

Since weather, climate, and the weather cycle know no national boundaries, international cooperation at a global scale is essential. With the rapid new development of instrumentation to quantify meteorological phenomenon and a growing constellation of weather satellites collecting real-time data in orbit, it is clear that there is much more data being collected and, thus, much more to be processed and stored. With better and easier ways to obtain and store information, there also comes a higher demand for ways of managing and analyzing all the data. This is vital not only to public weather services and applications in agriculture, aviation, shipping, environment, and water issues, but to many other important areas as well (Menze, 2012).

Proper processing and use of key data has incalculable benefits for humankind's well-being, providing vital information for advance warnings that save lives and reduce damage to property and increasingly to help preserve the environment. Global weather data exchange is essential for climate monitoring and for better understanding the world's weather system to help prepare and protect human populations from adverse and extreme weather events. The effective use of this data might be perhaps tomorrow or perhaps decades in the future.

6.7 Meteorological Operational Satellites

The Meteorological Operational Satellite (MOS) program is a worldwide initiative to provide satellite weather data services, monitor the climate and improve weather forecasts. In fact, this program was formally integrated by the major states that provide global MOS service, as members of World Meteorological Organization (WMO). Therefore, the coordinator of all MOS programs and services is WMO together with major member states, such as the US National Oceanic and Atmospheric Administration (NOAA), the European Organization for the Exploitation of Meteorological Satellites (Eumetsat), the Russian Federal Service for Hydrometeorology and Environmental Monitoring (Roshydromet), China Meteorological Administration (CMA), India Meteorological Department of the Indian Space Research Organization ISRO), and Japan Meteorological Agency (JMA), etc.

The space Program's objective is to promote availability and utilization of satellite data and products for weather, climate, water and related applications to WMO members. Thus, it coordinates environmental satellite matters and activities throughout all WMO programs and gives guidance on the potential of remote-sensing techniques in meteorology, hydrology and related disciplines.
The WMO Space Program activities are divided into four parts: Observation capabilities; Earth Observation (EO) products and applications; Access to weather data and products; and Information and capacity building. A web-based resource Ocean Surface Current Analyses Real-time (OSCAR) has been developed to record the characteristics of the space-based observation system in support of the Rolling Review of observation Requirements (RRR), which contains technical descriptions of more than 500 satellites and 700 instruments and is accessible at: www.wmo.int/oscar. Through the SCOPE-CM (Climate Monitoring), SCOPE-NWC (Nowcasting), Severe Weather Forecasting Demonstration Project (SWFDP), and RGB workshop, product development and generation have been enhanced. In addition, WMO Members, within the WMO Space Program, are coordinating their efforts for space weather warning services, as a most important issue of MOS activities.

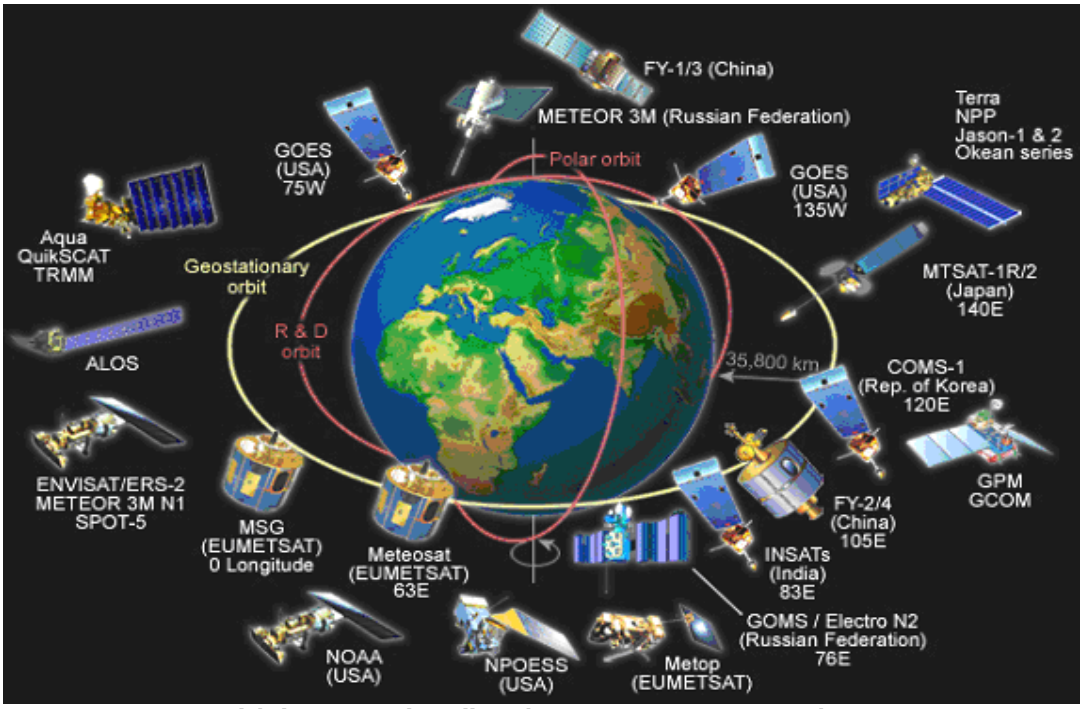

Figure 6. 26 Global Operational Satellite Observation System Coverage by COMET 2011

The OSCAR Satellite Status lists the status of current and future satellites contributing to the WMO Integrated Global Observing System (WIGOS). This information is extracted from OSCAE/Space (Observing Systems Capability Analysis and Review Tool). For further information, it is possible to go directly to the tool, which offers search, filter and export all facilities and addresses to a larger number of Earth observation satellites. Thus, the links in the tables also lead directly to OSCAR/Space. For more details on the satellites, e.g., payload characteristics, data access or telecommunication frequencies, it is necessary to click on the respective name.

Figure 6.26 shows the major MOS constellations presented by the Cooperative Program for Meteorological Education and Training (COMET), which was started with activities in the frame of WMO University Corporation for Atmospheric Research (UCAR) in 1989. This figure includes GEO, PEO and LEO (R&D Orbit), but does not include two meteorological satellites in High Elliptical Orbit (HEO) known as the Russia Arctica and the future Canadian Polar Communications and Weather (PCW) spacecraft.
In the period of 2012 to 2015, WMO started with the implementation of the WMO Integrated Global Observing System (WIGOS), which provides a new framework for WMO observing systems and the contributions of WMO to co-sponsored observing systems. However, it is important to recognize that WIGOS is not replacing the existing observing systems, but is rather an over-arching framework for the evolution of these systems which will continue to be owned and operated by a diverse array of organizations and programs. The WIGOS group will focus on the integration of governance and management functions, mechanisms and activities to be accomplished by contributing observing systems, according to the resources allocated on a global, regional and national level.

The Plan for the Implementation of WIGOS (WIP) (available under “Basic Documents” in all WMO languages) addresses the necessary activities to establish an operational WIGOS by

the end of the period 2012-2015, as per the direction of the WMO Congress. It identifies and describes the following activity areas:

(a) Management of WIGOS implementation; (b) Collaboration with WMO and co-sponsored observing systems; (c) Design, planning, and optimized evolution of WIGOS observing components; (d) Integrated observing system operation and maintenance; (e) Integrated quality management; (f) Standardization, system interoperability, and data compatibility; (g) WIGOS operational information resource; (h) Data and metadata management, delivery, and archival; (i) Capacity development,; and (j) Communication and outreach.

The WIP also addresses a number of additional activities that would substantially improve the operational capabilities of WIGOS beyond the 2012-2015 implementation. The WIP also addresses a number of additional activities that would substantially improve the operational capabilities of WIGOS beyond the 2012-2015 implementation; however, these activities are dependent on resources in addition to the regular budget. If these activities are not completed, WIGOS can still be considered operational. The resulting system will, however, be less effective in achieving its goals and benefits to members will be reduced or delayed.

Satellite status and plans operated by CGMS Members are listed in a set of tables that are maintained by the WMO Space Programme office on behalf of CGMS. The tables indicate the current status of on-orbit satellites along with the plans for future ones including launch date, orbital characteristics, payload and operational status, if relevant. Hyperlinks enable navigation to more detailed information from the relevant satellite agency as well as to the online OSCAR (Observing System Capabilities Analysis and Review) tool, which contains detailed information on instruments, satellites, or high-level gap analysis. Information is available for both Operational and Research and Development (R&D) in GEO, HEO, PEO sun-synchronous and LEO satellite orbits, which contribute or have the potential to contribute - to the space-based component of the Global Observing System (GOS).

This chapter will introduce the following MOS of National Oceanic and Atmospheric Administration: US National Oceanic and Atmospheric Administration (NOAA), European Organization for the Exploitation of Meteorological Satellites (Eumetsat), Russian Federal Service for Hydrometeorology and Environmental Monitoring (Roshydromet), China Meteorological Administration (CMA), Indian Space Research Organization ISRO) and Japan Meteorological Agency (JMA).

6.7.1 NOAA Meteorological Satellites

On 3 October 1970, NOAA was formed under the US Department of Communications (DOC) and developed for better protection of life and property from natural hazards, for a better understanding of the total environment and for exploration and development leading to the intelligent use of our marine resources.

Specifically, NOAA’s mission is to describe and predict Earth’s environment to safeguard lives and property and to contribute to national economics and environmental health. In order to support and fulfill this mission, NOAA gathers environmental data around the world and from space.

Operating the country’s environmental satellite program, NOAA is responsible for developing and applying space-based Earth remote sensing and cloud imagery for NOAA’s

National Weather Service (NWS) forecasts. The NWS is responsible for weather warning services, providing forecasts, and other products for the purposes of protection, safety, and general information. Within NOAA, the National Environmental Satellite, Data, and Information Service (NESDIS) office operates the satellites and manages the processing distribution, as well as the archiving of the data. It distributes on a global basis more than 3.5 billion vital bits of data and images to forecasters daily. Data is used for various applications, including oceanography, agriculture, forest fire detection, volcanic ash monitoring, monitoring atmospheric ozone, and storm prediction.

Over time, NOAA's satellites have evolved from serving solely as weather satellites to environmental satellites for broad applications, thus enhancing our understanding of climate variability and society's ability to plan and respond. Its role with regard to monitoring space weather has also expanded over time. The NOAA's operational activities, such as weather prediction, routinely and reliably generate specific services and products that meet predefined accuracy, timeliness, and scope/format requirements.

In addition to providing cloud images for daily television weather forecasts, the information is also disseminated or made available to a variety of users in the public, private, and academic sectors. Operational systems must be developed to withstand risk and operate without interruption to provide measurements with predefined accuracy and timeliness requirements. The NOAA service represents the US investment in satellite technologies and infrastructure to routinely collect data and transmit operational information about Earth's environment (weather, climate, oceans).

The NOAA satellite constellation consists of complementary operational environmental satellites, including GOES and POES. Both types of satellites are critical to the global weather network and Cospas-Sarsat Search and Rescue (SAR) service. As noted above, the NESDIS processes and distributes more than 3.5 billion vital bits of data and images to meteorologists and forecasters globally, and it does so under demanding standards of timeliness and quality. Further in doing so, it is constantly working to accurately combine polar and geostationary satellite data. This mission is being achieved by virtue of greatly upgraded data processing and analysis installations, enhanced ground facilities, and data sharing agreements with military weather services. The primary customer of these data remains the NWS, which adopts satellite data to perform weather forecasts for the public, television, radio, and weather advisory services. Satellite information is also shared with various federal agencies, other countries (e.g., Japan, Russia, European Space Agency members, and the United Kingdom Meteorological Office) and the private sector.

6.7.1.1 NOAA Sun-synchronous PEO Meteorological Satellites of WIGOS

As stated earlier, TIROS-1 was launched on 1 April 1960 . It was the first US weather satellite capable of monitoring Earth and helping weather forecasts. As an experimental spacecraft, TIROS-1, in its 78-day operating period, sent back nearly 23,000 pictures of Earth and its ever-shifting cloud cover from an altitude of about 700 km. This satellite was equipped with both wide and narrow-angle television cameras, one low-resolution and one high-resolution, which relied on reflected solar radiation, capable of operating only during the daytime.

To assist in overcoming these limitations, as well as for other purposes, TIROS-2 was launched on 23 November 1960 , carrying several radiometers in addition to two of the same

television cameras used on TIROS-1. One of these radiometers measured the energy emitted by Earth in the water vapour window with wavelength intervals from 8 to 12 μm. The TIROS experimental system continuously launched ten satellites successfully between 1960 and 1965. It provided early warning of severe tropical storms, hurricanes and typhoons.

From TIROS-8, launched on 23 December 1963, the APT camera system and ground stations were tested. The APT camera utilizes a very slow-scan vidicon compared to the TV camera. By virtue of the 2 kHz bandwidth of the APT system, TIROS-8 offered the capability of transmitting direct, real-time TV pictures to a series of relatively inexpensive ground stations located around the world. This technique provided an instantaneous view of local area weather from a satellite passing overhead. In accordance with the NASA-NOAA's USWB agreement, TIROS-9, the first weather satellite to be launched into Sun-synchronous orbit, was a NASA-financed, modified TIROS satellite, orbited to test the new configuration that would eventually be incorporated in the operational series.

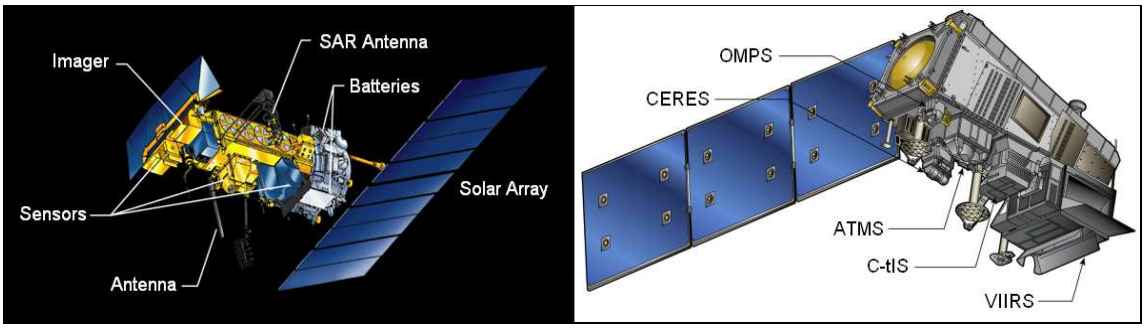

Figure 6. 27 PEO Meteorological Satellites NOAA-19 and NPP/Suomi by NOAA 2004

In the meantime, TIROS-10 and series ESSA 1-10 of Environmental Science Services Administration (ESSA) were launched. The first satellite of Nimbus 1-7 series was launched in 1965 to test advanced meteorological sensor systems and for collecting atmospheric science data. Then 5 satellites of Improved TIROS Operational System (ITOS) series, 4 satellites of Next Generation TIROS-N/NOAA series and finally 11 satellites of Advanced TIROS-N (ATN)/NOAA series were launched. The last satellite of this series is 12th NOAA-19 satellite, which contains the SARSAT-12 and Argos-3 payloads.
In this sequence, the following current NOAA meteorological satellites will be introduced:

1. NOAA-19 - The POES began with NOAA-K (NOAA-15), which was launched on 13 May 1998. With a suite of instruments, this series, like its precursors, was able to measure many parameters of Earth's surface and atmosphere. This included observations of cloud cover, incoming solar protons, positive ions, electron-flux density and the energy spectrum at the satellite's altitude. The satellites could also receive, process, and retransmit data from beacon transmitters and automatic Data Collection Platforms (DCP) on land, ocean buoys, or aboard free-floating balloons. The primary instrument on POES was the 3rd generation instrument of AVHRR (AVHRR/3), which is the latest version of the sensor with six channels (three solar channels in the visible-near infrared region and three thermal infrared channels). Thus, NOAA-N Prime (NOAA-19) was the last in the series of Advanced TIROS-N (ATN) satellites launched on 6 February 2009, which is shown in Figure 6.27 (Left). This satellite also carries payloads for the SARSAT-12 and Agros-3 Search and Rescue (SAR) satellite programs. Like its predecessors, NOAA-N' provides global images of clouds and surface features and vertical profiles of atmospheric temperature and humidity for use in numerical weather and ocean forecast models, as well as data on ozone distribution in the

upper part of the atmosphere and near-Earth space environments. This information is important for the marine, aviation, power generation, agriculture and other communities. Except for the AVHRR/3 instrument, this satellite carries onboard High Resolution Infrared Radiation Sounder (HIRS/4), and the Advanced Microwave Sounding Unit (AMSU-A), which were designed for a three-year mission. The Solar Backscatter Ultraviolet Spectral Radiometer (SBUV/2) was designed for a two-year mission, and the Microwave Humidity Sounder (MHS) was designed for a five-year mission.

2. NPP/Suomi – The first National Polar-orbiting Partnership (NPP)/Suomi satellite was launched on 20 October 2011 as a first of US Joint Polar Satellite System (JPSS) series, formerly known as the National Polar-orbiting Operational Environmental Satellite System (NPOESS), which was meant to be a replacement for both the DMSP and POES satellite programs, shown in Figure 6.27 (Right). Main payloads of this satellite will include five key instruments, a Visible/Infrared Imager/Radiometer Suite (VIRRS), a Cross-track Infrared Sounder (C-tIS), an Advanced Technology Microwave Sounder (ATMS), an Ozone Mapping and Profiler Suite (OMPS) and Clouds and the Earth's Radiant Energy System (CERES). It provides PEO missions in the afternoon orbit for civil regional and global weather/climate requirements.

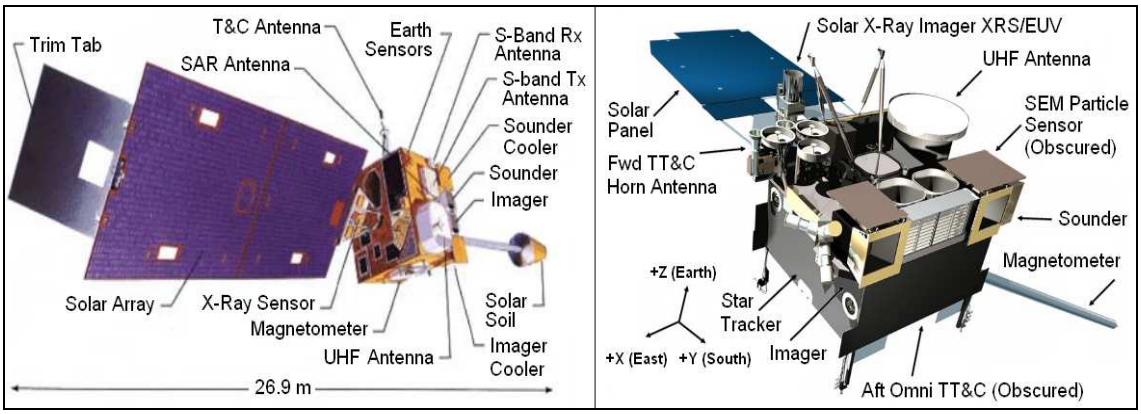

Figure 6. 28 NOAA GEO Meteorological Satellites GOES I-M and GOES N-P Series by NOAA 2004

6.7.1.2 NOAA GEO Meteorological Satellites of WIGOS

The United States also maintains geosynchronous weather satellites that orbit the equatorial plane of Earth at a speed matching Earth's rotation. This allows them to hover continuously over one position on the surface at an altitude of about 35,800 km above Earth. Thus, in the mid-1960s, the first successful experimental geosynchronous communications satellites of the Syncom project and the first series of three operational meteorological satellites (ESSA-1 to ESSA-3) were successfully launched. In the meantime, the series of ATS, SMS and GOES satellites were launched.

1. GOES I-M and M-P Series - The GOES 8-12 (GOES I-M) series were launched in the period between 1994 and 2001. This prototype is shown in Figure 6.28 (Left), while the prototype of modern series GOES N-P (GOES 13-15) is shown in Figure 6.28 (Right). The series of GOES 89 to 12 were successfully launched between 1994 to 2001. These two generations of satellites viewed Earth 100% of the time and took continuous images and soundings, and provide the Cospas-Sarsat GEOSAR service globally for maritime, land and aeronautical applications. The GOES-13 spacecraft was launched on 24 May 2006, representing the first of the next generation of GOES satellites. However, the GOES N-P spacecraft had an advanced attitude control system using star trackers, a spacecraft optical bench, and improved Imager and Sounder instruments for navigation and registration. Old

generations of GOES satellites have been a critical component of this ongoing weather monitoring program, aiding forecasters in achieving more precise and timely forecasts. The US operates two geostationary meteorological satellites, with one observing the East Coast and another observing the West Coast, thus achieving complete and overlapping national coverage. NOAA, with help from NASA, has established a continuous and long-term remote sensing capability for the nation based on a combination of polar and geostationary platforms. This service has proven useful in monitoring and predicting severe weather, such as tornadoes, tropical cyclones, and flash floods in the short-term and climate trends indicated by sea surface temperatures, biomass burning, and cloud cover in the longer term. Finally, this system continues to improve with new technological innovations and sensors, resulting in improved observations of the weather system to protect property, health, public safety, and development.

2. GOES R-U Series - For future geostationary satellites, new GOES-R is expected to be launched in 2016 with a mission design life until 2027. Therefore, it will have a tremendous improvement on current GOES capabilities by including a suite of advanced instruments to provide higher spectral, spatial and temporal information, then real-time mapping of total lightning activity, improved severe weather forecasting and solar monitoring capabilities.

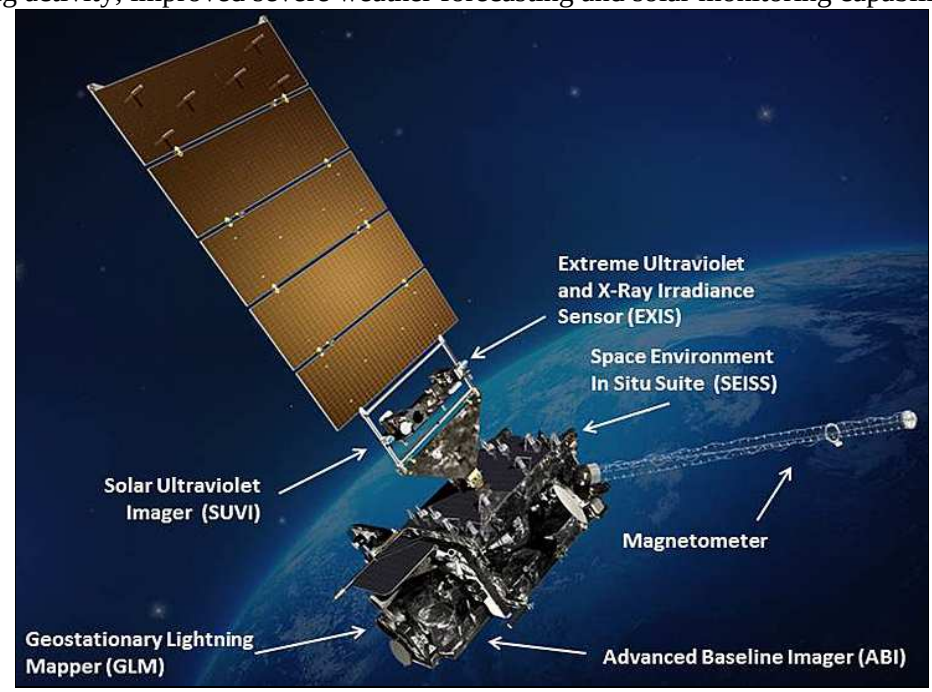

Figure 6. 29 Forthcoming NOAA GEO Meteorological Satellites GOES R-U by NOAA 2012

The GOES-R series of satellites will include GOES-R, S, T and U, This prototype is shown in Figure 6.29. This GOES will continue to be collaboratively developed and acquired jointly between NOAA and NASA. The next GOES-R series of satellites will extend the operation of the GOES satellite system over the next few decades. In addition, the GOES-R spacecraft bus will be 3-axis stabilized and designed for 10 years of on-orbit operation preceded by up to 5 years of on-orbit storage. It will provide near-continuous observations as well as vibration isolation for the Earth-pointed optical bench and high-speed spacecraft-to-instrument interfaces designed to maximize data collection. The cumulative time that GOES-R science data collection (including imaging) is interrupted by momentum management, station keeping and yaw flip maneuvers will be under 120 minutes/year. Thus, this represents a nearly two order of magnitude improvement compared to current GOES satellites.

The GOES-R Unique Payload Services (UPS) consist of transponder payloads that provide communications relay services in addition to primary mission data. The UPS suite consists of the Data Collection System (DCS), the High Rate Information Transmission/Emergency Managers Weather Information Network (HRIT/EMWIN), GOES-R Rebroadcast (GRB), and the Search and Rescue Satellite Aided Tracking (SARSAT) System.

The Emergency Managers Weather Information Network (EMWIN) is a direct service that provides users with weather forecasts, warnings, graphics and other information directly from the National Weather Service in near-real time. The GOES EMWIN relay service is one of a suite of methods to transmit these products to end users. The HRIT service provides broadcast of low-resolution GOES satellite imagery data and selected products to remotely located user HRIT terminals.

As an integral part of the international SAR satellite program called Cospas-Sarsat, NOAA operates the Search and Rescue Satellite Aided Tracking (SARSAT) System to detect and locate mariners, aviators and other recreational users in distress almost anywhere in the world at any time and under almost any conditions. This system uses a network of satellites to detect and locate distress signals from emergency beacons onboard vessels, vehicles, aircraft and from handheld personal locator beacons.

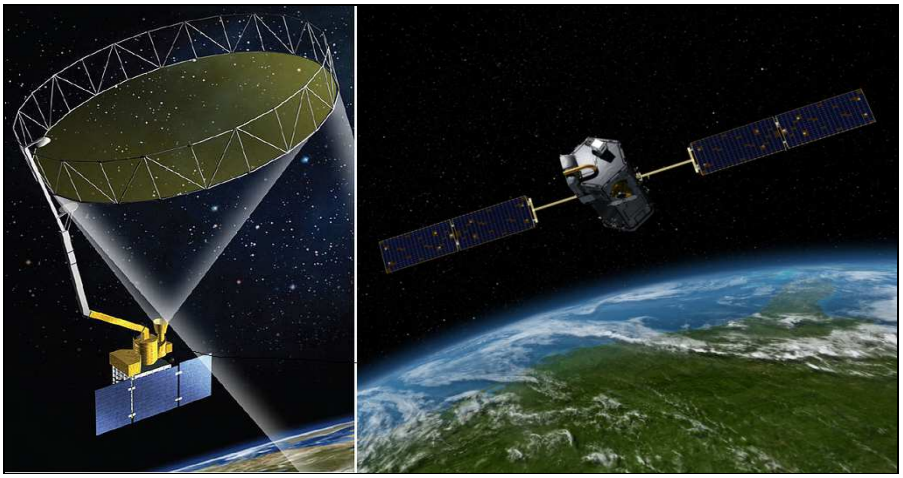

Figure 6. 30 Current NOAA LEO Meteorological Satellites SMAP and OCO-2 Series: by NOAA 2004

6.7.1.3 NOAA LEO Meteorological Satellites of R&D

The NOAA Low Earth (LEO) weather satellites are operated in a special polar orbit as a Sun synchronous orbit. In a sun synchronous orbit, the satellite passes over the same spot on Earth each day at the same time. The satellites are operated in pairs with one satellite making a morning pass and the other satellite making an afternoon pass. This pattern ensures that every spot on the Earth is observed by a NOAA weather satellite at least every six hours and typically every four hours. Figure 6.26 presents R&D Orbit as an LEO used by SMAP, OCO-2 and other similar satellites, while Figure 6.30 (Left) and Figure 6.30 (Right) illustrate image of both operational LEO meteorological satellites SMAP and OCO-2, respectively.

There are many other operational LEO meteorological satellites operated by single or group meteorological organization. This Satellite Status may be found in the list maintained by WMO on behalf of CGMS at: http://www.wmo.int/pages/prog/sat/satellitestatus.php.

6.7.2 Eumetsat Meteorological Satellites

Soon after, several individual successful experiments with meteorological satellites of some European countries became evident. Although Western European countries could invest in research and space-related activities, olely national projects would not be able to compete with the major superpowers. European involvement in meteorological satellite programs became possible with the founding of the European Space Research Organization (ESRO) in 1962, which, together with the European Launcher Development Organization (ELDO), became the precursor to the European Space Agency (ESA). ESA was founded in 1975 when the ELDO effort proved ineffective in developing a European launcher. It was thus decided that an integrated effort for research and development for Europe would likely be more successful, and, thus, the highly successful ESA was born.
Meteosat became the European meteorological program in GEO that was initiated in 1972 by the eight-nation ESRO. Throughout 1980, there were discussions about a suitable structure for managing operational satellite meteorology involving the heads of meteorological services across Europe. In March 1983, an intergovernmental conference held in Paris agreed to form the European Organization Eumetsat, which would assume financial responsibility for the Meteosat Operational Program (MOP) series of spacecraft, together with ground segment operations.

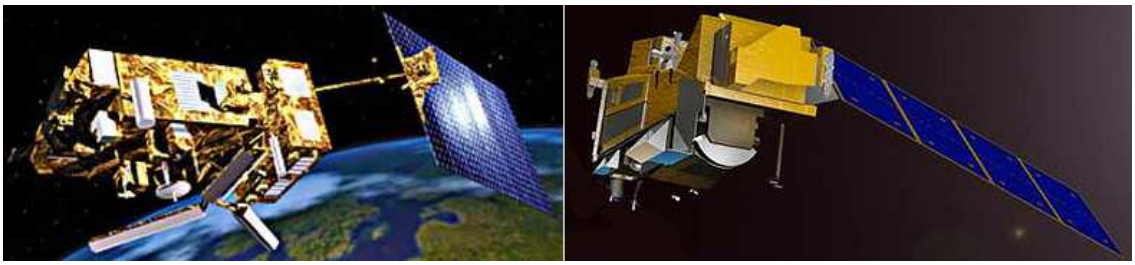

Figure 6. 31 Eumetsat PEO Meteorological Satellites MeTop A-B and MeTop C-SG Series by Eumetsat 2009

On 1 January 1987, responsibility for the operation of the Meteosat satellites was transferred from ESA to Eumetsat, which formally took over direct responsibility for the reception, processing, dissemination, and archiving of European meteorological satellite data. In May 1991, the decision was made that Eumetsat would establish its own independent ground segment to replace the system established by ESA in 1977. In 1995, Eumetsat implemented the Meteosat Transition Program (MTP), which was the first program fully developed under Eumetsat control, including provision and launch of additional satellites, development of a new ground system and handling routine operations. Thus, this covered the period from the phasing out of the MOP and to the start of the second-generation meteorological satellite program. On 15 November 1995, Eumetsat gained control of the Meteosat satellites in orbit, following 18 years of ESA operations.

6.7.2.1 EUMETSAT Sun-synchronous PEO Meteorological Satellites of WIGOS

After the growth of Europe's meteorological capacity and mastering of geostationary orbit, the need for a polar-orbiting system soon became apparent, in order to provide more detailed measurements of the atmosphere and improved observational coverage. In November 1998,

building upon the POES program, an agreement called the Initial Joint Polar System (IJPS) was established. The Eumetsat Polar System (EPS) is the European contribution to the IJPS. With a series of European and US Sun-synchronous polar-orbiting satellites, Europe's EPS system takes over the morning orbit service from the current series of NOAA satellites, while the NOAA 18-19 POES system continues to be responsible for the afternoon service.

The EPS program consists of the Meteorological Operational (MetOp) satellite program of Europe mission series of four polar-orbiting satellites. Figure 6.31 (Left) illustrates the prototype of two operational MetOp-A and -B, while Figure 6.31 (Right) illustrates the image of two projected MetOp-C and –SG series of PEO meteorological satellites, which are planed to be launched in 2016 and 2021, respectively.
The MetOp-A spacecraft was primarily designed to provide continuous, long-term datasets, in support of operational meteorological forecasting and global climate monitoring. This satellite series was also to provide enhanced monitoring capabilities to fulfill the additional requirements of studying Earth's climate system as expressed in a number of international cooperative programs, such as Global Climate Observing System (GCOS), International Geosphere and Biosphere Program (IGBP) and World Climate Research Program (WCRP). It is complementary to the NOAA POES system, the Eumetsat/ESA MSG system and the ESA Environment Satellite (ENVISAT) system.

The MetOp-A satellite was launched on 19 October 2006 as Europe's first polar orbiting satellite used for operational meteorology. Subsequently, satellite MetOp-B was launched on 17 September 2012. The satellites carry a payload comprising 11 scientific instruments and two of which support SAR services of SARSAT and Argos. In order to provide data continuity between MetOp and NOAA POES several instruments are carried on both fleets of satellites.

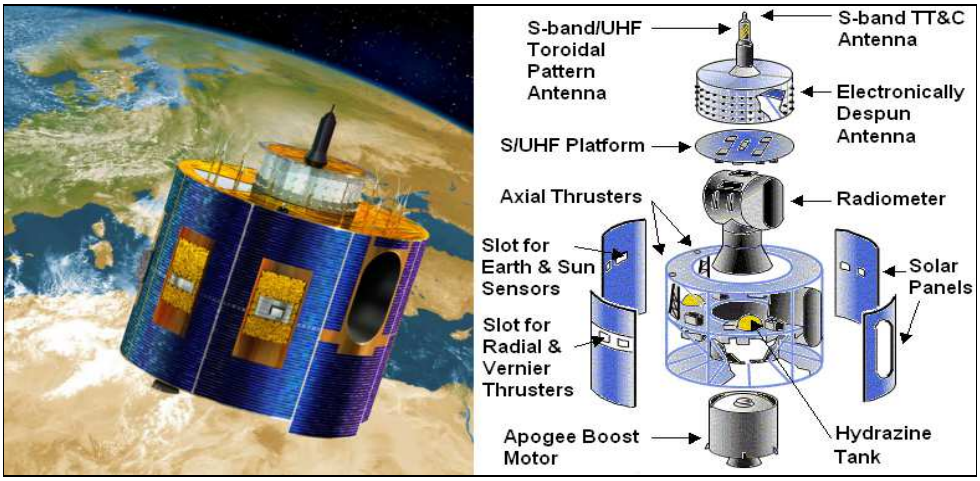

Figure 6. 32 Eumetsat GEO Meteorological Satellites MSG 1-4 Series by Eumetsat 2009

6.7.2.2 EUMETSAT GEO Meteorological Satellites of WIGOS

On 15 November 1995, Eumetsat gained control of the Meteosat satellites in orbit, following 18 years of ESA operations. Meteosat-7, the only satellite in this program, was launched on 2 September 1997, and had a similar design and capability to its six predecessors. The GEO Meteosat 1-7 satellites are often referred to as the first generation of Meteosat satellites. The next generation of Eumetsat GEO satellites are as follows:

1. Meteosat Second Generation (MSG) Satellites – This system was established in June 1994 with a first launch in 2002 and operational services in 2004, under cooperation between Eumetsat and ESA to ensure the continuity of GEO meteorological observations. The series of MSG 1-4 satellites except meteorological payloads they have onboard GEOSAR transponders. Figure 6.32 (Left) shows the MSG 1-4 series, and Figure 6.32 (Right) illustrates the main components of the same satellite. Provisions were made for the procurement of four geostationary meteorological satellites and provision for their launch and operation until 2020. Thus, the first of the second-generation missions began with the launch of MSG-1, later renamed to Meteosat-8, on 28August 2002. However, the primary objective of MSG is to ensure continuity of atmospheric and space observation from GEO satellites at 0° longitude and no equatorial inclination, as part of a worldwide, operational meteorological satellite system, consisting of four polar-orbiting and five geostationary satellites.

All MSG satellites are designed for the needs of now-casting applications and numerical weather prediction. The spacecraft body is cylindrical-shaped, 3.2 m in diameter and 2.4 m high. In order to maintain its pointing toward Earth, its sensors are constantly spinning in an anti-clockwise motion at 100 RPM in relation to its platform that spins at the exact same speed in the clockwise motion in GEO orbit at an altitude of 35,870 km. Primary payload instruments, include the Spinning Enhanced Visible and InfraRed Imager (SEVIRI) and the Geostationary Earth Radiation Budget (GERB) instruments, which support operational when compared to the first generation satellites.

The MSG satellite provides twelve imaging channels instead of three, a higher spatial and temporal resolution, as well as extra services, such as improved measurement instrument and communication services. They also provide more frequent and comprehensive data collection with a baseline repeat cycle of 15 min. The series of MSG satellites make up the Eumetsat flagship program and provide improved data downloads that contain almost twenty times as much information as that from the first generation of satellites (Eumetsat, 2009).

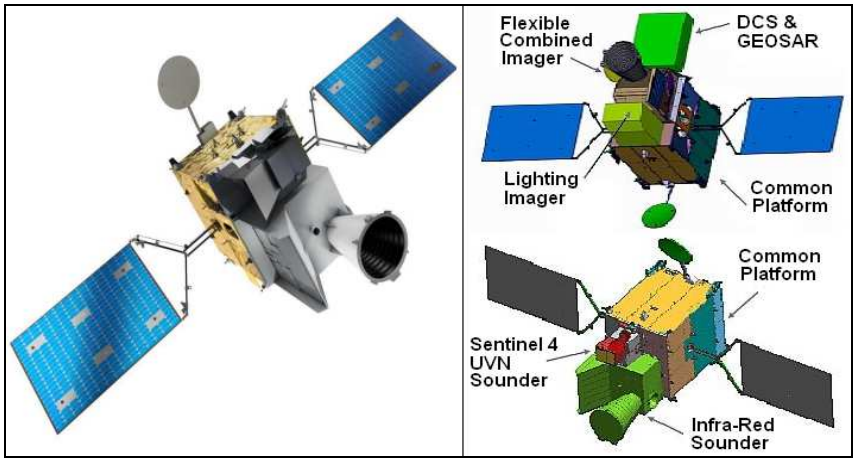

Figure 6. 33 Eumetsat GEO Meteorological Satellites MTG-I 1-2 Series by Eumetsat 2009

1. Meteosat Third Generation (MTG) Satellites – The first satellite of this series MTG-I-1 or Meteosat-12 is planned to be launched in 2019. This satellite prototype for all MTG-I 1-2 or Meteosat 12-17 is presented in Figure 6.33 (Left), while Figure 6.33 (Right) presents in two projections all main components of the same series of MTG satellites. Thus, MTG-I 1-2

and MTG-S 1-2 except meteorological payloads they have onboard Sentinel 4A and 4B transponders.
The MTG series will comprise of six satellites, from which four will provide an enhanced imaging system, along with the development of expanded ground segment and satellite operations. The MTG-I satellite will carry the Flexible Combined Imager (FCI) and an imaging lightning detection instrument called the Lightning Imager (LI). Two sounding satellite platforms (MTG-S) will carry an interferometer called the Infra-red Sounder (IRS), and the Ultraviolet Visible Near-infrared (UVN) sounder among other instruments. The platform will be a three-axes body stabilized with instruments pointing at Earth for 100 % of their orbit time. The addition of a second sounding satellite platform is a key innovation of the new MTG program. This capability will enable not just imaging of weather systems but also the ability to profile the atmosphere layers and to perform chemical composition studies.

6.7.3 Roshydromet Meteorological Satellites

The history of the Russian satellite program can be traced back to the world's first ever successfully launched artificial satellite Sputnik-1, which is illustrated in Figure 6.34. Then, during the Cold War, maintaining up-to-date information about weather conditions was necessary for supporting military strategic planning.

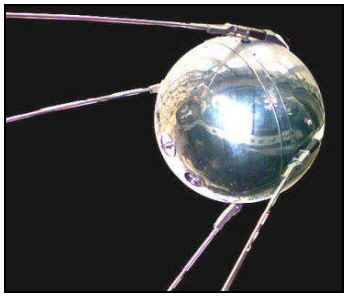

Figure 6. 34 Soviet Sputnik-1 by Ilcev 2005

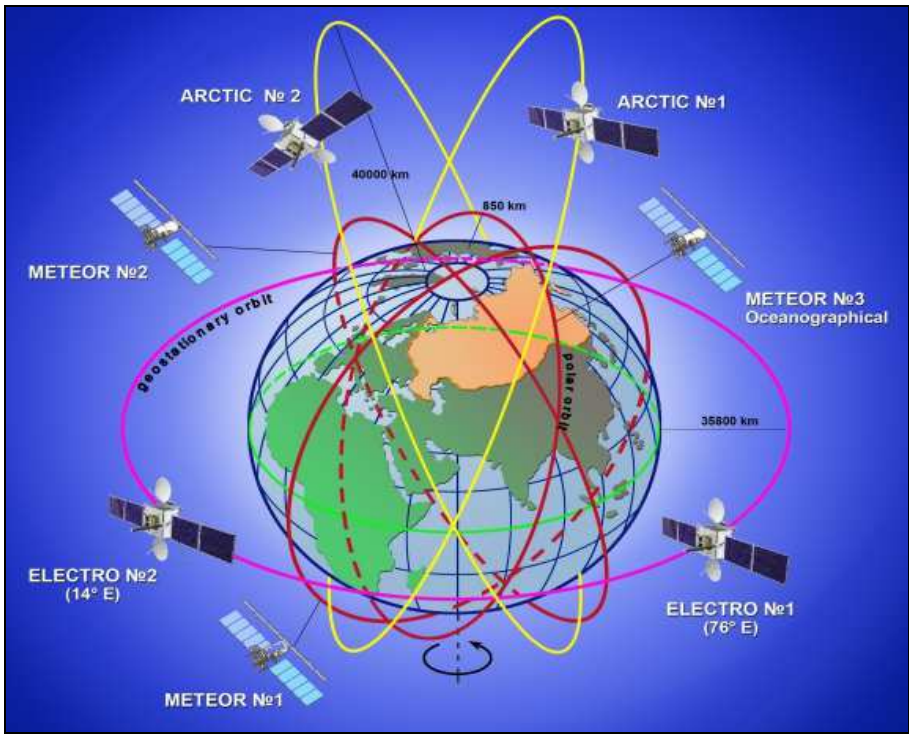

Figure 6. 35 Russian Constellation by Roshydromet 2009

On 30 October 1961, the Soviet government issued a decree ordering the development of an experimental meteorological network known as the Meteor satellite series, which became the nation's first operational polar-orbiting satellites for environmental and weather monitoring In the meantime, were developed four meteorological satellite constellations, such as PEO, GEO and HEO, illustrated in Figure 6.35, while LEO constellation was developed recently.

As stated earlier, today, within the Russian Federation and its main agency Roscosmos, the sponsoring agency of the meteorological program is Roshydromet organization. This entity is the national central agency that provides relevant environmental and climate information to the public, various industrial organizations and decision-making bodies. It is a service in the Ministry of Natural Resources and Environment and it oversees public services related to meteorological and other geophysical processes. The Meteor satellite series began in 1969 and was designed and developed by the All-Russian Scientific and Research Institute of Electro-mechanics (VNIIEM) of Moscow.

Prior to the Russian meteorological program, experimental scientific satellites were launched with the Kosmos series. The designation Kosmos is a generic name given to a large number of Soviet Union and, subsequently, Russian satellites, the first of which was launched in 1962. As of 2013, Russia has launched more than 2,485 Kosmos satellites with some Sputnik and Meteor satellites also given the Kosmos designation. The first experimental orbiting meteorological satellite was Kosmos-44 launched on August 28, 1964. It was the first in a series of prototype weather satellites used mainly to test basic spacecraft hardware, including a three-axis attitude control system, cremnium-based solar panels, and thermal protection systems. Kosmos-44 transmitted the first TV images of cloud cover.

A series of nine analogous Kosmos experimental satellites were launched from 1965 to 1969. These meteorological satellites served as test vehicles to develop and improve prototypes of

TV and Infrared (IR) cloud cameras and actinometrical instruments. Besides, the subsequent launches of Kosmos-122, Kosmos-144, and Kosmos-156 formed the first Soviet Union experimental weather-forecasting network.

Interim experimental weather satellite instrumentation included two vidicon cameras for daytime monitoring, a high-resolution visible and infrared radiometer for day and night imaging, as well as an array of narrow- and wide-angle radiometers. However, these radiometers were used to measure the intensity of radiation reflected from the clouds and oceans, the surface temperatures of Earth and cloud tops and the flux of thermal energy from the Earth-atmosphere system into space. Assembly and testing of satellites continued to take place at VNIIEM, while analogous Kosmos satellites were launched until 1968, when the succeeding series was officially named Meteor-1 in 1969.

Modern Russian program of Earth Observation Satellites provides the following satellite meteorological constellations: PEO, GEO, HEO and LEO.

6.7.3.1 Roshydromet Sun-synchronous PEO Meteorological Satellites of WIGOS

Originally developed in the 1960s, the Meteor PEO satellite series was designed to monitor atmospheric and sea-surface temperatures, humidity, radiation, sea ice conditions, snow cover and cloud patterns. The designations of the series Meteor-1, -2, and -3 define different payload configurations, improved spacecraft platforms and different orbits. In total, the Meteor-1 program launched 42 satellites into PEO between 1964 and 1981. The satellites were designed to last for 6 months and frequently replaced. This resulted in an average of 3.4 launches per year for these satellites. On-board sensors consisted of the television-type optical instrument, TV infrared instrument, and a radiation budget sensor. Somewhat similar to the NOAA-TIROS series, the Meteor series provided a daily weather review for more than two-thirds of the globe, observation of cloud patterns, ice cover, and atmospheric radiation.
Meteor 1-1 was the first operational weather satellite of the Meteor series launched on 3 March 1969, with a main mission of cloud observation. This satellite had a mass of 1,300 kg with a length of 5 m and diameter of 2.5 m and was placed at an orbital altitude of 560 km with two large solar panels attached to the sides, as illustrated in Figure 6.14 (Left). The satellite carried two vidicon cameras for daytime photography, a scanning high-resolution infrared radiometer for day and night photography and an actinometric instrument for measuring Earth's radiation field. Accordingly, data were transmitted directly to ground receiving stations and analyzed by the Hydrometeorological Center in Moscow.

The successors of Meteor 1-1 satellites include the Meteor-Priroda, Meteor-2, Meteor-3 and Meteor-3M. The second generation Meteor-2 series comprised of 21 operational satellites launched in July 1975 over a period of 8 years until 1993 with improved design and performance compared to Meteor-1. Operational design lifetime was planned to be extended from 6 months to 1 year with direct data transmission to receiving ground stations.

Both Meteor-1 and –2 series were launched into non-Sun-synchronous polar orbit with an inclination of 81 to 82°. Thus, the main improvement represented by the Meteor-2 was the introduction of infrared temperature/humidity sounding radiometric sensors that were able to build global vertical temperature maps. The satellite instrument package contained three TV visual/infrared scanners, a five-channel scanning radiometer, and a Radiation Measurement Complex (RMC) device for measuring radiation flux densities in near-Earth space. In fact, the Meteor system provided fast-reaction weather forecasting and was able to distinguish

characteristics of ice cover even in the Arctic Ocean, which proved to be useful for ship navigation and military planning.

At the beginning of the 1970s, gradual demilitarization of the Meteor-Priroda program (Meteor-P) had begun with the goal of orienting space technologies towards civilian remote sensing purposes. The Meteor-P series consisted of six satellites intended to demonstrate new instrumentation, mainly for multispectral land observation. These 5 satellites were actively spin-stabilized over three axes with a design lifetime extended to 2 years of operation.

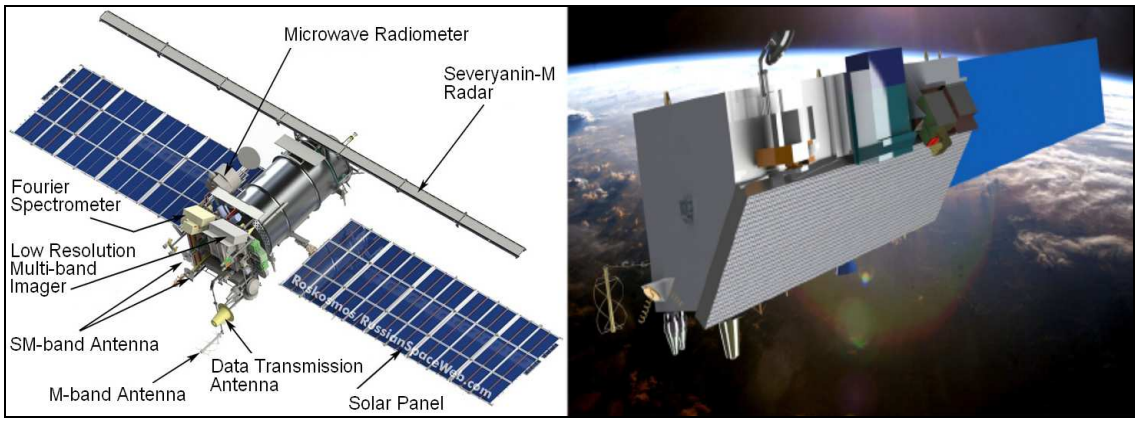

Figure 6. 36 Russian PEO Satellite Meteor-M1 and Meteor-MP1 by Roshydromet 2009

The third generation of seven Meteor-3 satellites series started with launching Meteor-3 (1a) on 27 November 1984, Meteor-3-1 on 24 October 1975 and last Meteor-3-6 on 25.01.1994. Measuring 1.4 m by 4.2 m in dimension, the satellites had a three-axis stabilization attitude control system enabling orientation accuracy to be up to 0.5°. The satellites were equipped with sophisticated instrumentation with multiple remote sensing instruments in addition to the weather-forecasting payloads. Since the satellites were placed into a higher altitude than the previous series, an extension of the instrument swath width with complete coverage of Earth's surface was achieved. The last two satellites of the series hosted foreign instruments for ozone and Earth radiation budget observations. For example, the Meteor-3-5/ TOMS-2 satellite was launched on 15 August 1991 carrying the Total Ozone Mapping Spectrometer (TOMS), as the first and last US-built instrument to fly on a Soviet spacecraft.

The follow-up Meteor-3M satellite program only involved one Meteor-3M-1 satellite, which was launched on 10 December 2001, significantly delayed by financial problems. Thus, it featured sensor improvements, such as a 1.4 km resolution visible channel and a ten-channel radiometer with 3 km resolution. This satellite was also in Sun-synchronous orbit and included experiments, such as a Stratospheric Aerosol and Gas Experiment (SAGE III) payload designed to measure vertical profiles of aerosol, ozone, and other constituents of the atmosphere. It also carried a set of multi-spectral scanning sensors and other instruments designed to measure temperature and humidity profiles, clouds, surface properties, and high energy particles in the upper atmosphere.

The Meteor-M series represents follow-on to the polar-orbiting meteorological mission to Meteor-3M. These satellites are designed as the next generation of Russian meteorological satellites. Meteor-M1 was launched on 17 September 2009, with six instruments, including imagers, sounders and a radar imaging system carried on-board, which is shown in Figure 6.36 (Left). It is capable of gathering multispectral imagery in the visible range, as well as

radar imagery of Earth's surface and to perform surveillance of Earth surface features and atmospheric conditions. On 8 July 2014, Meteor-M2 was launched and in two years Meteor-M3 satellite will be launched, and will be equipped with new-generation phased antenna radar for ocean monitoring. Russian space officials have planned to orbit as many as two Meteor-M satellites by 2017 and to begin launching a new-generation Meteor-MP satellite series beginning in 2016. This prototype is shown in Figure 6.36 (Right). The primary mission of Meteor-M is similar to those for NOAA/ NPOESS and EPS/MetOp series.

According to the Federal Space Program, the development of new Meteor-MP constellation has been started in 2011. The spacecraft mass is 3300 kg and deployed size 21,5×3,2×4,4 m will consist of meteorological and oceanographic satellites. Meteor-MP payload will be basically similar to Meteor-M series payload, but with improved instrument performance.

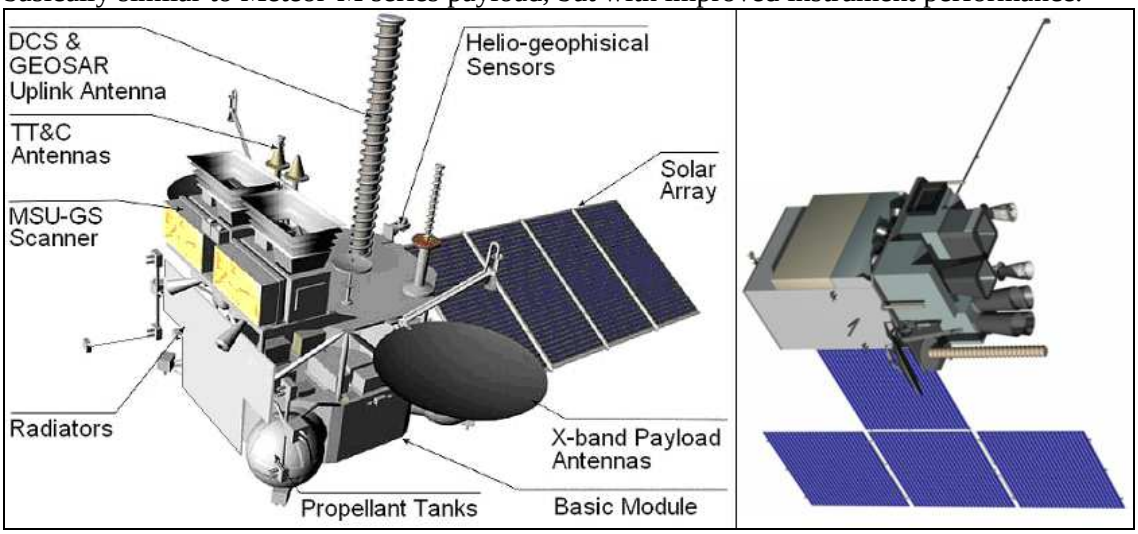

Figure 6. 37 Russian GEO Satellite Electro-L 1-2 and Electro-M 1-2 by Roshydromet 2009

6.7.3.2 Roshydromet GEO Meteorological Satellites of WIGOS

In addition to PEO meteorological satellites, Russia develops and operates GEO spacecraft to monitor Earth and the space environment. Thus, Geostationary Operational Meteorological Satellite-1 (GOMS-1), also referred to as Electro-1, represents Russia's first series of operational meteorological satellites in GEO orbit, and has also led Russia to join the international geostationary weather-monitoring group. The program began in 1994 and was developed by Roscosmos and operated by Roshydromet. The spacecraft and instruments were developed by VNIIEM as the prime contractor.

The primary objectives of the GOMS-1 spacecraft were to acquire in real-time television images of Earth's surface and cloud cover in the visible and infrared regions of the spectrum, to measure the radiation levels and magnetic field of the space environment and to measure vertical temperature profiles and cloud cover. Payload instruments included a radiation measurement system and scanning TV radiometer. The communications system obtained and retransmitted information via Russian and international Data Collection Platforms (DCP), which were then exchanged among ground stations to the user community. The GOMS-1 spacecraft was launched on 31 October 1994, but experienced initial problems with attitude control and never became fully operational. Limited operational capability was recovered in 1996, although visible imagery could not broadcast due to technical issues with the sensors.

Electro-L 1-3 is a new generation GEO meteorological mission developed by Roshydromet, Roscosmos and the Scientific Research Center of Space Hydrometeorology "Planeta". The launch of Electro-L1 on 1 January 2011 became a substantial contribution to Russian weather forecasts, which is shown in Figure 6.37 (Left). Electro-L2 and L3 have to be launched in 2016/17, so all three GEO satellites have to provide a new wide variety of data for weather analysis and forecasting on both a global and regional scale. The primary objectives of Electro-L are to provide multispectral imagery of the global and regional atmosphere in both visible and infrared frequencies, and to collect heliospheric, ionospheric, and magnetospheric data, as well as providing data for climate change and ocean monitoring. Data collection services were provided from self-timed DCP to the ground segment. The main instrumental payload is an optical imaging radiometer, which provides image data in three visible and near-infrared channels and in seven infrared channels. Thus, unlike NASA/NOAA GOES satellites, Electro-L captures images in the infrared, as well as the visible near infrared spectrum, providing valuable information about cloud movement and vegetation cover.

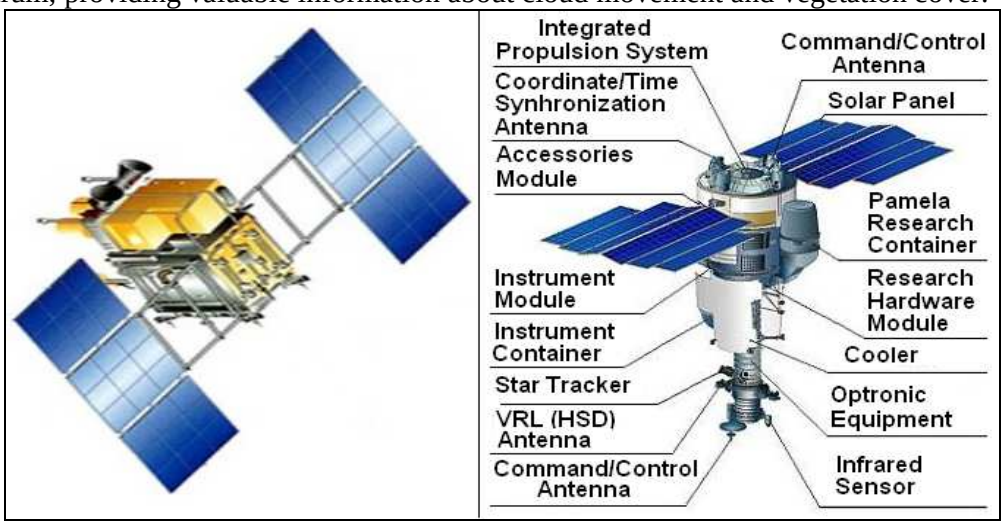

Figure 6. 38 Russian LEO Satellite Kanopus-V 1-2 and Resurs-P 1-2 by Roshydromet 2009

The design life of Electro-L satellites is expected to be 10 years with a replacement policy based on launching satellites at roughly five-year intervals. Future generations of Russian GEO weather satellites include Electro-M1 and M3 series, which is shown in Figure 6.36 (Right). Both will contribute to Russia's goal to strengthen its weather satellite network and provide accurate weather analysis and forecasting both for its territory and worldwide.

6.7.3.3 Roshydromet LEO Meteorological Satellites of R&D

The Russian space agency Roscosmos together with Roshydromet started with new projects of small LEO observation satellite carrying onboard a wide range of imaging and other special sensors to represent a unique feature for a remote-sensing satellite. Moreover, a joint operation of already developed Kanopus-V and Resurs-P satellites could provide unmatched capabilities in the imaging of the Earth's surface. All data acquired by LEO satellites, processed and distributed by the Research Center for Earth Operative Monitoring (NTs OMZ) in Moscow.

Kanopus-V1 (Vulcan) – This is an Earth observation mini satellite mission of Roscosmos and Roshydromet/Planeta which was launched on 22 July 2012, and which is shown in Figure 6.38 (Left). The second in Vulcan series is Kanopus-V2 launched on 27 December

2014. The overall objective of both satellites is to monitor Earth's surface with highly operational observation of specified regions, land, forestry, agriculture, water and coastal resources; atmosphere, ionosphere and magnetosphere to detect and study the probability of strong earthquake occurrence; man-made and natural emergencies including natural disasters and hydrometeorological phenomena; including mapping, detection of forest fire seats, and large environmental pollutant emissions.

2. Resurs-P2 – This new LEO special program is a Russian commercial Earth observation satellite capable of acquiring high-resolution imagery up to 1.0 m, which is shown in Figure 6.38 (Right). In fact, the spacecraft was launched on 26 December 2014, and will be operated by Roscosmos along with the Resurs-P1 satellite launched in 2013. The satellite is designed for multi-spectral remote sensing of the Earth's surface aimed at acquiring high-quality visible images in near real-time as well as on-line data delivery via radio link and providing a wide range of consumers with value-added processed data. Additionally, the satellite carries the Nuklon high-energy particle detector developed by the Moscow Sate University for detecting cosmic radiation.

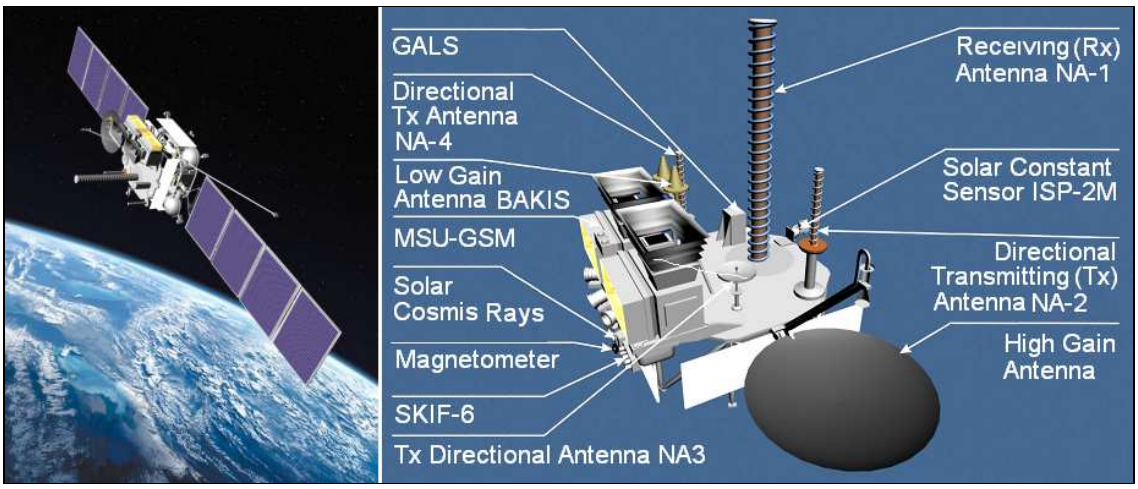

Figure 6. 39 Russian HEO Arctica-M (1-2) Satellite and Payload by Roshydromet 2009

6.7.3.4 Roshydromet HEO Meteorological Satellites of R&D

Russia is developing a unique HEO satellite network dedicated to monitoring of the Arctic. With her territory stretching thousands of kilometers along the Arctic Ocean, Russia faces many challenges when trying to balance the economic development and the environmental protection of her vast northern regions. In particular, traditional communications and weather forecasting satellites "hanging" over the Equator are ill suited for serving high-latitude areas of the globe. To focus latest space capabilities on this crucial, yet hard-to-reach region, Russian engineers proposed a multi-purpose constellation dubbed Arctica (Arktika), which will consist of two satellites in HEO known as Molniya.

The Arctica network will be employed to perform a variety of remote-sensing tasks, such as monitoring of environmental conditions, and also provide reliable communications and navigation across this inhospitable but economically crucial region. Figure 6.39 (Left) shows the HEO satellite Arctica-M1 and Figure 6.39 (Right) illustrates the components of Artica-M1 payload, which has to be launched in 2017. Arctica-M2 satellite is a planet for launching in 2019, and, in the meantime, the next generation of two HEO satellite constellations Arctica-MS and Arctica-R will be developed.

6.7.4 CMA Meteorological Satellites

China's meteorological satellite program is called Feng-Yun (FY), meaning wind and cloud, which consists of both polar-orbiting and geostationary series. The China Meteorological Administration's (CMA) National Satellite Meteorological Center (NSMC) was founded in 1971 and is tasked with the responsibility of satellite operations and developing the ground segment. It is authorized to develop and operate the national satellite meteorological service for addressing weather and climate issues. Its main responsibilities include developing and operating the Chinese meteorological satellite system, providing an information service to disseminate satellite data for climate prediction, forecasts, and warning, and implementing satellite engineering project contracts.
The CMA contracts the China Aerospace Science and Technology Corporation (CASC) to develop, design and launch the Feng-Yun satellites, while the NSMC maintains overall system operations. The funding body in China is the Ministry of Aerospace. FY-odd numbers (FY-1, FY-3, etc.) are applied to generations of PEO satellites, whereas FY-even numbers (FY-2, FY-4, etc.) refer to the geostationary series.

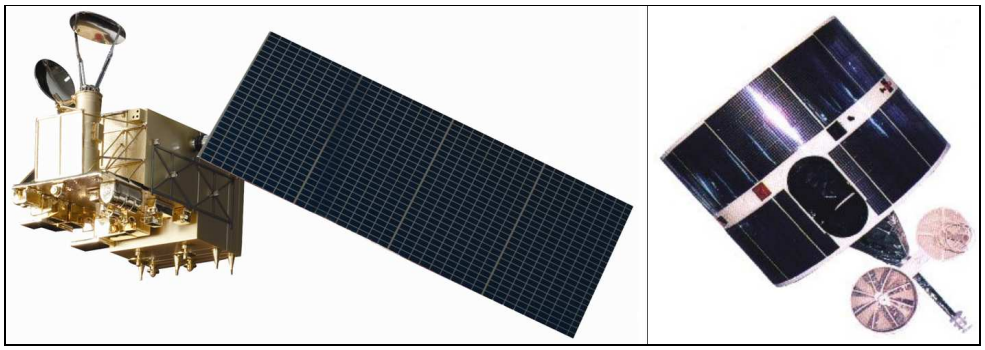

Figure 6. 40 Chinese Feng Yun PEO (FY-3) and GEO (FY-2) Meteorological Satellites by WMO, 2013

The Feng-Yun satellites have played important roles in oceanography, agriculture, forestry, hydrology, aviation, navigation, environmental protection, and national defense, in order to fulfill the public service and information needs of Chinese society and national economy. The main objectives of the Feng-Yun program are to establish a comprehensive operational meteorological satellite system with the combination of PEO and GEO constellations, as well as a ground monitoring and data sharing system.

6.7.4.1 CMA Sun-synchronous PEO Meteorological Satellites

China's PEO meteorological satellite program began with the first-generation FY-1 series that were built by the Shanghai Institute of Satellite Engineering. They were three-axis stabilized and powered by two solar arrays. The first FY-1A PEO satellite was successfully launched into Sun-synchronous orbit on 7 September 1988, FY-1B on 3 September 1990, FY-1C on 10 May 1999 and the last series FY-1D on 15 May 2002. The primary payload contains a Multichannel Visible Infrared Scanning Radiometer (MVISR) for multi-purposes imagery and a Space Environment Monitor (SEM) for space weather observations. This instrumentation enabled the satellites to acquire global visible and infrared cloud imagery for weather forecasting. Although the two satellites suffered from some malfunctions, they nevertheless laid a solid foundation for the next generation of operational PEO satellites.

With the experience from the first experimental FY-1 satellites, the last three operational satellites FY-3A (launched on 27 May 2008), FY-3B (launched on 4 November 2010) and

FY-3C (launched on 23 September 2013) represented upgraded versions, which are shown in Figure 6.40 (Left). These satellites had significant improvements of imaging instruments, including the MVISR that now had ten channels. Thus, the advanced design enabled more powerful observations of clouds, land, and ocean. Examples of application areas of the observation data included the monitoring of drought, snow cover, floods, forest and grassland fires, dust storms, and sea ice.

6.7.4.2 CMA GEO Meteorological Satellites

The Chinese GEO meteorological program was initiated in the 1980s with the development of the FengYun2 (FY-2) satellite series by the NSMC and operated by the CMA. Its design involved dual spin-stabilized geostationary spacecraft with rotation velocity of 100 rpm. The first experimental GEO meteorological satellite FY-2A was successfully launched on 10 June 1997. This satellite is shown in Figure 6.40 (Right). Besides, the follow-up experimental satellites FY-2B, FY-2C, FY-2D, FY-2E, FY-2F and FY-2G were launched on 31 December 2014. The last FY-2 series FY-2H and next generation FY-4A have to be launched in 2017, while the launching of FY-4B is planned in 2018 and FY-4C in 2020.

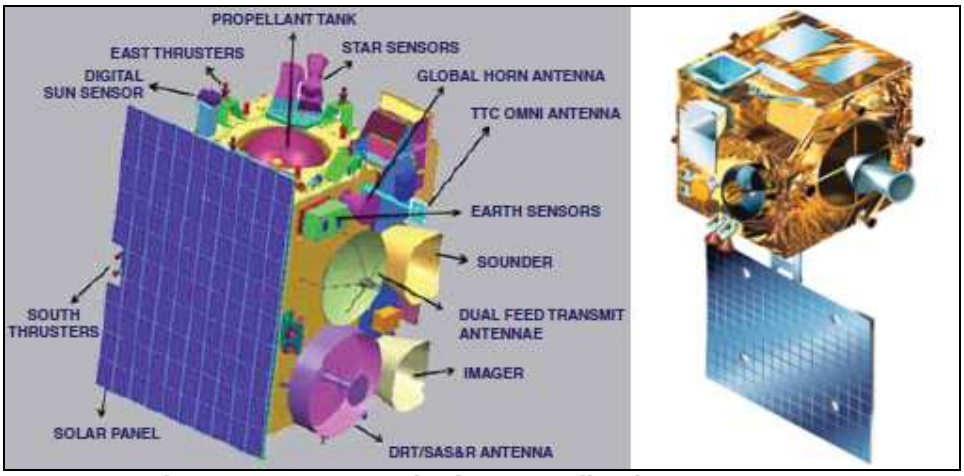

Figure 6. 41 Indian GEO INSAT-3D and Kalpana-1 Satellites by ISRO 2014

The main satellite payload FY-2 series was the Stretched Visible and Infrared Spin-Scan Radiometer (S-VISSR), which is an opto-mechanical system with different image scanning modes. This satellite was capable of cloud imagery of five spectral channels (one visible and four infrared). This improved the satellite's capability for detecting and calculating water vapour contents, temperature resolution data and ice cloud detection and sea temperature estimation. These satellites were able to capture hourly visible, infrared and water vapour disk images of Earth's surface, including several subsystems for data circulation, command and data acquisition, data transmission, weather facsimile and data collection service. In addition, the new generation of these satellites can also generate daily image data and products used for environmental monitoring and weather forecasting services. Derived products include the atmospheric motion vector, sea surface temperature, and surface albedo.

6.7.5 ISRO Meteorological Satellites

India has developed its own satellite series of meteorological and environmental observation in both GEO and LEO/PEO orbits since the1970s. The Indian Space Research Organization (ISRO) was established in 1969 as the primary space agency of the Indian government with

the primary objective of advancing space technology and its applications for national benefit. It is responsible for the development and operations of all types of Indian satellites and instruments, while satellite meteorological data are processed and disseminated by the India Meteorological Department (IMD) as the principal agency responsible for meteorological observations, weather forecasting, and seismology.

6.7.5.1 ISRO GEO Meteorological Satellites

The INSAT (Indian National Satellite) system of the ISRO is the first multipurpose GEO satellite system that was developed not only for meteorological applications but also for telecommunications, television broadcasting, and search and rescue services. The INSAT series of 1A, 1B, 1C and 1D began with the launch of INSAT-1A on 10 April 1982 and the next generation of INSAT series 2A, 2B and 2E started with the launch of INSAT-2A on 9 July 1992. The newest generation of INSAT series 3A (launched on 9 April 2003), 3C (on 23 January 2002 and last series INSAT 3D was launched on 25 July 2013, which is shown in Figure 6.41 (Left). To date, meteorological, telecommunication and television services were frequently designed for combined INSAT payloads. However, advantages of developing separate satellite payloads exclusively dedicated to meteorology were recognized.

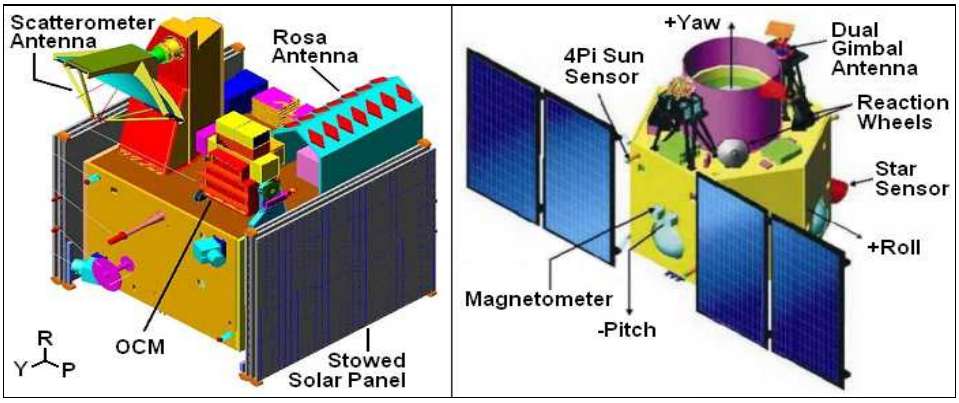

Figure 6. 42 Indian LEO Oceansat-2 and Cartosat-2 Satellites by ISRO 2014

MetSat-1, as shown in Figure 6.41 (Right), is India's first dedicated meteorological satellite launched by ISRO using a Polar Satellite Launch Vehicle (PSLV) into geostationary orbit on 12 September 2002. However, it was later renamed to Kalpana-1 in honor of Dr. Kalpana Chawla, an Indian-born NASA astronaut who had died in the US Space Shuttle Columbia disaster. Kalpana-1 was considered to be a cost-effective solution for providing meteorological payloads and services from geostationary orbit. In fact, this satellite served to set the policy for future INSAT missions to be configured separately for meteorological and communication payloads.

6.7.5.2 ISRO PEO and LEO Meteorological Satellites

Complementing GEO meteorological satellites, India has also developed a long series of sun synchronous PEO and LEO satellites beginning with the Indian Remote Sensing (IRS) system. This series started in the mid-1980s. The first generation satellites IRS-1A and -1B were launched successfully during 1988 and 1991 to provide Earth observation services for India. The initial program of Earth observation imaging was extended to other environmental applications with the addition of payload sensors and instruments. Then, a second-generation IRS-1C was launched in 1995, and a similar IRS-P3 in 1996. These satellites carried imaging

instruments to measure in four spectral channels, mainly in the visible and near infrared, such as the Multispectral Opto-electronic Scanner (MOS).

The next generation of IRS-P4 or Oceansat-1 was launched on 26 May 1999, and this satellite is dedicated exclusively to ocean monitoring. It was envisaged to provide service continuity for the operational users of Ocean Color Monitor (OCM) data global weather forecasting. The OCM payload is a solid-state camera designed to operate in eight narrow spectral bands. The camera is used to collect data on chlorophyll concentration, phytoplankton blooms, atmospheric aerosols, and particulate matter. A second payload is a Multi-channel Scanning Microwave Radiometer (MSMR) for collecting data on sea surface temperature, wind speed, cloud water content, and water vapour content in the atmosphere above the ocean. OceanSat-1 completed its mission after serving for 11 years. Oceansat-2 was designed to provide follow-on services for Oceansat-1 with enhanced application potential for studying surface winds, ocean surface strata, chlorophyll concentration, phytoplankton blooms, atmospheric aerosols and suspended sediments in water. This satellite was launched on an Indian PSLV rocket on 23 September 2009, into a Sun-synchronous orbit, which is shown in Figure 6.42 (Left).

The new generation ISRO Cartosat-2 LEO satellite was launched on 10 January 2007, which is shown in Figure 6.42 (Right). Follow up missions are Cartosat-2A (launched on 28 April 2008) and Cartosat-2B (launched on 12 July 2010). The objective is to provide high resolution imagery (1 m, with an event monitoring capability) from a highly agile spacecraft.

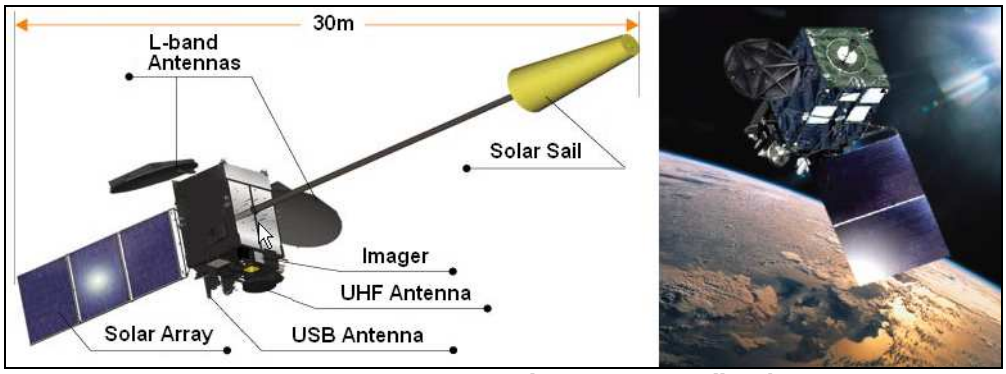

Figure 6. 43 Japanese GEO MTSAT-2 and Himawari-8 Satellites by JMA 2014

6.7.6 JMA GEO Meteorological Satellites

The Japan Meteorological Agency (JMA) is responsible for collecting and reporting weather data and forecasts in Japan, as well as observation and warning of natural hazards, such as earthquakes, tsunamis and volcanic eruptions. It has been operating employing GEO meteorological satellites since 1977, which have provided weather data for the prevention and mitigation of weather-related disasters, especially for monitoring typhoons and other weather conditions in the Asia-Oceania region.

The Japanese Geostationary Meteorological Satellite (GMS) series, which is also known as “Himawari” (“sunflower”), was the first national satellite program of Japan for weather and environmental observations in geostationary orbit. It was operated by the JMA with the Japan Aerospace Exploration Agency (JAXA - formerly NASDA) as the spacecraft and launch service provider. The operational meteorological program consisted of five satellites in total, beginning with the launch of GMS-1 on 14 July 14 1977, from a NASA Delta rocket from

Cape Canaveral. The GMS spacecraft were spin-stabilized in geostationary orbit at a nominal position of 140°E longitude and with a design lifetime of 5 years. Mission objectives were to provide weather watch capabilities by a two-channel Visible-Infrared Spin Scan Radiometer (VISSR), collection of meteorological data from Data Collection Platforms (DCP), direct broadcast of cloud images, and monitoring of solar particles with a SEM.
With a design life of 5 years, GMS-5 was due to be replaced by a successor program called MTSAT (Multifunction Transport Satellite) in November 1999. The series was procured by the Japan Civil Aviation Bureau (JCAB) to provide Augmentation GNSS program and JMA, while being funded by the Japanese Ministry of Land, Infrastructure and Transport (MLIT).
However, due to launch failure, the MTSAT-1 satellite was destroyed and left Japan without weather satellite imagery. Thus, the replacement spacecraft, MTSAT-1R (Himawari-6) was launched on 26 February 2005 with meteorological service operations switched over from GOES-9 to MTSAT-1R on 8 June 2005. MTSAT-1R performs full disk observations every 30 min with imaging channels consisting of a visible band and four infrared bands. Routine products of MTSAT included an hourly atmospheric motion vector, clear sky radiance, cloud grid information, sea surface temperature, aerosol optical thickness and snow/ice index and this satellite also carried onboard GNSS transponder for augmentation of GPS signals (JMA, 2014).

MTSAT-2 (Himawari-7) was launched on 18 February 2006 into GEO and on 1 July 2010, MTSAT-2, as shown in Figure 6.43 (Left), became operational for meteorological services, while MTSAT-1R is being kept on standby. Thus, MTSAT-2 has the same imaging channels as MTSAT-1R and provides similar imagery. The upcoming Hinawari-8, as shown in Figure 6.43 (Right) was launched on 7 October 2014, and Himawari-9 satellites are being prepared for launch in 2016 to sustain and improve continuous satellite observations for the purposes of disaster prevention, weather forecasting and now-casting.

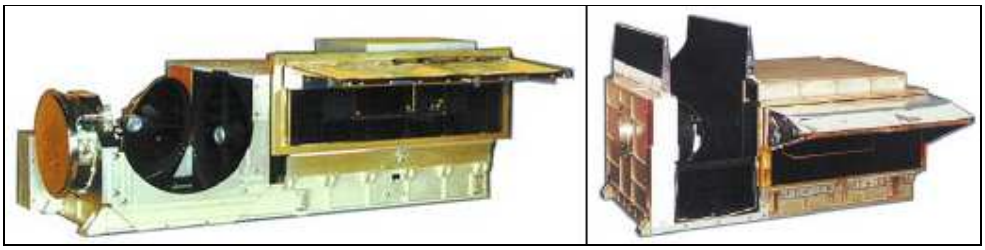

Figure 6. 44 AVHRR and HRIRS Instruments by NOAA 2009

6.8 Meteorological Satellite Instrumentation

The main components of meteorological satellites are different instrumentations, with which the basic radiometric observation and measurements are made. This instrumentation is today upgraded onboard current meteorological satellites, which are sources of weather data that different consumers will most likely use. The next context will introduce some of major operational instrumentation on current and future meteorological satellites. The most important issue in satellite weather observation and imaginary is to provide archive or location where satellite data are stored and processed.

6.8.1 Meteorological Instrumentation onboard PEO Satellites

All meteorological PEO satellites are equipped onboard with different imager and sounding instruments, which are helping for gathering meteorological data and images by the ground Earth receiving stations. All instruments and transponders are situated in the satellite bus.

6.8.1.1 Advanced Very High Resolution Radiometer (AVHRR)

The AVHRR onboard satellite instrument is an across track scanning radiometer that senses the Earth's outgoing radiation from horizon to horizon in six channels (three solar channels in the visible-near infrared region and three thermal infrared channels), with a spatial resolution of 1 km at nadir. This means that it makes calibrated measurements of upwelling radiation from small areas (scan spots or pixels) that are scanned across the subsatellite track, as shown in Figure 6.44 (Left). Images or pictures are constructed by displaying successive scan lines on photographic film or on a computer display. The operation of the AVHRR is representative of many scanning radiometers onboard different PEO/LEO satellites. The AVHRR, like its predecessor, the Very High Resolution Radiometer (VHRR), which flew on the previous generation of NOAA satellites (the ITOS series), consists of a rotating scan mirror, a telescope, internal optics, detectors and electronics. The scan mirror is elliptical with a major axis of 29.46 cm and a minor axis of 20.96 cm.

6.8.1.2 High-resolution Infrared Radiation Sounder (HIRS)

The High Resolution Infrared Radiation Sounder 2 (HIRS/2) is derived from the HIRS/1, which flew onboard PEO NOAA satellites, as illustrated in Figure 6.44 (Right). The primary differences between the HIRS/2 and the AVHRR are: (1) the HIRS/2 has many more channels (20) than does the AVHRR (4 or 5); and (2) the HIRS/2 has much coarser resolution (42 km) than the AVHRR (1.1 km). These differences are due to the different requirements of the two instruments. The AVHRR is designed to make images, in which the horizontal structure of the atmosphere is most important, whereas the HIRS/2 is used for soundings, in which the vertical structure of the atmosphere is most important.

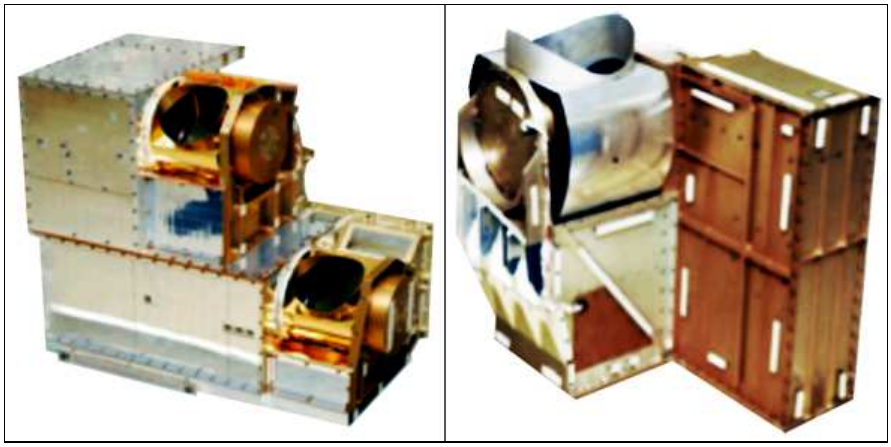

Figure 6. 45 AMSU-A1 and AMSU-A2 Instruments: by NOAA 2009

6.8.1.3 Advanced Microwave Sounding Unit (AMSU)

The Advanced Microwave Sounding Unit (AMSU) is a multi-channel microwave radiometer installed on PEO meteorological satellites. The instrument examines several bands of microwave radiation from the atmosphere to perform atmospheric sounding of temperature and moisture levels. This unit is derived from the Microwave Sounding Unit (MSU) and produced the following models:

1. AMSU-A1 – This instrument measures scene radiance in the microwave spectrum, which is shown in Figure 6.45 (Left). The data from this instrument are used in conjunction with the

HIRS to calculate the global atmospheric temperature and humidity profiles from the Earth's surface to the upper stratosphere, approximately a 2-millibar pressure altitude (48 km or 29.8 mi). The data are used to provide precipitation and surface measurements including snow cover, sea ice concentration, and soil moisture.

2. AMSU-A2 – This instrument is a cross-track scanning total power radiometer, which is shown in Figure 6.45 (Right). It is divided into two physically separate modules, each of which operates and interfaces with the spacecraft independently. Module A-1 contains 13 channels and Module A-2 contains two channels. The instrument has an IFOV of 3.3° at the half-power points providing a nominal spatial resolution at nadir of 48 km (29.8 mi). The antenna provides a cross-track step scan, scanning ± 48.3° from nadir with a total of 30 Earth fields-of view per scan line. The instrument completes one scan every 8 seconds.

3. AMSU-B – This unit offers five channels between 89 and 183.3 GHz, has a spatial resolution near nadir of 15 km and is primarily intended for moisture sounding. The spot size of both sub-instruments becomes larger and more elongated toward the edges of the swath. When the two instruments are used together, there are roughly 9 AMSU-B fields-of-view in a 3x3 array corresponding to each AMSU-A field-of-view.

6.8.1.4 Stratospheric Sounding Unit (SSU)

Long-term changes in stratospheric temperatures are important for interpreting the radiative effects of anthropogenic emissions of ozone depleting substances and greenhouse gases. Satellite measurements of stratospheric temperature now span more than 30 years, which potentially can provide valuable information on temperature trends since 1979. To achieve these values, the Stratospheric Sounding Unit (SSU) is a special satellite instrument designed to retrieve temperatures in the stratosphere. Its immediate predecessor is the Pressure Modulator Radiometer (PMR) flown on NOAA satellites, such as Nimbus 6. Therefore, stratospheric temperature records inferred from SSU are inconsistent to resolve these values.

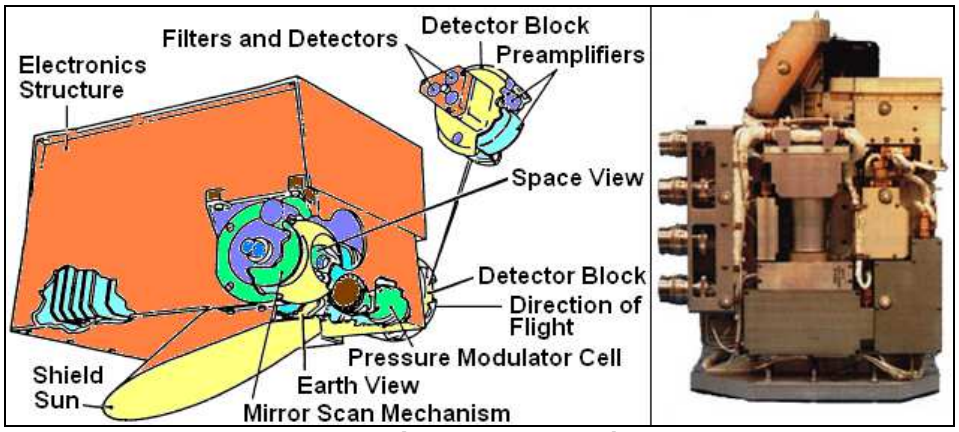

Figure 6. 46 SSU and SBUV Instruments by NOAA 2009

The SSU, as illustrated in Figure 6.46 (Left), is supplied by the United Kingdom Meteorological Office. In fact, the SSU is a scanning radiometer like all the instruments discussed above. Its scan mirror steps in 10° increments for 8 steps from 35° left to 35° right of the satellite track. Each step takes 4 s, and an entire scan line takes 32 s. Since the field of view of the radiometer is 10°, the scan spots are contiguous in the cross track direction, but there is an under lap in the along-track direction. Also, the SSU scans only about two thirds as far out as does the HIRS/2 and the AMSU. Thus, the outermost HIRS/2 and AMSU scan spots have no corresponding SSU data.

6.8.1.5 Solar Backscatter Ultraviolet Radiometer (SBUV)

Onboard the Advanced TIROS I satellites (NOAA 9 and NOAA 11) is the Solar Backscatter Ultraviolet Radiometer 2 (SBUV/2), which is the successor to the SBUV/1. The SBUV/2, as illustrated in Figure 6.46 (Right), was built by the Aerospace Systems Division of Ball Corporation in Boulder, Colorado. Its purpose is to estimate the global ozone distribution by measuring backscattered solar radiation in the ultraviolet Hartley-Huggins bands.

The SBUV/2 unit actually consists of two instruments, namely, the Monochrometer as the primary instrument that measures the Earth radiance directly and selectively the Sun when a diffuser is deployed, and the Cloud Cover Radiometer (CCR) that detects clouds that would contaminate the signal. The CCR measures the 379-nm wavelength and is co-aligned to the monochrometer. The output of the CCR represents the amount of cloud cover in a scene and is used to remove cloud effects in the monochrometer data. Neither of these instruments scan spatially, they simply view nadir. The field of view of the instruments is 11.3°, which means that the scan spot has a 168 km diameter on the Earth. The Monochrometer can be operated in either discrete mode or sweep mode during this time (NOAA, 2012).

Therefore, the SBUV/2 measures the ultraviolet solar irradiance itself. It is calibrated with an onboard mercury lamp with eight emission lines in the wavelength range of the instrument: 184.0, 253.7, 302.2, 313.2, 365.0, and 404.7 nm. For instance, the lamp can be positioned such that it shines directly into the optics, or such that it first reflects from the diffuser plate, thus checking the properties of the diffuser. This instruments measure solar irradiance and Earth radiance (backscattered solar energy) in the near ultraviolet spectrum (160 to 400 nm). The following atmospheric properties are measured from this data:

- The global ozone concentration in the stratosphere to an absolute accuracy of 1 percent;
- The vertical distribution of atmospheric ozone to an absolute accuracy of 5 percent; and
- The long-term solar spectral irradiance from 160 to 400 nm Photochemical processes and the influence of "trace" constituents on the ozone layer.

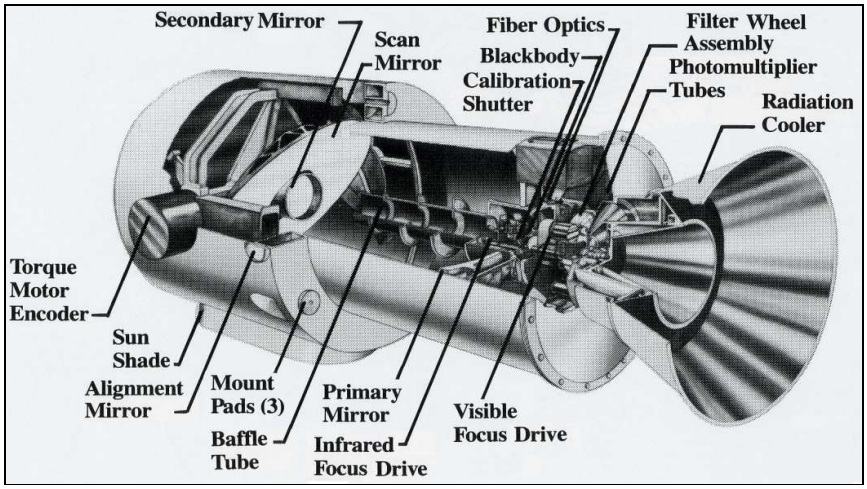

Figure 6. 47 VAS Instruments by NOAA 2004

6.8.2 Meteorological Instrumentation onboard GEO Satellites

The GOES satellites generally have three major subsystems, such as Space Environment Monitor (SEM), TT&C subsystem and satellite meteorological instrument. The SEM is quite different from the SEM on board the NOAA satellites. Thus, it includes a magnetometer, a solar X-ray sensor and an energetic particle monitor. The instrument package is designed to study solar activity and the Earth's magnetic field. The TTC has several functions including transmission to Earth of data collected by the satellite instruments, satellite command, relay of data from Earth-based Data Collection Platforms (DCP) and relay of weather facsimile (WEFAX) charts.

6.8.2.1 Visible and Infrared Spin Scan Radiometer (VISSR)

Prior to GOES-4, the meteorological instrument on GOES was the Visible and Infrared Spin Scan Radiometer (VISSR). On GOES-4-7, the primary instrument has been the VISSR Atmospheric Sounder (VAS), which has sounding capabilities in addition to the VISSR imaging capabilities. The VAS instrument, as shown in Figure 6.47, was designed and built by Santa Barbara Research Center, a subsidiary of Hughes Aircraft. **.** The GOES 4-7 satellites have spun and de-spun portions. Thus, the de-spun portion includes the antennas for communication with Earth. The VAS resides in the spun portion of the satellite and its optical axis coincides with the principal axis of the satellite.

The VAS is a radiometer with 8 visible channel detectors and 6 thermal detectors that detect infrared radiation in 12 spectral bands. Besides, a filter wheel in front of the detector is used to achieve the spectral selection. The spatial resolution is 0.9 kilometer in the visible and 7 or 14 kilometers in the infrared depending on the detector used. Full Earth disk coverage is accomplished by spinning in the west to east direction at 100 rpm and by stepping a scan mirror from north to south. Additional VAS instrument characteristics are summarized.

The VAS has three operating modes: VISSR, Multispectral Imaging (MSI) and Dwell Sounding (DS). The operational VISSR mode is used by NOAA/NESS for its operational products, which include a visible picture and an 11 micrometer infrared (channel 8) picture at half hour intervals. The MSI mode combines the operational VISSR capability (visible plus infrared window) with two additional spectral channels to provide half hourly full Earth disk imagery of atmospheric water vapour, temperature, and cloud distribution. The DS mode is used primarily for sounding to obtain the temperature and moisture profiles. In this mode, multiple spins on the same scan line in a given band are averaged to obtain the required signal to noise ratio for sounding.

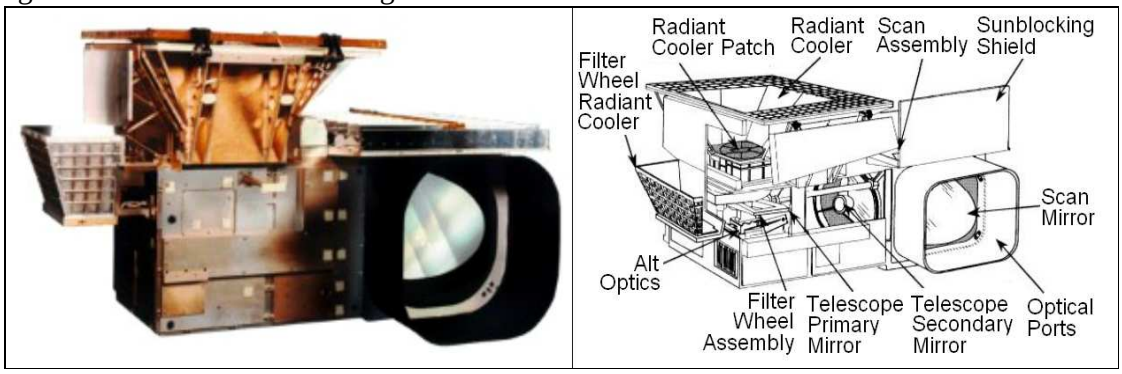

Figure 6. 48. GOES I-M and N-O-P Imager by NOAA 2009

6.8.2.2 GOES-I/P Imager

The GOES I-P imager is a multispectral imaging radiometer, built by the US ITT Industries company. Its objectives are: operational meteorology and climatology (one channel in the VIS and four channels in the IR range). Furthermore, the GOES Imager measures radiant and solar-reflected energy from sampled areas of the Earth by means of a servo driven, two-axis gimbaled mirror scanning system in conjunction with a Cassegrain telescope. Thus, the imager's multispectral channels can simultaneously sweep an 8-kilometer (5 statute mile) north-to-south swath along an East-to-West/West-to-East path, at a rate of 20^0 degrees (optical) East-West per second. This translates into being able to scan a 3000 by 3000 km (1864 by 1864 miles) "box" centered over landscape in just 41 seconds. The actual scanning sequence takes places by sweeping in an East-West direction, stepping in the North-South direction, than sweeping back in a West-East direction and stepping North-South, sweeping East-West, and so on.
The imager instrument, as shown in Figure 6.48 (Left), consists of electronics, power supply and sensor modules. The sensor module containing the telescope, scan assembly and detectors, is mounted on a baseplate external to the spacecraft, together with the shields and louvers for thermal control, as shown in Figure 6.48 (Right). Furthermore, the electronics module provides redundant circuitry and performs command, control and signal processing functions. It also serves as a structure for mounting and interconnecting the electronic boards for proper heat dissipation. The power supply module contains the converters, fuses and power control for interfacing with the spacecraft electrical power subsystem. The electronics and power supply modules are mounted inside the spacecraft on the internal equipment panel.

Therefore, the GOES Imager is a multi-channel instrument designed to sense radiant and solar-reflected energy from sampled areas of the Earth. In such a way, the instrument can produce full-Earth disc images, sector images that contain the edges of the Earth, and various sizes of area scans completely enclosed within the Earth scene using a flexible scan system. Scan selection permits rapid continuous viewing of local areas for monitoring of mesoscale (regional) phenomena and accurate wind determination.

6.8.2.3 GOES-I/P Sounder

The GOES I-P sounder was also designed and developed by ITT Industries Inc. The sounder instrument is a 19-channel discrete-filter radiometer, designed to sense the emitted thermal energy and reflected solar energy from sampled areas of the Earth's surface and atmosphere to provide data for computing vertical profiles of temperature and moisture, surface and cloud-top temperatures and ozone distribution.

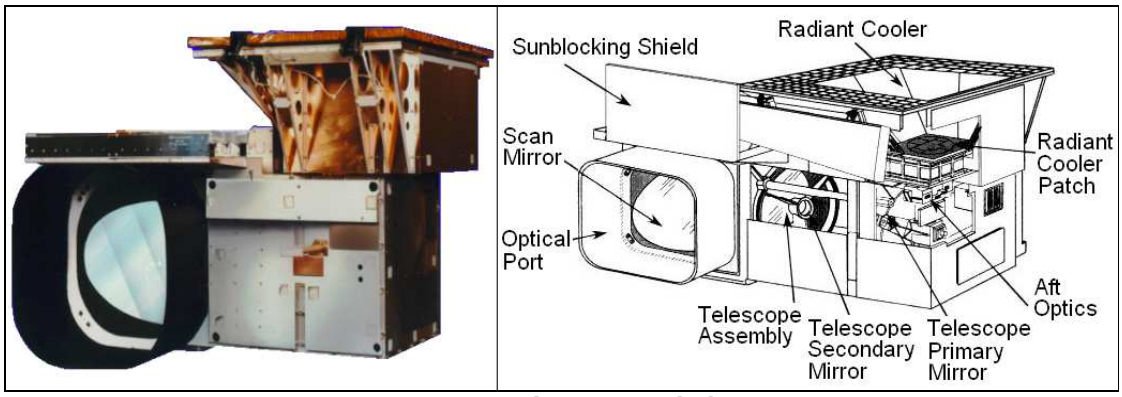

Figure 6. 49 GOES I-M and N-O-P Sounder by NOAA 2009

The Sounder looks at conditions in "columns" of the atmosphere - cylindrical sections that extend from the Earth's surface to the upper reaches of the atmosphere. The Sounder is shown in Figure 6.49 (Left) and its components are shown in Figure 6.49 (Right). The Sounder has 4 sets of detectors (visible, long wave IR, medium wave IR, short wave IR), while the incoming radiation passes through a set of filters before reaching the detectors. It operates by means of a scan mirror that steps across the disk of the Earth in a West-to-East and East-to-West direction along a North-to-South path as the filter wheel rotates. The filter wheel has 18 filters, each of which corresponds to a particular band or wavelength in the electromagnetic spectrum. Each filter allows only energy with a particular wavelength to reach the detectors. All 18 filters and the visible band are sampled during each rotation, which occurs 10 times per second.

The GOES I-M Sounder is a 19-channel radiometer that senses specific data parameters for atmospheric temperature and moisture profiles, surface and cloud top temperature, and ozone distribution. The atmospheric profiles that are produced are very similar to what has been achieved for decades using balloon-borne radiosondes. However, the satellite Sounder system is able to achieve a greater number of profiles, and many more locations than is possible with a ground-based balloon system. The Sounder consists of electronics, power supply and sensor modules. The sensor module containing the telescope, scan assembly and detectors, is mounted on a baseplate outside the main structure of the spacecraft, together with shields and louvers for thermal control. The electronics and power supply modules are mounted inside the spacecraft on the internal equipment panel.

6.8.2.4 Spinning Enhanced Visible and InfraRed Imager (SEVIRI)

The Eumetsat MSG GEO spin stabilized GEO satellites are designated to provide accurate weather monitoring data through its primary instrument, i.e., the Spinning Enhanced Visible and InfraRed Imager (SEVIRI), which has the capacity to observe the Earth in 12 spectral channels and records data in a 15 minute cycle. Eight of these channels is in the thermal infrared, providing among other information, observations of the temperatures of clouds, land and sea surfaces at approximately 5 km resolution with a 15 minute duty cycle. This Group for High Resolution Sea Surface Temperature (GHRSST) dataset produced by Meteo France CMS is derived from the SEVIRI instrument on the first MSG satellite (Meteosat-8). Skin Sea Surface Temperature (SST) data are calculated from the infrared channels of SEVIRI unit at full resolution on an hourly basis. Remapping of original pixel size to 11.6 km resolution is made by spatial averaging, and a 3-hourly temporal resolution SST is created by

averaging the hourly SSTs having the best confidence level. Data from different MSG satellites are not averaged together.

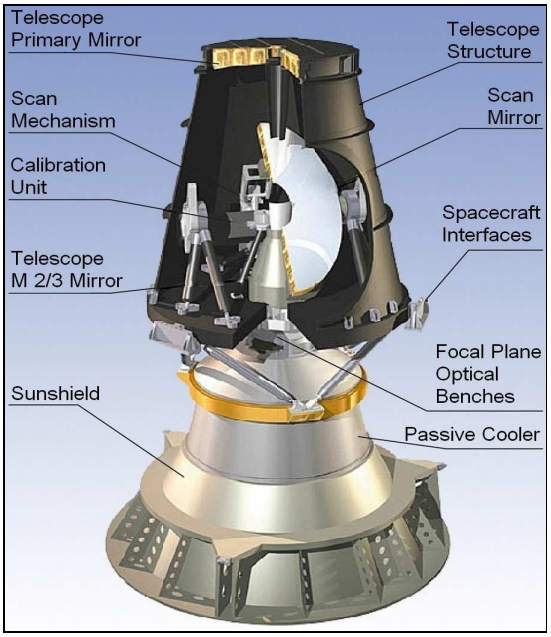

Figure 6. 50 SEVIRI by Schmid 2011

The SEVIRI instrument, as shown in Figure 6.50, is a 50 cm-diameter aperture, line-by-line scanning radiometer, which provides image data in four Visible and Near-InfraRed (VNIR) channels and eight InfraRed (IR) channels. **.** The resolution of the high-resolution visible light channel measures 1 km at the sub-satellite point (compared to 2.5 km on the previous Meteosat). A key feature of this imaging instrument is its continuous imaging of the Earth in 12 spectral channels with a baseline repeat cycle of 15 min. The imaging sampling distance is 3 km at the sub-satellite point for standard channels, and down to 1 km for the High Resolution Visible (HRV) channel. The instrument has a mass of about 260 kg and power consumption of about 150 Watts.

6.8.3 Meteorological Instrumentation onboard Aircraft and Stratospheric Platforms

The Gimballed Limb Observer for Radiance Imaging of the Atmosphere (GLORIA) is a newly developed unique atmospheric remote sensing instrument that bridges the gap from scanning to imaging in the infrared spectral domain. This is realized by combining a classical Fourier Transform Spectrometer (FTS) with a 2-D detector array tailored to the FTS needs.
Imaging allows the spatial sampling to be improved by up to an order of magnitude when compared to state of the art limb scanning instruments. In addition to the limb mode, the instrument can also perform nadir measurements. The GLORIA instrument is designed to operate on various high altitude research platforms, such as aircraft, stratospheric balloons and airships (SCP).

The GLORIA instrument is a German airborne imaging FTS, which is capable of operating on various airborne platforms. The main scientific focus is on the dynamics and chemistry of the UTLS (Upper Troposphere and Lower Stratosphere) region. The instrument is capable of measuring in limb and nadir geometry and has flexibility in terms of spatial and spectral sampling. At this point, the limb sounding mode is used to explore transport processes

between different compartments of the atmosphere that take place on scales satellite instruments are not able to resolve.

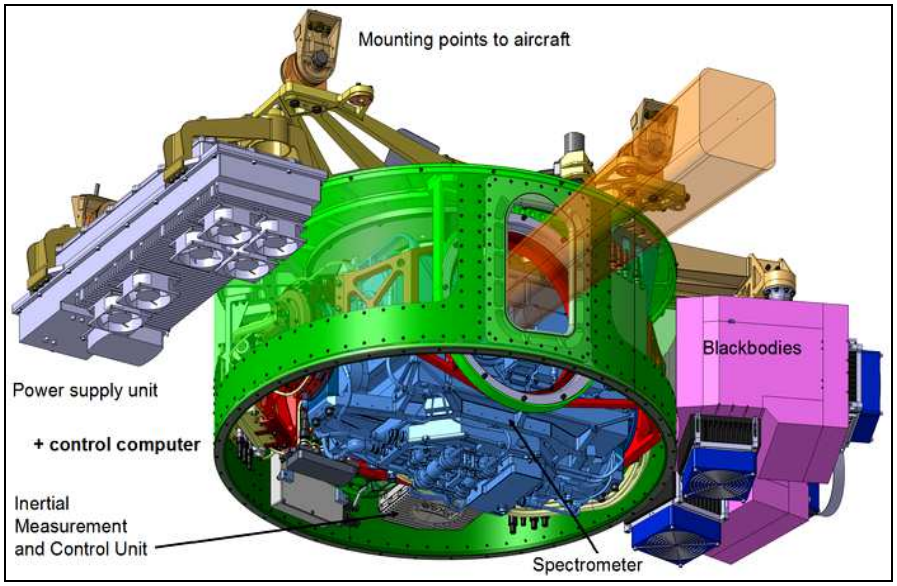

Figure 6. 51 GLORIA by KIT 2008

The GLORIA instrument, which is shown in Figure 6.51. is a joint development of the Helmholtz Large Research Facilities Karlsruhe Institute of Technology (KIT) and Research Centre Jülich (FZJ) and it builds upon the heritage of KIT and FZJ in developing and operating IR limb sounders (CRISTA, MIPAS).. Since GLORIA is exposed to the hostile environment of the UTLS with mutable low temperature and pressure, the in-flight blackbody for Radiometric calibration system has to be carefully designed to cope with those adverse circumstances.

The GLORIA FTS subsystem is realized as a classical Michelson Interferometer. The optical setup of the interferometer is straightforward and simple: the radiation enters through an insulating double germanium window; amplitude splitting is performed by a dielectric beam splitter on a potassium chloride substrate, two Zerodur cube corners, one fixed and one linearly moveable act as retro reflectors.

The Gimbal Frame and the Pointing Control systems enable nadir and three different limb view acquisition modes: Calibration**,** Chemistry (high spectral resolution) and Dynamics (high spatial resolution, tomography) Mode. The GLORIA subsystem is based on a flexible concept tailored to support different scientific scenarios and aims, so a 3-axis compensation of platform movements and other noise sources are mandatory.

The electronics subsystem is a distributed network of intelligent electronic components that are responsible for command and control of the whole instrument, for data acquisition, for housekeeping data generation and for power management. The intelligent units communicate via an internal LAN and additional direct links for time critical communication.

6.9 Meteorological Satellite Image Interpretation

The purpose of meteorological satellite image interpretation is to relate significant features in the image to physical processes that are occurring, or have occurred, in the atmosphere. For

example, meteorologists want to identify clouds. The shape or texture of the cloud or the proximity to geographic features on the Earth's surface can tell us much about the dynamics occurring in the atmosphere. The simple existence of a cloud on a satellite image can lead all meteorologists to a number of conclusions or questions, such as, what was the mechanism for formation of the cloud?

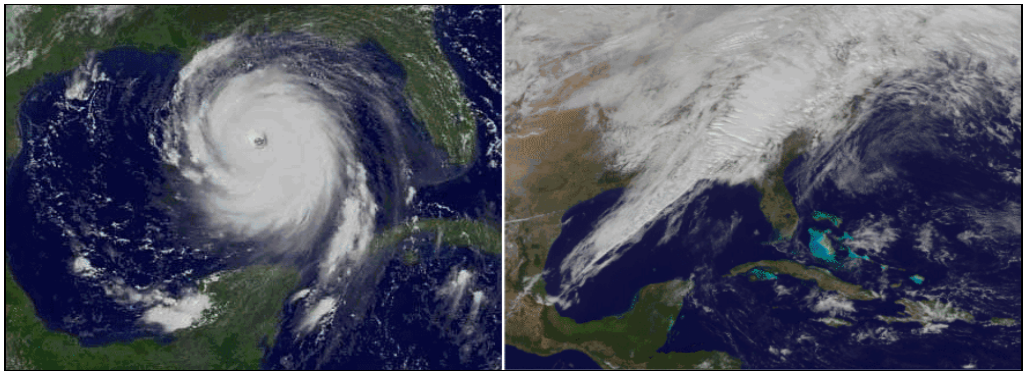

Figure 6. 52 Visible Imagery by NOAA 2004

The formation mechanism could be mechanical lifting, it could be convection due to heating, or the cloud could be the residual of a cloud mass that has been adverted far from its point of origin. Image interpretation can give meteorologists some clues to help identify the mechanism. Thus, knowledge can, in turn, help all interested stakeholders to determine the present and future hydrodynamic state of the atmosphere. The objectives of image interpretation are to: (1) detect and identify features such as clouds or other obscuring or radiating phenomena on the image; and (2) determine the physical mechanisms that produce or sustain those features.

The term satellite imagery can be used to describe two similar and yet unique displays: photo and digital. It is important to differentiate between the two. Photo images are easy for an analyst to handle, but digital images can be processed in many more ways, as some analysis techniques work only on digital images. Satellite imagery that is typically stored on magnetic or optical media is referred to as digital imagery, due to the nature of the collection and archive process (Schmetz, 2002).

The resolution of a satellite instrument can be defined as the size of the smallest element in the Earth scene that can be resolved by the instrument. It is a function of the field of view of the sensor optics and the distance to the Earth's surface. The resolution of a satellite instrument is usually for the satellite subpoint. It is important to note that the resolution of the satellite instrument may be quite different from the resolution of an image produced from the data. By using a filter, placed in front of the satellite sensor, radiation can be measured at specific wavelengths. The filter allows radiation within a narrow segment of the electromagnetic spectrum, called a spectral interval, to reach the sensor. Most meteorological satellites make measurements in the visible and infrared portions of the electromagnetic spectrum. There are four common types of imaginary:

6.9.1 Visible Imagery

Visible images represent the amount of sunlight being reflected back into space by the clouds or by the Earth's surface. Cloud free land and water will typically be dark while clouds and snow appear bright. Thicker clouds have a higher reflectivity and appear brighter than thinner

clouds. However, it is difficult to distinguish among low and high level clouds in a visible satellite image. For this distinction, infrared satellite images are useful. Thus, visible images cannot be used when no solar light is available.

The first imaging sensors aboard meteorological satellites measured radiation in the visible band (0.4-0.7 μm). Figure 6.52 (Left) illustrates the visible image of Hurricane Katrina, which happened in the Gulf of Mexico on 31 August 2005. Figure 6.52 (Right) shows a visible image from the GOES-13 weather satellite done on 3 February 2012. Visible imagery generally offers the highest spatial resolution and provides us with a view of the Earth that closely matches our senses.

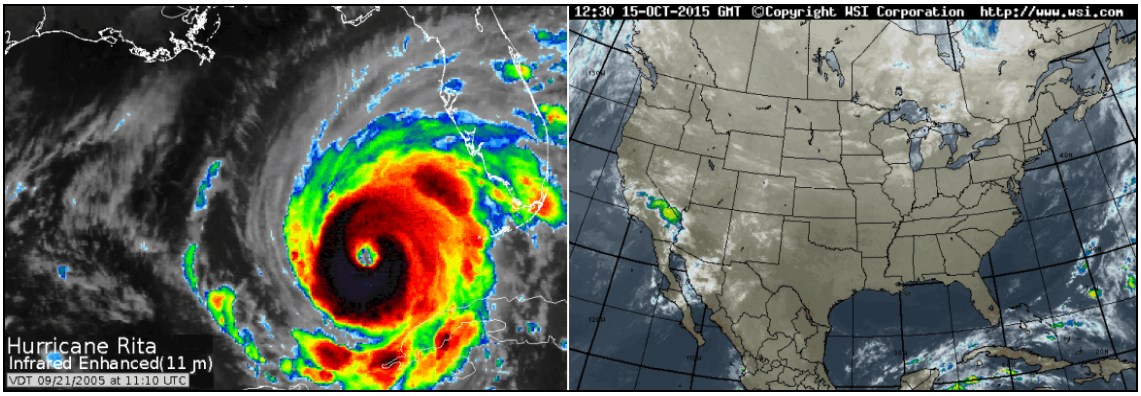

Figure 6. 53 Infrared Imagery by NOAA 2004

Land, clouds and ocean are easily discernible. One obvious limitation to visible data is that they are available only from the sunlit portion of the Earth. However, one exception to the daytime-only limitation is a sensitive instrument such as Operational Linescan System (OLS) on board the Defense Meteorological Satellite Program (DMSP) satellites, which can sense features that are illuminated at night by moonlight.

6.9.2 Infrared Imagery

Infrared images represent the infrared radiation emitted by the clouds or by the Earth's surface, which actually are measurements of temperature. For an infrared picture, warmer objects appear darker than colder objects. Cloud free areas will typically be dark, but also very low clouds and fog may appear dark. Most other clouds are bright, while high-level clouds are brighter than lower level clouds. Figure 6.53 (Left) shows the infrared image of Hurricane Rita that occurred in the Gulf of Mexico on 21 September 2005, while Figure 6.53 (Right) shows an infrared image of clouds over United States on 15 October 2015. The infrared channels are most often between 1 and 30 μm range. The most common infrared band for meteorological satellites is in the 10-12.5 μm window, in which the atmosphere is relatively transparent to radiation upwelling from the Earth's surface. Thus, when the word infrared is used alone to describe an image, it is nearly always in the 10-12.5-/xm window rather than in another portion of the electromagnetic spectrum.

Since infrared radiation can be related to the temperature of the emitting body and because the troposphere generally cools with height, this helps us interpret the atmospheric processes occurring within the scene. In this case, an important characteristic of the infrared channels is

their ability to provide images at night. This provides continuous coverage of cloud evolution over a full 24-hour period. Normally, in image processing, images are displayed such that the greater the radiance, the brighter the pixel. In satellite meteorology, however, infrared images are normally inverted, that is, the larger the radiance from an element, the darker the pixel. In this way, clouds, which are usually colder than the surface, appear white and the warmer ground or ocean surface appears darker than clouds, as in visible images.

6.9.3 Water Vapour Imagery

Water vapour images represent the amount of water vapour in the mid and upper atmosphere. Water vapour images are useful for pointing out regions of moist and dry air, white regions on the imagery representing more moisture than dark regions. The water vapour channels are so named because the satellite measures radiation in water-vapour absorption bands. Several wavelengths can be used, but the most common is centered around 6.7 μm.

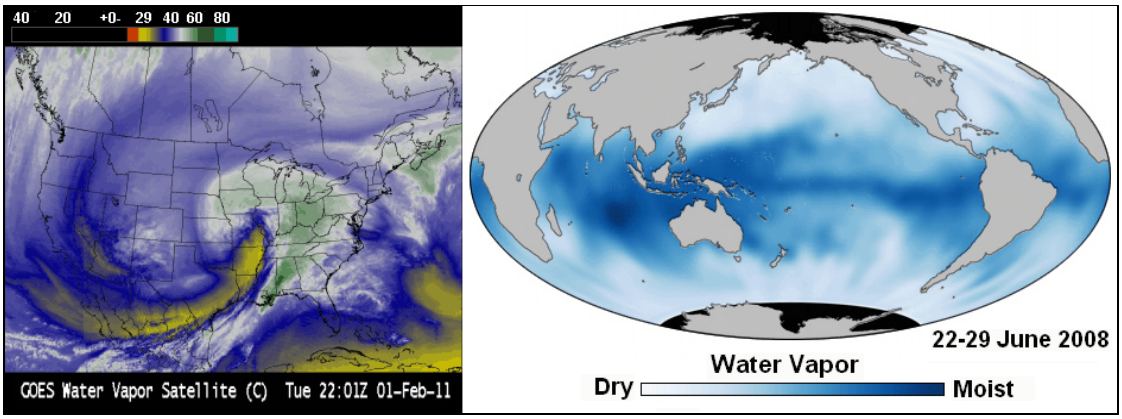

Figure 6. 54 Water Vapor Imagery by NOAA 2009

At this wavelength, most of the radiation sensed by the satellite comes from the atmospheric layer between 300 and 600 hPa, thus, it measures middle levels of the troposphere. It is noteworthy that the highest clouds can be seen, but surface features cannot be detected because this is not a window channel. Instead, dramatic swirls and eddies of water vapour are seen where high clouds are not present. Water-vapour imagery is commonly looped to display motions in cloud-free regions of the atmosphere.

Figure 6.54 (Left) presents a particularly large storm on 2 February 2011, which impacts a swath of the US over 2500 miles long and 700 miles wide with snow, sleet and ice from New Mexico to Maine, with snowfall amounts as high as 27.0 inches at Antioch, Illinois. As the storm developed, the water vapour imagery displayed a very pronounced dry slot, along with an extensive cloud shield. Figure 6.54 (Right) shows the First Global Water Vapour Map from the NASAC Ocean Surface Topography Mission *(*OSTM*)* produced between 22 and 29 June 2008. Figure 6.54 also illustrates Water Vapour Image by European satellite Meteosat-1.

One way to qualitatively interpret water-vapour imagery is to say that it approximates the relative humidity of the midtroposphere. Consider a bright area and a dark area in a water vapour image. In the bright area, the satellite measures less radiance than in the dark area. Less radiance means either that the atmosphere is colder at the same level as in the dark area or that there is more water vapour present in the bright area so that the satellite senses a higher, and, therefore, colder level. In either case, the relative humidity is likely to be higher

in bright areas than in dark areas. Bright and dark areas may also indicate rising and sinking motions, respectively.

6.9.4 Microwave Imagery

Microwave radiation via weather satellite is sensitive to an array of surface and atmospheric parameters, including precipitation, cloud water, water vapour, water droplet phase, soil moisture, surface temperature, atmospheric temperature, and ocean surface wind speed. In addition, many regions of the microwave spectrum are available for remote sensing. Then, all microwave instruments measure polarized radiation, and polarization is a factor in the microwave radiation emitted by some of the above atmospheric and surface phenomena. Very roughly, we can say that 19 GHz is a window region and provides a measurement of surface radiance in clear sky areas. The 22-GHz channel is sensitive to water vapour. Thus, the 37-GHz channels are attenuated by clouds and rain, and the 85-GHz channels can be used to identify ice clouds and snow. For example, the very cold temperatures, seen at 85 GHz in Plate 2 in Indiana, Ohio, and across the South, are probably thunderstorms.

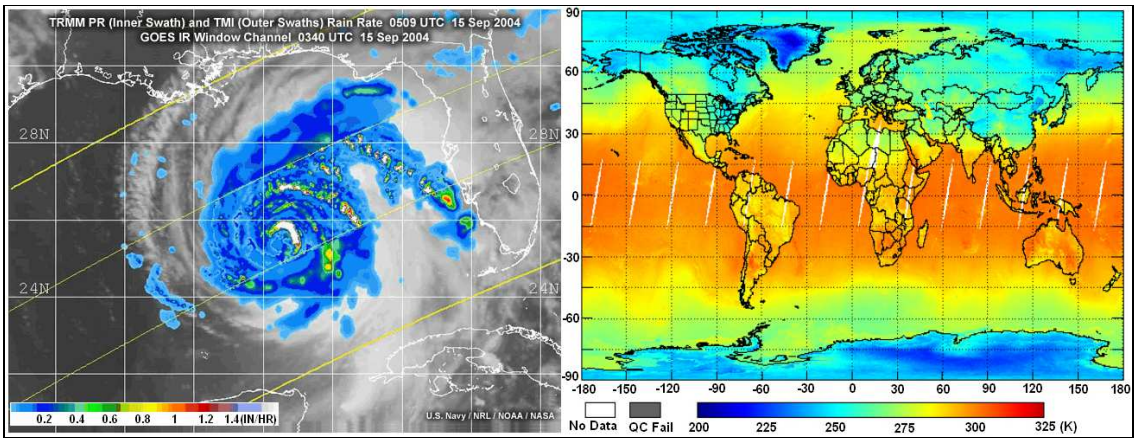

Figure 6. 55 Microwave Imagery by NOAA 2009

These channels are often used in combination to produce products, such as precipitation images. A great deal of current research is devoted to understanding and fully utilizing the information contained in microwave images.

The samples of satellite microwave images are shown in Figure 6.55. Figure 6.55 (Left) illustrates the TRMM (Tropical Rainfall Measuring Mission) satellite mission done on 15 September 2004, which includes an active radar that measures precipitation at discrete heights and is capable of operating at a higher horizontal resolution than current passive microwave instruments. The infrared and microwave rain rate composite image of Hurricane Ivan, shown here, illustrates the increased horizontal resolution available with active microwave instruments. More detailed structures become apparent within the inner swath, taken by the higher resolution TRMM Precipitation Radar, when compared to the outer swaths, which are from the lower resolution TMI (TRMM Microwave Imager) instrument. Figure 6.55 (Right) presents Suomi NPP ATMS surface skin temperatures for descending (midnight) orbits on 3 January 2012 and Suomi NPP ATMS surface skin temperatures for descending (midnight) orbits on 3 January 2012. This is microwave images produce primarily two-dimensional products, often displayed as images or maps. Sea and land surface temperature plots are an example of these data types.

CHAPTER SEVEN

REGIONAL METEOROLOGICAL SERVICE VIA SCP

This chapter introduces the development of Stratospheric Communication Platforms (SCP) or High Altitude Platforms (HAP) and their scientific potential to be deployed and integrated with current meteorological satellite networks. In particular, remote sensing and observation applications of SCP are presented in terms of information retrieval. The first section describes the basic concepts and types of SCP stations. The second section presents an overview of salient features of the SCP orbital parameters and suggested data acquisition technologies. The third section discusses the scenario of data analysis acquired and transmitted by SCP to the Direct Readout Ground Earth Stations.

7.1 Introduction

The SCP stations have been a concept that envisaged the use of unmanned airships and aircraft for the relay of telecommunication signals with a variety of applications including meteorological observations. For the past decades, SCP technologies, in general, have demonstrated specific inherent advantages, e.g., advanced microwave power transmission due to modern solar power systems, with widespread and diverse present and future space applications ranging from communication networks to Earth system sciences, sensing and meteorological observations. These SCP airships or aircraft operating in the stratosphere have payloads, transceivers and sensors that are capable of delivering a range of services including communications, emergency services and remote sensing (Aragon-Zavala et al, 2008).

SCP stations are more cost effective solutions than satellite systems. For instance, 6 cost effective platforms will cover a territory of South Africa with significant overlapping, as shown in Figure 7.1. In addition, SCP stations are a viable competitor or complement to terrestrial infrastructures and also satellite systems due to inherent restrictions related to, e.g., environmental and health constraints and the astronomical costs of terrestrial masts and satellites, respectively.

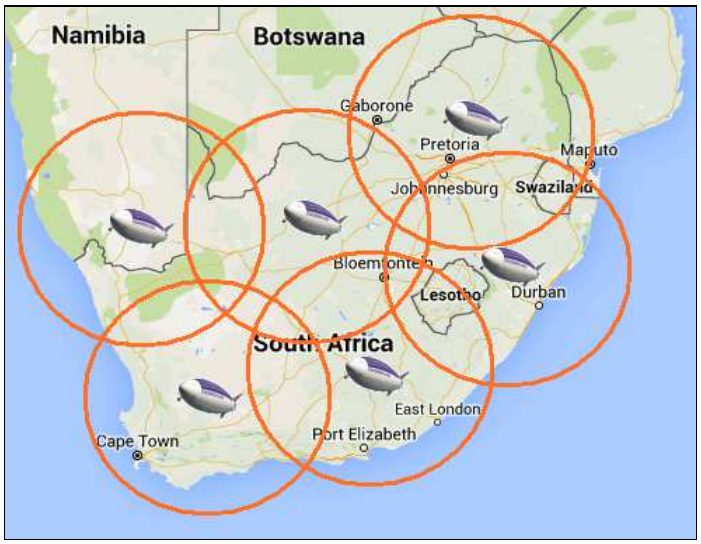

Figure 7. 1 Possible Coverage of South Africa by 6 SCP Stations by Ilcev 2015

For remote sensing and observation applications, a good example is a prototype known as High Altitude Long Endurance (HALE) aircraft that was proposed to offer an alternative and many advantageous solutions to manned airborne and satellite systems. The HALE platform had wide coverage, capable for providing meteorological observation, continuous coverage, a 15 to 20 cm spatial resolution as well as high spectral and radiometric resolution. The platform was designed to consist of a payload with Multispectral Digital Camera (MDC), LIDAR, Digital Thermal Camera (DTC) and Synthetic Aperture Radar (SAR).

Deployment of space remote sensing and weather observations network, in general, based on SCP space stations, and, in particular, based on High Altitude Platforms (HAP) of airships or Unmanned Aerial Vehicles (UAV) of aircraft has gained a significant momentum through several initiatives where space vehicles and telecommunications payloads have been researched and adopted. This initiative results in more efficient and more cost effective solutions of proposed SCP stations for Meteorological and Weather (WX) Observations applications.

The next section will introduce and propose the possibility of special SCP implementation as an alternative to the current satellite systems, their integration and as a complementary fast-evolving technology to improve weather observation systems especially in developing countries. The advantages of this initiative in relation to the meteorological and weather observation, proposals of an observation framework for weather observation via SCP and its modern requirements are taken into consideration.

7.1.1 Overview to SCP Stations

The SCP station is the last space technology and technique suitable for the development of low altitude communications for fixed, mobile, Global Navigation Satellite Systems (GNSS) augmented and meteorological applications, including military solutions. The SCP systems are unmanned or manned on solar or fuel energy aircraft and unmanned on solar power airships only, both carrying payloads onboard with transponders, antenna systems and TT&C equipment. With regards to the meteorological observation, SCP stations are able to carry onboard all kinds of observation instrument, sensors and payloads mentioned in Chapter 6.

A few very cheap remote controlled and solar powered airships can cover a territory of some region or country including urban, suburban and remote areas, farms, forests, meteorological centres and other rural environments with a low density of population. There are four general telecommunications architectures, which can be used to deliver communications and meteorological observation data and service to consumers.

Two of these architectures are space-based Geostationary Earth Orbit (GEO) and Non-GEO satellite communication systems and the other two are terrestrial rooftop cellular-like radio millimetre wave radio repeaters and stratospheric relay platforms. The SCP network offers better communication solutions than all cellular systems, with greater speed of transmission than even optical modes, with better roaming, without shadowing problems and disturbances inside buildings and servicing will cost less.

Moreover, the SCP mission can be integrated with current satellite communications or meteorological systems, because airships and aircraft stations are more autonomous and discrete systems, more cost effective and will be the best solution for military and all civilian

applications. Whereas, the delays through satellite network nodes, even through Low Earth Orbit (LEO) or Medium Earth Orbit (MEO) satellite nodes, are too long for many interactive applications, delays are 25 or 1,000 times longer for LEO or GEO than for High Altitude Long Operation (HALO) Networks, respectively. In fact, the HALO parameters are similar to a variety of metropolitan environment spectrum bands of the Local Multipoint Distribution Service (LMDS) band near 28 GHz.

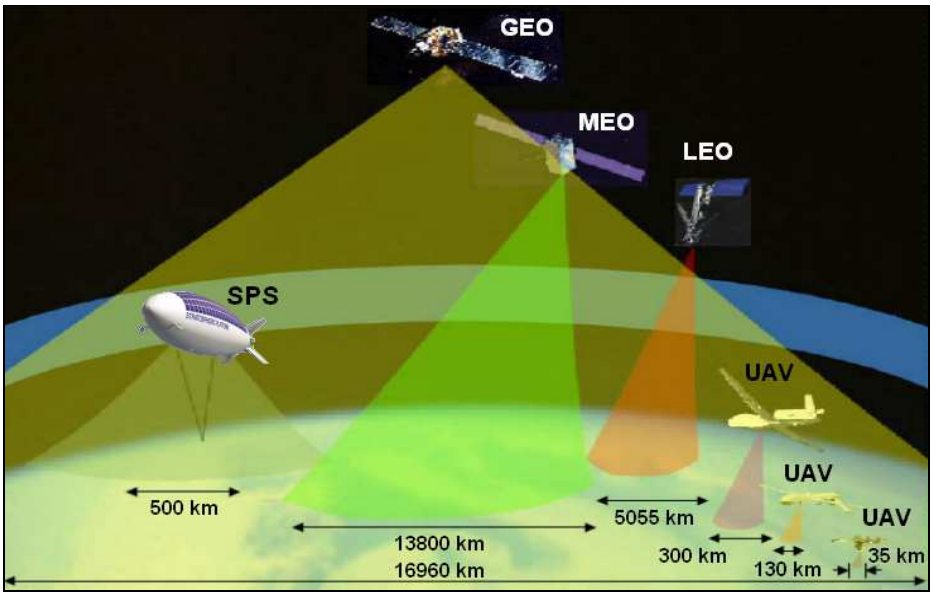

Figure 7. 2 Possible Coverage of Satellite, SCP and UAV Systems by Ilcev 2011

For instance, the HALO Broadband SCP Millimeter Wavelength (MMW) Network of the Angel Company provides data densities nearly one thousand times higher than proposed satellites (see **Table 7.1)**, while having round trip time delays appropriate for interactive broadband services.

Table 7. 1 Comparison of Data Density and Signal Delays in Ilcev 2011

Node Type	Node Data Density		Round Trip Delay	
	Min ($Mb/s/km^2$)	Max ($Mb/s/km^2$)	Min (millisec)	Max (milieu)
LMDS	3	30	0.003	0.060
Halo	2	20	0.10	0.35
LEO (Broadband)	0.002	0.02	2.50	7.50
GEO	0.0005	0.02	200	240

The increasing demands for modern, reliable and cost effective communication services grow very rapidly. Figure 7.2 shows different types of space communication systems, such GEO, MEO and LEO constellations, including SCP and different altitude UAV stations. A pressure on the radio spectrum can, therefore, be a trigger to a move towards higher frequency bands, which are less heavily congested. The use of millimeter wavelengths implies Line-Of-Sight (LOS) propagation for satellite and other space communication systems compared with lower frequencies solutions. Thus, the local obstacles will cause some problems because each user needs to have a LOS in during communication.

In recent years, a novel wireless concept, which also needs LOS, has been attracting much attention in the telecommunications community. As stated earlier, these systems are the SCP aircrafts or aircraft based on reusable unmanned or manned air vehicles, carrying transponders with antenna systems and operating in the stratosphere in an almost quasi stationary position at altitudes up to 25 Km above the Earth's surface. Such altitudes have not been used much by telecommunication services except for those related to scientific researches. However, these systems are acting as very low altitude spacecraft and have both azimuth and elevation angles. Elevation angles are providing better coverage and penetration in the building or shadowing than one tower of cellular system.

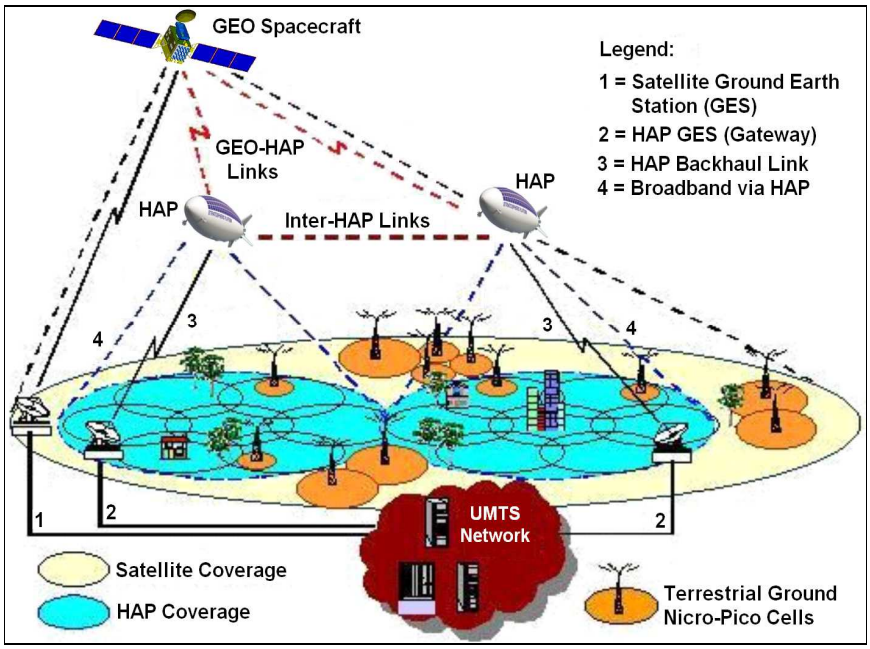

Figure 7. 3 Integration of Satellite, SCP Airship and Cellular Systems by Antonini et al 2003

7.1.2 Integration of Space and Terrestrial Networks

The combination of GEO and Polar Earth Orbit (PEO) meteorological (weather) satellites is one of the most important parts of the existing Global Weather Observation (GWO). The existing meteorological satellites are used to observe the Earth environments, sea surfaces, ocean currents and atmosphere from the space. They gather information about temperature, pressure, water vapour and critical trace gases (i.e., carbon dioxide) in the Earth's atmosphere through Vertical Atmospheric Sounder (VAS) for both nowcasting and future weather forecasts. The GEO spacecraft uses a circular orbit of about 36 thousand kilometers above the equator following the direction of the Earth's rotation. Satellites in GEO are far away from Earth that causes communication latency to become significant. Thus, the PEO spacecraft, at an altitude of approximately 1000 km, passes above or nearly above both poles once in a 12-hour period, so satellites in such an orbit can observe the full Earth's surface twice a day, which is, sometimes, not enough to provide observation. Due to the importance of the real-time accurate observations in weather forecasting, GEO is mostly used because it provides continuous observations every fifteen minutes, while polar orbit satellites only provide two observations a day, with better resolutions of images. There are new coming LEO and High Elliptic Orbit (HEO) meteorological satellites, which also participated in meteorological and climatological observations. Due to the importance of the real-time accurate observations in weather forecasting, GEO is mostly used because it provides

continuous meteorological observations every fifteen minutes, although resolutions of their images are not as high as PEO resolutions (Emanuela et al, 2006).

The last mile of new technology and techniques are SCP airships and aircraft, which provide more cost effective and reliable local Earth and meteorological observations by providing images with the highest resolution and with greater speed transmission to ground stations. The integration of the GEO satellite and SCP constellations of airships are shown in Figure 7.3. This integrated network can be connected to the Universal Mobile Telecommunications System (UMTS) and to GES terminals interfaced to GEO or SCP (HAP) constellations, for instance, distribution of meteorological data and images.

To provide greater coverage, many SCP (HAP) stations have to be connected via microwave or optical Inter-Platform Links (IPL), similarly used by the Iridium mobile communication system. Architecture of an integrated terrestrial-platform-satellite network can be designed according to the deployment choices, namely, the traffic from the cell sites may be backhauled in three different ways: through the Cellular Network Operators (CNO), which are integrated with the terrestrial telecommunication backhaul, via the HAP operator's terrestrial backhaul and satellite link. This architecture may use IPL to backhaul entire integrated traffic.

Satellites, especially GEO satellites, compared to SCP systems, are very expensive tools and, therefore, world researchers and service operators, especially in developing countries, are looking for more cost effective and affordable solutions. The ground station for weather observation system is very expensive to be located in all the corners worldwide, which is still inhibited by high latency, down times and it cannot be accessible in all the areas. Thus, all of the above mentioned factors affecting weather observation networks indirectly affect the economy and the understanding of weather and climate change (Ilcev, 2005). Economy is affected where a budget gets committed on inadequate decisions made from poor observations. Satellite observation has been used not for only weather forecasting, but also climate change detection and atmospheric research. Most of these observation needs are not feasible especially from developing countries.

This requires some innovative ways to fulfill the above-mentioned requirements that will be affordable, reliable and easy to maintain that can be easily integrated with the current weather observation network. At this point, many developed countries are providing research and experiments with new HAP or UAV worldwide, which initiatives may be followed by many developing countries in Africa including South Africa.

7.2 Weather Observation via Satellites and HAP

As stated in Chapter 6, the first whether commercial satellite Vanguard-2 was launched in February 1959. It was designed to measure cloud cover and resistance, but a poor axis of rotation and its elliptical orbit kept it from collecting a notable amount of useful data. In April 1960, NASA launched TIROS-1, which operated for 78 days and proved to be much more successful than Vanguard 2. Thus, because of these successful projects and experiments with weather satellites, the World Meteorological Organization (WMO) may start with new projects of the deployment of SCP stations for meteorological observation and imaging.

The SCP stations are a significant concept that has been proposed several decades ago for telecommunications and other services for local and even regional applications. The SCP

airships are stationary and operate at the stratosphere at an altitude between 16 and 30 km, to take advantage of usually lower winds facilitating location keeping. In all the regions worldwide, frequency bands of 47.2 - 47.5 GHz and 47.9 - 48.2 GHz are assigned to systems using HAP and UAV stations. Airships had been modeled not as the successor to either the terrestrial or satellite systems but as a complementary system. **Table 7.2** presents the differences between airships, unmanned aircraft and manned aircraft.

7.2.1 Multifunctional SCP Networks

The denomination of HAP airships and UAV aircraft stations was defined in the World Radio Communications Conference (WRC) in 1997, in the Radio Regulations (RR) No. S1.66A as a station located on an object at an altitude of 20 to 50 Km and at a specified, nominal, fixed point relative to the earth [WRC-122, 97]. In this definition, it has not been determined yet if the object is manned or unmanned or even how it is powered. Several countries proposed many alternative technologies for the development of such an object in the stratosphere (Ilcev, 2011).

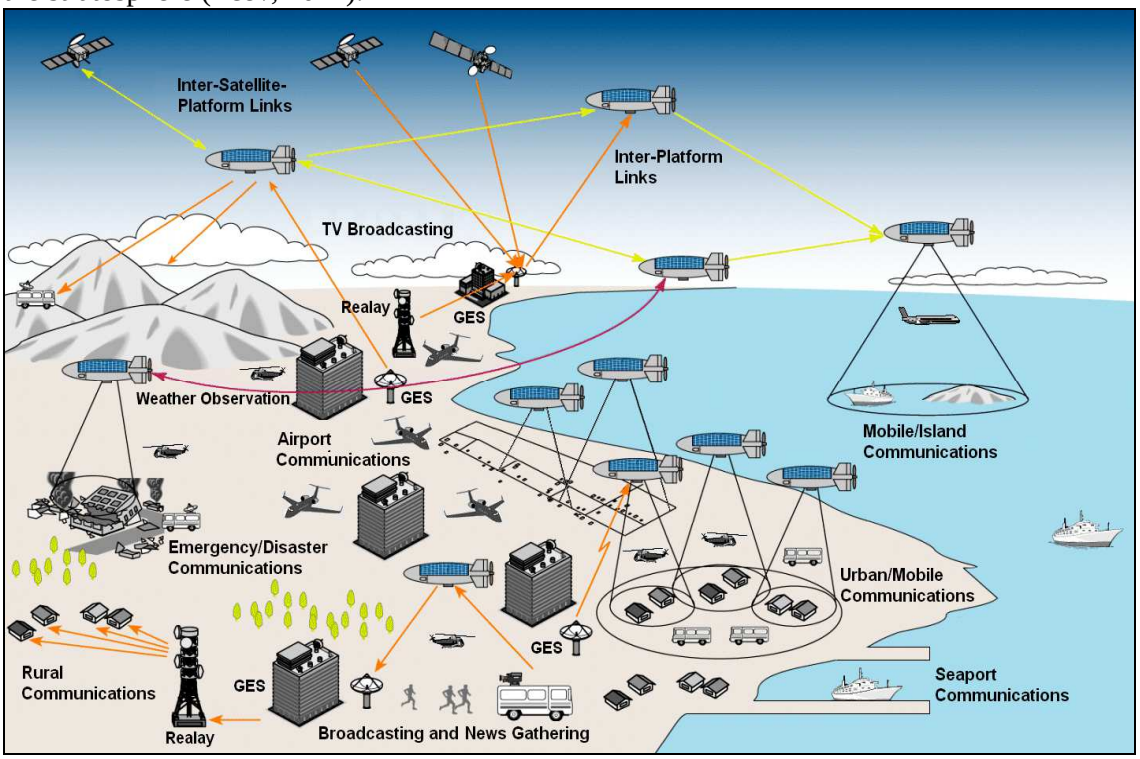

Figure 7. 4 Multipurpose SCP Airships Network by Ilcev 2011

Table 7. 2 Comparisons of SCP (HAP) Systems in Ilchenko 2004

Sources	Airship (Unmaned)	Solar-Powered UAV	Maned Aircraft
Size	Lenght 150 - 200 m	Wingspan 35 - 70 m	Lenght ≈ 30 m
Total Weight	≈ 30 ton	≈ 1 ton	≈ 2.5 ton
Power Source	Sollar (+Fuel) Cells	Sollar (+Fuel) Cells	Fossil Fuel
Flight Duration	Up to 5 Years	7 - 14 days	Up to 18 Hours
Position Keeping (Radius)	Within 1 km Cube	1 - 3 km	4 km
Coverage at Altitude of 20-30 km	500 - 600 km	500 - 600 km	Up to 500 km
Mission Payload	1000 - 2000 kg	50 - 300 kg	Up to 2000 kg
Power for Mission	≈ 10 kW	≈ 3 kW	≈ 40 kW
Example	China, Japan, Korea, ATG, Lockheed Martin, SkyStation etc.	Helios, Pathfinder Plus (Aero Vironment), Helipat (Europe) etc.	HALO (Angel Technologies), M-55 (Geoscan)

The HAP and UAV stations have to be positioned well above commercial airplane corridors of 10 km and at an altitude that is high enough to provide service to a large area or spot footprint, providing telecommunication, broadcasting and environment observation services with minimal ground network infrastructure.

The common vision of multipurpose observation and communication systems predicts that it will contain one or more SCP airships with inter links to the spacecraft, as illustrated in Figure 7.4. However, the same network can be developed without interlinks, so all platforms have to communicate via GES terminals or Gateways located in the overlapping areas. The SCP stations will provide service via area (regional) or spot coverage cells for mobile and fixed networks using GES or Fiber backhauls. The SCP multipurpose networks will provide service for broadcast, broadband, communication, surveillance, emergency, meteorological and other users.

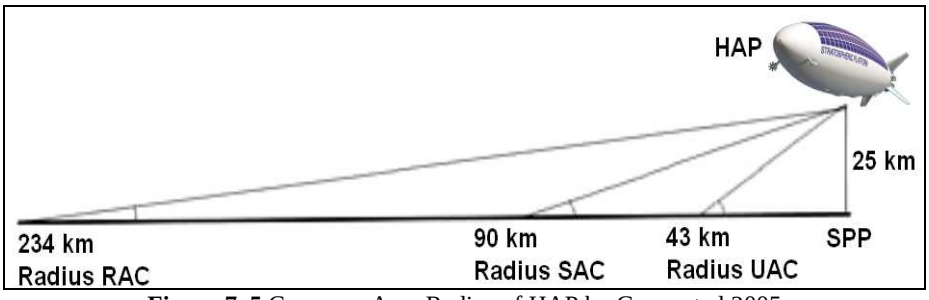

Figure 7. 5 Coverage Area Radius of HAP by Grace et al 2005

The systems based on HAP and UAV stations SCP represent a technological alternative that has been under study and development for the last several years, although the investigation of unmanned aerial vehicles had started at a few universities and research centres in the world as early as the late 1950s. At this point, these systems could have many advantages compared with terrestrial and satellite systems, while, at the same time, avoiding many of the pitfalls [ITU-Q/2, 98], which can be solved. Various applications and services are planned to be provided by platform stations that could be classified as narrowband or broadband service, depending on the bandwidth required. Different subscribers will transmit their information directly to the platform or vice versa for communications, broadband, weather information and other broadcastings, where onboard switching devices will route traffic directly to other subscribers within the same platform coverage area or through heterogeneous networks.

Various applications and services are planned to be provided by HAP and UAV stations that could be classified as narrowband or broadband service, depending on the bandwidth required, for reliable Communication, Navigation and Surveillance (CNS), remote sensing and weather observations. Different fixed and mobile subscribers will transmit their Voice, Data and Video over IP (VDV) and messages for all applications directly to the platform, where onboard platform switching devices will route traffic directly to other subscribers within the same platform coverage area with possible overlapping platform network or through heterogeneous networks. On the other hand, the stratospheric HAP or UAV will provide weather observation and transmit images to the ground stations for processing (Struzak, 2007).

The platform stations also experience less propagation delay with regards to satellite systems. In comparison with the cellular system, platform and satellite systems suffer less from shadowing and multipath distortions because they are exposed to high angle-of-arrival signals (elevation angles). Each platform station can deploy onboard a multi-beam antenna capable of projecting numerous spot beams within its potential coverage area.

The platforms act as the highest cell tower in urban areas, but an area of up to 600 km will require one or two platforms only. In a system based on HAP or UAV stations, the platform is positioned above the ground to create a radio electric coverage and service area of up to 500 km in diameter. The ITU-R defines three coverage areas: Urban Area Coverage (UAC), Suburban (SAC) and Rural (RAC), which are determined by the position of the ground receiver; i.e., coverage depends on the minimum elevation angle accepted from the subscriber's location and the distance from the Sub-Platform Point (SPP). These areas are shown in Figure 7.5, while some important parameters related to them are listed in **Table 7.3**, where **h** represents height above ground level.
Currently there are two well-established methods for providing wireless and space communication services. The first method is terrestrially based systems, as it is widely used in VHF/UHF radio systems and the second method is the space systems using GEO and PEO satellites including both HAP and UAV stratospheric platforms. Cellular radio systems can be used for transmissions of meteorological images on shorter distances between UAV and ground meteorological station.

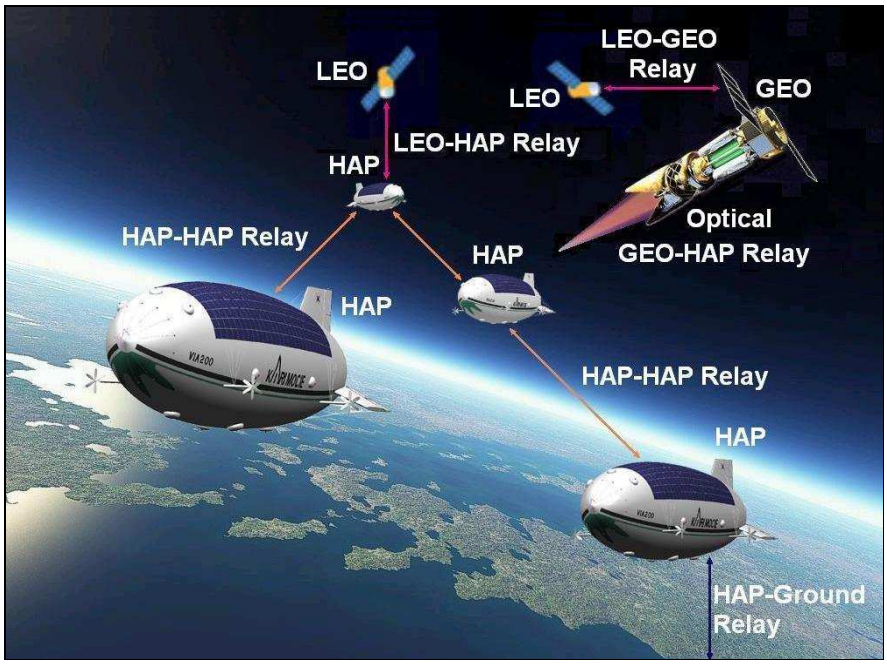

Figure 7. 6 Relay Satellite Optical Links via SCP/HAP by Ilcev 2011

Table 7. 3 Characteristics of Coverage Area Radius for HAP in Struzak 2007

Areas	Elevation Angle (degree)	Coverage Radius (Km)	
		h = 21 Km	h = 25 Km
UAC	90 - 30	0 - 36	0 - 43
SAC	30 - 15	36 - 76.5	43 - 90.5
RAC	15 - 5	76.5 - 203	90.5 - 234

However, for transmission of weather observation images via SCP, International Telecommunications Union (ITU) frequency designation bands such as frequencies at L, X, Ku and Ka-band can be used.

7.2.2 Satellite Optical Downlink and High Speed Data Link via HAP

Optical links offer significantly higher bandwidth, but they are blocked by clouds. As a consequence downlinks from satellites to a ground station have a limited availability depending on the cloud situation over a site. For Non-Earth Observation (EO) applications like communications or broadcast, a nearly hundred percent availability is required for the satellite link. This problem can be solved by using a relay station in the form of an HAO station, which has to be positioned above the clouds in about 20 km altitude. Besides, an optical link from the satellite to the HAP would have 100% availability for Non-EO and EO applications, as it is not hindered by clouds. The final “last mile” to the ground could then be bridged by a standard Micro Wave (MW) or optical point-to-point link as used today in terrestrial applications, but with a large bandwidth compared to a satellite link due to the short distance. An optical link in parallel to the MW link could increase the bandwidth of the last 20 km several times during cloud-free conditions (Tozer, 2003).

Figure 7.6 illustrates two scenarios for optical downlinks from two LEO satellites, namely, relay link from a LEO satellite to the ground via HAP relay (left) and from a LEO satellite over a GEO satellite and a SCP (right).

In addition, the “last mile” downlink from the HAP to a ground station would be either bridged by a high-bandwidth optical or microwave link. In the SCP Relay scenario, the data is sent directly via HAP to the ground (HAP-GND). In the case of the GEO satellite (GEO-HAP) Relay, the data is first transmitted to a GEO satellite and then via HAP to the ground.

However, the link to HAP-ground can be established by an optical link or alternatively by an MW link and provide full availability. Link duration between the LEO satellite and the HAP will be up to 12 minutes for each contact, with about 3-15 contacts depending on the geographic latitude of the HAP. In order to increase contact times, a GEO satellite time would be about half of the LEO orbit, i.e., about 12 hours per day. From the GEO satellite, the data would be transmitted on a continuous link to the HAP. The increased link duration would be at the cost of significantly longer link distances with a more stringent link budget and the additional expenses of an GEO satellite.

7.2.3 Technical and Geometry Aspect of SCP

From the geometrical point of view, the SCP system would enable communication services that take advantage of the best features of both terrestrial and satellite multipurpose communications. In addition, however, the system could bring advantages of its own, not available in current systems.

The most important advantages of employing SCP are high elevation angles, broad coverage, low propagation delay, low-cost operation, easy and incremental deployment and the ability to move around in an emergency situation. Although immature, airship technology, the stabilization system and onboard antenna technology of the platform are challenges that have to be investigated. The SCP is expected to avoid some inherent limitations of the traditional systems and to provide a backbone to cellular systems. Some of the challenges include a huge number of base stations required by the terrestrial system, limitation of the minimum cell size on the ground involved in a GEO satellite system, and the handover problem faced by LEO/MEO satellite system. The ITU has allocated the spectrum to this system at 2 GHz for 3G mobile systems, 48/47 GHz for the usage worldwide, and 31/28 GHz band is allocated to certain Asian countries.

Moreover, the SCP station is designed to have capability of flying in stratosphere at about 20 and 30 km for long endurance on-station, fed only by solar energy, offering the possibility to play the role of artificial satellites, with the advantages of being close to earth and more flexible. In fact, such platforms are attracting increasing interest for a variety of applications such as delivering a wide range of communication services to rural and remote areas lacking in telecommunications infrastructure (either wired and wireless), provision of basic emergency communications systems to areas hit by catastrophes or just supply of broadband telecommunication services to residential zones, with a relative low cost, quick deployment and acceptable data rate. It is also expected that the SCP would deliver a high quality TV broadcasting, voice, data, video and imaging transmissions for general and meteorological communication systems. The flexibility of the system allows its utilization for remote sensing and for earth observation purposes as well.

As stated earlier, those attractive features may not be characteristics of the conventional terrestrial and satellite systems. Thus, to provide multifunctional and reliable space communications, it will be necessary to provide integration of satellite and SCP networks, together with cellular networks. However, the SCP stations may be used to serve the users in the urban environment not only in LOS conditions but also in shadow situations. Although the SCP may enjoy many advantages not possessed by the terrestrial and satellite communication systems, there are still unreported important matters that have to be proven before the deployment of this system.

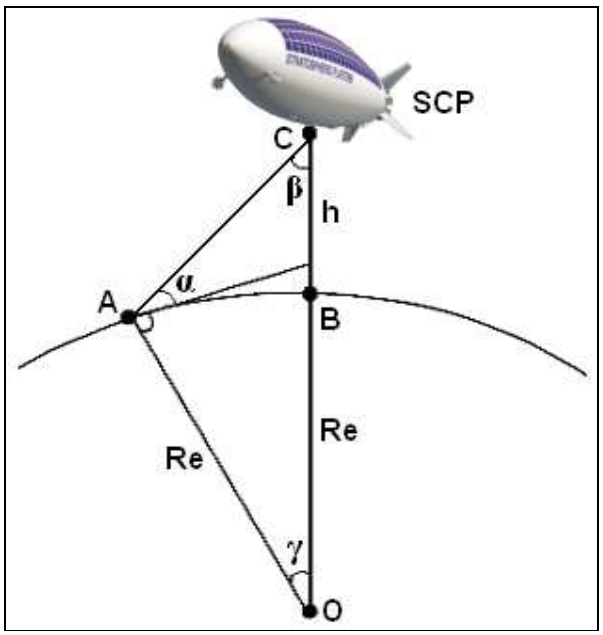

Figure 7. 7 Geometry Aspect of SCP by Aragon-Zavala et al, 2008

One important matter is the channel characteristic of the communication link between the SCP and mobile users on the ground. This thesis deals with the channel modeling and characterization as well as an investigation of the propagation aspects of the communication link for mobile users using the concept of SCP stations.

It is important first to look at the system geometry of SCP, as shown in Figure 7.7, before design and evaluate its communication characteristic so that the difference from other systems describes the geometry of the SCP system by involving the Earth's curvature. The SCP System is positioned at an altitude *h* (point C of SCP) with the sub-platform point, that is, the point vertically below the intended platform location is in point B. Besides, point A denotes the position of a user served by the SCP station having an elevation angle α. Point O in the figure represents the Earth's centre and R_e is the Earth's radius. Thus, from the principle of trigonometry, it can be expressed that:

$$OA/\sin\beta = OC/\sin(90 + \alpha) - OC/\cos\alpha \quad (7.1)$$

$$\sin\beta = (R_e/R_e + h)\cos\alpha \quad (7.2)$$

Assuming the Earth's surface is a perfect sphere, the arc AB indicates the radius (*d*) of SCP coverage on the ground and might be expressed through the following equation:

$$AB = R_e \gamma \quad (7.3)$$

Let us consider the triangle OAC. The total angle of the triangle is 180^o so that the angle γ can satisfy this equation

$$\gamma = 90^0 - \beta - \alpha \quad (7.4)$$

After substitution of relations (12.2.) to (12.4.), it will be able to rewrite the radius of the SCP coverage by the following relation:

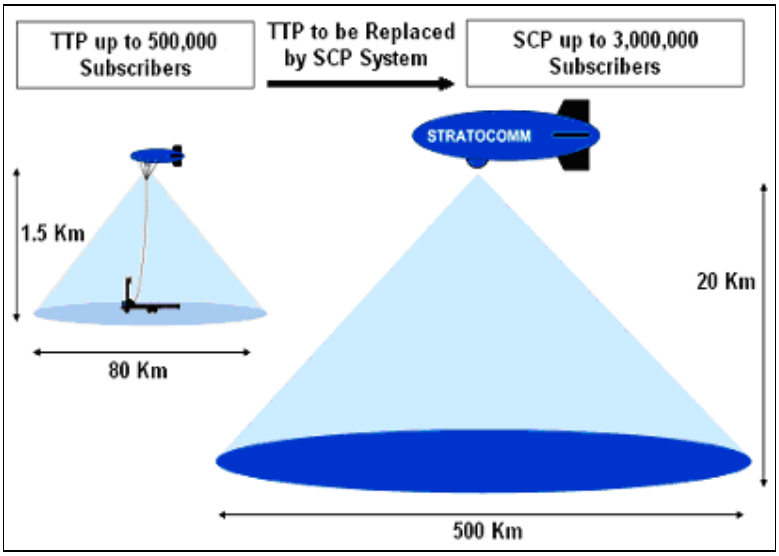

Figure 7. 8 Transition from TTP to SCP by Ilcev 2005

$$d = R_e \{\cos^{-1} [(R_e/R_e + h) \cos \alpha] - \alpha\} \quad (7.5)$$

According to the above geometrical analysis, the SCP at 20 Km altitude has the capability to cover an area on the ground up to 504 km in radius for 0^0 of elevation angle. In this sense, Figure 7.8 shows a radius of coverage area as a function of an elevation angle with the assumption of a platform altitude of 20 km. In this altitude, the SCP can, therefore, be considered as an ultrahigh-altitude tower compared with a terrestrial radio tower. As a result, the SCP can easily provide LOS communication with a high elevation angle, whereby the links are relatively free of the influence of obstacles. The antenna and the radio equipment can be made smaller because the electric power required for transmission can be decreased. Furthermore, there is minimal voice delay when used for voice for telephone service or the like, because the stratospheric platform is much closer to the ground than satellites, and, hence, the delay propagation is almost not an issue in this system.

7.3 SCP Space Segment

Several developed countries in the world are now proposing many alternative technologies for the development of space segment of SCP objects in stratosphere. The SCP stations have to be positioned well above a commercial airplane at an altitude that is high enough to provide service to a large area or spot footprint, providing communication, broadcasting, tracking, detecting, meteorological and environment Earth observation services with minimal ground network infrastructure.

There have been several recent developments in the space platforms arena of SCP scenario, especially for design of data transfer and the surveillance system on many international borders has demonstrated them to be a reliable and proven technology. In fact, a number of trials of small-scale airship have been conducted by companies in Japan, USA and Switzerland (StratoComm). Several programs are now focusing on space platforms providing fixed and mobile wireless broadband and communications using local WiMAX and WiFi services. In the interim, the StratoComm Corporation, formed in 1992, has designed network for the Transitional Telecommunication Project (TTP) tethered system as a means to immediately enhance telecommunications capacity in under-served areas.

This network became commercially available to provide service for about half a million customers and seamless transition from the aerostat-based systems to its SCP network that will serve about three million customers.

As a result, the SCP can easily provide LOS communication with a high elevation angle, whereby the links are relatively free of the influence of obstacles. The antenna and the radio equipment can be made smaller because the electric power supply required for transmission can be decreased.

Furthermore, there is minimal voice delay when used for voice for telephone service or the like including data transfer, because the stratospheric platform is much closer to the ground than satellites, and, hence, the delay propagation is almost not an issue in this system. The StratoComm platform is a Lighter-Than-Air (LTA) aerostat system positioned at an altitude point of approximately 1,500 meters over the region to which it is providing wireless telecommunications services. The aerostat is connected via high-strength steel and Kevlar tether to the ground cite, thereby maintaining its position and ability to support subscriber services, as well as providing access to power, operational control and data service via fiber optic cable and electrical conductors embedded within the tether.

The transitional aerostat station is approximately 37 meters in length and 12 meters at its widest point. It meets all US FAA requirements, including the presence of an emergency flight termination system and proper lighting. The aerostat carries an internally designed telecommunications payload weighing approximately 225 Kg, which is capable of supporting subscribers by broadband fast Internet, voice, data and video transmission with various combinations in a coverage area of 80 Km in diameter.

Figure 7.8 shows the transition from the old TTP to more the advanced SCP system. The SCP station doesn't interfere with aircrafts' flights, because the SCP system is located over 10 Km. However, the airship leverages LTA technology which is made of very high strength and lightweight materials. In addition, a platform is accompanied by advanced propulsion systems that maintain proper positioning and is equipped with autonomous navigation, Telemetry Tracking and Command (TT&C) and communications payload stabilization systems. An airship, located at 20 km position over Earth, is able to cover about 400 km radius areas. The SCP airship can be launched by deploying a specified volume of helium separated from the air to maintain its shape. As it rises, the helium expands and, at the proper altitude, displaces all of the air within the STS. Once it is in the stratosphere, the SCP is remotely controlled and moved into its determined position. The integration of solar cells, batteries and fuel cells provides power for the SCP airship during the five-year planned deployment. The SCP also incorporates TT&C and redundant systems to serve as back-up measures, and features that are designed to provide the airship with a high level of

availability, reliability and safety. The STS is designed to hold approximately 1,000 kg of communication payload capable of supplying focused fixed and mobile broadband, narrowband and wireless backbone services to approximately 3 million subscribers. However, the SCP airships are ideal networks for local or regional mobile communication, tracking and monitoring solutions.

The SCP configurations can be dynamically changed in milliseconds to reallocate capacity as needed, such as to highly trafficked commuter routes during peak travel times, to business districts on weekdays or to stadiums during events. In general, there are two main solutions of SCP, aircraft and airships divided into four categories:

1. Manned aircraft on fuel, which are flying in small circles as SCP and in any destination for observation and imaging applications around 48 hours or until fuel lasts;
2. Unmanned aircraft on fuel, which can fly until fuel lasts;
3. Unmanned plane on solar power can fly for a minimum 6 month period before requiring maintenance; and
4. Unmanned airship on solar power can hover in a certain position for a minimum of 6 months and has to be landed for maintenance, and will be replaced by another airship.

Figure 7. 9 Prototype of HAP Aircraft Altus by AVCS/NATO 2014

7.3.1 SCP Aircraft Networks

The new aircraft projects offer cost-effective systems by using special unmanned and solar powered engines with an estimated endurance of several months and piloted aircraft with fuel engine propulsion for operating on a daily basis, known as Unmanned Aerial Vehicles (UAV). This system will be more effective by development new systems such as: General Atomic, Halostar/Halo, Heliplat/HeliNet Hale, SkyTower Global and other forthcoming networks. These UAV networks are ideal for broadcasting, mobile tracking, meteorological observation and remotes sensing solutions.

Building upon its worldwide leadership in the new design, manufacture and deployment of UAV, the General Atomics Aerial Vehicle Communications System (AVCS) is developing the next generation of SCP aircraft. The research team of the General Atomic together with the NASA, the US Navy and the Department of Energy (DOE) developed a prototype high-altitude aircraft, Altus, for the future AVCS Network project, as illustrated in Figure 7.9 (Left).

This stratospheric aircraft will be ideal for Telecommunications Relay, Cellular Relay and Commercial Applications. At first, Altus was deployed in support of atmospheric research for the DOE, with future plans to use the high altitude capabilities to understand the genesis of and predict hurricane paths and damage potential, as well as many other advanced scientific applications.

The first unmanned, high altitude solar-electric aircraft designed under the NASA project was Pathfinder, as shown in Figure 7.9 (Right), which was developed in 1995 with a wingspan of about 29.87 m which flew to 15.39 and 21.79 km in 1995 and 1997, respectively. A second modified UAV Pathfinder program, known as Pathfinder-Plus, with a bigger wingspan of 36.88 m, flew to 24.44 km. This record flight was the 39th consecutive successful flight test of the Pathfinder platform. The next-generation of aircraft Centurion was a wingspan of 62.78 m, which was test flown in 1998. The wingspan was then further extended to 75.28 m and the previous model of aircraft was renamed the Helios prototype.

7.3.2 SCP Airship Networks

The new airship projects offer cost-effective systems for SCP by using special unmanned and non-fuel solar cell-powered balloons with an estimated endurance of several months. Thus, in comparison with aircraft and airship systems, it is difficult to say which one will be better for the future reliablility of the SCP. There are several airships such as: SkyStation Global Network, SkyLARK Network, StratCon (StratoSat) Global Network, TAO Network, etc.

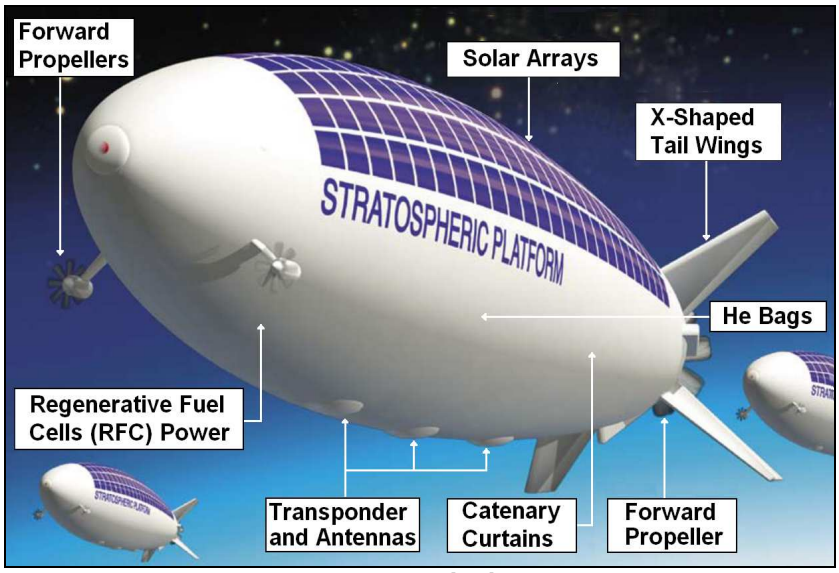

Figure 7. 10. SCP Airship by TAO 2006

A Research and Development (R&D) program on SCP airship is in progress since April 1998. The final goal of this project is to realize the SCP airship, being capable of a long duration station-keeping flight at about 20 Km in the stratosphere. The achievements will enable advanced wireless fixed and mobile communications, digital direct broadcasting, modern broadband transmission and high-resolution observations and monitoring of the remote, rural and global environment. This advanced SCP program is promoted in collaboration with the Communications Research Laboratory of Japan (CRL), National Space Development Agency of Japan (NASDA), Japan Marine Science and Technology

Centre (JAMSTEC) and the Telecommunications Advancement Organization (TAO) of Japan.

The stratospheric platform is an unmanned airship kept at a stratospheric altitude of about 20 km for multimedia communications, tracking monitoring and remote sensing. It is equipped with communications payload, observation sensors or other equipment. The SCP system is designed similar to a satellite space segment as a relay station to receive signals from ground stations using feeder links and to retransmit them to subscribers using service links. Therefore, an airship, like a satellite, is carrying a payload with corresponding transponders and antenna system. The launch of SCP into position is much simpler than putting a satellite into any orbit. After careful preparation in the hanger space, the airship is launched in 4 ascent phases through the troposphere and interface location point in the stratosphere and, finally, it shifts to the station-keeping position. The recovery phase goes in the opposite direction, namely, the airship is slowly moved from the station-keeping position towards the interface point and descends down to the ground in 4 descent phases (Aragon-Zavala et al, 2008).

The airship construction has a semi-rigid hull of ellipsoidal shape, with an overall length of about 200 m, as shown in Figure 7.10. It is composed of an air-pressurized hull for maintaining a fixed contour and internal special bags filled with the buoyant helium gas. Two air ballonets are installed inside the hull to keep the airship at a required attitude. For a load balance to the lifting force, catenary curtains are connected to the lower rigid keel, directly attached to the envelope. Propulsive propellers of SCP are mounted on both the stem and stern of the airship and tail fins are installed on the rear end of the hull. A solar photovoltaic power system of solar cells and Regenerative Fuel Cells (RFC) are provided to supply a day/night cycle of electricity for airship propulsion.

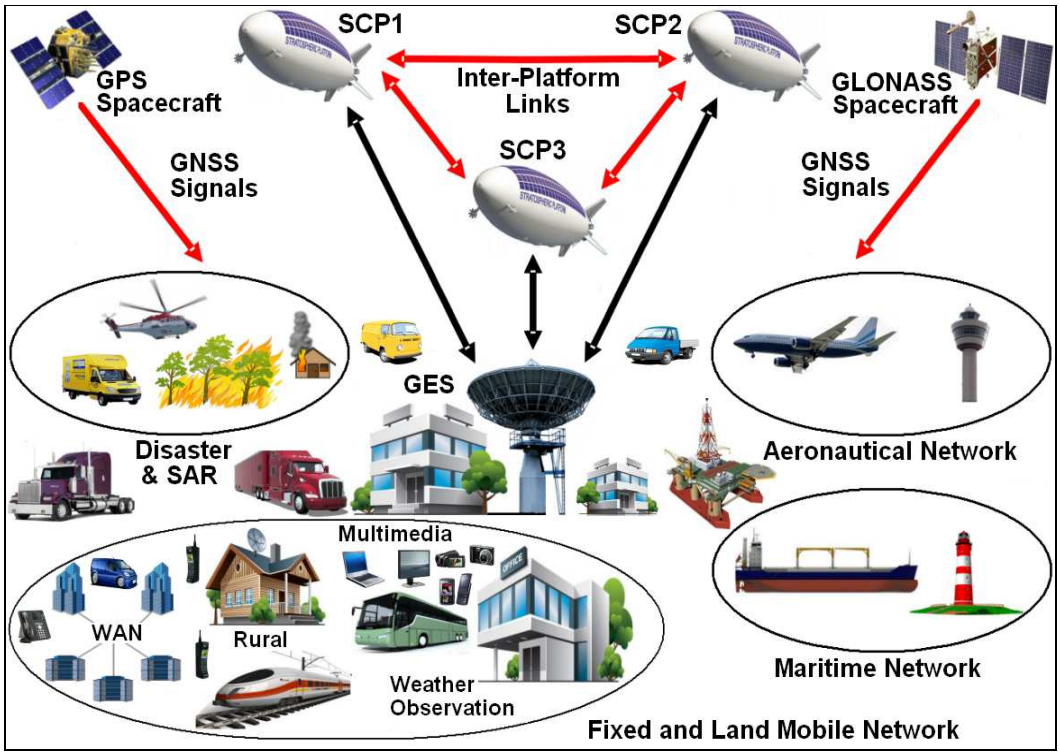

Figure 7. 11 Different Networks via SCP by Ilcev 2013

The length of an airship, in general, is about 250 m and 60 m diameter. This is about 4 times as long as the Jumbo jet passenger airplanes whose weight is about 32 tons. Thus, 50% of the weight corresponds to those of structures and membrane materials. Hence, solar arrays and fuel batteries, related to the electric power system, are also heavy. The weight of mission equipment is supposed to be about 1 ton.

The necessary condition for an airship to float at a certain altitude is that the gravity and buoyancy forces, which are exerted on the airship, are in a state of equilibrium. When the shape and volume of the airship are supposed to be constant, unlike a balloon, the buoyant force, at an altitude of 20 km, becomes about 1/15 that at sea level. Accordingly, a buoyancy of 15 times is necessary for equilibrium. Therefore, in order to float an SCP station in the stratosphere, it is necessary to make the weight of the airship light and to make the buoyancy as large as possible. Inside the airship, there are several internal bags filled with He gas to obtain enough buoyancy.

7.4 SCP Ground Segment

A complete inter-platform link, CNS, fixed and mobile broadband multimedia service, including a meteorological program with all applications, is presented in Figure 7.11. In fact, fixed ground terminals can be a self-contained portable or office PC configuration with a modem, or as an integrated part of an advanced LAN or WAN, laptop, video, fixed telephone set in office or public and mobile or cellular phone equipment.
On board the airship, there is mission equipment to provide Multimedia and Broadcasting for Fixed and Mobile communications including an Earth observation, Weather Monitoring and Disaster Monitoring System. So, the airship is expected to have the following features:

1) Communication, Navigation and Surveillance (CNS) network of GNSS augmented and not augmented systems, which can be useful for some meteorological solutions and have been proven to improve the accuracy of weather prediction models.

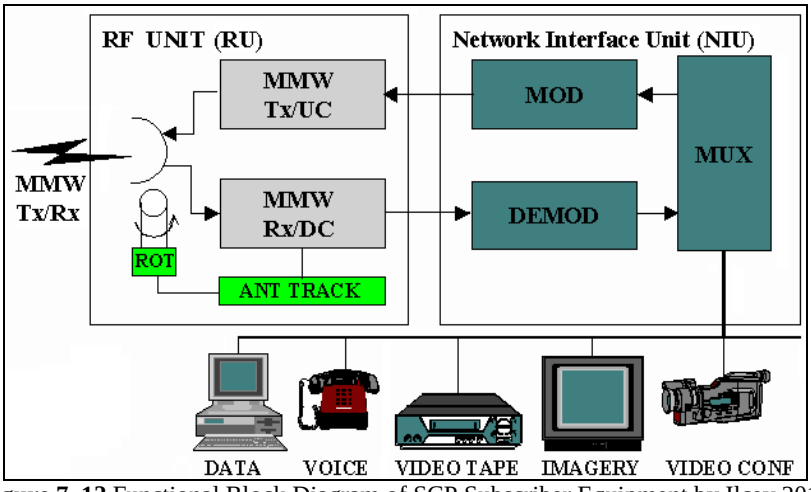

Figure 7. 12 Functional Block Diagram of SCP Subscriber Equipment by Ilcev 2013

2) Broadband communications and broadcasting of Voice, Data and Video (VDV), including weather imaging, are possible with small-sized and very low-power terminals, because of much shorter propagation distances compared with satellite systems.
3) High-quality, reliable and very cost-effective space communications and broadcasting are possible with a smaller number of ground stations, due to significantly better LOS

conditions, less wave-blocking and multi-path effects compared with existing ground telecommunication systems. Meanwhile, compared with satellite systems, the propagation distance of SCP is shorter by about 1/1800. Consequently, as Electro Magnetic (EM) radiation propagation losses and delay distortions become much smaller, and broadband platform communications and broadcasting are possible with smaller sized and lower power fixed and mobile terminals.

4) By establishing Interplatform Links (IPL), high-speed communications and broadcasting networks, comparable to optical fiber systems will be possible, including different novel communications.

5) Optimum communication configurations links are possible owing to the flexible operations of airship SCP systems, which can enable expansion to a world fixed, mobile and military communications system, including weather observation.

The CSP system is designed for fixed and mobile multimedia two-way communications systems. In addition, various remote-sensing and weather observation services will be available for radio wave observations, aerial photographs, meteorological imaging and so on. The ground segment consists of GES or Gateways and fixed, semi-fixed and mobile terminals, with onboard corresponding auto tracking and focusing antenna systems for all applications, respectively.

Mobile systems for CNS via GES will offer maritime, land, aeronautical and personal applications including GNSS access. At this point, mobile user terminals can be PC/laptop portable or fixed configurations interfaced to the SCP transceiver with adequate antennas or self-contained mobile or portable/in vehicle transceiver units with mobile auto tracking antenna and personal handheld terminals with built-in antenna.

In Figure 7.12 shows the prototype of fixed and mobile SCP equipment and their services. The mobile SCP equipment and system will provide two-way commercial, distress, emergency and safety communications for ships, fishing boats, road vehicles, rails and aircraft integrated with GEO and GNSS systems. In the framework of this service, there will be additional activities like buoy and lighthouse control, marine pollution, investigation, warnings and Search and Research (SAR) missions. Figure 7.12 shows the prototype of fixed and mobile SCP equipment and their services.

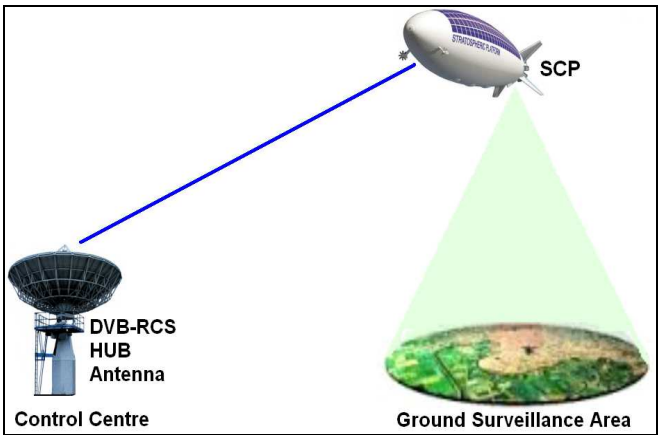

Figure 7. 13 Weather Observation via SCP Station by Ilcev and Sibiya 2015

Land mobile equipment and systems will provide services for all kinds of vehicles like trains, buses, trucks and cars, including personal mobile units, cellular service and emergency

communications for natural disasters, which can be enhanced with equipment for tracking and navigation facilities. The SCP has to substitute or integrate current cellular systems.

Aeronautical mobile equipment and systems will provide commercial, safety and distress service for all kinds of aircraft integrated with GEO, GPS and other GNSS to provide CNS networks and service.

The broadcasting system using the SCP airship constellation will provide: **1)** digital broadcasting; **2)** complementary terrestrial digital broadcasting to fixed and mobile SCP stations; **3)** terrestrial rebroadcasting programs; **4)** relay broadcasting of HDTV including radio programs; **5)** movable broadcasting on demand, using mobile equipped stations; **6)** broadcasting for limited suburban regions, isolated islands, rural and remote places; **7)** field pickup from the SCP; and **8)** emergency news and observations.

7.5 Weather Observation and Communication of Data via SCP

Weather satellites carry different types of onboard cameras, Space Synthetic Aperture Radar (SSAR) and other instruments pointed toward Earth's atmosphere and surface. They can provide advance warning of severe weather and are a great aid to weather forecasting.

Observations and monitoring of the entire Earth's atmosphere, ocean, land and the related environment via stratospheric platforms form the foundation for the production of weather, climate, water and related environmental services. Development of weather and climatology observations via stratospheric platforms, as presented in Figure 7.13, requires deployment of one or more HAP airships or even UAV aircraft with adequate equipment onboard. Onboard SCP spacecraft is necessary to deploy onboard communication payload, which contains a transmitter, receiver and antenna known as a transponder. Payloads may carry satellite transponders, such as Transparent or Bent-pipe and more complex Regenerative transponder or modern VSAT Spacecraft Transponders, for Digital Video Broadcasting-Return Channel via Satellite (DVB-RCS) service. On the other hand, SCP needs some sort of control, monitoring and maintenance of payload, transponders, propellant system, electrical power, correction of position and maneuvering. In effect, to provide all the above-listed requirements, SCP also incorporates Telemetry, Tracking and Command (TT&C) remotely to transmit data and maintain redundant systems to serve as back-up measures, and features that are designed to provide SCP with a high level of availability, reliability and safety.

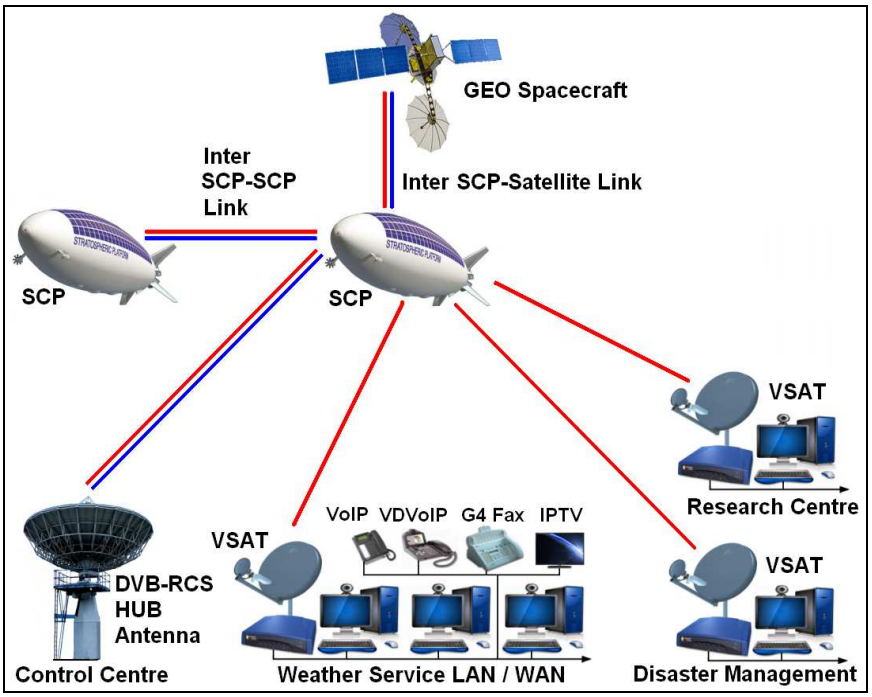

Figure 7. 14 Space/Ground Segment via DVB-RCS for Weather Observation by Ilcev and Sibiya 2015

The position of SCP is usually higher than all commercial flight corridors, so,practically, airships do not interfere with commercial aircrafts' flights, because they are located over 10 km. Airship itself leverages Lighter-Than-Air (LTA) technology which is made of very high strength and lightweight materials. It is accompanied by advanced propulsion systems that maintain proper positioning and equipped with autonomous navigation, radio-controlled command and communications payload stabilization systems.
The stratospheric airship is launched using a specified volume of helium separated from the air to maintain its shape. As the SCP rises, the helium expands and, at the proper altitude, displaces all of the air within the platform. Once it is in the stratosphere, the SCP is remotely controlled and moved into a right determined position. A combination of solar cells, batteries and fuel cells will power the SCP during its minimum 6 months planned deployment.

Thus, the SCP airship is being designed to hold approximately 1,000 kg of communications payload accompanied with other onboard subsystems for surveillance and weather remote sensing, imaging and observations capable of supplying fixed ground stations and observatories by meteorological data and images. On the other hand, the main SCP configurations can be dynamically changed in very short time, to reallocate capacity, to reprogram tasks and to provide new requirements as needed.

The meteorological information, images and climate observation data are essential for weather and forecasting observation centres, which will conduct research to improve services, assessing changes in the climate system and for developing and new operating structures. This will improve information for weather and climate dependent sectors such as agriculture, forestry, water, transport, tourism, construction, mining and energy, in support of communities' efforts to reduce disaster risks and to adapt for climate variability and changes. Meteorological observation and weather monitoring via SCP airships is also one of the pillars of the global framework for climate services.

The proposed space segment for weather observation and communication network for transmission of data and images comprises SCP airships and GEO satellites with Very Small Aperture Terminals (VSAT) Spacecraft Transponders, as shown in Figure 7.14.

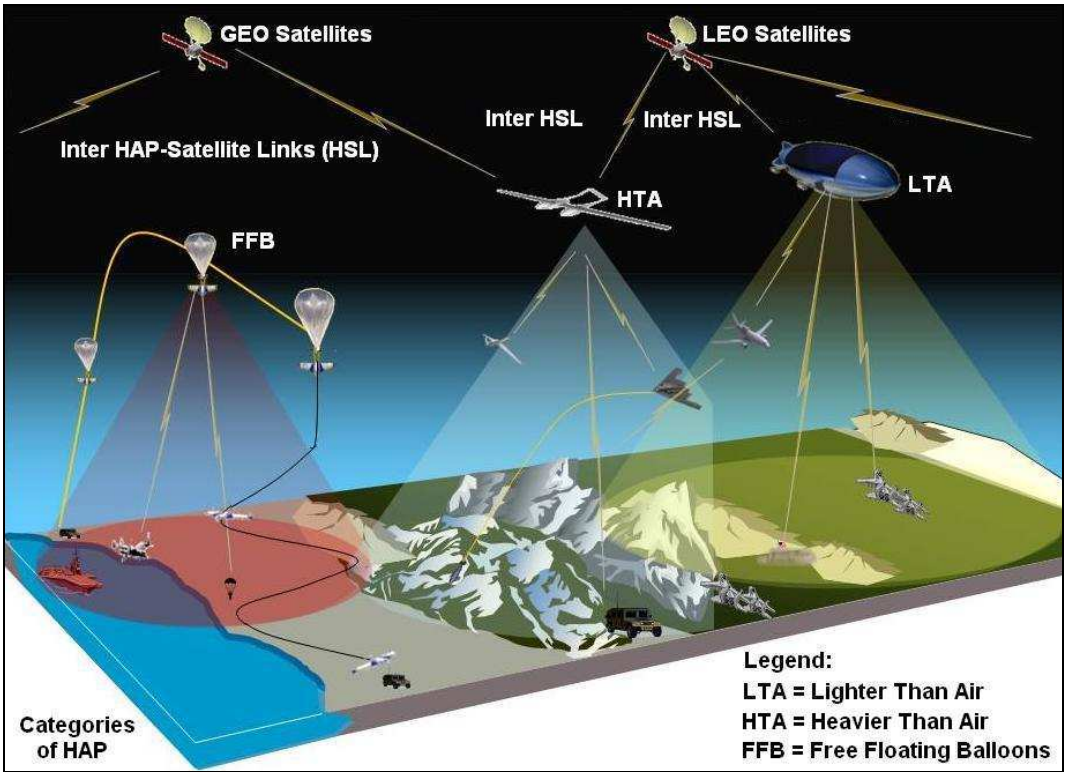

Figure 7. 15. Integrated Satellite and SCP Networks by Ilcev and Sibiya 2015

The communication between these SCP stations and GEO satellites is via optical links. In fact, SCP space stations receive weather and observation data from GEO satellites and forward the data to the HUB antenna and Control Centre via up-links (red lines) and down-links (blue lines). Thus, the ground segment is composed of the DVB-RCS HUB antenna, Control Centre connected to the remote VSAT stations, such as Research Centre, Disaster Management, Weather Service LAN/WAN and other observation and weather centres. Ground Control Centre is dedicated to control ground HUB with antenna, manage SCP stations and provide very redundant and reliable data transfer and backup.

The connection between the VSAT ground segment and the SCP stations is established via Digital Video Broadcasting - Return Channel via Platform (DVB-RSP) similar to DVB-RCS scenario. The connections between VSAT modem is conducted via LAN or WAN and new WiFi or WiMAX to the peripheral of equipment such as Voice over IP (VoIP), VDVoIP, G4 Fax and IPTV configurations. Otherwise, the principal task of the ground Control Centre is to process, backup meteorological information and disseminate processed data to weather and forecasting. It also monitors and manages the operations of the stratospheric platforms.

7.6 Integrated Satellite and SCP Networks for Weather Observation

The modern SCP network, as presented in Figure 7.13, will be deployed together with terrestrial and GEO/LEO and even Medium Earth Orbits (MEO) satellites networks to provide another degree of flexibility for system integration that can be easily adjusted to the

needs of the weather and metrological observations and forecasting. In fact, SCP stations will play a complementary role in future weather and forecasting infrastructures such as Free Floating Balloons (FFB), Heavier Than Air (HTA) and Lighter Than Air (LTA) satellites. This integration may be also interfaced with the existing terrestrial, cellular and mobile systems to provide easy deployment and roll out of the 3G and beyond 4G services.

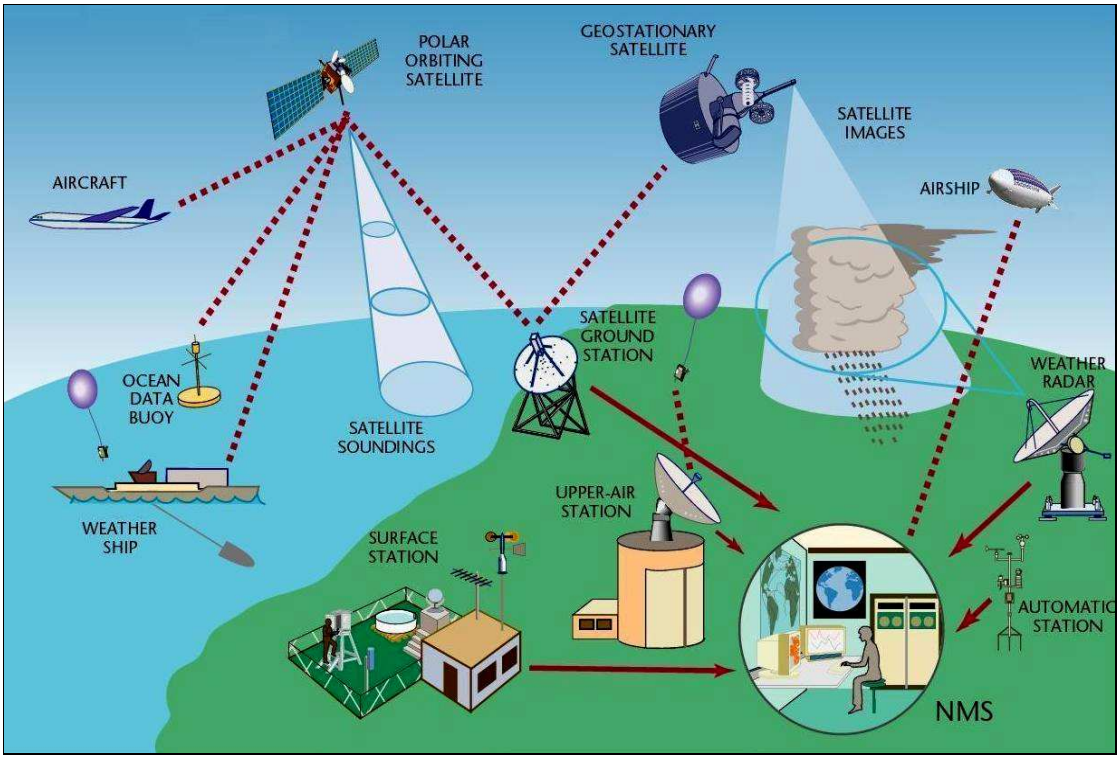

Figure 7. 16 Global Integrated Weather Observing System and Network by Ilcev and Sibiya 2015

The modern integration of advanced multimedia service over heterogeneous networks is one of the key objectives in the development of future communication systems for weather and observation integrations. Anyway, satellites have played an important role in some niche markets, such as navigation and localization services, broadcast and some specific applications such as Earth observation and remote sensing. However, despite its advantages in terms of coverage and bandwidth, the level of penetration of infrastructures of satellite communications in the current telecommunications infrastructure is still low. Two of the main limits in the performance of satellite broadband communications are the throughput degradation of TCP/IP over the existing satellite links, as well as the limited satellite capacity in point-to-point mode (Fidler et al, 2010).

While SCP stations present some advantages over satellite and terrestrial systems, they present some limitations as well. For example, SCP coverage area is limited to a radius of approximately 200 – 400 km considering an elevation angle of 15º. Therefore, all these negative effects and disadvantages of GEO/PEO satellites and SCP stations will be lees presented if proper integration occurs in the future, as shown in Figure 7.16.

7.7 Typical Aspects of SCP Orbital Parameters, Coverage and Data Rates

Orbital parameters are important considerations in the design of a typical SCP station. For remote sensing and observation applications, the PEGASUS platform orbital design concept

could be considered as a viable option. In particular, a summary of the orbital parameters is given in **Table 7.4**, and the orbital period equation is as follows:

$$T_0 = 2\pi (R_p + H) \sqrt{R_p + H/g_s R_p^2} \quad (7.5)$$

Where H = satellite orbital altitude; R_p(~6378 km) = radius of the Earth and g_s (~9.81 ms^{-2}) = gravitational acceleration. This equation can be re-written as in the following equation:

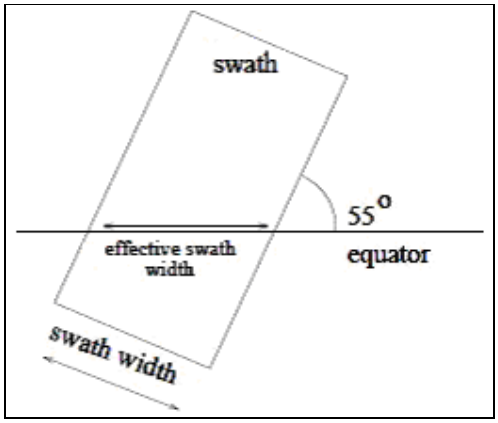

Figure 7. 17. Swatches at Equator Crossing by Ilcev 2011

Table 7. 4 Orbital and Design Parameters

Orbital Parameter	Value	Remark
Orbital Period		T_0
Inclination Angle	55^0	
Altitude	14 -20 km	
Revisit Time	16 per day	
Spatial Resolution	20 cm	
Data Transmission		Consider Tracking and Data Relay Option

$$T_0 = 2\pi r \sqrt{r/gR_p^2} \quad (7.6)$$

where r(=h+R_p) is the satellite distance from the Earth's centre. Accordingly, for SCP h~18 km, the approximate orbital period is 1.4133 hours. The orbital velocity of this satellite is derived from the following equation yielding a value of approximately 7879 ms^{-1}:

$$v = \sqrt{gR_p^2/r} = 2\pi r/T_0 \quad (7.7)$$

Now suppose that the SCP system considered has a swath width (w) of 50 km (see Table 7.4), the minimum number of ascending passes required to cover the entire equator is calculated by dividing the perimeter of the equator by the effective swath width (this is the length along the equator covered by the swath crossing at a given inclination angle). Given that the inclination angle (θ) is 55^0 and w is 50 km, the effective swath width (w_e) is ~61 km based on equation:

$$w = w/\sin\theta \quad (7.8)$$

Figure 7.17 shows swath and effective swath values' width at the equator crossing of SCP airships. The perimeter of the equator is 40074 km, which are presented by the following equations, whose minimum number of ascending passes is ~657:

$$P = 2\pi R_p \quad \text{and} \quad P_a = 2\pi R_p / w_e \tag{7.9}$$

By considering both ascending and descending passes, the satellite swath width crosses the equator twice in every orbit implying that the required time is cut to half. The time required to acquire the calculated coverage can be calculated from the following equation, yielding approximately 38.68 days:

$$T_c = P_a \cdot T_0 \tag{7.10}$$

To calculate the data rate, the pixel spacing and resolution, the number of spectral channels and sampling bits has to be taken into consideration. In the present case, the SCP system has a pixel spacing of 30 m, the data rate (at one byte samples) for the different channels (say 5) is measured in area covered per unit time. The rate of coverage (r_c) and coverage per orbit (c_0) are calculated as given in the following relation. In this regard, the area covered per orbit is obtained as ~2.44 *10^6 km^2:

$$Rc = v w_e R_p / r \quad \text{and} \quad c_0 = 2\pi R_e w_e \tag{7.11}$$

If it is approximated that there are 16 orbits per day, then the SCP acquires an area of 3.9113 *10^7 km^2 per day. In order to calculate the data rate (d_r), the number of lines per second (l_s) is multiplied by the number of samples per line (s_l), the bits per samples (b_r) and the number of channels (N), as expressed in the following equation:

$$d_r = v R_p / r \cdot w_e / r_p^2 \cdot N b_r \tag{7.12}$$

7.7.1 Sensor Characteristics

Given the number of necessary sensor system onboard SCP stations, a push-broom system configuration is proposed. Thus, the sensor types are determined by the target applications.
In this instance, a suite of satellite sensors consisting of Minimum Distance Classification (MDC), Light Detection and Ranging (LIDAR), Digital Thermal Monitoring (DTM) and Synthetic Aperture Radar (SAR) will be capable of providing remote sensing applications ranging from Earth observation (mapping, fires, crop monitoring, crisis management due to, e.g., flooding) and atmospheric remote sensing (e.g., water vapour and aerosol studies). The sensor specifications are given in **Table 7.5.**

Table 7. 5 Suit of Proposed Sensors

Sensor type	Bands	Spatial
MDC	20 bands in NVIR	20 cm
LIDAR		
DTC	2 thermal IR	1.5 m
Bi-SAR		2.5 m

7.7.2 Data Analysis for Remote Sensing Applications in SCP

Using data analyzes will be possible to solve some non-linear nature problems in space observations, such as ozone, aerosol and water vapour and clouds.

7.7. 2.1 Non-linear Nature Problems in Remote Sensing

Desired phenomena of interest in most remote sensing applications are a function that manifests in a quantity that is remotely or indirectly observed. For instance, recovery of a geological structure is possible through seismic exploration while recovery of the atmospheric vertical structure is through satellite/SCP observations of upwelling radiation. Additionally, the recovery of aerosols in the atmosphere is through particle size distributions, which have unique signature of scattered radiation or cross-sectional information. In all these examples, information retrieval for atmospheric or the Earth's system can be modeled simply as:

$$S = F(M) \tag{7.13}$$

Where S = signature when EM waves interact with a medium (M), F = functional (non-linear, in most instances) that describes absorption, scattering, emission or even polarization. Thus, the concern of remote sensing is to characterize M and this is only true taking the inverse of above equation. Since the medium under investigation often consists of many unknown parameters, it leads to the same radiation signature emanating from various physical combinations. Hence, the inverse problems in remote sensing are inherently difficult to solve because the solutions are non-unique. However, the following analysis demonstrates the background to scientific information retrieval from SCP data for various atmospheric studies. This complex analysis will be limited to water vapour, aerosols and cloud characteristics.

Considering sunlit incident at the atmosphere and SCP measurement system located in the stratosphere, the scattered radiation is given as:

$$dF_\lambda(z) = F_\lambda dz \sec\theta \left[k_\lambda \rho(z) + \sigma_{s,R}(\lambda) N(z) + \sigma_{e,m}(\lambda) N_a(z)\right] \tag{7.14}$$

Where values θ = solar zenith angle, k = absorption coefficient associated with molecules, ρ = density of molecules, while values σ_s and σ_e are the Rayleigh scattering cross-section and Mie extinction coefficient, respectively. The number of molecules and aerosols at a given height z are given by N(z) and $N_a(z)$, respectively. The following equation is the solution to the previous equation with the following relation:

$$\ln\left[F_\lambda(0)/[F_\lambda(\infty)]\right] = -\int_{\infty}^{0} k(\lambda)\rho(z)\sec\theta dz - \left[\tau^R(\lambda)\sec\theta + \tau^M(\lambda)\sec\theta\right] \tag{7.15}$$

Where $\tau^{R,M}$ = optical depths associated to Rayleigh/Mie scattering/extinctions.

1. Ozone –Equation (7.14) solves the problem with K(λ) and ρ(Z) being the absorption coefficient due to ozone and density of ozone at altitude Z. However, the following equation is used to retrieve total ozone in the atmosphere:

$$\Omega = \int^{\infty} \rho(z)\, dz \tag{7.16}$$

Given that the ozone is concentrated around ~22 km, then θ≡Z (the solar zenith angle at 22km). The SCP sensor system ought to be tuned to resolve the ozone absorption band (also called the Hartely-Huggins). However, at this absorption band, there is also some absorption from other atmospheric molecules. Taking the differences of equation (7.15) at two wavelengths where the aerosol optical depths will be considered equal and substituting in Equation (7.16), results in the following equation:

$$\Omega = \{\ln[F_{\lambda 1}(\infty)/F_{\lambda}(\infty)] - \ln[F_{\lambda 1}(0)/F_{\lambda}(0)] - m[\tau^{R}(\lambda_1) - \tau^{R}(\lambda_2)]\}/\sec Z\,[k(\lambda_1) - k(\lambda_2)] \quad (7.17)$$

In this equation, only the unknown quantities, i.e., $F_{\lambda 1,2}(0)$, can be measured on the ground by, e.g., Dobson spectrometers.

2. Aerosols – To retrieve aerosol information, it will be necessary to set molecular absorption to zero and the solution reduces to the the following equation:

$$F_{\lambda}(0)/F_{\lambda}(\infty) = e^{Q} \quad \text{where } Q = [-\tau^{R}(\lambda) - \tau^{M}(\lambda)]\,m \quad (7.18)$$

Where τ^{M} is a function of the number of particles as well as the particle size distribution and can. therefore be solve for while τ^{R} is theoretically calculated.

3. Water Vapour and Clouds – Cloud and precipitation properties are often retrieved from satellite observations based on what is commonly referred to as forward models. There are three main classes of these forward models. The first class consists of determining the property of clouds measuring the transmission at predefined radiation source attenuation. In the second class, emission from of IR and/or microwave radiation is used to characterize the property under investigation. However, in the third class, scattering radiation from clouds and precipitation is used to derive their inherent properties.
The amount of precipitable water vapour in the path of the sun to SCP can be derived from measurements of incoming solar flux at two wavelengths in the Near Infrared Radiation (NIR) water vapour band. Firstly, the outside of the water vapour band (λ_1) is given by:

$$F_{\lambda 1}(0)/F_{\lambda 1}(\infty) = e^{Q} \quad \text{where } Q = [-\tau^{R}(\lambda 1) - \tau^{M}(\lambda 1)]\,m \quad (7.19)$$

The solution to Equation (7.15) for the water vapour band (λ_2) is given by;

$$F_{\lambda 2}(0)/F_{\lambda 2}(\infty) = e^{Q} \quad \text{where } Q = \{[-\tau^{R}(\lambda 2) - \tau^{M}(\lambda 2)]\,m - K\sqrt{\mu M}\} \quad (7.20)$$

Where μ = the precipitable water vapour, $K\sqrt{\pi S_0 \alpha/\delta}$, so α and δ being the mean line intensity, half-width and spacing, respectively. One can solve for μ if the extinction of molecules and aerosols are closely identical, in which case the dividing equation (7.19) and (7.20) gives:

$$\mu = (\ln q_0/q_{\infty}/K^2 M; \quad q_0 = F_{\lambda 2}(0)/F_{\lambda 1}(0); \quad \text{and} \quad q_{\infty} = F_{\lambda 2}(\infty)/F_{\lambda 1}(\infty) \quad (7.21)$$

In order to remote sense clouds, one ought to understate cloud particle size distribution, complex index of refraction, particle phase, particle size and cloud optical depth. However, cloud reflection properties near the absorption band (i.e., the visible wavelengths) are dependent on optical depth (this is the cloud optical depth). Reflection from clouds at NIR wavelengths is largely dependent on cloud particle size. In the following presentation, we derive observation equations for the most important parameters that characterize the radiative

properties of clouds, i.e., optical depth (τ), particle size or effective radius (r_e) and the Liquid Water Content (LWC). In order for SCP to have this capability, the sensors ought to be able to resolve the emission and/or the multiple scattering. In this case, the attenuation of the initial radiance as the radiation passes between the cloud base and cloud top is manifests optical thickness of the cloud layer given by the following equation:

$$\tau_\lambda = \int_{z^b}^{z_t} b_{e,\lambda}\,(z)\,dz \qquad (7.22)$$

The extinction coefficient is then given by the following equation:

$$b_{e,\lambda} = \int_0^{\lambda} Q_{e,\lambda}\, A_r\, N_r\, dr \qquad (7.23)$$

where values $Q_{e,}$ N_r and A_r are the efficiency factor, particle size distribution and project area, respectively.
This, considering water drops with radius r, $A_r \sim \pi r^2$ and $Q_e \sim 2$ (this is a geometrical optics approximation). As a result, equation (7.23) reduces further and substituted into Equation (7.22) to obtain as follows:

$$\tau_\lambda = \int_{z^b}^{z_t} 2\pi \left[\int_0^{\infty} r^2\, N_r dr\right] dz \qquad (7.24)$$

The liquid water content, on the other hand, is retrieved based on differential emission of microwave radiation by clouds and water vapour. In particular, the retrieval algorithm shown in equation (7.26) is based on the inverse of the general radiative transfer given in equation (7.25), where τ, I_b, and μ are the optical depth (derived from absorption), the radiance of surface below the cloud layer and cosine of the view angle, respectively. Furthermore, $B(T_c)$ is the plank blackbody function referenced to a cold temperature T_c given by:

$$I_{obs} = I_b e^{-\tau/\mu} + b(T_c)\,[1 - e^{-\tau/\mu}] \qquad (7.25)$$

$$\tau = -\,\mu \ln\,[T_{obs} - T_c/T_b - T_c] \qquad (7.26)$$

The microwave optical depth is given as the sum of water vapour contribution, the liquid water droplet contribution and contribution from other gases. These contributions are given as term one, two and three, respectively, in the following equation:

$$\tau = KvW + K_l LWP + \tau_g \qquad (7.27)$$

7.7.2.2 Retrieval Algorithms for Remote Sensing and Earth Observation for SCP

The information retrieval algorithm will be different for each sensor type. Therefore, two categories of information retrieval algorithms suitable for SCP are proposed. Category one consists of a suite of algorithms for atmospheric remote sensing (Stephens and Kummerow,

2007). Additionally, Kokhanovsky (2002) reviews modern aerosol retrieval algorithms based on reflected solar light intensity and polarization.

For category two, the algorithms are dedicated for earth observation including land surface temperature, flood and fire detection. Thus, Earth observation retrieval algorithms have been widely used. For example, the Moderate Resolution Imaging Spectroradiometer (MODIS) active fire detection algorithm, described by Giglio et al, (2003) which uses brightness temperatures derived from MODIS 4µm and 11 µm, has been reported in numerous literature studies. The algorithm utilizes a number of reflectance channels and set conditions to classify each pixel as fire, non-fire, missing data, water and unknown pixels.

The SCP can be involved in active fire detection observation and will consider a similar, yet improved detection rate. Some of the instruments deployed onboard the SCP airship are the SAR and LIDAR systems. In this regard, these sensors would be utilized to detect floods and flood extent based on the near-real time flood detection algorithm using a split-based automatic thresholding procedure reported by Martinis et al,(2009); Martins (2011); Martins (2011) and Cossu (2009).

Figure 7. 18 Samples of Visible, Infrared and Vapor Images via Satellite by NOAA 2009

7.8 Satellite Imagery Instruments onboard SCP Stations

When a sensor onboard satellite or airship looks down at the Earth, it senses the radiation from an elliptical area within the sensor's field of view. Operational forecasters use three main types of satellite meteorological imagery, such as: Visible (VIS), Infrared (IR) and Water Vapour (WV), which are described in **Chapter 6**. All three types can be installed onboard SCP stations and used as imaginary instruments. Figure 7.18 shows samples of VIS **(Left),** IF **(Middle)** and WV **(Right)** images done by NOAA meteorological satellites. Thus, to provide a complete image of US territory via SCP stations, it will be necessary to deploy about 40 airships in the stratosphere. The resolution of images made via the ACP airship should be much better, because one airship, for instance, will cover the area of Florida.

As the sensor scans across the landscape, the individual fields of view are composited into the geographical image used by weather forecasters. Thus, this field of view determines the image resolution. Strictly speaking, image resolution refers to the smallest viewable area at the satellite's subpoint. Thus, the field of view gets larger as you move away from that subpoint. The resolution varies with wavelength and instrument type. In general, visible imagery resolution is around 2.5 km while IR imagery resolution is around 5 km.

Single onboard airship images are useful in analyzing what is happening in the atmosphere, but a series of images, shown in sequence, i.e., animated, often reveal features that may not be obvious from one image alone. When an observer views image animation, he/she doesn't need to capture the entire image at one time. It will be necessary to focus on one feature and

follow it for several loops, and then has to switch to another feature and view it. This approach allows observer to see more detail in the satellite animation.

1. Basic Interpretation of Visible Imagery - Visible imagery is derived from solar radiation reflected from the Earth and atmosphere. The radiation is in the 0.4μ - 0.7μ range. Images are available during daylight hours, while some satellites can sense low intensity visible light at night, but these data are not routinely used by operational meteorologists. The standard VIS imagery is black and white in colour. White is used for the brightest and most reflective energy received by the sensor, while black displays the least reflective values. Shades of grey are used between the two extremes. The brightness sensed by VIS depends upon the albedo of the underlying surface, the intensity of the solar beam (which is a function of the day of the year and the solar angle) and the relative position of the Sun and the satellite. The relative brightness implies something about what observers are viewing on the VIS image. However, low brightness is associated with the ocean, lakes and the background Earth while medium brightness values come from land, including forests and deserts areas. Clouds produce high brightness, displayed in white or light grey. Thus, with the better resolution available in VIS imagery, you often see some vertical structure in the clouds and cloud layers. For example, the shadow of one layer upon another is frequently seen around sunrise and sunset when the solar angle is low. Thunderstorm tops that protrude above the anvil can also be seen. Cloud texture and cellular patterns are easily distinguished.

2. Basic Interpretation of Infrared Imagery – The IR or conventional thermal infrared imagery is derived from terrestrial radiation emitted by the Earth, cloud tops and entire atmosphere in the 10μ - 12μ range. It is available 24 hours a day. Values are a measure of the temperature of the emitting surface, with some modification due to absorption and reemission as the radiation passes through the atmosphere. The standard IR display was black and white in the early days of imagery, but later has been modified with colour enhancement for easier interpretation. On the black and white scale, white is used for the colder temperatures and black for the warmer clouds. Thus, this scale choice allows clouds, which have colder tops, to appear white, similar to the white associated with clouds on visible imagery. Temperatures also allow the relative height of the cloud tops to be estimated. However, image enhancement is a process that modifies the infrared temperature values with colours or shades of grey to emphasize specific features and improve interpretation. The concept of image enhancement is used with many image types including radar and non-weather data. The enhancement process of images displays specific colours (or shades of grey) for specific temperature bands. Colours for adjacent bands are selected to maximize the contrast between bands. This selection of colours tends to emphasize or enhance specific features on the image.

3. Basic Interpretation of Water Vapour Imagery - Water vapour imagery is derived from radiation emitted by water vapour at wavelengths not in an atmospheric window in range of 6μ - 7μ, and is available 24 hours a day. The stronger the signal seen by the WV sensor, the higher in the atmosphere is the moisture located. Most WV radiation originates from moisture in the upper troposphere (600-300 mb layer). If the upper troposphere is dry, WV radiation can come from layers as low as 800 mb. The standard WV display is in black and white but, as with the IR, is usually colour enhanced to highlight specific features. On the black and white scale, white is used for higher sensor values implying more moisture in the upper troposphere. Darker colours indicate that the upper troposphere is dry and that radiation from moisture in the lower parts of the troposphere is reaching the satellite.

7.9 Satellite Optical Downlink and High Data Link via SCP

Optical links offer significantly higher bandwidth, but they are blocked by clouds. As a consequence, downlinks from satellites to a ground station have a limited availability depending on the cloud situation over a site. For non-Earth Observation (EO) application like communications or broadcast, a nearly hundred percent availability is required for the satellite link. This problem can be solved by using a relay station in the form of an SCP, which has to be positioned above the clouds in about 20km altitude.

Besides, an optical link from the satellite to the SCP would have 100% availability, as it is not hindered by clouds. The final "last mile" to the ground could then be bridged by a standard MW point-to-point link as used today in terrestrial applications, but with a large bandwidth compared to a satellite link due to the short distance. An optical link parallel to the MW link could increase the bandwidth of the last 20km several times during cloud-free conditions.

Link availability to the GEO satellite would be about half of the LEO orbit, i.e., about 12 hours per day. From the GEO satellite, the data would be transmitted on a continuous link to the SCP airship stations. The increased link duration would be at the cost of significantly longer link distances with a more stringent link budget and the additional expenses of a GEO satellite.

For the meteorological communication scenario of integrated space, GEO, LEO and SCP airships and aircraft will be anticipated via a mobile ad-hoc network consisting of several Optical Ground Stations and optical mobile stations, such as ships and airplanes, which are illustrated in Figure 7.18.

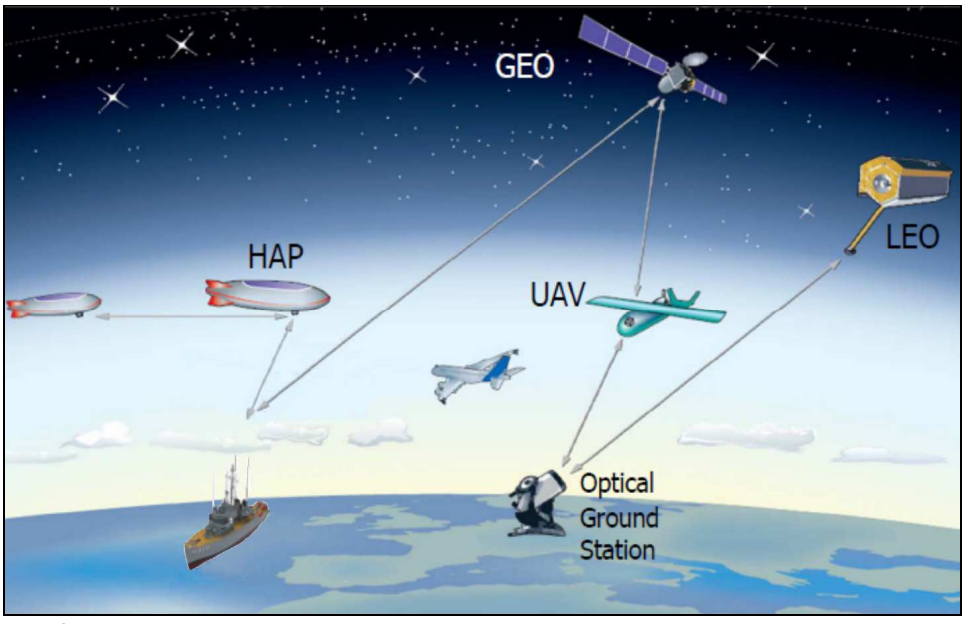

Figure 7. 19 Future Space Meteorological Integrated Optical Links via SCP Stations by Ilcev 2013

Typical link distances can be read out of Figure 7.19. For inter-SCP connections, maximum distances are in the range of 400 km. For long links, it is important to ensure that the lowest point of the link will not be too close to the ground. In general, link blockage probability due

to clouds increases with lower altitudes. Without considering unfrequented weather situations like thunderstorms, thick clouds typically occur below 6 km altitude.

Each SCP station optically connected to satellites can be seen as a network node and some are connected to the terrestrial network via RF satellite-links. When direct downlinks to terrestrial nodes are required. These should preferably be realized with microwave frequencies due to the high probability of cloud blockage of optical downlinks. While optical signals can transverse thin clouds in the upper troposphere (with some Decibel attenuation penalty), the thick water clouds in the lower atmosphere act as opaque obstacles.

The Free-Space Optics (FSO) applications are less favourable for supporting meteorological transmissions via SCP stations, due to the intrinsic limitations of the FSO communication systems, in particular limited availability due to link blockage (e.g. from clouds for altitudes lower than 10 km) and latencies (between tens of milliseconds to several seconds depending on the link topology) due to link establishment procedures. The main use of FSO systems should be for connections from or into the terrestrial data networks via SCP and satellites and for interconnection between ACS en-route that cruise above the cloud layer. Application areas and scenarios for meteorological optical communication are inter-SCP stations links that are used to build up an ad-hoc network in high dense areas. Optical connection of SCP stations with the ground stations or while climbing is less reliable due to high cloud blockage probability for the space optical link. Finally, high-speed connections to the space-backbone meteorological communications network via SCP or satellites are also supposable.

CHAPTER EIGHT

GROUND SEGMENT

This chapter recalls the reasons why the ground segment of meteorology and climatology is so important to the global Weather (WX) system, including economy and the contribution of meteorological satellites and the new stratospheric platforms to those disciplines.

One of the major functions of the meteorological satellite and stratospheric platform systems is the collection of daily environmental data from Data Collection Platforms (DCP). This co-ordination, needed to define a truly international system of data collection from these space meteorological structures, has been conducted under the auspices of the Coordination Group for Meteorological Satellites (CGMS) The International Data Collection System (IDCS) Users' Guide contains a complete description of the international system. In fact, it provides specifications and guidelines for the design of space meteorological platforms, describes the procedures for certification and admission and details the operational support provided for these platforms.

8.1 Introduction

Meteorological observations via satellites and new stratospheric platform solutions, data and services have become essential for both meteorology and climatology, continuing the two fundamental concepts of data exchange and international cooperation, which have been traditional for more than 150 years. They provide vital data at frequent intervals over wide areas, in the context of the international cooperation needed to ensure adequate worldwide data coverage. Thus, co-operation in the establishment meteorological satellite systems exists at three levels. The first level is local through one country only willing to establish short-range coverage for collecting meteorological data from the stratospheric aircraft or airships. The second level is the regional level through one country or those countries, which have come together to establish their own meteorological satellite system that ensures the continuity of the weather system and the availability of data over nearly one quarter of the planet. The third level of co-operation is on a global scale of integrated local and regional meteorological satellite and space platform systems, which ensures the availability of satellite and platform data over the entire Earth (Haan, 2008).

Satellites provide all countries worldwide with a unique and long sought after opportunity to look at Earth from space. These spacecraft now enable ground meteorological stations to observe and measure the many forces of nature, which converge on our planet. Mankind can now observe the global nature of the environmental and weather factors which interact to form the complex systems we call Earth. In fact, from the unique vantage point of space, sophisticated environmental and weather satellites are able to bring information about cloud formation and movements, precipitation amounts, temperatures, ocean currents, sea surface temperatures, air and water pollutants, drought and floods, severe weather/storm conditions, vegetation, insect infestations, ozone content of the atmosphere, volcano eruptions and other factors that affect our daily lives. They have also provided us with less tangible aesthetic values, which help shape attitudes about the environment of this planet. This global attitude is, perhaps, just as important as the hard data that the satellites and platforms may provide.
Much of this information is transmitted from meteorological satellites or platforms via direct readout to ground stations where it can be displayed and analyzed. The direct readout service

is pioneered more than 45 years ago by the first weather satellites and have been expanded and operated in the US by the National Oceanic and Atmospheric Administration (NOAA).

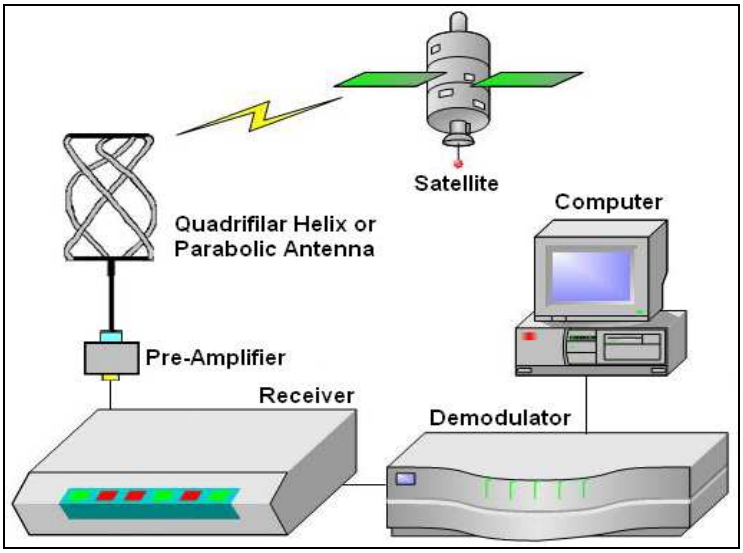

Figure 8. 1 Direct Readout GES by NOAA 2009

8.1.1 Direct Readout Ground Earth Stations (GES) Infrastructure

Thousands of direct readout ground stations have been purchased or built to receive the direct readout transmissions from these satellites, such as the sample of typical GES components in operation of PEO satellite, as shown in Figure 8.1. Each GES can integrate other electronic devices, different antenna systems, some software and has to be integrated to the Terrestrial Telecommunication Network (TTN). Government and military agencies, companies, private industries and a variety of private individuals including ham radio operators, students and faculty are operating ground Earth stations. Perhaps, the fastest growing use of this data is within the educational community. Many researchers, teachers with their students at all levels within educational institutions have discovered the benefits of these satellites.

The innovative lecturers are using real time data to teach a variety of curriculum materials including the sciences, electronics, engineering, computer sciences, social studies, geography and art. Exposure to this exciting world of Earth remote sensing and observation can help retain students, motivate them toward higher education and expand career possibilities to areas unheard of a few years ago. This publication is designed to provide a broad spectrum of potential users with the basic information needed to establish and operate a direct readout ground station and understand the imagery provided by Earth-orbiting weather satellites.

Technological advances in microelectronics and computer software applications over the past decades have made it rather simple to assemble and use a basic direct readout ground station for meteorological satellite and space platform observations. Early techniques used in these technologies were surplus radio receivers to receive the satellite signals and old photographic facsimile drum recorders to reproduce the Automatic Picture Transmission (APT) or Weather Facsimile (WEFAX) imagery. On the other hand, today, it is possible to purchase modern off-the-shelf, state of the art commercial meteorological products for the same cost as the older surplus equipment and an inexpensive personal desktop computer can perform most of the functions originally performed by additional hardware.

When planning the installation of a direct readout system,the following issues must be considered:

- To purchase a complete “turn-key” system from a commercial source;
- To purchase individual components (antenna, receiver, demodulator, software, etc.) and assemble a system;
- To assembly the direct readout station primarily for low-resolution regional imagery (APT), or to require higher resolution or global capabilities (LRIT, HRPT and GVAR); and
- To realize the financial considerations and limitations for assembling all components and complete direct readout system.

Most newcomers to weather-satellite imagery start by assembling the PEO receiving station for the APT imagery. Starting with a basic analog APT mode allows the user to become more familiar with satellite image reception techniques, receiving satellite radio telemetry from a fast-moving platform in space, learning the techniques of predicting satellite orbits and acquisition of signal timing and analyzing weather patterns and temperature variations in the visible and infrared direct readout imagery. In fact, as one gains practical experience with meteorological satellite image reception and as the application requirements change, one may migrate to the higher resolution digital Low-Rate Information Transmission (LRIT), High Resolution Picture Information (HRIT), High Resolution Picture Transmission (HRPT) and GOES Variable format (GVAR) data transmitted by the US Geostationary Operational Environmental Satellites (GOES) commercial systems (Menzel, 2012).

A basic direct readout station typically contains components such as: Antenna, Preamplifier, Radio, receiver, Demodulator card to “decode” the satellite signal; Display system to view the satellite imagery (typically a personal computer); A storage system (computer disk, tape) to store and archive the satellite imagery; Computer software to manipulate the imagery (image enhancement); and A method to predict when the satellite will be in view of the GES.

Each component will be described in further detail in the following chapters. The more advanced direct readout systems (LRIT, HRPT, GVAR) utilize the same basic components, although the antenna, receiver design and demodulation system differ due to the nature of the radio frequencies required to transmit and demodulate the high-speed digital imagery.

Several different types of antennas may be used for polar orbiting reception of APT imagery, such as omnidirectional and directional, which require tracking systems.

8.1.2 Direct Readout Transmissions from Meteorological Satellites

In the early 60’s, satellite pictures received from the weather satellites were analyzed by the US Weather Bureau meteorologists, and the results, in the form of hand drawn nephanalyses (cloud depiction charts), were transmitted to major forecast centers throughout the United States and overseas. These cloud charts, sent by conventional landline or radio facsimile circuits, often reached these centers too late to be of any practical value in forecasting the weather. The weather satellite direct broadcasting system, or more commonly called Direct Readout Service (DRS), was developed to overcome this problem. Remotely sensed data are transmitted directly from PEO or GEO weather satellites in real time to forecasting centers and ground stations within signal of transponders from the Advanced Very High Resolution Radiometer (AVHRR), Advanced TIROS Operational Vertical Sounder (ATOVS) and other sensors. The weather satellite images were designed with a format that could be received and

reproduced by relatively inexpensive ground station equipment and the data is transmitted free of charge to anyone with the appropriate receiving and display equipment.

The DRS systems are an integral component of both the PEO and GEO meteorological satellites, including new stratospheric platforms. Each of these satellite platforms can provide a high resolution and lower resolution image data product. These systems include APT, HRPT and Direct Sounder Broadcasts (DSB) from the PEO satellites, and LRIT and GOES GVAR data format from the GEO satellites. Today, the majority of the world's users of weather satellite imagery acquire them through the use of these direct readout systems. Over 120 countries and approximately 8,000 known (and an estimated several thousand more unknown) ground stations rely on these daily transmissions of meteorological data. On the other hand new stratospheric aircraft and airship platforms are also able to provide DRS via special ground infrastructures.

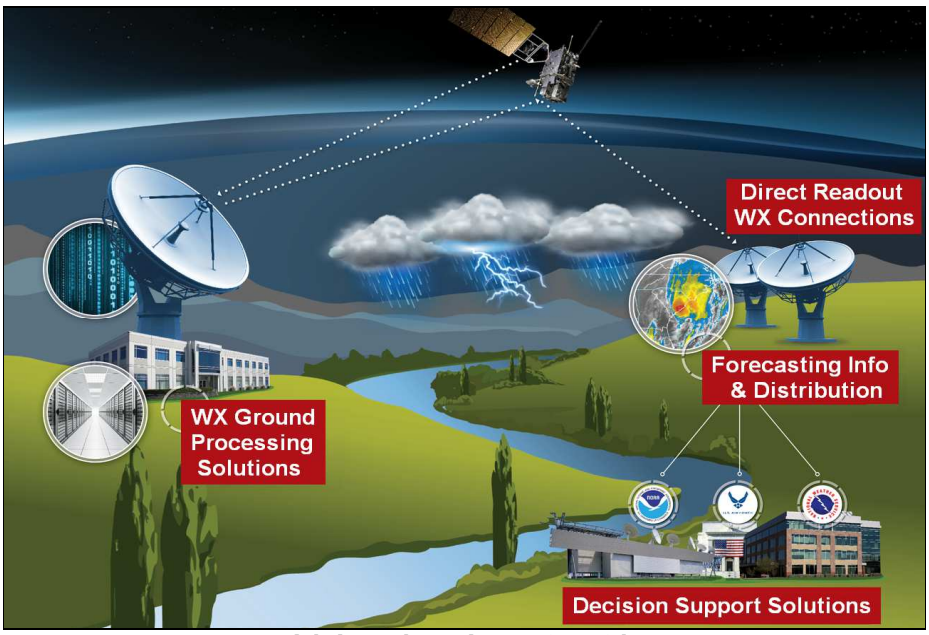

Figure 8. 2 Global Weather Solutions (GWS) by Harris 2015

Figure 8.2 illustrates the DRS system that provides Global Weather Solutions (GWS) for sustainable weather (WX), forecasting and climatology observation via meteorological satellites. The GWS systems are a family of affordable satellite and sensor data receiving and processing WX solutions for leveraging environmental intelligence data to assure weather prepared world. It is important to explore the family of WX solutions containing direct readout WX connections, WX ground processing solutions, forecasting information and distribution and decision support solutions, to get ready for the new generation of environmental satellites and the unprecented influx of high-resolution data they will deliver.
The first APT system was pioneered on TIROS-VIII as one of the early PEO metrological satellites. Several US weather offices were equipped to receive transmissions from this kind of satellites and plans for building relatively simple, low cost ground receiving stations that were widely distributed to foreign meteorological services. By 1965, radio amateurs (HAMS) were designing weather stations for home reception and publishing design information in popular electronic magazines. Interest and activity in receiving direct readout transmissions by members of the academic community also developed. Today, polar orbiting satellites launched by the United States continue to transmit images of the Earth via APT and HRPT. These have been joined by the Russian Meteor and Chinese Feng Yun spacecraft with similar

meteorological transmission systems. This is fortunate because a ground station capable of receiving data from the US polar orbiting satellites can also receive images from satellites of other countries as well (GSFC, 2009).

8.1.3 Direct Readout PEO Ground Earth Station (GES)

Due to the rotation of the Earth, satellites in PEO can be received in GES not more often than 3 to 4 times per day. Data received at those times thus belong to measurements made 6 hours (mean value for 4 contacts being equally distributed over the day) or more before the contact. The same satellites appear over the poles during each orbit, about 15 times per day. If all these possible satellite contacts are used for data reception, then the measurement data is available after not more than 95 minutes. It is this fast availability, which allows the use of data in time critical applications.

Figure 8. 3 Main Types of PEO GES Terminals and Antennas by Kongsberg 2015

The PEO GES Terminal is situated in any given position of certain PEO satellite footprint together with adequate tracking satellite dish antenna. Depending on the construction of the GES infrastructure. each satellite antenna can be installed next to the GES building or on its roof. The PEO meteorological GES infrastructure may employ different antenna systems such as omnidirectional Quadrifilar Helix Antenna (QHA), directional Parabolic or Crossed Yagi antenna and so on. There are three types of PEO infrastructures with their principal electronic components and antenna systems:

1. PEO GES with Tracking Satellite Receiving S/L/X-band Antenna – This GES meteorological satellite tracking antenna is a parabolic antenna, designed by the German producer SCISYS Deutschland GmbH to receive satellite meteorological data and images from NOAA, Feng-Yun, OrbView and METOP PEO satellites, which are shown in Figure 8.3 (Left). The GES infrastructure uses 2.4, 2.8 and 3.0m X/Y axis tracking satellite S, L and X-band reflector antenna system. The antenna system is operated in program track mode, in fact, the pass of the satellite will be pre-calculated to reduce the cost of the tracking system by avoiding the need for expensive auto-tracking systems. The satellite receiver is prepared for the reception of PEO satellite data and it contains a QPSK Demodulator and a Viterbi Decoder. The data are sent to the station computer via a serial to parallel converter. Thus, the software on the GES computer reads the data via a high-speed interface board and executes the Consultative Committee for Space Data Systems (CCSDS) processing. The data are fed into the higher level processing software like IMAPP, IPOPP or CSPP. The realization of the frame synchronizer and Reed-Solomon decoder as software solution reduces the total system

costs. The background processing performs all activities like pass prediction, antenna control and reception automatically, so that the system operates unattended. The PEO tracking antenna consists of the following components: parabolic reflector, X/Y type pedestal, DC servo motor drives, limit switches, electromechanical brake, shaft encoders, Motor Control Unit (MCU), Antenna Interface Unit (AIU) and power and control cabling.

The X/Y antenna pedestal provides a program-controlled automatic tracking system allowing for movement in both, X and Y directions. DC antenna motors, driven by a 4-quadrant pulse width modulation system in conjunction with digital shaft encoders, allow full servo position control. The motors drive the axes through a primary gearbox and a cycloid zero backlash transmission unit. Primary and secondary limit switches at all extreme positions increase overall safety. The pedestal is designed to be mounted on a stable foundation, such as a concrete pad, fastened in place by suitable threatened rods and is connected to the control equipment by the appropriate power and control cables. However, the maximum distance between the pedestal and the motor control unit is 75m. Using special cabling set, it may be extended up to 130m (Orbit, 2014).

The tracking satellite antenna can be used with unshielded parabolic reflectors ranging from 2.4 up to 3.0m sizes. Electrical features of this antenna are: Frequency Range 1.7 - 2.1/7.7 1 8.3 GHz (L/S/X-band), Gain 26dB (X-band), Beam Width 5.0° (L-band) and 1.0° (X-band). Environmental features of this antenna are: Temperature -30° to +50^{o}C; Operational Wind 100km/h and Survival Wind 150km/h.

2. PEO GES with Tracking Satellite Receiving L-band Antenna – From meteorological, oceanography and environmental observations to disaster management, TeraScan GES of the US SeaSpace Corporation with L-band antenna system are the complete acquisition and data processing solution for every major direct-broadcast PEO satellite, as shown in Figure 8.3 (Middle). This GES infrastructure can use the S and X-band as well. This type of GES receiver and antenna provides Weather Decision Support (WDS) for local and hemispheric images from PEO meteorological satellites that are directly broadcast to the ground. Similar to the previous solutions, this WDS system also automatically receives, processes and displays meteorological and maritime forecast data tailored to the vessel's operating areas of interest. The GES receiver utilizes a 1.5 m antenna reflector mounted on a 3-axis positioner installed inside a 2.0 m radome.

3. PEO GES with Tracking Satellite Receiving 2.4m - 4.2m L/S/X-band Antenna – The MEOS GES of Kongsberg Spacetec AS manufacturer is a PEO multi-mission, flexible and modular turnkey system for acquisition, archiving, processing, analysis and distribution of satellite meteorological data. This GES is providing support for the following meteorological PEO satellites: NOAA, FY-1, FY-3A or3B, METOP, NPP and others. This station supports direct broadcast reception in L, S and X-bands, and it supports the C and Ku-band reception through Eumetcast for NOAA and METOP satellites. The front-end system of this GES provides the functionality to track the satellite, receive the radio frequency and deliver data to the ingest system, which includes the following units: Antenna, Feed/downconverter; Digital receiver/bit synchronizer; and Satellite tracking controller. The parabolic reflector MEOSTM Antenna is available from 2.4 to 4.2m in L, S and X-bands, which are illustrated in Figure 8.3 (Right). The basic package ingests data from the front-end system and provides all the necessary tools for basic GES processing and operations. Data are pre-processed and stored into a Unix-file system in mission specific formats or as Level 0, 1 and map-projected products in HDF 5 format. All data are archived in a product database. Map-projected products can be viewed with the visualization software package known as MEOS VImSat. It

is a fast, operational viewing tool containing functions, such as accessing archived products, zooming, printing, image enhancements, format converting and overlaying graphics.

Raw data files and higher-level products may be distributed over LAN/WAN to other users. All operations are automatic and easily configurable, including management of disk space and retrieval of processing parameter files. Thus, the system has advanced capabilities for monitoring the system. All status information is written to disk as log reports. This gives a unique capability to do diagnostics locally as well as remotely, and to generate reception quality reports. This basic package contains a Quick Look Viewer showing incoming data in real time, with the possibility to show selected channels, perform image enhancement, and view a previous dissemination and to display multiple missions.

8.1.4 Direct Readout GEO Ground Earth Station (GES)

The GEO GES Terminal is situated in any given position of certain GEO satellite footprint between latitudes of 75^{o} North and 75^{o} South, together with satellite parabolic reflector dish antenna systems. Depending on the construction of the GES site, each satellite antenna can be installed next to the GES building or on its roof. There are two types of GEO infrastructures with their main components and antenna systems:

Figure 8. 4 Main GEO GES Terminals and Antennas by Harris 2015

1. GEO GES with Tracking Satellite Receiving L-band Antenna – The early 2016 launch of the first GOES-R satellite begins a new era in satellite weather information. This system will provide valuable earth imagery at four times the pixel resolution, three times the spectral data, and five times faster coverage than the current satellites. As a result, the new-generation GOES-R Rebroadcast (GRB) system will provide substantially greater nowcasting capability than the legacy GVAR service. Thus, the Harris Corporation's WxConnect GRB system delivers a direct connection from the GOES-R series satellites to the GES terminal, enabling access to all collected data, at full resolution, in the shortest time feasible over all other methods of obtaining new generation GOES meteorological data. This exclusive processing architecture and software was designed and implemented for low latency processing to support mission critical applications with fast access to newly received weather data.

Modular and scalable GES terminal of WxConnect GRB system, as shown in Figure 8.4 (Left), includes options for a 3.7, 4.5 or 6.5m satellite L-band reflector parabolic antenna and

a high-power processing system providing high availability and secure reception of enhanced environmental data from the GOES-R satellite system. **.** Deployment services include antenna and processing equipment installation, connected to the GES terminal and providing system trial. Optional product generation and algorithm development support are available to complete the GOES-R weather data solution. In addition, this GES terminal and antenna can provide high-performance DVB-S2 demodulation for robust operation in high adjacent signal environments.

The similar MEOS GES with parabolic antenna of Norway producer Kongsberg Spaced AS is a multimission, flexible and modular turnkey system for acquisition, archiving, processing, analysis and distribution of meteorological data using advanced package software. Thus, the system provides the functionality to receive the radio frequency and deliver data to the ingest system. The front end system of GEO GES includes: Antenna, Feed/Downconverter and Digital receiver/bit-synchronizer. Depending on the customer's requirements, **Table 8.1** shows the types of meteorological satellites, their antenna sizes and working frequency bands:

Table 8. 1 Type of Antennas and Frequency Bands in Kongsberg 2014

Frequencies	**L-band**	**Ku-Band** (Europe)	**C-band** (Africa/ America)
Antenna sizes in m	3.8	1 - >	2.4 - >
MTSAT	+		
FY-2	+		
MSG	*	+	+

Therefore, all three GEO meteorological satellites, the Japanese MTSAT, Chinese FY-2 and European MSG, are using L-band, while the MEOS MSG Ground Station supports reception relayed via Ku-band (EUTELSAT 9A/10A) and C-band (AtlanticBird) satellites for DVB-S2 transmissions. The ground station also supports L-band reception directly from the MSG satellite, an option, which may become available in the future.

2. GEO GES with Tracking Satellite Receiving L/S/X-band Antenna – The MEOS GEO GES with Antenna of producer Kongsberg Spaced AS comes with dish sizes from 3.0, 3.8, 4.3 up to 5.0 m, as shown in Figure 8.4 (Right). This antenna is situated in plastic radome to be protected from influence of very harsh environment. This GES gives sufficient margin for data reception from direct readout and remote sensing satellites. Thus, designed for optimal maintainability and reliability, the MEOS satellite antenna utilizes the most modern industrial components available today. **Table 8.2** shows different sizes of optional GES antenna, frequency bands and other characteristics:

Table 8.2 Size of Antennas and Frequency Bands in Kongsberg 2014

Standard Reflector Sizes				
	3.0 m	**3.8 m**	**4.3 m**	**5.0 m**
L Band G/T (1700)[2]	10 dB/K	12 sB/K	13 dB/K	14 dB/K
S Band G/T (2400)[2]	13 dB/K	15 dB/K	16 dB/K	17 dB/K
X Band G/T (8200)[2]	25 dB/K	27 dB/K	28 dB/K	29 dB/K
Pointing error	0.09° rms[3]			
Pointing resolution	0.005° on both axis			
Velocity	6 deg/s			
Wind speed operational	40 m/s	27 m/s	Radome recommended	
Wind speed survival	56 m/s	56 m/s	Radome recommended	
Travel				
X-axis: Mechanical ± 90 deg, Tracking ± 87 deg Y-axis: Mechanical ± 90 deg, Tracking ± 87 deg				

Key features of this GEO antenna are as follows: Pedestal connected to indoor unit by optical fiber; TCP-IP on fiber cable between pedestal and indoor unit Cable length is about 3 km; Single or dual band configuration available; Designed for L, S, and X-band missions; Dish size is 3.0 to 5.0; Employed X/Y geometry for lower stress to drive chain with X/Y pedestal for elimination of overhead keyhole; Extensive monitoring and control capabilities; In-field diagnostics and alignment tools; Remote and local monitoring and control available; Real time and historic status available; Java based graphical user interface; MEOS Connect ready for integration in a ground station network; Stable antenna control unit running Linux, which is supporting 24/7 operations without operator intervention; Resumes operation automatically after a power break; Self test and remote diagnostics; Robust computers and servo units; and Low failure probability

8.2 METEOCast Interactive Broadcasting GEO DVB-RCS GES

The Digital Video Broadcasting-Return Channel via Satellite (DVB-RCS) or DVB-S and DVB-S2 broadcasting technique are the ETSI standards, which define the complete air interface specification for two-way satellite broadband Very Small Aperture Terminal (VSAT). Low cost VSAT can provide highly dynamic and demand-assigned transmissions, such as fixed and mobile communications, meteorological data transfer and so on (Hughes, 2008).

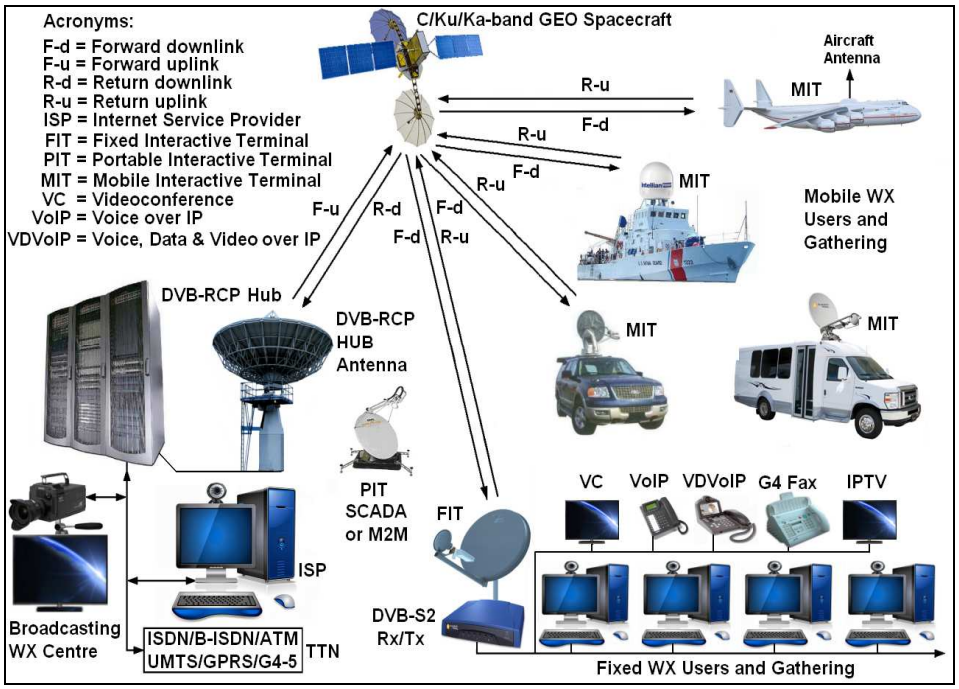

Figure 8. 5 DVB-RCS Weather (WX) Network by Ilcev 2011

The existing commercial DVB-RCS and DVB-S2 broadcasting service,as shown in Figure 8.5 provides Voice, Data and Video (VDV) transmissions via commercial GEO satellites for fixed, mobile and other applications, including satellite SCADA (M2M) system. .

The EUMETCast broadcast system for Environmental Data is a multi-service dissemination system based on standard DVB TV technology. It uses commercial communication GEO satellites to multicast files (data and products) to a wide user community. Thus, EUMETCast is EUMETSAT's contribution to GEONETCast. This concept fully supports the family of DVB based satellite receiving systems for the meteorological user community using DVB commercial telecommunication satellites like Eutelsat, SES-6 and AsiaSat-4. Moreover, the Meteorological Satellite Centre (MSC) of Japanese agency JMA is using its own commercial communication satellite, JCSAT-2A/2B, for the dissemination of meteorological data and images at C-band, which are known as HimawariCast. This agency uses its own multifunctional satellite MTSAT-2 for the same purpose, because this satellite has onboard communication, meteorological and GNSS/CNS transponders and uses the L, Ku and Ka-bands.

Within the current EUMETCast system configuration, the server side is implemented at the EUMETCast uplink site (Usingen, Germany), and the client side is installed on the individual EUMETCast reception stations. The telecommunication providers supply the DVB multicast distribution. Encoded LRIT/HRIT data and product files are transferred via a dedicated communication line from Eumetsat to the uplink facility where they are transmitted to a GEO communication satellite for broadcast to user receiving stations. Each receiving station decodes the signal and recreates the user data/products according to a defined directory and file name structure. In its current configuration, EUMETCast operates two turn-around systems. The turnaround service provider receives the DVB satellite signal from one satellite and retransmits it, without unpacking the DVB C-band turn-around service for EUMETCast Africa from its uplink site in Fucino (Italy) and Globecast provides the C-band turn-around service for EUMETCast Americas from its uplink facility in Paris (France). Further information about EUMETCast and its services is provided on the EUMETSAT Web page or

in the Technical Document TD-15. As the missions are encrypted, every user needs to have a license agreement with EUMETSAT or its national weather service.

Figure 8. 6 DVB-RCS Hub Terminals and Multiband Antenna by Hughes 2012

The same scenario can be used for new proposed Global Meteorological Broadcasting (GMB) such as retransmission of meteorological LRIT/HRIT data, products and images via commercial GEO satellites transponder and SCP stations to customers received by DRS and transmissions of meteorological data from ground DCP via GEO satellites to the DRS infrastructures. This proposal named as the METEOCast system was developed by the Research Centre in Space Science and Postgraduate Studies at the Durban University of Technology (DUT) and contains two the following scenarios, as shown in Figure 8.5:

1. METEOCast Forward DVB-RCS Uplink for Data Retransmission – This system has to provide retransmission of meteorological data and images from Broadcasting WX Centre of Direct Readout Service (DRS) and send them to the DVB-RCS Hub at C, Ku or Ka-band. Then, the Hub server encapsulates DRS data, which are sent to the GEO communication satellite Rx by the forward uplink Hub reflector dish antenna. The communication GEO satellite broadcast data are received from the uplink station to the VSAT stations as fixed and mobile users (FIT and MIT) on the ground by the forward downlink Tx. The VSAT receiving antenna and Low-noise Block Downconverter (LNB) receive the data from the communication satellite and send the information to the DVB-S2 Rx. The VSAT Rx then converts the data into IP packets and sends them to the computers (PC) integrated in the Local Area Network (LAN), as shown in Figure 8.7. The METEOCast professional client unencapsulates the data for storage in any directory on the PC memory. The Forward DVB-RCS Uplink solution is shown in Figure 8.5.

All wanted meteorological information by METEOCast users can be sent in any real time and space via Hub to GEO communication satellite. The two types of Hub stations: i.e., Advantech is shown in Figure 8.6 (Left) and Hughes in Figure 8.6 (Right). The Hub ground antenna, as shown in Figure 8.6 (Middle), transmits all forward uplinks DVB-RCS information to the ground users via GEO satellite Tx and receives all return uplink DVB-S2 information from ground users via GEO satellite Tx.

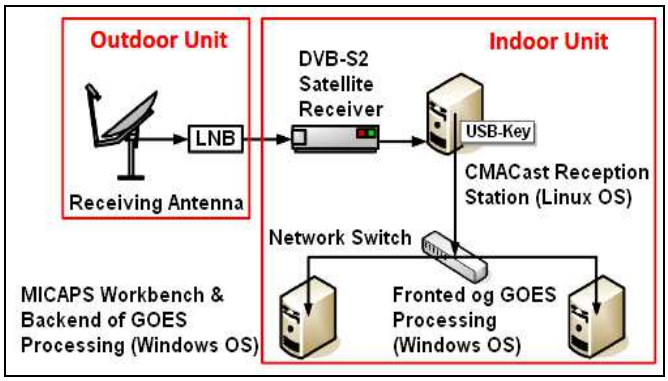

Figure 8. 7 GOES DVB-S2 Rx by GAO 2013

Figure 8. 8 DVB-S2 VSAT Units and Antenna by Advantech 2015

The features of the Advantech next generation DVB-RCS VSAT Hub Discovery 300 are as follows: Multi-transponder and multi-satellite support; Up to 1Gb/s of 5 x 200 Mb/s Forward Links capacity with 5:1 redundancy; Up to 3 x 240 Mb/s Return Links per rack capacity; Geographical redundancy and satellite roaming; Support for up to 45,000 VSAT terminals; Optimized for IP and multimedia content including MPEG4 video; Open standard design of DVB-RCS and DVB-S2 for return links; DVB-S, DVB-S2 and DVB-S2X for forward links; The VSAT Hub is frequency independent that its onboard processors can be operated in any frequency band (e.g., Ku, Ka, C, X-band or hybrids of these); The switching mechanism, on the return link, between the DVB-RCS TDMA system and the DVB-S/S2/TCC SCPC modes is customer controlled and can be commanded by the Hub Operator; and so on.

The features of Hughes HN VSAT Hub are as follows: The base configuration can be readily expanded to accommodate multiple 121 Mb/s forward channels and over 70 Mb/s of return channel traffic; Multicast data delivery, four levels of IP traffic prioritization and their any combination; Multimedia applications including MPEG4 video; This VSAT Hub provides star TDM/TDMA connectivity; SCPC/MCPC replacement links; and so on.

2. METEOCast Return DVB-S2 Uplink for Data Transmission – This system is designed to provide transmission of meteorological data and images from fixed, mobile and portable Data Collection Platforms (DCP) VSAT stations (FIT, MIT and PIT) using C, X, Ku or Ka-band, depending on the model. The PIT station can be an ordinary VSAT station or can be SCADA Machine-to-Machine (M2M) VSAT connected to the DCP terminal. The converted data from IP packets in DCP terminal VSAT Tx send them to the GEO communication satellite Rx by the return uplink VSAT dish antenna. Then, the GEO communication satellite Tx sends received DCP data to the VSAT Hub antenna by the return downlink. Finally, the VSAT Hub (GES) distributes this data directly to the BWC or to ground users via Internet and TTN The Return DVB-RCS Uplink solution is shown in Figure 8.5.

The samples of VSAT transceiving stations that can be used for both GEO METEOCast forward and return uplink configurations are shown in Figure 8.8: Advantech VSAT station **(Left)**, Advantech VSAT reflector antenna **(Middle)** and Hughes VSAT station **(Right)**.
In the similar way, the same Advantech or Hughes VSAT stations can be installed onboard the Mobiles, but to provide GEO METEOCast forward and return uplinks have to be connected to special tracking mobile VSAT antenna, which are shown in Figure 8.9: shipborne antenna **(Left)**, vehicleborne antenna **(Middle) and** airborne antenna **(Right)**.

Figure 8. 9 Mobile DVB-S2 VSAT Antennas by Orbit 2015

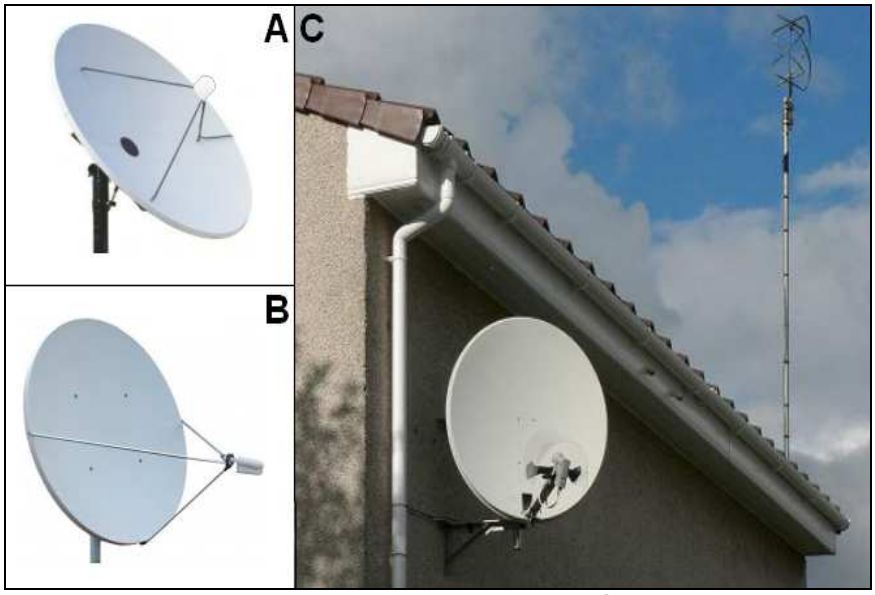

Figure 8. 10 DVB-S2 Receiving VSAT Antennas by Dartcom 2015

8.3. METEOCast Receiving Broadcasting GEO DVB-RCS Stations

As stated before, customers and different users can now receive data from Eumetsat via a TV broadcasting satellite Eutelsat-10A as an alternative way to either direct reception from the Meteosat transponders or using the Internet to download the data. This WX service is called EUMETCast and it is provided by a TELLICAST server. Just like direct reception, the data is only broadcast once in the certain time and day by schedule via DVB-RCS transmissions. To receive this EUMETCast information, it will be necessary to provide DVB-S2 VSAT Rx stations with adequate antennas. The DVB-S2 C-band antenna is shown in Figure 8.10 (A), Ku-band receiving antenna is shown in Figure 8.10 (B) and Figure 8.10 (C) illustrates the Ka-band receiving satellite dish for GEO EUMETCast and QFH antenna for PEO satellite APT service over Europe. Thus, subsets of this data are also broadcast via C-band satellites providing coverage to Africa and some of the Americas.
For receiving only VSAT of LRIT or HRIT data on C-band a 2.4m, 3.0m or 3.7m parabolic dishes and LNB can be used. The sample of C-band LNB is shown in Figure 8.11 (Left). The

TechniSat SkyStar 2 internal PCI DVB-S2 receiver card for EUMETCast C-band service, which can be installed in PC, is shown in Figure 8.11 (Middle) and TBS 6983 internal PCIe DVB-S2 receiver card for C and Ku-band HimawariCast is shown in Figure 8.11 (Right).

The two DVB-S2 receivers recommended by EUMETCast are SR1 desk mount Ku-band version, as shown in Figure 8.12 (Left) and rack mount Ku-band version, as shown in Figure 8.12 (Right). In addition, the TBS 6983 PCIe card of DVB-S2 receiver can be used.

It is possible to receive service from Meteosat, GOES, MTSAT, Metop, AVHRR, ATOVS and EUMETCast DVB-S2.

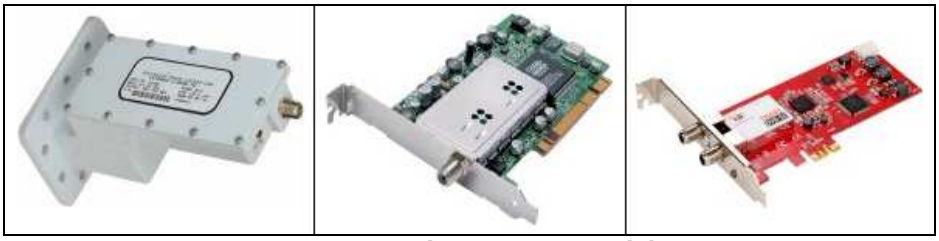

Figure 8. 11 DVB-S2 LNB and PC Receiving Cards by Dartcom 2015

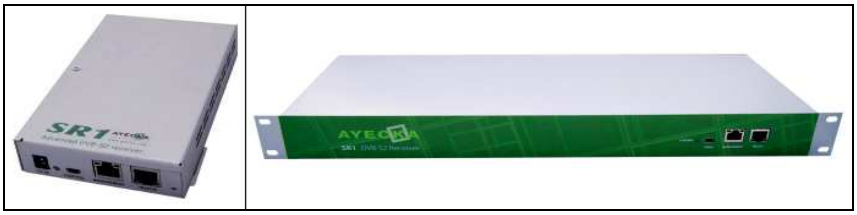

Figure 8. 12 DVB-S2 Deck and Rack Receivers by Ayecka 2015

To provide a universal system for receiving service from the Broadcasting GEO DVB-RCS Stations, it will be necessary to establish a global casting METEOCast service proposed by the DUT Research Centre in Space Science. The METEOCast global casting of meteorological LRIT and HRIT data has to integrated with the existing METEOCast, HimawariCast and other GEO meteorological satellite casting in unique and interoperable METEOCast global system.

8.4 Direct Readout GES Indoor Equipment

This section will introduce the following main indoor equipment in GES for meteorological Direct Readout Service (DRS):

1. DRS Indoor PEO Equipment – The X-band PEO satellite indoor devices are providing affordable, high performance and end-to-end solution for receiving and processing X-band data from Terra and Aqua (MODIS), Suomi-NPP, FengYun-3 and other meteorological and observation satellites. This solution is a cost-effective migration path from existing L-band systems to X-band for the next generation of meteorological and Earth observation satellites. However, a combined X/L-band option allows reception and processing of data from both X-band and L-band satellites using the same antenna system. If reception of NOAA HRPT, Metop AHRPT or FengYun-3 AHRPT data is also required using the same antenna system, additional RF components and receiver rack modules can be supplied. to
The new X-band PEO satellite meteorological data are essential for the accurate monitoring of global weather and climate patterns. It is also invaluable for remote sensing weather and

climate patterns work, such as detecting forest fires, monitoring ocean currents and mapping land use. However, X-Band reception systems have always tended to be very expensive to purchase and maintain. They also normally require specialized installation procedures and building works. With the help of research institutions, the Dartcom producer developed a lower cost X-band system which still offers performance and features competitive with much more expensive products. Dartcom has achieved lower costs with a smaller antenna, state-of-the-art RF components, tight tolerances and advanced software. Figure 8.13 (Left) shows the receiver rack, high-rate demodulator and ingest PC running by the Dartcom Polar Orbiter Ingester software. The Processor PC running RT-STPS, Simulcast, IPOPP and the FY3L0pp/FY3L1pp software are illustrated in Figure 8.13 (Right).

Figure 8. 13 DRS Receiving Rack and Processor PC by Dartcom 2015

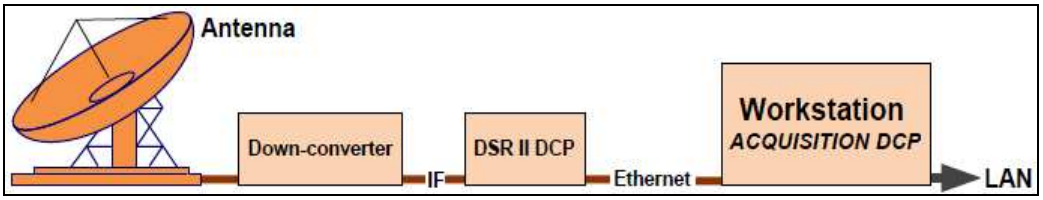

Figure 8. 14 Indoor Components of GEO GES by SCISYS 2014

The DRS Indoor PEO Equipment contains the following components: Modular receiver rack (4U rack mount); High-rate demodulator (1U rack mount); 2kVA UPS (tower or 2U rack mount); Ingest PC (midi-tower or 4U rack mount) running 64-bit Windows with Dartcom Polar Orbiter Ingester software; Processor PC (midi-tower or 4U rack mount) running NASA RT-STPS, Simulcast, IPOPP and CMA FY3L0pp/FY3L1pp software; Optional visualization PC (midi-tower or 4U rack mount); and 6U desktop or optional 22U floor-standing cabinet for complete rack-mounted system. However, the modular receiver rack contains the following removable modules: LNB power supply; XDC programmable downconverter; USB hub and serial adapters; GPS receiver; Switch mode power supply; Optional USB interfaces for reception of L-Band services.

The DRS Indoor PEO Equipment works in such a way that the antenna system automatically tracks X-Band satellites and receives direct broadcast RF transmissions, which are focused into the scalar feed horn by the parabolic dish, amplified by the low-noise amplifier, and then fed to the block down-converter. This converts the signal to a lower frequency to minimize cable loss and feeds it to the XDC programmable downconverter in the receiver rack, where it is converted to a common frequency and fed to the high-rate demodulator.

The demodulator converts the RF signal back to a binary data stream which is then Viterbi decoded, byte-aligned and transferred via USB to the Polar Orbiter Ingester software running on the ingest PC. This detects the Attached Synchronization Markers (ASM) in the

data stream and extracts the Consultative Committee for Space Data Systems (CCSDS) frames, which are then derandomised, Reed-Solomon decoded and demultiplexed into Virtual Channel Data Units (VCDU). The VCDU is automatically transferred via a TCP socket to the RT-STPS software running on the processor PC, which processes them live and displays a preview in the Simulcast software. The IPOPP software automatically processes the resulting data sets into level 0, 1 and 2 data and products.

2. DRS Indoor GEO Equipment – The SCISYS Data Collection Platform (DCP) DRS GES includes the digital receiver DSR II and a workstation and software, as shown in Figure 8.14. The DRS GCP indoor equipment has been designed to provide state of the art technology capable of receiving data from all current METEOSAT or GOES DCP channels. The design of this ground weather station is based on only one dedicated Hardware (HW) component. The DRS II Antenna, feed and down-converter are standard for L-band reception. Most of the DCP functions are implemented in adequate software. Thus, this design allows easy and cost effective up-grade to a multi-channel system by adding standard PC and Acquisition DCP software licenses. The DCP unit is designed against worst-case specifications to allow proper operations under all circumstances for all data rates from 100 to 2400 Baud (SCISYS, 2014).

A typical DRS hardware GES system consists of antenna, feed, Low Noise Amplifier (LNA) Downconverter and the dedicated SCISYS Digital Satellite Receiver DRS II providing the functionality of a complex analogue to the digital converter. The output of the receiver is a stream of 16 bit I/Q complex samples at 500 kHz sample rate resulting in about 2.5 MB/s network transfer including some monitoring data and time stamping. The receiver is connected to a standard PC via a fast Ethernet interface. None of the HW components needs any maintenance or adjustment during normal operations.

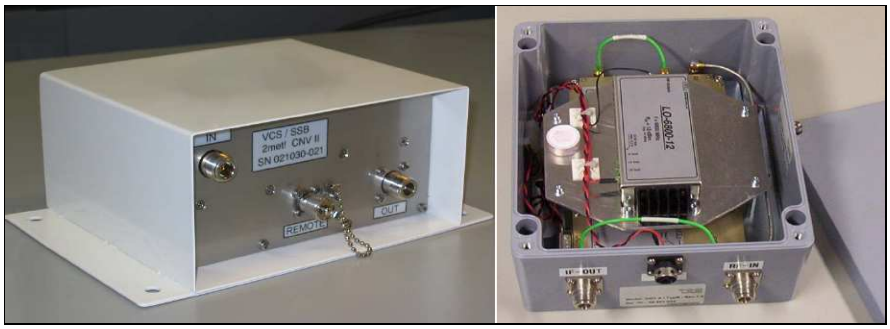

Figure 8. 15 LNA and X-band Downconverters by SCISYS 2014

Figure 8.15 (Left) shows High Performance L-Band CNV II LNA/down-converter of the SCISYS Company. It has been designed to cope with the current series of GEO meteorological satellites for direct dissemination in L-Band and to reduce influences from external sources working under outdoor environmental conditions. The down-converter unit is self-contained with the LNA and all other associated systems, which include Pre-LNA filter, power, local oscillator frequency reference, etc, within a single enclosure. The down-converter amplifies the received signal from the antenna and converts it to a suitable frequency for further processing in DSR II. Thus, a high performance, low-loss pre-LNA filter prevents unwanted frequency components from entering the signal path, while maintaining an exceptional low noise figure. In addition, this assembly provides suitable signals for the remote S-meter assembly used to provide the S/N information necessary for adjusting the antenna pointing direction. The unit is designed for outdoor use. The local

oscillator used for the frequency conversion is based on a high stability Temperature Compensated Crystal Oscillator TCXO.

Figure 8.15 (Right) shows the High Performance X-band Down-converter SCISYS CNV X Type B. This down-converter has been designed to cope with current and future series of GEO platforms for direct dissemination in X-band working under outdoor environmental severe conditions. It amplifies the received signal from the LNA and converts the RF signal from X-band to L-band for connection to a receiver, for example, the DSR III model. Thus, a built-in image rejection filter reduces the unwanted image signals by approximately 20dB. As an option, a four (4) section cavity filter in front of the mixer provides the highest image rejection while maintaining a suitable passband bandwidth for later JPSS extensions. The local oscillator used for the frequency translation is based on a high stability TCXO.

Figure 8.16 (Left) shows the Multimission Meteorological Satellite Data Receiver DRS II of SCISYS Company. This multimission satellite receiver exploits the experience from the digital baseband processing used for the Meteosat User Station Baseband Module (MUBM). It provides a fast Ethernet interface for TCP/IP connection to any host system, whose implementation allows for reception of several meteorological satellites. It supports data rates from 75 Kb/s (MTSAT/LRIT) up to 3.5 Mb/s (AHRPT) of METOP satellites. The extremely low losses of 0.4 dB for the LRIT/HRIT missions at the operating point (Eb/N0 = 2.8dB) are realized by a mostly digital design. The main functions are: 2nd conversion of the IF signal including antialiasing filtering; coherent BPSK/QPSK/PM demodulation; baseband-pulse shaping; symbol/bit synchronization; Viterbi decoding (if is applicable); and data buffering and provision of monitoring information.

Figure 8. 16 LNA and X-band Downconverters by SCISYS 2014

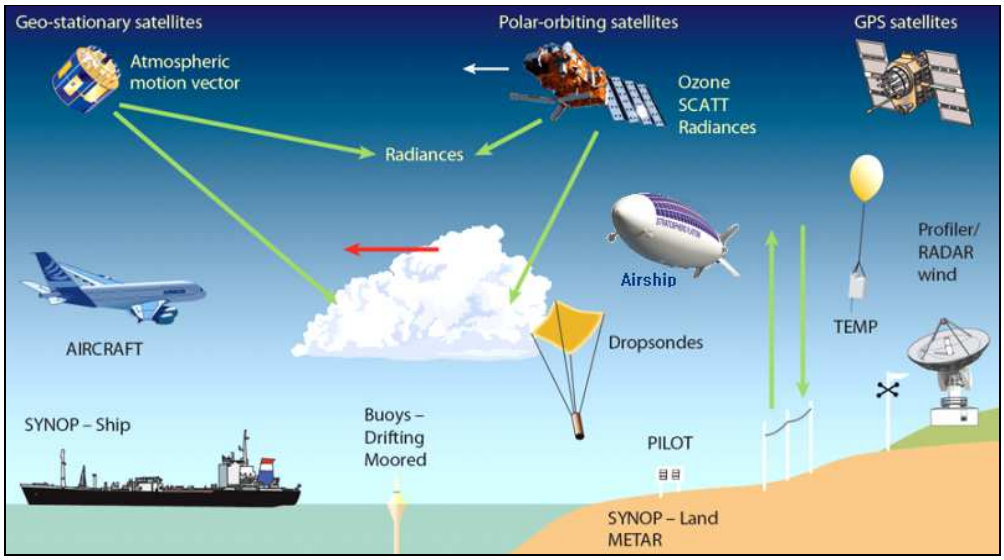

Figure 8. 17. Global Integrated Meteorological Observation Systems by WMO 2013

Figure 8.16 (Right) shows the SCISYS adaptable satellite Telemetry Receiver DSR III, which receives and processes high-rate data streams up to 90 Mb/s directly from GEO broadcasting Earth Observation satellites. It operates on various modulation/coding formats and provides advanced monitoring capabilities, and allows reception of several Earth Observation Satellites. In average, it supports data rates from 0.5 Mb/s up to 80 Mb/s, pending on the modulation/coding formats of 45 Mb/s with Viterbi, of 78 Mb/s with Reed Solomon RS (255,233) only. The receiver supports advanced monitoring capabilities and comprehensive user programmability using various utility programs. Its main functions are: standard IF input of 1-1.5 GHz or a fixed 720M Hz IF; Modulation is BPSK/QPSK/OQPSK/8PSK; Software frame synchronization to various standards, CCSDS or special formats; Viterbi decoding for R=1/2 K=7 operation (ESA/NASA standard) in BPSK mode like "serial" mode (TERRA) or QPSK like "parallel" mode (MSG HRIT); and Provision of monitoring information.

The Acquisition DCP Software comes with everything the customer needs,i.e., high reliability at affordable price. The User's friendly graphical Man Machine Interfaces (MMI) set-up the system without long training phases and reduce management overhead. The Demodulator modules with Beacon Tracking are realized completely in software. Thus, the application includes channel selection and frequency correction as well as matched filtering, Automatic Generation Control (AGC) and timing correction. The channel selection can be easily performed by a control MMI. The status of each demodulator and the beacon are displayed on a monitoring MMI. The DCP Message Data can be retrieved via a standard TCP/IP socket interface. Support for multiple pilot tones is provided and the automatic removal of phase and amplitude ripple is induced by the Electronically Despun Antenna (EDA) effect of spinning satellites.

8.5 Future Worldwide Integration of Direct Readout and Broadcast Services

Weather forecasts have always relied on accurate observations of the current weather. Modern numerical weather prediction is no different and makes extensive use of integrated terrestrial and satellite observations, as illustrated in Figure 8.17. These observations provide atmospheric, ocean and land surface information. Satellites now provide most data, although more traditional observations are still important.
Therefore, this integration contributes to the future development of the global observing system both through assessing the potential impact of new data and by pioneering the use of new satellite data including data from SCP airships. The variety, quality and reliability of satellite observations are still changing rapidly, however, some modern types are now very well established. Satellite instruments are very complex and often making many thousands of individual observations simultaneously at the same location, and requiring sophisticated techniques to interpret the information they contain.

Observations, in particular from PEO and GEO satellites, combined with new airship platforms and the improved Earth meteorological surface system modeling and advances in data assimilation techniques, in general, make a major contribution to improve the medium range weather forecast skill.

The US National Oceanic and Atmospheric Administration (NOAA) is in the process of transitioning its current direct broadcast services to the most up-to-date digital formats. In this way, the new Global Specifications for Low Rate Information Transmission (LRIT) and the Advance High Rate Picture Transmission (AHRPT) digital formats are intended to

improve the quality, quantity, and availability of meteorological data from direct broadcast meteorological satellites.

The transition of the NOAA direct readout services takes place across several spacecraft constellations. In fact, this will encompass many years of development, coordination and implementation. Replacement of the analog Weather Facsimile (WEFAX) with the new digital LRIT, in 2005, started a transition period that will culminate with the implementation of the GOES Re-Broadcast (GRB) service on the GOES-R spacecraft constellation. The current direct broadcast services of NOAA will change dramatically in data rate values, data content, frequency allocation and field terminal configurations.

8.5.1 Current NOAA Broadcast Services

The current direct readout services are derived from satellite sensor data from NOAA's geostationary GOES and polar POES meteorological satellite systems. The NOAA's GOES direct readout services include Low Rate Information Transmission (LRIT) and VARiable (GVAR) broadcasts, while, the POES system for direct readout services include the analog Automated Picture Transmission (APT) and digital High-Rate Picture Transmission (HRPT) transmissions.

8.5.1.1 Low Rate Information Transmission (LRIT) Broadcast Services

The LRIT broadcasting is a communications transponder service provided through the GOES spacecraft. This low-rate digital service involves the retransmission of low-resolution data, polar-orbiter satellite imagery and other meteorological data through the GOES satellites to relatively low cost receiving units within receiving range of the satellite. The low-resolution geostationary and polar satellite images are produced at the NOAA Environmental Satellite Processing Center (ESPC) facility in Suitland, Maryland. This GOES imagery is created from the retransmitted GVAR data received at the facility.

The ESPC ingests these retransmitted GVAR data streams through a Front End Processor. Based on an automated schedule, the data are divided into sub-areas, reduced in spatial resolution, if necessary, and enhanced according to predefined look-up tables. The resultant LRIT products and imagery (IR and visible) are referred to as sectors which are spatial subsets of the full earth disc corresponding to an area of interest to weather forecasters. The generated sectors are then sent from the ESPC as digital product via dedicated telephone lines to the Wallops CDA station for transmission through the GOES spacecraft.

On the current on-orbit spacecraft suite (GOES 10-13) and the planned launch missions of GOES O/P, the LRIT service will continue to support a 128 kbps service. In the GOES-R era, LRIT or HRIT will provide a 455 kbps broadcast service. The LRIT service complies with the CGMS Global Specification for LRIT/HRIT (CGMS, 1999).

8.5.1.2 GOES Variable (GVAR) Broadcast Services

With its two operational satellites, the GOES system is covering North, Central and South America and their neighbouring ocean environments including the central and eastern portions of the Pacific Ocean and the central and western portions of the Atlantic Ocean. NOAA acquires raw data from its two primary instruments used to carry out the main

mission. The Imager is a multi-channel instrument that senses radiant energy and reflected solar energy from the Earth's surface and atmosphere.

The Sounder is a multi-channel instrument that provides data through vertical atmospheric temperature and moisture profiles, surface and cloud top temperatures and ozone distribution. These instruments scan the Earth according to the sector commanded. Raw data from these instruments are downlinked to the ground to be processed into GVAR formatted data. The GVAR data is up-linked to its corresponding GOES satellite, together with auxiliary data inputs from additional ground equipment, for global re-broadcast to users.

The GVAR data format is primarily used to transmit Imager and Sounder meteorological and climatological data. Other functions of GVAR data include transmission of calibration data, satellite navigation data, administrative and operational text messages. The GVAR format was developed because the AAA format used for the early spin-stabilized GOES spacecraft would severely limit the capabilities of the Imager and Sounder data for the new three-axis stabilized spacecraft platform. The AAA format used a fixed-length transmission. Thus, the GVAR format supports variable scan line lengths. The last GVAR mission will be supported by GOES-P scheduled for launch in October 2009.

8.5.1.3 Automated Picture Transmission (APT) Broadcast Services

The APT service provides a reduced resolution data stream from the Advanced Very High Resolution Radiometer (AVHRR) instrument. Besides, any two of the AVHRR channels can be chosen by ground command for processing and ultimate output to the APT transmitter. A visible channel is used to provide visible APT imagery during daylight, and one IR channel is used constantly (day and night). A second IR channel can be scheduled to replace the visible channel during the nighttime portion of the orbit.

The analogue APT signal is transmitted continuously and can be received in real time by relatively unsophisticated, inexpensive ground station equipment while the satellite is within radio range. The characteristics of the transmitted signal remain unchanged in the NOAA KLM satellite series from those in the TIROS-N series (NOAA 8 - 14), while there is a minor change in the data format to account for the modified channel 3 on the AVHRR/3 instrument beginning with NOAA-K.

With the launch and operation of the METOP1 satellite, the morning (AM) APT service was replaced with the Low Rate Picture Transmission (LRPT) broadcast. Since the failure of the LRPT transponder, NOAA will continue to support both the morning (AM) and the afternoon (PM) polar-orbiting missions with its APT service. The last of the APT missions will be supported by NOAA-N' scheduled for launch in March 2009.

Otherwise, the APT service is used by the NOAA weather satellites and some Russian weather satellites in PEO constellations to transmit satellite weather photos.

8.5.1.4 High Rate Picture Transmission (HRPT) Broadcast Services

The HRPT service installed on the NOAA satellites has for some two decades been the main source of high quality data from PEO meteorological satellites at major user stations or User Earth Stations (UES) throughout the world. The data stream not only contains full resolution

images in digital format from the AVHRR instrument but also the atmospheric information from the suite of sounding instruments.

Through a HRPT terminal, an environmental user can acquire data from three or more consecutive overpasses twice each day from each satellite, giving high resolution data coverage of a region extending to about 1500 km radius from the user station. The imagery gives a snapshot of the meteorological conditions and can also be used for many land and ocean applications, while the sounding data give detailed atmospheric data that may be processed and used in regional Numerical Weather Prediction (NWP) models.

The NOAA HRPT system provides data from all NOAA-K, L, M, N, and N' spacecraft instruments at a transmission rate of 665,400 BPS. All information necessary to calibrate the instrument outputs is also included in the data stream. The real-time transmissions in S-band (at around 1700 MHz) include the digitized unprocessed output of the dedicated sensors.

8.5.1.4 Advanced Very High Resolution Radiometer/3 (AVHRR/3) Broadcast Services

The AVHRR/3, with its 1.1 km resolution, dominates the data rate of the HRPT broadcast. Five spectral channels out of a possible range of six are transmitted in full resolution at any one time, together with relevant calibration data. Channels 3A and 3B cannot be transmitted at the same time. The selection is made by the Satellite Operations Command Center (SOCC) via telemetry control. The onboard processor also generates Global Area Coverage (GAC) and Local Area Coverage (LAC) formats from the original AVHRR data. This data are stored onboard and downloaded separately from the real-time data stream transmitted by HRPT.

8.5.2 Future Direct Readout Services

As future environmental satellites improve their monitor and observing capabilities, they will produce far more data than the current satellite series. The GEO and PEO environmental satellite constellations will employ new downlink frequency allocations, larger bandwidths, and faster data rates. Environmental data users must employ new field terminal receivers unique to that particular broadcast service.
Over the last nine years, NOAA has been developing the National Polar-orbiting Operational Environmental Satellite System (NPOESS). The advanced visible and infrared imagers and microwave sounders that are being developed for NPOESS spacecraft will deliver higher spatial and temporal resolution data to meet user validated requirements for 55 atmospheric, oceanic, terrestrial and solar-geophysical parameters enabling more accurate short-term weather forecasts and severe storm warnings, as well as serving the weather data continuity requirements for improved global climate change assessment and prediction.

The Integrated Program Office (IPO) has developed a Memorandum of Agreement (MOA) for providing two direct data links to Field Terminal users, one for High Rate Data (HRD) in X-band at 20 Megabits per second (Mb/s), and one for Low Rate Data (LRD) in L-band at 3.5 Mb/s. The IPO plans to demonstrate prototype NPOESS HRD and LRD terminals as a guide to users in modifying or replacing their existing terminals, and will distribute nonproprietary HRD/LRD versions of Field Terminal Interface Data Processor Segment (IDPS) software.
The current field terminals used throughout NOAA and the worldwide civilian community will not be capable of receiving NPOESS data in their current configurations. For example,

the planned LRD frequency and data rate are substantially higher than the current Automatic Picture Transmission (APT). OSDPD is working with users to ensure that the IPO's proposals address all user requirements and that an integrated test strategy is developed to evaluate end-to-end interoperability.

8.5.2.1 High Rate Data (HRD) Broadcast Services

The NPOESS HRD broadcast service will be a complete, full resolution data set containing all sensor data and auxiliary data necessary to generate all NPOESS Environmental Data Records (EDR) and is intended to support users at regional hubs. The HRD broadcast service will be transmitted at X-band frequencies, at a data rate of about 20 Mb/s, and will require a bandwidth of nearly 50 MHz, with a receive antenna aperture not to exceed 2.0 meters in diameter. The IPO has reviewed alternative spectrum availability and has determined that the WARC-97 EESS X-band allocation at 7750-7850 MHz is suitable for this application.

8.5.2.2 Low Rate Data (LRD) Broadcast Services

The NPOESS LRD broadcast will be a subset of the full NPOESS sensor data set and is intended for NOAA and worldwide users of field terminals (land and ship-based, fixed and mobile environmental data receivers operated by different users and surface receivers operated by other federal agencies, worldwide weather services, and other international users). Some data compression (Lossy or Lossless) may be employed for the LRD link. The LRD L-band broadcast will provide data at a rate of about 4.0 Mbps (nominally 3.88 Mbps) at 1702.5/1706.5 MHz with full Consultative Committee for Space Data Systems (CCSDS) convolutional coding, Viterbi decoding, and Reed Solomon encoding/decoding into a tracking receive antenna aperture not to exceed 1.0 meter diameter.

The LRD broadcast will be available on two selectable channels to accommodate multiple NPOESS spacecraft in the same orbit during life-cycle replacement. The NPOESS LRD broadcast parameters (frequency, bandwidth, data rate, and data content) have been selected to satisfy NOAA requirements for low-rate, real-time direct broadcast, as well as be closely compatible with the satellite broadcast parameters for the Advanced High Resolution Picture Transmission (AHRPT) format that has been accepted and approved by the Coordinating Group on Meteorological Satellites (CGMS) and will be used on the European Organization for the Exploitation of Meteorological Satellites (EUMETSAT) Metop spacecraft. Thus, the NPOESS LRD service will include data required to satisfy the U.S. user specified highest priority EDR mode for real-time broadcast.

Fifteen additional lower priority EDR values will also be included in the LRD broadcast. While the eight high priorities EDR modes will be produced at the LRD "objective" level of performance, including data latency of two minutes for imagery EDR processing and 15 minutes or less for the other EDR, these lower priority EDR will be produced between threshold and objective levels with less stringent latency requirements.

8.6 Weather Ground Processing of Satellite Meteorological Data

Leveraging proven meteorological satellite Ground Segment technology for weather and climatology observations, the service designers of modern ground meteorological processing solutions address the significant challenges associated with the new generation of weather and environmental satellites and the expanding sources of environmental intelligence. Each

weather mission benefits from the ability to leverage a range of sources and translate these into mission-specific intelligence for both civil and military missions.

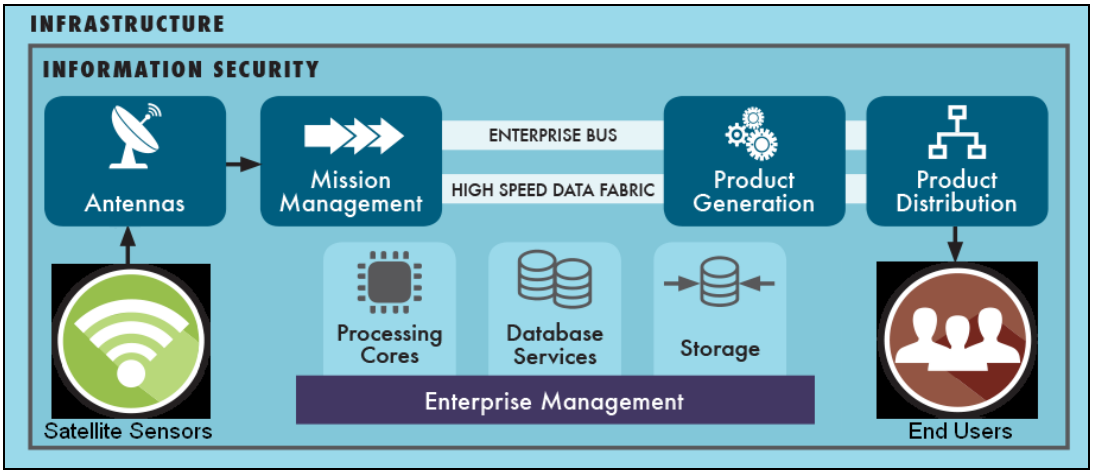

Figure 8. 18 Meteorological Modular Ground Processing Systems by Harris 2015

Thus, an enterprise ground system provides the optimal framework for the future, and experts designed, delivered and tested the modern ground system using this concept. In fact, these new ground solutions employ common algorithms and shared computing resources, within a comprehensive service-oriented architecture to affordable access, process and distribute data and products from a variety of satellite sensor data sources, including dedicated satellites, hosted payloads, ancillary data, mesonets and more.

The benefits of unified solutions in the establishment of weather ground processing are as follows:

1. System Consolidation – This effort minimizes the total cost of ownership of the complete systems' landscape by removing stovepipes and replacing them with an integrated and unified flexible system;
2. Operational Efficiency – This is a solution that applies scalable/extensible service-oriented architecture to affordable access, process, and distribute data and products from any applicable environmental satellite;
3. Operational Readiness – This decreases the time to availability when introducing new technologies and launching new services by deploying agile processes and systems, easily adaptable to changing requirements;
4. Acceleration of New Capabilities – This factor eliminates redundant acquisitions, utilizes a common baseline and allows business processes to be streamlined; and
5. System Security – This is needed to provide security design methodology to ensure that customers' systems will not suffer denial-of-service attacks and eliminates the downtime of operations due to hackers with malicious intents.

Modular ground processing components and solutions offer scalable, off-the-shelf, affordable and reliable solutions to address key elements of modern ground processing systems, which are shown in Figure 8.18. From components to end-to-end solutions, these solutions are scaled to fit the specific mission needs to all customers in satellite meteorology.

8.6.1 Meteorological Satellite Ground Program and Service

Given that South Africa and entire Africa is in the coverage area of the European Eumetsat system, here will be introduced its Meteosat system, as a representative of the Global Meteorological Satellite System (GMSS). The Meteosat system is defined by a number of overlapping cooperation programs, which establish the respective legal and financial frameworks during particular periods. These programmatic arrangements do not affect the user community to any great extent, but are often referred to and are recalled for the sake of completeness.

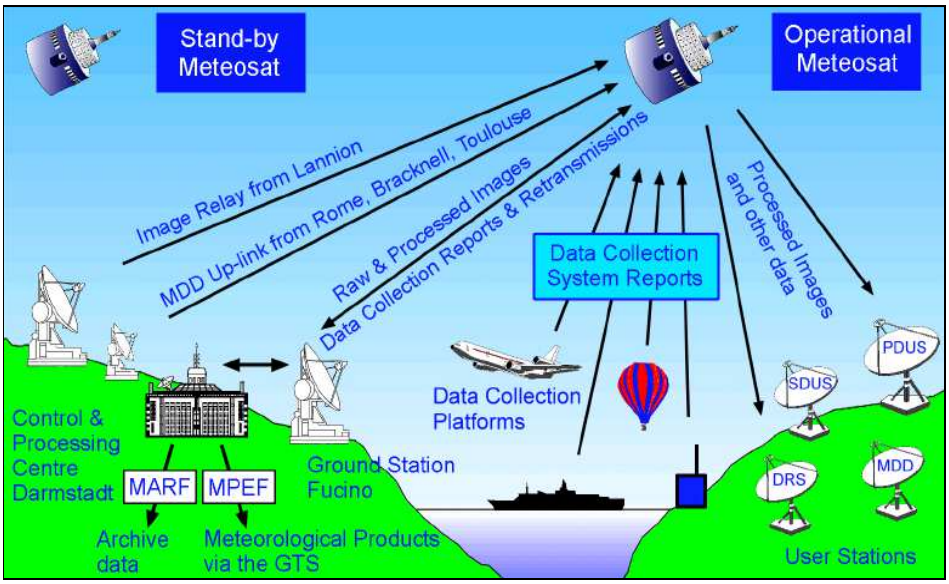

Figure 8. 19 Main Services of Meteosat System by Eumetsat 2009

The development and early operation of Meteosat was covered by a series of ESA programs until 1983. These ensured the development of the two original flight models, and of the prototype, which was later refurbished and flown as Meteosat-3. When Eumetsat was defined in 1983, ESA initiated the Meteosat Operational Programme (MOP) and, from 1987, this was conducted as a joint program, under the overall authority of Eumetsat. Thus, this program provided the framework for the construction and launch of three further Meteosat satellites.
Since it had been decided that a new generation of satellites would not be immediately available by the end of the Meteosat Operational Programme, Eumetsat implemented the Meteosat Transition Programme (MTP), which includes the provision and launch of a further satellite of the same design. It has since been agreed to extend MTP Operations until 2003 to provide an overlap with the next generation of satellites (MSG). The current Meteosat system, as defined in this document, is, therefore, operated within the MTP framework.

The main service provided by the Meteosat system is the generation of images of the Earth, showing its cloud systems both by day and by night and the transmission of these images to the users in the shortest practical time. There are several other important supporting services summarized in the following sections and described in more detail in the next chapter.

The main services of the Meteosat system are shown in Figure 8.19. The principal components are: Meteorological Archive and Retrieval Facility (MARF), Meteorological Products Extraction Facility (MPEF), Primary Data User Station (PDUS), Secondary Data

User Station (SDUS), Meteosat Data Retransmission System (DRS) and Meteorological Data Distribution (MDD).

8.6.2 Earth Imaging

The Meteosat radiometer is the principal payload of the satellite. It provides the basic data of the Meteosat system in the form of radiances from the visible and infrared parts of the EM spectrum. These form images of the full earth disc, as seen from geostationary orbit. Thus, the radiometer operates in the following three spectral bands:
- 0.45 to 1.0 µm – Is the visible band (VIS) used for imaging during daylight?
- 5.7 to 7.1 µm – Is the water vapour absorption band (WV) used for determining the amount of water vapour in the middle atmosphere?

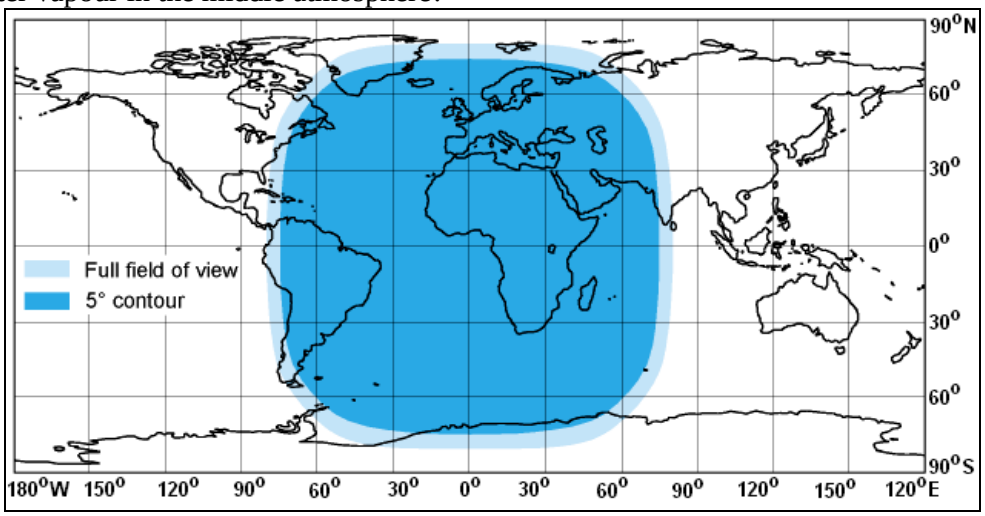

Figure 8. 20 Telecommunications Coverage Area of Meteosat by Eumetsat 2009

- 10.5 to 12.5 µm – Is the thermal infrared (window) band (IR) used for imaging by day and by night and also for determining the temperature of cloud tops and of the ocean's surface?

Otherwise, Earth images are generated at 30 minute intervals from meteorological space to ground segment. Each image is transmitted from the satellite to the Primary Ground Station (PGS) Fucino in Italy and relayed to the central facilities in Germany for further processing, distribution and archiving. As can be seen from the illustrations in Chapter 6, each image covers a substantial portion of the Earth, centered at the sub-satellite point, which is over the equator and normally at 0^o longitude. In this way, using these images, meteorological features can be identified and weather patterns tracked out to nearly 70^o of the great circle arc from the sub-satellite point. The distorted perspective introduced by the Earth's curvature makes quantitative use of the data less satisfactory at large distances from the sub-satellite point, but quantitative products are generated routinely for distances of at least 60^o of the great circle arc.

8.6.3 Image Dissemination

Meteosat is equipped with High Power Amplifiers used to transmit processed Earth images and other meteorological information to user stations located anywhere within the field of view of Meteosat, as shown in Figure 8.20. The dissemination schedule is dominated by the transmission of Meteosat imagery in all three spectral bands.

However, these images are complemented by the International Data Collection System (IDCS), which receives data from other meteorological GEO satellites, including the US satellites GOES-E and GOES-W over the western Atlantic and eastern Pacific, Japan's GMS satellite over the western Pacific, Chinese FY-2 over Eastern Pacific and the Russian GOMS satellite over the Indian Ocean, as shown in Figure 8.21. Images from other satellites will be added as available, so that, with a single receiver and antenna system, the Meteosat user station can acquire images covering most of the globe.

The satellite carries two independent dissemination channels used to transmit image data with minimum delay to two classes of user stations. Digital data are transmitted to Primary Data User Stations (PDUS), which are intended to serve the larger meteorological centres and research centres, while analogue data are transmitted to the less complex Secondary Data User Stations (SDUS), widely implemented in smaller meteorological centres as well as in many schools and by private individuals.

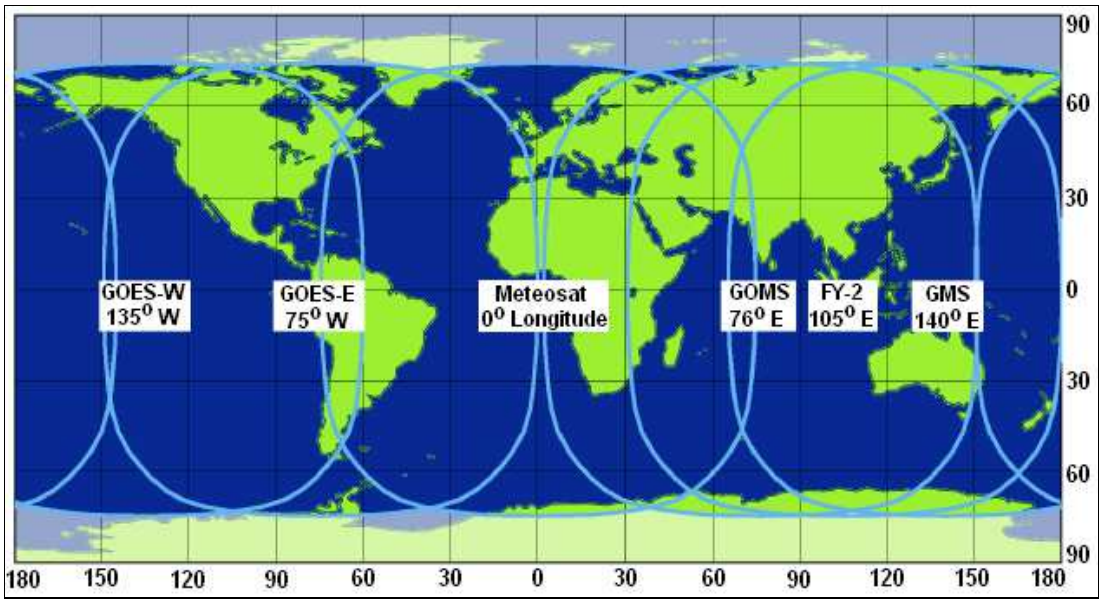

Figure 8. 21 International Data Collection System by Eumetsat 2009

8.6.4 Meteorological Data Collection and Distribution

Besides its main dissemination channels, Meteosat provides a further 66 telecommunication channels used for the relay of environmental data from automatic or semi-automatic Data Collection Platforms (DCP). Regional DCP stations may be located anywhere within the Meteosat field of view, as shown in Figure 8.20, and are served exclusively by the Meteosat Data Collection System (DCS), which relays the data through the satellite to the Primary Ground Station (PGS) for onward distribution.

The so-called International DCP (IDCS) stations are mobile platforms, such as ships and aircraft. These can move anywhere in the world and are supported through the IDCS stations, which are co-ordinated by all of the geostationary meteorological operators. The DCP data are distributed by a variety of means. In this instance, the Meteosat DCP Retransmission Data System (DRDS) broadcasts DCP data directly to small user terminals, while meteorological data from many DCP stations are also transmitted over the Global Telecommunication System (GTS) of the World Meteorological Organization (WMO).

Additional Meteosat satellite telecommunication links are used for the transmission of conventional meteorological data, including observations in meteorological transmission codes and meteorological charts containing both data analyses and forecasts. In fact, this is Meteosat's unique Meteorological Data Distribution (MDD) service. The data are transmitted directly to the satellite through three independent up-link sites located at meteorological centres in France, Italy and the UK, and received by small user terminals.

8.6.5 Meteorological and Climatological Products

The Meteorological Products Extraction Facility (MPEF), which is located in the Eumetsat headquarters, makes use of the satellite digital Meteosat image data to generate a variety of quantitative meteorological and climatological products. At this point, the meteorological products include wind vectors obtained through the automatic tracking of clouds as they move through the atmosphere. The Cloud Motion Winds (CMW) are of great importance as inputs to the computer models used for numerical weather prediction, especially over tropical areas where there are few other observations of atmospheric dynamics.

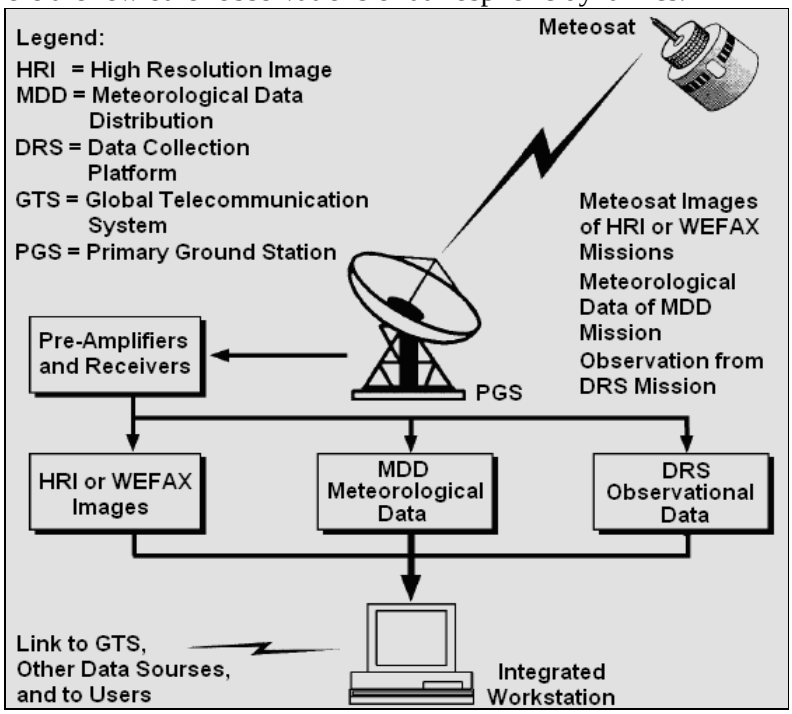

Figure 8. 22 MOSAIC Concept of Integrated User Facility by Eumetsat 2009

The Meteosat facility also generates several climate products, including the data needed for the International Satellite Cloud Climatology Project (ISCCP). Thus, clouds form a vital part of the Earth's climate system helping to insulate the Earth from excessive solar radiation during the day and to reduce heat loss from the planet at night. The ISCCP model, to which Meteosat contributes, has been systematically storing global cloud coverage parameters since 1983 and is a major resource for climate studies.

8.6.6 Meteorological Archiving and Retrieval

The final component of the Meteosat system is the Meteorological Archive and Retrieval Facility (MARF), which is also located within the Eumetsat headquarters in Darmstadt. This facility has been archiving all Meteosat image data and derived products in digital format

since 1995. It provides a comprehensive data retrieval service including on-line access to the data catalogues and other information.

The digital data are written to Digital Linear Tape (DLT), each having the capacity to store several days' images. This is a different medium from that used to store images before 1995 and the same retrieval mechanism cannot be used to directly retrieve the data archived prior to that date. However, the older data, extending back to 1977, remain available and can be retrieved using independent systems. A project to systematically transfer the old data from some 40,000 tapes and cartridges to the newer medium will take some years to complete.

8.7 Meteosat Operational Systems for data Acquisition and InterChange (MOSAIC)

The Eumetsat MOSAIC meteorological concept is not a separate service but indicates how all of the real time Meteosat services can be brought together at a user site to provide a consolidated "one-stop shopping" service, meeting many of the data requirements of small meteorological centres, as shown in Figure 8.22.
A single antenna system may be used to receive frequent image data from Meteosat and from other satellites around the world. The same antenna can be used as a DRS terminal to receive environmental data from data collection platforms located within the region of interest and can also form part of an integrated MDD terminal for the reception of other meteorological data. Furthermore, modern computer workstations or personal computer systems can be used to display, store and print all of the data in a cost efficient way.

Low cost disk storage systems may be used to provide a local satellite meteorological image archive. Many meteorological centres have all of these facilities, which may be combined into a single integrated facility.

8.7.1 Meteosat PGS System Frequencies

The spacecraft has a comprehensive telecommunications capability, which can be described under two headings:

1. System frequencies used for raw image reception, telemetry, tracking telecommands and for spacecraft orbit determination, described in this section; and
2. User accessible frequencies, described in the following section: S-band in the range 2098 - 2110 MHz and L-band in the range 1675 - 1690 MHz are the frequency bands used for system related functions.

These include row image transmission from the spacecraft to the PGS in cite Fucino, transmission of telemetry data from the spacecraft and telecommands to the spacecraft, transmission of DCP reports from the spacecraft to the Primary GES, up-link of image dissemination data from the PGS to the spacecraft, up-link of MDD data from a maximum of four ground stations, and ranging signals transmitted between the PGS in Fucino, spacecraft and the Land-Based Transponder (located in French Guiana), used for determination of the precise location of the satellite in orbit.

The normal data rate of the raw image data from the spacecraft to the PGS is 333 Kb/s, which is achieved through onboard buffering of each line of image data during the Earth scan so that it may be transmitted during the much longer period (20 times as long) when the radiometer is viewing space. However, if this onboard buffering were disabled, then an

alternative direct transmission would be used at a data rate of 2.7 Mb/s. Thus, all of these transmissions are intended for point-to-point transmissions between the satellite and the Eumetsat PGS or Back-up Ground Station (BGS) and are not broadcast for general use. For security and copyright reasons, the transmissions are not available to the user community and are strictly reserved for system use.

8.7.2 Meteosat UGS System Frequencies

Data transmissions to User Ground Stations (UGS) form part of the essential service of Meteosat and the frequencies used are, of course, available to registered users. The L-band is for user-related functions, including the following frequencies required to receive the specified Meteosat service:

- 1691.0 MHz WEFAX analogue image dissemination and the DRDS;
- 1694.5 MHz HRIT of digital image dissemination, with arrangement of a few WEFAX transmissions; and
- 1695.605 - 1695.935 MHz MDD, with up to four channels spaced at 30 kHz.

In addition, Data Collection Platforms may be given access to one of the 66 up-link channels in the UHF band between 402.0 and 402.2 MHz with 3 kHz channel separation. A channel and precise time slots for data transmission are assigned to each individual DCP when registration is accepted.

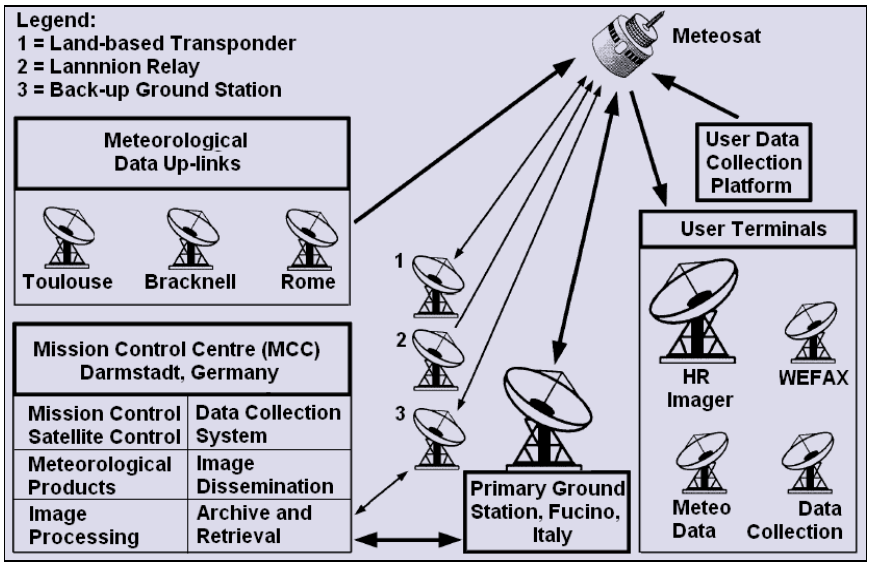

Figure 8. 23. Block Diagram of Meteosat System by Eumetsat 2009

8.8 Meteosat Ground Segment Facilities

The Meteosat ground segment, as shown in Figure 8.23, consists of a number of major components at different locations, which include: Primary Ground Station (PGS), located in Italy, serves for all normal communications with the spacecraft; Mission Control Centre (MCC) located in Germany, where the complete system is monitored and controlled, and all data processing is undertaken; Back-up Ground Station (BGS), used in emergencies for monitoring and control of the spacecraft; Lannion facility, used to up-link image data from satellites other than Meteosat; Up-link sites for the MDD service, used to broadcast

meteorological data through Meteosat; Land-Based Transponder (LBT), used for orbit determination; and the user (UGS) facilities, located at user sites and under the direct control of the relevant users. The Meteosat ground segment consists the following subsegments:

1. Meteosat Primary Ground Station (PGS) – This PGS was established in Fucino with its facility fully owned by Eumetsat located within a commercially operated centre, which includes a major antenna farm serving many satellite systems, as shown in Figure 8.24.

Figure 8. 24. Meteosat Antennas at the Fucino PGS by Eumetsat 2009

The actual PGS site is in a wide valley in the mountains some 150 km east of Rome. Thus, the PGS serves as the main channel of communications with the Meteosat satellites and is an essential component of the Meteosat system.

2. Meteosat Back-up Ground Station (BGS) – This is a separate station located in Cheia, near Brasov, Romania, which can be used in emergencies for satellite control purposes, but only the PGS has the operational capability to support the main user services, handling the raw image transmissions from the satellite and re-transmitting the processed images back through the satellite to the users. The PGS also uniquely supports many other user-related functions and has the capability to act as the Back-up Satellite Control Centre (BSCC), in the event of severe problems at the Mission Control Centre (MCC) in the Eumetsat headquarters or failure of the main communications links between the MCC and PGS. To accomplish these vital tasks, a considerable amount of redundancy is incorporated in the station, which, to a great extent, can function completely automatically. No operating staff is normally required at the PGS; engineering support is available for maintenance purposes only during normal working hours, while normal operations are supervised by the MCC in Darmstadt, Germany (SCISYS, 2014).

3. Antenna and Monitoring Control – Two fully steerable 13.2 metre diameter parabolic antennas, as shown in Figure 8.24, are located at the PGS and used exclusively to support all communications with Meteosat. Each antenna is capable of supporting all the transmissions and data reception required for one Meteosat spacecraft and is used for TT&C, raw image reception, processed image dissemination, DCS and for monitoring MDD service. Thus, the antennas are situated within a few tens of metres away from a building used exclusively for the Meteosat equipment.

The control of the PGS is actually executed by a local monitor and control system located in Fucino and interacting with the MCC in Darmstadt. The PGS can operate in two different

modes: remotely, under the control of the MCC; or through use of the system consoles in Fucino. This flexibility ensures maximum reliability in case of problems.

4. Equipment and DCP Retransmission System – The Fucino PGS is fully equipped to handle two complete Meteosat spacecraft, with additional redundancy of key components. The only exception to this philosophy is the support for the DCS, since it is envisaged that only one spacecraft would support this service. All of the 66 DCP channels can be supported simultaneously, with primary and back-up DCS systems.

Whilst most of the Meteosat data processing is performed at the MCC in Darmstadt, one service is conducted entirely within the PGS, namely, the DRDS. DCP messages received in the PGS are selected according to a pre-defined list and are then transmitted directly from the PGS to the spacecraft in the gaps between the transmissions of individual WEFAX image dissemination formats. This normally ensures the delivery of DCP messages within four minutes of observation to any user having a DRS data reception terminal. In addition to this DRS activity, all DCP messages received at the PGS are transmitted to the MCC for further processing and distribution, depending on the requirements of each operator.

5. Back-up Satellite Control Centre – Also located at the PGS is a BSCC established as a functional extension of the MCC in Darmstadt. At this point, in an emergency, it could be used in standalone mode to monitor and control the spacecraft and the PGS, as well as to perform all essential flight dynamics activities. It is not designed to support the Meteosat user services but does ensure the safety of the spacecraft until the problem is solved. The BSCC can also be used in parallel with the MCC to operate the PGS and to monitor the spacecraft.

6. Mission Control Centre (MCC) – This is a special dedicated facility incorporated in the operations wing of the Eumetsat headquarters building in Darmstadt, Germany. Dedicated communications links connect it to the PGS in Fucino and to the BSCC station in Cheia near Brasov, Romania. The MCC is the core of the Meteosat ground segment. The entire system is controlled from the MCC and this is also where all of the central processing is conducted.

Figure 8. 25 Mission Control Centre by Eumetsat 2009

Facilities are installed for the monitoring and control of the main components of the Meteosat system, including the spacecraft, PGS, main communication links and the MCC itself, which is shown in Figure 8.25. Additional facilities of MCC are used to generate meteorological products from the Meteosat image data, to archive the images and products, and to monitor the end-to-end performance of the system from the point of view of an end-user.

7. Image Processing - Apart from the control function, a primary task of the Core Facility is to process the image data in real-time. Raw images are received from the PGS and processed line-by-line to remove image imperfections, as shown in Figure 8.26. In particular, the data

from the various onboard sensors are realigned by resampling in order to make the image from each set of detectors coincide with the other images. At the same time, sampling removes the slight perturbations caused by the movement of the spacecraft, thereby rectifying the image so that it appears to come from the nominal location of the spacecraft. Adjustments to the individual data values are made according to calibration information, then the image is passed to the dissemination PC for immediate relay to users and to the meteorological computers for further processing.

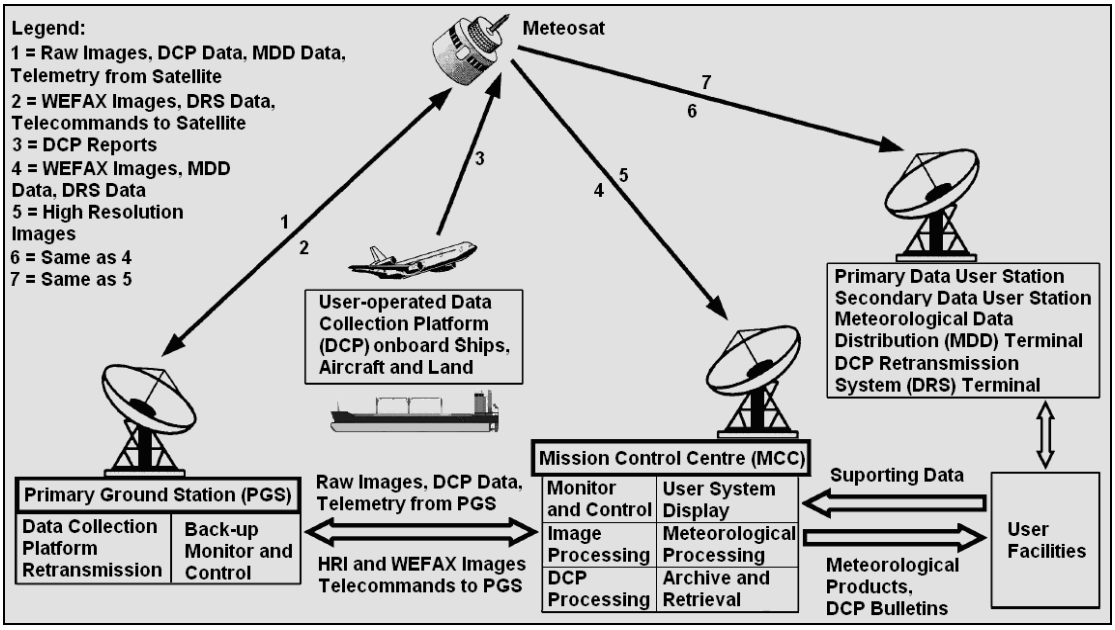

Figure 8. 26 Meteosat Min System Data Flows by Eumetsat 2009

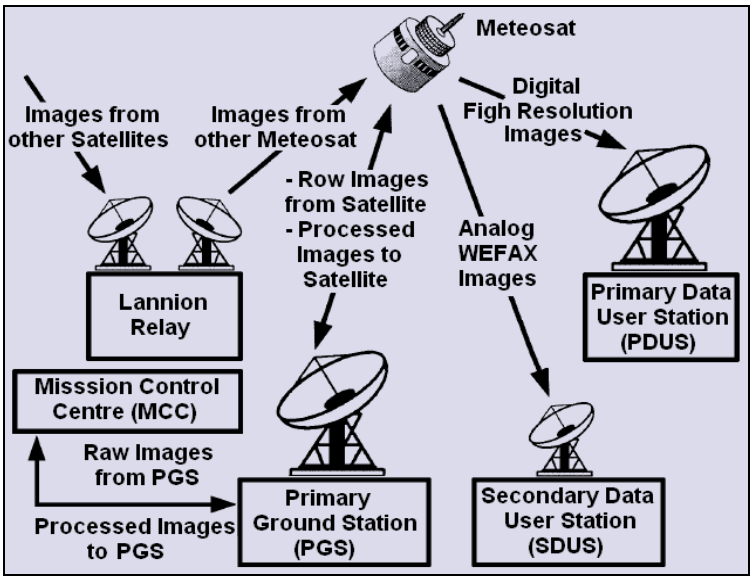

Figure 8. 27 Block Diagram of Meteosat Dissemination System: by Eumetsat 2009

8. Image Dissemination – The dissemination of Meteosat images is also prepared in the Core Facility of the Mission Control Centre using dedicated workstations, as shown in Figure 8.27. Processed images are cut into individual formats ranging in size from the full earth disc to segments covering Europe or smaller areas. These formats are prepared according to a pre-

defined schedule for the two Meteosat dissemination channels and sent back down the communications links to Fucino for uplink to the spacecraft and then transmitted to the users. The aim is to make the processed image data available to the users with the minimum of delay. Priority is given to the European sectors, for which the processing is completed and dissemination started within three minutes of the completion of image acquisition. Transmission of the image covering the full Earth disc starts four minutes later, and the full earth imagery data are normally fully available on the users' computer systems within a maximum of 20 minutes from the completion of image acquisition.

9. User Station Display Facility – The dissemination of processed images is the primary function of the Meteosat system and is accomplished strictly according to a pre-defined schedule matching user requirements. The operation of the central service is monitored by the Core Facility of the MCC but there may be rare occasions when the disseminated images may be subject to some distortions or errors, which are not readily detected by the mission monitoring computers.

The operation of the central service is monitored by the Core Facility of the MCC but there may be rare occasions when the disseminated images may be subject to some distortions or errors, which are not readily detected by the mission monitoring computers. Alternatively, the system at a user site may itself have problems and the user needs to know if there is a problem with the local terminal or with the central facilities. Accordingly, a complete User Station Display Facility (USDF) is co-located with the Core Facility. The USDF has its own independent antenna and receiving system, together with a display system shown in Figure 8.28, so that it can independently monitor the final results of the image dissemination system. The received images from both communications channels are displayed on monitors and are used as a final check on quality. The details of the received data are also monitored by the USDF computers and passed back to the Core Facility for analysis and comparison with the transmitted data. By this means, the system operators can, at any stage, be aware of any problem in the complete system and take immediate action to rectify the situation.

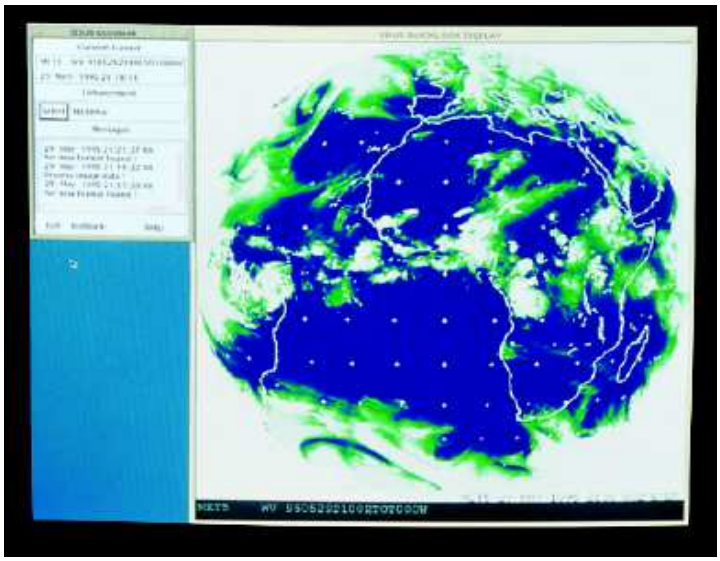

Figure 8. 28 User Display Screen for Monitoring Image Reception by Eumetsat 2009

8.9 User Earth Stations (UES) onboard Mobiles

The UES terminals can be installed onboard ships, land vehicles and aircraft. Aircrafts can use the same equipment as ships or vehicles use, but the antenna has to be flat or installed in the tail of aircraft.

8.9.1 Weather Decision Support (WDS) Systems for Automatic Satellite Tracking

The Weather Decision Support (WDS) infrastructures are special ground satellite antenna and receivers that are receiving from meteorological satellites images direct broadcast to the fixed and mobile ground stations. These WDS installations can be some locations on the ground or onboard vessels and vehicles, whose task is to process and produce received local and hemispheric weather images for government, corporate, personal and private customers.

8.9.1.1 Shipboard Satellite Weather Receiving 0.61m L and S-band Antenna

The WDS shipboard receiver is receives and produces local and hemispheric weather images from the meteorological satellites that are directly broadcast to the vessel and other customers. In addition to satellite data, the WDS system automatically receives, processes and displays meteorological and maritime forecast data tailored to the vessel's operating areas of interest. The TeraScan L and S-band Shipboard System utilize a 0.61 m flat plate phased array antenna mounted on a 3-axis positioner installed inside a 0.90 m radome. The radome size has been carefully matched to the antenna to minimize weight and overturning moment. Figure 8.29 presents the Shipboard Satellite Weather Receiving 0.61m Antenna **(Left)** and WDS Shipboard GUI **(Right)**.

Ideal for shipboard operations where space is at premium, the 0.61m Weather Decision Support (WDS) System automatically tracks satellites while in ship motion. It is designed to receive and process data from current Polar Earth Orbiting (PEO) meteorological satellites.
The WDS system comes with specialized software that automatically receives oceanographic products. The Graphical User Interface (GUI) displays as a special human computer interface that was developed with the mariner user in mind for more easy operations during any surrounded weather conditions.

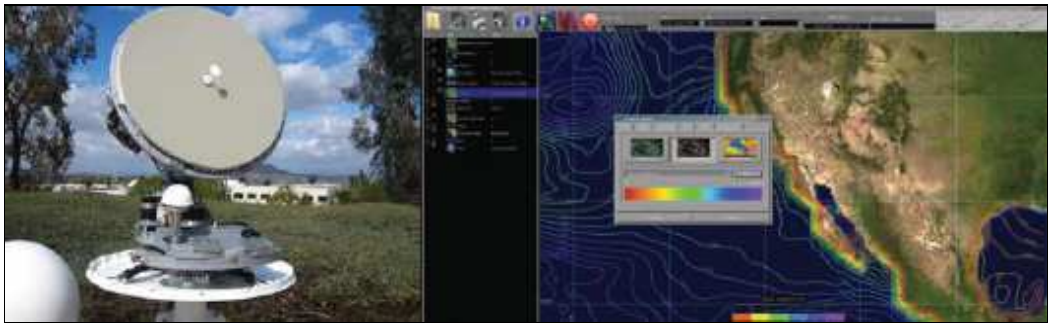

Figure 8. 29 Shipboard Satellite Weather Receiving 0.61m Antenna and WDS Shipboard GUI: by SeaSpace 2011

The key features of both L and S-band shipboard satellite weather receiving antenna are:

- High reliability for mission critical operations;
- Theater-wide coverage;
- Low maintenance cost and power consumption;
- Unique feed and compact design;
- Multi-mission with L and S-band capability;
- Oceanographic Specific GUI; and
- Automated data processing.

Figure 8.30 presents Cloud Top Temperature Characteristics and Infrared (IR) Cloud Data with blue colour enhancements. It is necessary to underline that meteorologists use colour-enhanced imagery as an aid in satellite interpretation. The colours enable them to easily and quickly see features that are of special interest. Usually they look for high clouds or areas with a large amount of water vapour.

In an IR image, cold clouds are high clouds, so the colours typically highlight the colder regions The IR enhancement 1 is shown in Figure 8.31 (Left) and the IR enhancement 2 is shown in Figure 8.31 (Right). The bar on the right side of the image indicates the pixel brightness values for the corresponding colour. The intensity value represents emitted infrared radiation. The intensity of a pixel is recorded as a digital number (for example, in these images the numbers range from 0 to 255). It is possible to determine temperatures using one of the formuli below:

If B > 176, T = 418 - B; or
if B <= 176, T = 330 - (B/2) (8.1)

Note that the resulting temperatures are in Kelvin.

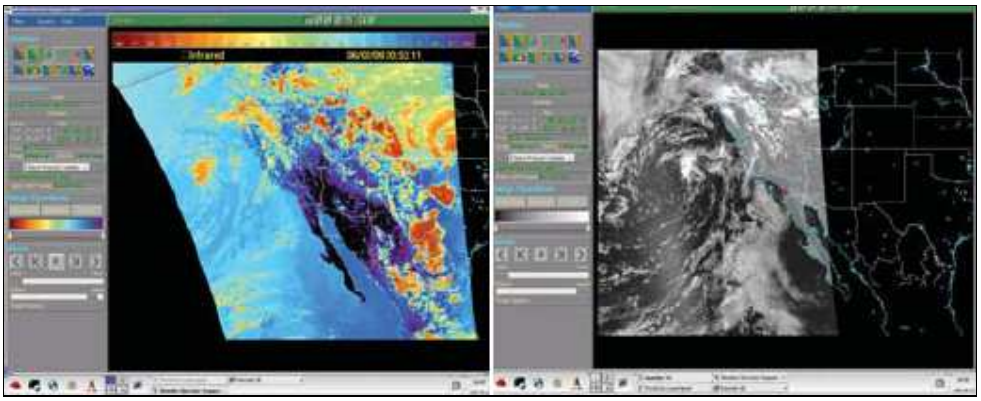

Figure 8. 30 Cloud Top Temperature and IR Cloud Data SeaSpace 2011

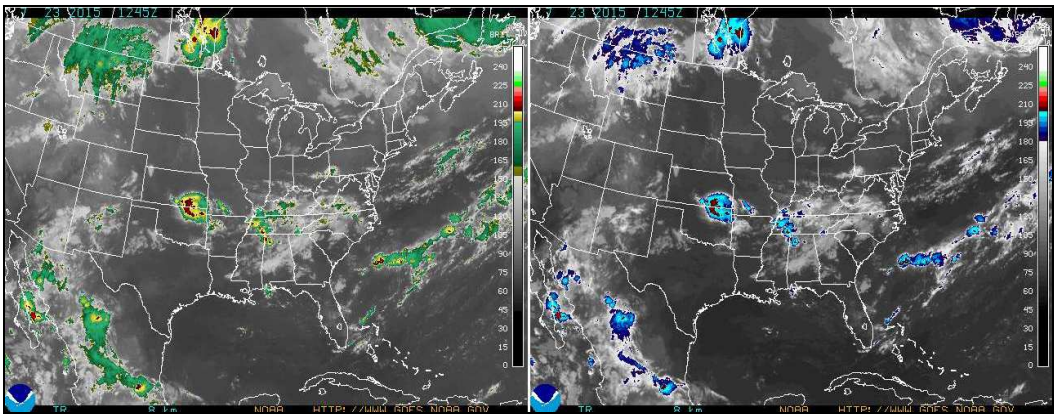

Figure 8. 31 IR Enhancement 1 and 2 by NOAA 2004

To calculate the resulting Kelvin temperature to Fahrenheit: (K - 273.15) x 1.8 + 32.00.
To calculate the resulting Kelvin temperature to Celsius: C = K - 273.
(B = Brightness value; T = Temperature; F = Fahrenheit; C = Celsius).

Both models WDS6100L (L-band) and S (S-band) have common components, such as feed, antenna pedestal, reflector, RF electronics, radome (top and base), basic spares kit, and O&M manual. The samples of shipborne and ground antennas are illustrated in Figure 8.32 (Left & Right), respectively. In addition, both types of WDS6100 antennas contain L-band or S-band feeds, antenna pedestals, reflectors, RF electronics, radomes (top and base), basic spares kits and Operation and Maintenance (O&M) Manual.

The L-band antenna, on the frequency band 1680 -1710 MHz, provides the following telemetries: NOAA does High Resolution Picture Transmissions (HRPT); FengYun (Chinese Weather Satellite) does Chinese High Resolution Picture Transmission (CHRPT); METeorological OPerational (METOP) Polar Eumetsat Satellite does Advanced High Resolution Picture Transmissions (AHRPT); and there is Low Rate Information Transmission (LRIT). Its antenna gain value is 17 dBic, aperture efficiency is 70%, noise temperature is 0.7 at 23°C, total system noise temperature is 85.7 K and system G/T is 0.26 dBK.

The L-band antenna, on frequency band 2200-2270 MHz, provides telemetries, such as Real Time Data (RTD) for the US Defense Meteorological Satellite Program (DMSP). The gain of this antenna is 20 dBic, system G/T is 2.69 dBK and other values are the same to the L-band antenna.

Figure 8. 32 Shipboard and Ground-based WDS6100 L and S-band Antennas SeaSpace 2011

Figure 8. 33 Shipboard 2.0 m Radome and Type of WDS Vessel by SeaSpace 2011

8.9.1.2 Shipboard Satellite Weather Receiving 1.5m L/S-band Antenna

This type of receiver and antenna also produces WDS for local and hemispheric weather images from meteorological satellites that are directly broadcast to the vessel. Similar to the previous solutions, this WDS system also automatically receives, processes and displays meteorological and maritime forecast data tailored to the vessel's operating areas of interest. The TeraScan L/S-band Shipboard System utilizes a 1.5m antenna reflector mounted on a 3-axis positioner installed inside a 2.0 m radome. The radome size of the antenna has been designed to reduce weight, overturning moment and site preparation requirements and costs. Low-loss, impedance-matched radomes enable operation in extreme environments without sacrificing RF performance. Each antenna system is perfectly balanced in all 3 axes and exhibits no inherent backlash.

There are no pointing and tracking errors associated with torsional stiffness since there is no strong wind loading on the tracking system and the velocities and accelerations are kept extremely low. The antenna automatically tracks satellites while the vessel is in motion, as shown in Figure 8.33 **(Left)** and type of vessel **(Right)**. It is designed to receive and process data from current L and S-band PEO meteorological satellites. This antenna system includes specialized software that automatically receives and processes data into oceanographic products, with a GUI display developed for use onboard vessels.

The key features of L/S-band shipboard satellite weather receiving antenna are:
- High tracking accuracies, low velocity and acceleration requirements;
- No keyhole losses at any elevations and completely balanced system;
- 3-axis, Elevation over Cross- Elevation over Azimuth configuration;
- Low-loss radome enclosure for all installations; and
- Integrated tracking receiver with Pulse Width Modulation (PWM) servo control system.

The PWM mode or Pulse Duration modulation (PDM) is a modulation technique used to encode a message into a pulsing signal. Although this modulation technique can be used to encode information for transmission, its main use is to allow the control of the power supplied to electrical devices, especially to inertial loads such as motors.

The 1.5 m shipboard L-band and L/S-band antennas contain L or L/S-band feed, antenna pedestal, reflector, RF electronics, antenna radome (top and base), basic spares kit and O&M manual. L-band input frequency is 1670 - 1720 MHz S-band input frequency 2166 - 2315 MHz. Thus, RF Performance G/T at S-band is 5.5 dBK minimum at 2240MHz and G/T at L-band is 5.0 dBK minimum at 1700MHz. Input signal power is -90 to -50 dBm, input frequency is 126 - 154 MHz and demodulation is BPSK-PSK.

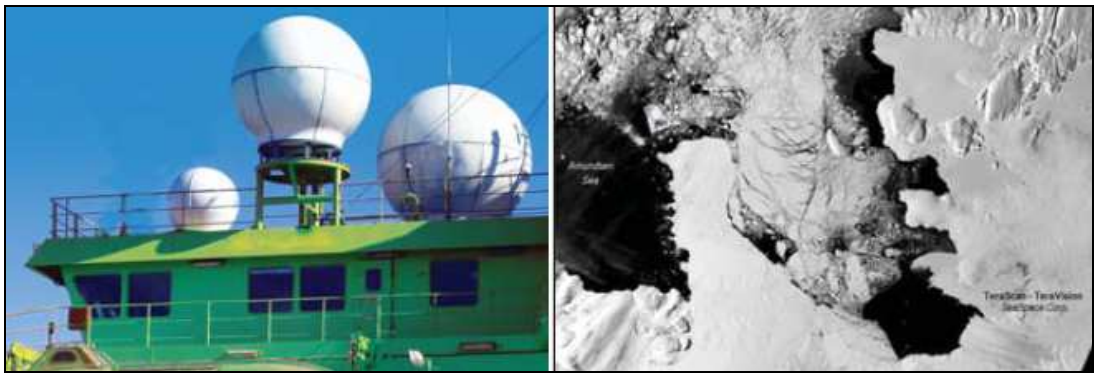

Figure 8. 34 Shipboard 2.4 m Radome and Iceberg Mapping in Antarctic by SeaSpace 2012

The system is supporting the following telemetries: NOAA HRPT, METOP and DMSP RTD, and also supports data encoding such as Non-Return to Zero (NRZ) formats, NRZ-S, NRZ-M and Phase Encoded Format (Biphase-L). This solution uses Linux OS, such as Red Hat Enterprise Linux (RHEL) and Community Enterprise Operating System (CentOS).

In telecommunication, the NRZ line is a binary code which is represented usually by a positive voltage, while zeros are represented usually by a negative voltage, with no other neutral or rest condition.

8.9.1.3. Shipboard Satellite Weather Receiving 2.4m L/S/X-band Antenna

The 2.4m multi telemetry WDS is configured with a tracking antenna and receiver for the reception of real-time weather images from meteorological satellites that are directly broadcast to the vessel. Real-time products include sea surface temperature for research, fishing, ice products for detecting ice edges and navigation support in the Polar Regions. Day-night band from Suomi-NPP (National Polar-orbiting Partnership) allow low-light detection at night and is useful for identifying illegal fishing. Infrared – visible products can be used for fog detection, storm tracking, course plot decisions and help to save fuel and avoid rough seas, while ocean chlorophyll maps can be used for research, pollution tracking

and fisheries. The system includes the necessary proprietary hardware and proven TeraScan software for the automated reception, processing, and visualization of products. This solution includes WDS specialized software that automatically receives and processes data into oceanographic products, with a GUI display developed for users onboard special vessels. The TeraScan system performs automated image navigation and geolocation for every major remote sensing satellite. A World Vector Coastline database and the TeraNav interactive navigation tool are included with each system. Figure 8.34 shows (central radome) a shipboard 2.4 m antenna **(Left)** and mapping of icebergs images in the Antarctic **(Left)**.

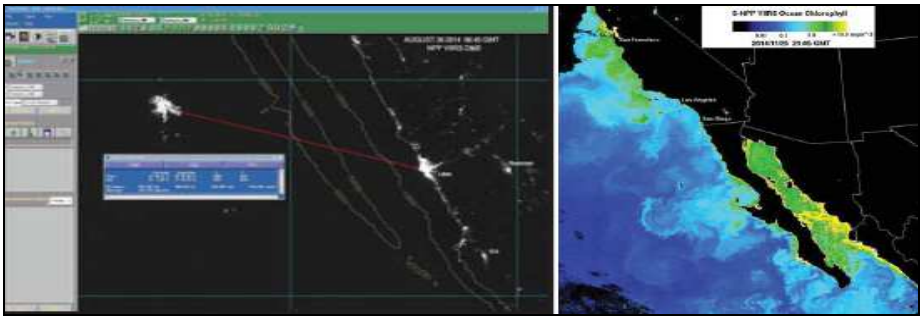

Figure 8. 35 NPP VIIRS Light Detection from Fisheries and TeraScan Color Imaging Data by SeaSpace 2011

Figure 8. 36 Vehicleboard 0.61m L-band Antenna and Ruggedized Laptop Mounted in Vehicle for WDS Processing by SeaSpace 2011

Figure 8.35 (Left) shows detection of nighttime lights from fishing fleets using NPP Visible Infrared Imaging Radiometer Suite (VIIRS) and Figure 8.35 (Right) illustrates meteorological data captured and processed by TeraScan for ocean colour used in monitoring primary productivity, pollution and fishing zones.

The key features of L/S-band shipboard satellite weather receiving antenna are:
- High tracking accuracies and stabilized positioner with continuous azimuth rotation;
- No keyhole losses at any elevation;
- 3-axis, Elevation over Cross-Elevation over Azimuth configuration;
- Completely balanced system and low maintenance cost and power consumption;
- Operation in extreme environments, Program Track and Autotrack Modes;

- High reliability for mission critical operations, easy to install, operate and maintain;
- End-to-End system solutions - Turn Key; and
- Automated capture and processing 24/7 and remote access control.

This solution uses Linux OS (RHEL and CentOS). Its input signal power is -90 to -50 L-band and -60 to -20 dBm at X-band. Input frequency is 126-154 MHz (L and S-Band), 720 MHz (X-Band) and demodulation types are: BPSK, SQPSK, USQPSK and QPSK.

8.9.1.4 TeraScan Satellite Acquisition System (TacSAS) THM

This WDS solution is ideal for commercial vehicle and military field operations, from mission planning to ordnance targeting service. The Tactical Satellite Acquisition System (TacSAS) provides both automated reception and processing of direct-broadcast weather and environmental data from the NOAA and DMSP series of Low Earth Orbit (LEO) satellites. Where time, transportation and manpower are at a premium, the entire dual-telemetry system fits into a HMMWV-sized vehicle and is easily deployed into a fully functional ground station within 10 minutes. The TacSAS provides joint mission interoperability, such as for naval, ground and air forces, and can now utilize identical equipment to exploit real-time satellite meteorological data, from imagery to vertical soundings. Thus, the TacSASTHM is designed to complement current deployments of TacSAS-FM terminals that receive and process data from GEO satellites (SeaSpace, 2011).

In the same way, this solution can be deployed for commercial land vehicles, whose vehicleboard 0.61m outdoor antenna is shown in Figure 8.36 (Left) and ruggedized indoor laptop mounted in the vehicle for WDS processing is shown in Figure 8.36 (Right).

The key features of L/S-band shipboard satellite weather receiving antenna are:

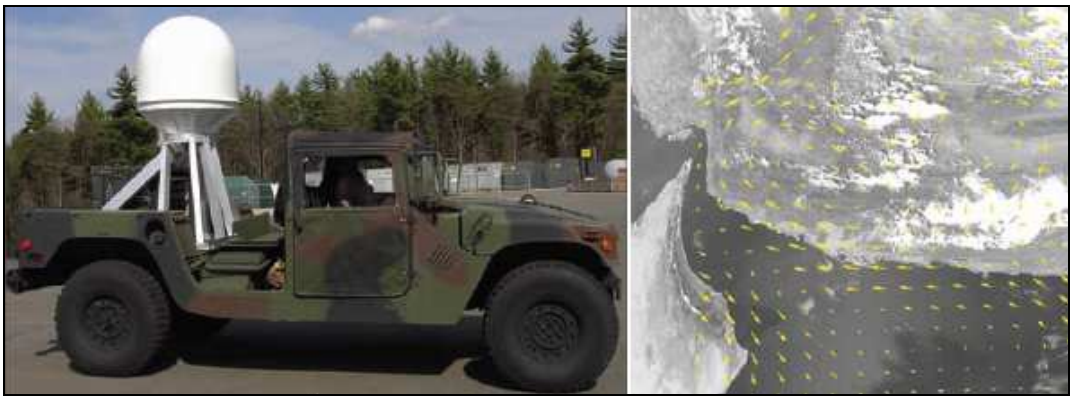

Figure 8. 37 THM Vehicleboard System in the Field and NOAA-16 AMSU Wind Speed Image by SeaSpace 2011

- High Resolution Data: Uses data acquired from the NOAA and MetOp (Meteorological Operation) satellites. Ground pixel size is 1km for visible and IR imagery, and 40km for microwave soundings;

- Wide Area Coverage: Data products include satellite's accurate and precise imagery and vertical profiles, covering greater than a 1,000 km radius, with profiles from ground level up to 20km altitude;
- LRIT Option: LRIT data are available when not acquiring NOAA/MetOp data;
- Low Observability: Less than 1m in height, fully camouflaged, and fully passive (no RF emissions);
- Proven Automated Performance: Timely and automatic generation and dissemination of data products for real-time decision making;
- Interactive Display. An intuitive graphical user interface includes the WDS interface and the TeraVision interface. Users can customize data viewing options; and
- No Consumables: Delivers timely and accurate weather satellite data without the use of expendables such as balloons.

Figure 8.37 (Left) illustrates the vehicleboard system in the field or may be any private or commercial vehicle, and Figure 8.37 (Right) illustrates the NOAA-16 satellite Advanced Microwave Sounding Unit (AMSU) Wind Speed Image. The size of the L-band satellite antenna is 0.61 m for receiving NOAA HRPT and MetOp data and to process them in the TeraScan Satellite Acquisition Module (TSAM) processor. The system also possesses the GPS antenna and receiver, and the tracking antenna is integrated with Selective Availability and Anti-Spoofing Module (SSASM).

8.9.2 HRPT/AHRPT Receives and Antenna System

The Dartcom HRPT/AHRPT Receivers and Antenna System provide very reliable, high performance land-based and marine mobile solutions for receiving, archiving, processing and displaying data from NOAA and Metop satellites, and optionally from FengYun-3 (L-Band) and DMSP (S-Band).

A number of land-based antennas are available (1.8 m, 1.2 m and radome-enclosed 1.5 m). A radome-enclosed 1.3 m antenna with active stabilization, which is illustrated in Figure 8.38 (Left), is suitable for marine use. Ingested data can be viewed and processed using the Dartcom IPAD/MicroPro software.

Moreover, outputs are also available for popular image processing software packages such as PCI Geomatica, ERDAS IMAGINE and ENVI/IDL, as well as standard interchange formats such as NOAA level 1B, EPS level 0 and GeoTIFF.

Figure 8. 38 Dartcom 1.3m Active-Stabilized Marine Antenna by SeaSpace 2011

8.9.3 HRPT/AHRPT 1.3m Marine Antenna System

This antenna is designed to track PEO satellites on moving vessels using a state-of-the-art active-stabilized X-Y pedestal to compensate for pitch, roll and yaw, as shown in Figure 8.38 (Right). It has a continuous axis movement to eliminate cable wrap problems without slip-rings or rotary joints. The pedestal's high speed and accuracy ensure that there is no "cone of silence" (data loss at high elevations).
The antenna has a 0.35 F/D ratio and 24.7dBi gain (S-band 27dBiC) to achieve a system G/T of better than 3.4dBK at 1.7GHz and 4.7dB/K at 2.252GHz, both at 5° elevation, and a bit error rate of better than 1:106 from 3.5° elevation.

The reflector is a 1.3m diameter prime focus aluminium parabolic dish finished in light grey paint (RAL 7044). An Integrated Feed Downconverter (IFD) is mounted at the focal point in a hermetically sealed unit, with more details in the Land-based antennas section for specifications. The dish and pedestal assembly is mounted inside a weather-tight glass fiber radome and base with access hatch.

The antenna control unit (ACU) is located below decks in 19" equipment racks with the receiver rack, ingest PC, UPS and network switch. The ACU provides fully automatic control of the pedestal using an advanced stabilization algorithm. Thus, full diagnostics and maintenance facilities are available on a colour TFT screen. This antenna is ISO9001/CE certified and has been designed to meet or exceed military standard (MIL-STD) specifications.

8.9.4 GEO Data Collection Platform (DCP)

Climatologic and synoptic meteorological surface data collected via DCP are used to create weather prediction models that describe the atmosphere and its changes over time. The data can be sent by the TX32 Satellite transmitter via GOES satellite, as shown in Figure 8.39.

Figure 8. 39 TX320 GOES Transmitter by Campbell Scientific 2013

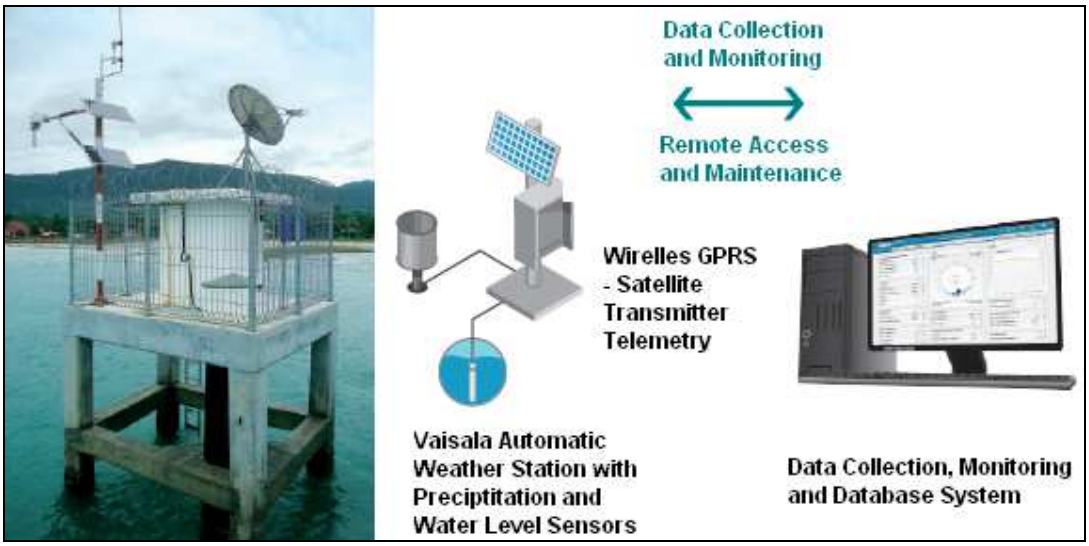

Figure 8. 40 Automatic Weather Station and Components by Vaisala 2015

Before transmission, meteorological data need to be collected, and a functional and exhaustive meteorological database for accurate models requires high quality observations of a variety of relevant measurements. This process is shown in Figure 8.40, with the AWS System **(Left)** and its Components **(Right)**. Automatic Weather Station (AWS) for DCP can be installed in offshore or onshore locations and onboard ships, whose main task is to collect local meteorological data and send them via GEO satellite to some Direct Readout Station. Each DCP station is specialized for the following tasks:

1. Hydrological measurement data is essential in the prediction and solution of flood, water pollution, drought and erosion problems. Some areas have plenty of water while other areas, afflicted by drought, go wanting.
2. Coastal weather stations produce meteorological data for sea weather forecasts and to warn ships and offshore operators about severe weather conditions. The same data is also used in regional and global computer models to help predict atmospheric changes and monitor ocean climate and the state of the oceans.
3. Agrometeorological Automatic Weather Station (AWS) systems measure in-site weather conditions in parallel with local forecasts. The objective is to produce weather data that enables optimal timing and control of all field operations. The data is gathered, stored, viewed and analyzed to enable more profitable decisions with less risk in farm management.
4. Weather can create significant disruptions in urban areas. Heavy rains can cause severe flooding, snow and freezing rain can disrupt transportation systems, and major storms with accompanying lightning, hail and high winds can cause power failures.

The main variables of hydrological measurements in AWS are: Precipitation; Water level (rivers, lakes, reservoirs, wells); Water temperature; Snow depth; Waterflow; Evaporation; Soil moisture; Ambient water quality, and so on. The sensors used in Vaisala AWS fulfill WMO's recommendation for accuracy.

CHAPTER NINE

SYSTEM ANALYSES AND CONCLUSION

In this chapter, the scientific potential of the integrated SCP system is discussed. In particular, a scenario analysis of data acquired by SCP is presented. It also covers the limitation and the contribution of this study, and includes the concluding remarks.

9.1 SCP-Borne Bistatic Synthetic Aperture RADAR

In the proposed configuration, a bistatic systhetic aperture (BiSAR) on the SCP would operate with a distinct transmitter (T_x) and receiver (T_r) that are mounted on separate platforms, as depicted in Figure 9.1. In particular, the SCP-borne receiver will consist of two channels. The first channel is dedicated for measuring signals directly emanating from the transmitter antenna sidelobes. As reported in Wang et al., (2008), the signals from the transmitter antenna sidelobes are used as reference signals vital for matched filtering and or for BiSAR time-frequency synchronisation compensation. The second channel is dedicated for remote sensing applications.

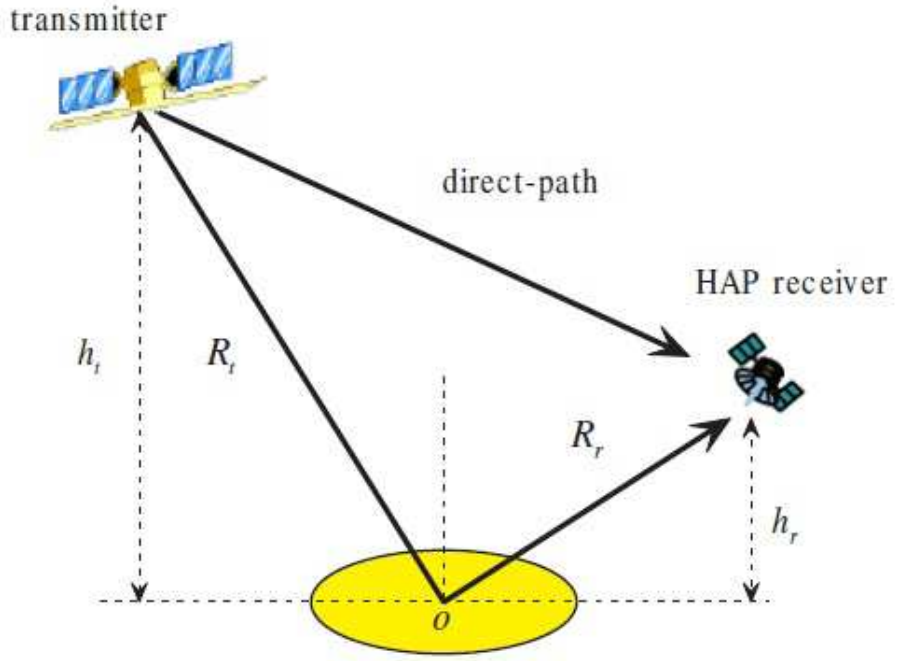

Figure 9. 1 Typical HAP-borne SAR system by Widiawan et al 2005

In order to utilize BiSAR for remote sensing applications, it is proposed that both the transmitting and receiving antennae be configured in such a way that their ground beams overlap. The resulting beam pattern influences the exposure time of the point target often analysed using imaging time and imaging coverage parameters. For instance, the image time (T_i) for a SCP-borne BiSAR is given in Equation (9.1).

$$T_i = \frac{D_{a,x} + D_{a,r}}{|v_x - v_a|} \tag{9.1}$$

In Equation (9.1), $v_{x|r}$ are the transmitter and receiver velocities. The illuminted ground coverage in the azimuth direction for the $T_{x|r}$ i.e., $D_{a,x|r}$ are given by Equation (9.2).

$$D_{a,x} \sim 2\frac{h_x}{\sin\gamma_x}\tan\left(\frac{\theta_{a,x}}{2}\right)$$
$$D_{a,r} \sim 2\frac{h_r}{\sin\gamma_r}\tan\left(\frac{\theta_{a,r}}{2}\right) \quad (9.2)$$

In Equation (9.2), $h_{x|r}$ are the altitudes, $\gamma_{x|r}$ are the incidence and $\theta_{a,x|r}$ are the antenna beam widths. The resulting coverage in the azimuth ($L_{az,ra}$) are given in Equation (9.3).

$$L_{az} = D_{a,r} - v_r T_i$$
$$L_{ra} = D_{r,r} \quad (9.3)$$
$$\sim 2\frac{h_r}{\sin\gamma_r}\tan\left(\frac{\theta_{r,r}}{2}\right)$$

Table 9.1 presents the proposed system parameters for BiSAR together with the corresponding imaging time and imaging coverages.

Table 9. 1 BiSAR system parameters

Parameter		Transmitter	Receiver
Carrier Frequency [GHz]		~ 9.6	~ 9.6 GHz
Range Bandwidth [GHz]		2	2 GHz
Swath Width [Km]		5	5
Squint angles [^{0}]		0 - 85	0-85
Beam width [^{0}]		1.78	1.78
Velocity [ms^{-1}]		150	40
Slant range at scene centres [Km]		13.1	23.1
Image time			
Imaging coverage	Azimuth		
	Range		

Numerous image formation algorithms for BiSAR have been reported in the literature. For example, the polar formatting algorithm (PFA) has been in Rigling and Moses (2004), the back-propagation (BP) is described in Ding and Munson (2002) while non-linear chirp scaling (NLCS) algorithm is reported in, e.g., Wong and Yeo (2001). For the SCP-borne BiSAR system proposed, the NLCS methodology described in, e.g., Wong and Shao (2013) is recommended. For the purposes of completeness, a brief theoretical background and image reconstruction are presented below.

A 2-D BiSAR image (spectrum) is often constructed from an approximation of a stationary-phase azimuth time derived from two quasi-monostatic phase histories which are a Tylor – expanded two quasi-monostatic phase history based on the methodology described in Loffeld et al (2004). In particular, the transmitted signal, $y_t(t)$, with inherent encoded wide bandwith (chirp) signal, P(t), and up-converted by the transmitter to the carrier frequency (f_c) is given

in Equation (9.4). The radar echo reflected from a point target experiences a time delay that is proportional to the range history, (R_τ), expressed in Equation (9.5).

$$y_t(t) = P(t)e^{j2\pi f_c t} \tag{9.4}$$

$$y_r\left(t,\tau;R_{r0},\tau_{r0}\right) = y_t\left(t - \frac{R(\tau)}{c_0}\right) \tag{9.5}$$

In Equation (9.5), τ_{r0} is the azimuth time when the target appears normal to the receiver track. Once the signal has been down converted, the demodulated signal is expressed in Equation (9.6)

$$y_r\left(t,\tau;R_{r0},\tau_{r0}\right) = P\left(t - \frac{R\tau}{c_0}\right)e^{2\pi j\frac{R(\tau)}{\lambda}} \tag{9.6}$$

Equation (9.6) can be transformed to a range-frequency domain ,with $P(f_r)$ being the Fourier Transform (FT) of P(t)) yielding Equation (9.7)

$$y_r\left(f_r,\tau;R_{r0},\tau_{r0}\right) = P\left(f_r\right)e^{-2\pi j\left(\frac{f_r+f_c}{c}\right)R(\tau)} \tag{9.7}$$

Equation (9.7) can now be transformed from the azimuth-time to azimuth-frequency domain (wherein f_a is the azimuth Doppler frequency) yielding Equation (9.8).

$$y_r\left(f_r, f_a;R_{r0},\tau_{r0}\right) = P\left(f_r\right)\int_{-\infty}^{\infty} e^{-2\pi j\left[\frac{f_r+f_c}{c}R(\tau)+f_a\tau\right]}d\tau \tag{9.8}$$

If the phase history, given in Equation (9.8), has a stationary phase point τ^* and using the principle of stationary phase, then Equation (9.8) can be written as follows:

$$\begin{aligned} Y\left(f_r, f_a\right) &= R\left(f_r\right)e^{-2\pi j\left(\frac{f_0+f_r}{c_0}R\left(\tau^*\right)-f_a\tau^*\right)} \\ f_a &= -\frac{f_r+f_a}{c_0}\left.\frac{\partial R(\tau)}{\partial\tau}\right|_{\tau=\tau^*} \\ &= -\frac{f_r+f_a}{c_0}\left[v_x\sin\varepsilon_x + v_r\sin\varepsilon_r\right] \end{aligned} \tag{9.9}$$

In Equation (9.9), the instantaneous squint angles are given by $\varepsilon_{x|r}$. As a result, the instantaneous bistatic range history is given at the azimuth time τ as follows:

$$R(\tau) = R_{x0}\cos\varepsilon_x + \left[R_{x0}\tan\varepsilon_{x0} - v_x\tau\right]\sin\varepsilon_x + R_{r0}\cos\varepsilon_r + \left[R_{r0}\tan\varepsilon_{r0} - v_r\tau\right]\sin\varepsilon_r \tag{9.10}$$

Where $\varepsilon_{x|r,0}$ denotes the instantaneous squint angles of the transmitter and receiver at zero-Doppler frequency. As a result, Equation (9.9) simplifies to

$$\begin{aligned} &Y\left(f_r, f_a\right) = P\left(f_r\right)e^{-2\pi jf'D} \\ &D = R_{x0}\cos\varepsilon_x + R_{x0}\tan\varepsilon_{x0}\sin\varepsilon_x + R_{r0}\cos\varepsilon_r + R_{r0}\tan\varepsilon_{r0}\sin\varepsilon_r \\ &f' = -\frac{f_0+f_r}{c_0} \end{aligned} \tag{9.11}$$

A two 2D inverse FT (IFT) of Equation (9.11) would yield a SAR image of a monostatic SAR system. For a BiSAR system, the transmitter and receiver can be configured such that they move at different velocities with a characteristic systhetic aperture time T_s such that;

$$\begin{aligned} & v_t \;\; » \; v_r; \\ & R_{x0} \;\; » \; v_r \tau; \\ & \tau \in \left\{ -\frac{T_s}{2}, \frac{T_s}{2} \right\} \end{aligned} \tag{9.12}$$

Additionally, an equivalent velocity, v_{eq} between the transmitter and receiver plat can be utilised for approximations given in Equation (9.13)

$$\begin{aligned} R_b(\tau) &= \sqrt{R_{x0}^2 + (v_x \tau)^2} + \sqrt{R_{r0}^2 + (v_r \tau)^2} \\ &\sim \sqrt{R_{x0}^2 + (v_{eq} \tau)^2} + R_{r0} \end{aligned} \tag{9.13}$$

Now the equivalent instantaneous azimuth Doppler f_a can be approximated in terms of the instantaneous angle between the transmitter and point target, $\emptyset_x$ as:

$$f_a = \frac{v_{eq}}{\lambda} \sin \phi_x \tag{9.14}$$

The following further approximations (for small $\emptyset_x$) can be considered:

$$\begin{aligned} & \lambda \frac{f_a}{v_{eq}} \;\; « \; 1 \\ & R_b(f_a, R_{x0}) = \frac{R_{x0}}{\cos \phi_x} + R_{r0} \\ & \sim R_{x0}[1 + C_s] + R_{r0} \\ & C_s = \frac{1}{\sqrt{1 - \left(\frac{\lambda f_a}{v_{eq}} \right)}} - 1 \end{aligned} \tag{9.15}$$

In Equation (9.15), C_s is the scaling factor in the chirp scaling algorithm (CSA).

The theoretical framework presented thus far suffices for SAR image reconstruction. The non-linear chirp scaling (NCS) framework is based on a step-wise processing of a transmitted signal of the form (with chirp rate k_r):

$$y_x(t) = e^{\left[j\pi \left(2 f_{c\theta} t + k_r t^2 \right) \right]} \tag{9.16}$$

At the receiver, the demodulated signal is given by;

$$y_r(t) = e^{\left\{ -j\pi \left[k_r \left(t - \frac{R_b(\tau)}{c_0} \right)^2 + 2 \frac{R_b(\tau)}{c_0} \right] \right\}} \tag{9.17}$$

The FT Equation (9.17) to the azimuth time τ leads to:

$$Y_r(t, f_a) = e^{\left\{ -j\pi k_{eq} \left[t - \frac{R_b(f_a; R_{x0})}{c_0} \right]^2 \right\}} \times e^{-j\pi \frac{\lambda R_{b0} f_a^2}{v_{eq}}} \times e^{-j2\pi f_a \frac{y_p}{v_{eq}}} \tag{9.18}$$

In Equation (9.18), $(x_p, y_p, 0)$ is the target coordinate and R_{b0} is the minimum bistatic range. In order to obtain the BiSAR image, the CS processing is considered using the phase term whereupon Equation (9.18) is transformed into 2D frequency domain using the First Fourier Transform (FFT). The resulting signal is then range compressed followed by the Inverse First Fourier Transform (IFFT). The effects of the inherent azimuth –variant Doppler chirp rate is accounted for by Dopper chirp rate correction after phase filtering. The resulting signal is Fourier Transformed in the azimuth direction and then weighted by a phase compensation term before applying an azimuth IFFT. A summary is the NCS as presented in the block diagram depicted in Figure 9.2.

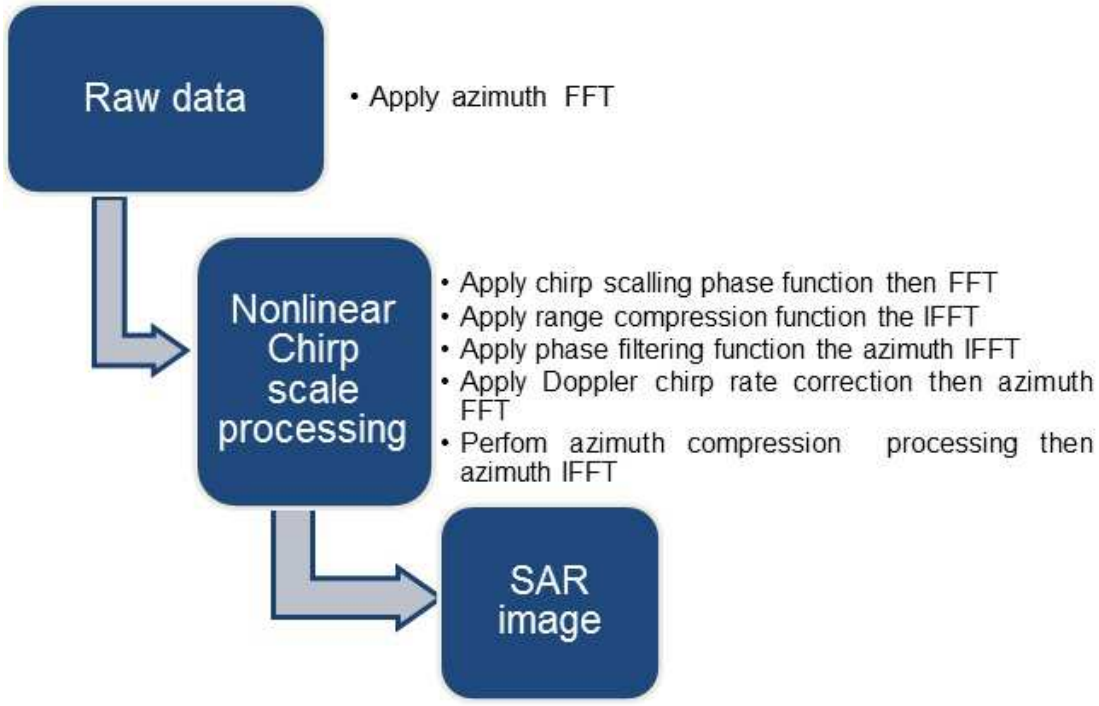

Figure 9. 2 Typical nonlinear chirp scaling algorithm for bistatic synthetic aperture radar image processing. Adopted from Wang et al., (2011) and Wang and Shao (2013)

9.2 SCP-Borne multispectral image analysis

To analyse the multispectral image acquired by SCP-borne system for earth observation, specific indexes applicable to the different land cover type of interest ought to be considered. For example, if the task is to discriminate vegetation from other land cover feature, mathematical operation, e.g., band ratioing is performed using selected bands. In particular, for SCP-vegetation index (hereafter HAP-NDVI), the channels corresponding to the infrared (say B4) and red regions (say B3) of the spectrum ought to be computed in a normalized index expressed in Equation (9.19).

$$HAP - NDVI = \frac{B4 - B3}{B4 + B3} \tag{9.19}$$

Similarly, to delineate water bodies (this can be rivers, dams or even flooded area), the stages involved are summarized in the flow chart depicted in Figure 9.3.

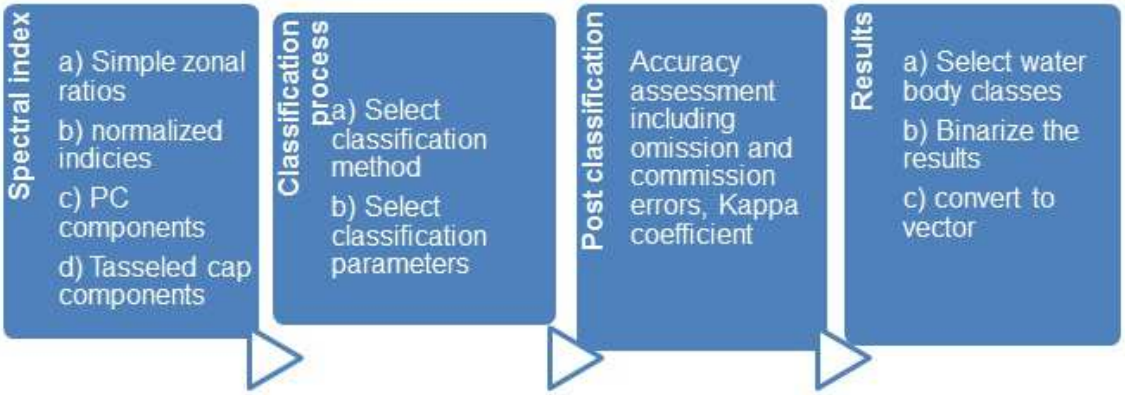

Figure 9. 3 Flowchart for water body delineation

For flood detection, two water indices are proposed, i.e., the Modified Normalized Water index (MNDWI) described in Xu (2006) and the Desert Flood index (DFI) reported in Wang (2007) expressed in Equation (9.20) and Equation (9.21).

$$MNDWI = \frac{B_G - B_{SWIR}}{B_G + B_{SWIR}} \tag{9.20}$$

$$DFI = \frac{B_G - B_{SWIR} + 0.1}{\left\{\left(B_G + B_{SWIR}\right)\left(NDVI + 0.5\right)\right\}}; \quad NDVI = \frac{B_{NIR} - B_R}{B_{NIR} + B_R} \tag{9.21}$$

The correction terms in Equation (9.21), i.e., *NDVI+0.5*, is used to reduce the effect of vegetation on *DFI* values. In particular, using NDVI negates the inclusion of vegetation as a water pixel especially in areas where water and vegetation proportions are in small proportions and, hence, not being able to be resolved. To demonstrate image processing based on Equations (9.20) and (9.21), Figure 9.5 and Figure 9.6 have been produced using the Matlab software for original RGB image, the MNWI and DFI, respectively.

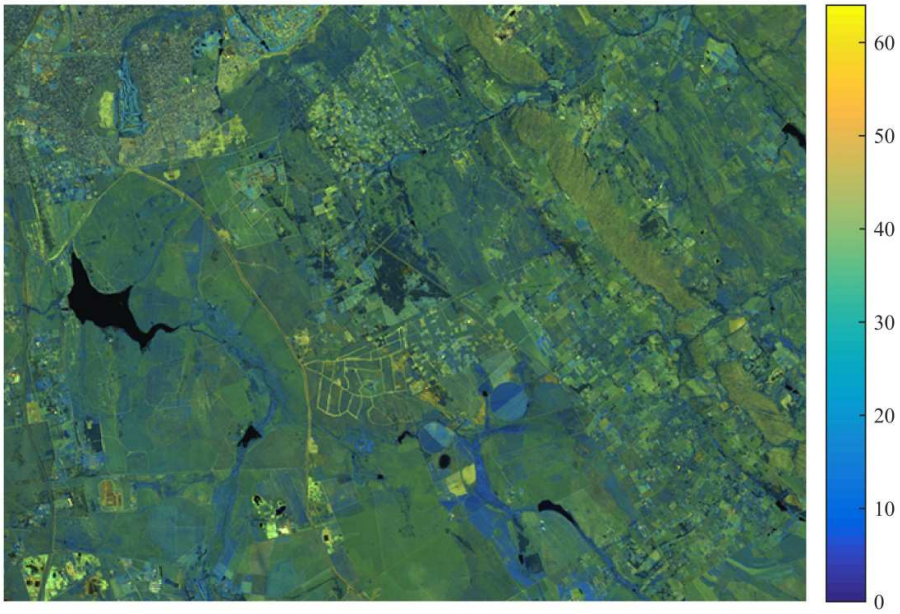

Figure 9. 4 Sub-set of the original image (Band 1, 2 and 3)

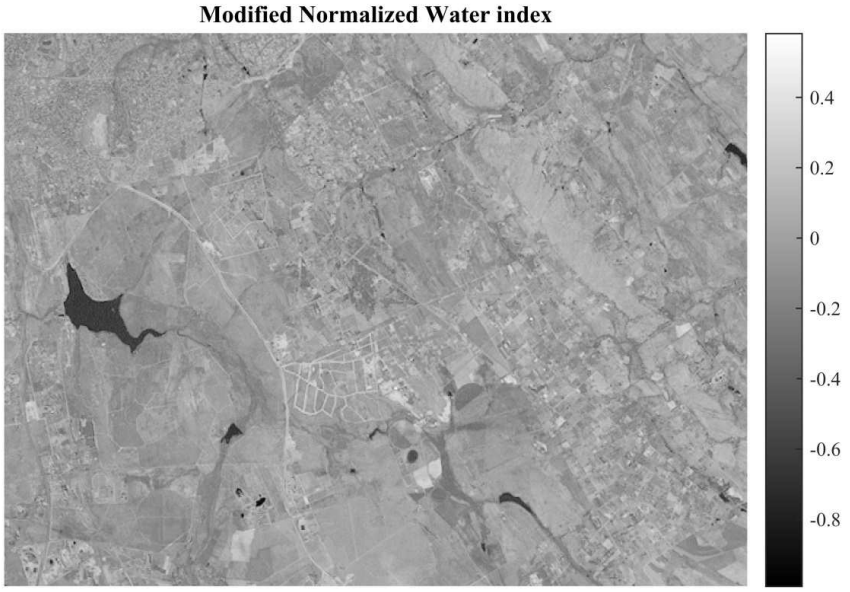

Figure 9. 5 Modified normalized water index

Figure 9. 6 Example of image processing for delineating flooded area using the desert flood index. Dark spots depict water

9.3 SCP-Borne LiDAR for flood detection

Airborne Light Detection and Ranging (LiDAR) measures laser light reflected from the surface. The LiDAR technology utilizes the concept of laser altimetry where a scanning pulsed laser scans the ground at a set horizontal resolution in order to derive high precision topographic mapping products with potential local or regional application studies. For instance, with regard to flood monitoring, the overarching contribution of the LiDAR system is in, e.g., a) validation as well as parameterize flood prediction models, and b) providing near real-time information for emergency flood relief management.

Small-footprint airborne LiDAR technology appears to be attractive because it provides fine-scale Digital Terrain Models (DTM) over a large coverage. This technology supports surveying hundreds of kilometers of shoreline and rivers with a high spatial-temporal resolution. It's very high vertical accuracy (<0.15 m) has opened up new possibilities of tackling very precise and specific problems, that were impossible to deal with before (Hladik and Alber, 2012; Collin et al., 2012). To this end, topographic airborne laser scanning has become an established technique to characterize the Earth surface since LidAR provides 3D point clouds allowing a fine reconstruction of the topography. For flood hazard modeling, the key step before terrain modeling is the discrimination of land and water surfaces within the delivered point clouds. Therefore, instantaneous shoreline, river borders, and inland waters can be extracted as a basis for more reliable DTM generation.

The proposed LiDAR system on board HAPS is configured to operate on the near-infrared channel (NIR). Data from the proposed LiDAR component is conceived to be suitable both for coasts and rivers and, therefore, a supervised classifier will be ideal. The core of the

workflow is designed in a 2D-raster mode in order to provide a fast classification, with a tailored learning step. It is expected that the approach is fully automatic, parameter-free, and versatile: no multi-echo, intensity, full-waveform or multi-spectral information is necessary. However, the system may require the setting of parameters at the different steps in data processing. Overall, the processing chain can be divided into the following three steps.

9.3.1 Computation of features of interest

Three families of features are utilized here, i.e., based on (i) the height, (ii) the local point density, and (iii) the local shape of the 3D point neighbourhood. To deal with any kind of lidar point cloud, the intensity/amplitude echo based features, i.e., information about the position of the 3D point within the current emitted lidar pulse are discarded. As a result, methodology uses only 3D point co-ordinates. For the feature computation stage, the single parameter to be tuned is the size of a 3D point neighbourhood. In this regard, given d as the point cloud density and n as the minimal number of points needed to calculate robust 3D descriptors, the radius *r* is defined in Equation (9.22),

$$r = \left(\frac{n}{\pi d} \right)^{0.5} \tag{9.22}$$

As reported in Smeeckaert et al. (2013), ten points are sufficient and a typical domain of $1 < r < 2$ can be realized. Additionally, the interpolation of the 3D point cloud features on a regular 2D grid allows to better handle the large data volume and high dimensionality of the raw point clouds. In the proposed SCP-LiDAR, the main areas of interest are the land-water interface, and, in particular, shallow waters. The larger the grid cell, the more inaccurate the classification. As a result, the point cloud is resampled at a resolution of 1 m which is sufficient for retrieving the land/water interface with a horizontal accuracy > 2 m. The mean value of each feature is selected as the final descriptor.

For feature description, the following 2D density-based features/parameters are used:

1) The height of LiDAR point (H_G)

   A first obvious attribute is the height of the lidar point with respect to the geoid, H_G. Note that H_G does not always help to discriminate water points in inland areas.

2) Local mean point density (D)

   This parameter is computed for each point, independently from the lidar strip to which they belong. Note that several neighbourhoods at different sizes can be computed, enhancing more or less land areas but also water areas at the nadir of the aircraft. This feature is particularly preferable for single lidar strip analysis. The neighbourhood increase allows to deal with overlap sensitivity (overlapped lidar strips locally increases point density). A 5×5 m offers a suitable trade-off. Nevertheless, this leads to the loss of small structures. In order to account for this limitation, the majority density (D_m) is computed, i.e., only lidar points from the strip and the highest number of lidar hits are taken into account. In order to avoid the sensitivity to the strip overlap, Equation (9.23) is considered:

$$D_m = \max_{str_1;str_2} \left\{ D_{str_1}; D_{str_2} \right\} = D_{\max} \quad (9.23)$$

3) The density ration (D_r)
This parameter is introduced to weight areas with unequal areas of strip sampling. Note that water bodies do not suffer from this problem. The parameter is computed, as given in Equation (9.24);

$$D_r = \frac{D_{\max} - D_{\min}}{D_{\max}} \in [0,1] \quad (9.24)$$

In Equation (9.24), D_{max} and D_{min} are point densities of each grid cell with the highest and lowest number of points, respectively.

4) In terms of computation of eigenvalue features ($\lambda_{1,2,3}$) (Demantk´e et al., 2011), a covariance matrix of the 3D coordinates is computed in a cylindrical vertical neighbourhood of fixed radius. Such a matrix provides three eigenvalues, i.e., λ_1, λ_2 and λ_3 (in descending order). These attributes allow to discriminate water surfaces, which are both horizontal and planar, from land, even for pixels lying on the ground. Two eigenvalue-based features were computed. The first one is the smallest eigenvalue, i.e., λ_3 (the volume). $\lambda_3 \cong 0$ accounts for for planar elements, $\lambda_3 > 0$ represents ground pixels, ground microreliefs and surface roughness) and $\lambda_3 >> 0$ accounts for 3D Earth surfaces. The second feature is the scatter, defined as $S = \lambda_3 / \lambda_1 \in [0, 1]$.

For the SCP-LiDAR application; in case of LiDAR data with multiple strips, the feature set is: $\{H_G, D_m, D_r, \lambda_3, S\}$. For single strips, the probable feature set would be: $\{H_G, D, \lambda_3, S\}$.

9.3.2 Learning procedure

The knowledge of the land/water interface is used to define the training pixels that are most likely to belong to each class. However, as this delineation may not be up-to-date or accurate enough, more representative training pixels are automatically selected using spatial reasoning. For non-parametric classifiers, such as the supervised Support Vector Machines (SVM), only samples lying on the edges of a given class distribution in data space contributes to the analysis. Here, the subset generation is carried out automatically using the scatter and the volume features. Extreme values are representative of land and water classes, respectively. High scatter values correspond to areas with significant vertical scattering such as vegetation and buildings. Lowest volume values indicate the flattest areas, i.e., water surfaces close to the flightline nadir. Thus, we retrieve pure pixels (hereafter called seeds) by thresholding volume and scatter cumulative distribution functions (computed with 500,000 pixels randomly taken). Gradient is computed on both curves. For the volume (scatter) curve, areas inferior (superior) to the highest gradient value are labelled as water and land seeds, respectively. However, seed distribution is not satisfactory. For water areas, few nadir points are selected whereas they are the most similar to land surfaces, while, for land regions, significant spatial heterogeneity exists and heterogeneous training pixels cannot be selected with such a method. Note that since they are not representative of both classes, they are only used as a basis for designing a more adapted training set.

9.3.3 Land/water classification

In the SCP-LiDAR classification scheme, Support Vector Machines classification are considered. In particular, the standard Gaussian kernel is selected and the SVM hyper-parameters are optimized with a simple grid search. Note that the SVM are limited to local classification of pixels, which results in noisy outputs. This is in spite of their ability to handle high-dimensional feature spaces. Several solutions are possible to overcome such limitation (Schindler, 2012). In the present system, the filtering approach is recommended. For each pixel, a new label is computed with respect to the weighted incoming labels of a given neighbourhood. In this scheme, the solution offers the advantage of linear growth of the computational cost with the number of pixels. The relaxation probabilistic framework, reported in Gong and Howarth, (1989), is adopted wherein both neighbourhood information and the probabilities of belonging to each class, as provided by libSVM (Wu et al., 2004), is taken into account. The proposed classification procedure is iterative wherein the probability values for each pixel are updated to ensure that they are closer to their neighbours. Thereafter, an energy membership is calculated for both classes. A label corresponding to the lowest value is assigned, as given in Equation (9.25)

$$E_l(i) = \sum_{j \in V(i)} G_\sigma \left(\| i - j \| \right) \circ E_l(j) . M_{i,j} \left[l, l_j \right] \tag{9.25}$$

In Equation (9.25), $G\sigma(.)$ is the weight of pixel j, where G_σ corresponds to the zero-mean Gaussian density function with variance σ^2 and $V(i)$ is the vicinity window (here a 5×5 window). Finally, M is called compatibility matrix since it measures the compatibility between pixel i with label l and pixel j with label l_j. Note that M defines a priori correlations between the probabilities of neighbouring points and corresponds to conditional probabilities verifying:

$$\begin{aligned} 0 \le M_{i,j} \left[l, l_j \right] \le 1 \\ \sum_j M_{i,j} \left[l, l_j \right] = 1 \end{aligned} \tag{9.26}$$

In this regard, the coefficients of M are empirically selected to ensure spatial homogeneity. However, in order to preserve water/land boundaries, the coefficients out of the matrix diagonal are not equal to 0.

9.4 Research contributions and concluding remarks

This section discusses the contributions that the study makes and how the SCP system formulated contributes to the body of knowledge on the use of SCP for Earth Observation.

9.4.1 Theoretical contribution

This study is a major theoretical contribution as it will enrich the literature on the utilization of SCP for remote sensing applications, in general, and earth observation, in particular. The study focused on the development of a conceptual framework for SCP with specific earth observation applications. The framework can be applied in the design of system capable of providing timely information on, e.g., extreme weather events such as flooding and veld fires. The designed framework is supported by conceptualized algorithm for information retrieval which can be used by other researchers as a reference to develop other models or be used in other studies to inform technology usage for different societal applications of SCP. Overall, the literature reviewed in this study in addition to the framework would enrich research in the SCP body of knowledge.

9.4.2 Practical contribution

The framework developed will assist policy makers in the field of Earth Observation to better understand how SCP could be utilized. This will assist them to devise better means of using SCP to improve and enhance space applications for sustainable development. The designed framework can be utilized by other scientists, engineers and researchers to simulate further thoughts on optimizing SCP designs capable for a wide range of environmental applications. The insights gained will then assist them in making informed decisions of improving the quality of SCP so as to provide better scientific and societal applications in support for, e.g., disaster management cycle: preparedness, response, recovery and mitigations.

9.5 Limitations of the study

Due to time and funding constraints, there were some limitations to this study. In particular, the work presented here is a demonstration of the SCP concept and information retrieval algorithm with applications in earth observation. The practical test of the algorithm is largely in-exhaustive.

9.6 Recommendations and future work

In order to address the gaps in the study reported in this dissertation, the following recommendations are proposed:

Future research can be conducted with focus on testing the robust nature of information retrieval. This study focused on the theoretical basis information retrieval. Several other factors that influence data acquisition and data quality have not been incorporated. This is highly recommended. The study also makes the following recommendations to stakeholders of space applications for earth observation:

All stakeholders should increase awareness on the visibility of SCP as cost-effective technology alternative to existing space technology.

Funding institutions should provide funding to support further research on SCP. The researcher recommends that future research can be conducted in order to enhance understanding of SCP potential as a viable option for various earth observation applications.

9.7 Conclusion

According to WMO, during 2014, temperatures in Africa were close to or above average in almost all areas where long-term records are available. The average anomaly across the entire continent was also higher than the long-term mean, but lower than the record value for 2010. There were notable heatwaves in South Africa, when high-temperature records were broken. The above still reflects the importance of weather data to be able to mitigate the risks that comes with weather patterns that are not normal. This research work introduced the alternative system for space weather observation based on integration of current PEO and GEO satellite systems with HAP airship. This integration also considers communication facilities for transmission of weather and observation data and images to the ground meteorological and forecasting stations and centres. These observations are also essential for conducting intensive research to improve services, assessing changes in the climate system

and for development of operating systems in weather and climate-dependent sectors such as agriculture, water, transport and energy, in support of communities' efforts to reduce disaster risks and adapt to climate variability and change.

LIST OF ACRONYMS

AIS	Automatic Identification System
AMSS	Aeronautical Mobile Satellite Service
APR	Automatic Position Report
APT	Automatic Picture Transmission
ARINC	Aeronautical Radio Incorporated
ARNSS	Aeronautical Radio Navigation Satellite Service
ASAS	African Satellite Augmentation System
ASP	Application Service Provider
ATC	Air Traffic Control
AWS	Automatic Weather Stations
CCD	Charge Coupled Device
CDMA	Code Division Multiple Access
CES	Coast Earth Stations
CMRC	Convectional Maritime Radio Communications
CNS	Communication, Navigation and Surveillance
CCIR	Consultative Committee on International Radio
CSC	Common Signaling Channel
DCS	Digital Selective Call
DCU	Display Control Unit
DDC	Digital Down Converter
DDP	Data Distribution Plan
DF	Direction Finding
DRS	Direct Readout Service
DSB	Direct Sounder Broadcasts
DVB-RCP	Digital Video Broadcasting-Return Channel via Platform
DVB-RCS	Digital Video Broadcasting-Return Channel via Satellite
DVB-S2	Digital Video Broadcasting-Second generation
EC	European Commission
EGNOS	European Geostationary Navigation Overlay System
EM	Electromagnetic
EMSO	Efficient Meteorological Space Observation
EOSS	Electro-Optical Space Surveillance
ESA	European Space Agency
FCC	Federal Communications Commission
FES	Fixed Earth Stations
FFT	Fast Fourier Transform
FSS	Fixed Satellite Service
GAVDL-B	GNSS Augmentation VDL-Broadcast
GCC	Gateway Control Centers
GCSS	Global Communication Satellite Systems
GEO	Geostationary Earth Orbits
GES	Ground Earth Station
GIO	Geosynchronous Inclined Orbits
GIRD	Group for Investigation of Reactive Movement
GLONASS	Global Navigation Satellite System
GMSC	Global Mobile Satellite Communications
GNSS	Global Navigation Satellite System
GPS	Global Positioning System

GSAR	Ground Synthetic Aperture Radar
GSAS	Global Satellite Augmentation Systems
HAP	High Altitude Platforms
HAPS	High Altitude Platforms Station
HEO	High Elliptical Orbit
HRPT	High Resolution Picture Transmission
HSC	High Speed Craft
HSD	High Speed Data
Hz	Hertz
IDC	International Data Centre
IHO	International Hydrographic Organization
IMCO	Intergovernmental Maritime Consultative Organization
IMO	International Maritime Organization
ISAR	Inverse Synthetic Aperture Radar
ISL	Inter-Satellite Link
ITS	Intelligent Transportation Systems
ITU	International Telecommunications Union
LADAR	Laser Detection and Ranging
LCD	Liquid Crystal Display
LEO	Low Earth Orbit
LES	Land Earth Station
LGA	Low Gain Antenna
LIDAR	Light Detection and Ranging
LMSS	Land Mobile Satellite Service
LNA	Low Noise Amplifiers
LOS	Line-of-Sight
LPA	Log Periodic Antenna
LRIT	Long Range Identification and Tracking
LRNSS	Land Radio Navigation Satellite Service
MCC	Master Control Center
MEO	Medium Earth Orbit
MMSC	Maritime Mobile Satellite Communications
MRNSS	Maritime Radio Navigation Satellite Service
MSAS	MTSAT Satellite-based Augmentation System
MSC	Mobile Satellite Communications
MSS	Mobile Satellite Systems
MSUA	Mobile Satellite Users Association
NCC	Network Control Centres
NCS	Network Coordination Stations
NOAA	National Oceanic and Atmospheric Administration
OTDM	Optical Time Division Multiplexing
OTS	Orbital Test Satellite
PEO	Polar Earth Orbit
PMSS	Personal Mobile Satellite Service
PVT	Position, Velocity and Time
R&D	Research and Development
RADAR	Radio Detection and Ranging
RADS-B	Radio Automatic Dependent Surveillance - Broadcast
R-AIS	Radio Automatic Identification System
RDSS	Radio Determination Satellite System

RF	Radio Frequency
RSAS	Regional Satellite Augmentation Systems
RW	Radio Waves
Rx	Receiver
SADS-B	Satellite Automatic Dependent Surveillance - Broadcast
SATFM	Satellite Asset Tracking and Fleet Management
SCC	Satellite Control Centre
SCP	Stratospheric Communication Platforms
SDL	Satellite Data Link
SMOS	Satellite Meteorological Observation Systems
SSAR	Satellite Synthetic Aperture Radar
TCU	Terminal Control Unit
TDM/TDMA	Time Division Multiple/TDM Access
TES	Transportable Earth Stations
TT&C	Satellite Tracking, Telemetry and Command
TTN	Terrestrial Telecommunication Network
TTP	Transitional Telecommunication Project
Tx	Transmitter
UAV	Unmanned Aerial Vehicle
UT	Universal Time
VDL	VHF Data Link
VES	Vehicle Earth Station
VRS	Vehicle Radio Stations
WAAS	Wide Area Augmentation System
WMO	World Meteorological Organization

REFERENCES

Advantech. 2015. *Discovery 300 Next Generation DVB-RCS VSAT Hub*. Available: [http://www.advantechwireless.com/wp-content/uploads/2014/09/PB-VSAT-HUB-D300-14248.pdf.]: accessed June 2015

Advantech. 2012. *Fixed, Mobile and Portable VSAT Units*. Available : [http://www.advantechwireless.com/products_/vsat/]: access on June 2015

Advantech. 2006. *Ground Satellite Antennas.*Available: [http://www.advantechwireless. com/products] accessed on June 2015

Advantech. 2009. *Theoretical Performance of DVB-S2 and DVB-S*. Available: [www.advantechwireless.com/wp-content/uploads/DVB-S2-theory.pdf]: accessed June 2015

Antonini, M., Cianca, E., De Luise, A., Pratesi, M. and Ruggieri, M. 2003. *Stratospheric Relay: Potentialities of New Satellite-high Altitude Platforms Integrated Scenarios.* Aerospace Conference, 2003. Proceedings. 2003 IEEE 3, 3_1211-3_1219

Aragon-Zavala, A. . Cuevas-Ruiz, J.L. and Delgado-Penin A. 2008. *High-Altitude Platforms for Wireless Communications.* Wiley, Chichester, UK.

Ayecka. 2015. *Advanced DVB-S2 Receiver*. Hod HaSharon, Israel.

Benesch, W. 2010. *60 Years Operational Satellites up to 2030*. Deutscher Wetterdienst, Offenbach am Main, Germany.

Berlin, P. 1988. *Geostationary Applications Satellite*. Cambridge: Cambridge University Press.

Blonstein, L. 1987. *Communications Satellites, The Technology of Space Communications.* Heinemann, London, UK.

Blyenburgh, V. P. 2006. *UAV Systems: Global Review*. Avionics 2006 Conference, 1-52, Amsterdam.

Camp, E. 2010. *Tiros-1/2 Ground Station*. Camp Evans Project Diana Site, Wall, New Jersey, USA.

Campbell Scientific. 2015. *TX320 GOES Satellite DCP Transmitter*. Logan, UT, USA.

Calcutt, D., Tetley, L. 2004. *Satellite Communications, Principles and Applications.* Elsevier, Oxford.

Chehade, W., Gur, B. , Spietz, P., Gorshelev, V., Serdyuchenko, A., Burrows J. P., and Weber M. 2013. *Temperature dependent ozone absorption cross section spectra measured with the GOME-2 FM3 spectrometer and first application in satellite retrievals*. Atmos. Meas. Tech., Vol. 6,pp. 1623-1632.

CHEOS. 2012. *The Space Earth Observation of China*. NSMC, CMA, Beijing, China.

Colozza, A. and Dolce, J.L. 2005. *High-Altitude, Long-Endurance Airships for Coastal Surveillance*. NASA, Cleveland, Ohio.

COMET. 2011. *Satellite Monitoring*. UCAR, Boulder, CO, USA.

Cossu, R., Schoepfer, E., Bally, Ph. and Fusco, L. 2009. *Near real-time SAR based processing to support flood monitoring.* J. Real-Time Image Processing. Vol.4(3), pp. 205- 218.

Dalgleish, D.I. 1989. *An Introduction to Satellite Communications*. IEE, Peter Peregrinus, London.

Dartcom. 2015. *GVAR System*",Yelverton, Devon, UK.

Dartcom. 2015. *HRPT, CHRPT and SeaWiFS System*. Yelverton, Devon, UK.

Dartcom. 2015. *LRIT/HRIT Multi Satellite System.* Yelverton, Devon, UK.

Davis, G. 2011. *History of the NOAA Satellite Program*. Silver Spring, Maryland, USA.

Divine, W. 2005. *The History and Science of Hurricanes.* Oxford University Press, Oxford, UK.

Dong, C.,Yang, J., Zhang, W., Yang, Z., Lu, N., Shi, J., Zhang, P., Lu, Y. and Cai, B. 2009. *An Overview of a New Chinese Weather Satellite FY-3A.* American Meteorological Society, Boston , MA, USA. Vol. 90(10), pp. 1531 -1544.

Elbert, B.R. 2001. *Ground Segment and Earth Station Handbook.* Artech House, Boston – London.

Emanuela, F., Massimiliano L., Marina M. and Fabrizio S. 2006. Integrated Services from High Altitude Platforms: a Flexible Communication System. *IEEE Communications Magazine*, 2:124-133.

Everaerts, J., Lewyckyj, N. and Fransaer D. 2004. *PEGASUS: Design of a Stratospheric Long Endurance UAV System for Remote Sensing*. The International Archives of the Photogrammetry, Remote Sensing and Spatial Information Sciences, Volume XXXV, Part B2.

Evans, B.G. 1991. *Satellite Communication Systems*. IEE, Peter Peregrinus, London.

Faller, K. 2005. *MTSAT-1R: A Multifunctional Satellite for Japan and the Asia-Pacific Region*. Proceedings of the 56th IAC 2005, Fukuoda, Japan.

Eumetsat. 2013. *TD 18 Metop Direct Readout AHRPT Technical Description.* Darmstadt, Germany.

Eumetsat. 2009. *A New Geostationary Meteorological Satellite System for the 21s t Century*. Darmstadt, Germany.

Eumetsat. 2009. *International Data Collection System User's Guide*. Darmstadt, Germany.

Eumetsat. 2009. *Meteosat Receiving Multi Satellite Data from the EUMETCast DVB-S2 Service*. Darmstadt, Germany.

Eumetsat. 2009. *TD 16 - Meteosat Data Collection and Distribution Service*. Darmstadt, Germany.

Feher, K. 1983. *Digital Communications, Satellite Earth Station Engineering*. Prentice-Hall, Englewood Cliffs, New Jersey, US.

Festo, D. 2015. *Satellite Orbits, Coverage and Antenna Alignment*. Quebec, Canada.

Fidler, F., Knapek, M., Horwath, J. and Leeb, W.R. 2010. *Optical Communications for High-Altitude Platforms*. Selected Topics in Quantum Electronics, IEEE Journal, pp: 1058 - 1070 Volume: 16.

Fransaer, D., Vanderhaeghen, F. and Everaerts J. 2004. *PEGASUS: Business Plan for a Stratospheric Long Endurance UAV System for Remote Sensing*. Accepted for The International Archives of the Photogrammetry, Remote Sensing and Spatial Information Sciences, Volume XXXV, Part B2.

Fujimoto, K. 2008. *Mobile Antenna Systems Handbook*. Artech House, London.

Harris. 2015. *GOES-R Rebroadcast (GRB) and GOES VARiable (GVAR) Service*. Melbourne, FL USA.

Heidorn, C.K. 2010. *TIROS-1: First Eye in the* Sky, *The Weather Doctor*. San Clemente, CA, USA, available: [http://www.islandnet.com/~see/weather/almanac/arc2009/ alm09sep .htm]: accessed May 2014.

Hughes. 2014. *Hughes HX260 Mesh/Star Broadband Router*. Germantown, MD, USA.

Hughes. 2008. *DVB-RCS C, Ku and Ka-band System*. Germantown, MD, USA.

Hughes. 2012. *HUB HN System*. Germantown, MD, USA.

Gagliardi, R.M. 1984. *Satellite Communications*. Van Nostrand Reinhold, New York.

GAO. 2013. *Geostationary Weather Satellites*. Government Accountability Office, Washington, DC.

Gatenby, P.V. and Grant, M.A.. 1991. *Optical Intersatellite Links*. ECE Journal, Vol. 3, No. 6, IEE, Stevenage.

Giglio, L., Descloitres, J., Justice, C. O. and Kaufman Y.J. 2003. *An Enhanced Contextual Fire Detection Algorithm for MODIS*. ELSEVIER, Remote Sensing of Environment 87, pp: 273–282.

Grace, D. and Mohorcic, M. 2011. *Broadband Communications via High-Altitude Platforms*. Wily, Chichester, UK.

Grace, D., Thornton, J., Guanhua, C. , Pallavicini, M. B. , and Lalovic, M. 2005. *CAPANINA - Communications from Aerial Platform Networks Delivering Broadband Information for All*. in IST Mobile Communications Summit Dresden, Germany.

Graeme, L.S. and Christian D.K. 2007. *The Remote Sensing of Clouds and Precipitation from Space*. A Review. J. Atmos. Sci., V o l : 64, p p : 3742–3765.

Grayzeck, E. 2015. *ATS Spacecraft*. NASA, Washington, DC.

GSFC. 1996. *GOES I-M Data Book*. National Aeronautics and Space Administration, Greenbelt, Maryland, USA.

GSFC. 2009. *GOES-N Series Data Book*. National Aeronautics and Space Administration, Greenbelt, Maryland, USA.

GT&T. 2003. *VSAT Equipment*. Louvain-La-Neuve.

Gordon, G. D. and Walter L.M. 1993. *Principles of Communications Satelites*. New York: John Wiley.

Haan, S. 2008. *Meteorological Applications of a Surface Network of GPS Receivers*, Universiteit Utrecht, Utrecht, Netherlands.

Holm, T. 2013. *Landsat: Building a Future on 40 Years of Success*. EROS Centre, Alameda, CA, USA.

Huurdeman, A.A. 1997. *Guide to Telecommunications Transmission Systems*. Artech House, New York, Boston, London.

Ilcev, D. S. 2013. *Global Aeronautical Communications, Navigation and Surveillance (CNS)*. Volume 1 & 2, AIAA, Reston.

Ilcev, D. S. 2005. *Global Mobile Satellite Communications for Maritime, Land and Aeronautical Applications*. Springer, Boston.

Ilcev, D.S. 2009. *Satellite DVB-RCS Standards for Fixed and Mobile Commercial and Military Applications*. Microwave Journal, Norwood, USA.

Ilcev, D.S. 2011. *Stratospheric Communication Platforms (SCP) as an Alternative for Space Program*. Aircraft Engineering and Aerospace Technology (AEAT) Journal, Emerald, Bingley.

Ilcev, D.S. and Sibiya S.S. 2015. *Weather Observation via Stratospheric Platform Stations*. IST-Africa Conference, Lilongwe, Malawi

Ilcev, D. S. 2011. *Global Mobile CNS*. Manual, Durban, DUT.

Ilcev, D. S. 205. *Satellite Meteorological Observation System*. Manual, Durban,DUT.

Ilchenko, M. E 2004. *Application of High-altitude Platform Systems in Regions of Disaster and Emergency* . 14th International Crimean Conference on Microwave and Telecommunications Technology, Sevastopol.

ISRO. 2014. *INSAT 3-D Observing Weather from Space*. ISRO, Bangalore, India.

ISRO. 2015. *INSAT 3-D and Cartosat-1*. NRSC, Bangalore, India.

ITU. 2008. *Use of Radio Spectrum for Weather, Water and Climate Monitoring and Prediction*. Geneva, Switzerland.

ITU. 1996. *Radiowave Propagation Information for Predictions for Earth-to-space Path Communications – Handbook.* Radiocommunication Bureau, Geneva.

Jayaraman, V. 2014. *Oceansat-2* , ISRO, Bangalore, India.

JMA. 2015. *MTSAT Multifunction Transport Satellite*. Japan Meteorological Agency, Tokyo, Japan.

Jones, J. 2013. *GNSS and Weather Forecasting*, Met Office, Potsdam, Germany.

Kadish, *J.E.* and East. Th.W.R. 2000. *Satellite Communications Fundamentals*. Artech House, Boston-London.

Kamel, A. 2003. *Japanese Advanced Meteorological Imager (JAMI)*. Space Systems, Loral, Palo Alto, CA, USA.

Kidder, S.Q. and Ham T.C. 1995. *Satellite Meteorology – An Introduction*. Academic Press, Sand Diego, USA.

Knapek, M., Horwath, J., Moll, F., Epple, B., Courville, N., Bischl, H. and Giggenbach. D. 2007. *Optical High-Capacity Satellite Downlinks via High-Altitude Platform Relays*. Proc. SPIE 6709, 67090E

Kongsberg. 2014 . *MEOS 3.0 m to 5.0 m L/S/X-band Antenna*. Tromso, Norway.

Kongsberg. 2015. *MEOS GEO DVB-A2 HimawariCast*. Tromso, Norway.

Kongsberg. 2015. *MEOS PEO and GEO Geostationary Ground Station*. Tromso, Norway.

Kramer, H.J. 2002. *Observation of the Earth and Its Environment: Survey of Missions and Sensors*. Springer, Boston.

Krovotyntsev, V. 2009. *Perspectives of Development of the Russian Meteorological Satellite Constellation*. Roshydromet, SRC Planeta, Moscow, Russia.

Lasaponara, R. and Masini, N. 2012. *Remote Sensing and Digital Image Processing*. Springer, Boston, New York, USA.

Launius, R. 2014. *The First Commercial Space Activity: Communication Satellites*. Telstar-1, Internet.

Maini, A.K. and Agrawal, V. 2007. *Satellite Technology - Principles and Applications*. John Wiley, Chichester.

Maral, G., ?????. 2009. *Satellite Communications Systems*. Wiley, Chichester.

Martinis, S., Twele, A. and Voigt S. 2009. *Towards operational near real-time flood detection using a split-based automatic thresholding procedure on high resolution TerraSAR-X data*. Natural Hazards and Earth System Sciences. Vol:9, pp:303- 314.

Martinis, S., Twele, A. and Voigt, S. 2011. *Unsupervised extraction of flood- induced backscatter changes in SAR data using Markov image modeling on irregular graphs*. IEEE. Trans. Geoscience Rem. Sens. Vol:49(1), pp:251-263.

Mason, D.C., Speck, R., Devereux, B., Schumann, G.J-P., Nea,l J.C. and Bates P.D. 2010. *Flood detection in urban areas using TerraSAR-X* . IEEE. Trans. Geoscience Rem. Sens. Vol: 48(2),pp: 882-894.

McGinnis, F.D. and Dries, M. 2009. *Meteorological Satellite Communications*. NASA/Eumetsat, Washington, DC.

Menzel, P. 2012. *Remote Sensing with Meteorological Satellites*. University of Wisconsin Academic Press, Medison, WI, USA.

NASA. 2009. *Helios Prototype Flying Wing*. Washington DC. Available : [http://www.nasa.gov/centers/dryden/multimedia/imagegallery/Helios/ED03-0152-60.html]

NASA. 2014. *History of the Blue Marble*. Earth Observatory, Washington, DC, US. Available: [http://landsat.gsfc.nasa.gov/].

Njoku, E.G. 2000. *Encyclopedia of Remote Sensing Earth Sciences Series*. Springer, New York.

NOAA. 2012. *Future of NOAA's Direct Readout and Direct Broadcast Services*. Washington, DC.

NOAA. 2004. *NOAA-N Satellite*. Suitland, Maryland.

NOAA . 2008. *Antenna and RF Systems Capabilities Handbook*. Suitland, MD, USA.

NOAA. 2009. *User's Guide for Building and Operating Environmental Satellite Receiving Stations*. Suitland, MD, USA.

Ohmori, S., Wakana, H. and Kawase, S. 1998. *Mobile Satellite Communications,* Artech House, ISBN: 0-89006-843-7, Norwood, MA, USA

Orbit . 2014. *Solutions of Meteorological Antenna Systems*. Netanya, Israel.

Pace, P., Aloi, G., De Rango, F., Natalizio, E., Molinaro, A. and Marano, S. 2004 . *An integrated satellite-HAP-terrestrial system architecture: resources allocation and traffic management issues. Vehicular Technology Conference, 2004. VTC 2004-Spring. 2004 IEEE 59th*, Vol.5 Volume: 5, pp: 2872 – 2875.

Pascall, S. C. and Withers, D. 1997. *Commercial Satellite Communications*, Focal Press.

Pranajaya, F. M., Zee, R. E., Cain, J. and Kolacz, R. 2010. *Nanosatellite Tracking Ships: Cost-Effective Responsive Space*. The 4S Symposium - Small Satellites Systems and Services, Funchal.

Pratt, T., Bostian, C.W. and Allnutt, J.E. 2002. *Satellite Communications*. 2nd Edition, John Wiley & Sons

Reckeweg, M. and Rohner, C. 2015. *Antenna Basic*. Rohde & Schwarz, München, Germany.

Richharia, M. 1995. *Satellite Communications System - Design principles*. Macmillan, Basingstoke.

Roddy, D. 1996. *Satellite Communications.* McGraw Hill, New York.

Rohner, C. 2013. *Antenna Basic* . Rohde & Schwarz, München, Germany.

Roscosmos. 2015. *Main Components of Russian Electro GEO Satellite*. Moscow, Russia.

Roshydromet. 2014. *High-elliptical Orbits Satellite System Arctica*. SRC Planeta, Moscow, Russia.

Roshydromet. 2009 . *Status of Current and Future Roshydromet Satellite Programmes*. State Research Centre on Space Hydrometeorology "Planeta", Moscow, Russia.

Rossow, B.W. 2015. *International Satellite Cloud Climatology Project.* NASA, Washington, DC.

Rublev, A. 2014. *Development and Application Perspectives of Space-Based Components in Roshydromet Observation Network*. Roshydromet (State Research Centre PLANETA), Moscow, Russia.

Schmetz, J. 2002. *An Introduction to Meteosat Second Generation (MSG).* American Meteorological Society, Washington DC.

Schmid, J. 2011. *The SEVIRI Instrument*. ESA/ESTEC, Noordwijk, Netherlands.

Schmidt, K. 2010. *World's First Weather Satellite Launched 50 Years Ago Today*. Rockville, MD, USA.

Schott, J.R. 1997. *Remote Sensing*. Oxford University Press, Oxford.

SCISYS. 2014. *Data Acquisition Software for PEO/GEO Observation Missions*. Bochum, Germany.

SeaSpace. 2011. *Mobile LEO Satellite Direct Readout*. Poway, CA, USA.

SeaSpace. 2012. *Shipboard Satellite Weather Receiving Antenna - 0.61m (L-band).* Poway, CA, USA.

Shang, L.D. and Gong, J., *Geospatial Technology for Earth Observation.* Springer, Boston.

Sheriff, R.E. and Fun Hu, Y. 2001. *Mobile Satellite Communication Networks.* John Wiley Sons Ltd, Chichester.

Singh, D. 2014. *Status Report on Current and Future Geostationary Indian Satellites.* Satellite Meteorology, New Delhi, India.

SSEC. 2006. *40 Years of Geostationary Satellite Research and Observations.* Space Science and Engineering Center", Madison, WI, USA.

Stacey, D. 2008. *Aeronautical Radio Communication Systems and Networks.* Wiley, Chichester.

Sun, Z. 2005 . *Satellite Networking - Principles and Protocols.* John Wiley, Chichester.

Tan, S.Y. 2014. *Meteorological Satellite Systems* . Springer, New York.

Tang, Y., Zhang, J. and Wang, J.2014. *FY-3A Meteorological Satellite and the Applications.* National Satellite Meteorological Center/National Center for Space Weather, China Meteorological Administration, Beijing 100081

TAO. 2006. *TAO Stratospheric Platforms Project* .Tokyo.

Thornton, J., Grace, D., Spillard, C., Konefal, T. and Tozer, T. C. 2001. *Broadband Communications from a High Altitude Platfoims*. IEE Electronics and Communications Engineering Journal, vol. 13, no. 3, pp. 138-144.

Uesawa, D. 2006. *Status of Japanese Meteorological Satellites and Recent Activities of MSC* . Proceedings of the 2006 EUMETSAT Meteorological Satellite Conference, Helsinki, Finland.

US. 2007. *SumbandilaSat.* University of Stellenbosch, Cape Town, RSA.

Vaisala. 2015. *Automatic Weather Station (AWS).* Malmö, Sweden.

Wang, S. 2007. *The Quantitative Research on Dynamic Changes between flood and Vegetation in Tarim river valley* . PhD, Beijing Normal University.

Wang, W-Q. 2011. *Near-Space Remote Sensing.* Springer, New York, USA.

West, R. 2014, *Soil Moisture Active and Passive Mission (SMAP).* NOAA, Washington, DC.

Widiawan, A., Tafazolli, R., Evans, B., Milas, V. and Constantinou, P. 2005. *Coexistence of high altitude platform station, satellite, and terrestial systems for fixed and mobile services*. in Proceedings of International Workshop on High Altitude Platform Systems, Athens, Greece.

WMO. 2013. *Guide to the Observing System*. World Meteorological Organization, Geneva, Switzerland.

Xu, H. 2006. *Modification of normalised difference water index (NDWI) to enhance open water features in remotely sensed imagery*. International Journal of Remote Sensing, vol: 27, pp: 3025-3033.

Yulsman, T. 2013 . *Historic First Weather Satellite Image.* NASA, Washington, DC.

Zhilin, V.A. 1988. *Mezhdunarodnaya sputnikova sistema morskoy svyazi – Inmarsat*. Sudostroenie, Leningrad, USSR.